The Evolution of the Sub-Cratonic Mantle Seen in Mantle Xenoliths

Simon Robert Burgess

BSc St. Andrews 1993

Thesis Submitted for the Degree of Doctor of Philosophy

The University of Edinburgh

1997

TABLE OF CONTENTS

Volume 2: Tables and Figures

Chapter 2

Petrology and Geochemistry of the Sub-Cratonic Mantle

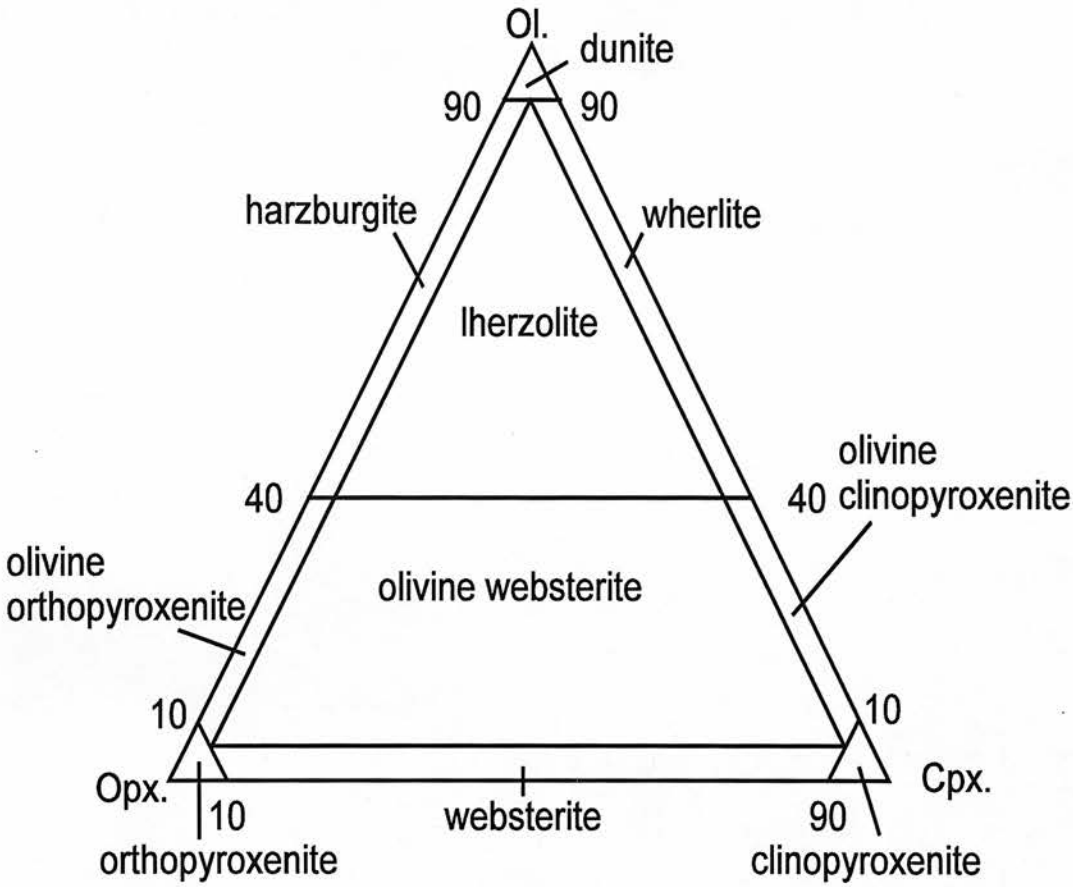

Fig. 2.1 Classification and nomenclature of ultramafic rocks, after Streckheisen (1975) Fig. 2.

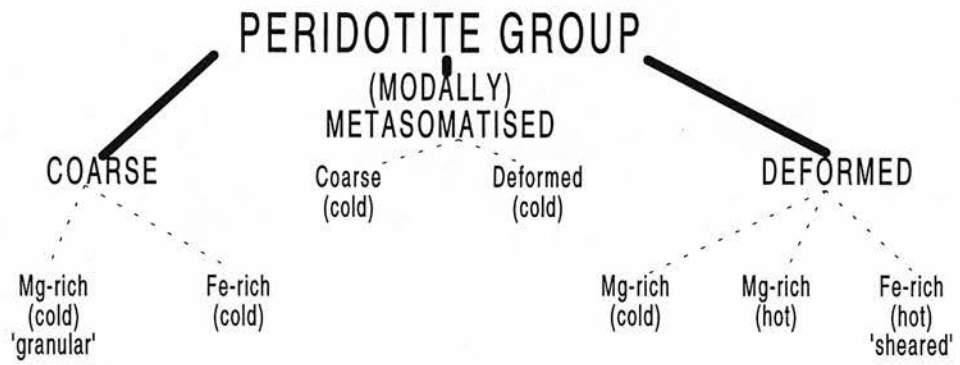

Fig.2.2 Classification of Peridotites after Harte (1983), Fig. 2.

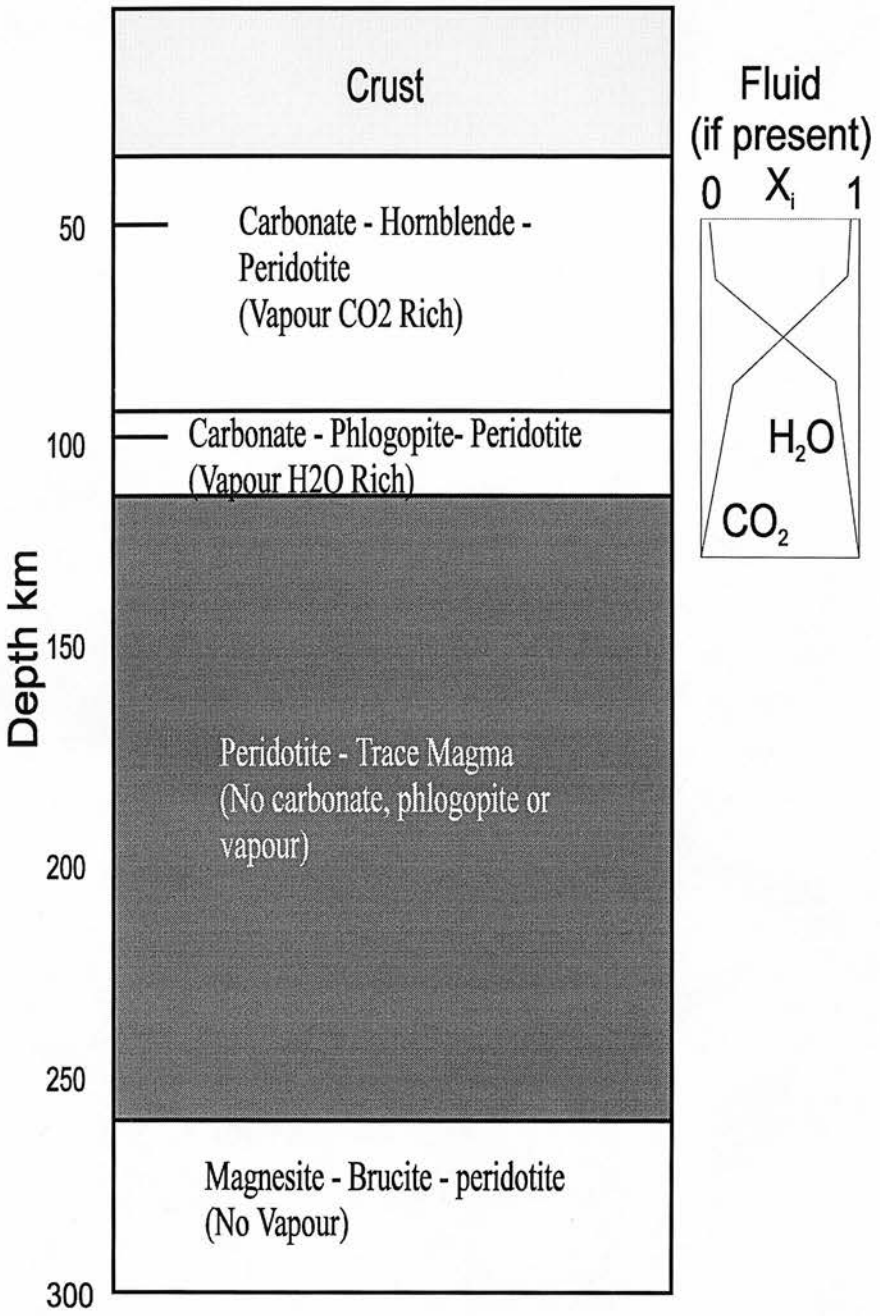

Fig. 2.3. A cross-section of the distribution of volatiles in mantle phases. Modified from Wyllie (1987), Fig. 313b. Inset (Modified from Schneider and Eggler 1986, Fig. 1) shows the composition of H_2O-CO_2 fluid at solidus temperatures, buffered by peridotite. Vertical scale for inset is identical to the main figure.

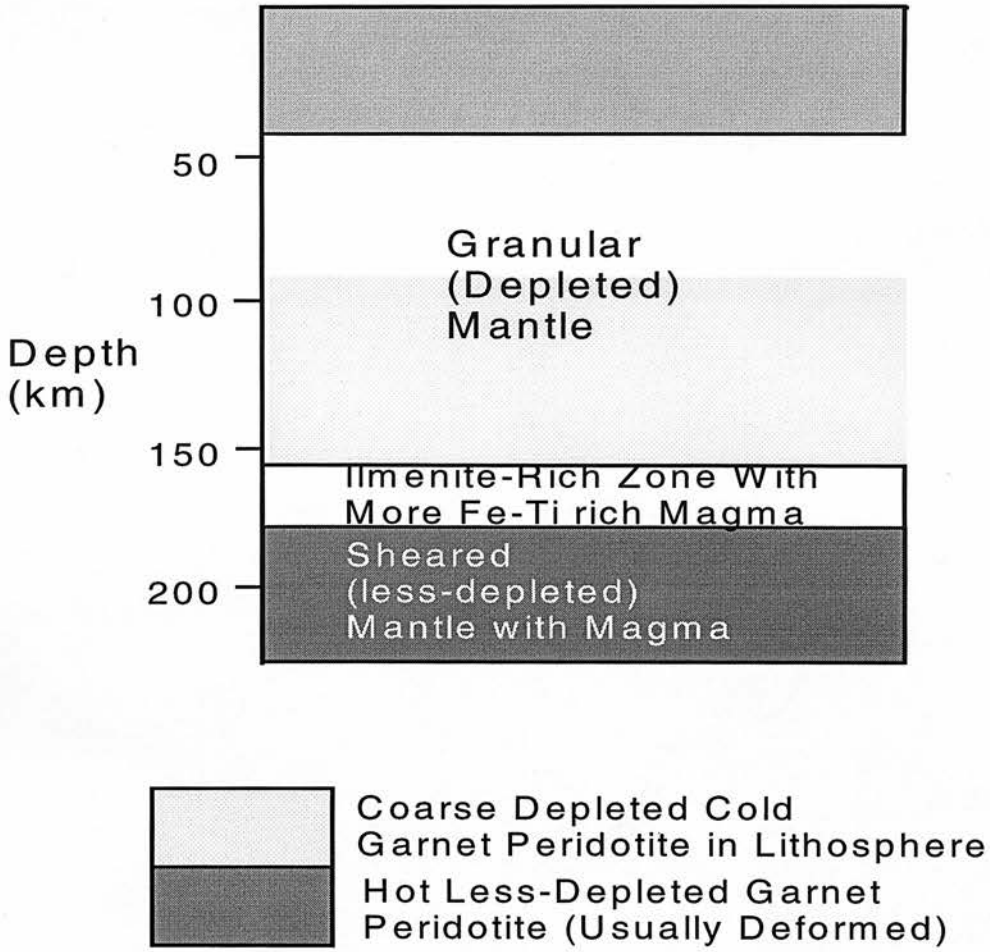

Fig. 2.4a Schematic cross-section of the crust and upper mantle based on the model of Nixon and Boyd (1973a,b).

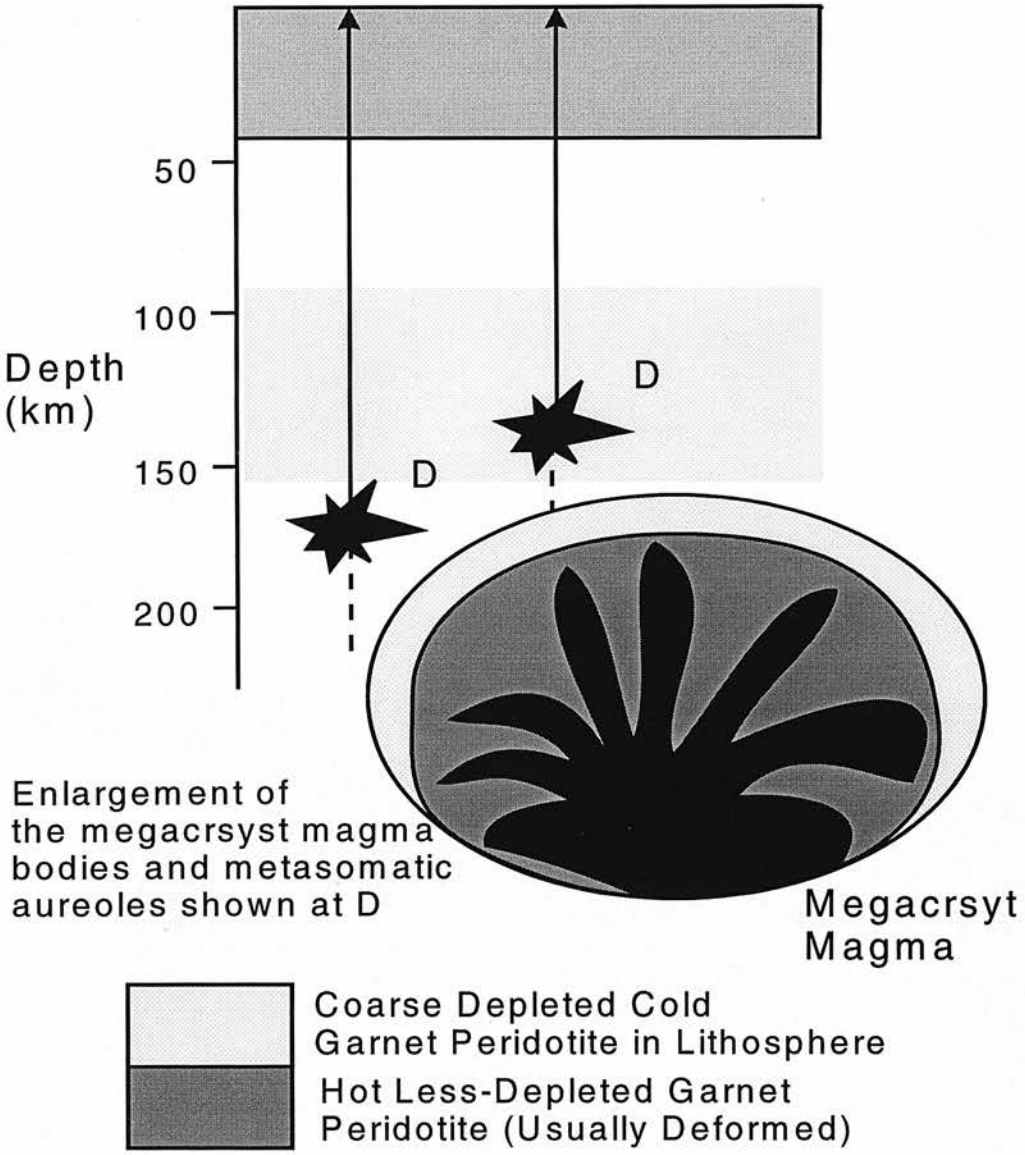

2.4b Schematic cross-section of the crust and upper mantle based on the model of Harte (1983). Solid vertical arrows indicate kimberlite eruption at some time following the formation of the megacryst magma. The vertical dashed lines indicate the derivation of the megacryst magma bodies from the asthenosphere.

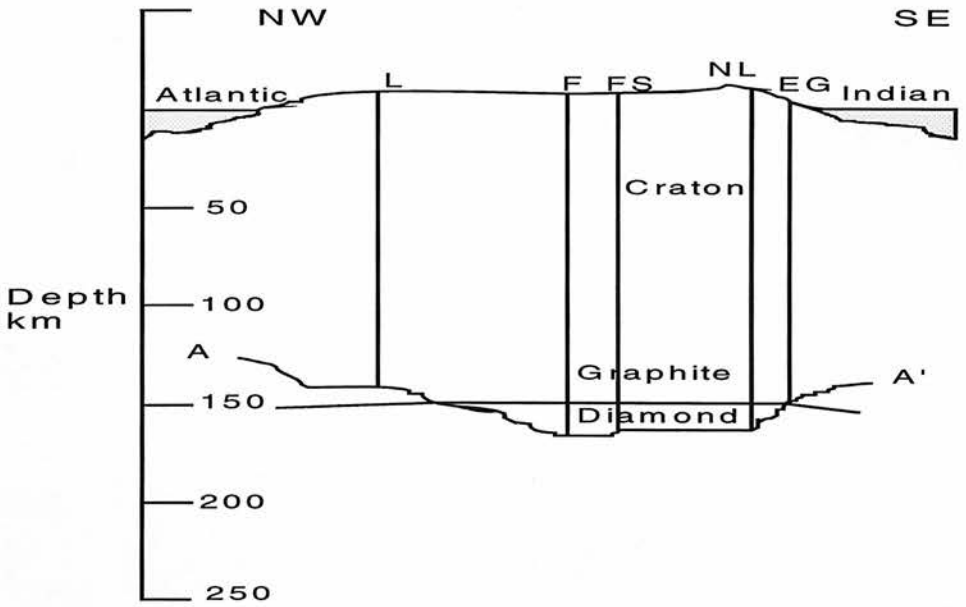

Fig. 2.5 Vertically exaggerated cross-section for the mantle below southern Africa, showing the depth to the inflected geotherm measured for xenoliths from five kimberlites: Louwrencia (L), Finsch (F), Frank Smith (FS), Northern Lesotho (NL) and East Griqualand (EG). Finsch, Frank Smith and Northern Lesotho are on craton. Based on Boyd and Gurney (1986) Fig. 6.

Chapter 3

Jagersfontein Xenoliths: A Summary of General Features and Previous Work

SAMPLE	P(BK)	T(CH)	P(BK)	T(K)	P(BK)	T(OW)	P(BK)	T(BM)	P(BK)	T(BK)	Group
J10	37	875	26	700	29	750	27	730	22	620	Low-T
J24	43	970	35	810	32	750	37	880	33	770	Low-T
J25	38	900	32	820	30	780	33	830	30	780	Low-T
J28	37	890			27	760					Low-T
J53	36	860	29	740	29	740	31	770	26	690	Low-T
J146	43	1030			45	1080					Medium-T
J157	38	970			36	920					Medium-T
JJG1728	32	930	44	1140	30	880	35	970	36	980	Medium-T
JJG1757	20	770			13	610					Low-T
JJG1761	39	1040			37	1000					Medium-T
JJG1780	34	940			31	900					Medium-T
JJG1781	37	1030			38	1040					Medium-T
JJG1795	38	980	50	1170	36	920	37	950	38	960	Medium-T

Table 3.1a. Equilibrium Pressures (kbar) and Temperatures (°C) for Jagersfontein Coarse Xenoliths
(BK) Brey and Kohler (1990) pressure:- Al in opx., temperature:- opx.-cpx. solvus.
(CH) Carswell and Harley (1989) temperature:- Mg-Fe gnt.-opx. exchange.
(K) Krogh (1988) temperature:- Mg-Fe gnt.-cpx. exchange.
(OW) O'Neill and Wood (1979) temperature:- Mg-Fe gnt.-ol. exchange.
(BM) Bertrand and Mercier (1985) temperature:- opx.-cpx. solvus.
Group corresponds to the sample classification used in this thesis, summarised in section 3.3.1.4.

SAMPLE	P(BK)	T(CH)	P(BK)	T(K)	P(BK)	T(OW)	P(BK)	T(BM)	P(BK)	T(BK)	Group
J18	43	1030			44	1070					High-T
J22	40	1100			41	1125					High-T
J26	55	1250	58	1300	55	1270	58	1300	60	1330	High-T
J31	45	1170	52	1270	47	1190	51	1260	52	1290	High-T
J33	51	1250	58	1350	55	1310	53	1280	55	1310	High-T
J34	57	1330	57	1330	60	1380	57	1330	58	1350	High-T
J36	60	1320	60	1320	60	1320	61	1330	63	1370	High-T
J37	49	1190	53	1250	60	1360	54	1270	56	1310	High-T
J38	57	1310	59	1340	57	1310	57	1310	59	1340	High-T
J42	52	1230	54	1260	53	1250	55	1270	57	1300	High-T
J47	69	1320	70	1330	62	1230	65	1270	68	1320	High-T
J51	65	1330	63	1300	60	1270	59	1230	62	1290	High-T
J104	48	1220	50	1260	48	1230	54	1320	55	1340	High-T
J107	43	1180			45	1220					High-T
J110	45	1169	56	1340	45	1160	55	1330	57	1360	High-T
J112	57	1350	55	1320	45	1160	52	1270	53	1280	High-T
J115	62	1360	58	1300	56	1270	60	1330	62	1360	High-T
J119	55	1240	59	1310	56	1250	54	1230	57	1270	High-T
J121	52	1220	53	1230	52	1220	57	1310	60	1340	High-T
J145	32	960	41	1220	34	1000	41	1220	42	1240	High-T
J159	47	1100			50	1150					High-T
JJG1776	54	1230	60	1320	55	1240	57	1270	60	1320	High-T
JJH11	48	1220	52	1280	53	1300	55	1340	57	1370	High-T
JJH19	47	1230			49	1270					High-T
JJH37	45	1190	51	1290	45	1190	52	1320	54	1340	High-T

Table 3.1b. Equilibrium Pressures (kbar) and Temperatures (°C) for Jagersfontein Deformed Xenoliths
(BK) Brey and Kohler (1990), (CH) Carswell and Harley (1989), (K) Krogh (1988), (OW) O'Neill and Wood (1979), (BM) Bertrand and Mercier (1985). See Table 3.1a
Group corresponds to the sample classification used in this thesis, summarised in section 3.3.1.4.

SAMPLE	P(BK)	T(BK)	Texture
J145	42	1240	Porphyroclastic
J119	57	1270	Mosaic
J112	53	1280	Porphyroclastic
J31	52	1290	Fluidal Mosaic
J51	62	1290	Porphyroclastic
J42	57	1300	Mosaic
J33	55	1310	Fluidal Mosaic
J37	56	1310	Porphyroclastic
J47	68	1320	Mosaic
JJG1776	60	1320	Porphyroclastc
J26	60	1330	Porphyroclastic
J104	55	1340	Fluidal Mosaic
J38	59	1340	Mosaic
J121	60	1340	Mosaic
JJH37	54	1340	Mosaic
J34	58	1350	Mosaic
J110	57	1360	Mosaic
J115	62	1360	Mosaic
J36	63	1370	Mosaic
JJH11	57	1370	Mosaic

SAMPLE	P(BK)	T(OW)	Texture
J145	34	1000	Porphyroclastic
J18	44	1070	Transitional
J22	41	1125	Fluidal Mosaic
J159	50	1150	Mosaic
J112	45	1160	Porphyroclastic
J110	45	1160	Mosaic
J31	47	1190	Fluidal Mosaic
JJH37	45	1190	Mosaic
J121	52	1220	Mosaic
J107	45	1220	Mosaic
J47	62	1230	Mosaic
J104	48	1230	Fluidal Mosaic
JJG1776	55	1240	Porphyroclastc
J119	56	1250	Mosaic
J42	53	1250	Mosaic
J51	60	1270	Porphyroclastic
J26	55	1270	Porphyroclastic
J115	56	1270	Mosaic
JJH19	49	1270	Mosaic
JJH11	53	1300	Mosaic
J33	55	1310	Fluidal Mosaic
J38	57	1310	Mosaic
J36	60	1320	Mosaic
J37	60	1360	Porphyroclastic
J34	60	1380	Mosaic

Table 3.2 Jagersfontein deformed xenoliths sorted in order of increasing temperature (°C) from the thermometers of (BK) Brey and Kohler (1990), and (OW) O'Neill and Wood (1979). The texture of each sample is given, to demonstrate the variation in degree of deformation with measured temparature.

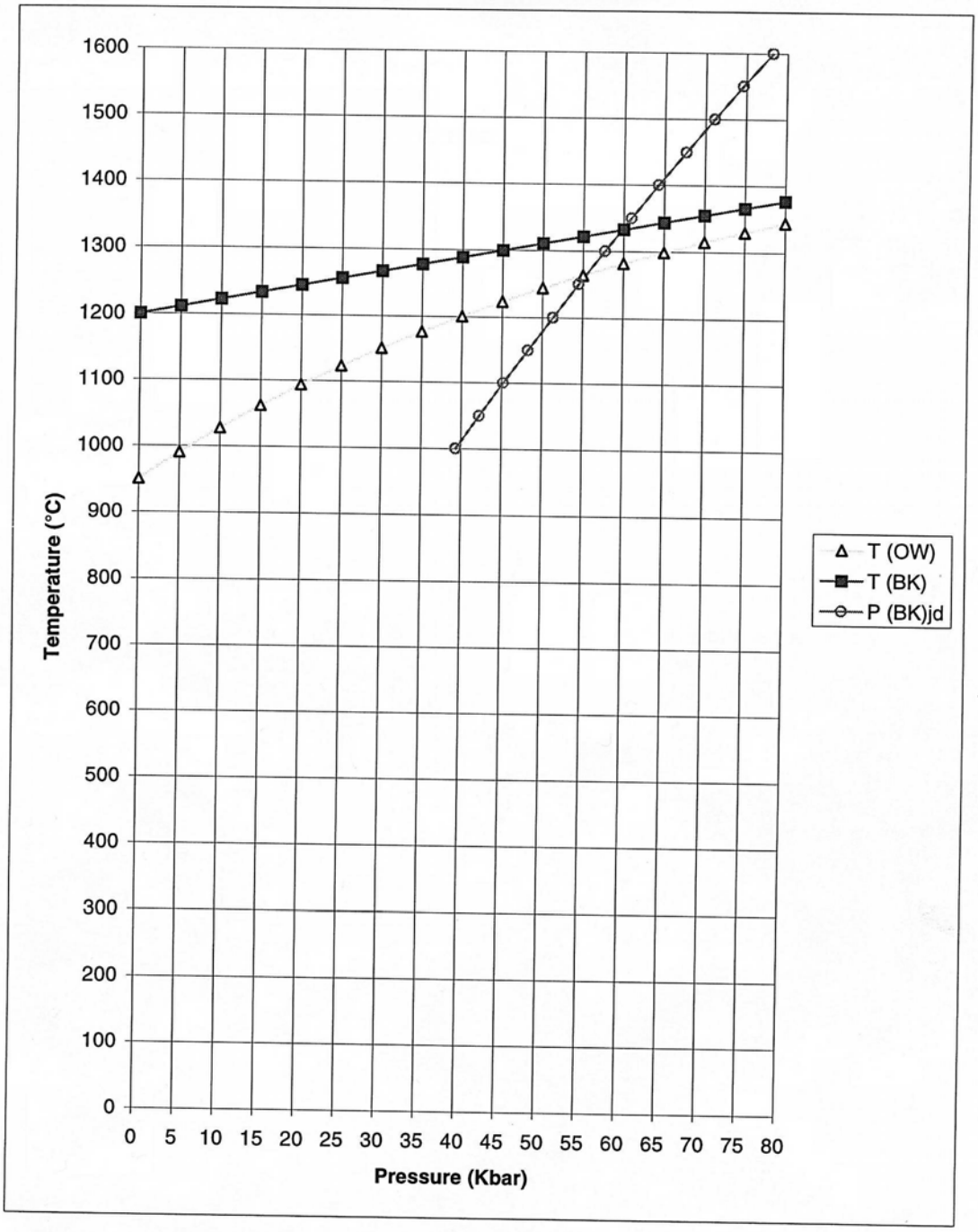

Fig. 3.1 Pressure-temperature arrays for (OW) O'Neill and Wood (1979), (BK) Brey and Kohler (1990) thermometers, and (BK) Brey and Kohler (1990) barometer. For (OW) thermometer and (BK) barometer: T=1270°C, P=55kbar; for (BK) thermometer and (BK) barometer: T=1330°C, P=60kbar. Sample is J26.

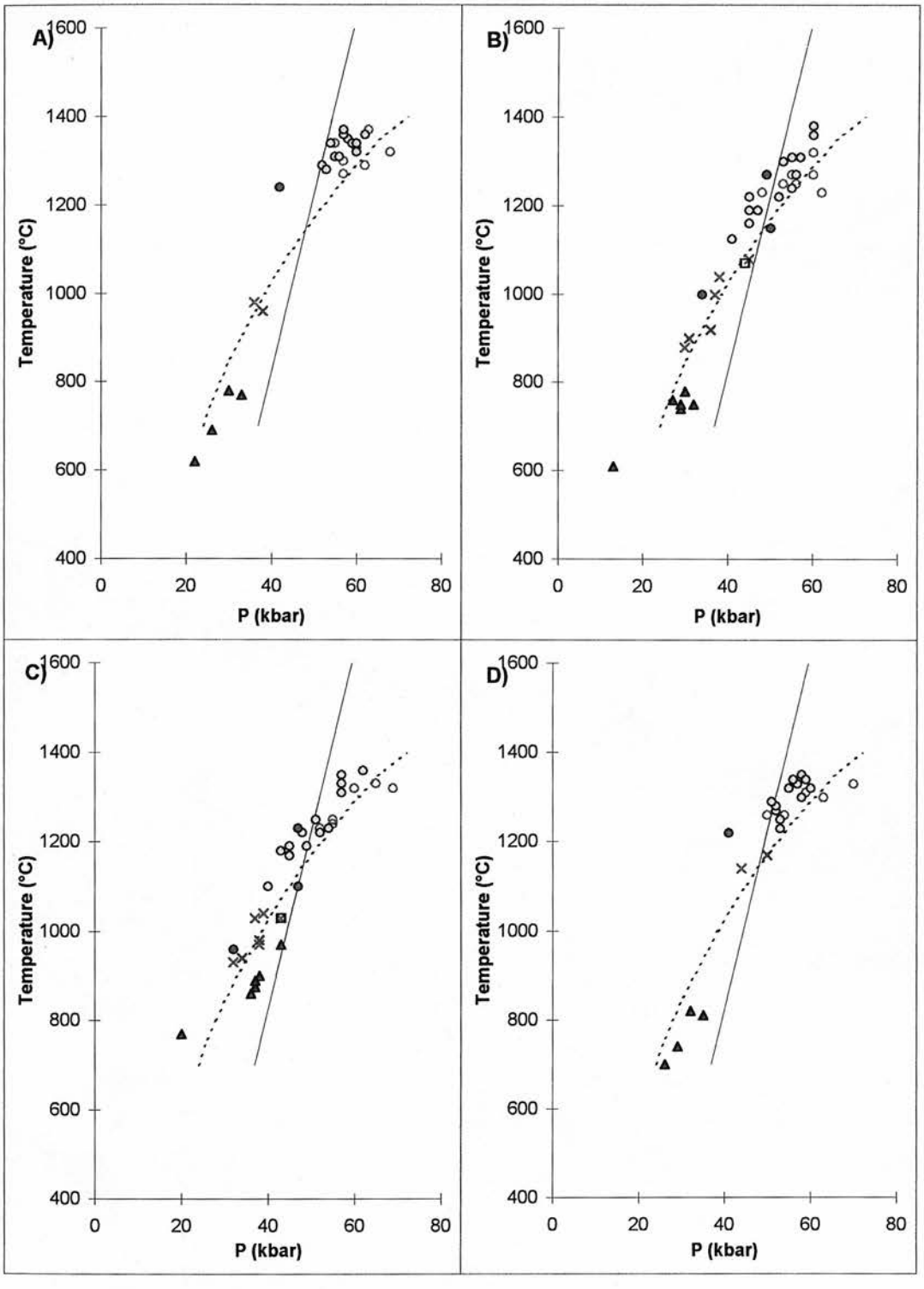

Fig. 3.2 Graphs of temperature against pressure for Jagersfontein xenoliths. Pressure calculations use Brey and Kohler (1990) barometer, thermometers are A) Brey and Kohler (1990) cpx-opx solvus, B) O'Neill and Wood (1979) Mg-Fe gnt-ol exchange, C) Carswell and Harley (1989) Mg-Fe gnt-opx exchange, D) Krogh (1988) Mg-Fe gnt-cpx exchange.
Symbols are: Coarse with G10 garnet, purple cross; Coarse with G9 garnet, red triangle; Coarse amphibole-bearing, green triangle; Coarse phlogopite-bearing, brown cross; Deformed with zoned garnets, blue circle; Deformed lherzolites, red circle; Deformed harzburgites, black open square; Deformed with G10 garnet, purple circle. The solid black line is the diamond-graphite equilibrium of Kennedy and Kennedy (1976), the dashed line is the 44mW/m2 conductive geotherm calculated by Kohler and Brey (1990) from the data of Chapman and Pollack (1977).

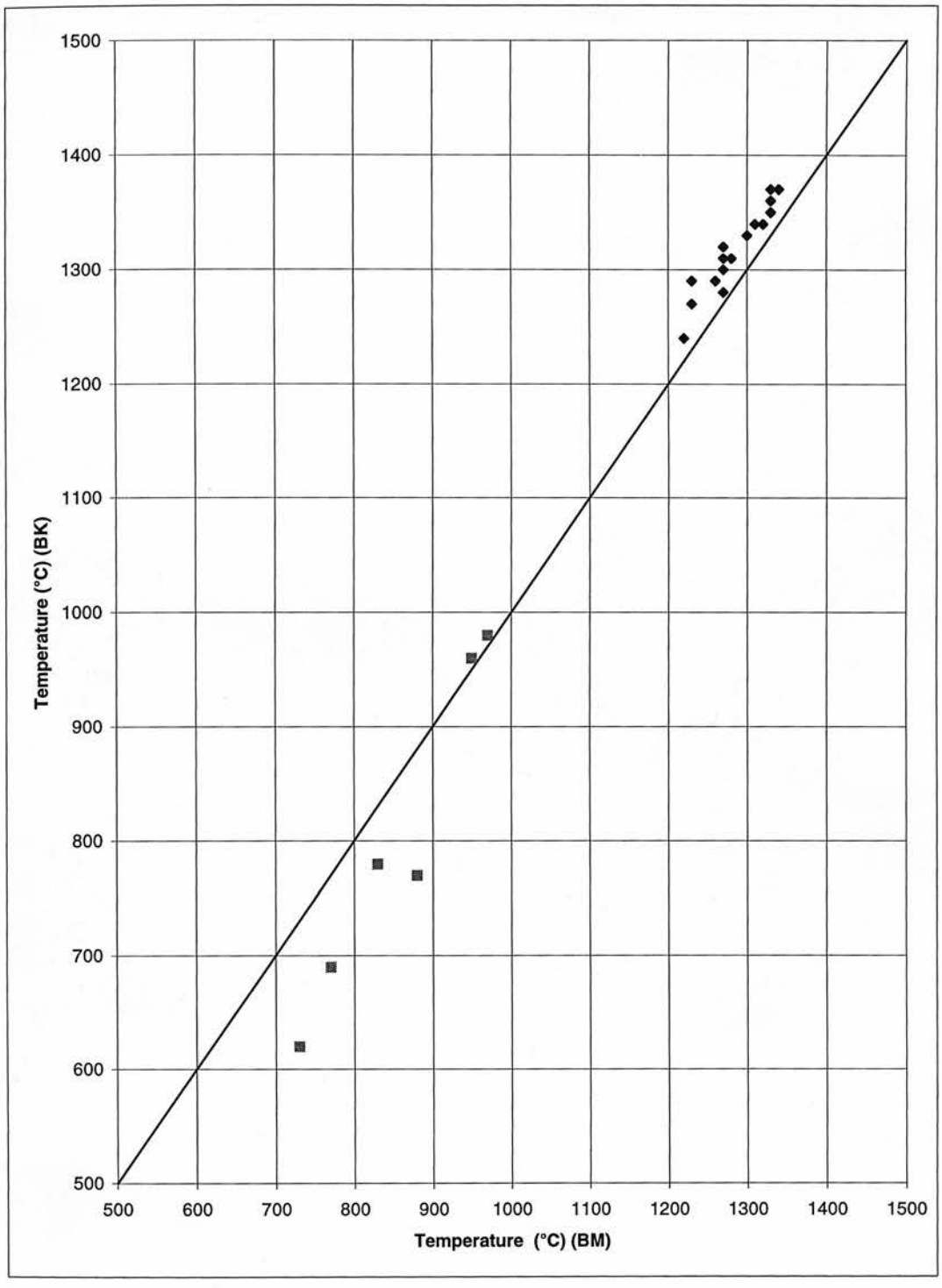

Fig. 3.3 A comparison of the temperature calibration of Brey and Kohler (1990), and Bertrand and Mercier (1985), for Jagersfontein xenoliths. Squares are coarse xenoliths, diamonds are deformed xenoliths. Data from Tables 3.1a and 3.1b.

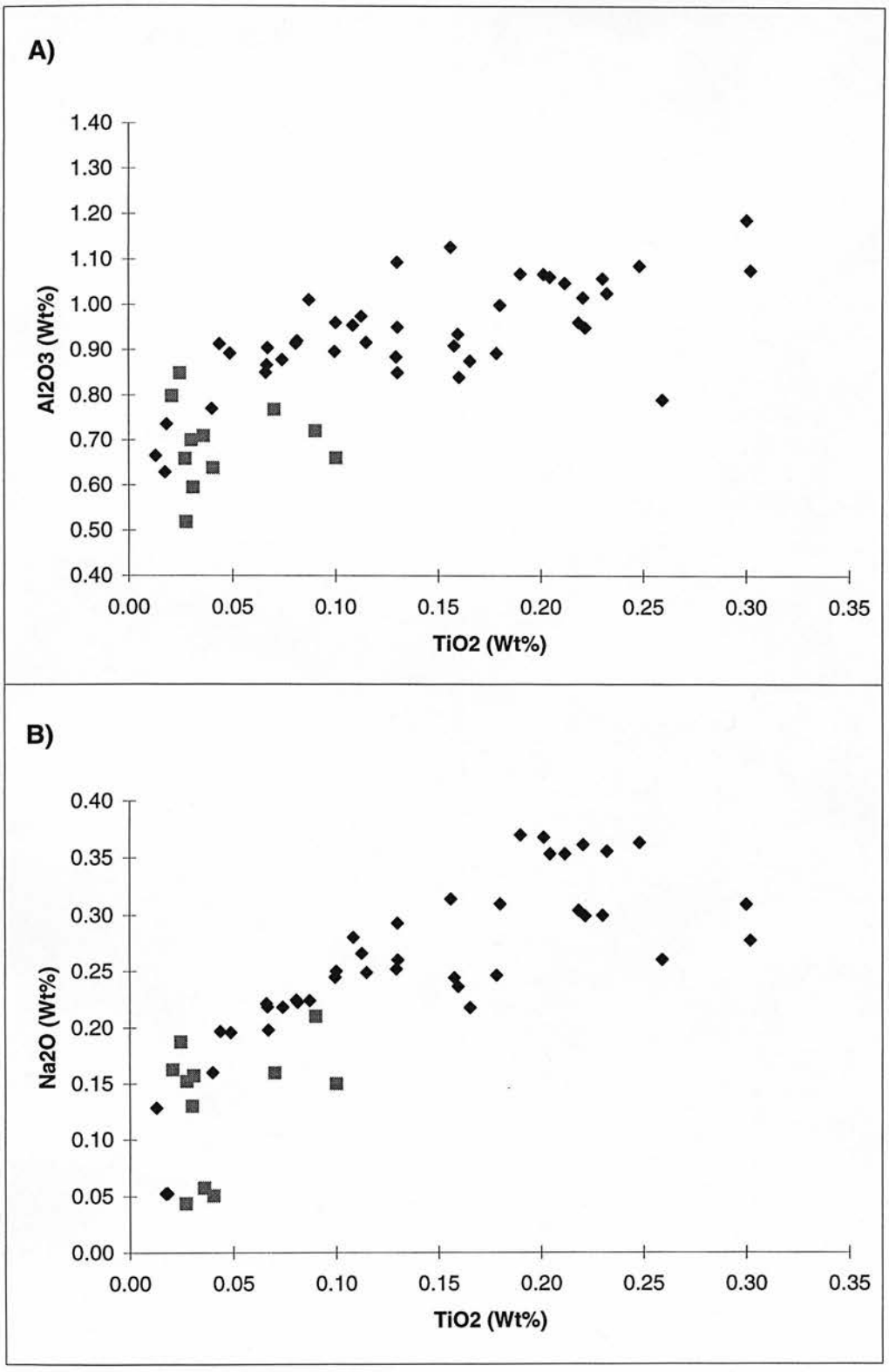

Fig. 3.4 A) Al2O3 against TiO2, and B) Na2O against TiO2 for orthopyroxenes from Jagersfontein xenoliths.
Data is from Table B.2. Squares are coarse xenoliths, diamonds are deformed xenoliths.

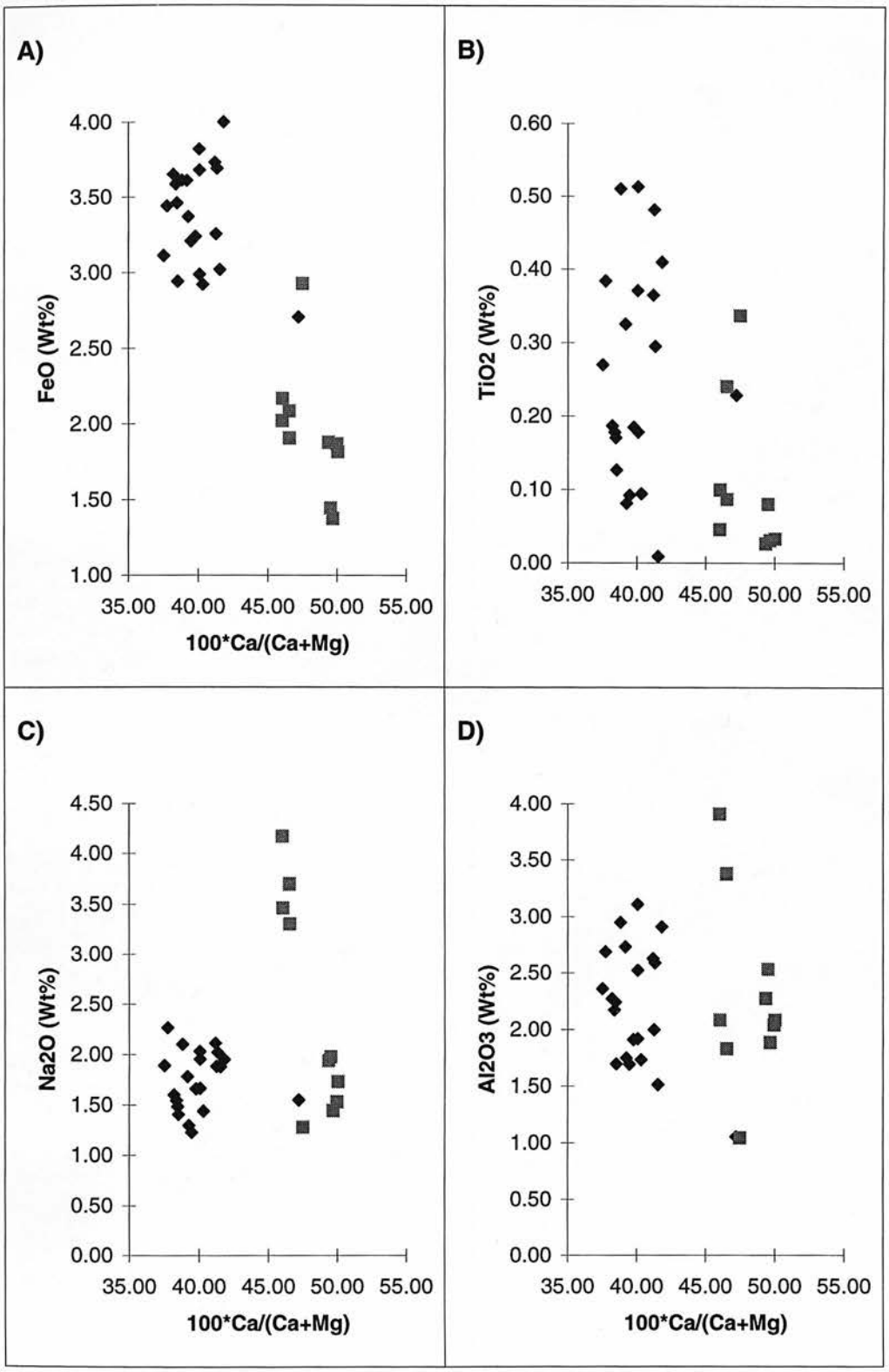

Fig. 3.5 A) FeO, B) TiO2, C) Na2O, and D) Al2O3 against 100*Ca/(Ca+Mg) or Ca number for clinopyroxenes from Jagersfontein xenoliths.
Data is from Table B.3. Squares are coarse xenoliths, diamonds are deformed xenoliths.

Chapter 4

Chemical Composition of Jagersfontein Garnets

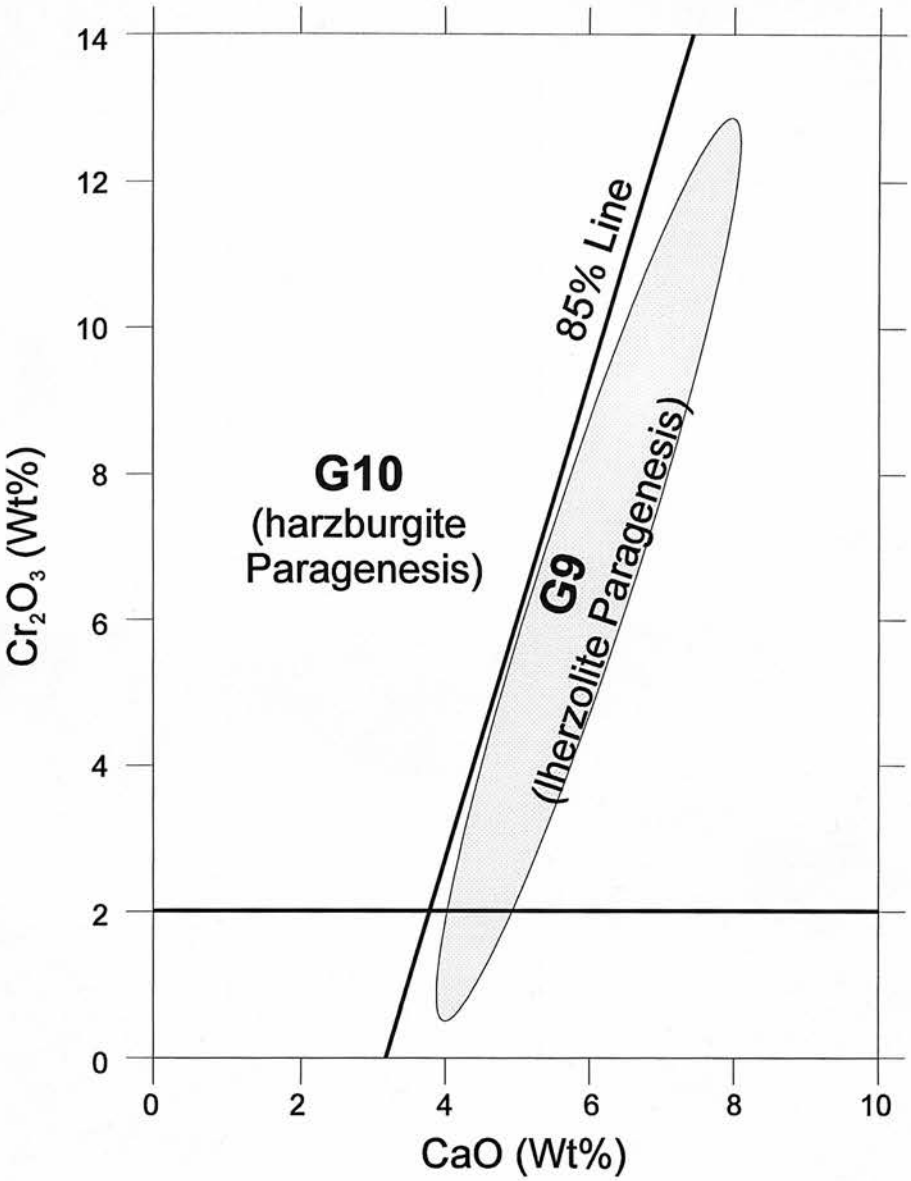

Fig. 4.1 Schematic representation of the Cr_2O_3 against CaO plot used to classify mantle garnet compositions. The two fields, G10-harzburgitic paragenesis, and G9-lherzolitic paragenesis are separated by the 85% line, derived from a study of diamond inclusion garnets from Finsch by Gurney (1984). Garnets to the left of this line plot in a field of variable CaO and Cr_2O_3, garnets to the right plot in a band, the 'lherzolite trend' shown by the grey area. The line at 2 wt% Cr_2O_3 is the arbitrary dividing line of Gurney (1984) which defines the field of garnets of eclogite paragenesis (<Cr_2O_3 2wt%).

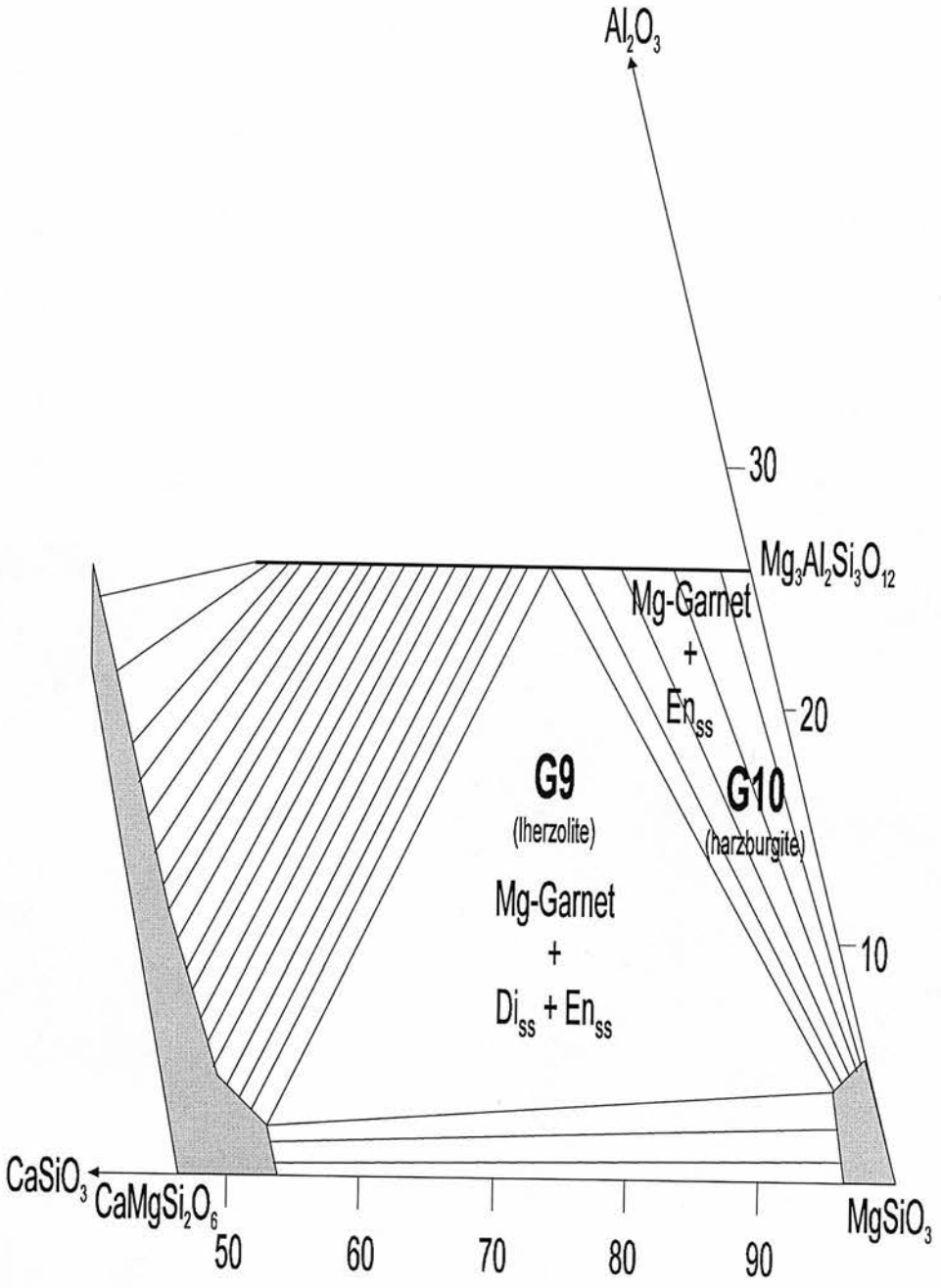

Fig. 4.2 Phase relations in the CMAS system at 1200°C and 30kbar. This is a schematic representation of part of Boyd (1970), Fig. 11. G10, harzburgite-paragenesis garnets are part of a two phase-univariant assemblage, so Ca may vary in concentration. G9, lherzolite-paragenesis garnets are part of a three phase-invariant assemblage, so have fixed Ca under these conditions. In this projection olivine is assumed to be present, but does not form solid solutions with pyroxene or garnet (see Boyd and Gurney 1986).

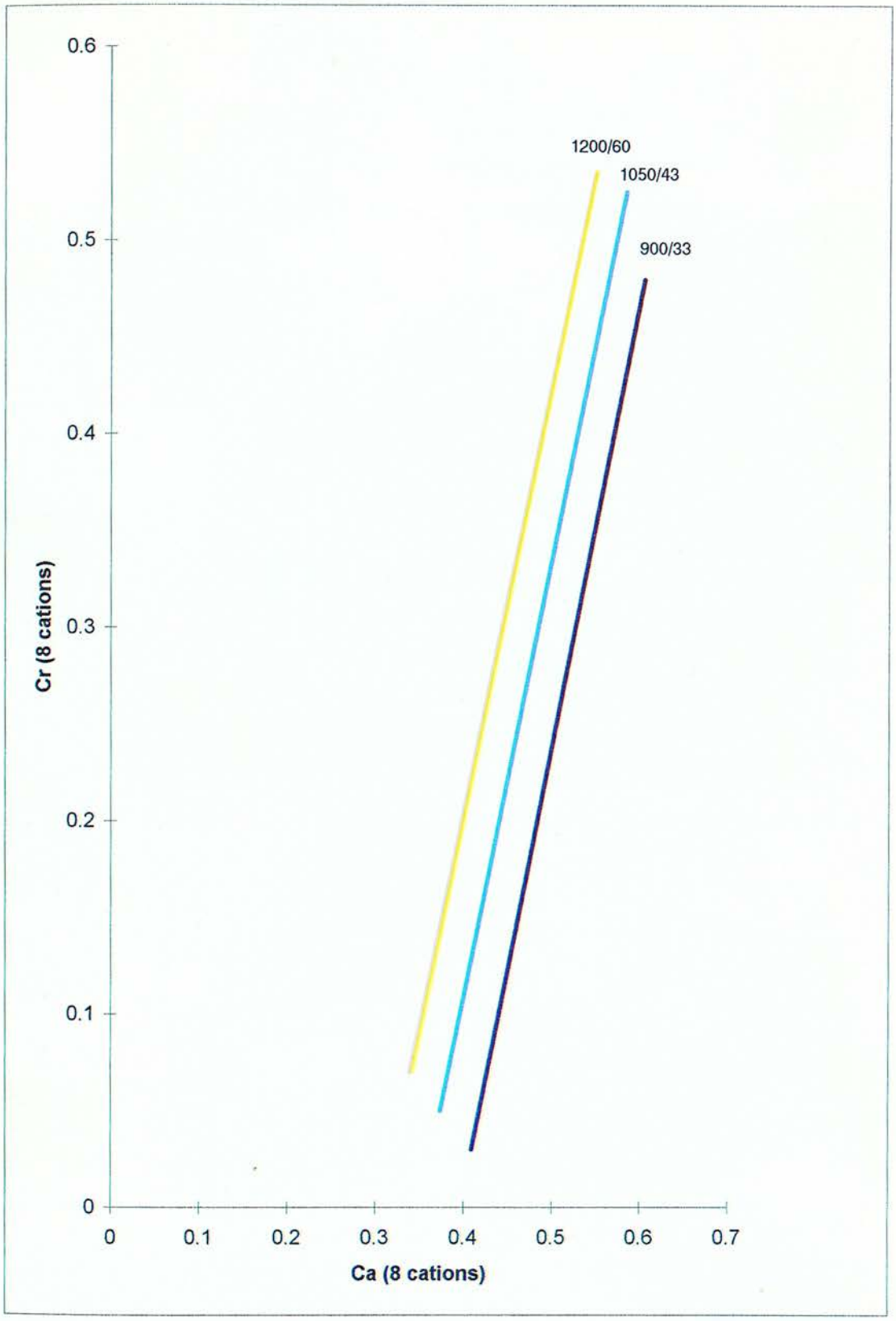

Fig. 4.3 Cr against Ca (based on 8 cations) for garnet in equilibrium with lherzolite assemblages modified from Brey (1991), Fig. 4. The lines link equilibrium compositions at a given pressure and temperature (burgundy 900°C/33kbar, sky blue 1050°C/43kbar, and yellow 1200°C/60kbar).

H:\jag12r9.xls

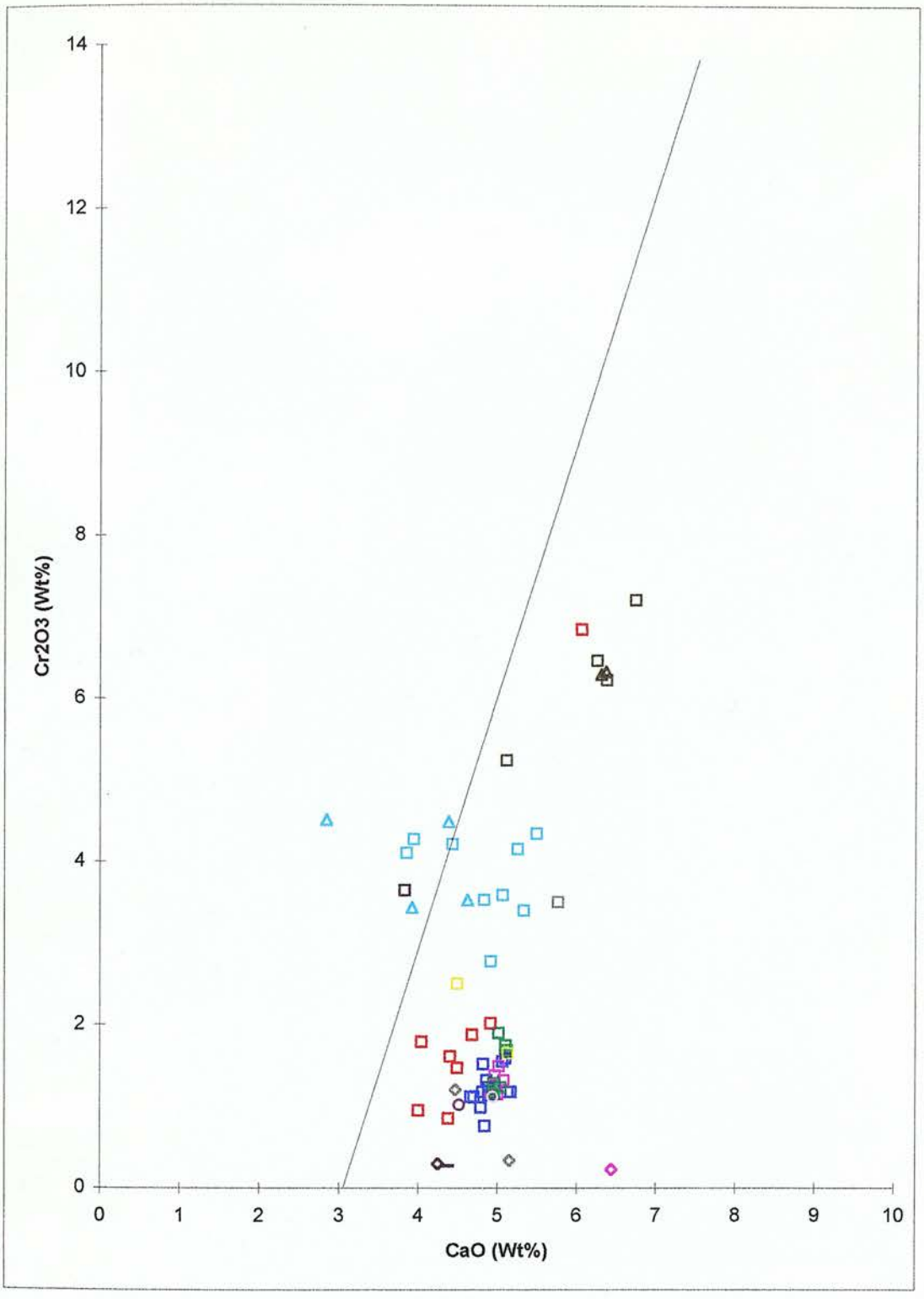

Fig. 4.4 Cr2O3 against CaO for garnets from alkali basalt hosted xenoliths and orogenic peridotites. Squares are lherzolites, circles garnet spinel lherzolites, triangles harzburgites, diamonds pyroxenites, bars wherlites. Sky blue symbols are from Lashaine (Reid et al. 1975, Rudnick et al. 1994), khakhi from Labait (Dawson et al. In Press), dark blue from Vitim (Ionov et al. 1992), pink from Khakasia (Sobolev 1995), green from Pali-Aike (Stern et al. 1989), burgundy from Marsabit, and grey Chyulu Henjes-Kunst and Altherr (1992), yellow from southern France (Albert and Brousse 1967, Berger and Brousse 1976), and red garnet serpentinites from the Czech Massif (Fiala 1965).
The black line is the 85% line of Gurney (1984).

H:\thesis\ca-cr.xls

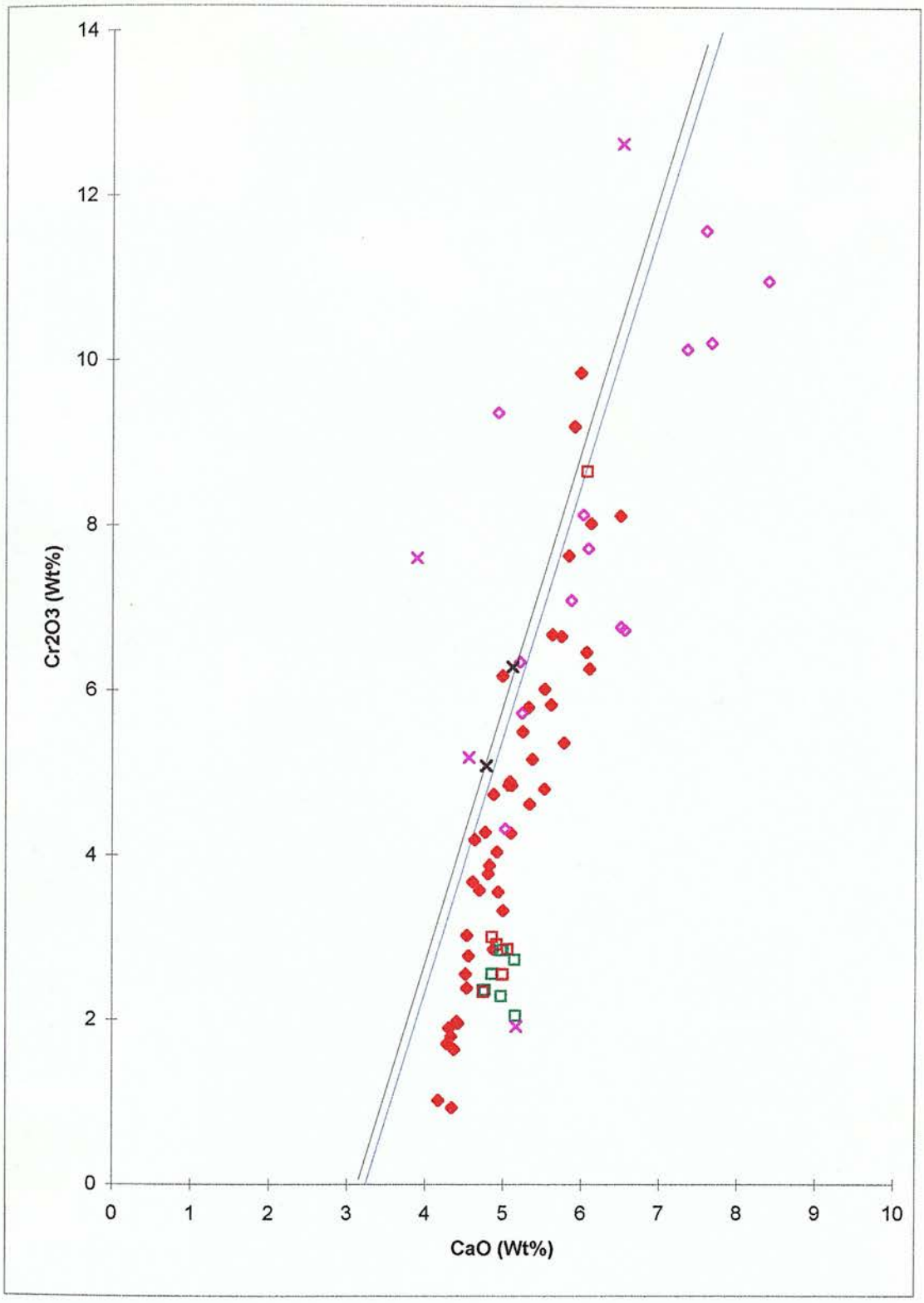

Fig. 4.5 Cr_2O_3 against CaO for Jagersfontein Garnets. Only homogeneous garnets are included in this plot. Red squares are coarse lherzolites, green squares are amphibole bearing coarse xenoliths, purple crosses are coarse harzburgites, brown crosses are phlogopite bearing coarse xenoliths, red diamonds are deformed lherzolites, purple diamonds are deformed harzburgites. The solid black line is the 85% line of Gurney (1984). The blue line is the division between G9 and G10 garnets for the Jagersfontein samples, based partly on trace element compositions (Chapter 7). Data from Table B.4a, Winterburn (1987) and Hops (1989).

H:\thesis\ca-cr.xls,sheet2

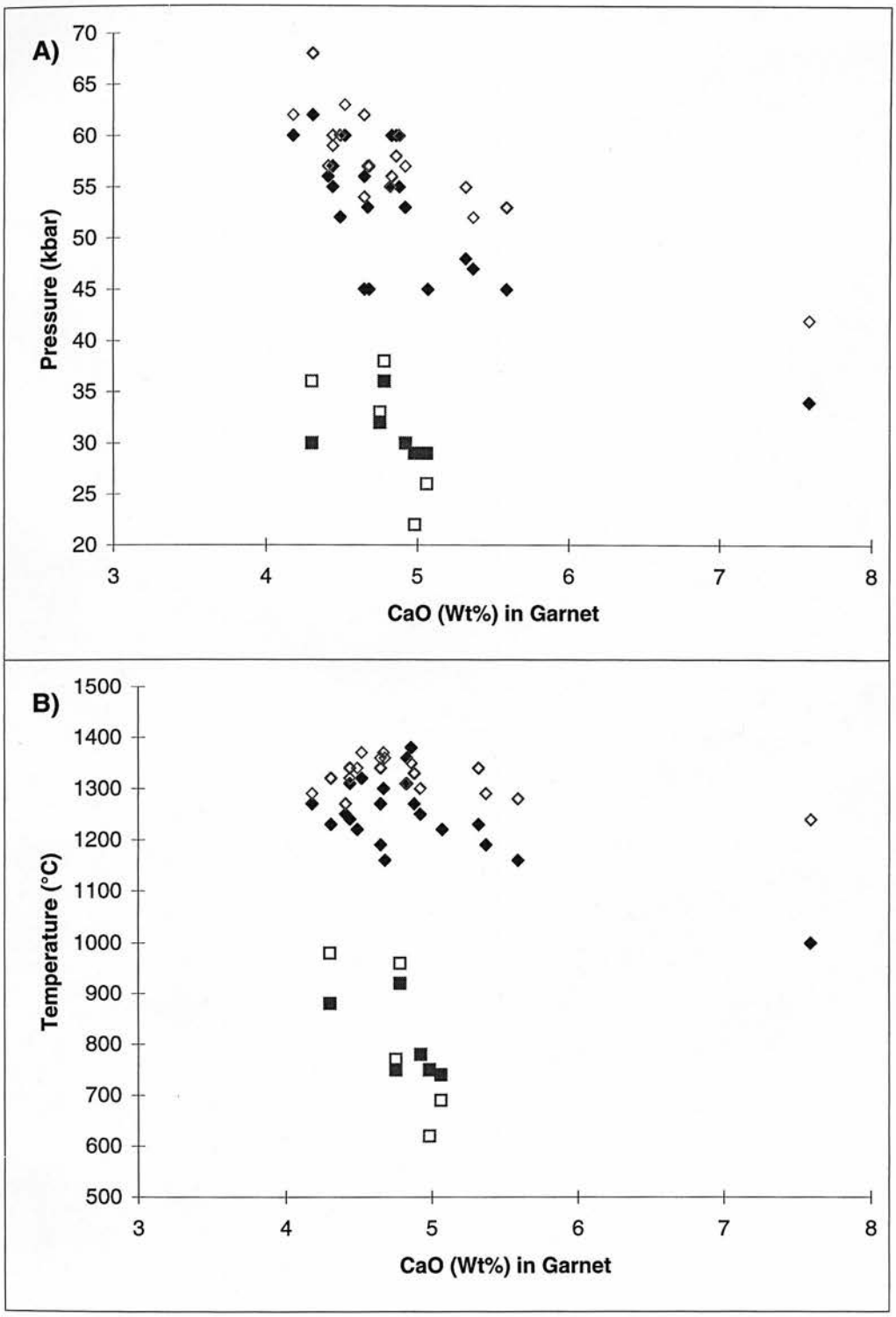

Fig. 4.6 A) Pressure, B) Temperature against CaO content in garnet for Jagersfontein xenoliths.
Filled symbols use Brey and Kohler (1990) barometer, and O'Neill and Wood (1979) thermometer, Open symbols use Brey and Kohler (1990) barometer and thermometer. Squares are coarse lherzolites, diamonds are deformed lherzolites. For zoned garnets rim compositions have been used.
Data is from Tables 3.1a,b, and B.4a.

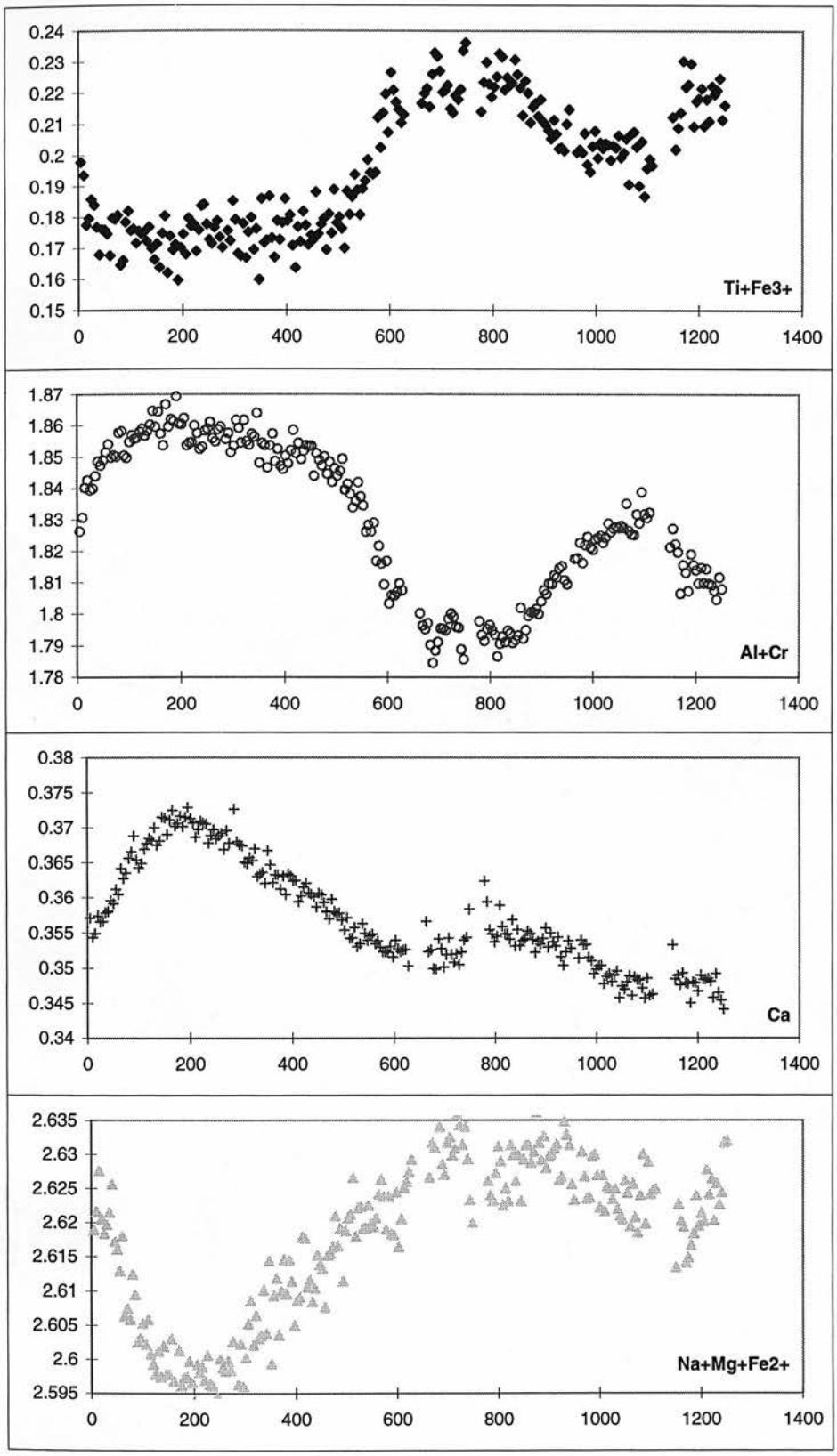

Fig. 4.7 Line Profile -1 Across JJH37 Garnet B (Fig. C.17a) recast to 8 cations. Fe3+/Fe2+ is calculated by the method of Ryburn et al. (1976). Profiles show the major substitutions on the Y-site: Cr + Al = Ti + Fe3+, and on the X-site: Ca = Na + Mg + Fe2+.

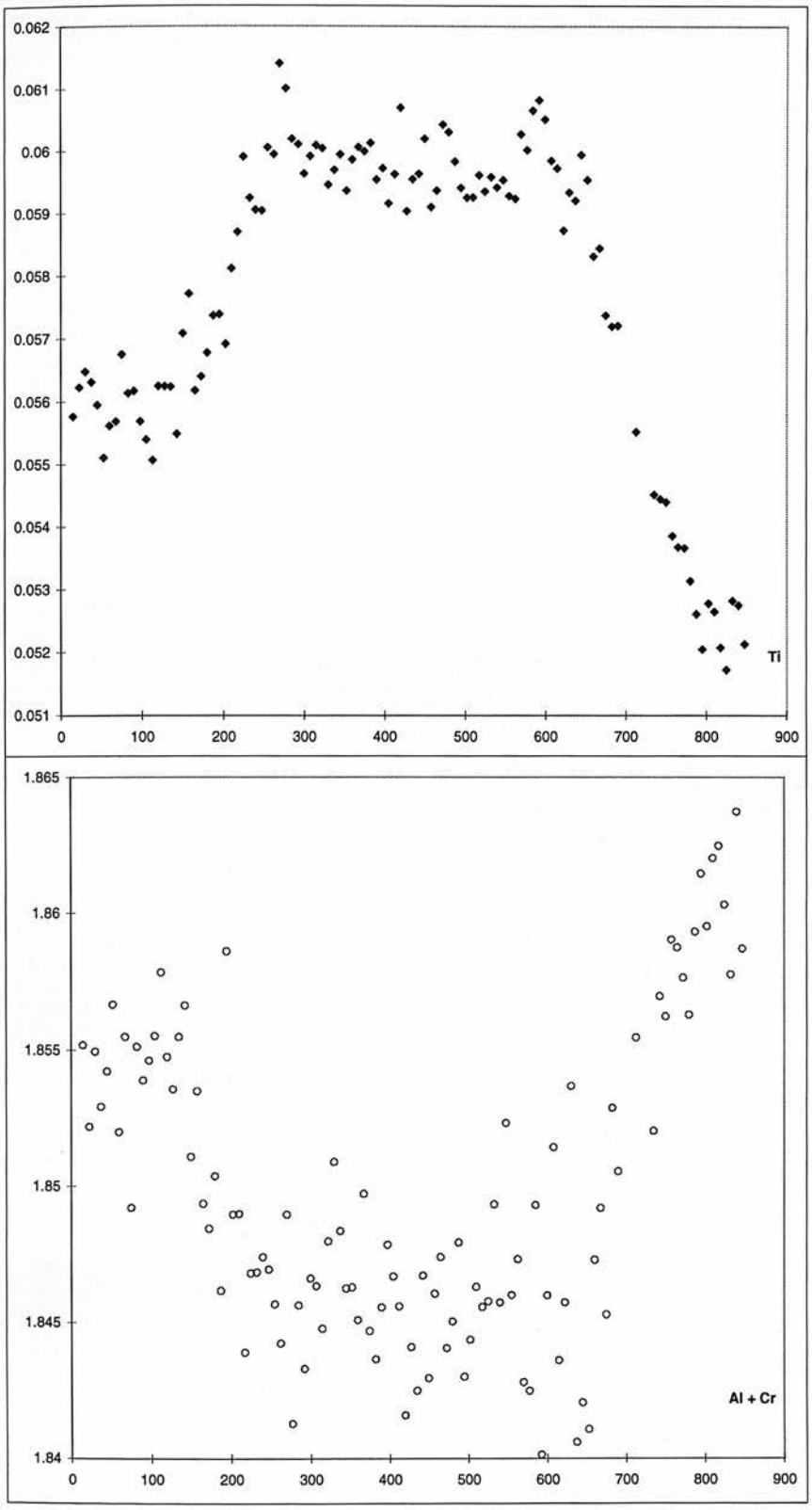

Fig. 4.8 Line profile across JJH37 Garnet D (Fig. C.19a) recast to 8 cations. Fe is assumed to be present solely as Fe2+. Variations of cations on the Y-site given here show that the substitution Cr + Al = Ti can be used to describe the chemical changes present.

Chapter 5

Geometry of Chemical Heterogeneities in Garnets

Sample	Type	Ti	Al	Cr	Fe	Mg	Ca	Na
J22C	Inflected	300		200		500	400	500
J22F2	Inflected	300	300	100				
J31-1	Diffusional	400		200			400	
J33	Diffusional	400		300	400	400	400	
J34A	Diffusional	500	500	500	750	750	500	500
J37	Inflected	500	100	200		250		
J38	Diffusional	300		100				
J107-1	Diffusional	700		600		1000		600
J107-2	Diffusional	600		600			600	
J110	Inflected	1000	300	500	300	1000	1000	300
J115	Ring	2000	1000	2000		2000	2000	
J121	Ring	2000	1500	1500				
JJG1728	Inflected		75	100	100			

Table. 5.1 Estimated diffusion distances (in μm) for heterogeneous garnets from Jagersfontein. Estimates are given for garnets which exhibit diffusion controlled exchange, inflected profiles, and ring zoning (see text).

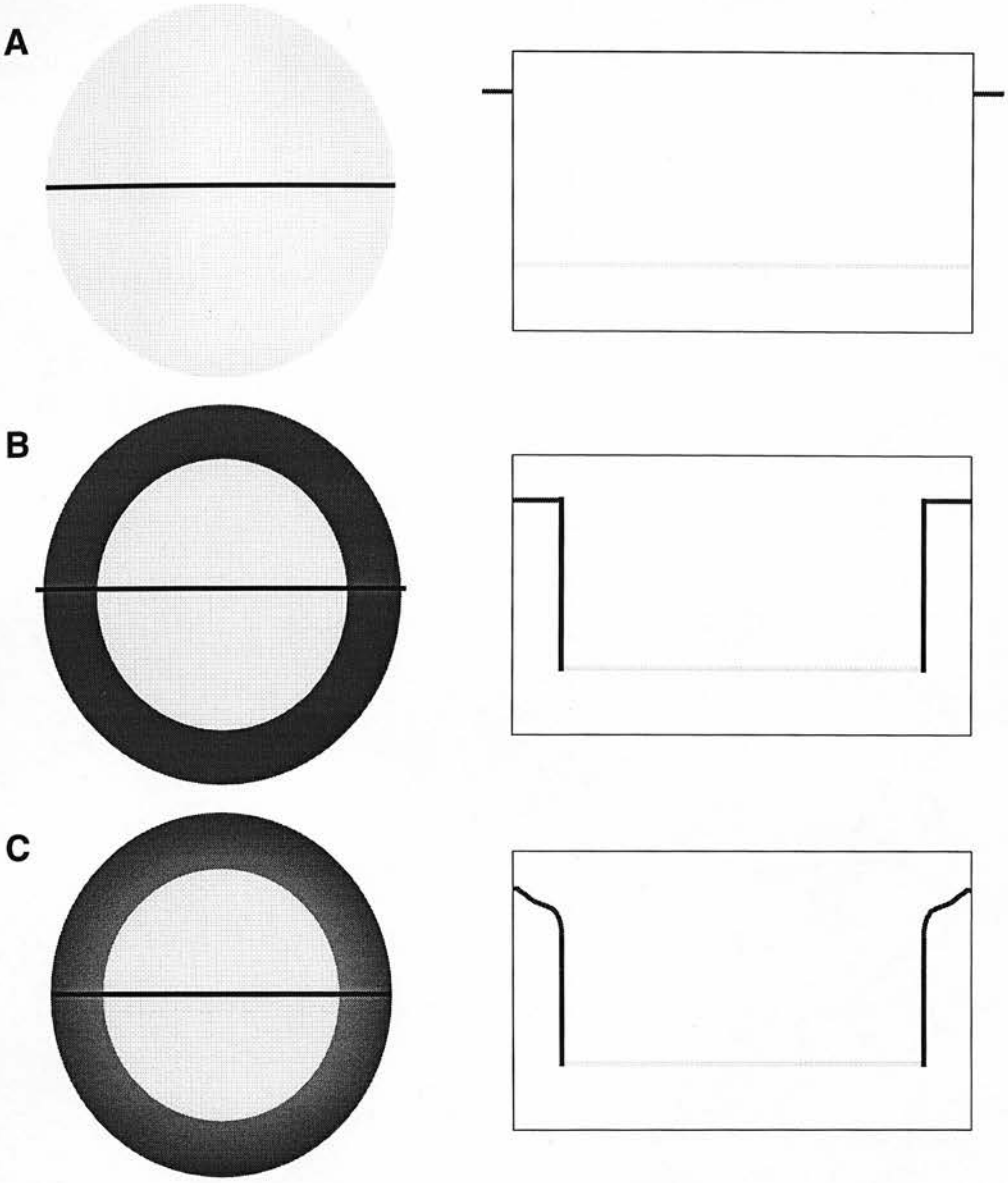

Fig. 5.1 Examples of major causes of chemical zoning within garnet. Each example shows a schematic representation of a spherical garnet grain, with a black line marking the position of a chemical profile, which shows the variation of the abundance of a component across the grain. **A.** The control of diffusion: A change in the chemical conditions of the matrix around a homogeneous grain, results in a change in the garnet composition which is in equilibrium with its surroundings (represented by the dark lines at the edge of the profile). The result is to drive diffusion between the grain and the surrounding matrix (Section 5.2.1). **B**. The control of growth at constant chemical conditions. A similar situation as described in A, except in this case chemical changes drive the growth of new garnet around the rim, of a composition which differs to that of the original grain. During growth the chemistry of the surrounding matrix is constant and therefore the composition of the overgrowth does not vary with distance. **C.** The control of growth during changing chemical conditions. This is an identical situation to that described in B, except that growth is the result of fractional crystallisation, and therefore occurs in constantly changing chemical conditions (Section 5.2.2).

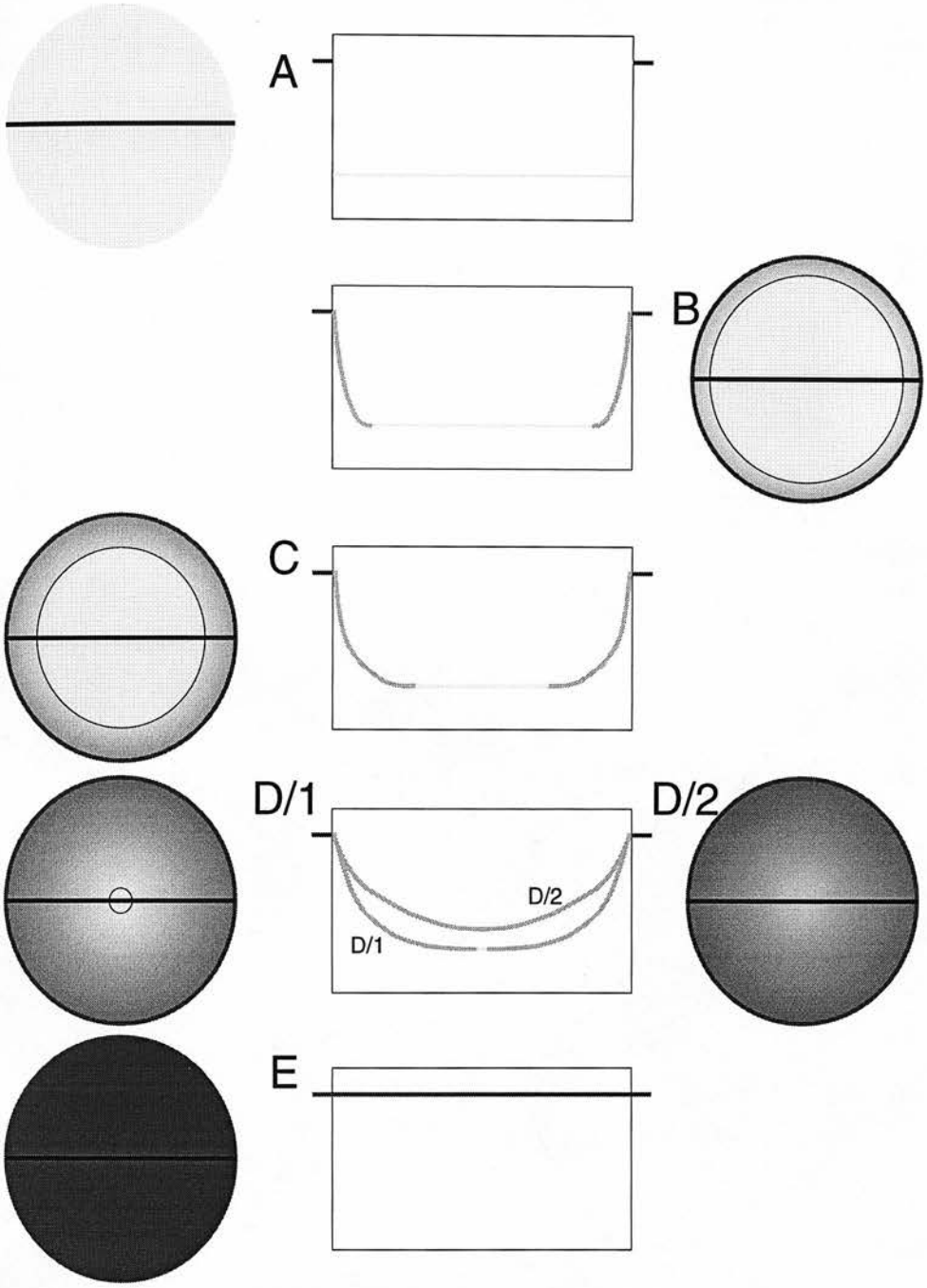

Fig. 5.2 Schematic representation of the changes in the chemistry, with time, of a concentric garnet grain, due solely to diffusion, driven by differences in chemical potential between the rim of the grain and its surroundings. At time A, the composition of garnet in equilibrium with the grain rim is altered due to changes in the surrounding matrix. The result is diffusional exchange between the rim and matrix. The resultant concentration gradient between core and rim is removed with time, as shown above for successive time intervals B, C, D/1, D/2, and E. The shape of the diffusion profile is characteristically concave for a component added at the grain rim. At Time E the grain has homogenised to a composition in equilibrium with the surrounding matrix.

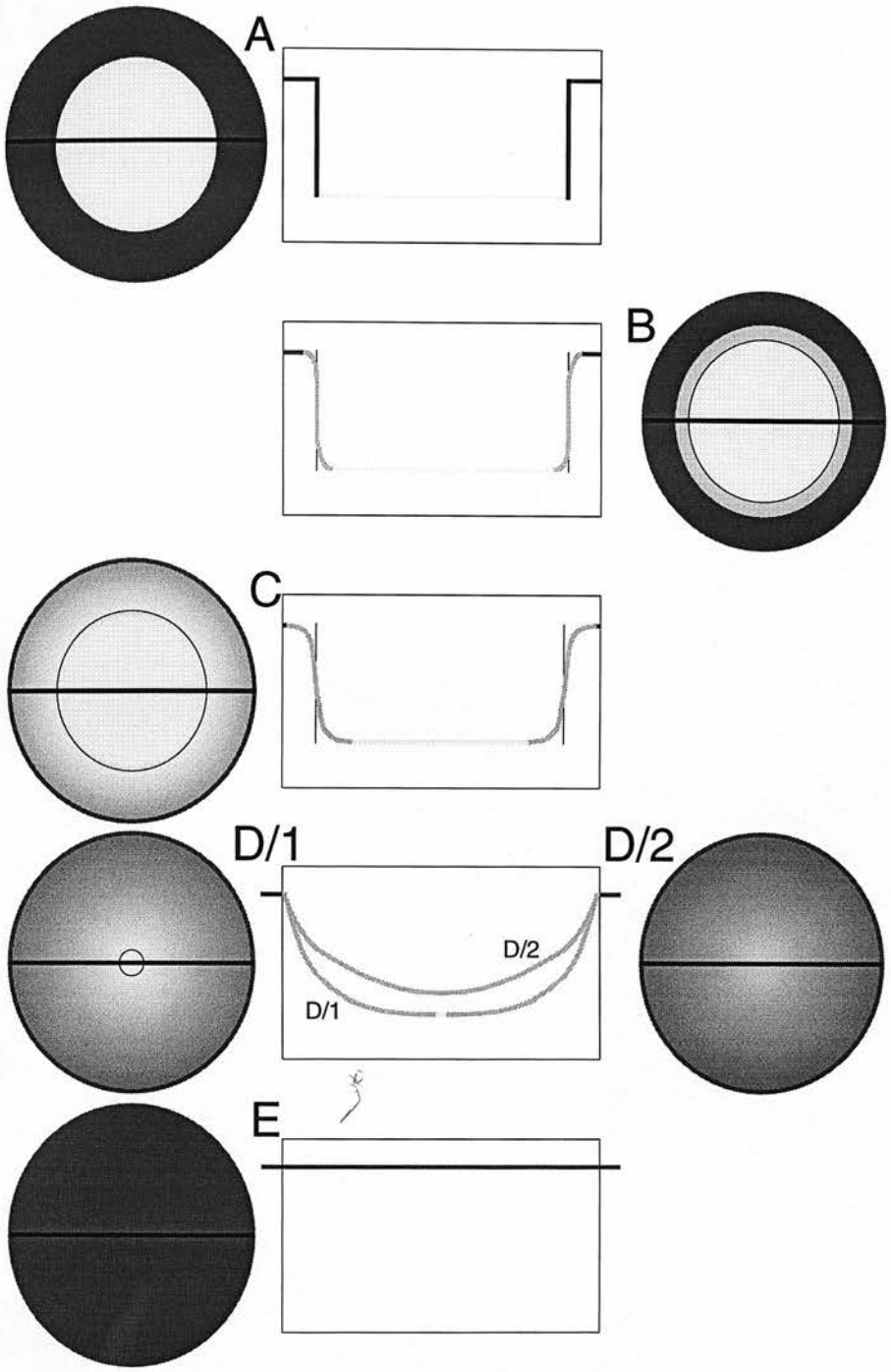

Fig. 5.3 Schematic representation of the changes in chemistry, with time, of a concentric garnet grain, due to a combination of growth and diffusion. At time A garnet of a new composition has formed an overgrowth around a garnet grain. The chemistry of the rim is maintained at constant composition, i.e. the position of chemical equilibrium with the surroundings remained constant during growth, which occurred at a rate significantly faster than diffusion. The step in chemical concentration resulting from this process is destroyed over time by diffusion. The characteristic inflection in the profile remains through time B, to time C when diffusion reaches the rim of this grain. After this time the chemical profile approximates to the diffusion only situation through time D/1 and D/2 until the grain homogenises at time E.

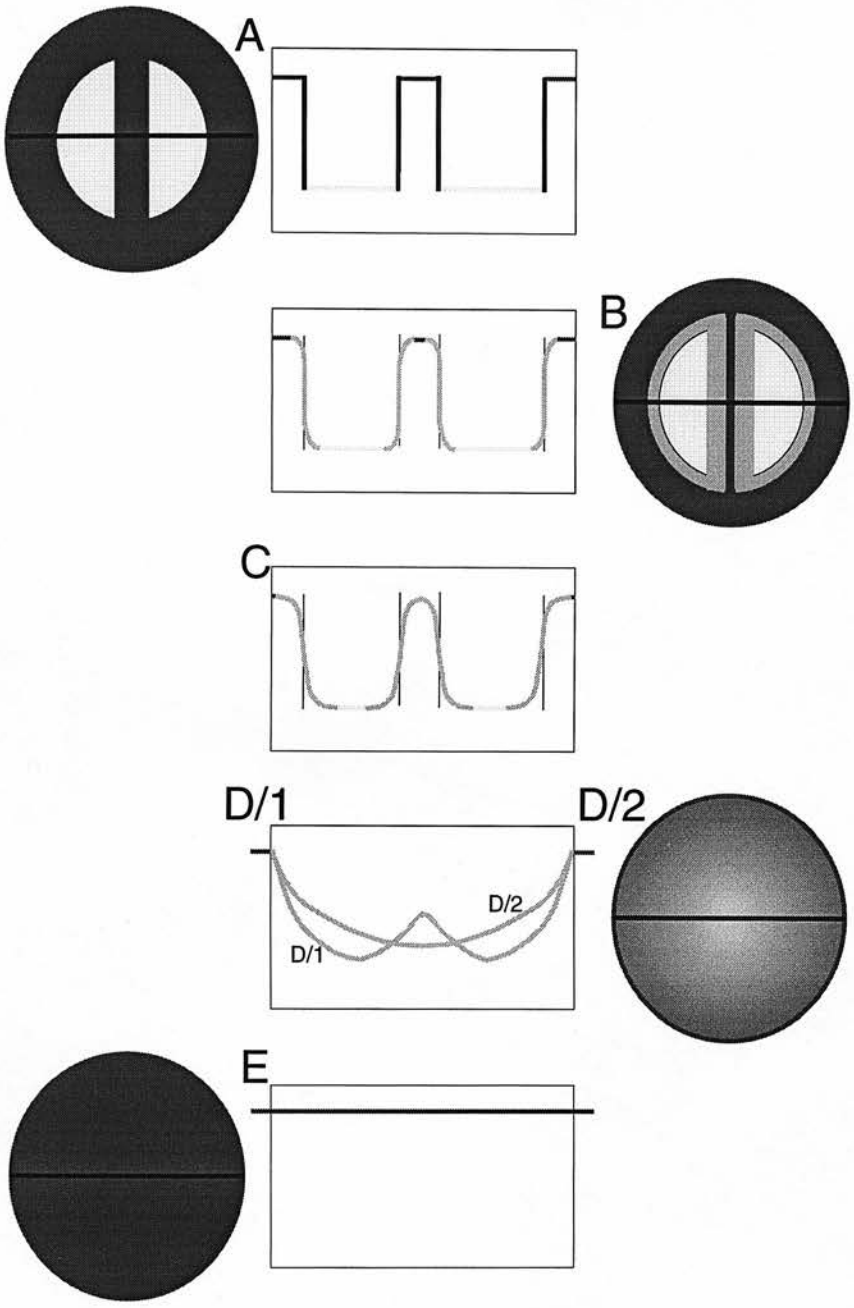

Fig. 5.4 Schematic representation of the changes in chemistry, with time, of a concentric garnet grain which has growth of a new composition in a crack through its centre, in addition to around its rim. At time A mineral growth has filled the crack to form a cross-cutting feature which is of identical composition to the rim overgrowth. The steps in concentration created are destroyed with time by diffusion. At times B and C diffusion has not removed clear evidence of either feature, however by time D/1 the inflection in the rim has been destroyed, though there is still evidence of the cross-cutting feature. As diffusion continues the cross-cutting feature will be lost (time D/2) and the grain will homogenise to be in equilibrium with the surrounding matrix (time E).

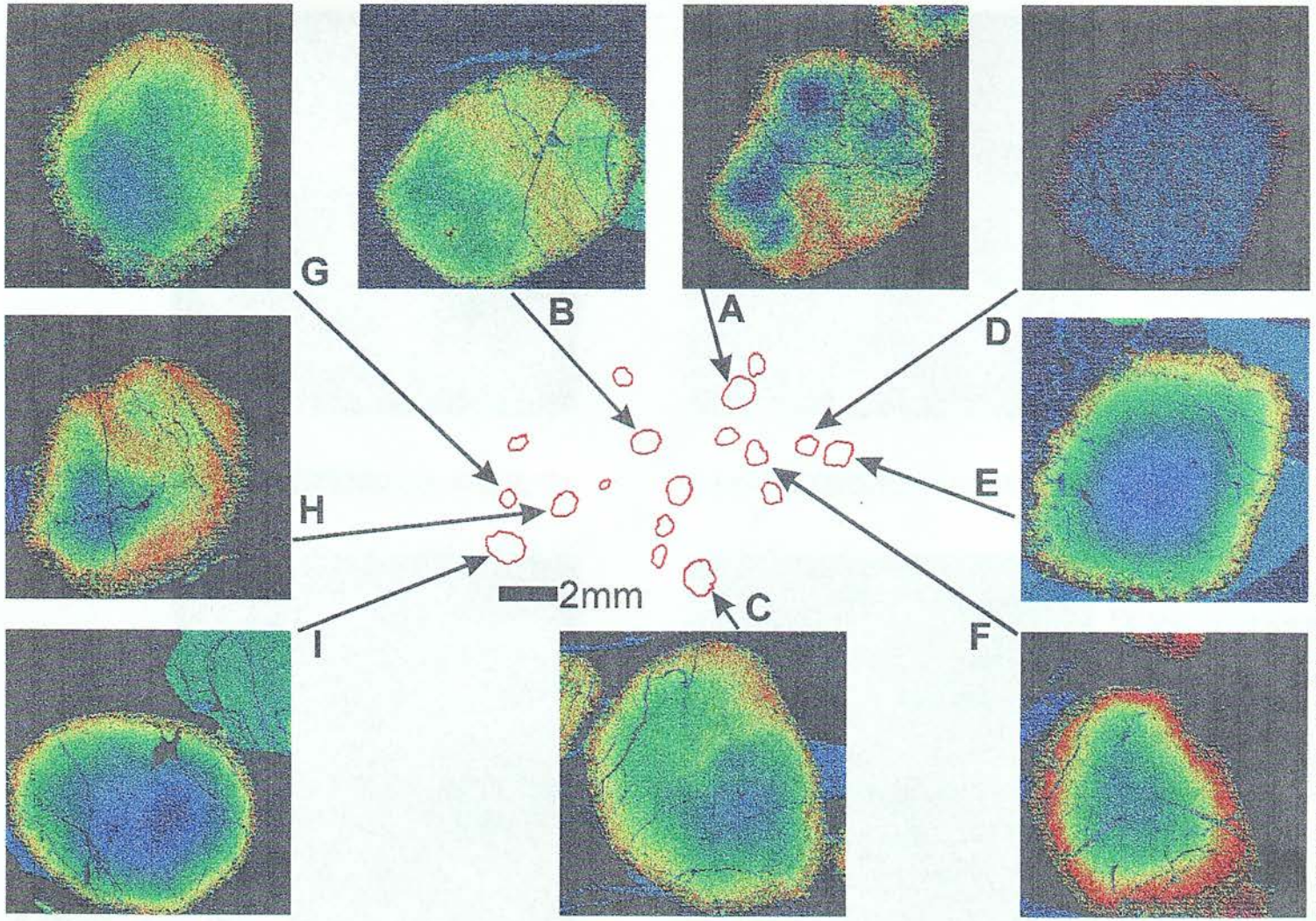

Fig. 5.5. Ti X-ray maps for nine garnets (A-I) from sample JJH37 placed in their spatial context. The centre diagram shows a schematic representation of the garnets present in the central region of the thin section. Note that this diagram is to scale, however the Ti X-ray maps are all scaled to be the same size, not their true size. Each X-ray map is orientated to the positions shown in the central diagram.

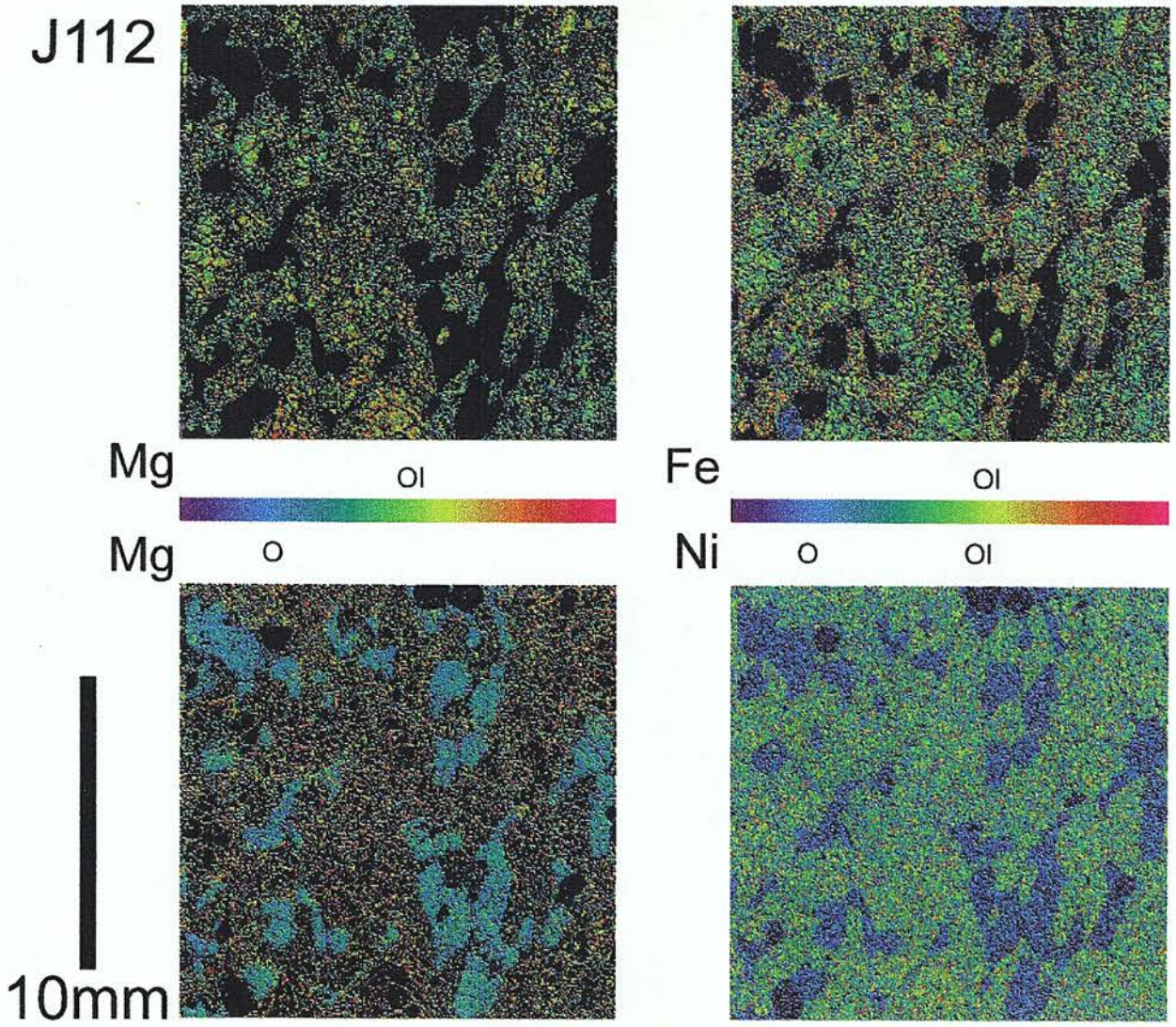

Fig.5.6. X-ray maps of Mg, Fe, and Ni for the matrix of sample J112. The Mg map is shown twice, scaled differently to show olivine, and orthopyroxene. The colours corresponding to the different phases are given. Ol = olivine, O = orthopyroxene. High levels of an element are shown by colours towards the red end of the spectrum.

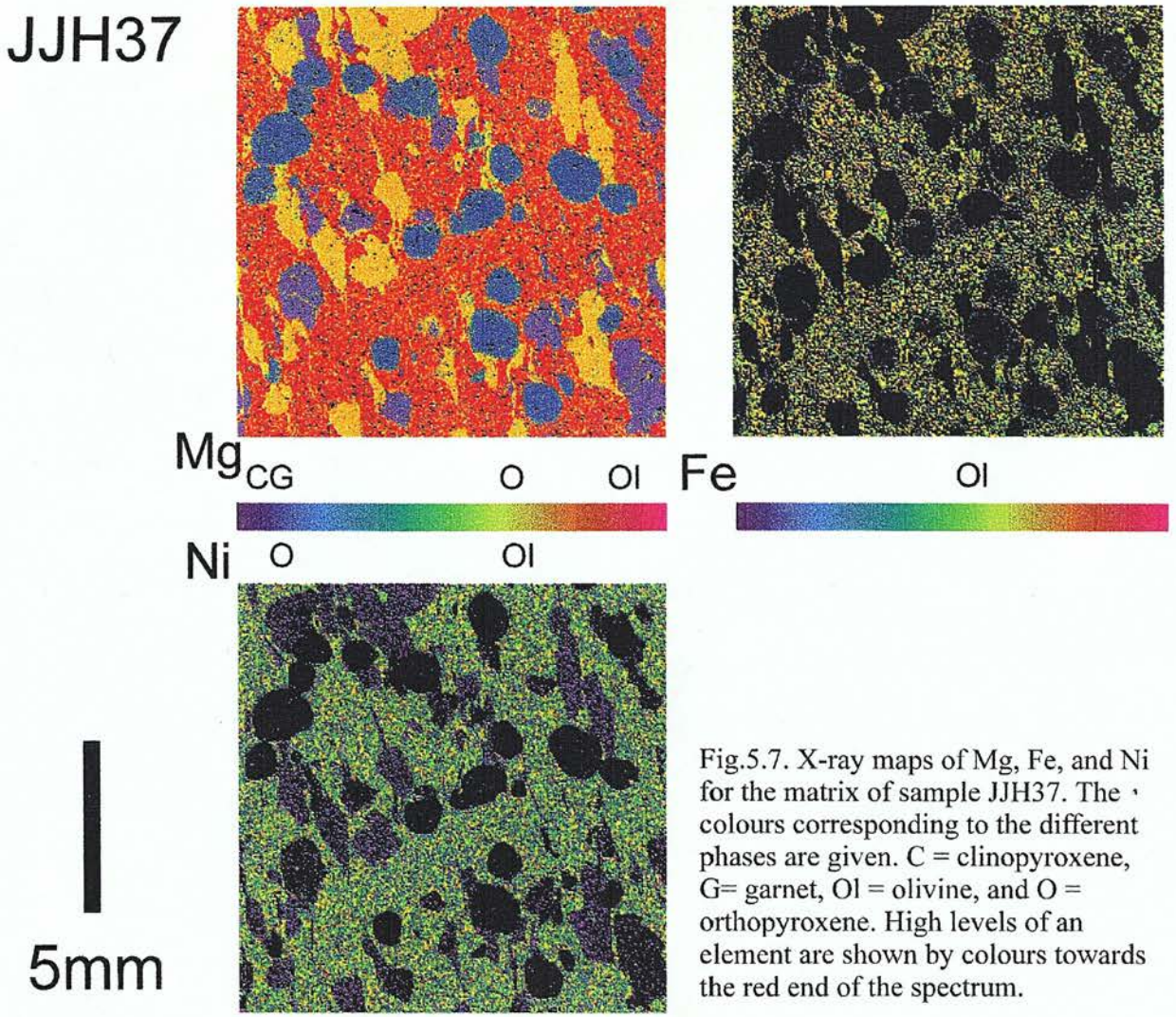

Fig.5.7. X-ray maps of Mg, Fe, and Ni for the matrix of sample JJH37. The colours corresponding to the different phases are given. C = clinopyroxene, G= garnet, Ol = olivine, and O = orthopyroxene. High levels of an element are shown by colours towards the red end of the spectrum.

Chapter 6

Major Element Substitutions Within Garnet

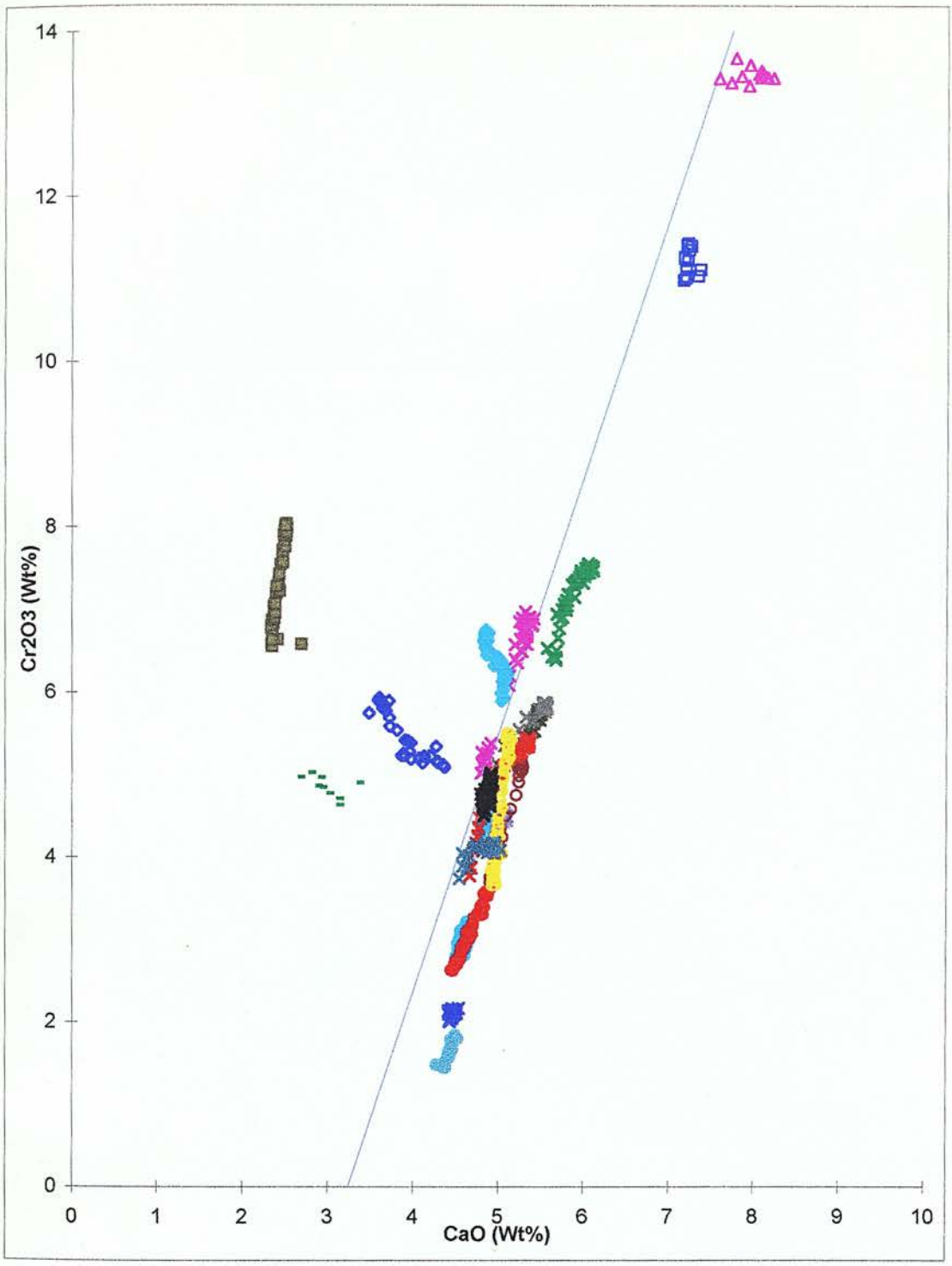

Fig. 6.1 Cr2O3-CaO plot for zoned Jagersfontein garnets. Crosses are Type I substitutions: pink J22, khaki J31, purple J33, sky blue J37, blue J38, grey J107, red J110, green J112, black JJH11, grey/blue JJH37. Circles are Type II substitutions, Type IIa open: burgundy J34, yellow J121a, Type IIb filled: sky blue J115, red J121, grey/blue JJG1776. Triangles are Type III substitutions: pink J145. Diamonds are Type IV and V substitutions: sky blue JJH19, blue JJG1728. Squares are Type VI substitutions: blue J146, khaki JJG2469. Green bars are garnet in JJG1728 kelyphite. See text for explanation of substitution types. Rims are low Ca, Types I, IIa III, and VI, high Ca Types IIb, IV, and V. The blue line is the G9-G10 boundary line from Fig. 4.5.

H:\j12r16.xls

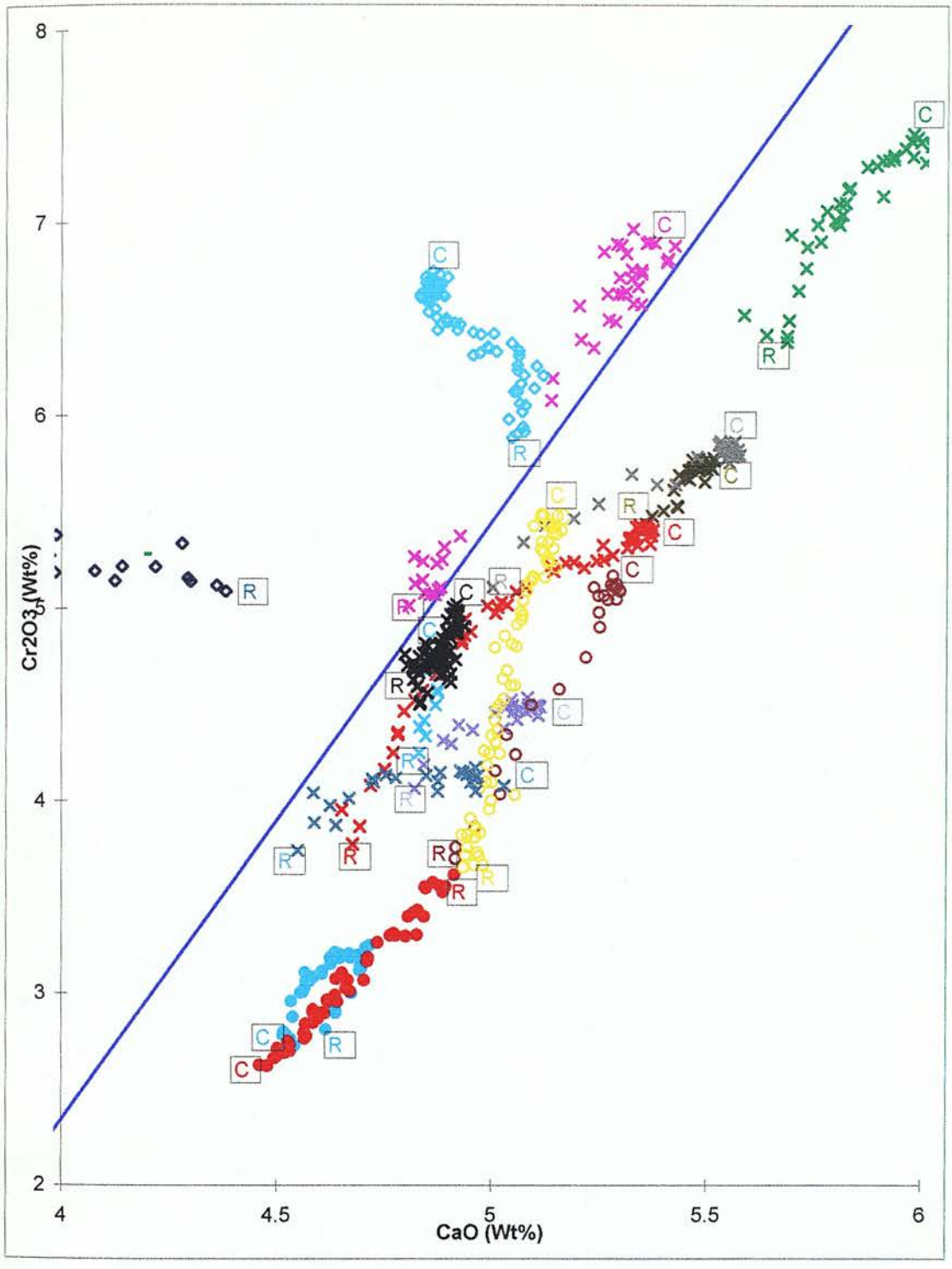

Fig. 6.2 Magnification of Cr2O3-CaO plot Fig. 6.1 for zoned Jagersfontein garnets. Symbols as for Fig. 6.1. Core (C) and rim (R) of each grain is also marked.

H:\j12r16.xls

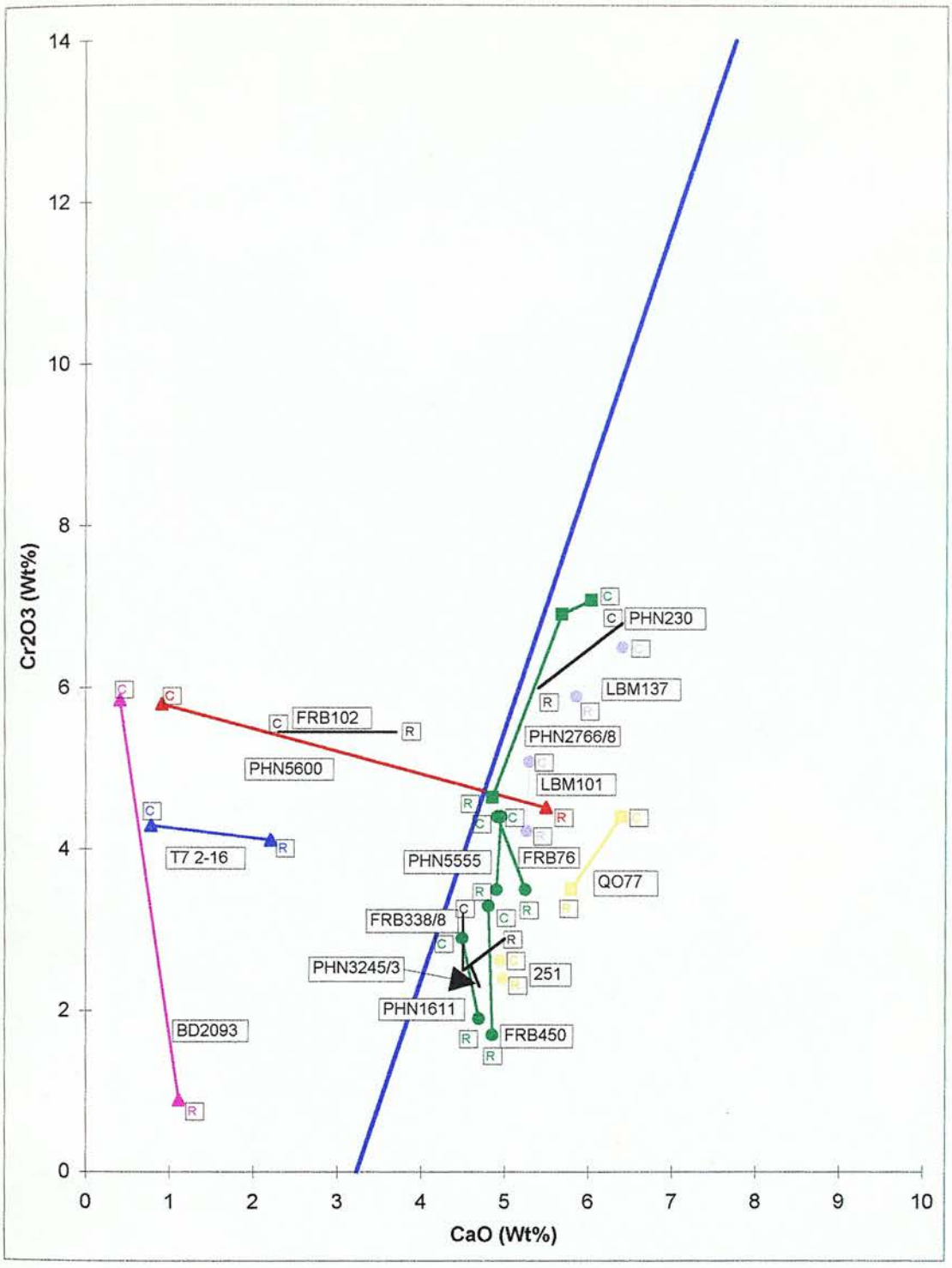

Fig. 6.3 Cr2O3-CaO plot for zoned garnets reported in the literature. Circles are from deformed xenoliths, squares from coarse xenoliths, triangles G10 garnets. Pink are from Liqhobong (Dawson et al. 1978), yellow from the Thumb (Smith and Ehrenberg 1984), purple from Matsoku (Harte et al. 1987), green from southern Africa (Smith and Boyd 1989), black from southern Africa (Smith and Boyd 1992), red from Jagersfontein (Boyd et al. 1993), and blue from Lashaine (Rudnick et al. 1994). The composition of cores (C) and rims (R) are plotted.
The blue line is the G9-G10 boundary line from Fig. 4.5

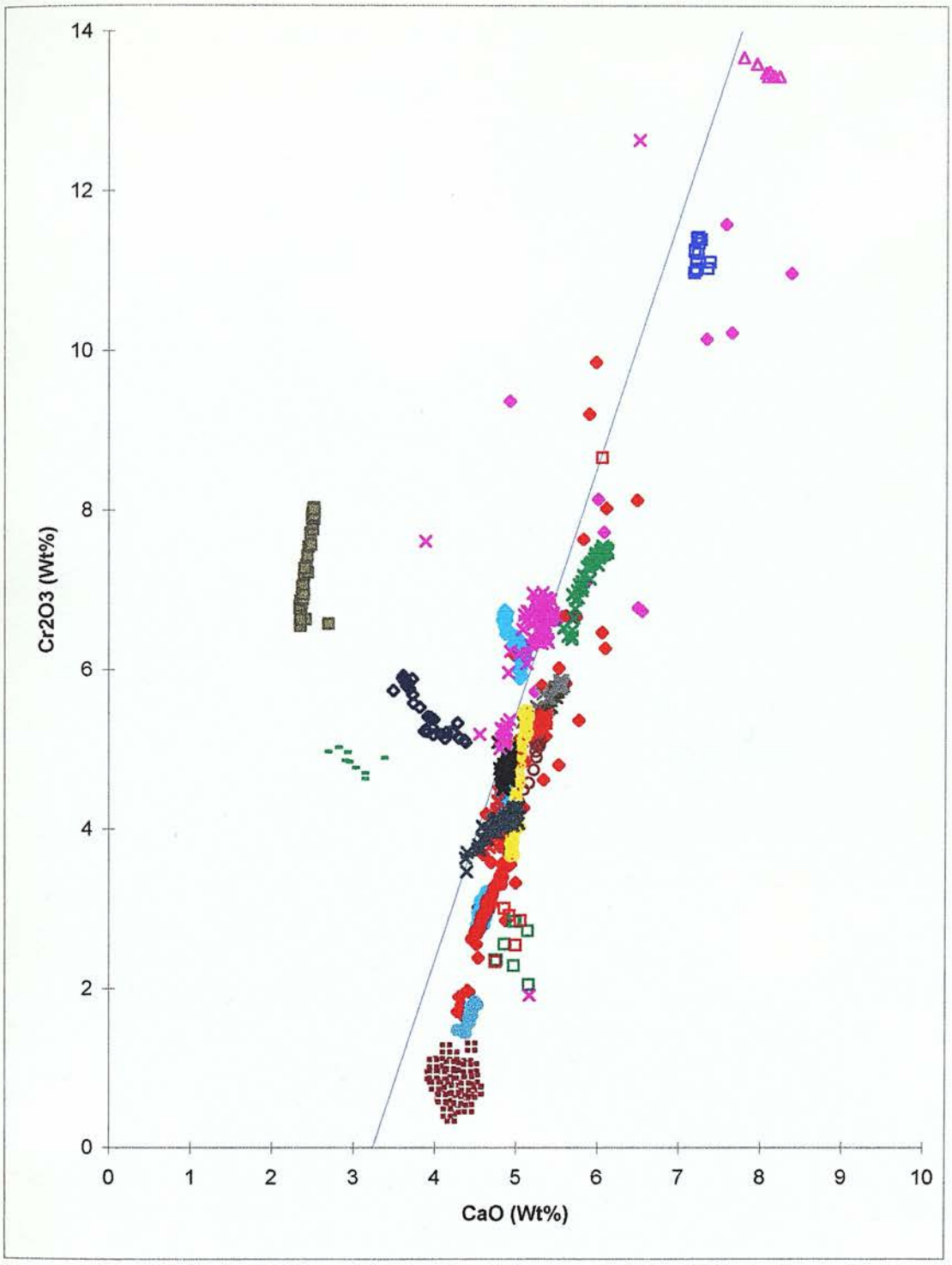

Fig. 6.4 Cr2O3-CaO plot for Jagersfontein garnets, a compilation of Fig. 4.5 for homogeneous garnets and Fig. 6.1 for zoned garnets. Jagersfontein Cr-poor megacrysts, white crosses on burgundy squares, are from Hops (1989). Other symbols as for Figs. 4.5 and 6.1.
The blue line is the G9-G10 boundary line from Fig. 4.5.

H:\thesis\ca-cr.xls

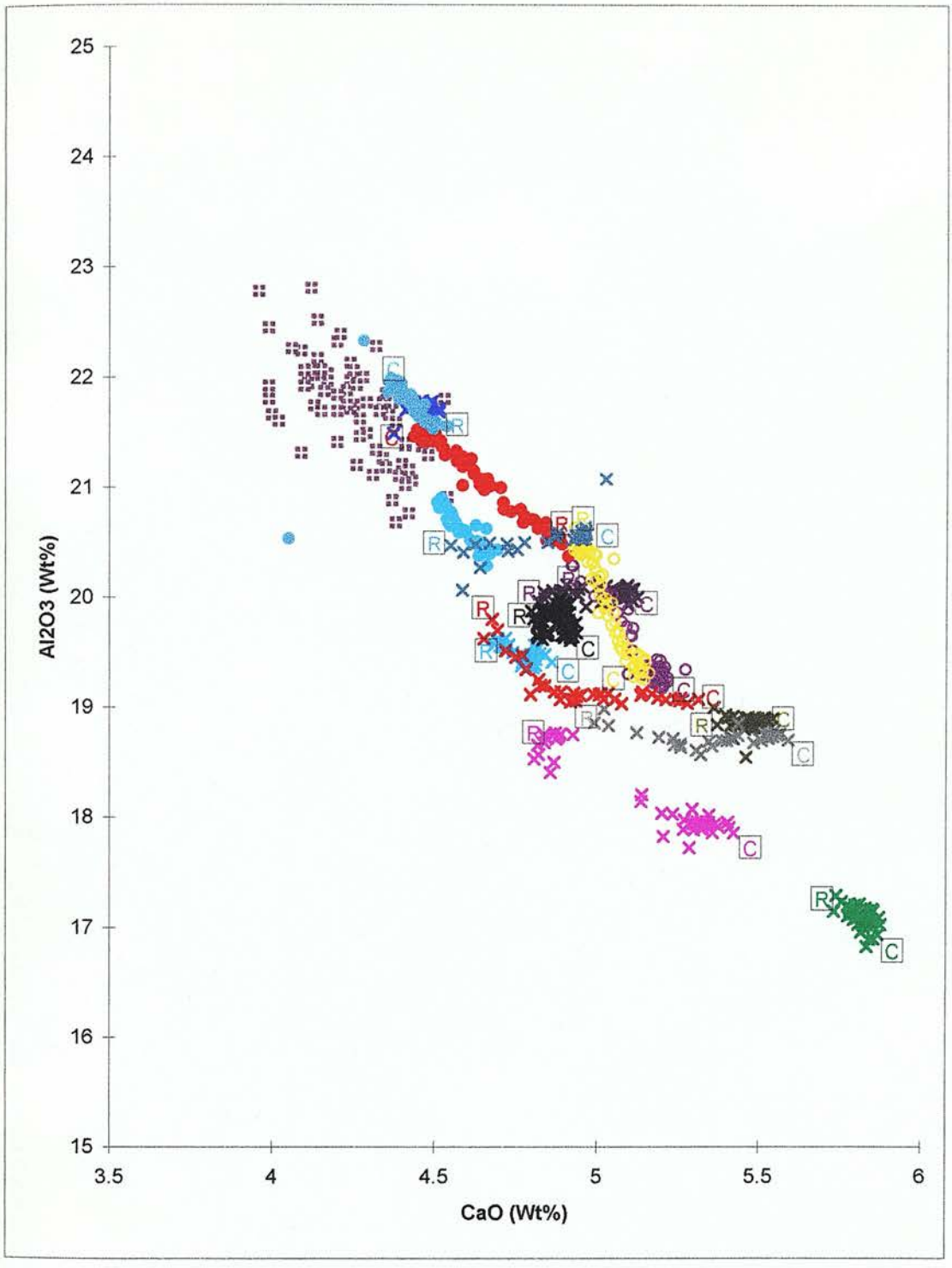

Fig. 6.5 Al2O3 against CaO for zoned Jagersfontein garnets showing Type I and II substitutions. Symbols as for Figs. 6.1 and 6.4. All Type I substitutions (Crosses) have Ca rich cores (C), and Ca poor rims (R). Type IIa substitutions are open circles, Type IIb are filled. Megacrysts (white crosses on burgundy square) are from Hops (1989)

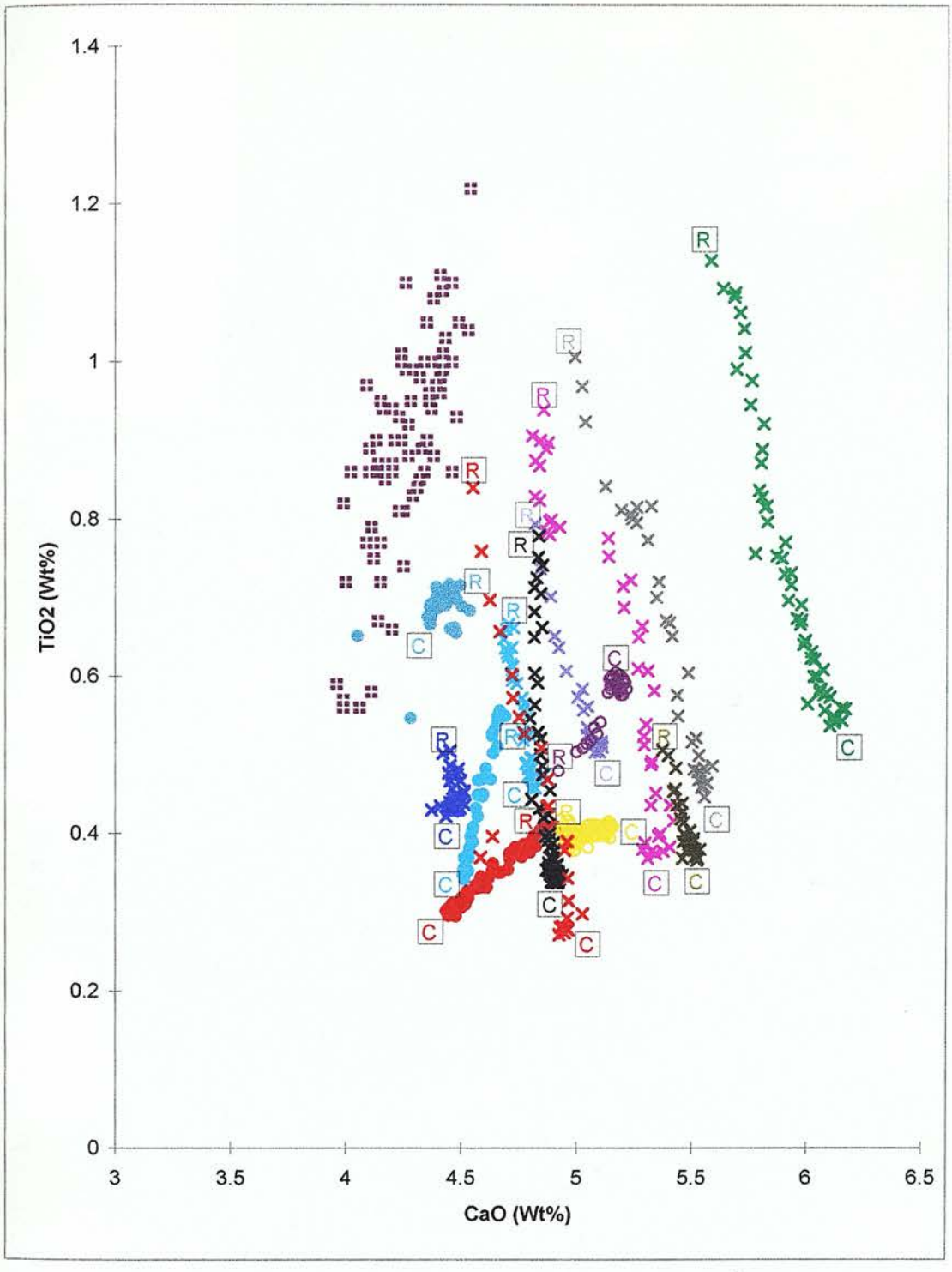

Fig. 6.6. TiO2 against CaO for zoned Jagersfontein garnets showing Type I and Type II substitutions. Symbols as for Figs. 6.1 and 6.4. All Type I substitutions (Crosses) have Ca poor rims. Type IIa substitutions are open circles, Type IIb are filled. Cores (C) and rims (R) are marked.
Megacrysts (white crosses on burgundy square) are from Hops (1989).

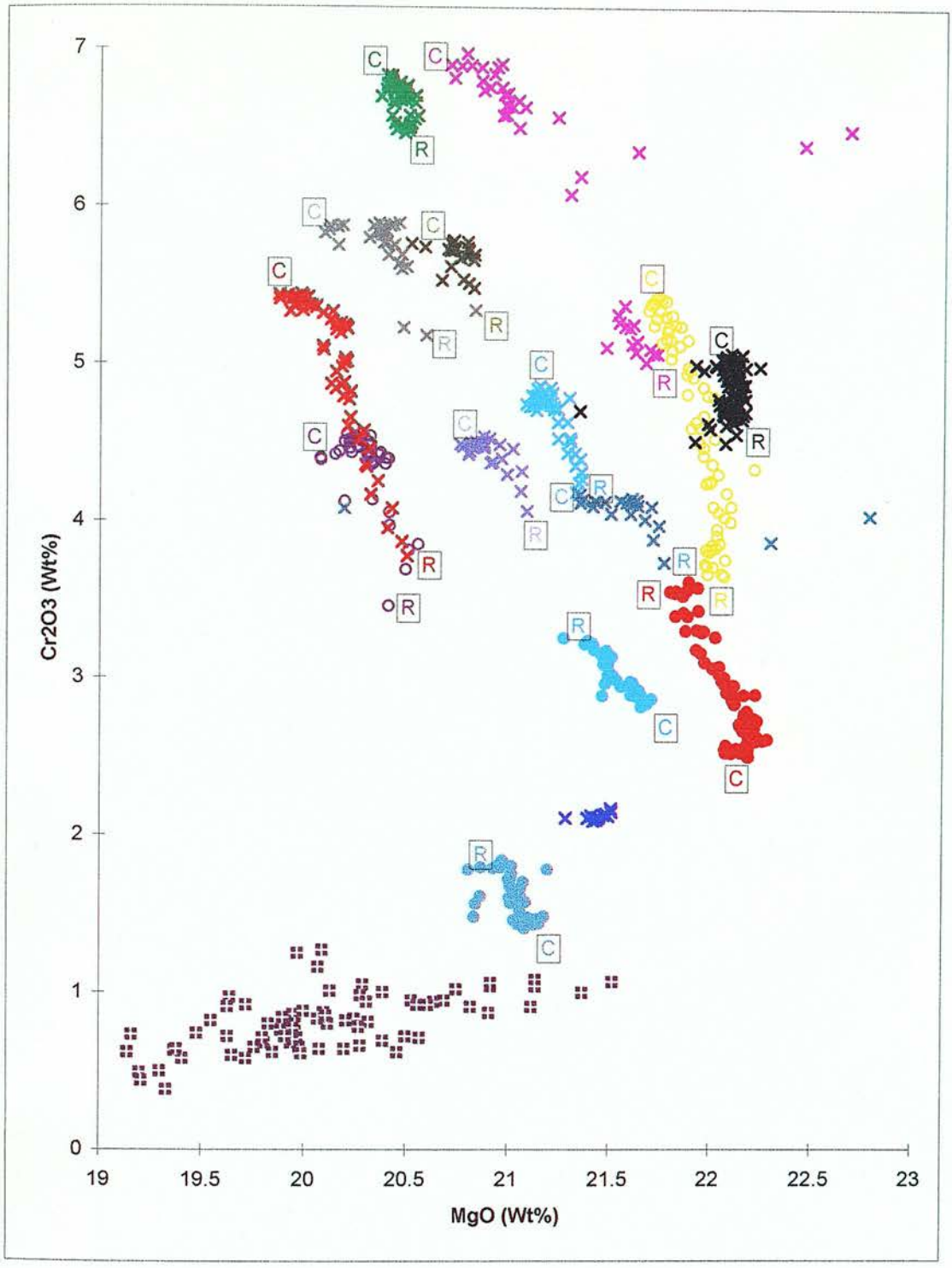

Fig. 6.7 Cr2O3 against MgO for zoned Jagersfontein garnets showing Type I and Type II substitutions. Symbols as for Figs. 6.1 and 6.4. All Type I substitutions (Crosses) have Ca poor rims. Type IIa substitutions are open circles, Type IIb are filled. Cores (C) and rims (R) are marked.
Megacrysts (white crosses on burgundy square) are from Hops (1989).

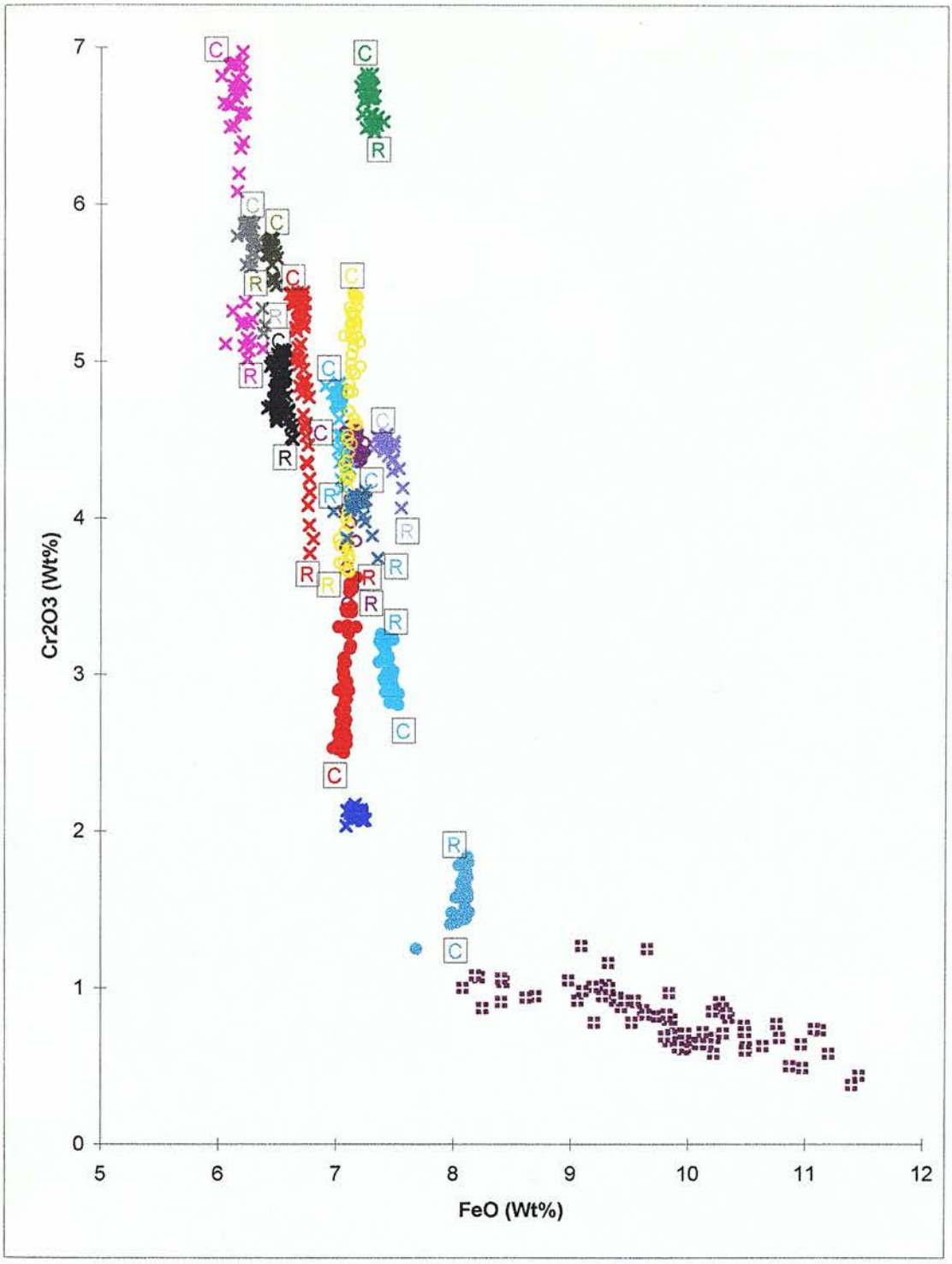

Fig. 6.8 Cr2O3 against FeO for zoned Jagersfontein garnets showing Type I and Type II substitutions. Symbols as for Figs. 6.1 and 6.4. All Type I substitutions (Crosses) have Ca poor rims. Type IIa substitutions are open circles, Type IIb are filled. Cores (C) and rims (R) are marked.
Megacrysts (white crosses on burgundy square) are from Hops (1989).

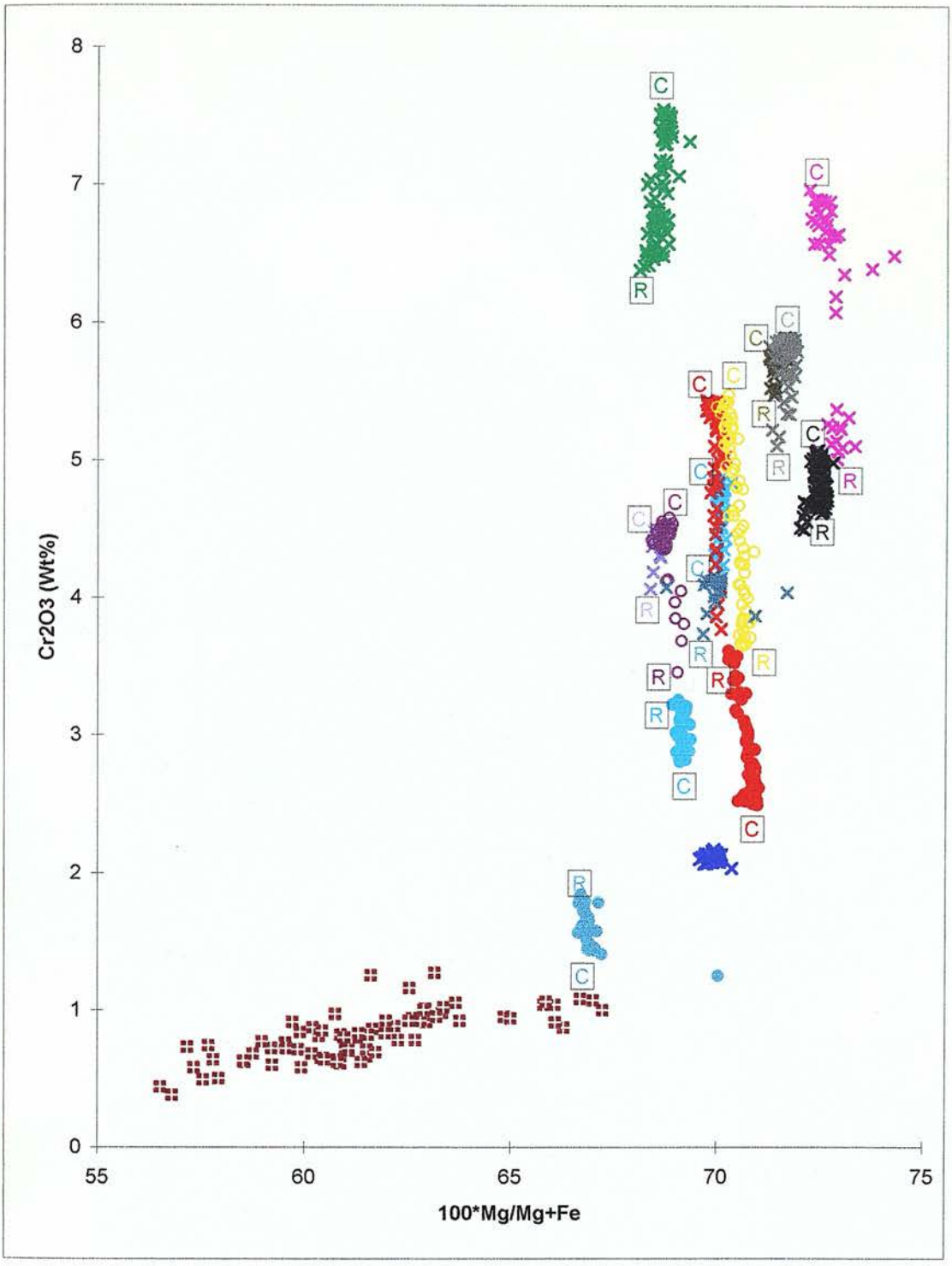

Fig. 6.9 Cr2O3 against 100*Mg/Mg+Fe for zoned Jagersfontein garnets showing Type I and Type II substitutions. Symbols as for Figs. 6.1 and 6.4. All Type I substitutions (Crosses) have Ca poor rims. Type IIa substitutions are open circles, Type IIb are filled. Cores (C) and rims (R) are marked.
Megacrysts (white crosses on burgundy square) are from Hops (1989).

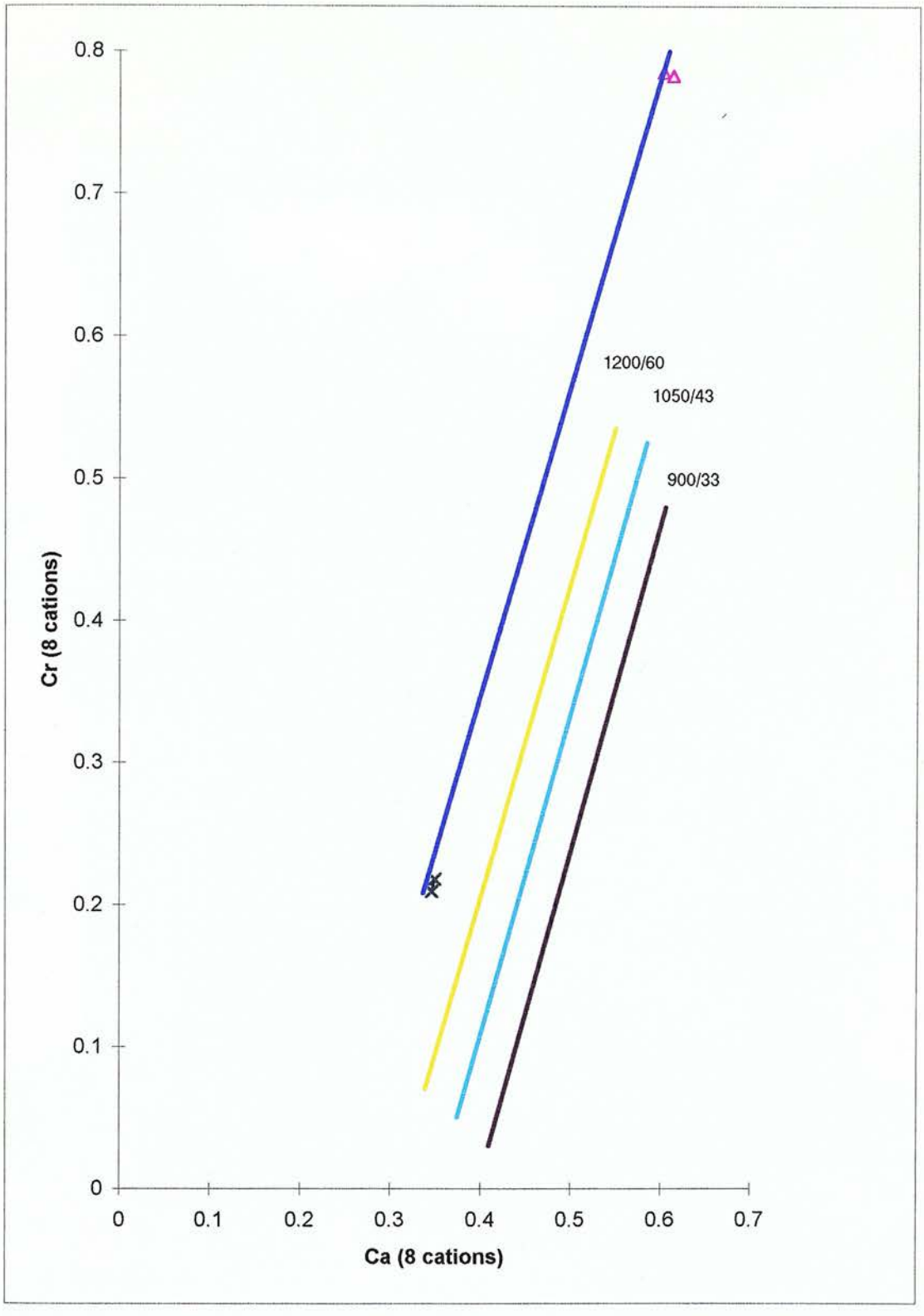

Fig. 6.10 Garnet Cr against Ca (based on 8 cations) modified from Brey (1991), Fig. 4. Lines of equal pressure and temperature (burgundy 900°C/33kbar, sky blue 1050°C/43kbar, and yellow 1200°C/ 60kbar) for garnet chemistry from Brey (1991). The blue line is the G9-G10 boundary from Fig. 4.5, recalculated using the rim compostions of J145 (1240°C/42kbar, pink triangles), and JJH37 Garnet I (1340°C/54kbar, blue/grey crosses).

Chapter 7

Trace Element Composition of Garnet

Sample	Texture	Mineralogy	Temp.Group	Garnet Type	Zoning Type
J22	Deformed	Garnet Harzburgite	High	G9	Type I
J24	Coarse-metasomatised	Garnet Amphibole Lherzolite	Low	G9	None
J25	Coarse	Garnet Lherzolite	Low	G9	None
J34	Deformed	Garnet Lherzolite	High	G9	Type II
J47	Deformed	Garnet Lherzolite	High	G9	None
J51	Deformed	Garnet Lherzolite	High	G9	None
J74	Megacryst	Garnet			
J75	Megacryst	Garnet			
J107	Deformed	Garnet Harzburgite	High	G9	Type I
J110	Deformed	Garnet Lherzolite	High	G9	Type I
J112	Deformed	Garnet Lherzolite	High	G9	Type I
J115	Deformed	Garnet Lherzolite	High	G9	Type II
J121	Deformed	Garnet Lherzolite	High	G9	Type II
J145	Deformed	Garnet Lherzolite	High	G10 (High-Cr)	Type III
J146	Coarse	Garnet Harzburgite	Medium	G10 (High-Cr)	Type VI
J157	Coarse	Garnet Harzburgite	Medium	G10	None
J159	Deformed	Garnet Harzburgite	High	G10 (High-Cr)	None
JJG1728	Coarse	Garnet Lherzolite	Medium	G10	Type V
JJG1757	Coarse	Garnet Harzburgite	Low	G9	None
JJG1761	Coarse	Garnet Harzburgite	Medium	G10	None
JJG1776	Deformed	Garnet Lherzolite	High	G9	Type II
JJG1780	Coarse	Garnet Phlogopite Harzburgite	Medium	G10	None
JJG1781	Coarse	Garnet Harzburgite	Medium	G10	None
JJG2469	Coarse	Garnet Dunite	?Medium	G10	Type VI
JJH19	Deformed	Garnet Harzburgite	High	G10/G9	Type IV
JJH37	Deformed	Garnet Lherzolite	High	G9	Type I

Table 7.1 Samples analysed for trace elements by ion microprobe
Notes: The temperature groups are defined in Chapter 3, and for each particular sample see Table 3.1.
The Garnet Type is based on the CaO-Cr2O3 chemistry, as discussed in Chapter 4.
Zoning Type refers to the major element substitution shown by garnet as defined in Chapter 6.

	La	Ce	Nd	Sm	Eu	Gd	Dy	Er	Yb	Lu
Olivine-melt		0.0005	0.001	0.0013	0.0016	0.0015	0.0017	0.0015	0.0015	
Opx-melt		0.003	0.0068	0.01	0.013	0.016	0.022	0.03	0.049	
Cpx-melt	0.061	0.092	0.199	0.276	0.31	0.3	0.386	0.344	0.43	0.357
Gnt-melt										
T=1400°C	0.0016	0.011	0.06	0.239	0.378		1.682	2.802		18.682
T=1300°C	0.0011	0.008	0.049	0.21	0.345		1.592	2.702		19.203
T=1200°C	0.0007	0.005	0.038	0.181	0.311		1.495	2.592		19.813
T=1100°C	0.0005	0.003	0.029	0.152	0.277		1.391	2.472		20.535
T=1000°C	0.0003	0.002	0.021	0.125	0.242		1.28	2.34		21.404
T=900°C	0.0002	0.001	0.017	0.099	0.206		1.162	2.194		22.269

Table 7.2 mineral-melt partition coefficients for some rare earth elements
Olivine-melt, Opx-melt, and Cpx-melt from Watt and Harte (1995 pers. comm) see text.
Gnt-melt data is calculated from Harte et al. (1996) Cpx-gnt data and above Cpx-melt data, see text.

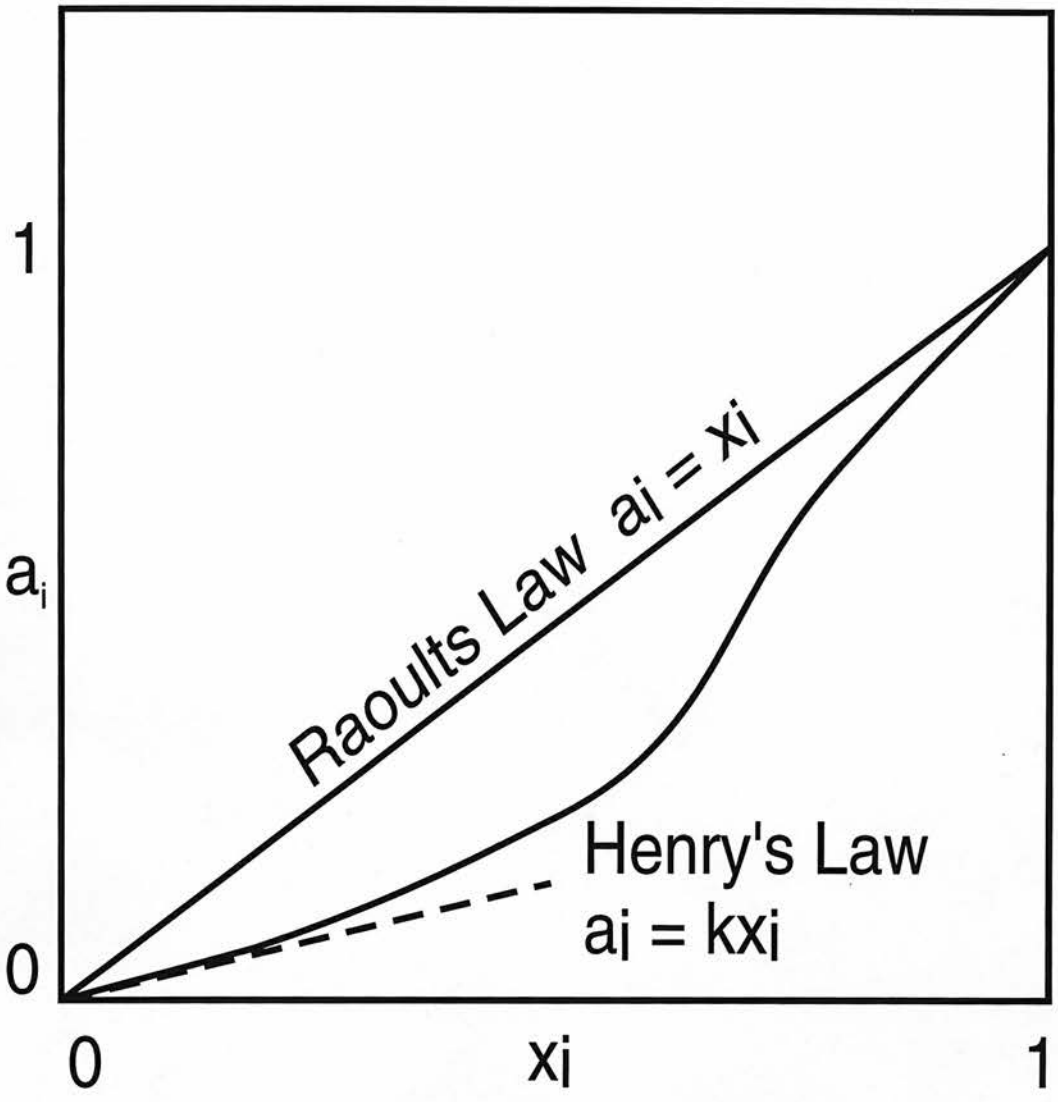

Fig.7.1. Schematic plot of chemical activity (a_i) against mole fraction (x_i) for a component i in an ideal and non-ideal solution (modified from Henderson 1982). The chemical activity of a component in an ideal solution is always equal to its mole fraction, and is said to follow Raoult's Law. In a non-ideal solution chemical activity of a component can only be predicted in three compositional ranges. When a component is absent from the solution, mole fraction and chemical activity are both zero. When the solution is pure, the mole fraction and the chemical activity of the constituent component are both one. At very small concentrations of a component the activity-composition curve approximates to a straight line, and the chemical activity is related to the mole fraction by a constant K. This region is the Henry's Law region.

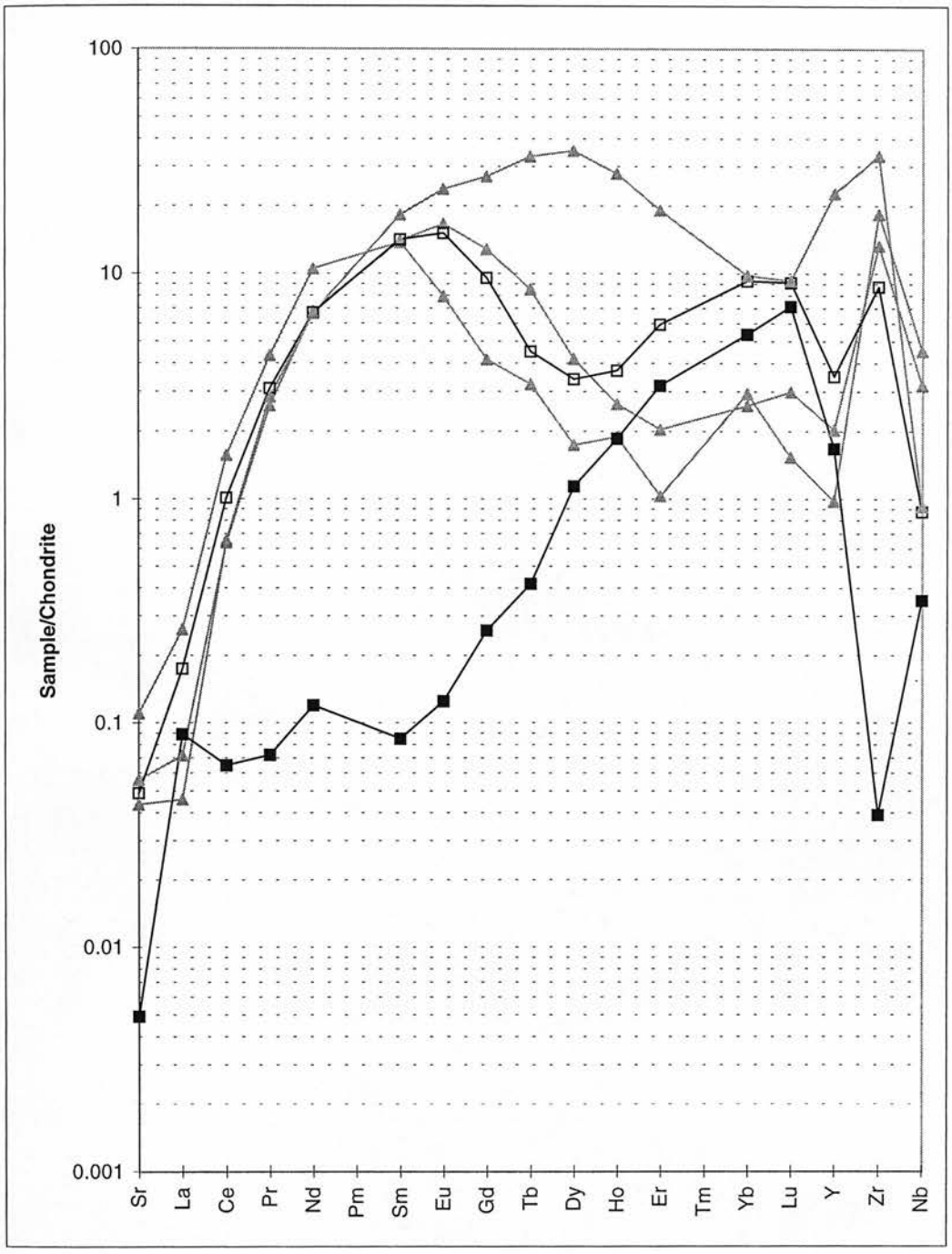

Fig. 7.2 Chondrite normalised 'spidergrams' for representative garnet cores from Jagersfontein coarse xenoliths. Black filled squares, average for coarse low-temperature xenoliths (J25, JJG1757), black open squares, coarse-low temperature metasomatised xenolith (J24), grey filled triangles coarse medium temperature xenoliths (J157, JJG1761, JJG1781). Data from Table D1, normalising values from Anders and Grevesse (1989).

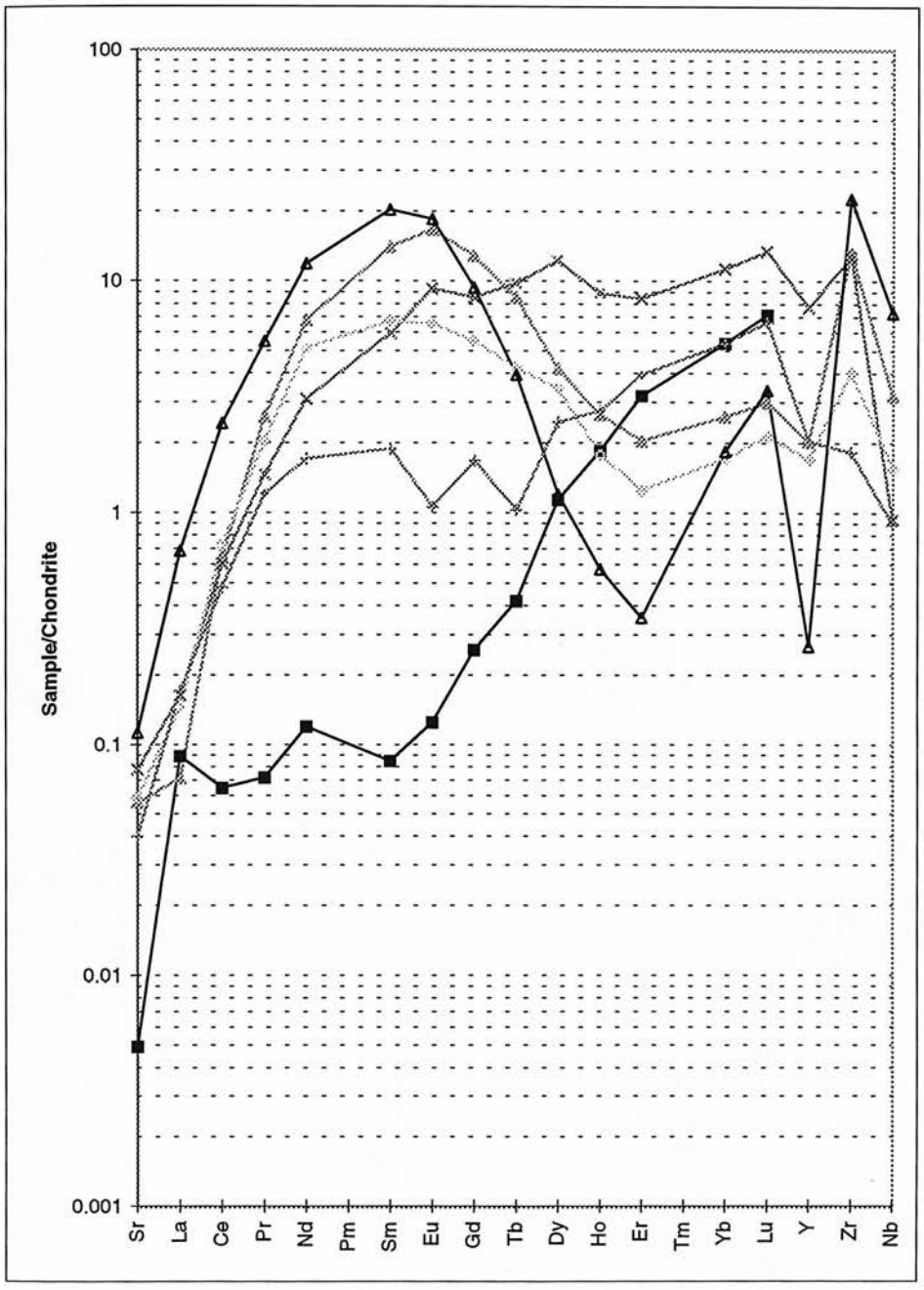

Fig. 7.3 Chondrite normalised 'spidergrams' for representative garnet cores from Jagersfontein coarse and deformed xenoliths. Black filled squares average for coarse low-temperature xenoliths (J25, JJG1757), grey filled triangles coarse medium-temperature xenolith (JJG1761), dark grey cross zoned G9 garnet from deformed xenolith (J110), light grey cross zoned G9 garnet from deformed xenolith (JJH37), black open triangle deformed high-Cr garnet (J145), light grey open diamond deformed G9-G10 transitional garnet (JJH19). Data from Table D1, normalising values from Anders and Grevesse (1989).

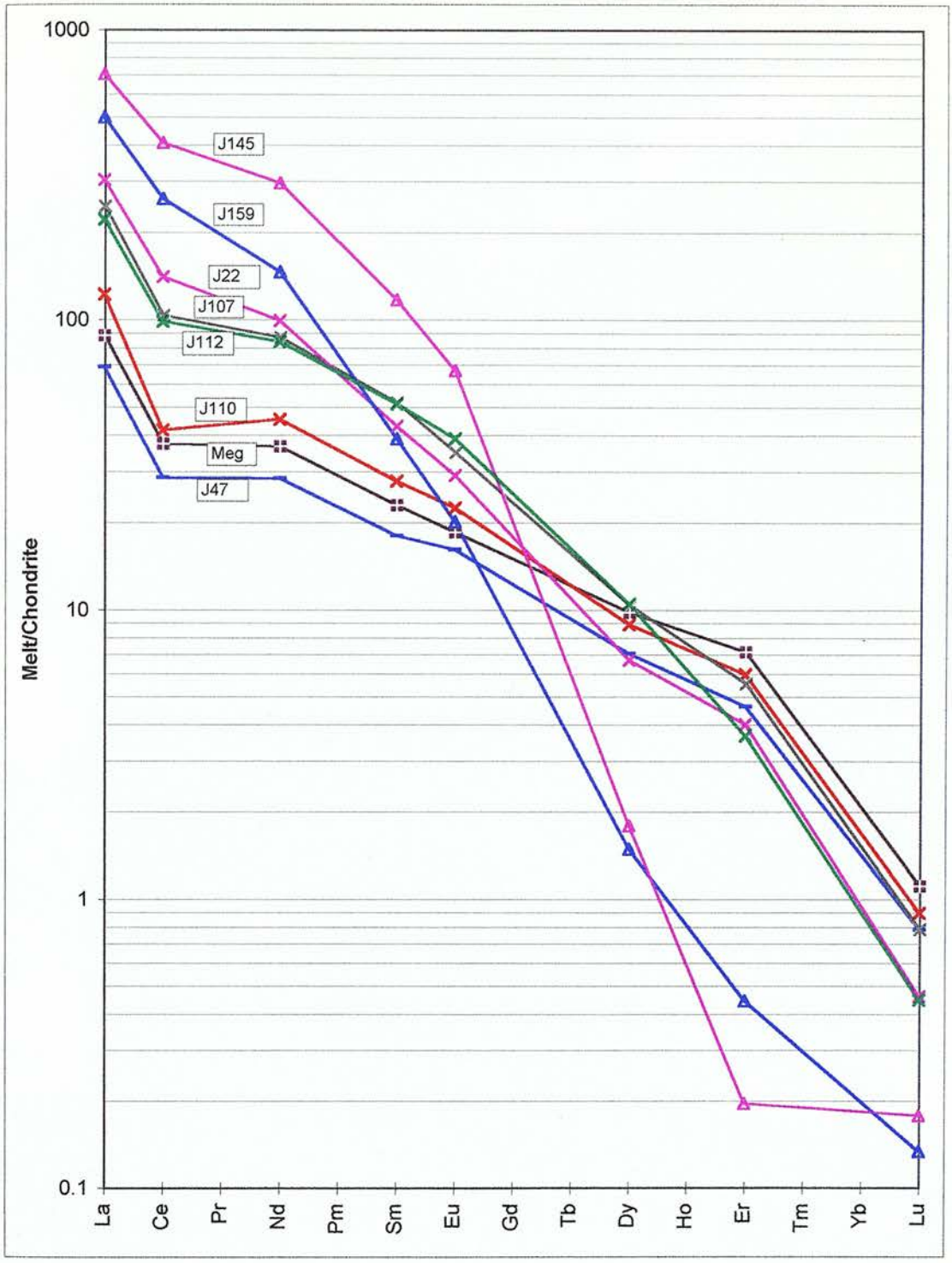

Fig. 7.4 REE composition of melts in equilibrium with rims of deformed Jagersfontein garnets. In order of increasing Cr2O3 content: burgundy cross J75 Cr-poor garnet megacryst, blue bar J47, red cross J110, grey cross J107, pink cross J22, green cross J112, blue triangle J159, pink triangle J145. White crosses on filled boxes are megacrysts, bars are homogeneous garnets, diagonal crosses are Type I substitution garnets, triangles are high-Cr G10 garnets.

C:\simon\traces\melts\
J75g.xls

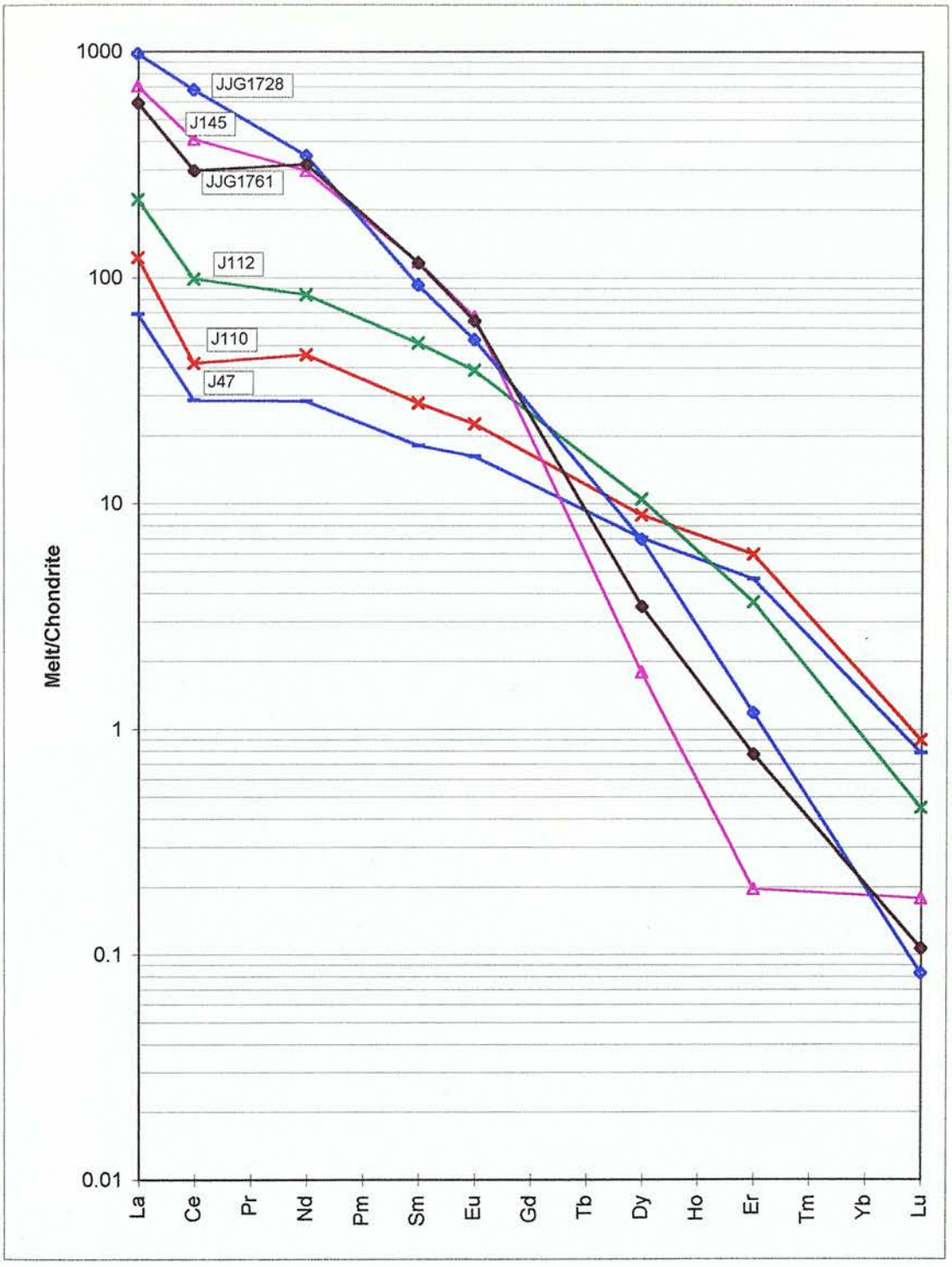

Fig. 7.5 REE composition of melts in equilibrium with rims of selected deformed and coarse G10 garnets. For deformed xenoliths, symbols are as in Fig. 7.4. Coarse G10 garnets are blue open diamonds JJG1728, brown closed diamonds JJG1761.

C:\simon\traces\melts\
J47g.xls

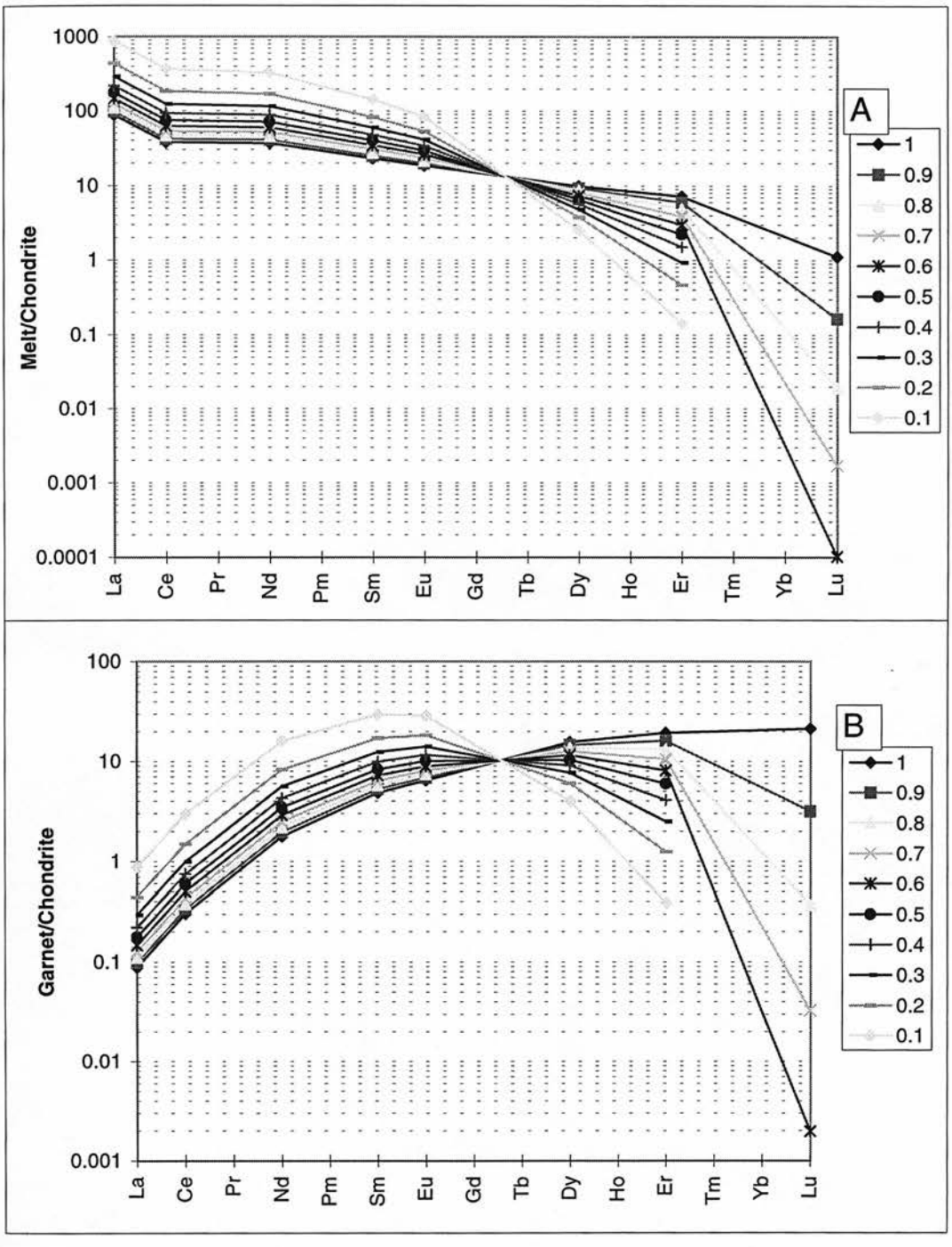

Fig. 7.6. REE compositions of melts and garnet in equilibrium with melts, during fractional crystallisation of garnet from the J75 'megacryst melt'.
A: compositions of the melt after succesive 10% fractions of garnet have been removed from F=1 (original melt), to F=0.1 (90% of melt crystallised)
B: compositions of garnet in equilibrium with the melt calculated for each 10% garnet fractionation shown above.

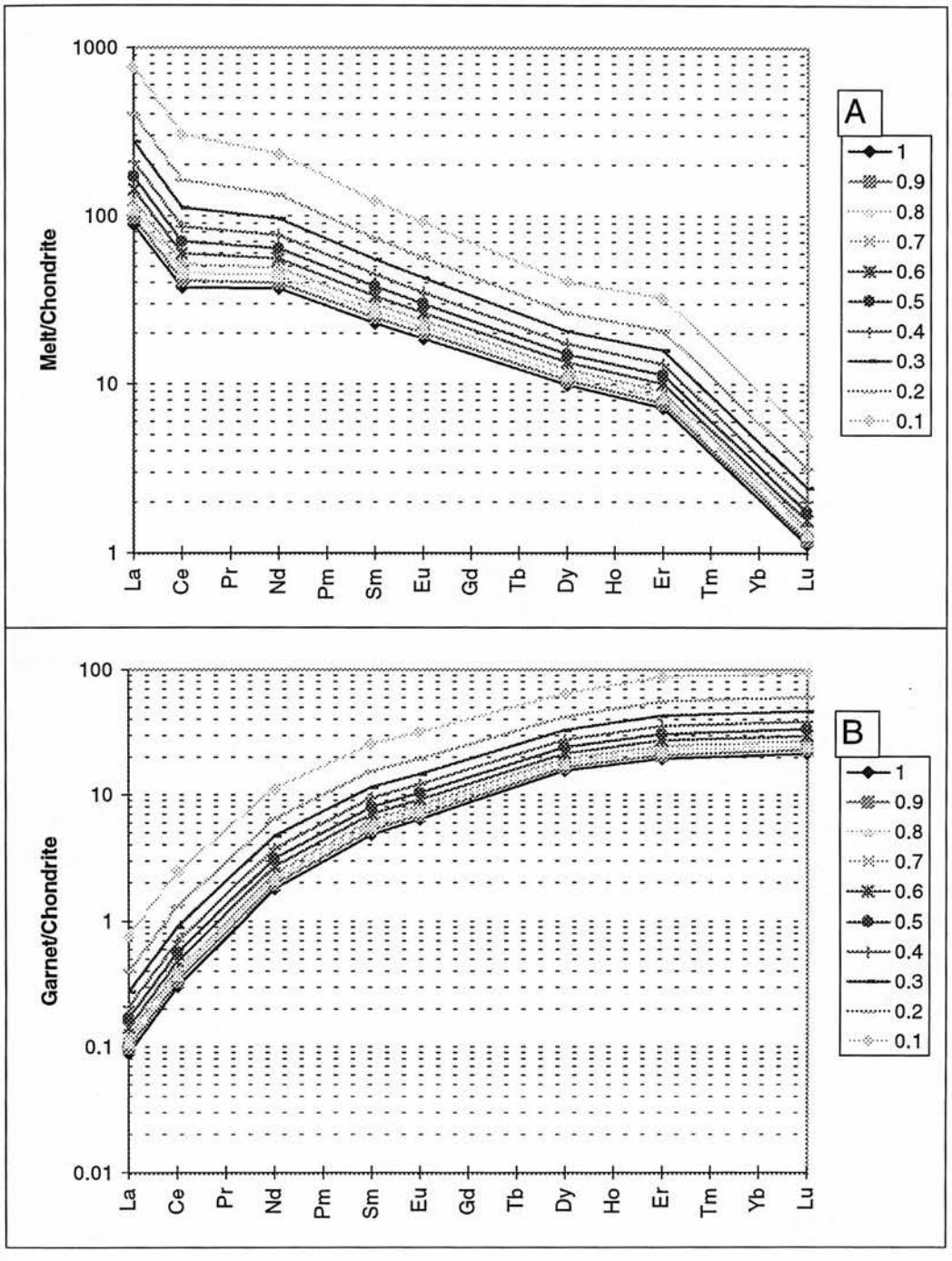

Fig. 7.7. REE compositions of melts and garnet in equilibrium with melts, during fractional crystallisation of clinopyroxene from the J75 'megacryst melt'.
A: compositions of the melt after succesive 10% fractions of clinopyroxene have been removed, from F=1 (original melt) to F=0.1 (90% of melt crystallised).
B: compositions of garnet in equilibrium with the melt calculated for each 10% clinopyroxene fractionation shown above.

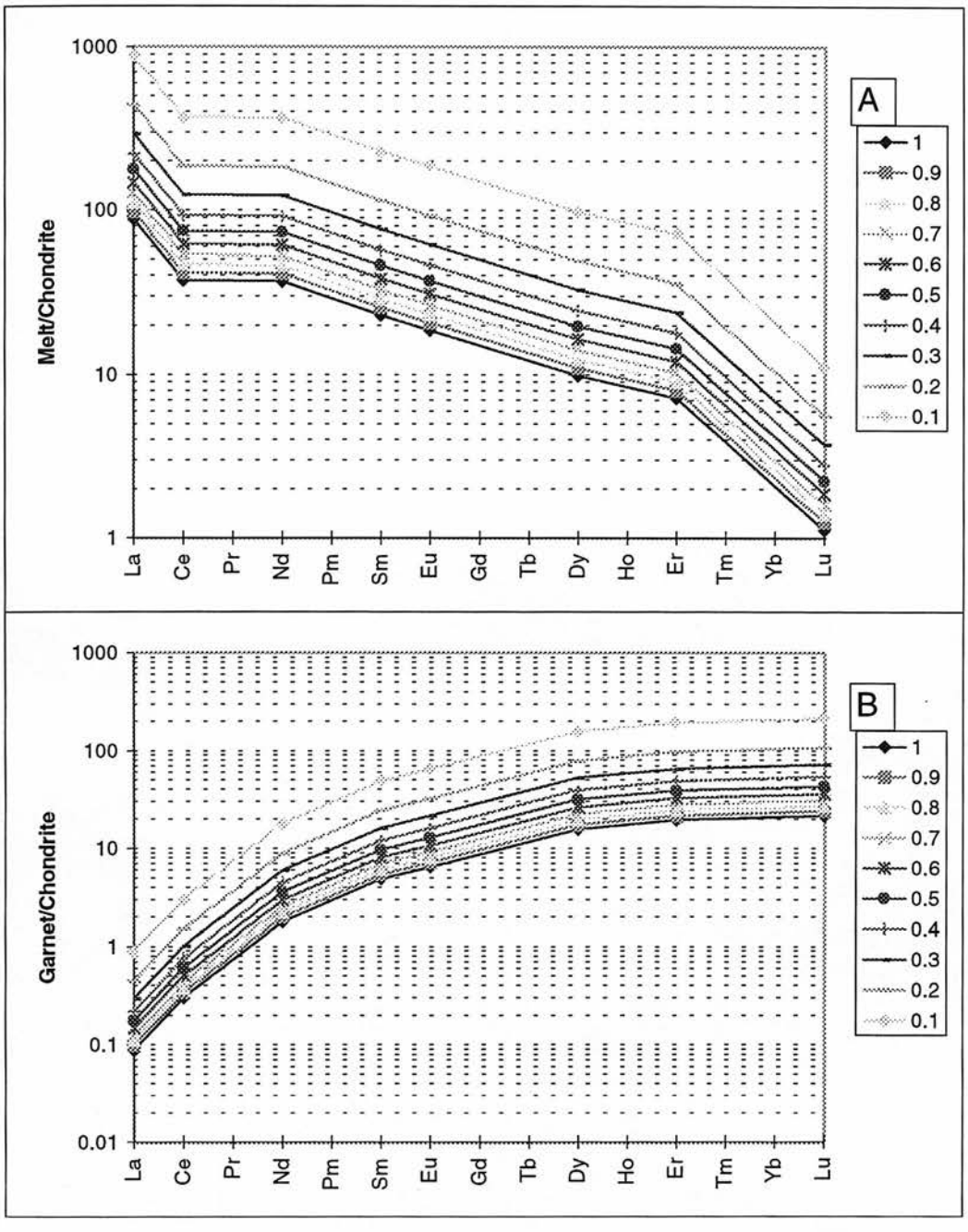

Fig. 7.8 REE compositions of melts and garnet in equilibrium with melts, during fractional crystallisation of olivine from the J75 'megacryst melt'.
A: compositions of the melt after successive 10% fractions of olivine have been removed, from F=1 (original melt), to F=0.1 (90% of melt has crystallised).
B: compositions of garnet in equilibrium with the melt calculated for each 10% olivine fractionation shown above.

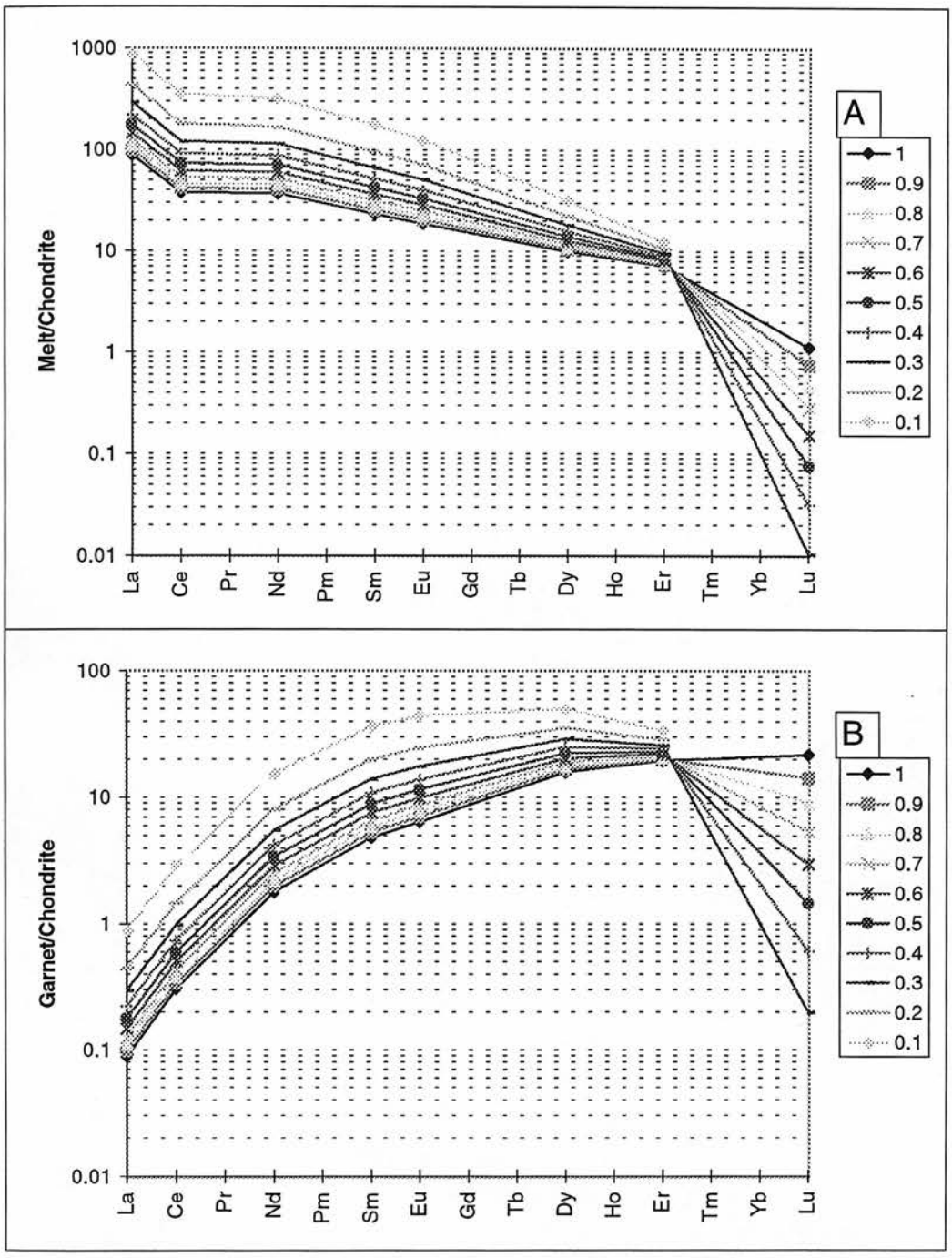

Fig. 7.9 REE compositions of melts and garnet in equilibrium with melts, during fractional crystallisation of 50% olivine, 25% garnet, and 25% clinopyroxene from the J75 'megacryst melt'.
A: compositions of the melt after succesive 10% crystal fractions have been removed, from F=1 (original melt), to F=0.1 (90% of melt crystallised).
B: compositions of garnet in equilibrium with the melt calculated for each 10% crystal fractionation shown above.

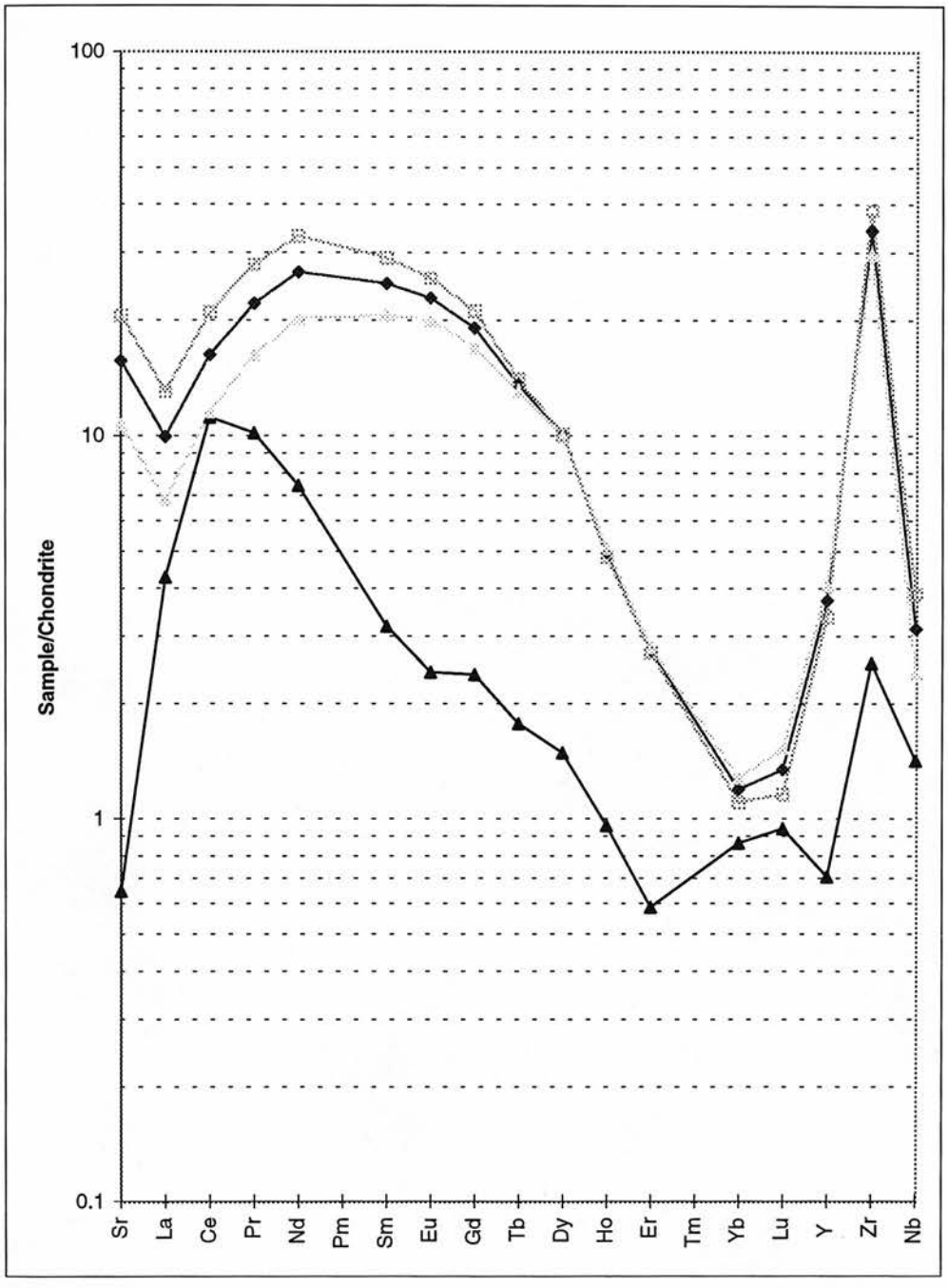

Fig. 7.10 Model trace element compositions for a prospective chemical reservoir for the formation of clinopyroxene and new garnet rims in coarse medium-temperature sample JJG1728. Grey triangles represent the composition of a mineral required to form a mix of 34% clinopyroxene and 64% new garnet by solid state reaction. Dark grey diamonds represent a 50-50% clinopyroxene garnet mix, and light grey squares a 66-34% clinopyroxene garnet mix. For comparison the composition of JJG1728 garnet cores (Black triangles), as a prospective trace element source reservoir is shown.

Fig. 7.11 Schematic Representations of REE compositions for mantle garnets

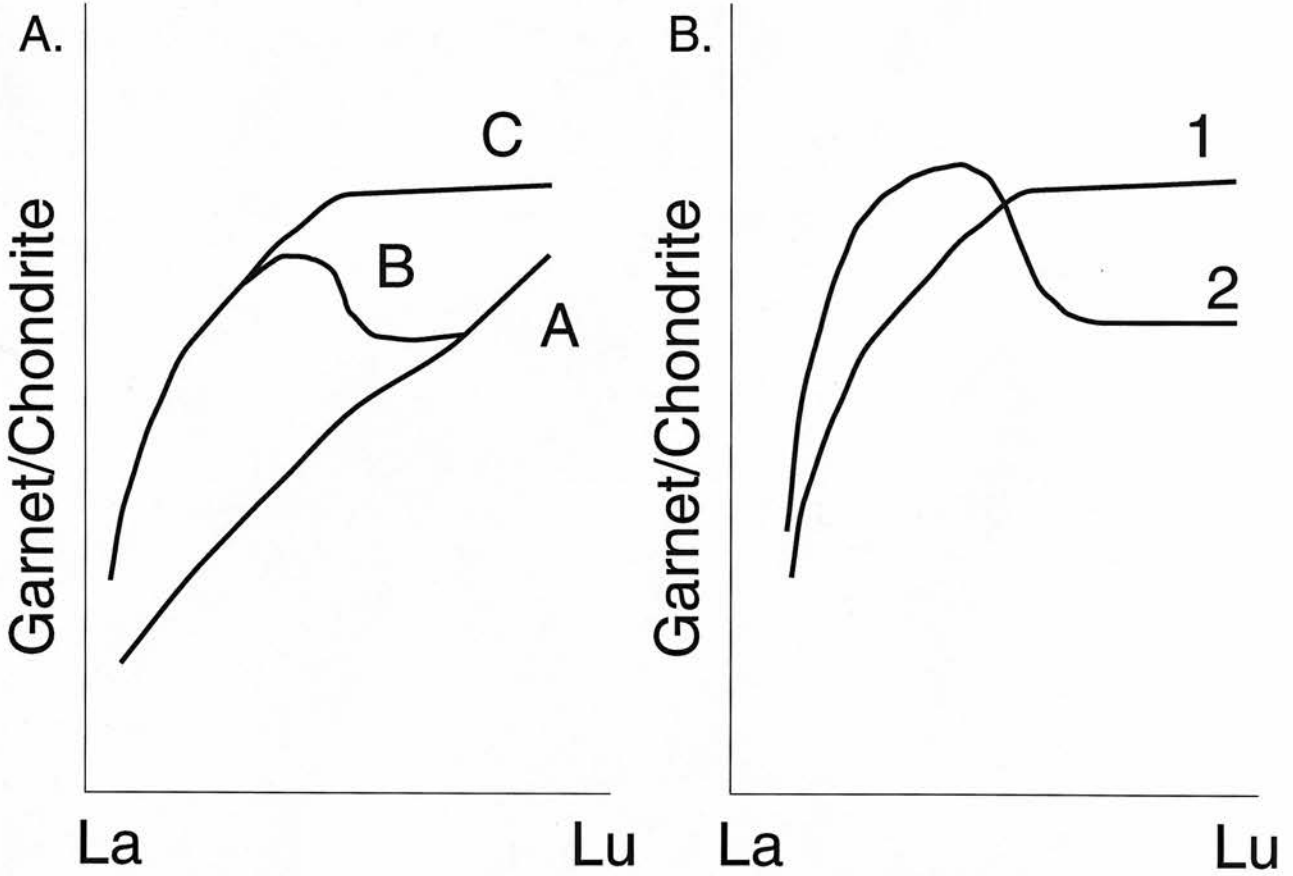

Partial Equilibrium Model, After Hoal et al. (1994), Fig. 4.
A refractory unmetasomatisd garnet, B partially equilibrated garnet with humped REE pattern, C metasomatised garnet with normal REE pattern

Compositions of Jagersfontein Garnets
1 Typical REE pattern of deformed G9 garnet,
2 Typical pattern of coarse G10 garnet.

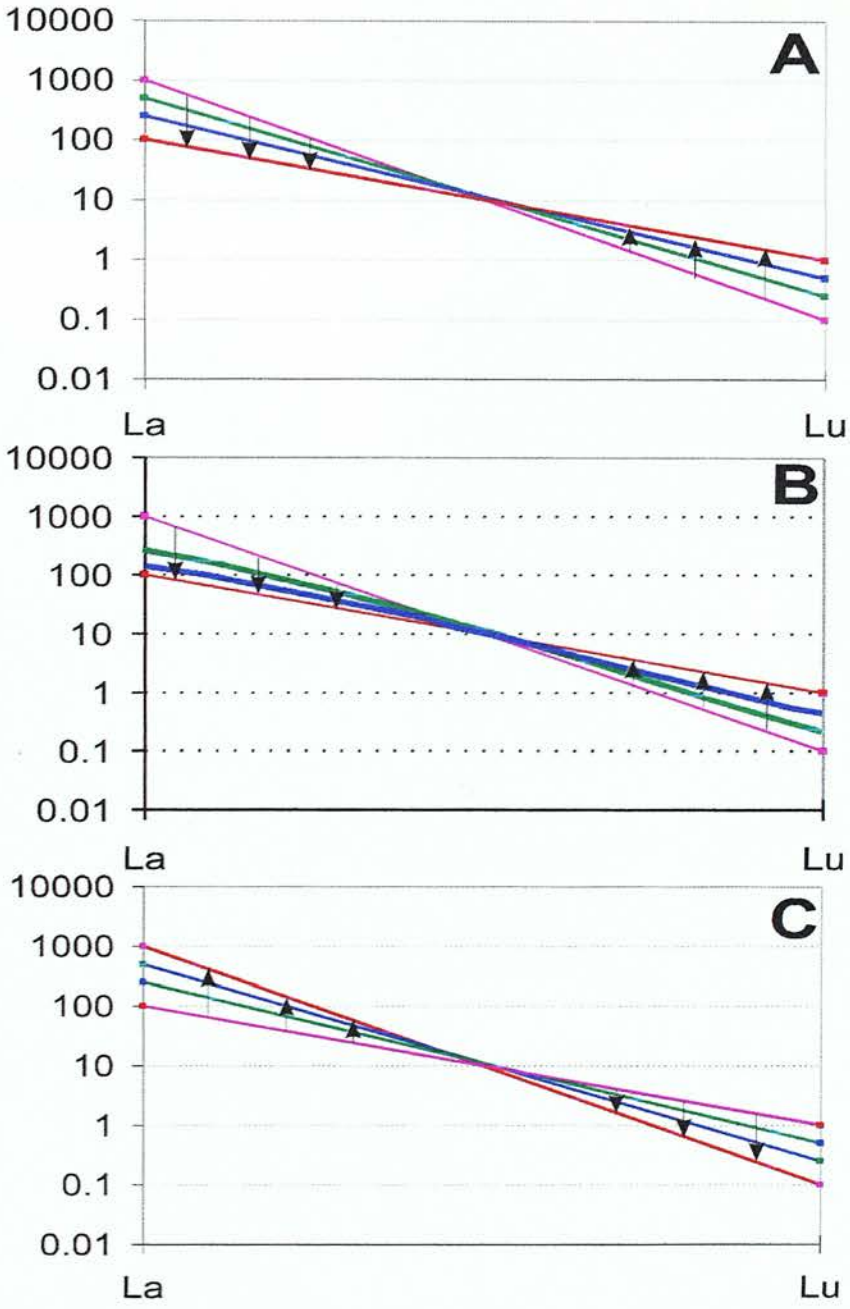

Fig. 7.12 Models of changing (chondrite normalised) REE compositions of metasomatic melts due to chromatographic processes. A. Compositional evolution of a 'megacryst melt' (red line) percolating through the Jagersfontein xenolith mantle. Melts are initially buffered to compositions in equilibrium with the matrix (pink line), and evolve toward the original melt composition with time (green and blue lines). B. Same as A. except LREE are evolving toward the original melt composition more quickly than HREE. C. Compositional evolution of a LREE-enriched metasomatic melt infiltrating an incompatible element depleted sub-cratonic lithosphere. In this case melts are initially buffered to LREE-depleted compositions (pink line), and evolve with time to the more LREE-enriched compositions of the original melt (green, blue and red lines). Freezing this metasomatic process before the mantle column is equilibrated to the melt composition, will yield a column in which the deepest samples are the most highly LREE-enriched.

Chapter 8

The Oxygen Isotope Composition of Jagersfontein Xenoliths

Sample	Phase (Population)	Sub-Population	No. of Analyses (n)	Mean	Standard Deviation about mean s.d	Standard Deviation of mean s.e.
J38	Garnet	Grain A	2	5.79	0.20	0.15
		Grain B	4	5.63	0.11	0.05
		Grain C	2	5.59	0.40	0.29
	Orthopyroxene	Grain D	6	5.54	0.09	0.04
		Grain E	9	5.50	0.10	0.03
J119	Garnet	Grain A	5	5.48	0.26	0.12
		Grain B	5	5.52	0.26	0.11
		Grain C	4	5.63	0.12	0.06
	Orthopyroxene	Porphyroclast	6	5.72	0.16	0.07
		Neoblast	4	5.63	0.09	0.04
J36	Garnet	Core	9	5.49	0.26	0.09
		Rim	10	5.63	0.19	0.06
J34	Garnet	Core	3	5.56	0.08	0.04
		Rim	9	5.61	0.19	0.06
J107	Garnet	Core	5	5.52	0.11	0.05
		Rim	4	5.59	0.14	0.07
Ion Probe Analyses						
J119	Olivine	Porphyroclast	19	5.1	1.0	0.2
		Neoblast	15	4.8	0.7	0.2
	Garnet	Grain 1	18	5.7	1.3	0.3
		Grain 2	14	5.5	0.9	0.2

Table 8.1 Statistical Analysis of laser fluorination and ion probe data for Jagersfontein xenoliths.
Standard deviations are σ-1 about the mean, and σ-1/root n of the mean.
Means of sub-populations are assumed to be identical if they are within two standard deviations of the mean of the population.

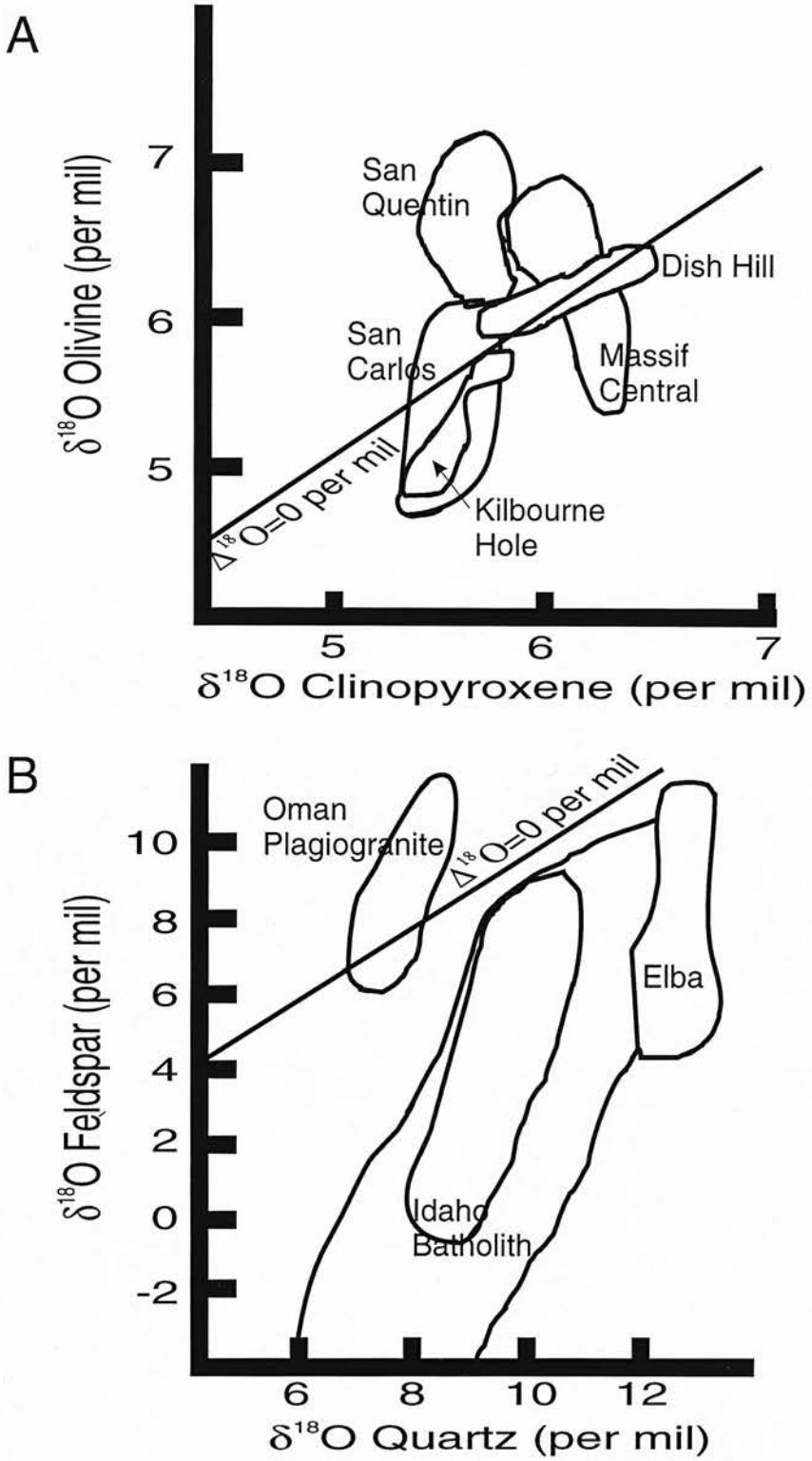

Fig. 8.1 Schematic representation of Gregory and Taylor (1986a) Fig. 1 (A) and Fig.2 (B). A shows $\delta^{18}O$ olivine versus $\delta^{18}O$ clinoproxene for spinel peridotites analysed by Kyser et al. (1981). B shows $\delta^{18}O$ feldspar versus $\delta^{18}O$ quartz for hydrothermally altered granites. Data for individual localities (clusters) show variations dominated by olivine/feldspar and therefore the data forms steep arrays crossing the $\Delta^{18}O=0$ per mil fractionation line.

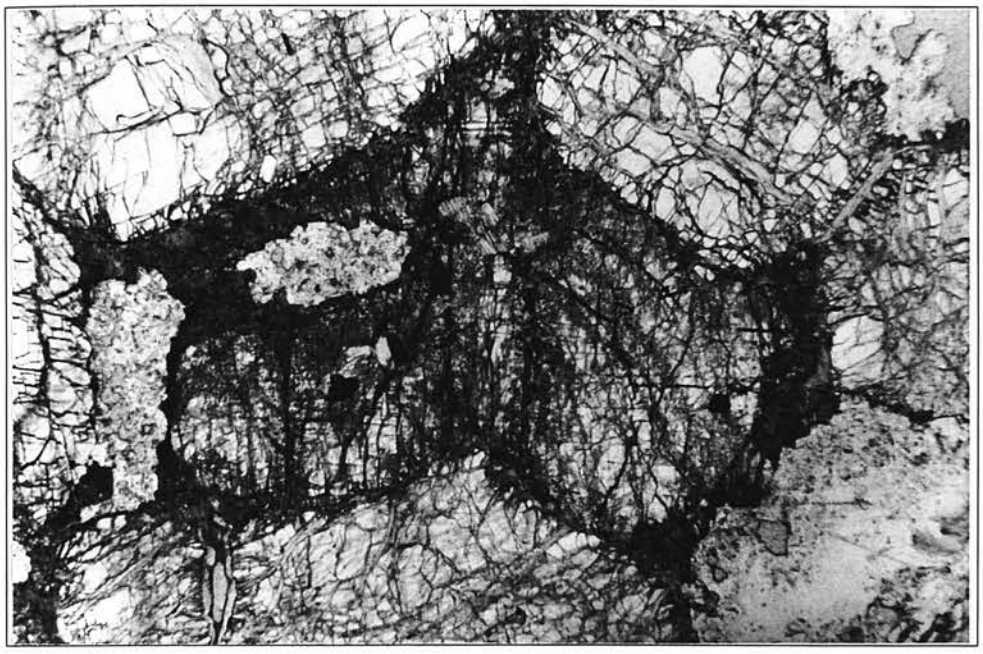

Fig. 8.2a Transmitted light photograph of a clinopyroxene grain from coarse medium-temperature phlogopite-lherzolite JJG1795. Alteration is clearly visible as cloudy patches within the grain. Surrounding grains are olivine. The right hand half of this grain was used in the TEM study. Magnification 15x.

Fig. 8.2b TEM image of an alteration vein in a clinopyroxene from coarse medium-temperature phlogopite-lherzolite JJG1795. The vein consists of a sheet silicate (probably serpentine) growing at right angles to the vein margin. Scale bar is 550nm.

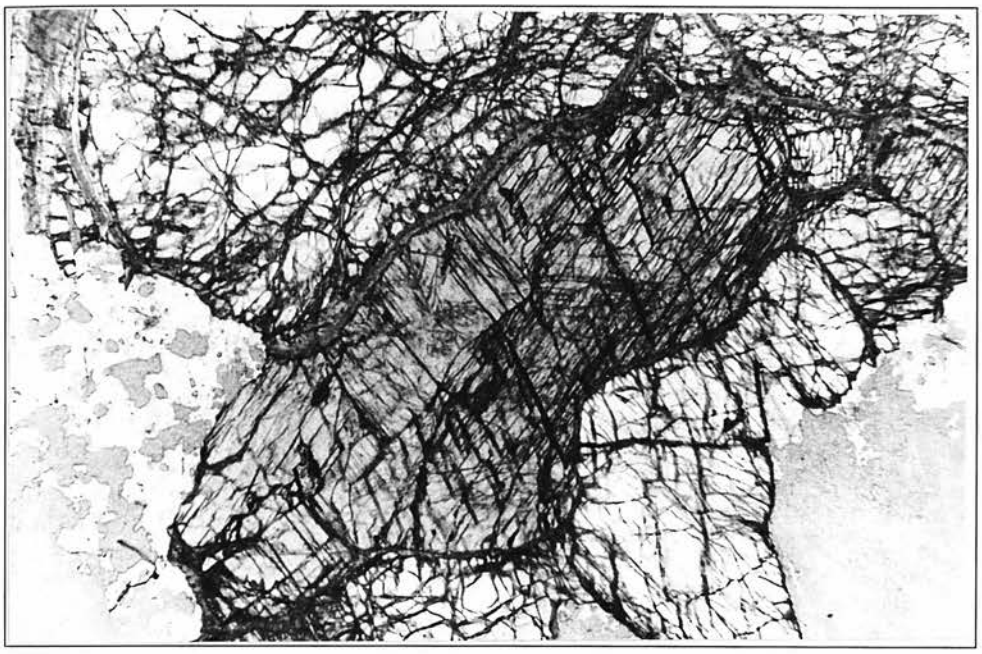

Fig. 8.2c Transmitted light photograph of a near basal section amphibole grain from coarse low-temperature phlogopite-amphibole-harzburgite JJG8. Visible alteration is dominantly confined to cleavages. Surrounding grains are olivine. The lower left half of this grain was used in the TEM study. Magnification 12x.

Fig. 8.2d TEM image of an alteration vein in an amphibole from coarse medium-temperature phlogopite-amphibole-harzburgite JJG8. The vein consists of a sheet silicate (probably serpentine) growing along cleavage planes. Scale bar is 900nm.

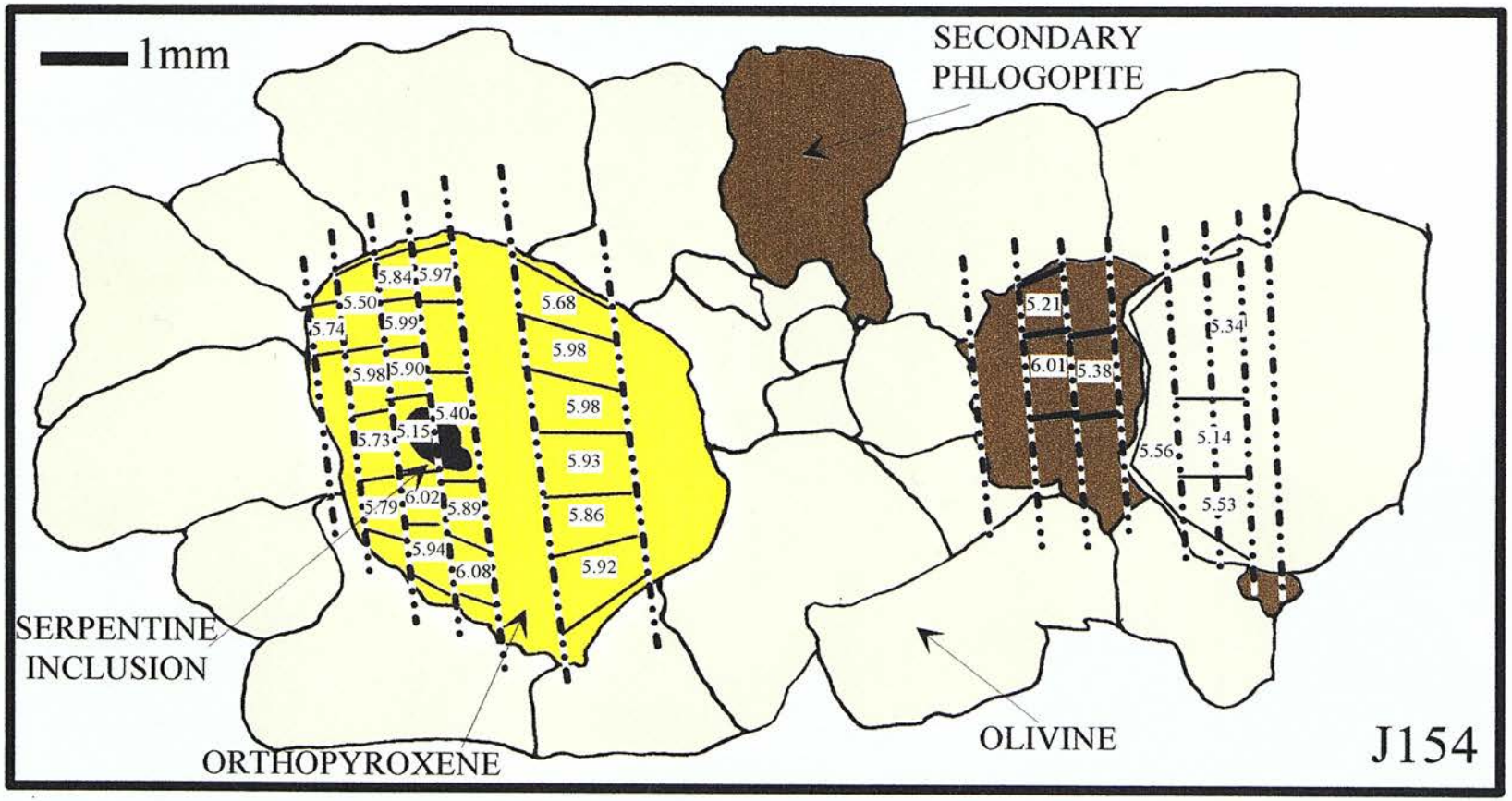

Fig. 8.3 Representation of detailed micro-sampling and analysis for a coarse harzburgite (olivine + orthopyroxene + secondary phlogopite) J154. Dashed lines represent saw cuts, microsamples are separated by solid lines. Oxygen isotope compositons are given in per mil-SMOW. The black inclusion in the orthopyroxene grain is serpentine. The low oxygen isotope composition of this inclusion is shown by the composition of the micro-samples in which this inclusion is contained.

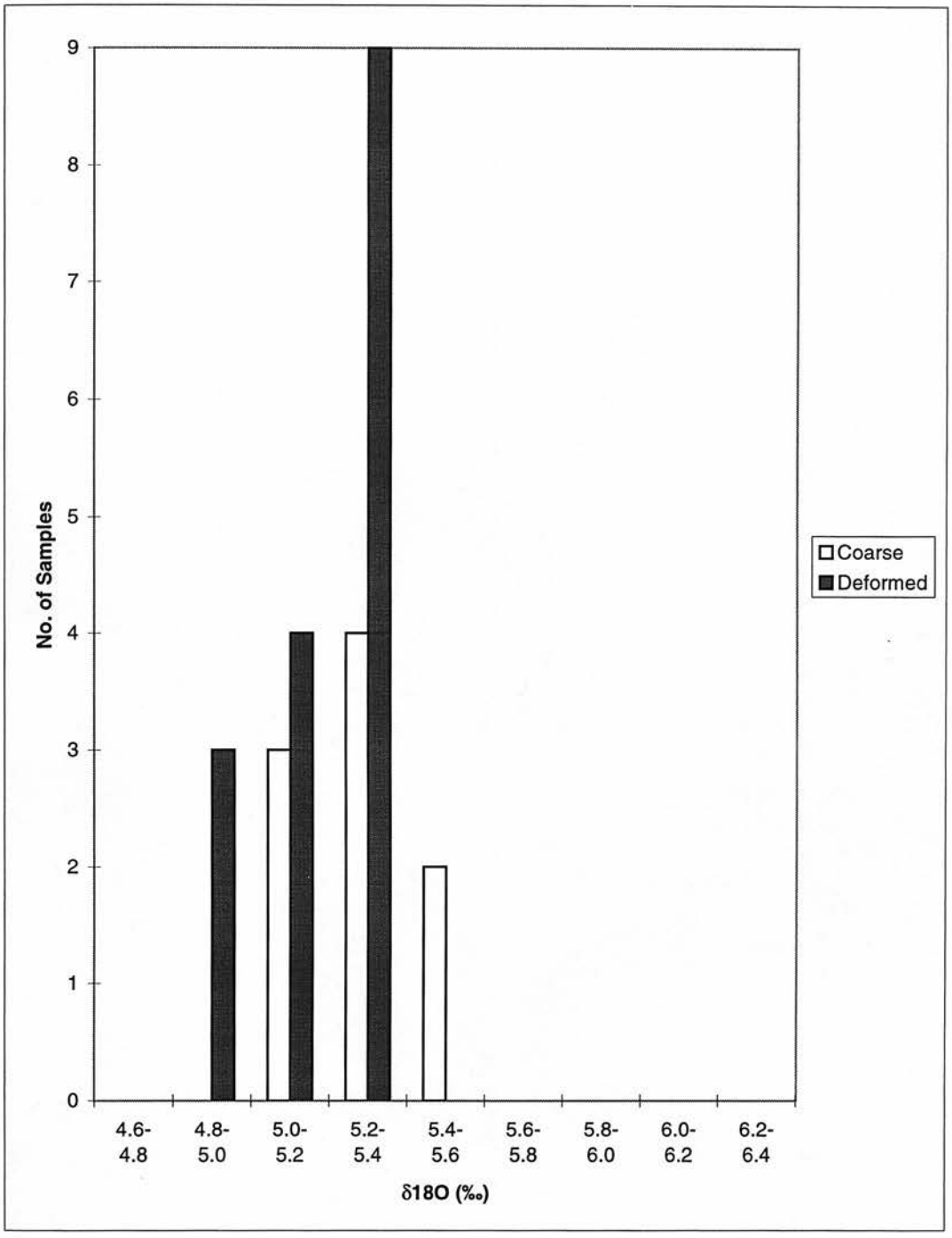

Fig. 8.4a Summary of mean oxygen isotope compositions for olivines from the Jagersfontein xenolith suite. Olivines from coarse xenoliths are in white, olivines from deformed xenoliths are in dark grey.

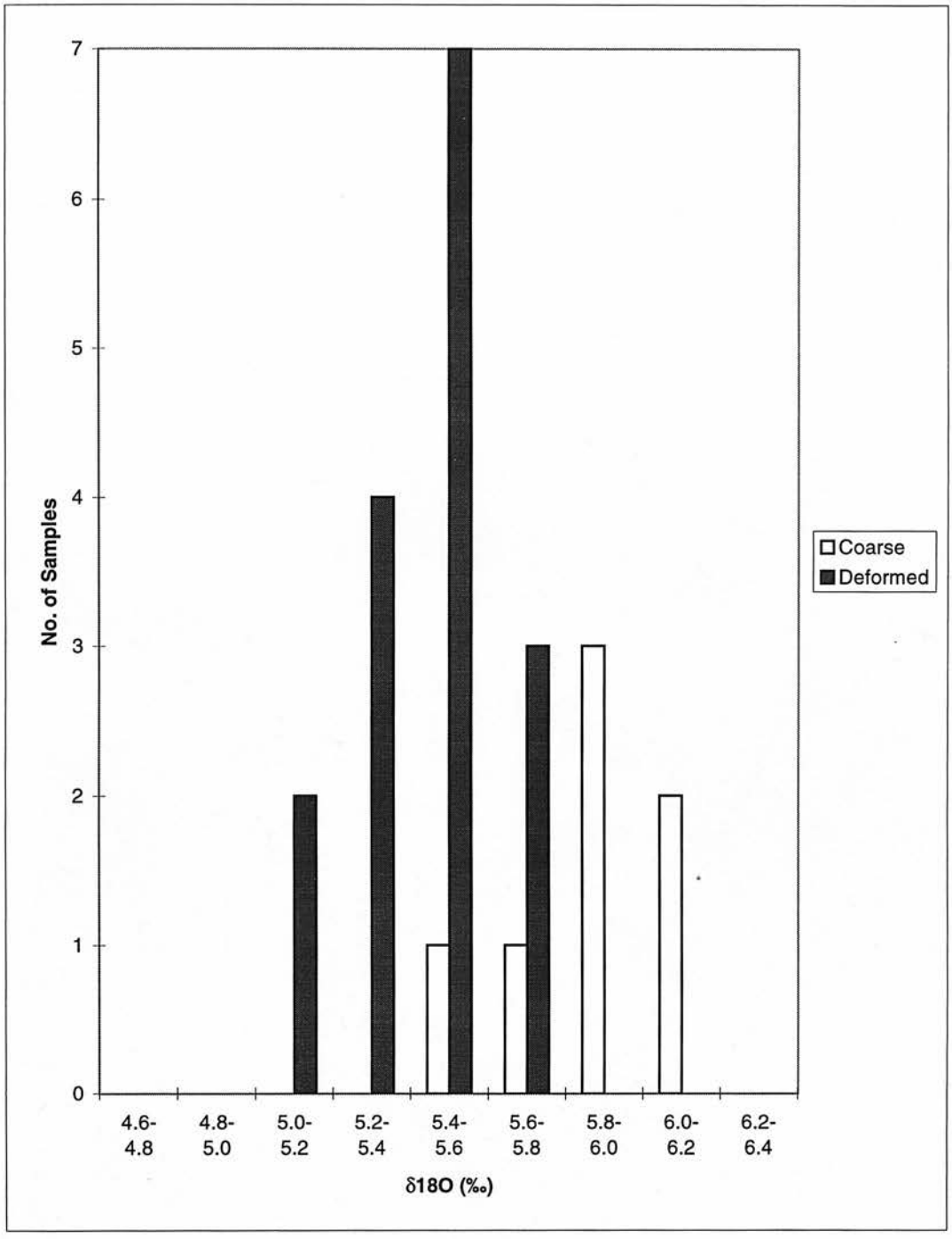

Fig. 8.4b Summary of mean oxygen isotope compositions for orthopyroxenes from the Jagersfontein xenolith suite. Orthopyroxenes from coarse xenoliths are in white, orthopyroxenes from deformed xenoliths are in dark grey.

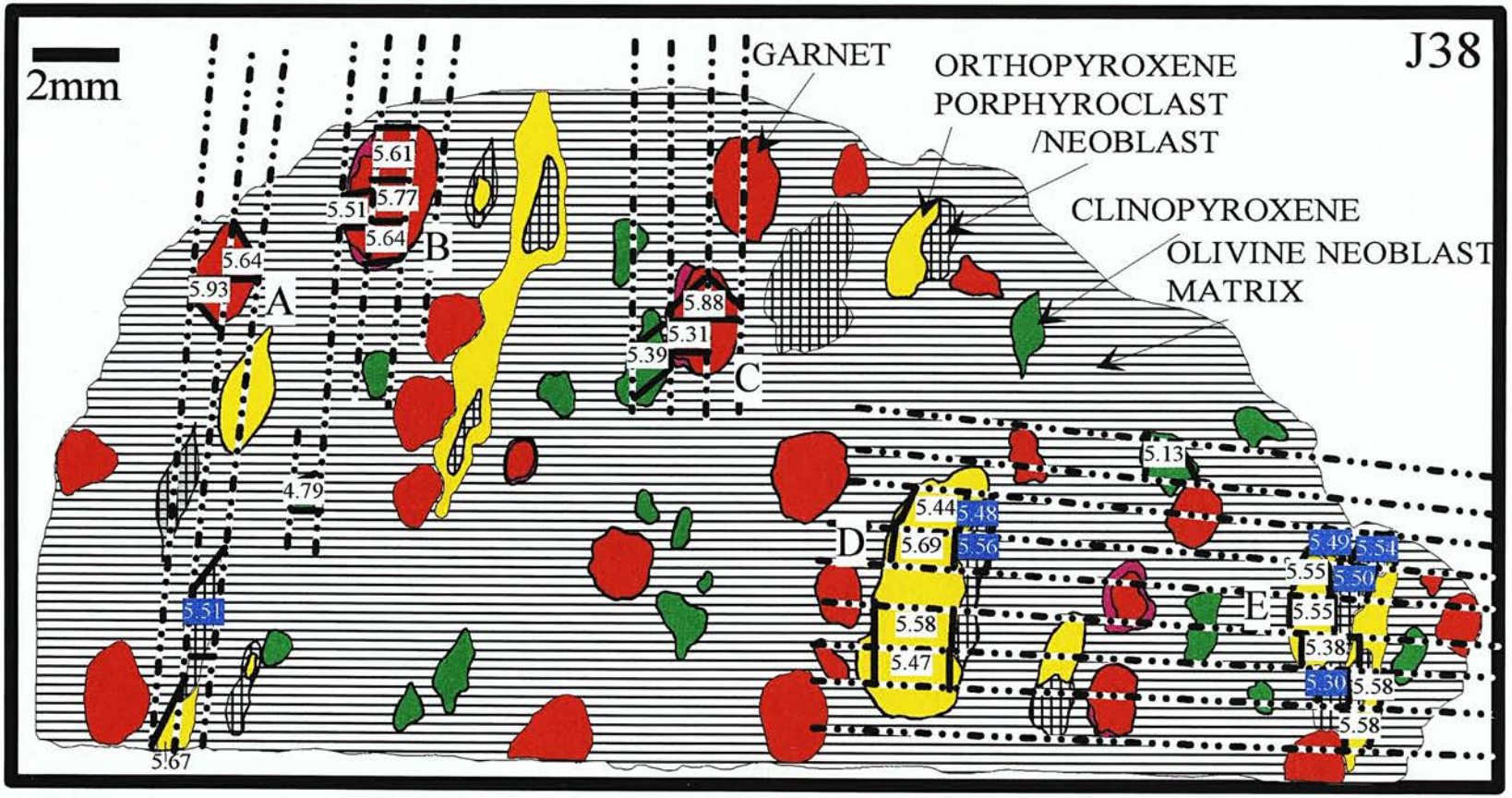

Fig. 8.5a Representation of detailed micro-sampling and analysis for the deformed garnet lherzolite xenolith J38. Dashed lines represent saw cuts, micro-samples are separated by solid lines. Oxygen isotope compositions are given in per mil-SMOW. Numbers in white with a dark background, are orthopyroxene samples which are dominated by neoblasts. Letters correspond to grains whose compositions are summarised in Table 8.1.

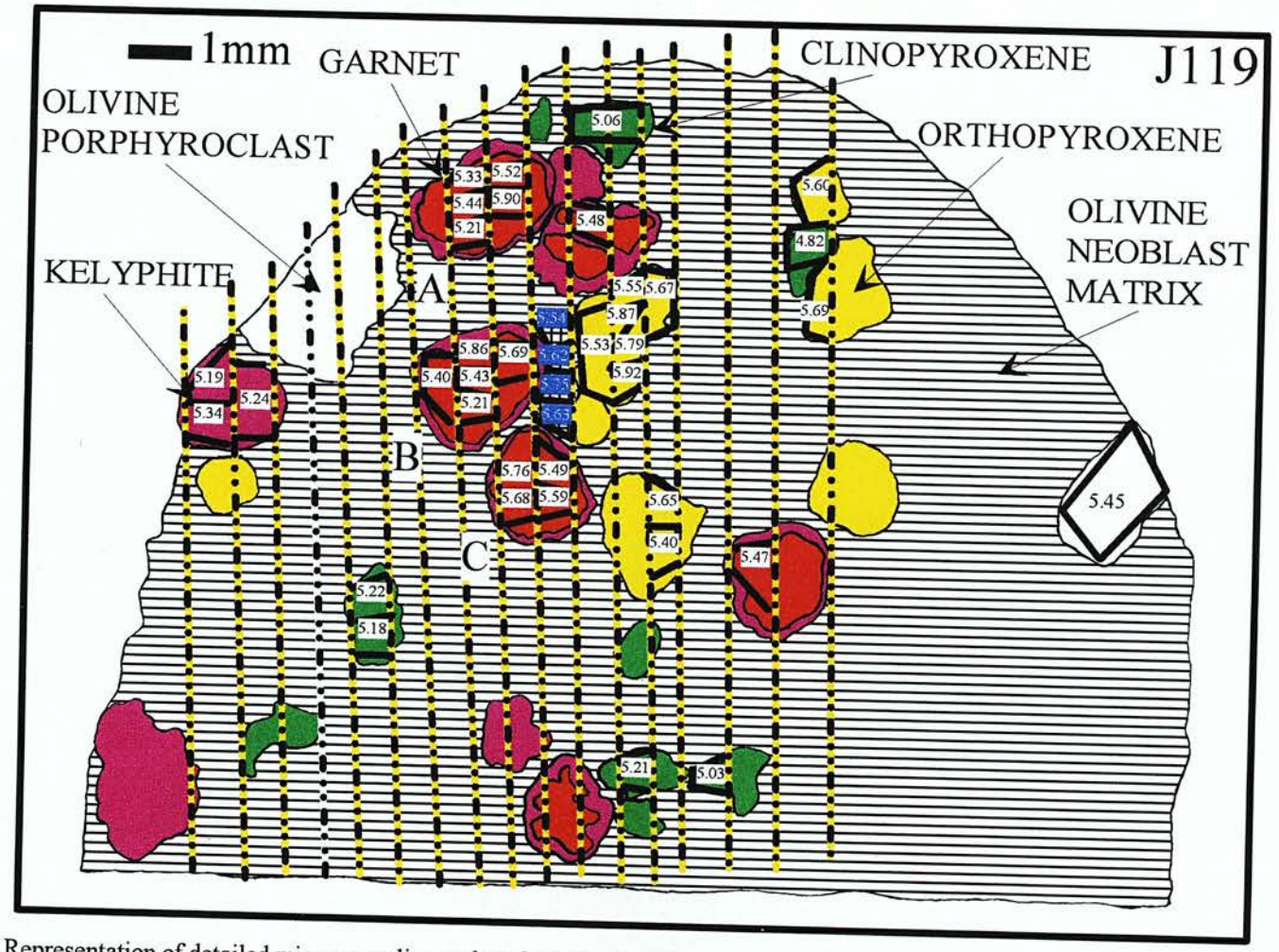

Fig. 8.5b Representation of detailed micro-sampling and analysis for the deformed garnet lherzolite xenolith J119. Dashed lines represent saw cuts, micro-samples are separated by solid lines. Oxygen isotope compositions are given in per mil-SMOW. Numbers in white with a dark background, are orthopyroxene neoblast analysis. Letters correspond to grains whose composition are summarised in Table 8.1

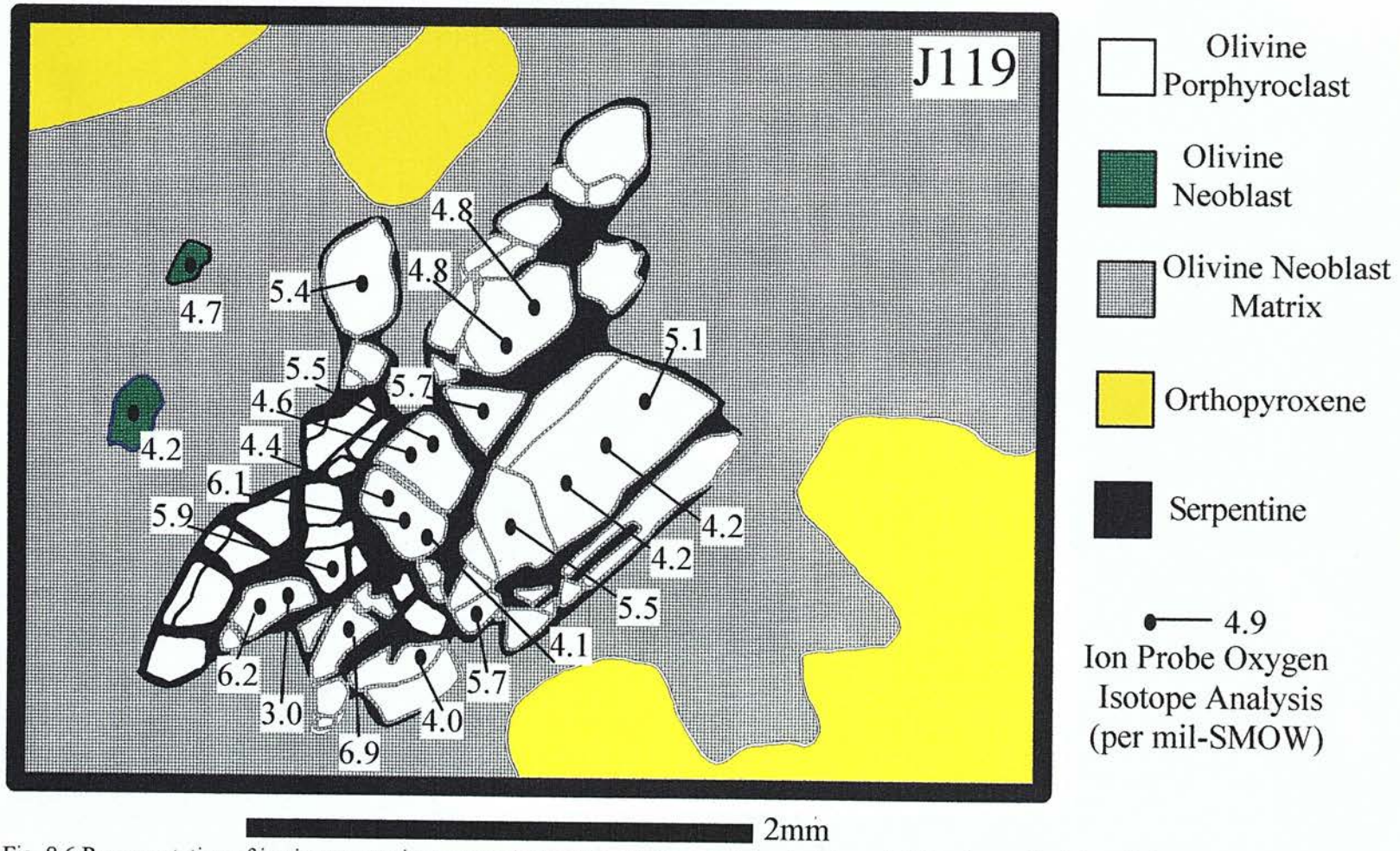

Fig. 8.6 Representation of in situ oxygen isotope analysis of an olivine porphyroclast from J119 by ion probe. The olivine neoblast/ serpentine matrix has been simplified for clarity. Two olivine neoblasts which have been analysed are shown.

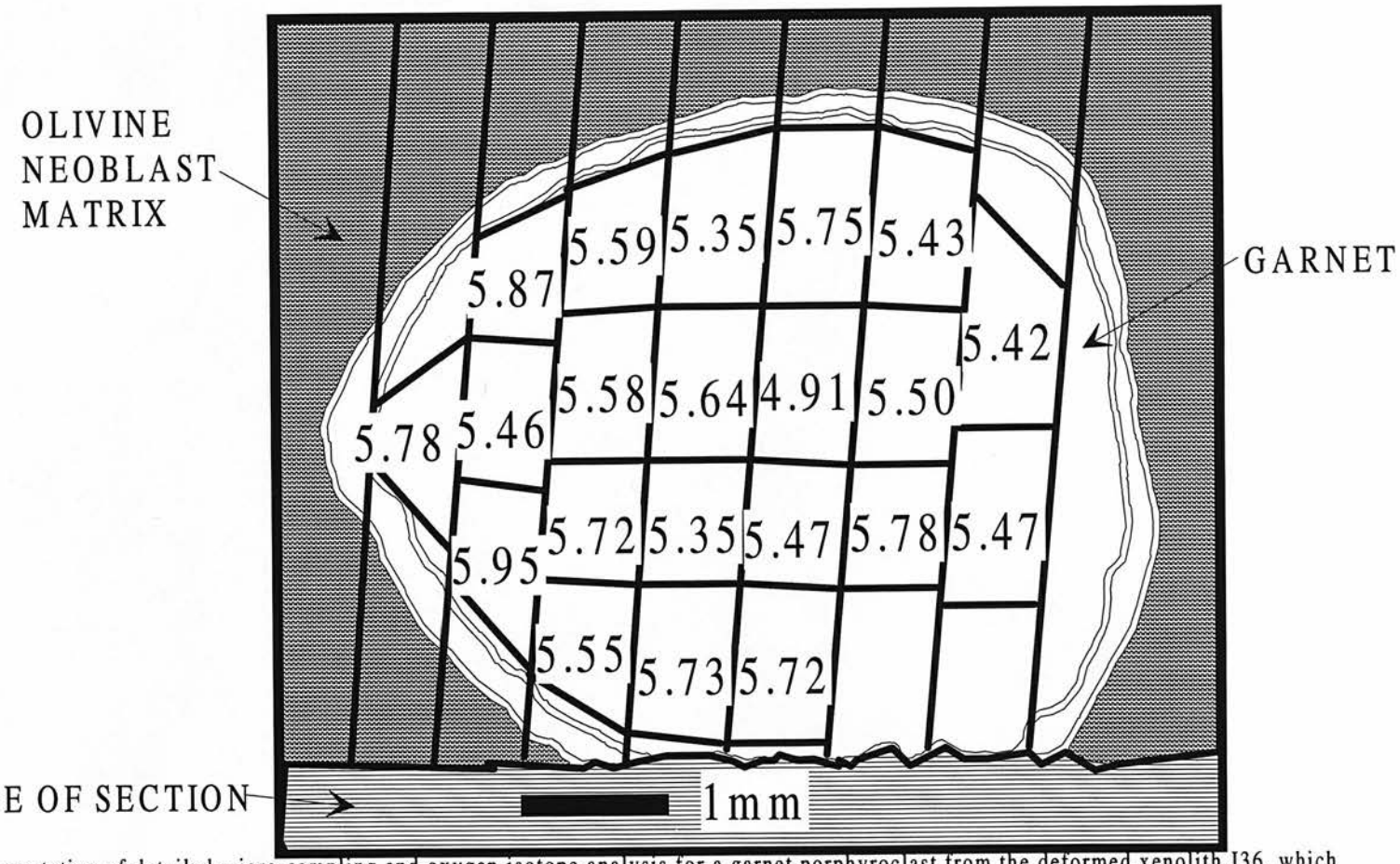

Fig. 8.7a Representation of detailed micro-sampling and oxygen isotope analysis for a garnet porphyroclast from the deformed xenolith J36, which is homogeneous with respect to major elements. Solid lines represent saw cuts, and separate individual micro-samples. Oxygen isotope compositions are given in per mil-SMOW.

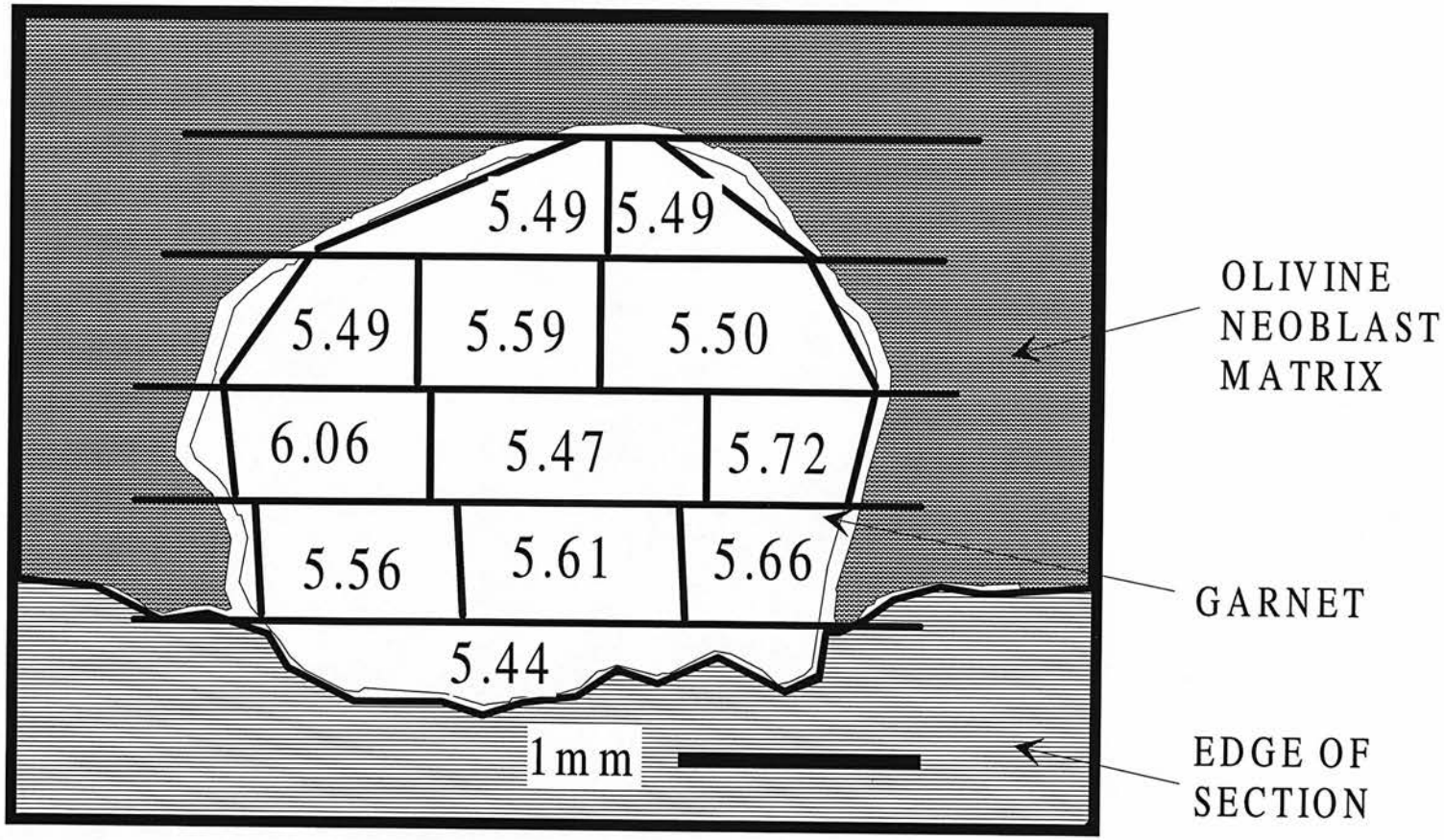

Fig. 8.7b Representation of detailed micro-sampling and oxygen isotope analysis for a garnet porphyroclast from the deformed xenolith J34, which is heterogeneous with respect to major elements. Solid lines represent saw cuts, and separate individual micro-samples. Oxygen isotope compositions are given in per mil-SMOW.

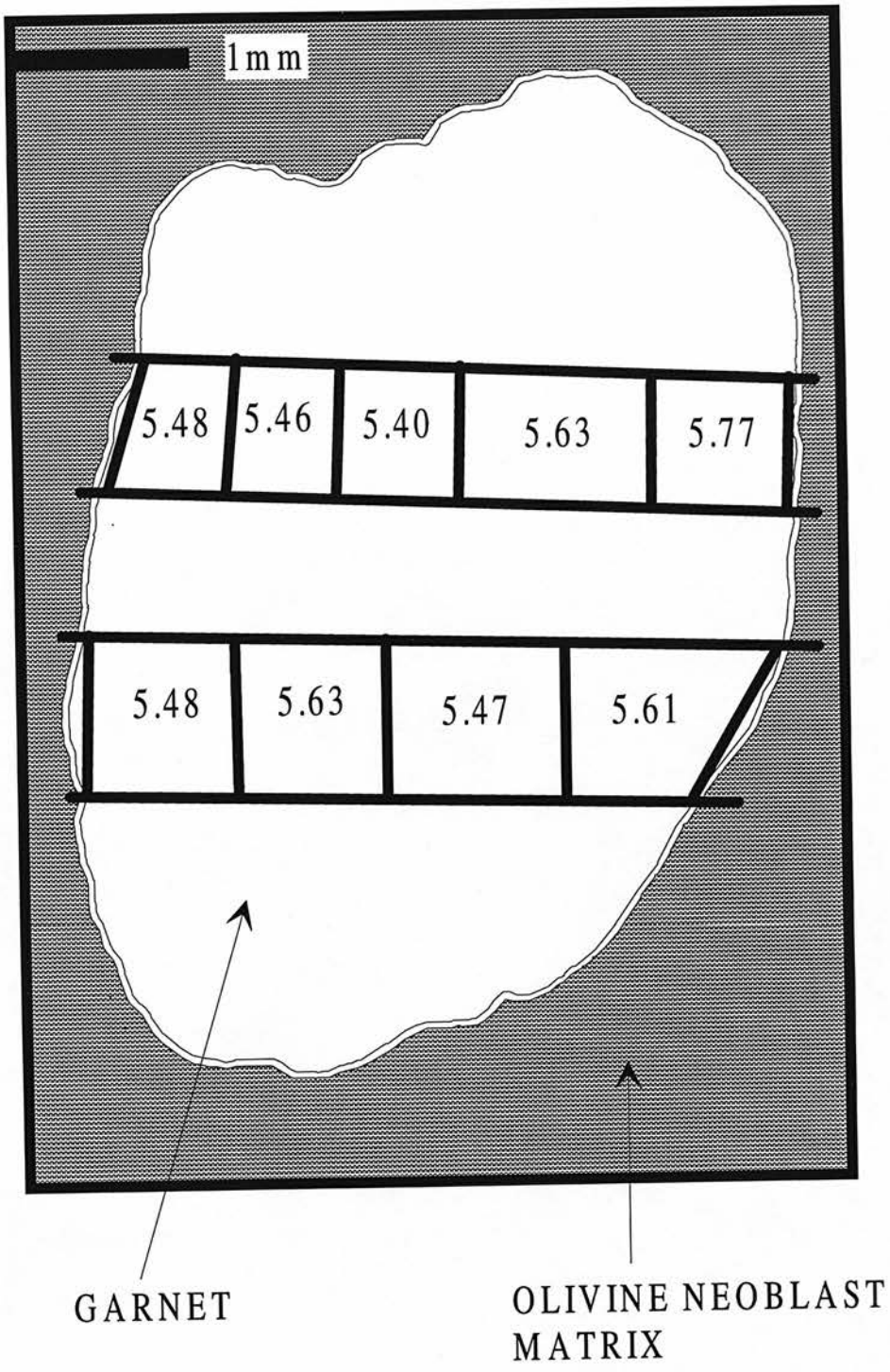

Fig. 8.7c Representation of detailed micro-sampling and oxygen isotope analysis for a garnet porphyroclast from the deformed xenolith J107, which is heterogeneous with respect to major elements. Solid lines represent saw cuts, and separate individual micro-samples. Oxygen isotope compositions are given in per mil-SMOW.

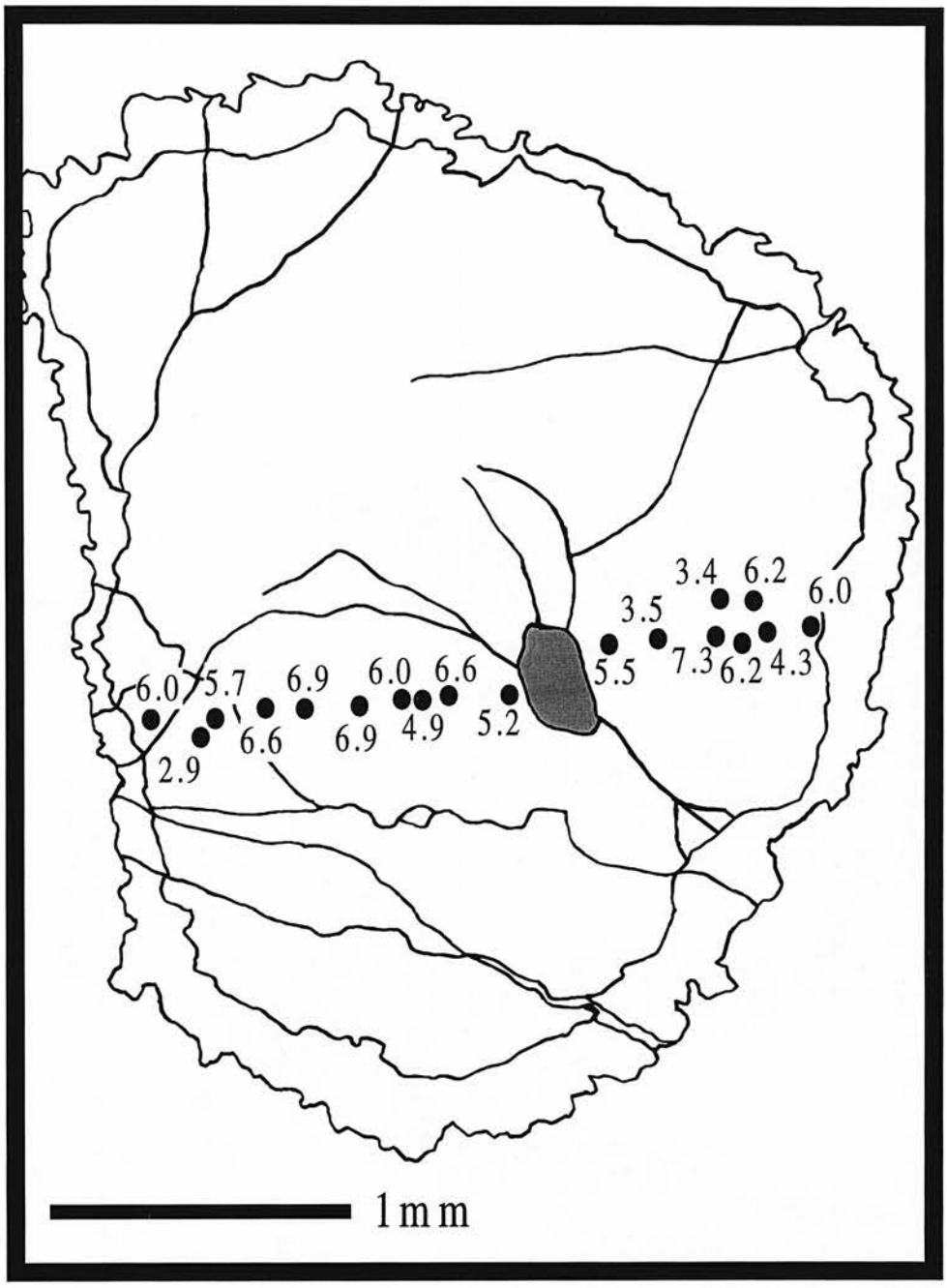

Fig. 8.8a Representation of in situ oxygen isotope analysis of garnet porphyroclast Grain One, from J119, by ion probe. Oxygen isotope compositions are given in per mil-SMOW. The inclusion shown is clinopyroxene. The rim around the grain is kelyphite.

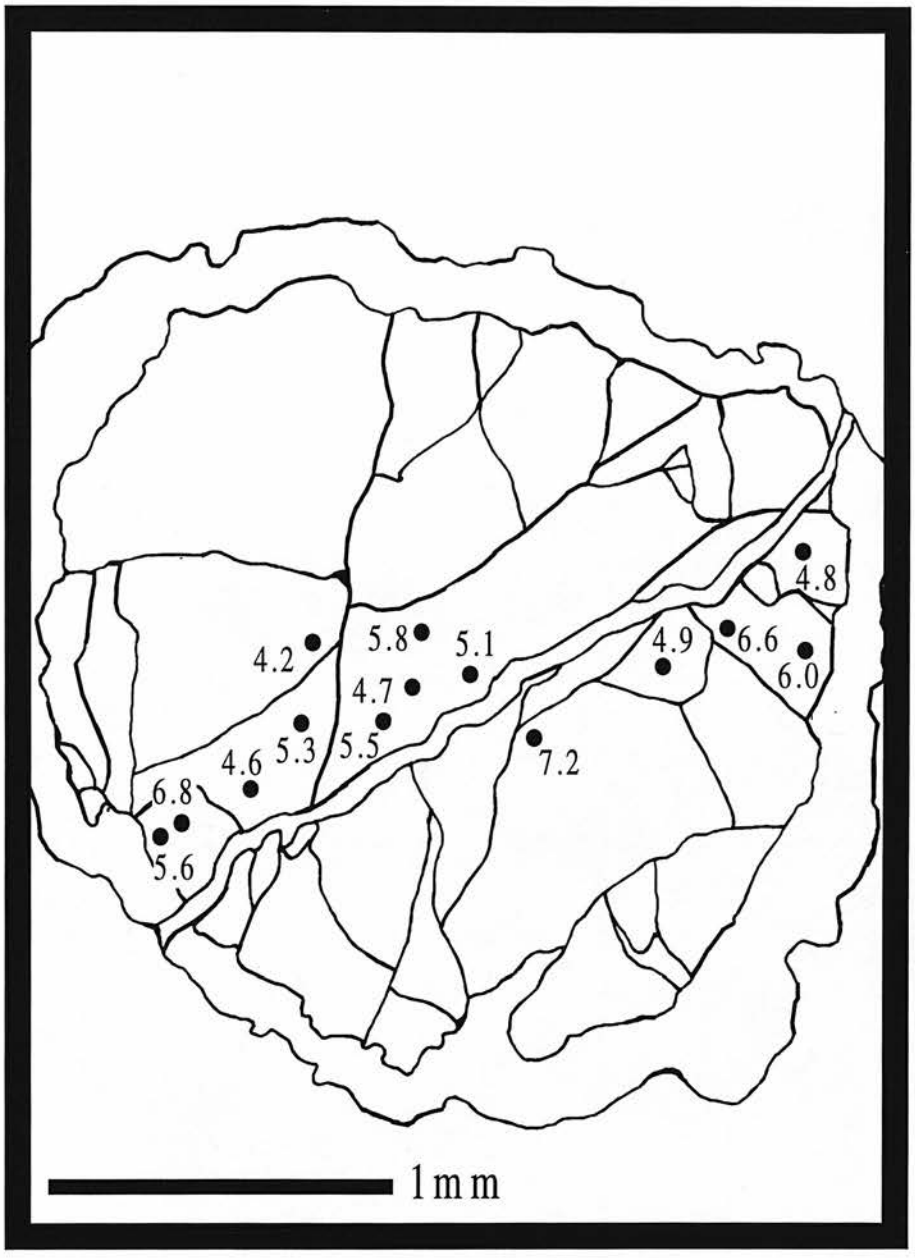

Fig. 8.8b Representation of in situ oxygen isotope analysis of garnet porphyroclast Grain Two, from J119, by ion probe. Oxygen isotope compositions are given in per mil-SMOW. The rim around the grain is kelyphite.

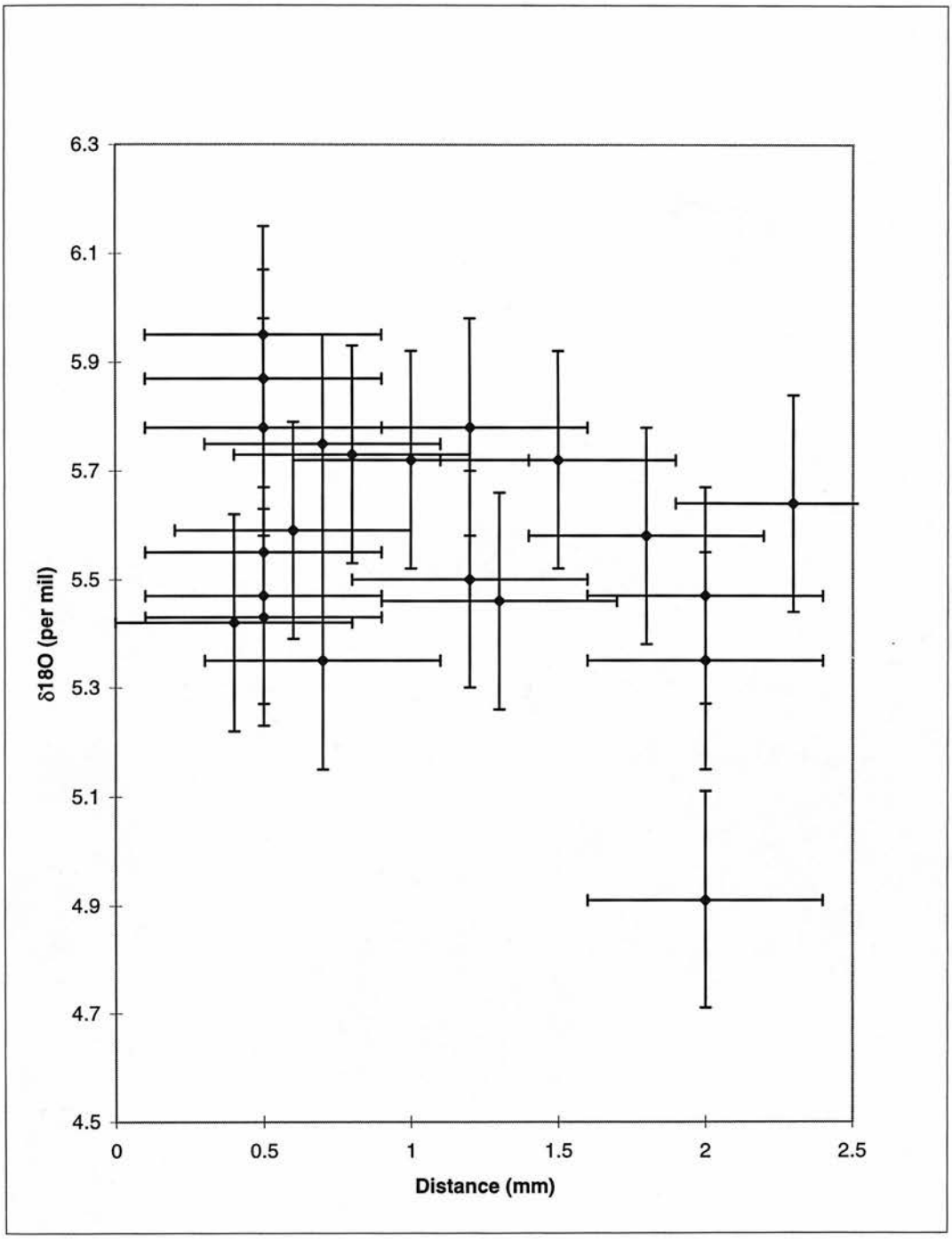

Fig. 8.9 Variation of oxygen isotope composition with distance from grain rim for a garnet porphyroclast from deformed sample J36. Y-errors are +/- 0.2‰ 2σ about the mean. X-error bars represent the typical maximum dimension of a micro-sample (0.8mm).

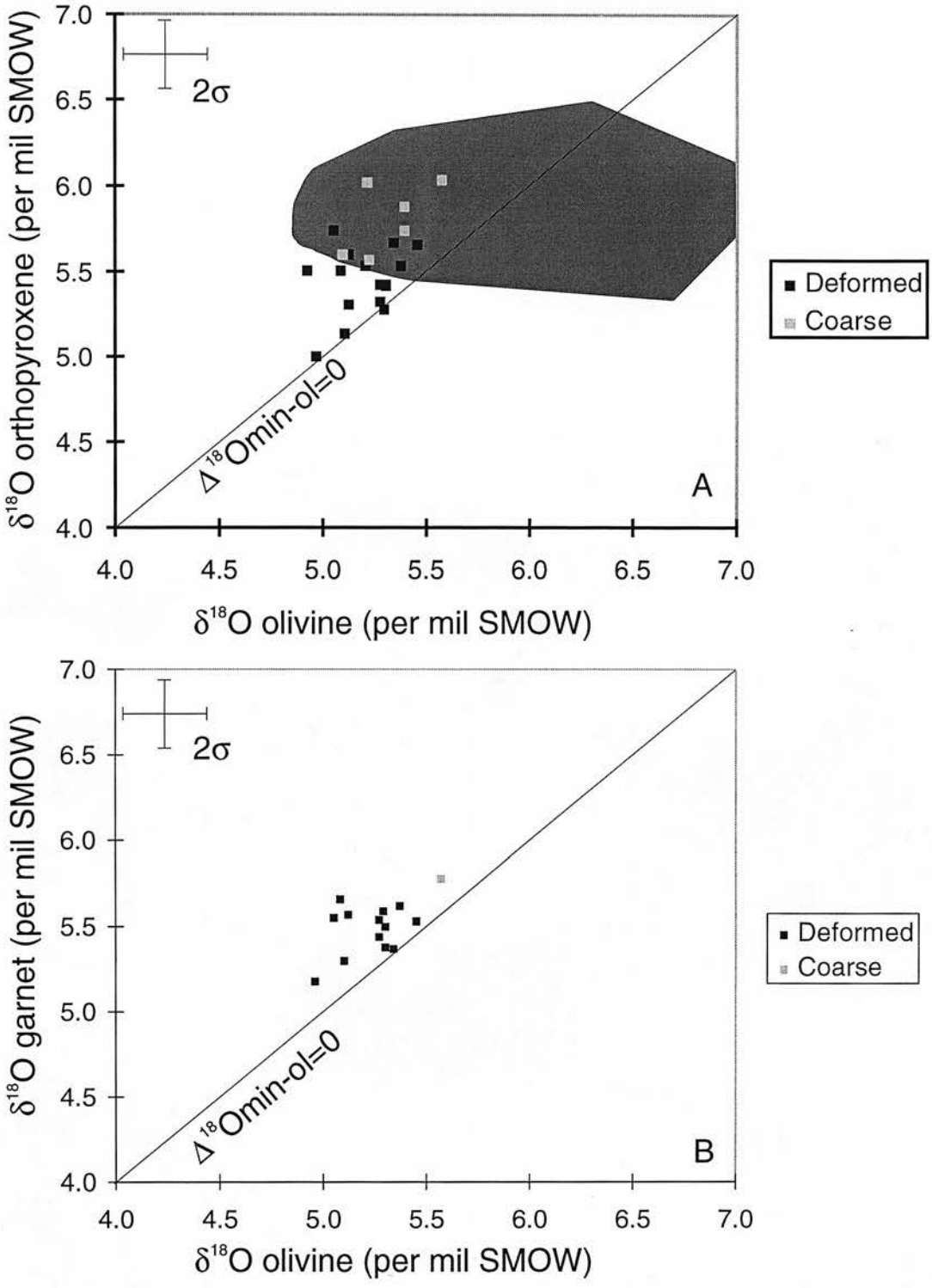

Fig. 8.10. A. $\delta^{18}O$ orthopyroxene versus $\delta^{18}O$ olivine, B. $\delta^{18}O$ garnet versus $\delta^{18}O$ olivine, for laserfluorination data. Each data point represents the mean of oxygen isotope analyses for a particular sample. In A the shaded area represents the conventional oxygen isotope data of Kyser et al. (1981).

Chapter 9

Summary, Wider Implications and Future Work

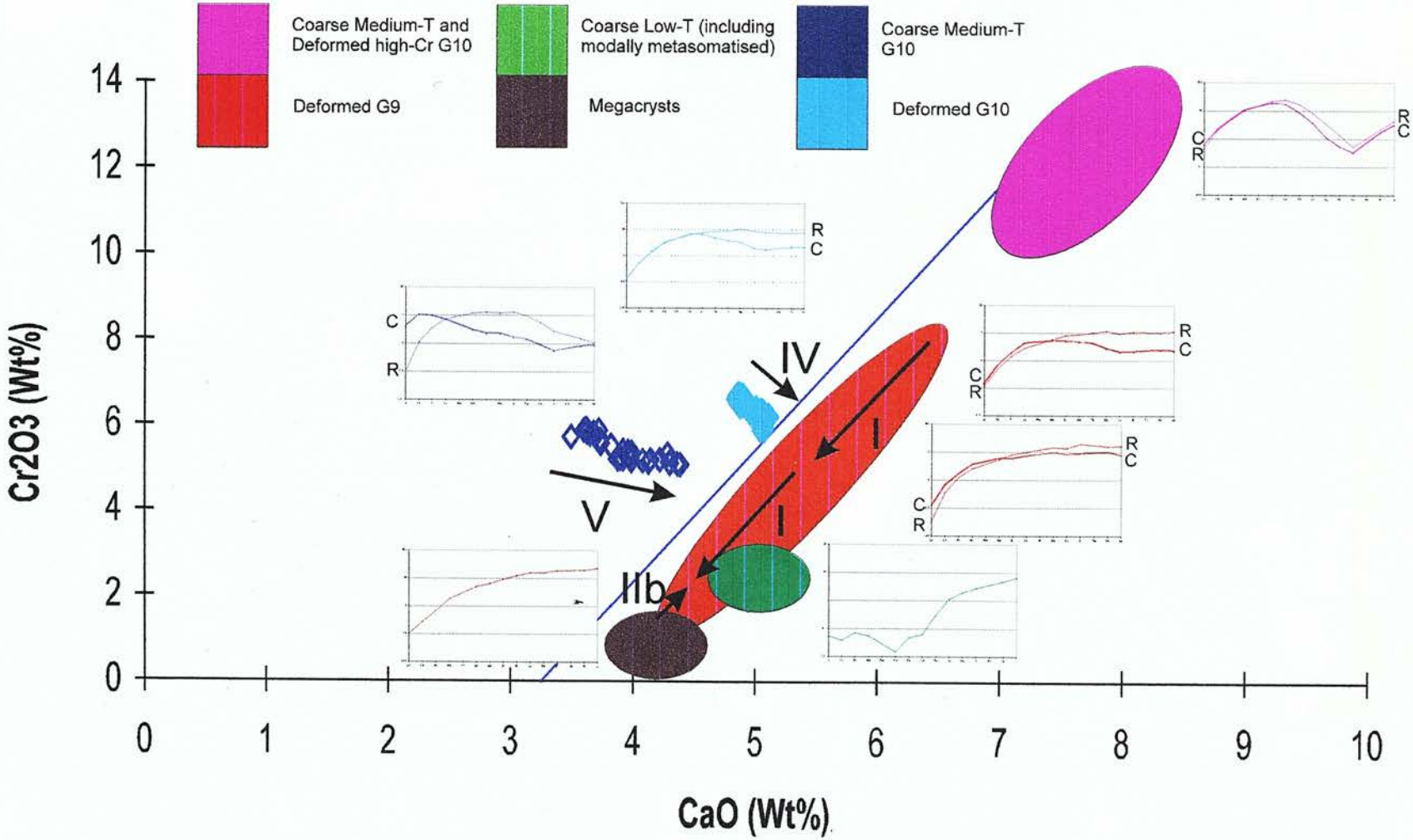

Fig. 9.1 Summary diagram of CaO-Cr2O3 and REE composition of Jagersfontein garnets. Chondrite normalised REE plots correspond to CaO-Cr2O3 compositions of the same colour. For heterogeneous garnets core (C) and rim (R) compositions are given. Arrows show direction of rimward change in CaO-Cr2O3, for different major element substitution types (Chapter 6).

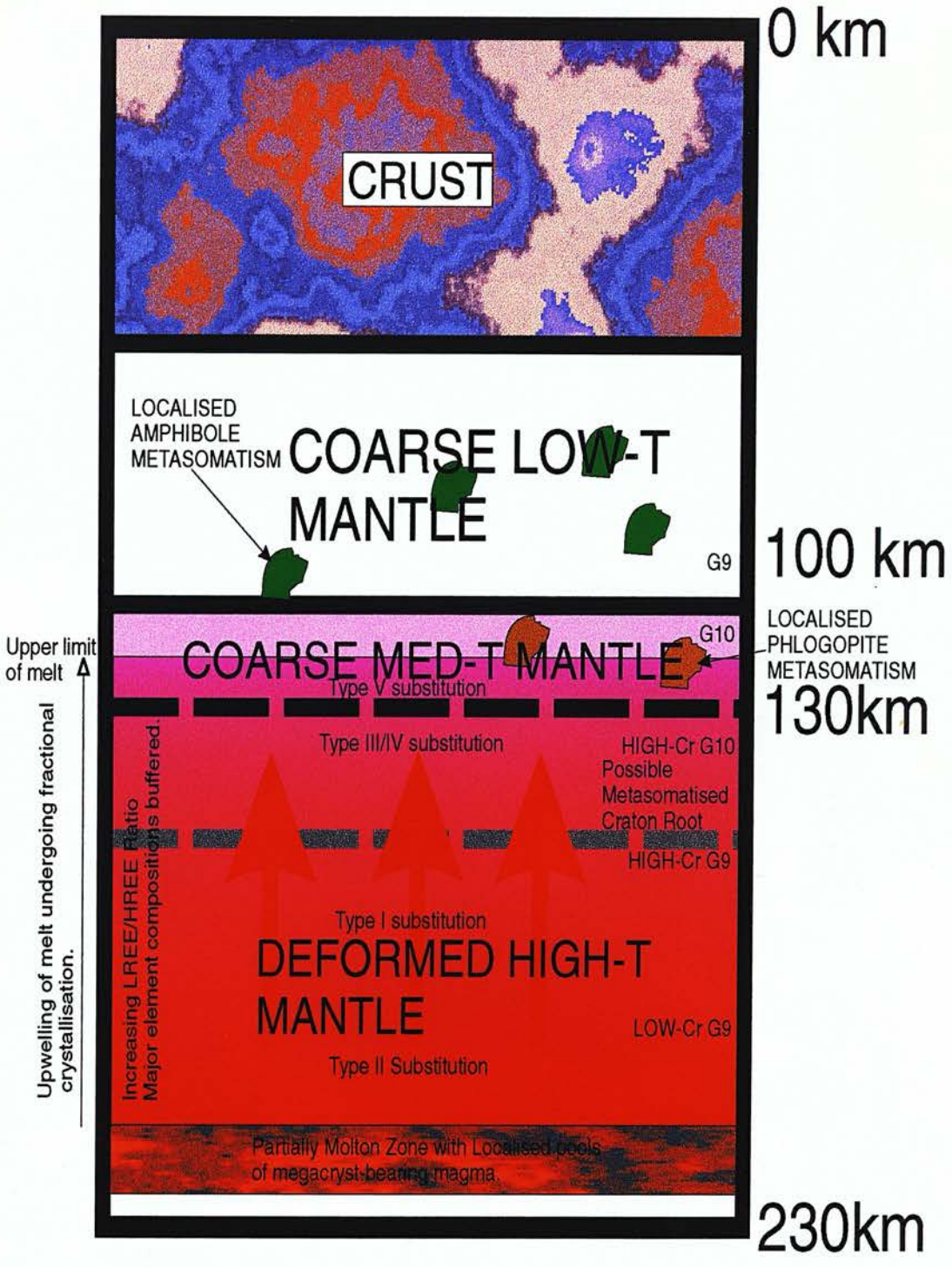

Fig. 9.2 Model of mantle under Jagersfontein at 90Ma.

Appendix A

Sample Methodology and Description

Sample	Suite	E-probe	Profile	Map	Trace El	Laser	Ion O	TEM
J10	Coarse	XXX						
J11	Coarse	XXX				XXX		
J12	Coarse	XXX				XXX		
J18	Deformed	XXX						
J22	Deformed	XXX	XXX	XXX	XXX	XXX		
J24	Coarse	X			XXX			
J25	Coarse	X			XXX			
J26	Deformed	XXX				XXX		
J28	Coarse	XXX				XXX		
J31	Deformed	XXX	XXX	XXX		XXX		
J33	Deformed	XXX	XXX					
J34	Deformed	XXX	XXX		XXX	XXX		
J36	Deformed	XXX				XXX		
J37	Deformed	XXX	XXX	XXX		XXX		
J38	Deformed	XXX	XXX			XXX		
J42	Deformed	XXX						
J47	Deformed	X			XXX			
J51	Deformed	X			XXX			
J52	Coarse	XXX						
J53	Coarse	XXX				XXX		
J74	Gnt Megacryst	XX			XXX			
J75	Gnt Megacryst	XX			XXX			
J104	Deformed	XXX						
J105	Deformed	X				XXX		
J107	Deformed	XXX	XXX	XXX	XXX	XXX		
J110	Deformed	XXX	XXX		XXX	XXX		
J112	Deformed	XXX	XXX	XXX	XXX	XXX		
J115	Deformed	XXX	XXX	XXX	XXX	XXX		
J119	Deformed	XXX	XXX		XXX	XXX	XXX	
J121	Deformed	XXX	XXX	XXX	XXX			
J145	Deformed	XXX	XXX	XXX	XXX	XXX		
J146	Coarse	X	XXX	XXX	XXX			
J154	Coarse	XXX				XXX		
J157	Coarse	X			XXX			
J159	Deformed	XXX			XXX	XXX		
JJG8/866?	Coarse	XXX				XXX		XXX
JJG853	Coarse	XXX				XXX		
JJG1728	Coarse	XX	XXX	XXX	XXX			
JJG1757	Coarse	X			XXX			
JJG1761	Coarse	X			XXX			
JJG1776	Deformed	XXX	XXX		XXX	XXX		
JJG1778	Coarse	XXX				XXX		
JJG1780	Coarse	XXX			XXX			
JJG1781	Coarse	X			XXX			
JJG1795	Coarse	XXX				XXX		XXX
JJG2469	Coarse	XXX	XXX		XXX	XXX		
JJH11	Deformed	X	XXX	XXX				
JJH19	Deformed	X	XXX	XXX	XXX			
JJH37	Deformed	X	XXX	XXX	XXX			

Table AA.1 Analytical techniques carried out on samples from Jagersfontein, reported in this thesis. E-probe is major element analysis by electron probe, for samples marked with X only some phases (typically garnet) were analysed. Profile is automatic WDS analysis across garnet grains. Maps are X-ray maps of garnet grains. Trace El is ion probe trace element analysis of garnet and clinopyroxene. Laser is laser fluorination oxygen isotope analysis. Ion O is ion probe oxygen isotope analysis. TEM is transmission electron microscopy of secondary alteration.

Sample	Thesis	Mineralogy	Texture
J10	Wint.	Garnet Amphibole Lherzolite	Coarse
J11	Wint.	Amphibole Dunite	Coarse
J12	Wint.	Lherzolite	Coarse
J18	Wint.	Garnet Harzburgite	Transitional
J22	Wint.	Garnet Harzburgite	Fluidal Mosaic
J24	Wint,	Garnet Amphbole Lherzolite	Coarse
J25	Wint,	Garnet Lherzolite	Coarse
J26	Wint,	Garnet Lherzolite	Porphyroclastic
J28	Wint,	Garnet Amphibole Lherzolite	Coarse
J31	Wint.	Garnet Harzburgite	Fluidal Mosaic
J33	Wint,	Garnet Lherzolite	Fluidal Mosaic
J34		Garnet Lherzolite	Mosaic
J36	Wint.	Garnet Lherzolite	Mosaic
J37	Wint,	Garnet Lherzolite	Porphyroclastic
J38	Wint.	Garnet Lherzolite	Mosaic
J42		Garnet Lherzolite	Porphyroclastic
J47	Wint.	Garnet Lherzolite	Mosaic
J51	Wint.	Garnet Lherzolite	Porphyroclastic
J52	Wint,	Amphibole Harzburgite	Coarse
J53		Garnet Lherzolite	Coarse
J74		Garnet Cr-poor megacryst	
J75		Garnet Cr-poor megacryst	
J104	Wint.	Garnet Lherzolite	Fluidal Mosaic
J105	Wint.	Garnet Lherzolite	Porphyroclastic
J107	Wint.	Garnet Harzburgite	Mosaic
J110		Garnet Lherzolite	Mosaic
J112		Garnet Lherzolite	Porphyroclastic
J115	Wint.	Garnet Lherzolite	Mosaic
J119	Wint.	Garnet Lherzolite	Mosaic
J121		Garnet Lherzolite	Mosaic
J145		Garnet Lherzolite	Fluidal Porph.
J146	Wint.	Garnet Harzburgite	Coarse
J154		Lherzolite	Coarse
J157	Wint,	Garnet Harzburgite	Coarse
J159	Wint.	Garnet Harzburgite	Mosaic
JJG8/866	Wint,	Phlogopite Amphibole Harzburgite	Coarse
JJG853	Wint,	Wherlite	Coarse
JJG1723	Wint.	Phlogopite Lherzolite	Coarse
JJG1728	Wint.	Garnet Lherzolite	Coarse
JJG1757	Wint.	Garnet Harzburgite	Coarse
JJG1761	Wint.	Garnet Harzburgite	Coarse
JJG1776	Wint,	Garnet Lherzolite	Porphyroclastic
JJG1778	Wint.	Harzburgite	Coarse
JJG1780	Wint.	Garnet Phlogopite Harzburgite	Coarse
JJG1781	Wint.	Garnet Harzburgite	Coarse
JJG1795	Wint.	Phlogpite Lherzolite	Coarse
JJG2469	Wint.	Garnet Dunite	Coarse
JJH11	Hops	Garnet Lherzolite	Mosaic
JJH19	Hops	Garnet Harzburgite	Mosaic
JJH37	Hops	Garnet Lherzolite	Mosaic

Table AA.2 Summary of petrography of the Jagersfontein samples investigated in this study. Samples whose descriptions are in the thesis of Winterburn (1987) are marked 'Wint.', and those which are described in the thesis of Hops (1989) are marked 'Hops'. Descriptions of other xenoliths are given in Appendix A. Sample nomenclature is discussed in Chapter 3, textural names follow Harte (1977) where Mosaic is mosaic porphyroclastic.

Appendix B

Electron Probe Analysis

Element	Crystal	Count times (s)		Background Offset	Standard
		Peak	Background		
Na	TAP	30	15	0.0075	Jadeite
Mg	TAP	30	15	0.0125	Periclase
Al	TAP	30	15	0.0075	Corundum
Si	TAP	30	15	0.0075	Wollastonite
K	PET	30	15	0.0100	Orthoclase
Ca	PET	30	15	0.0075	Wollastonite
Ti	PET	30	15	0.0100	Rutile
Cr	LiF	30	15	0.0100	Cr Metal
Mn	LiF	30	15	0.0100	Mn Metal
Fe	LiF	30	15	0.0100	Fe Metal
Ni	LiF	30	15	0.0100	Ni Metal

Table AB.1 Conditions for electron probe WDS analysis.
Elements are given in order of atomic number. Diffracting crystals used were thallium acid phthalate (TAP X2), pentaerythritol (PET), and lithium fluoride (LiF). Count times are given in seconds for both peak and background positions. Background positions are on the positive (low energy, long wavelength) side of the element peak, and are given in $\sin\Theta$.

	Error (Wt%)				
	Autoprofile Garnet	J26 Garnet	J26 Olivine	J26 Cpx	J26 Opx
Current (nA)	80	19.3	19.3	19.3	19.3
SiO_2	41.63±0.05	41.90±0.09	40.35±0.09	54.71±0.09	57.23±0.10
TiO_2	0.59±0.01	0.32±0.01	0.02±0.01	0.09±0.01	0.07±0.01
Al_2O_3	19.21±0.03	20.25±0.06	0.04±0.01	1.69±0.02	0.90±0.02
Cr_2O_3	5.28±0.03	2.86±0.05	0.05±0.02	0.74±0.03	0.24±0.02
FeO	6.87±0.03	6.68±0.06	8.18±0.07	3.21±0.04	4.93±0.05
MnO	0.3±0.01	0.28±0.02	0.12±0.02	0.12±0.02	0.12±0.01
MgO	21.02±0.03	21.73±0.07	50.29±0.10	19.51±0.06	34.56±0.08
CaO	5.02±0.02	4.88±0.03	0.07±0.01	17.71±0.06	1.18±0.02
NiO		0.03±0.01	0.42±0.02	0.08±0.02	0.14±0.02
Na_2O	0.08±0.01	0.04±0.01	0.03±0.01	1.23±0.03	0.20±0.01
K_2O				0.02±0.01	

Table AB.2 Theoretical precision for electron probe WDS analysis.
Errors given are for an average 20 automatic profiles across garnet grains (80nA), and for garnet, olivine, clinopyroxene and orthopyroxene analysis in normal mode (20nA). These errors are 1σ, in weight percent of the oxide, calculated from individual sample analysis (see text).

	Element Detection Limit (ppm)				
	Autoprofile Garnet	J26 Garnet	J26 Olivine	J26 Cpx	J26 Opx
Current (nA)	79.5	19.3	19.3	19.3	19.3
Si	44	92	85	86	97
Ti	60	111	111	101	108
Al	39	79	59	59	63
Cr	96	205	171	188	174
Fe	98	209	198	195	205
Mn	96	188	183	187	176
Mg	41	88	99	76	91
Ca	59	115	107	119	114
Ni		230	220	221	220
Na	66	136	140	137	131
K		123	116	114	118

Table AB.3 Detection limits for electron probe WDS analysis.
Detection limits are given for a typical garnet analysis in autoprofile mode (80nA), and for garnet, olivine, clinopyroxene, and orthopyroxene analysis in normal mode (20nA).
Detection limits are in ppm for the element, calculated from individual sample and standard analysis (see text).

Table B.1a Olivine-Wt% Oxide Totals
Coarse Xenoliths

	SiO_2	TiO_2	Al_2O_3	Cr_2O_3	FeO	MnO	MgO	CaO	NiO	Na_2O	K_2O	Total	100*Mg/(Mg+Fe)	
J10	40.65				7.35	0.10	51.51	0.02	0.38	0.02		100.02	92.58	
J11	40.43	0.02	0.02		8.32	0.14	50.51		0.28			99.72	91.54	
J12	40.20				8.10	0.08	50.63		0.43			99.43	91.76	
J24	41.30				8.20		51.40		0.44			101.34	91.78	W
J25	41.14				8.12		49.42		0.47			99.15	91.56	W
J28	40.35	0.02	0.02	0.04	8.52	0.11	50.41		0.38			99.83	91.34	
J52	40.73	0.02		0.03	6.90	0.08	52.07		0.39			100.21	93.08	
J53	40.75	0.02			7.30	0.08	51.29	0.02	0.42	0.03		99.91	92.60	
J146	40.43	0.10		0.16	8.56	0.24	50.13					99.62	91.26	W
J154	40.48	0.02	0.02	0.05	6.29	0.10	51.90	0.02	0.37	0.02		99.26	93.63	
J157	41.10		0.03		6.13	0.10	51.87					99.23	93.78	W
JJG8	40.18				8.96	0.12	50.06		0.38			99.70	90.87	
JJG853	40.15	0.04			9.52	0.12	49.25	0.04	0.29	0.02		99.44	90.21	
JJG1723	40.72	0.02		0.05	6.79	0.11	51.76	0.02	0.42			99.88	93.15	
JJG1728	40.79				6.55	0.08	51.86		0.43	0.02		99.73	93.39	
JJG1757	41.23		0.03		6.60	0.09	51.13					99.08	93.25	W
JJG1761	40.67			0.04	5.55	0.04	52.31					98.61	94.38	W
JJG1778	40.66		0.02		6.85	0.09	51.52	0.03	0.43	0.02		99.61	93.06	
JJG1780	40.82		0.02	0.03	6.61	0.09	51.09		0.38	0.02		99.06	93.23	
JJG1781	40.83				6.82	0.04	50.80					98.49	92.99	W
JJG1795	40.46	0.03		0.03	6.75	0.10	51.78	0.02	0.39	0.03		99.59	93.18	
JJG2469	40.62		0.02	0.06	5.76	0.09	52.46	0.03	0.34			99.37	94.19	

Table B.1a Olivine-Wt% Oxide Totals
Deformed Xenoliths

	SiO_2	TiO_2	Al_2O_3	Cr_2O_3	FeO	MnO	MgO	CaO	NiO	Na_2O	K_2O	Total	100*Mg/(Mg+Fe)	
J18 P	39.95	N.D.	0.03	0.05	6.62	0.09	52.06	0.03	0.42	0.02		99.26	93.34	
J18 N	41.15				10.50		49.74		0.43			101.82	89.41	W
J22 N	40.50	0.05	0.05	0.04	7.49	0.13	51.45	0.06	0.40	0.02		100.18	92.45	
J26 P	40.35	0.02	0.04	0.05	8.18	0.12	50.29	0.07	0.42	0.03		99.58	91.63	
J26 N	40.48	0.03	0.04	0.05	8.25	0.13	50.35	0.09	0.42	0.03		99.86	91.58	
J31 N	40.09	0.03	0.03	0.07	7.90	0.11	50.69	0.06	0.39	0.04		99.42	91.95	
J33N	40.29	0.05	0.05	0.04	9.74	0.11	49.42	0.09	0.41	0.04		100.24	90.04	
J34P	40.18	0.02	0.04	0.05	9.14	0.14	49.94	0.08	0.40	0.02		99.99	90.69	
J34 N	40.18	0.02	0.06	0.04	9.16	0.13	49.88	0.09	0.39	0.03		99.98	90.66	
J36 N	40.27	0.04	0.04	0.05	9.33	0.12	49.51	0.08	0.40	0.03		99.86	90.44	
J37 P	39.99	0.04	0.05	0.05	9.18	0.10	49.45	0.07	0.34	0.03		99.32	90.56	V
J37 N	40.02	0.04	0.05	0.06	9.24	0.11	49.39	0.09	0.34	0.04		99.37	90.50	
J38 N	40.41	0.04	0.05	0.05	9.12	0.12	49.65	0.08	0.40	0.03		99.95	90.66	
J42 P	40.41	0.03	0.04	0.05	7.87	0.10	50.62	0.06	0.36	0.03		99.58	91.97	
J42 N	40.38	0.04	0.04	0.06	7.92	0.10	50.57	0.07	0.35	0.03		99.56	91.92	
J47 N	41.15				9.77	0.15	48.98		0.42			100.47	89.93	W
J51 N	40.82				10.74	0.11	47.64		0.48			99.79	88.77	W
J104 N	40.21	0.03	0.03	0.06	7.77	0.12	50.87	0.07	0.39	0.03		99.59	92.11	
J105 P/N	40.52				8.53	0.14	49.74	0.08				99.01	91.22	W
J107 N	40.26	0.05	0.04	0.07	7.91	0.09	50.78	0.06	0.33	0.05		99.62	91.96	
J110 N	40.17	0.05	0.04	0.04	8.36	0.12	50.19	0.07	0.38	0.03		99.44	91.45	
J112 P	40.05	0.03	0.03	0.07	8.57	0.11	49.87	0.06	0.35	0.03		99.17	91.20	
J112 N	39.99	0.02	0.03	0.06	8.89	0.13	49.44	0.08	0.35	0.04		99.03	90.83	
J115 N	40.27			0.05	9.15	0.07	49.71					99.25	90.64	W
J119 P	39.96	0.03	0.04		9.89	0.11	49.17	0.06	0.31	0.04		99.61	89.86	
J119 N	40.04	0.04	0.04		9.93	0.11	49.32	0.06	0.34	0.04		99.92	89.84	
J121 N	40.27		0.04	0.05	8.69	0.12	49.81	0.09	0.36	0.03		99.47	91.08	
J145 P	40.57		0.03	0.09	8.70	0.12	49.96	0.05	0.35	0.03		99.90	91.10	
J145 N	40.36		0.03	0.11	8.66	0.13	49.74	0.08	0.37	0.04		99.51	91.10	
J159 N	40.20		0.03	0.04	8.49	0.13	49.95	0.07	0.38			99.29	91.30	
JJG1776 N	40.18	0.04	0.03		9.97	0.11	49.23	0.07	0.33	0.02		99.99	89.80	
JJH11 P/N	41.21			0.04	8.07	0.10	50.00	0.07	0.36			99.85	91.69	H
JJH19 P/N	41.28			0.07	7.88	0.11	50.28	0.05	0.37			100.04	91.92	H
JJH37 P/N	40.02				9.16	0.12	49.27	0.05	0.36			98.98	90.55	H

Table B.1b Olivine- No. of ions in formula, to 4O
Coarse Xenoliths

	Si	Ti	Al	Cr	Fe	Mn	Mg	Ca	Ni	Na	K	Total	
J10	0.99	0.00	0.00	0.00	0.15	0.00	1.87	0.00	0.01	0.00	0.00	3.01	
J11	0.99	0.00	0.00	0.00	0.17	0.00	1.84	0.00	0.01	0.00	0.00	3.01	
J12	0.99	0.00	0.00	0.00	0.17	0.00	1.85	0.00	0.01	0.00	0.00	3.01	
J24	0.99	0.00	0.00	0.00	0.16	0.00	1.84	0.00	0.01	0.00	0.00	3.01	W
J25	1.01	0.00	0.00	0.00	0.17	0.00	1.81	0.00	0.01	0.00	0.00	2.99	W
J28	0.99	0.00	0.00	0.00	0.17	0.00	1.84	0.00	0.01	0.00	0.00	3.01	
J52	0.99	0.00	0.00	0.00	0.14	0.00	1.88	0.00	0.01	0.00	0.00	3.01	
J53	0.99	0.00	0.00	0.00	0.15	0.00	1.86	0.00	0.01	0.00	0.00	3.01	
J146	0.99	0.00	0.00	0.00	0.18	0.00	1.83	0.00	0.00	0.00	0.00	3.01	W
J154	0.99	0.00	0.00	0.00	0.13	0.00	1.89	0.00	0.01	0.00	0.00	3.01	
J157	1.00	0.00	0.00	0.00	0.12	0.00	1.88	0.00	0.00	0.00	0.00	3.00	W
JJG8	0.99	0.00	0.00	0.00	0.18	0.00	1.83	0.00	0.01	0.00	0.00	3.01	
JJG853	0.99	0.00	0.00	0.00	0.20	0.00	1.81	0.00	0.01	0.00	0.00	3.01	
JJG1723	0.99	0.00	0.00	0.00	0.14	0.00	1.87	0.00	0.01	0.00	0.00	3.01	
JJG1728	0.99	0.00	0.00	0.00	0.13	0.00	1.88	0.00	0.01	0.00	0.00	3.01	
JJG1757	1.00	0.00	0.00	0.00	0.13	0.00	1.86	0.00	0.00	0.00	0.00	3.00	W
JJG1761	0.99	0.00	0.00	0.00	0.11	0.00	1.90	0.00	0.00	0.00	0.00	3.01	W
JJG1778	0.99	0.00	0.00	0.00	0.14	0.00	1.87	0.00	0.01	0.00	0.00	3.01	
JJG1780	1.00	0.00	0.00	0.00	0.14	0.00	1.86	0.00	0.01	0.00	0.00	3.00	
JJG1781	1.00	0.00	0.00	0.00	0.14	0.00	1.86	0.00	0.00	0.00	0.00	3.00	W
JJG1795	0.99	0.00	0.00	0.00	0.14	0.00	1.88	0.00	0.01	0.00	0.00	3.01	
JJG2469	0.99	0.00	0.00	0.00	0.12	0.00	1.90	0.00	0.01	0.00	0.00	3.01	

Table B.1b Olivine- No. of ions in formula, to 4O
Deformed Xenoliths

	Si	Ti	Al	Cr	Fe	Mn	Mg	Ca	Ni	Na	K	Total	
J18 P	0.98	0.00	0.00	0.00	0.14	0.00	1.90	0.00	0.01	0.00	0.00	3.02	
J18 N	0.99	0.00	0.00	0.00	0.21	0.00	1.79	0.00	0.01	0.00	0.00	3.01	W
J22 N	0.98	0.00	0.00	0.00	0.15	0.00	1.86	0.00	0.01	0.00	0.00	3.01	
J26 P	0.99	0.00	0.00	0.00	0.17	0.00	1.84	0.00	0.01	0.00	0.00	3.01	
J26 N	0.99	0.00	0.00	0.00	0.17	0.00	1.83	0.00	0.01	0.00	0.00	3.01	
J31 N	0.98	0.00	0.00	0.00	0.16	0.00	1.85	0.00	0.01	0.00	0.00	3.02	
J33N	0.99	0.00	0.00	0.00	0.20	0.00	1.81	0.00	0.01	0.00	0.00	3.01	
J34P	0.99	0.00	0.00	0.00	0.19	0.00	1.83	0.00	0.01	0.00	0.00	3.01	
J34 N	0.99	0.00	0.00	0.00	0.19	0.00	1.82	0.00	0.01	0.00	0.00	3.01	
J36 N	0.99	0.00	0.00	0.00	0.19	0.00	1.81	0.00	0.01	0.00	0.00	3.01	
J37 P	0.99	0.00	0.00	0.00	0.19	0.00	1.82	0.00	0.01	0.00	0.00	3.01	V
J37 N	0.99	0.00	0.00	0.00	0.19	0.00	1.82	0.00	0.01	0.00	0.00	3.01	
J38 N	0.99	0.00	0.00	0.00	0.19	0.00	1.81	0.00	0.01	0.00	0.00	3.01	
J42 P	0.99	0.00	0.00	0.00	0.16	0.00	1.85	0.00	0.01	0.00	0.00	3.01	
J42 N	0.99	0.00	0.00	0.00	0.16	0.00	1.85	0.00	0.01	0.00	0.00	3.01	
J47 N	1.00	0.00	0.00	0.00	0.20	0.00	1.78	0.00	0.01	0.00	0.00	3.00	W
J51 N	1.01	0.00	0.00	0.00	0.22	0.00	1.75	0.00	0.01	0.00	0.00	2.99	W
J104 N	0.98	0.00	0.00	0.00	0.16	0.00	1.86	0.00	0.01	0.00	0.00	3.02	
J105 P/N	1.00	0.00	0.00	0.00	0.18	0.00	1.82	0.00	0.00	0.00	0.00	3.00	W
J107 N	0.98	0.00	0.00	0.00	0.16	0.00	1.85	0.00	0.01	0.00	0.00	3.01	
J110 N	0.99	0.00	0.00	0.00	0.17	0.00	1.84	0.00	0.01	0.00	0.00	3.01	
J112 P	0.99	0.00	0.00	0.00	0.18	0.00	1.83	0.00	0.01	0.00	0.00	3.01	
J112 N	0.99	0.00	0.00	0.00	0.18	0.00	1.82	0.00	0.01	0.00	0.00	3.01	
J115N	0.99	0.00	0.00	0.00	0.19	0.00	1.83	0.00	0.00	0.00	0.00	3.01	W
J119 P	0.99	0.00	0.00	0.00	0.20	0.00	1.81	0.00	0.01	0.00	0.00	3.01	
J119 N	0.99	0.00	0.00	0.00	0.20	0.00	1.81	0.00	0.01	0.00	0.00	3.01	
J121 N	0.99	0.00	0.00	0.00	0.18	0.00	1.83	0.00	0.01	0.00	0.00	3.01	
J145 P	0.99	0.00	0.00	0.00	0.18	0.00	1.82	0.00	0.01	0.00	0.00	3.01	
J145 N	0.99	0.00	0.00	0.00	0.18	0.00	1.82	0.00	0.01	0.00	0.00	3.01	
J159 N	0.99	0.00	0.00	0.00	0.17	0.00	1.83	0.00	0.01	0.00	0.00	3.01	
JJG1776 N	0.99	0.00	0.00	0.00	0.20	0.00	1.80	0.00	0.01	0.00	0.00	3.01	
JJH11 P/N	1.00	0.00	0.00	0.00	0.16	0.00	1.82	0.00	0.01	0.00	0.00	3.00	H
JJH19 P/N	1.00	0.00	0.00	0.00	0.16	0.00	1.82	0.00	0.01	0.00	0.00	3.00	H
JJH37 P/N	0.99	0.00	0.00	0.00	0.19	0.00	1.82	0.00	0.01	0.00	0.00	3.01	H

Table B.2a Orthopyroxene- Wt% Oxide Totals
Coarse Xenoliths

	SiO_2	TiO_2	Al_2O_3	Cr_2O_3	FeO	MnO	MgO	CaO	NiO	Na_2O	K_2O	Total	100*Mg/(Mg+Fe)
J10	57.69		0.68	0.21	4.61	0.11	36.38	0.18	0.08	0.04		99.98	93.35
J12	57.19		0.70	0.24	5.06	0.11	35.74	0.20	0.09	0.04		99.36	92.64
J24	58.00		0.61	0.25	5.15		35.40	0.16				99.57	92.45 W
J25	57.83		0.73	0.26	5.01		34.88	0.43				99.14	92.54 W
J28	57.36	0.04	0.71	0.26	5.34	0.13	35.57	0.19	0.09	0.06		99.75	92.23
J52	57.86		0.67	0.20	4.39	0.11	36.70	0.21	0.08	0.02		100.25	93.71
J53	57.73	0.03	0.66	0.23	4.57	0.11	36.22	0.19	0.12	0.04		99.89	93.38
J146	59.55	0.10	0.66	0.51	5.09	0.14	35.41	0.90		0.15		102.51	92.54 W
J154	57.66	0.03	0.60	0.41	3.84	0.10	36.28	0.33	0.09	0.16		99.50	94.39
J157	57.89	0.03	0.70	0.36	3.77	0.09	36.23	0.28		0.13		99.48	94.48 W
JJG 8	55.77	0.04	0.64	0.21	5.96	0.15	37.01	0.18	0.12	0.05		100.13	91.71
JJG1723	58.02	0.03	0.52	0.37	4.13	0.11	36.30	0.35	0.12	0.15		100.10	93.99
JJG1728	57.44	0.02	0.85	0.45	3.98	0.11	36.11	0.32	0.12	0.19		99.58	94.18
JJG1757	57.14		1.60	0.55	4.27	0.08	35.05	0.43		0.11		99.23	93.60 W
JJG1761	57.54		0.78	0.56	3.43	0.05	36.15	0.27		0.16		98.94	94.94 W
JJG1778	56.11		2.61	0.98	4.47	0.11	34.85	0.66	0.09	0.04		99.92	93.29
JJG1780	57.69	0.02	0.80	0.40	4.04	0.09	35.60	0.32	0.10	0.16		99.22	94.01
JJG1781	56.95	0.09	0.72	0.59	4.19	0.09	35.22	0.64		0.21		98.70	93.74 W
JJG 1795	57.46	0.07	0.77	0.44	4.12	0.13	36.06	0.34	0.11	0.16	0.02	99.68	93.98

Table B.2a Orthopyroxene- Wt% Oxide Totals
Deformed Xenoliths

	SiO_2	TiO_2	Al_2O_3	Cr_2O_3	FeO	MnO	MgO	CaO	NiO	Na_2O	K_2O	Total	100*Mg/(Mg+Fe)
J18 P	56.99	0.01	0.67	0.48	3.92	0.10	36.35	0.59	0.13	0.13		99.37	94.29
J22 P	57.11	0.22	1.02	0.48	4.51	0.11	35.04	0.98	0.14	0.36		99.98	93.26
J22 N	57.04	0.21	1.05	0.51	4.55	0.14	35.00	1.00	0.14	0.35		100.00	93.20
J26 P	57.23	0.07	0.90	0.24	4.93	0.12	34.56	1.18	0.14	0.20		99.57	92.59
J31 P	56.90	0.10	0.90	0.41	4.73	0.11	34.81	1.10	0.14	0.24		99.44	92.92
J31 N	56.85	0.11	0.92	0.43	4.81	0.11	34.54	1.14	0.13	0.25		99.30	92.75
J33 P	57.18	0.22	0.95	0.33	5.79	0.13	34.12	0.99	0.13	0.30		100.14	91.31
J33 N	57.06	0.22	0.96	0.35	5.82	0.13	33.96	1.10	0.13	0.30		100.02	91.23
J34 P	57.29	0.08	0.92	0.25	5.42	0.13	34.14	1.17	0.13	0.22		99.74	91.82
J34 N	57.35	0.09	1.01	0.27	5.48	0.11	34.19	1.23	0.12	0.22		100.08	91.75
J36 P	57.11	0.11	0.97	0.23	5.60	0.13	34.07	1.18	0.13	0.27		99.81	91.55
J36N	57.09	0.11	0.95	0.24	5.63	0.12	33.87	1.25	0.12	0.28		99.68	91.47
J37 P	57.00	0.13	0.88	0.31	5.16	0.12	34.43	1.10	0.13	0.25		99.53	92.24
J38 P	57.08	0.13	1.09	0.22	5.50	0.13	33.92	1.19	0.13	0.29		99.68	91.67
J38 N	57.18	0.16	1.13	0.21	5.51	0.13	33.92	1.31	0.12	0.31		99.98	91.64
J42 P	57.10	0.07	0.85	0.34	4.76	0.11	34.90	1.06	0.11	0.22		99.51	92.89
J42 N	56.89	0.08	0.91	0.34	4.76	0.10	34.72	1.12	0.12	0.22		99.27	92.86
J47 P/N	58.34	0.16	0.84	0.15	5.99	0.11	34.32	0.91				100.82	91.08 W
J51 P/N	57.88	0.13	0.85		6.63	0.13	33.52	0.93	0.17			100.24	90.01 W
J104 P	57.06	0.07	0.88	0.43	4.78	0.13	34.77	1.09	0.14	0.22		99.57	92.83
J104 N	57.26	0.07	0.87	0.44	4.72	0.13	34.88	1.06	0.15	0.22		99.79	92.94
J105 P/N	57.63	0.04	0.77	0.31	5.05	0.14	34.92	0.83		0.16		99.85	92.49 W
J107 P	56.98	0.23	1.03	0.44	4.78	0.11	34.43	1.06	0.12	0.36		99.54	92.78
J107 N	56.94	0.25	1.09	0.45	4.81	0.12	34.39	1.10	0.12	0.36		99.65	92.72
J110 P	56.87	0.20	1.06	0.38	5.05	0.12	34.12	1.12	0.12	0.35		99.39	92.34
J110 N	56.74	0.20	1.07	0.38	5.09	0.13	34.02	1.13	0.12	0.37		99.25	92.26
J112 P	57.34	0.26	0.79	0.42	5.21	0.13	33.80	0.95	0.13	0.26		99.30	92.04
J112 N	56.73	0.30	1.08	0.49	6.03	0.13	32.99	1.15	0.14	0.28		99.32	90.70
J115 N	56.81	0.10	0.96	0.23	5.81	0.09	34.22	1.18		0.25		99.65	91.30 W
J119 P	57.04	0.18	0.89	0.17	6.00	0.12	34.34	0.87	0.10	0.25		99.96	91.07
J119 N	57.08	0.17	0.88	0.16	6.01	0.11	34.44	0.84	0.10	0.22		100.00	91.08
J121 P	57.16	0.05	0.89	0.27	5.23	0.11	34.14	1.17	0.13	0.20		99.34	92.09
J121 N	57.20	0.04	0.91	0.28	5.21	0.13	34.13	1.23	0.11	0.20		99.44	92.10

Table B.2a Orthopyroxene- Wt% Oxide Totals
Deformed Xenoliths Continued

	SiO_2	TiO_2	Al_2O_3	Cr_2O_3	FeO	MnO	MgO	CaO	NiO	Na_2O	K_2O	Total	100*Mg/(Mg+Fe)
J145 P	57.34		0.80	0.59	5.26	0.13	34.71	0.90	0.11	0.24		100.07	92.17
J145 N	57.17		0.71	0.61	5.21	0.14	34.53	0.87	0.13	0.24		99.60	92.20
J159 P	57.41	0.02	0.63	0.38	5.10	0.12	35.06	0.96	0.12	0.05		99.86	92.45
J159 N	57.13	0.02	0.74	0.44	5.11	0.14	34.84	1.00	0.12	0.05		99.59	92.40
JJG1776 P	57.19	0.16	0.91	0.19	5.97	0.12	34.27	0.91	0.11	0.24		100.08	91.09
JJG1776 N	57.12	0.16	0.94	0.18	5.98	0.11	34.32	0.91	0.12	0.24		100.06	91.10
JJH11 P/N	57.73	0.13	0.95	0.36	4.84	0.12	34.96	1.02		0.26		100.37	92.79 H
JJH19 P	57.38	0.18	1.00	0.40	4.68	0.11	34.45	1.00		0.31		99.51	92.92 H
JJH19 N	56.90	0.19	1.07	0.45	4.83	0.10	34.23	1.17		0.37		99.31	92.66 H
JJH37 P	57.23	0.23	1.06	0.28	5.54	0.10	33.93	0.99		0.30		99.66	91.61 H
JJH37 N	56.98	0.30	1.19	0.29	5.53	0.12	33.42	1.06		0.31		99.20	91.50 H

Table B.2b Orthopyroxene- No of ions in formula, to 6O
Coarse Xenoliths

	Si	Ti	Al	Cr	Fe	Mn	Mg	Ca	Ni	Na	K	Total
J10	1.97	0.00	0.03	0.01	0.13	0.00	1.86	0.01	0.00	0.00	0.00	4.01
J12	1.97	0.00	0.03	0.01	0.15	0.00	1.84	0.01	0.00	0.00	0.00	4.01
J24	1.99	0.00	0.02	0.01	0.15	0.00	1.81	0.01	0.00	0.00	0.00	3.99 W
J25	2.00	0.00	0.03	0.01	0.14	0.00	1.79	0.02	0.00	0.00	0.00	3.99 W
J28	1.97	0.00	0.03	0.01	0.15	0.00	1.83	0.01	0.00	0.00	0.00	4.01
J52	1.97	0.00	0.03	0.01	0.13	0.00	1.87	0.01	0.00	0.00	0.00	4.01
J53	1.98	0.00	0.03	0.01	0.13	0.00	1.85	0.01	0.00	0.00	0.00	4.01
J146	1.99	0.00	0.03	0.01	0.14	0.00	1.77	0.03	0.00	0.01	0.00	3.99 W
J154	1.98	0.00	0.02	0.01	0.11	0.00	1.86	0.01	0.00	0.01	0.00	4.01
J157	1.98	0.00	0.03	0.01	0.11	0.00	1.85	0.01	0.00	0.01	0.00	4.00 W
JJG 8	1.93	0.00	0.03	0.01	0.17	0.00	1.91	0.01	0.00	0.00	0.00	4.06
JJG1723	1.98	0.00	0.02	0.01	0.12	0.00	1.85	0.01	0.00	0.01	0.00	4.01
JJG1728	1.97	0.00	0.03	0.01	0.11	0.00	1.85	0.01	0.00	0.01	0.00	4.01
JJG1757	1.97	0.00	0.06	0.01	0.12	0.00	1.80	0.02	0.00	0.01	0.00	4.00 W
JJG1761	1.98	0.00	0.03	0.02	0.10	0.00	1.85	0.01	0.00	0.01	0.00	4.00 W
JJG1778	1.93	0.00	0.11	0.03	0.13	0.00	1.79	0.02	0.00	0.00	0.00	4.01
JJG1780	1.98	0.00	0.03	0.01	0.12	0.00	1.83	0.01	0.00	0.01	0.00	4.00
JJG1781	1.98	0.00	0.03	0.02	0.12	0.00	1.82	0.02	0.00	0.01	0.00	4.01 W
JJG 1795	1.97	0.00	0.03	0.01	0.12	0.00	1.85	0.01	0.00	0.01	0.00	4.01

Table B.2b Orthopyroxene- No of ions in formula, to 6O
Deformed Xenoliths

	Si	Ti	Al	Cr	Fe	Mn	Mg	Ca	Ni	Na	K	Total
J18	1.96	0.00	0.03	0.01	0.11	0.00	1.87	0.02	0.00	0.01	0.00	4.02
J22 P	1.96	0.01	0.04	0.01	0.13	0.00	1.80	0.04	0.00	0.02	0.00	4.02
J22 N	1.96	0.01	0.04	0.01	0.13	0.00	1.79	0.04	0.00	0.02	0.00	4.02
J26	1.98	0.00	0.04	0.01	0.14	0.00	1.78	0.04	0.00	0.01	0.00	4.01
J31 P	1.97	0.00	0.04	0.01	0.14	0.00	1.79	0.04	0.00	0.02	0.00	4.01
J31 N	1.97	0.00	0.04	0.01	0.14	0.00	1.78	0.04	0.00	0.02	0.00	4.01
J33 P	1.97	0.01	0.04	0.01	0.17	0.00	1.75	0.04	0.00	0.02	0.00	4.01
J33 N	1.97	0.01	0.04	0.01	0.17	0.00	1.75	0.04	0.00	0.02	0.00	4.01
J34 P	1.98	0.00	0.04	0.01	0.16	0.00	1.76	0.04	0.00	0.01	0.00	4.00
J34 N	1.98	0.00	0.04	0.01	0.16	0.00	1.76	0.05	0.00	0.01	0.00	4.01
J36 P	1.97	0.00	0.04	0.01	0.16	0.00	1.76	0.04	0.00	0.02	0.00	4.01
J36N	1.98	0.00	0.04	0.01	0.16	0.00	1.75	0.05	0.00	0.02	0.00	4.01
J37 P	1.97	0.00	0.04	0.01	0.15	0.00	1.78	0.04	0.00	0.02	0.00	4.01
J38 P	1.97	0.00	0.04	0.01	0.16	0.00	1.75	0.04	0.00	0.02	0.00	4.01
J38 N	1.97	0.00	0.05	0.01	0.16	0.00	1.74	0.05	0.00	0.02	0.00	4.01
J42 P	1.97	0.00	0.03	0.01	0.14	0.00	1.80	0.04	0.00	0.01	0.00	4.01
J42 N	1.97	0.00	0.04	0.01	0.14	0.00	1.79	0.04	0.00	0.02	0.00	4.01
J47	1.99	0.00	0.03	0.00	0.17	0.00	1.75	0.03	0.00	0.00	0.00	3.99 W
J51	1.99	0.00	0.03	0.00	0.19	0.00	1.72	0.03	0.00	0.00	0.00	3.99 W
J104 P	1.97	0.00	0.04	0.01	0.14	0.00	1.79	0.04	0.00	0.01	0.00	4.01
J104 N	1.97	0.00	0.04	0.01	0.14	0.00	1.79	0.04	0.00	0.01	0.00	4.01
J105	1.98	0.00	0.03	0.01	0.15	0.00	1.79	0.03	0.00	0.01	0.00	4.00 W
J107 P	1.97	0.01	0.04	0.01	0.14	0.00	1.77	0.04	0.00	0.02	0.00	4.01
J107 N	1.97	0.01	0.04	0.01	0.14	0.00	1.77	0.04	0.00	0.02	0.00	4.01
J110 P	1.97	0.01	0.04	0.01	0.15	0.00	1.76	0.04	0.00	0.02	0.00	4.01
J110 N	1.97	0.01	0.04	0.01	0.15	0.00	1.76	0.04	0.00	0.02	0.00	4.01
J112 P	1.99	0.01	0.03	0.01	0.15	0.00	1.75	0.04	0.00	0.02	0.00	3.99
J112 N	1.98	0.01	0.04	0.01	0.18	0.00	1.71	0.04	0.00	0.02	0.00	4.00
J115 N	1.97	0.00	0.04	0.01	0.17	0.00	1.77	0.04	0.00	0.00	0.00	4.02 W
J119 P	1.97	0.00	0.04	0.00	0.17	0.00	1.77	0.03	0.00	0.02	0.00	4.01
J119 N	1.97	0.00	0.04	0.00	0.17	0.00	1.77	0.03	0.00	0.01	0.00	4.01
J121 P	1.98	0.00	0.04	0.01	0.15	0.00	1.76	0.04	0.00	0.01	0.00	4.00
J121 N	1.98	0.00	0.04	0.01	0.15	0.00	1.76	0.05	0.00	0.01	0.00	4.00

Table B.2b Orthopyroxene- No of ions in formula, to 6O
Deformed Xenoliths Continued

	Si	Ti	Al	Cr	Fe	Mn	Mg	Ca	Ni	Na	K	Total	
J145 P	1.97	0.00	0.03	0.02	0.15	0.00	1.78	0.03	0.00	0.02	0.00	4.01	
J145 N	1.98	0.00	0.03	0.02	0.15	0.00	1.78	0.03	0.00	0.02	0.00	4.01	
J159 P	1.98	0.00	0.03	0.01	0.15	0.00	1.80	0.04	0.00	0.00	0.00	4.01	
J159 N	1.97	0.00	0.03	0.01	0.15	0.00	1.79	0.04	0.00	0.00	0.00	4.01	
JJG1776 P	1.97	0.00	0.04	0.01	0.17	0.00	1.76	0.03	0.00	0.02	0.00	4.01	
JJG1776 N	1.97	0.00	0.04	0.00	0.17	0.00	1.77	0.03	0.00	0.02	0.00	4.01	
JJH11	1.98	0.00	0.04	0.01	0.14	0.00	1.78	0.04	0.00	0.02	0.00	4.01	H
JJH19 P	1.98	0.00	0.04	0.01	0.13	0.00	1.77	0.04	0.00	0.02	0.00	4.00	H
JJH19 N	1.97	0.00	0.04	0.01	0.14	0.00	1.77	0.04	0.00	0.02	0.00	4.01	H
JJH37 P	1.98	0.01	0.04	0.01	0.16	0.00	1.75	0.04	0.00	0.02	0.00	4.00	H
JJH37 N	1.98	0.01	0.05	0.01	0.16	0.00	1.73	0.04	0.00	0.02	0.00	4.00	H

Table B.3a Clinopyroxene- Wt% Oxide Totals
Coarse Xenoliths

	SiO_2	TiO_2	Al_2O_3	Cr_2O_3	FeO	MnO	MgO	CaO	NiO	Na_2O	K_2O	Total	100*Ca/(Ca+Mg)
J10	54.39	0.03	1.88	1.29	1.37	0.06	16.31	22.39	0.04	1.44		99.21	49.67
J12	53.95	0.03	2.08	1.60	1.82	0.05	15.75	21.95	0.04	1.73		99.00	50.04
J24	54.70		2.04	1.70	1.87		15.70	21.80		1.53		99.34	49.95 W
J25	54.92	0.03	2.27	1.90	1.88		15.63	21.19		1.94		99.76	49.36
J53	54.41	0.08	2.53	1.74	1.44	0.06	15.60	21.28	0.07	1.98		99.19	49.51
J154	54.54	0.09	1.83	4.72	1.91	0.08	14.80	17.93	0.06	3.30		99.27	46.54
JJG853	54.14	0.34	1.04	1.43	2.93	0.11	16.77	21.10	0.04	1.28		99.19	47.49
JJG1723	54.50	0.10	2.08	4.84	2.17	0.10	14.58	17.30	0.04	3.46	0.03	99.20	46.03
JJG1728	54.41	0.05	3.91	4.06	2.02	0.04	13.86	16.44	0.05	4.17		99.00	46.01
JJG1795	54.25	0.24	3.38	3.64	2.08	0.11	14.32	17.33	0.04	3.70		99.09	46.52

Table B.3a Clinopyroxene- Wt% Oxide Totals
Deformed Xenoliths

	SiO_2	TiO_2	Al_2O_3	Cr_2O_3	FeO	MnO	MgO	CaO	NiO	Na_2O	K_2O	Total	100*Ca/(Ca+Mg)
J26	54.71	0.09	1.69	0.74	3.21	0.12	19.51	17.71	0.08	1.23	0.02	99.11	39.47
J31	54.33	0.18	1.92	1.49	2.99	0.10	18.87	17.56	0.09	1.66	0.04	99.21	40.08
J33	54.50	0.51	2.52	1.29	3.68	0.13	18.04	16.79	0.06	1.95	0.02	99.50	40.09
J34	54.59	0.17	2.24	0.87	3.46	0.14	19.32	16.80	0.09	1.48	0.02	99.19	38.47
J36	54.87	0.19	2.27	0.74	3.65	0.12	19.14	16.47	0.10	1.60	0.05	99.19	38.21
J37	54.48	0.19	1.91	1.20	3.24	0.12	18.88	17.35	0.09	1.66	0.03	99.14	39.78
J38	54.71	0.33	2.73	0.71	3.61	0.12	18.84	16.89	0.09	1.78	0.03	99.83	39.18
J42	54.69	0.09	1.73	1.13	2.92	0.12	19.05	17.91	0.07	1.44	0.04	99.20	40.33
J47	55.10	0.30	2.59	0.80	3.69		17.57	17.22		2.02		99.29	41.34
J51	55.47	0.41	2.91	0.55	4.00		17.43	17.43		1.95		100.15	41.82 W
J104	54.70	0.13	1.70	1.51	2.94	0.10	19.55	17.05	0.07	1.41	0.04	99.18	38.54
J110	54.40	0.38	2.69	1.39	3.44	0.11	18.55	15.65	0.08	2.27	0.03	98.98	37.75
J112	54.68	0.48	2.00	1.61	3.25	0.13	17.48	17.09	0.08	1.88	0.03	98.72	41.27
J115	54.90	0.18	2.17	0.71	3.59	0.09	19.19	16.65	0.07	1.54	0.02	99.11	38.40
J119	54.64	0.37	2.63	0.80	3.73	0.11	17.70	17.25	0.07	2.11	0.03	99.43	41.19
J121	54.85	0.08	1.74	0.81	3.37	0.13	19.41	17.47	0.07	1.30	0.03	99.25	39.27
J145	54.48	0.01	1.51	2.46	3.02	0.12	17.80	17.60	0.08	1.88	0.04	98.98	41.54
JJG1776	54.42	0.37	3.11	0.77	3.82	0.10	18.03	16.76	0.06	2.03	0.03	99.51	40.06
JJH11	55.07	0.27	2.36	1.36	3.11	0.11	19.28	16.11		1.89		99.56	37.52 H
JJH37	54.80	0.51	2.95	1.12	3.61	0.11	18.12	16.00		2.10	0.04	99.36	38.82 H

Table B.3b Clinopyroxene- No. of ions in formula, to 6O
Coarse Xenoliths

	Si	Ti	Al	Cr	Fe	Mn	Mg	Ca	Ni	Na	K	Total
J10	1.98	0.00	0.08	0.04	0.04	0.00	0.89	0.87	0.00	0.10	0.00	4.01
J12	1.98	0.00	0.09	0.05	0.06	0.00	0.86	0.86	0.00	0.12	0.00	4.02
J24	1.99	0.00	0.09	0.05	0.06	0.00	0.85	0.85	0.00	0.11	0.00	3.99 W
J25	1.99	0.00	0.10	0.05	0.06	0.00	0.84	0.82	0.00	0.14	0.00	4.00
J53	1.98	0.00	0.11	0.05	0.04	0.00	0.85	0.83	0.00	0.14	0.00	4.01
J154	1.99	0.00	0.08	0.14	0.06	0.00	0.81	0.70	0.00	0.23	0.00	4.01
JJG853	1.98	0.01	0.05	0.04	0.09	0.00	0.92	0.83	0.00	0.09	0.00	4.01
JJG1723	1.99	0.00	0.09	0.14	0.07	0.00	0.79	0.68	0.00	0.25	0.00	4.01
JJG1728	1.98	0.00	0.17	0.12	0.06	0.00	0.75	0.64	0.00	0.29	0.00	4.02
JJG1795	1.98	0.01	0.15	0.11	0.06	0.00	0.78	0.68	0.00	0.26	0.00	4.02

Table B.3b Clinopyroxene- No. of ions in formula, to 6O
Deformed Xenoliths

	Si	Ti	Al	Cr	Fe	Mn	Mg	Ca	Ni	Na	K	Total	
J26	1.98	0.00	0.07	0.02	0.10	0.00	1.05	0.69	0.00	0.09	0.00	4.01	
J31	1.97	0.00	0.08	0.04	0.09	0.00	1.02	0.68	0.00	0.12	0.00	4.02	
J33	1.97	0.01	0.11	0.04	0.11	0.00	0.97	0.65	0.00	0.14	0.00	4.01	
J34	1.98	0.00	0.10	0.02	0.10	0.00	1.04	0.65	0.00	0.10	0.00	4.01	
J36	1.98	0.01	0.10	0.02	0.11	0.00	1.03	0.64	0.00	0.11	0.00	4.01	
J37	1.98	0.01	0.08	0.03	0.10	0.00	1.02	0.67	0.00	0.12	0.00	4.02	
J38	1.97	0.01	0.12	0.02	0.11	0.00	1.01	0.65	0.00	0.12	0.00	4.02	
J42	1.98	0.00	0.07	0.03	0.09	0.00	1.03	0.70	0.00	0.10	0.00	4.01	
J47	1.99	0.01	0.11	0.02	0.11	0.00	0.95	0.67	0.00	0.14	0.00	4.00	
J51	1.99	0.01	0.12	0.02	0.12	0.00	0.93	0.67	0.00	0.14	0.00	4.00	W
J104	1.98	0.00	0.07	0.04	0.09	0.00	1.05	0.66	0.00	0.10	0.00	4.01	
J110	1.97	0.01	0.11	0.04	0.10	0.00	1.00	0.61	0.00	0.16	0.00	4.02	
J112	1.99	0.01	0.09	0.05	0.10	0.00	0.95	0.67	0.00	0.13	0.00	4.00	
J115	1.99	0.00	0.09	0.02	0.11	0.00	1.04	0.65	0.00	0.11	0.00	4.01	
J119	1.98	0.01	0.11	0.02	0.11	0.00	0.96	0.67	0.00	0.15	0.00	4.02	
J121	1.99	0.00	0.07	0.02	0.10	0.00	1.05	0.68	0.00	0.09	0.00	4.01	
J145	1.99	0.00	0.06	0.07	0.09	0.00	0.97	0.69	0.00	0.13	0.00	4.01	
JJG1776	1.97	0.01	0.13	0.02	0.12	0.00	0.97	0.65	0.00	0.14	0.00	4.02	
JJH11	1.98	0.01	0.10	0.04	0.09	0.00	1.03	0.62	0.00	0.13	0.00	4.01	H
JJH37	1.98	0.01	0.13	0.03	0.11	0.00	0.97	0.62	0.00	0.15	0.00	4.00	H

Table B.4a Garnet- Wt% Oxide Totals
Coarse Xenoliths

	SiO_2	TiO_2	Al_2O_3	Cr_2O_3	FeO	MnO	MgO	CaO	NiO	Na_2O	K_2O	Total
J10	41.51		22.14	2.29	8.12	0.54	20.15	4.98		0.02		99.75 W
J24	41.31	0.02	21.85	2.36	8.93	0.47	19.76	4.75		0.02		99.48
J25	41.40	0.02	21.56	2.92	8.77	0.50	19.76	4.92				99.86
J28	41.33	0.03	21.01	2.85	8.95	0.52	19.35	5.00		0.02		99.05
J53	41.55	0.05	21.22	2.86	8.14	0.47	19.94	5.06		0.02		99.31
J146 C	40.58	0.51	14.63	11.25	7.25		18.75	7.19		0.04		100.20
J146 R	40.61	0.71	14.41	11.06	7.42		19.02	7.25		0.05		100.53
J157	41.85	0.06	20.33	5.19	6.24		22.06	4.56		0.04		100.34
JJG1728 C	42.26	0.03	19.88	5.96	6.58		22.20	3.53		0.03		100.47
JJG1728 R	42.24	0.05	20.39	5.14	6.57		21.91	4.30		0.04		100.64
JJG1757	41.94	0.02	23.00	1.92	8.21		20.72	5.17		0.02		100.99
JJG1761	41.66	0.07	18.70	7.61	5.32		22.97	3.89		0.04		100.25
JJG1780	41.58	0.09	19.54	6.29	6.64		21.51	5.11		0.05		100.81
JJG1781	40.42	0.29	14.47	12.64	6.12		20.13	6.51		0.04		100.62
JJG1795	41.09	0.16	19.79	5.09	6.55	0.39	21.09	4.78		0.06		98.99
JJG2469 C	41.64	0.11	18.40	7.96	5.51		23.42	2.51				99.55
JJG2469 R	41.98	0.10	19.45	6.65	5.41		23.76	2.34				99.68

Table B.4a Garnet- Wt% Oxide Totals
Deformed Xenoliths

	SiO_2	TiO_2	Al_2O_3	Cr_2O_3	FeO	MnO	MgO	CaO	NiO	Na_2O	K_2O	TOTAL
J18	40.33	0.03	17.07	8.14	5.82	0.32	20.61	6.01	0.04	0.02	0.02	98.41
J22 C	41.61	0.24	18.47	6.49	6.17		20.90	5.27				99.14
J22 R	41.72	1.01	18.78	5.40	6.26		21.25	4.87				99.28
J26	41.90	0.32	20.05	2.86	6.68	0.28	21.73	4.88	0.03	0.04		98.77
J31 C	41.51	0.37	18.93	5.89	6.35		20.54	5.51				99.09
J31 R	41.76	0.50	18.99	5.60	6.38		20.72	5.37				99.34
J33 C	40.48	0.51	20.07	4.49	7.39		20.85	5.10		0.09		98.99
J33 R	40.54	0.79	19.96	4.07	7.55		21.09	4.82		0.11		98.94
J34 C	41.90	0.59	19.30	4.50	7.13		21.26	5.20				99.87
J34 R	42.25	0.48	20.52	3.31	7.00		21.72	4.86				100.13
J36	41.84	0.60	20.26	2.56	7.36	0.26	21.56	4.52	0.04	0.07		99.07
J37 C	41.34	0.46	19.55	4.75	7.05	0.32	21.27	4.81		0.06		99.60
J37 R	41.52	0.70	19.70	4.25	7.10	0.31	21.41	4.83		0.07		99.88
J38 C	42.33	0.44	21.74	2.09	7.21		21.60	4.48				99.88
J38 R	42.27	0.56	21.83	2.01	7.29		21.90	4.44				100.30
J42	41.61	0.29	19.64	4.04	6.39	0.28	21.60	4.92	0.03	0.05		98.84
J47	41.76	0.60	21.32	1.90	8.20	0.31	21.14	4.31		0.09		99.63
J51	42.58	0.77	22.20	1.02	8.95		21.38	4.18		0.10		101.18
J104	41.09	0.34	18.44	5.80	6.26	0.28	21.31	5.32		0.04		98.87
J105	42.16	0.23	19.65	4.85	7.00	0.35	20.86	5.07				100.17 W
J107 C	41.57	0.45	18.93	5.82	6.31		21.23	5.51				99.82
J107 R	41.74	0.99	18.94	5.30	6.44		21.55	5.07				100.02
J110 C	41.65	0.53	18.92	5.43	6.65		19.91	5.36				98.45
J110 R	41.99	0.96	19.80	3.78	6.78		20.51	4.68				98.49
J112 C	41.32	0.57	17.74	7.49	6.91		19.57	6.08				99.69
J112 R	41.22	1.15	17.98	6.39	7.27		20.01	5.69				99.70
J115 C	41.69	0.34	21.03	2.78	7.56	0.30	21.89	4.55		0.06		100.19
J115 R	41.49	0.53	20.85	2.89	7.49	0.30	21.79	4.65		0.06		100.04
J119	41.61	0.68	21.09	1.98	8.08	0.29	21.42	4.41	0.03	0.09		99.68
J121 C	42.73	0.30	21.52	2.55	7.05		21.87	4.37		0.03		100.41
J121 R	42.68	0.41	20.54	3.58	7.16		21.48	4.49		0.04		100.36
J145 C	40.35	0.06	13.15	13.45	7.33		17.72	8.16		0.03		100.23
J145 R	40.41	0.07	13.21	13.42	7.41		18.16	7.59		0.04		100.31

Table B.4a Garnet- Wt% Oxide Totals
Deformed Xenoliths Continued

	SiO_2	TiO_2	Al_2O_3	Cr_2O_3	FeO	MnO	MgO	CaO	NiO	Na_2O	K_2O	TOTAL
J159	40.35	0.03	15.23	10.23	6.90	0.35	18.52	7.65	0.02		0.01	99.31
JJG1776 C	42.13	0.71	21.88	1.43	8.07		20.99	4.41				99.61
JJG1776 R	42.13	0.65	21.63	1.84	7.95		20.85	4.44				99.48
JJH11 C	42.01	0.34	19.68	4.99	6.53		22.06	4.87		0.06		100.53
JJH11 R	41.98	0.73	19.58	4.48	6.56		22.31	4.67		0.08		100.38
JJH19 C	41.48	0.28	18.38	6.72	6.28		21.85	4.86		0.06		99.90
JJH19 R	41.42	0.97	18.05	5.89	6.40		22.16	5.05		0.12		100.06
JJH37 C	41.26	0.15	20.55	3.96	7.13	0.29	21.39	5.16		0.06		99.95
JJH37 R	41.30	0.93	20.28	3.62	7.56	0.34	21.31	4.65		0.12		100.09
J74	41.69	1.14	21.25	0.76	10.85		20.46	4.34		0.12		100.61
J75	41.88	0.97	21.69	0.75	10.50		20.45	4.18		0.12		100.53

Table B.4b Garnet- No. of ions in formula, to 12O
Coarse Xenoliths

	Si	Ti	Al	Cr	Fe	Mn	Mg	Ca	Ni	Na	K	Total
J10	2.97	0.00	1.87	0.13	0.49	0.03	2.15	0.38	0.00	0.00	0.00	8.03 W
J24	2.98	0.00	1.86	0.13	0.54	0.03	2.12	0.37	0.00	0.00	0.00	8.03
J25	2.98	0.00	1.83	0.17	0.53	0.03	2.12	0.38	0.00	0.00	0.00	8.03
J28	3.00	0.00	1.80	0.16	0.54	0.03	2.09	0.39	0.00	0.00	0.00	8.02
J53	3.00	0.00	1.80	0.16	0.49	0.03	2.14	0.39	0.00	0.00	0.00	8.02
J146 C	2.99	0.03	1.27	0.66	0.45	0.00	2.06	0.57	0.00	0.01	0.00	8.02
J146 R	2.98	0.04	1.25	0.64	0.46	0.00	2.08	0.57	0.00	0.01	0.00	8.03
J157	2.97	0.00	1.70	0.29	0.37	0.00	2.34	0.35	0.00	0.01	0.00	8.03
JJG1728 C	3.00	0.00	1.66	0.33	0.39	0.00	2.35	0.27	0.00	0.00	0.00	8.00
JJG1728 R	2.99	0.00	1.70	0.29	0.39	0.00	2.31	0.33	0.00	0.01	0.00	8.02
JJG1757	2.96	0.00	1.91	0.11	0.48	0.00	2.18	0.39	0.00	0.00	0.00	8.03
JJG1761	2.97	0.00	1.57	0.43	0.32	0.00	2.44	0.30	0.00	0.01	0.00	8.03
JJG1780	2.96	0.01	1.64	0.35	0.40	0.00	2.28	0.39	0.00	0.01	0.00	8.04
JJG1781	2.96	0.02	1.25	0.73	0.37	0.00	2.20	0.51	0.00	0.01	0.00	8.04
JJG1795	2.97	0.01	1.69	0.29	0.40	0.02	2.27	0.37	0.00	0.01	0.00	8.03
JJG2469 C	2.98	0.01	1.55	0.45	0.33	0.00	2.50	0.19	0.00	0.00	0.00	8.01
JJG2469 R	2.98	0.01	1.63	0.37	0.32	0.00	2.52	0.18	0.00	0.00	0.00	8.01

Table B.4b Garnet- No. of ions in formula, to 12O
Deformed Xenoliths

	Si	Ti	Al	Cr	Fe	Mn	Mg	Ca	Ni	Na	K	Total
J18	2.97	0.00	1.48	0.47	0.36	0.02	2.26	0.47	0.00	0.00	0.00	8.05
J22 C	3.01	0.01	1.57	0.37	0.37	0.00	2.25	0.41	0.00	0.00	0.00	8.00
J22 R	3.00	0.05	1.59	0.31	0.38	0.00	2.28	0.38	0.00	0.00	0.00	7.99
J26	3.02	0.02	1.70	0.16	0.40	0.02	2.33	0.38	0.00	0.01	0.00	8.04
J31 C	3.00	0.02	1.61	0.34	0.38	0.00	2.22	0.43	0.00	0.00	0.00	8.00
J31 R	3.01	0.03	1.61	0.32	0.38	0.00	2.23	0.42	0.00	0.00	0.00	8.00
J33 C	2.94	0.03	1.72	0.26	0.45	0.00	2.26	0.40	0.00	0.01	0.00	8.05
J33 R	2.94	0.04	1.71	0.23	0.46	0.00	2.28	0.37	0.00	0.02	0.00	8.05
J34 C	3.00	0.03	1.63	0.26	0.43	0.00	2.27	0.40	0.00	0.00	0.00	8.02
J34 R	3.00	0.03	1.72	0.19	0.42	0.00	2.30	0.37	0.00	0.00	0.00	8.02
J36	3.01	0.03	1.72	0.15	0.44	0.02	2.31	0.35	0.00	0.01	0.00	8.03
J37 C	2.98	0.03	1.66	0.27	0.42	0.02	2.28	0.37	0.00	0.01	0.00	8.04
J37 R	2.98	0.04	1.67	0.24	0.43	0.02	2.29	0.37	0.00	0.01	0.00	8.04
J38 C	3.00	0.02	1.82	0.12	0.43	0.00	2.28	0.34	0.00	0.00	0.00	8.01
J38 R	2.99	0.03	1.82	0.11	0.43	0.00	2.31	0.34	0.00	0.00	0.00	8.02
J42	3.00	0.02	1.67	0.23	0.39	0.02	2.32	0.38	0.00	0.01	0.00	8.03
J47	2.99	0.03	1.80	0.11	0.49	0.02	2.25	0.33	0.00	0.01	0.00	8.03
J51	2.99	0.04	1.84	0.06	0.53	0.00	2.24	0.31	0.00	0.01	0.00	8.03
J104	2.99	0.02	1.58	0.33	0.38	0.02	2.31	0.41	0.00	0.00	0.00	8.04
J105	3.01	0.01	1.66	0.27	0.42	0.02	2.22	0.39	0.00	0.00	0.00	8.01 W
J107 C	2.99	0.02	1.60	0.33	0.38	0.00	2.27	0.42	0.00	0.00	0.00	8.02
J107 R	2.99	0.05	1.60	0.30	0.39	0.00	2.30	0.39	0.00	0.00	0.00	8.01
J110 C	3.03	0.03	1.62	0.31	0.40	0.00	2.16	0.42	0.00	0.00	0.00	7.97
J110 R	3.03	0.05	1.69	0.22	0.41	0.00	2.21	0.36	0.00	0.00	0.00	7.96
J112 C	3.00	0.03	1.52	0.43	0.42	0.00	2.12	0.47	0.00	0.00	0.00	7.99
J112 R	2.99	0.06	1.54	0.37	0.44	0.00	2.16	0.44	0.00	0.00	0.00	8.00
J115 C	2.97	0.02	1.77	0.16	0.45	0.02	2.32	0.35	0.00	0.01	0.00	8.06
J115 R	2.96	0.03	1.75	0.16	0.45	0.02	2.32	0.36	0.00	0.01	0.00	8.05
J119	2.98	0.04	1.78	0.11	0.48	0.02	2.29	0.34	0.00	0.01	0.00	8.05
J121 C	3.01	0.02	1.79	0.14	0.42	0.00	2.30	0.33	0.00	0.00	0.00	8.01
J121 R	3.02	0.02	1.72	0.20	0.42	0.00	2.27	0.34	0.00	0.00	0.00	8.00
J145 C	3.00	0.00	1.15	0.79	0.46	0.00	1.97	0.65	0.00	0.00	0.00	8.03
J145 R	3.00	0.00	1.16	0.79	0.46	0.00	2.01	0.60	0.00	0.01	0.00	8.03

Table B.4b Garnet- No. of ions in formula, to 12O
Deformed Xenoliths Continued

	Si	Ti	Al	Cr	Fe	Mn	Mg	Ca	Ni	Na	K	Total
J159	2.99	0.00	1.33	0.60	0.43	0.02	2.05	0.61	0.00	0.00	0.00	8.04
JJG1776 C	3.00	0.04	1.84	0.08	0.48	0.00	2.23	0.34	0.00	0.00	0.00	8.00
JJG1776 R	3.01	0.03	1.82	0.10	0.47	0.00	2.22	0.34	0.00	0.00	0.00	8.00
JJH11 C	2.99	0.02	1.65	0.28	0.39	0.00	2.34	0.37	0.00	0.01	0.00	8.04
JJH11 R	2.98	0.04	1.64	0.25	0.39	0.00	2.36	0.36	0.00	0.01	0.00	8.04
JJH19 C	2.98	0.01	1.56	0.38	0.38	0.00	2.34	0.37	0.00	0.01	0.00	8.04
JJH19 R	2.97	0.05	1.53	0.33	0.38	0.00	2.37	0.39	0.00	0.02	0.00	8.05
JJH37 C	2.96	0.01	1.74	0.22	0.43	0.02	2.29	0.40	0.00	0.01	0.00	8.06
JJH37 R	2.96	0.05	1.71	0.20	0.45	0.02	2.27	0.36	0.00	0.02	0.00	8.04
J74	2.98	0.06	1.79	0.04	0.65	0.00	2.18	0.33	0.00	0.02	0.00	8.05
J75	2.99	0.05	1.82	0.04	0.63	0.00	2.17	0.32	0.00	0.02	0.00	8.04

Appendix C

X-ray Mapping

Appendix C: Major Element Profiles and X-ray Maps Across Heterogeneous Garnet Grains

Quantitative major element profiles and X-ray maps are presented in Figs. C.1-27. The profiles and X-ray maps are organised in sample order, with the deformed samples followed by the coarse samples. For samples where both line profiles and X-ray maps have been collected, the figures are ordered so the X-ray map immediately follows the corresponding line profile. Where possible, the position of the line profiles have been marked on the X-ray maps, with an arrow pointing in the direction the profile was collected (i.e. from left to right on the line profile). For grains where more than one profile has been collected, these profiles are labelled '-1' and '-2'

Line Profiles

Line profiles are shown as a combination of seven elements (as oxides in weight %), TiO_2, Al_2O_3, Cr_2O_3, Total FeO, MgO, CaO, and Na_2O, except for some profiles where Na_2O was not analysed, so SiO_2 is shown instead. Distances for the line profiles are measured in μm.

symbols used:-

Black Diamonds:	TiO_2
Grey Triangles:	Al_2O_3
Dark Grey Circles:	Cr_2O_3
Diagonal Crosses	FeO (Total)
Open Squares	MgO
Horizontal Crosses	CaO
Open Triangles	Na_2O or SiO_2

X-ray Maps

X-ray maps for each grain consist of images of three or four elements. The elements mapped are a combination from Mg, Al, Ca, Ti, Cr and Fe. They are positioned from top left to bottom right in order of increasing atomic number, with

the exception that Ca is placed last. The variation in each image is shown by a false colour spectrum, representing a qualitative scale from purple (low concentration) through blue, green, yellow, orange, to red (high concentration). This false colour spectrum is reproduced between the images, and where possible the corresponding nominal abundance range of the oxide of the element (in weight %) in the grain is matched to the spectrum.

Fig. C.1a J22C

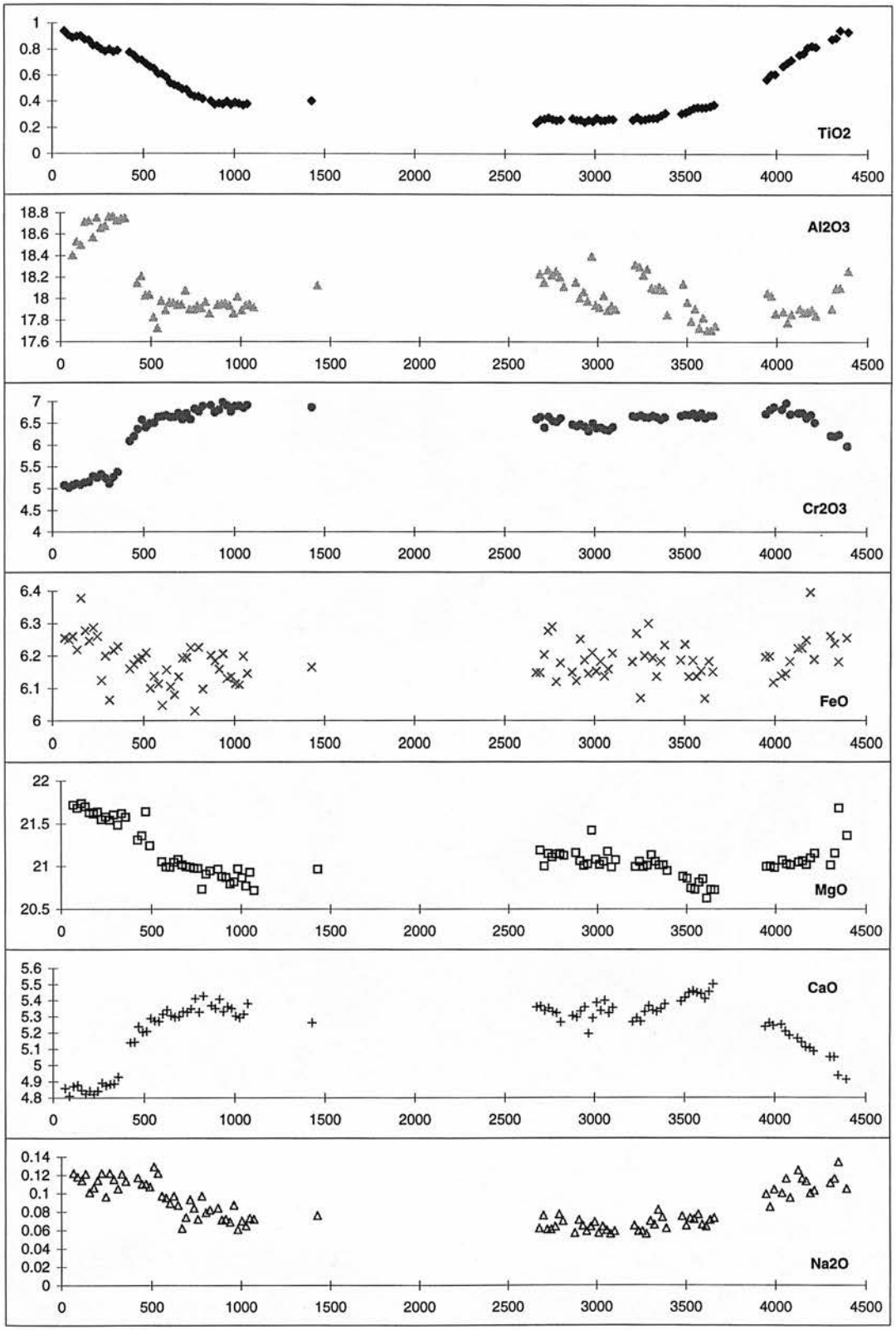
TiO2
Al2O3
Cr2O3
FeO
MgO
CaO
Na2O
0
500
1000
1500
2000
2500
3000
3500
4000
4500

Fig. C.1b
J22C

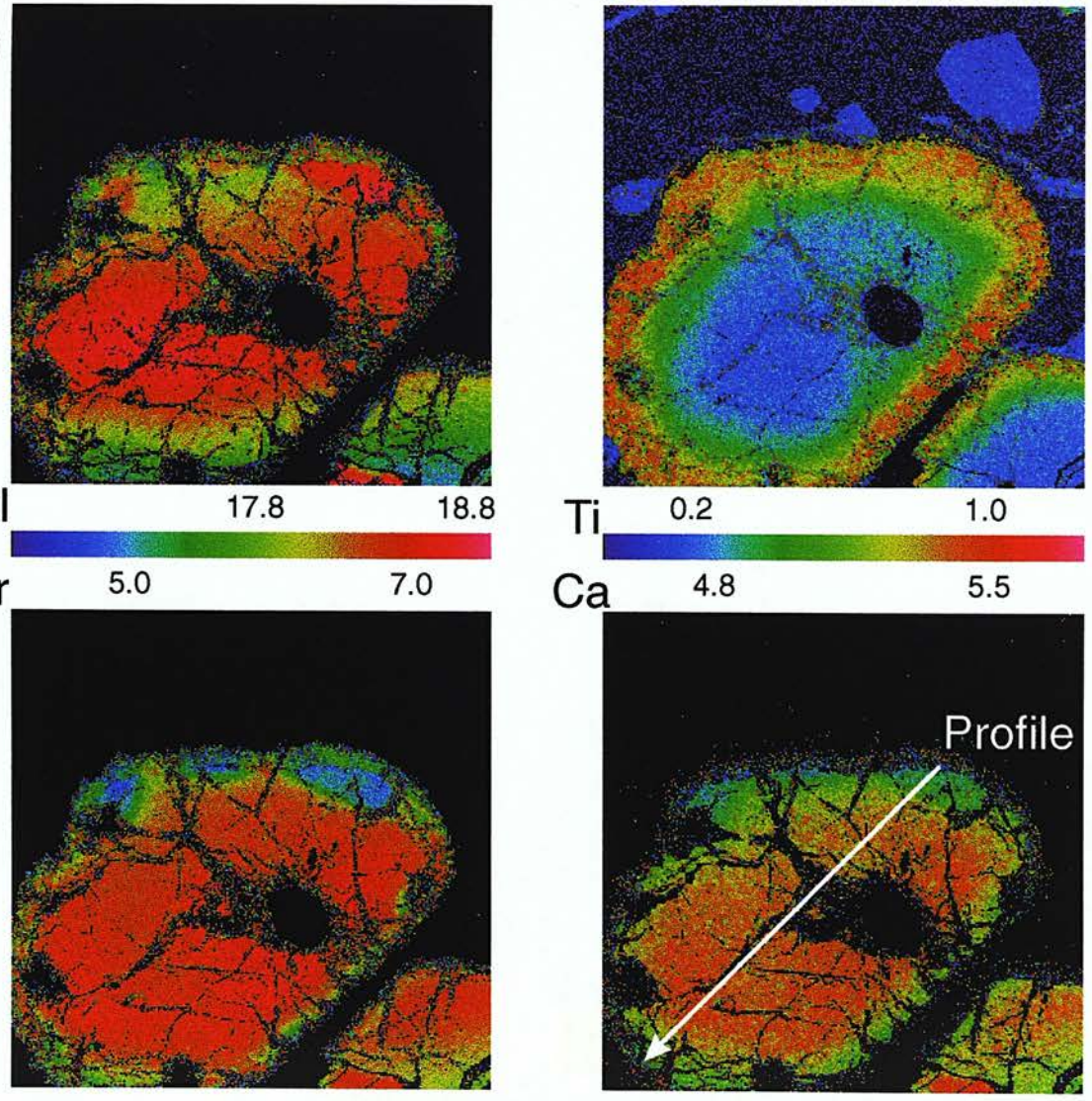

Fig. C.1c
J22F/1

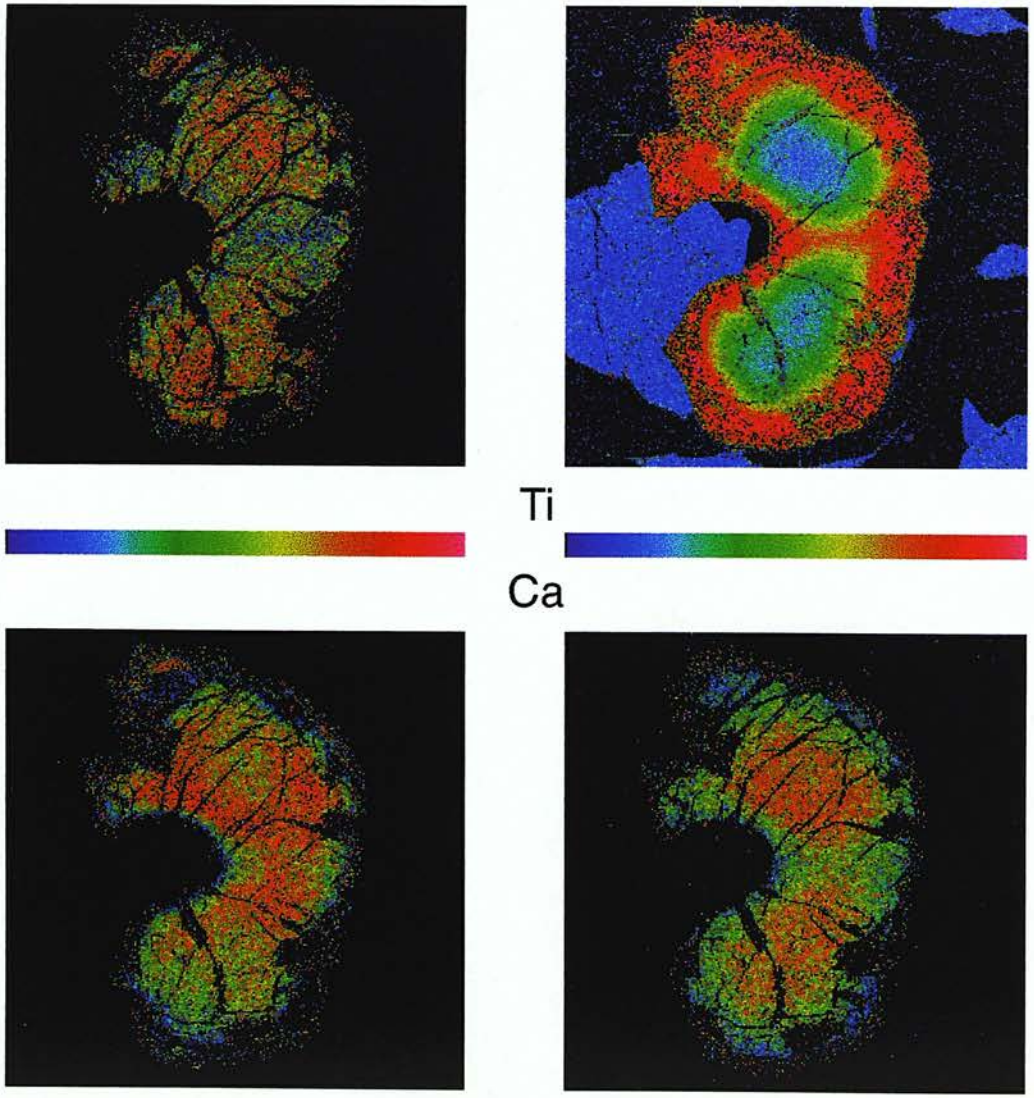

Fig. C.1d J22F/2

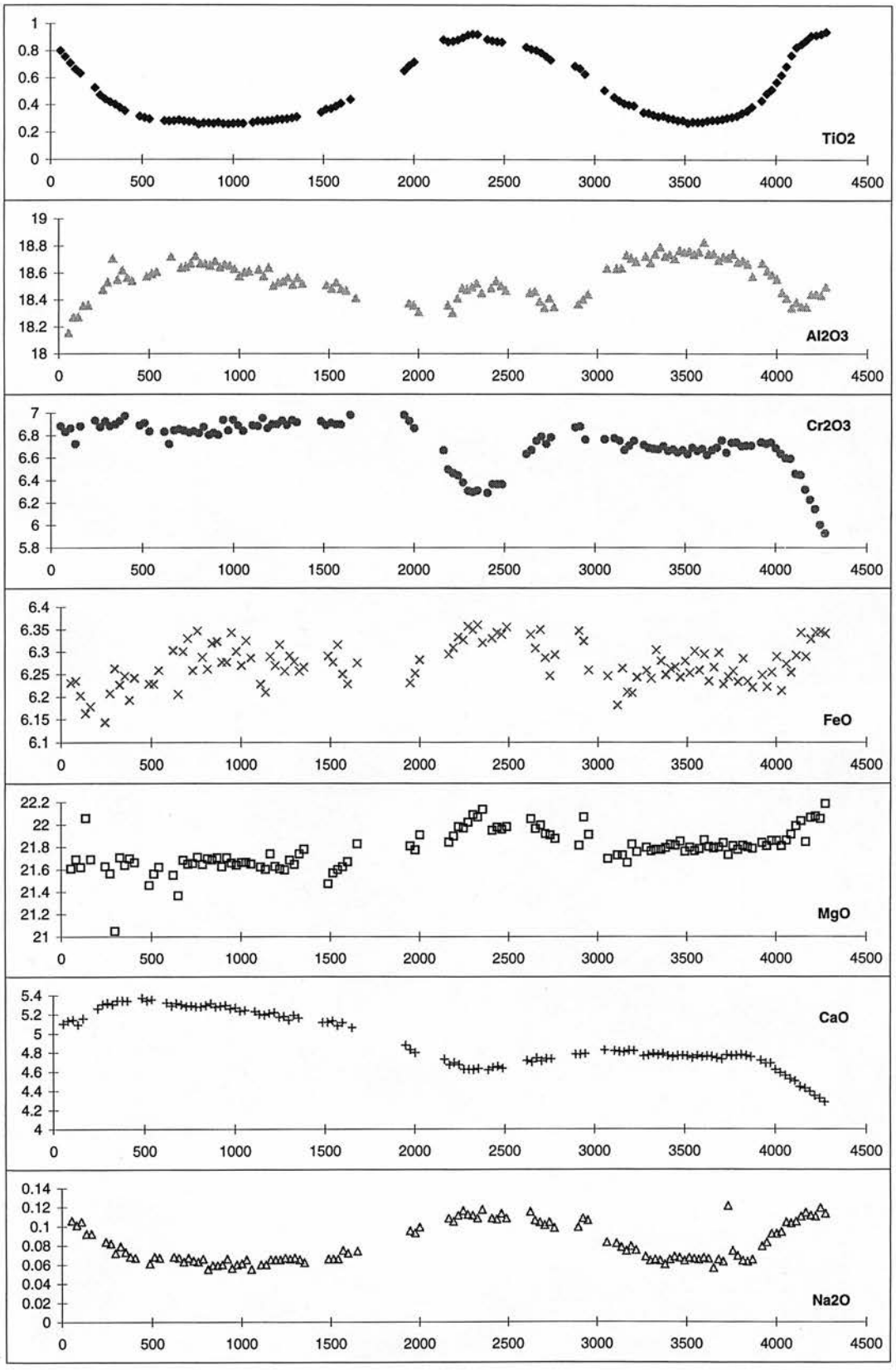

H:\jag12r3.xls

Fig. C.1e
J22F/2

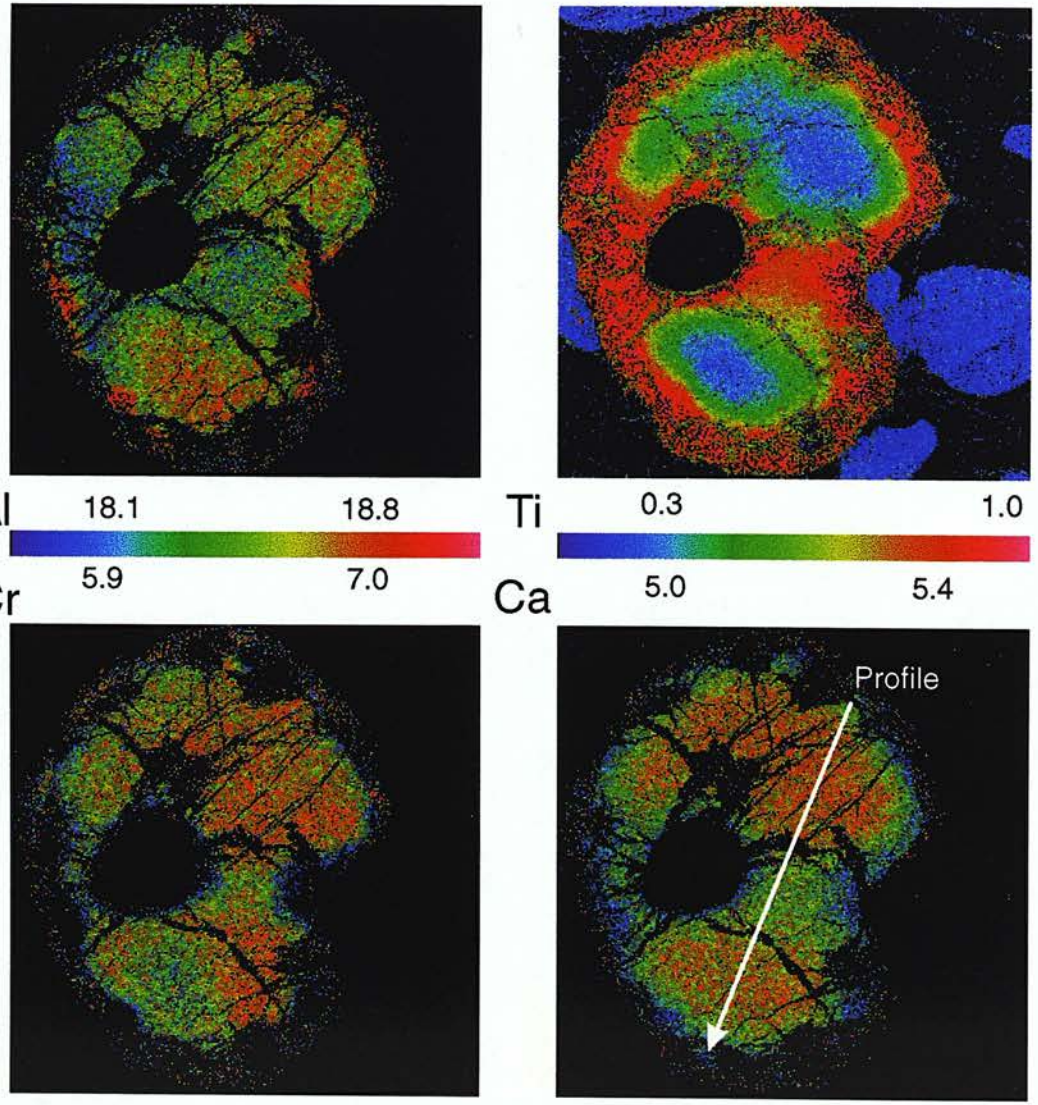

Fig. C.1f
J22F/3

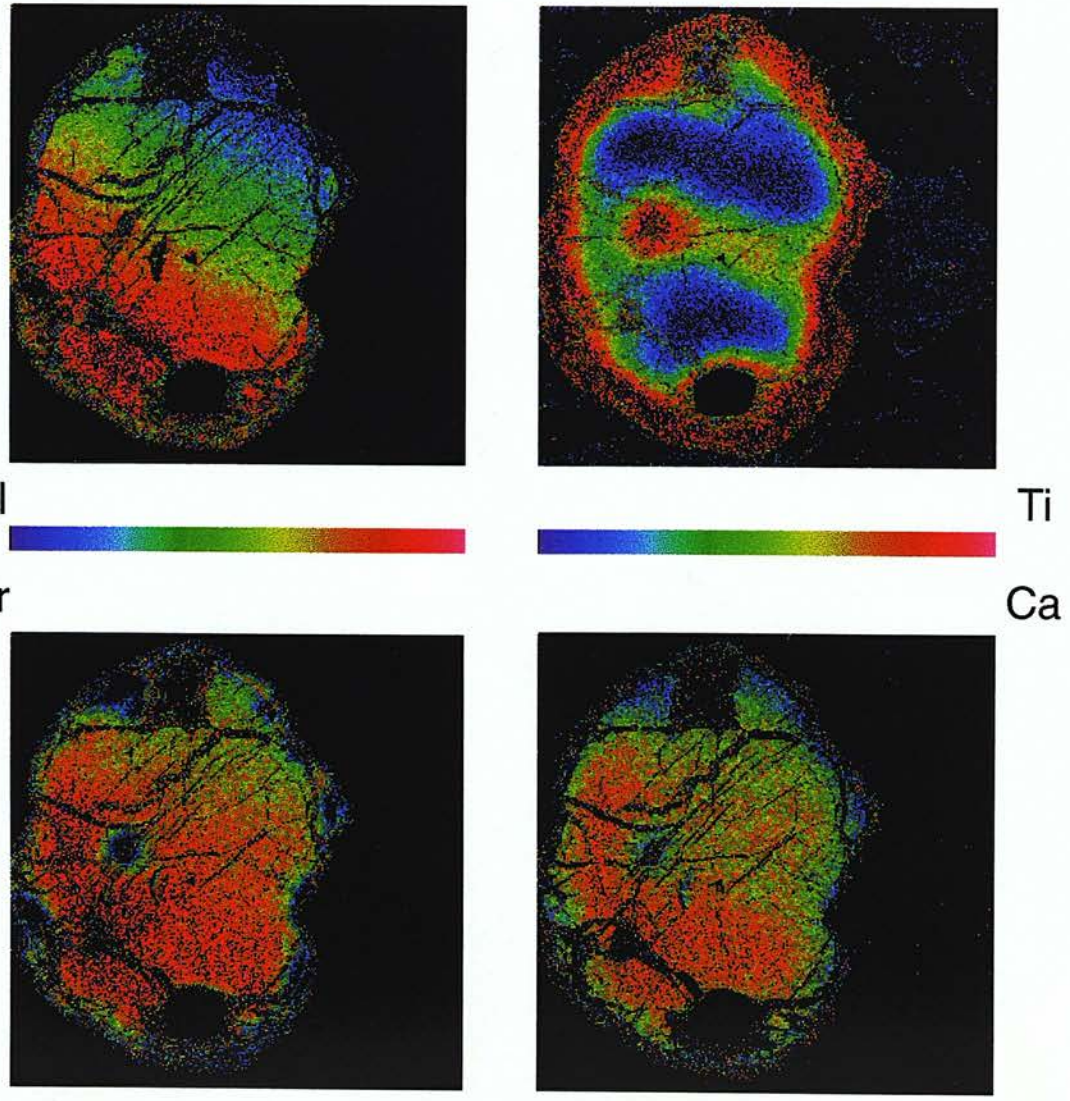

Fig. C.1g J22F/4

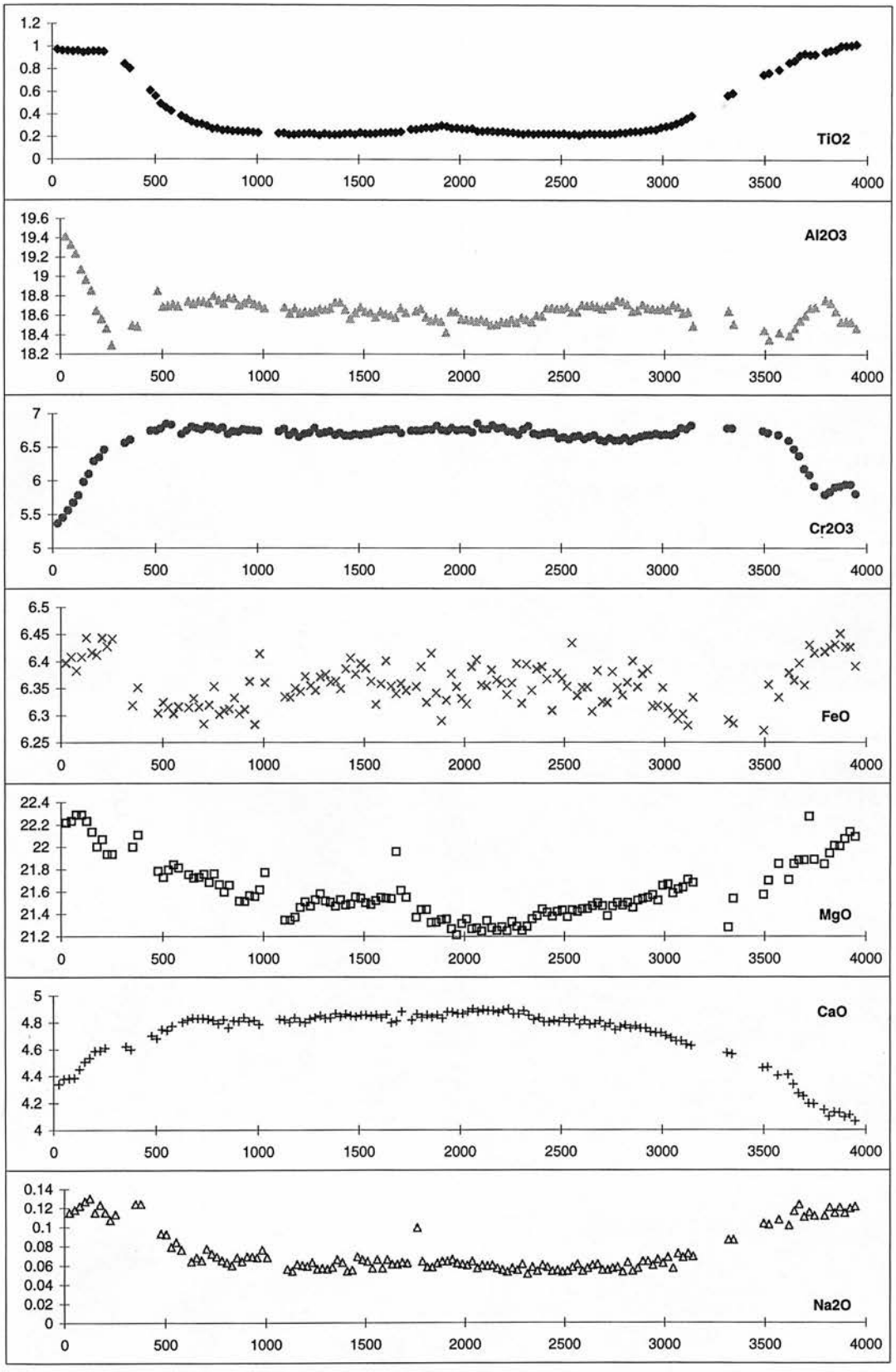

H:\Jag12r4.xls

Fig. C.1h
J22F/4

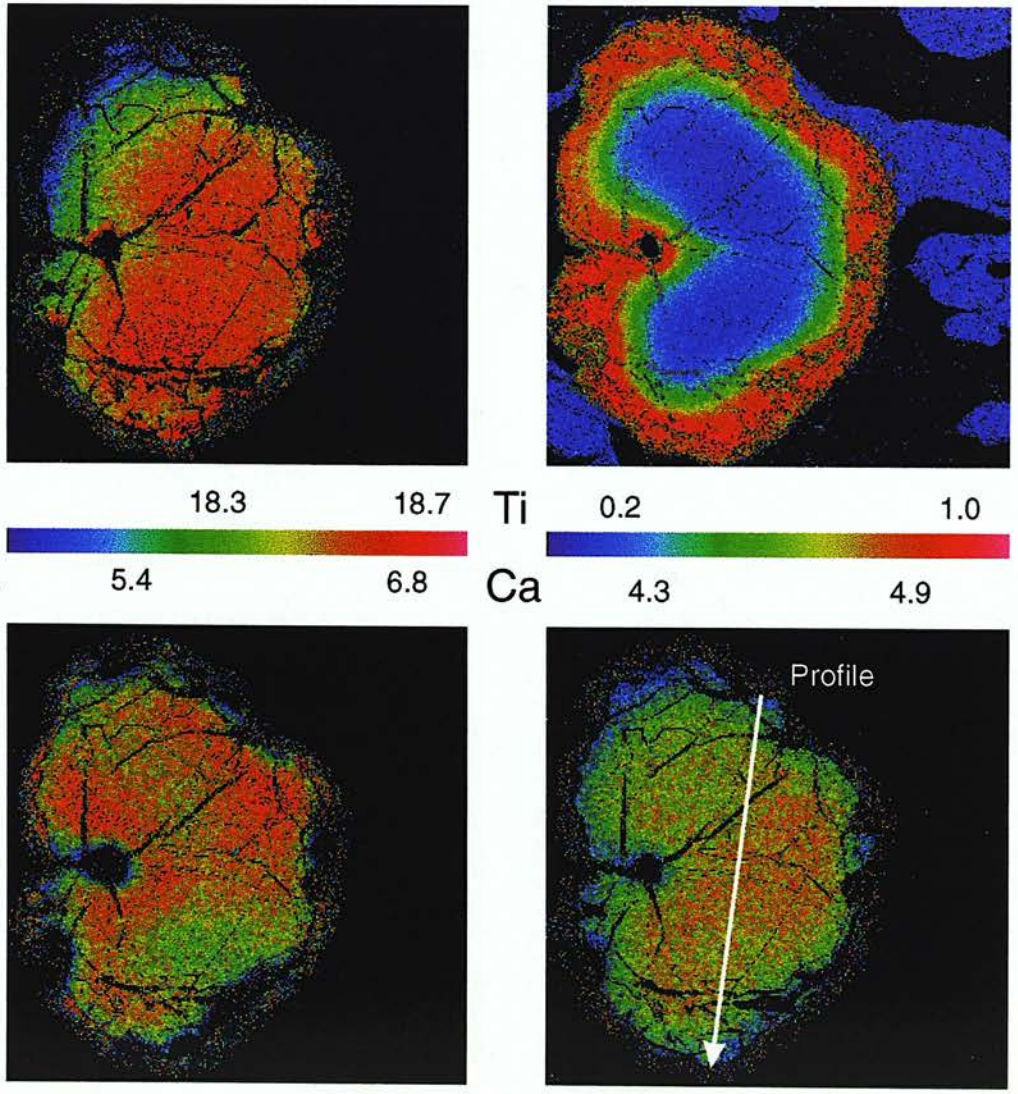

Fig. C.1i
J22

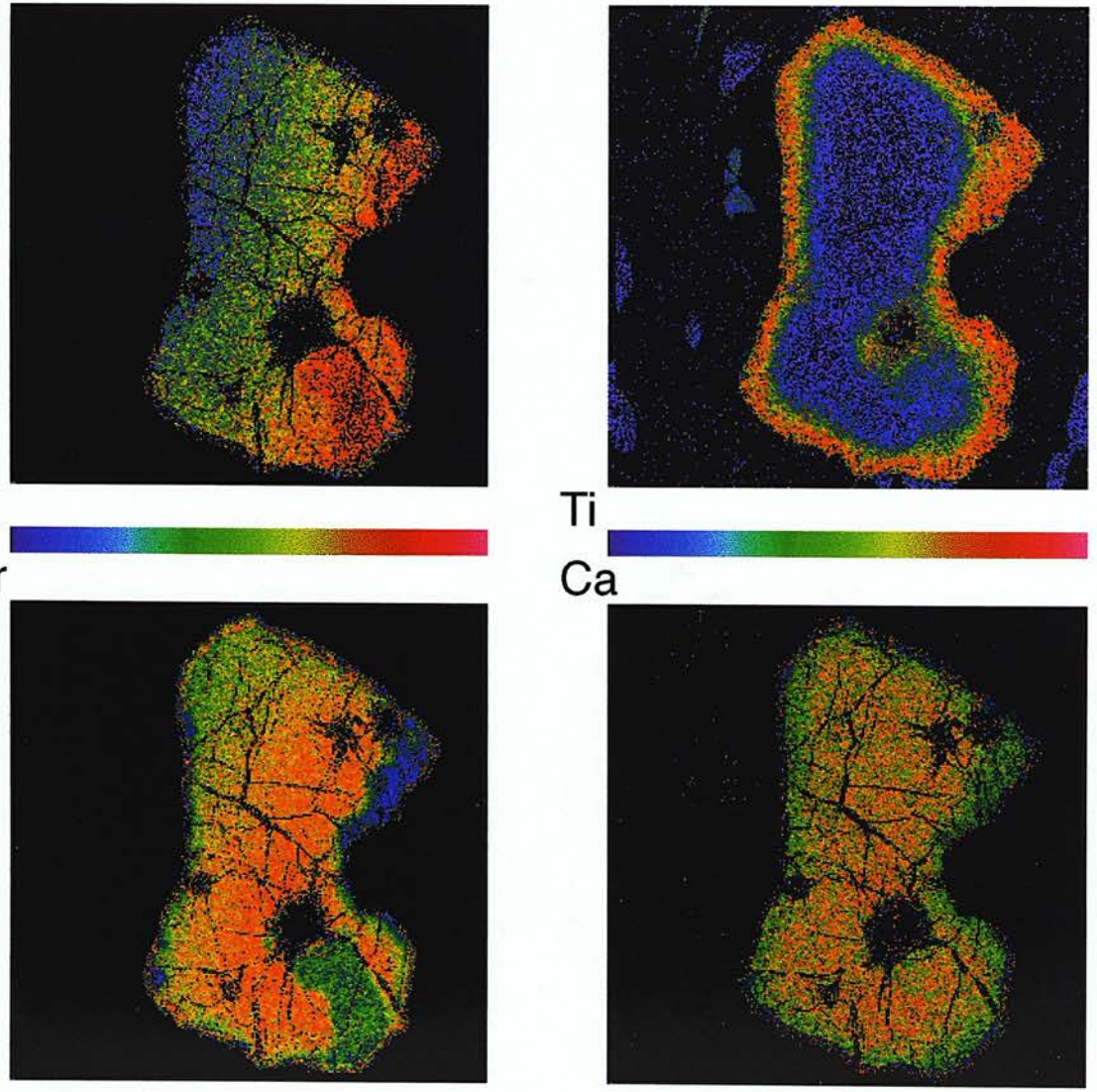

Fig. C.2a J31 -1

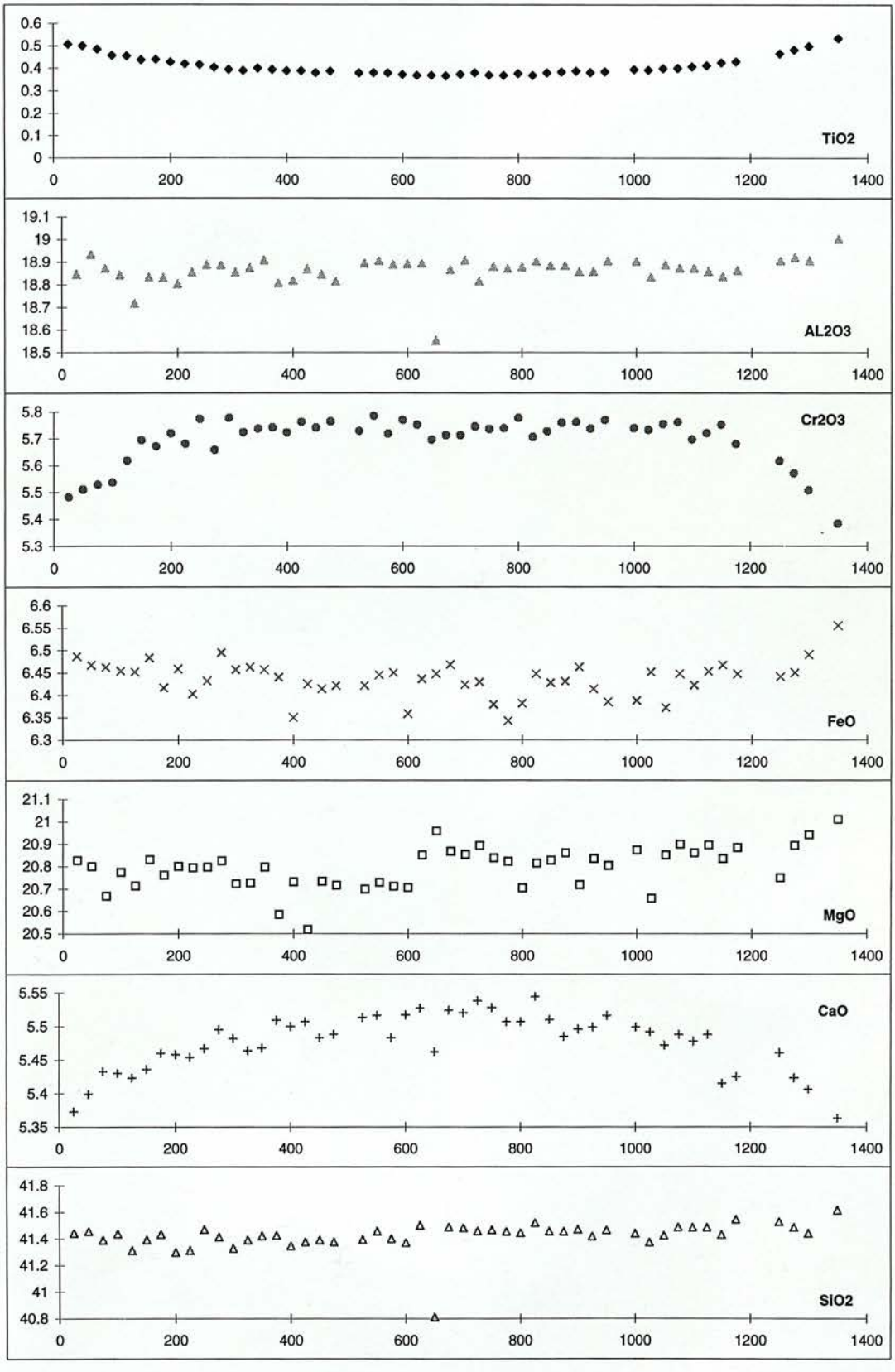

Fig. C.2b J31 -2

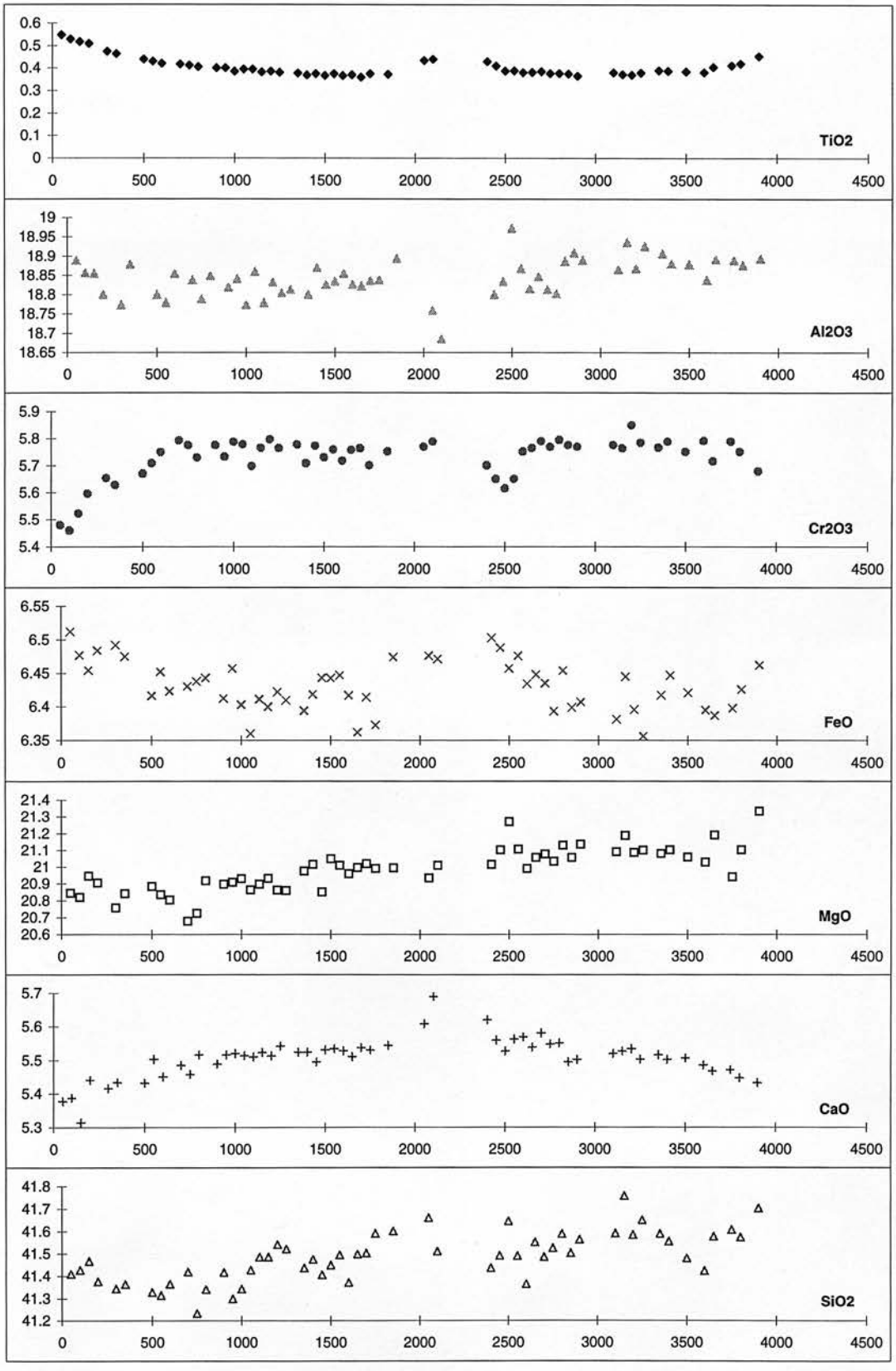

Fig. C.2c
J31

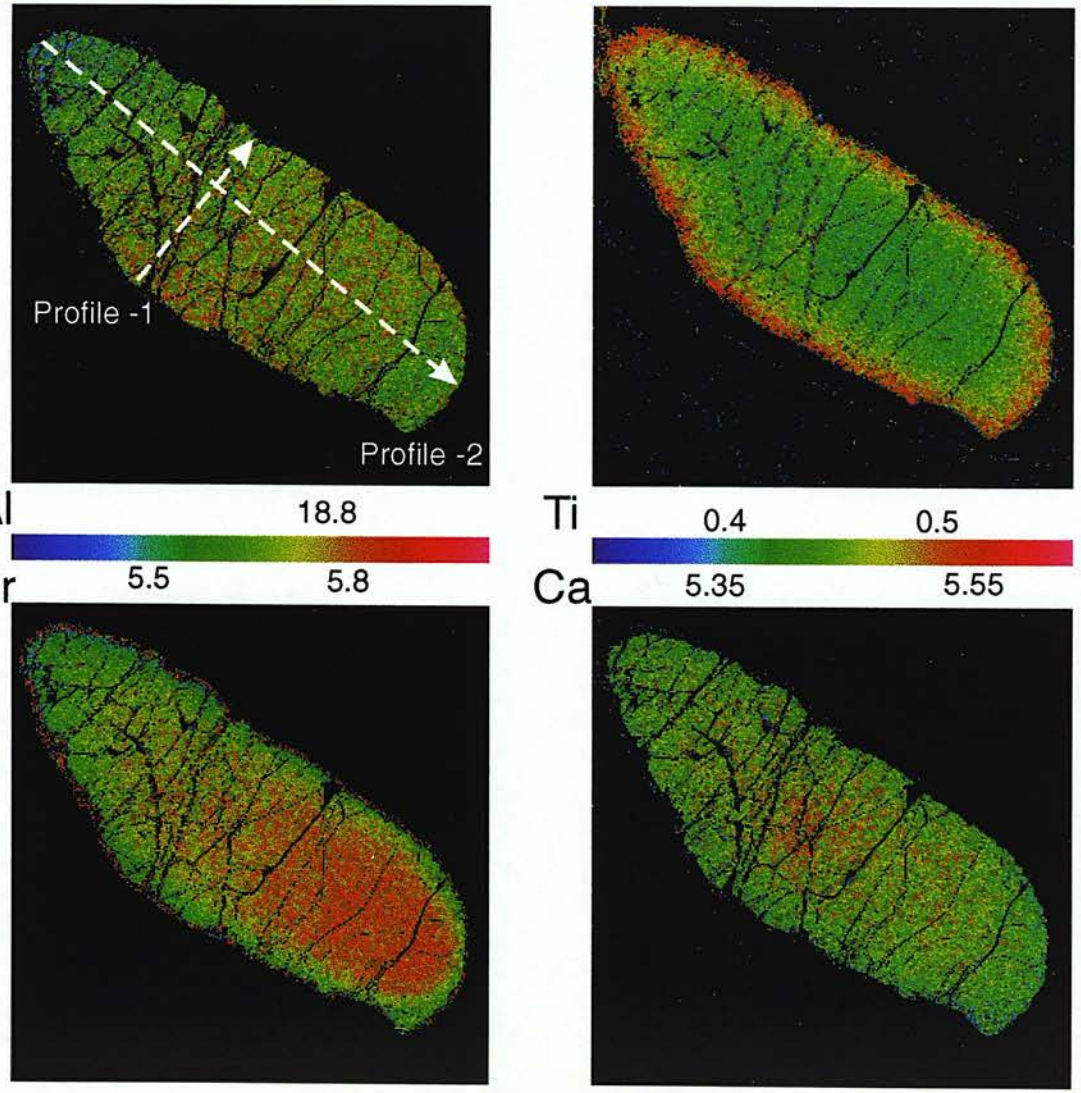

Fig. C.3 J33

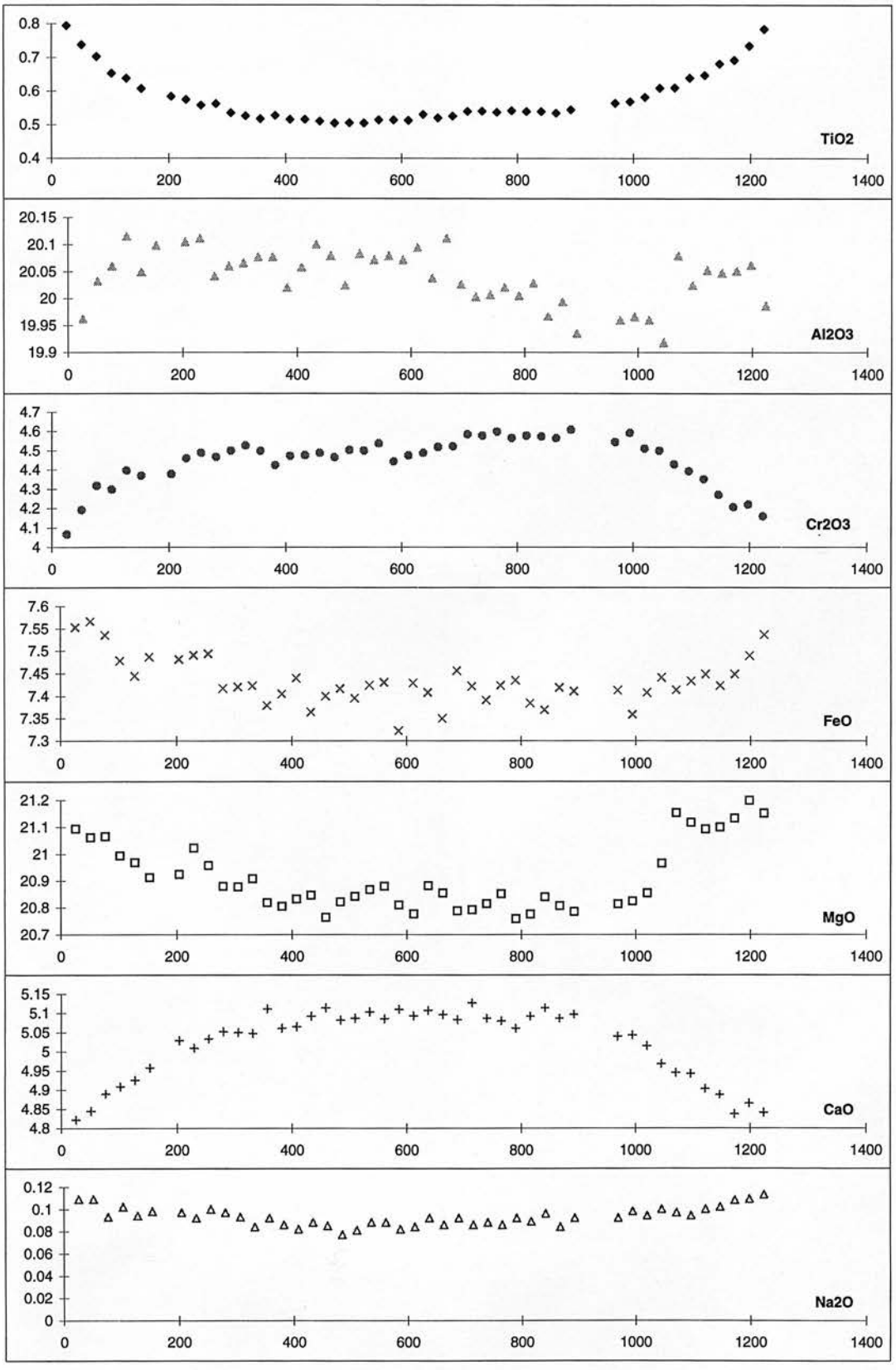

H:\j5rn30.xls

Fig. C.4a J34A

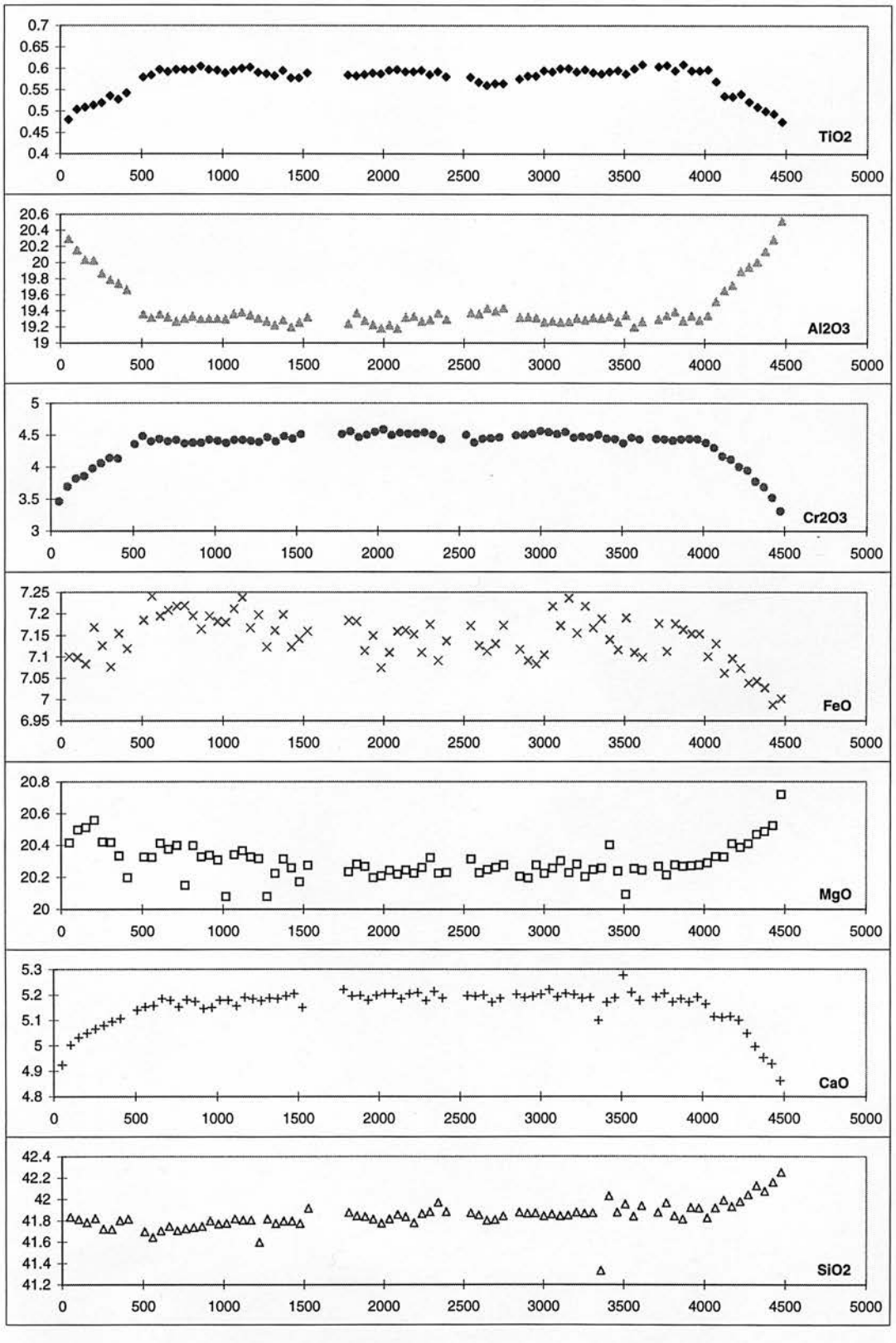

H:\jag5run6.xls

Fig. C.4b J34B Garnet A

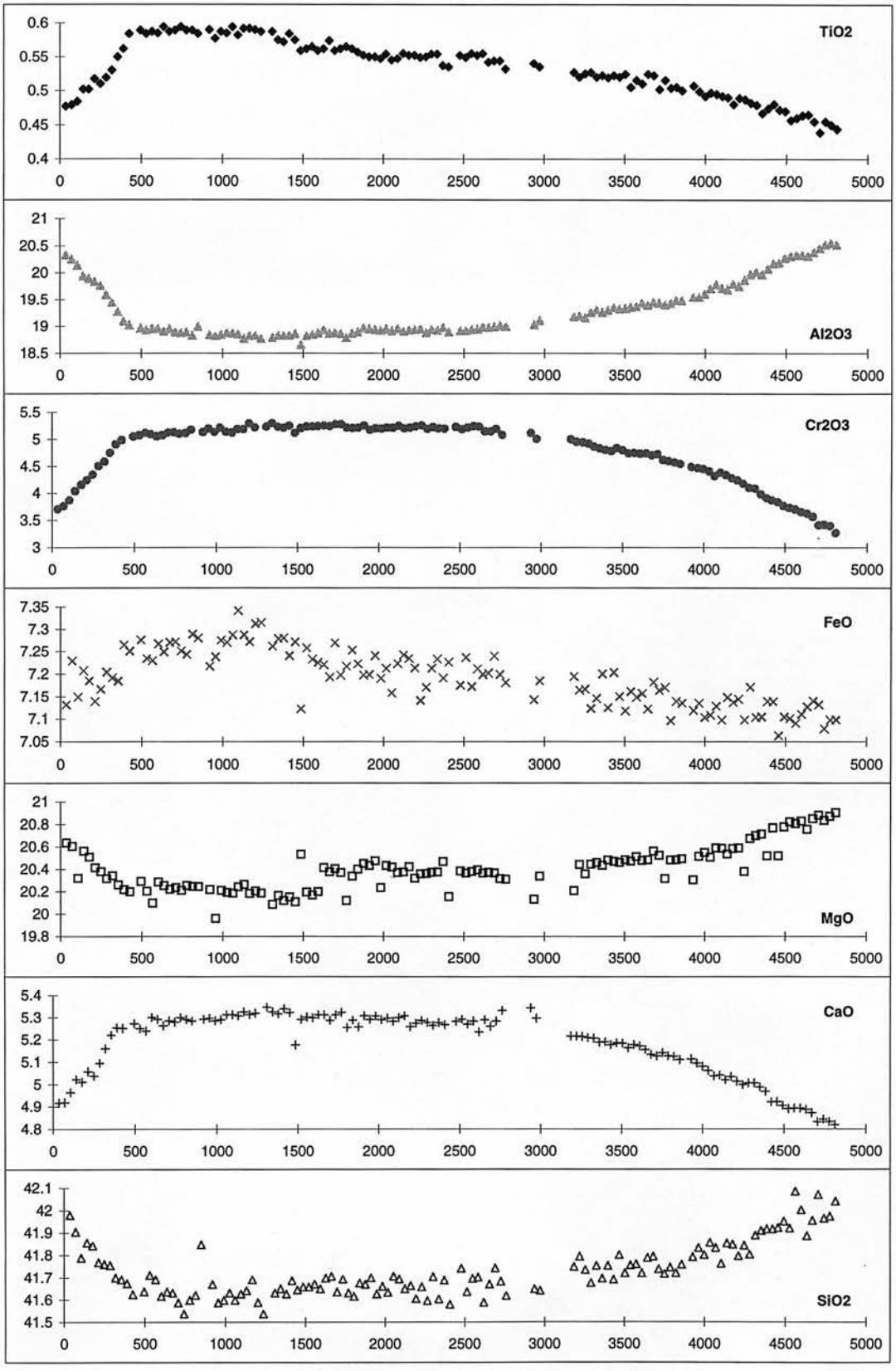

H:\jag5run8.xls

Fig. C.4c J34B Garnet B

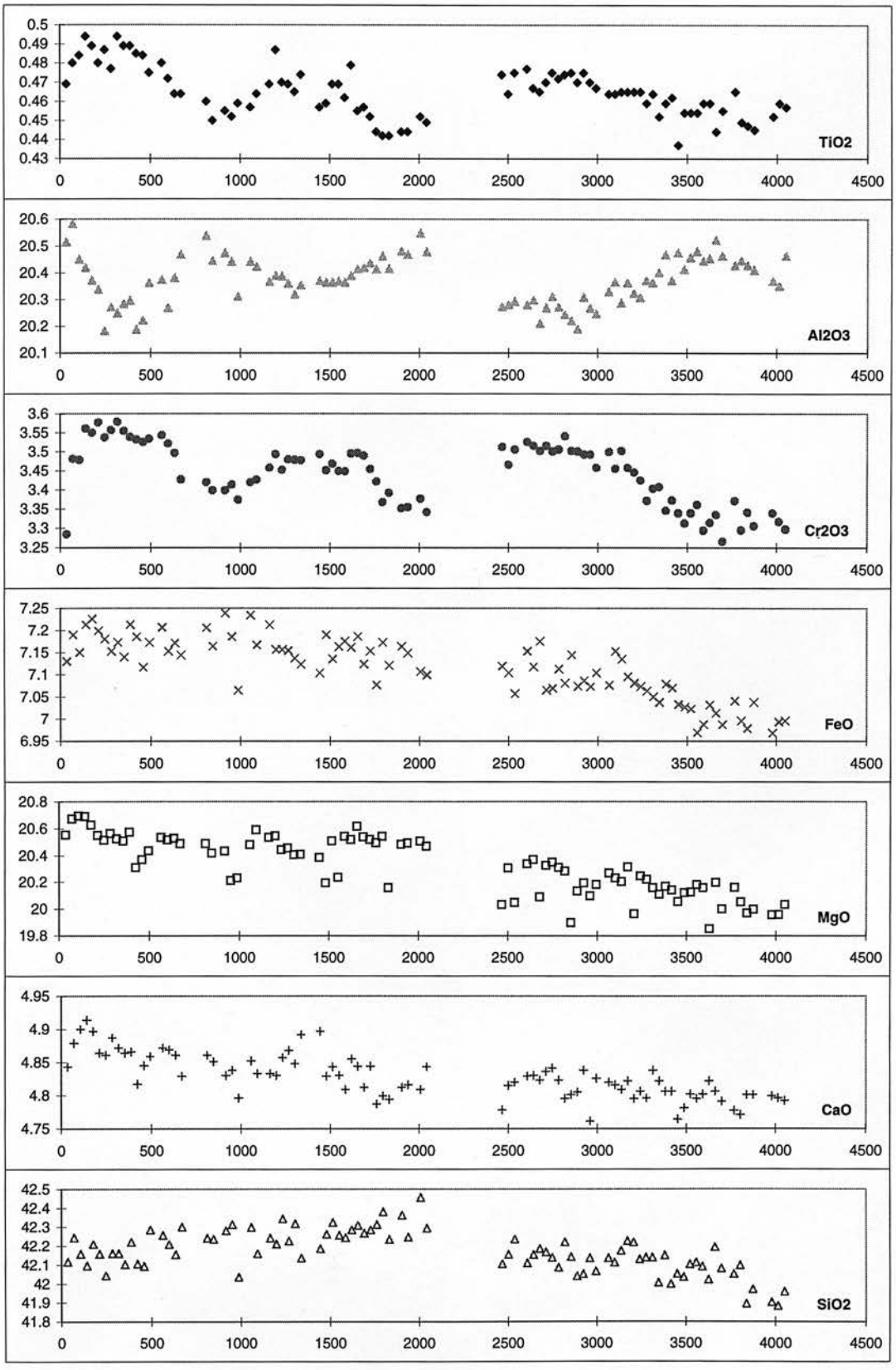

H:\j5rn28.xls

Fig. C.4d J34B Garnet C

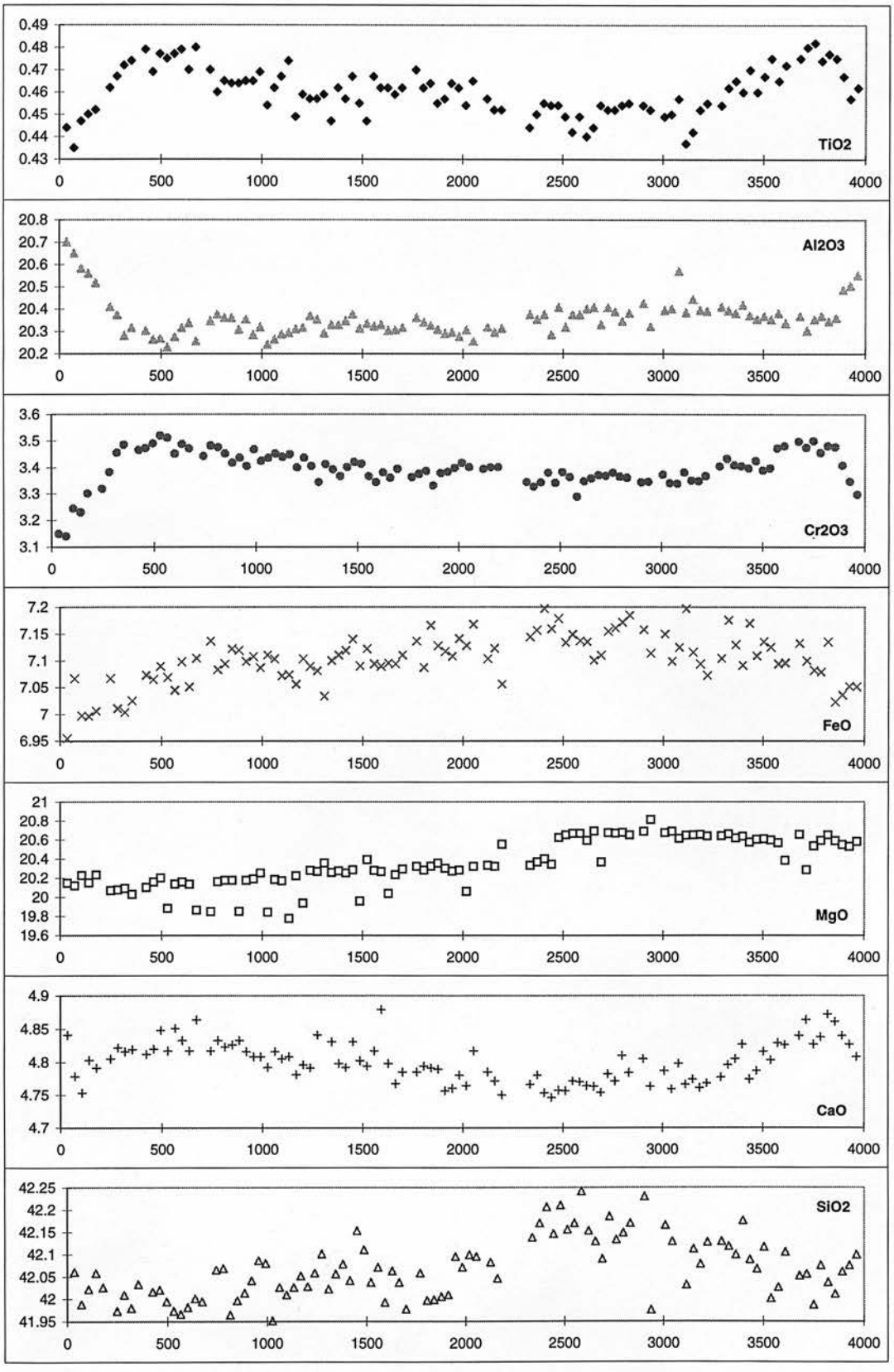

H:\j5rn29.xls

Fig. C.5a J37

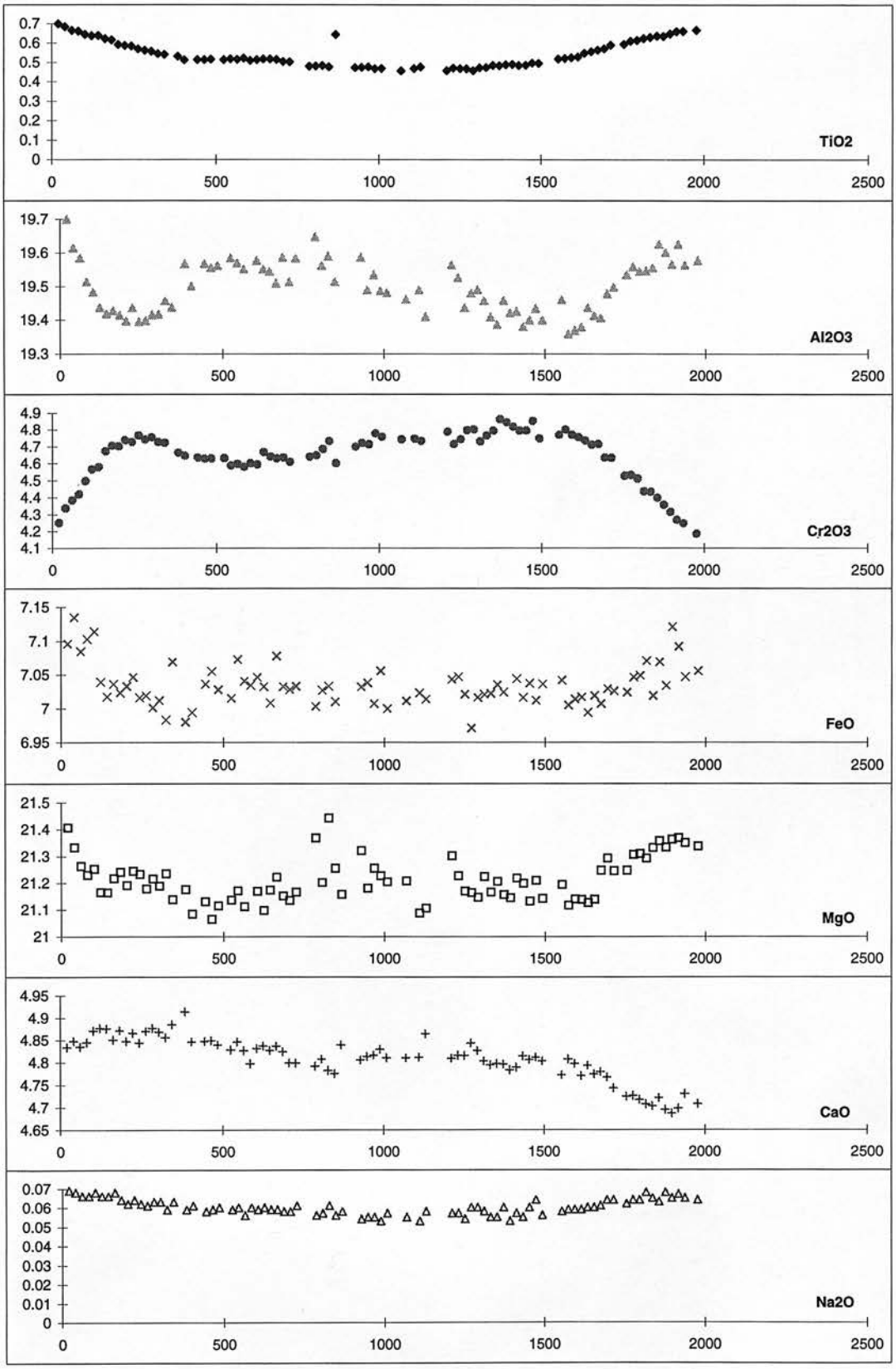

Fig. C.5b
J37

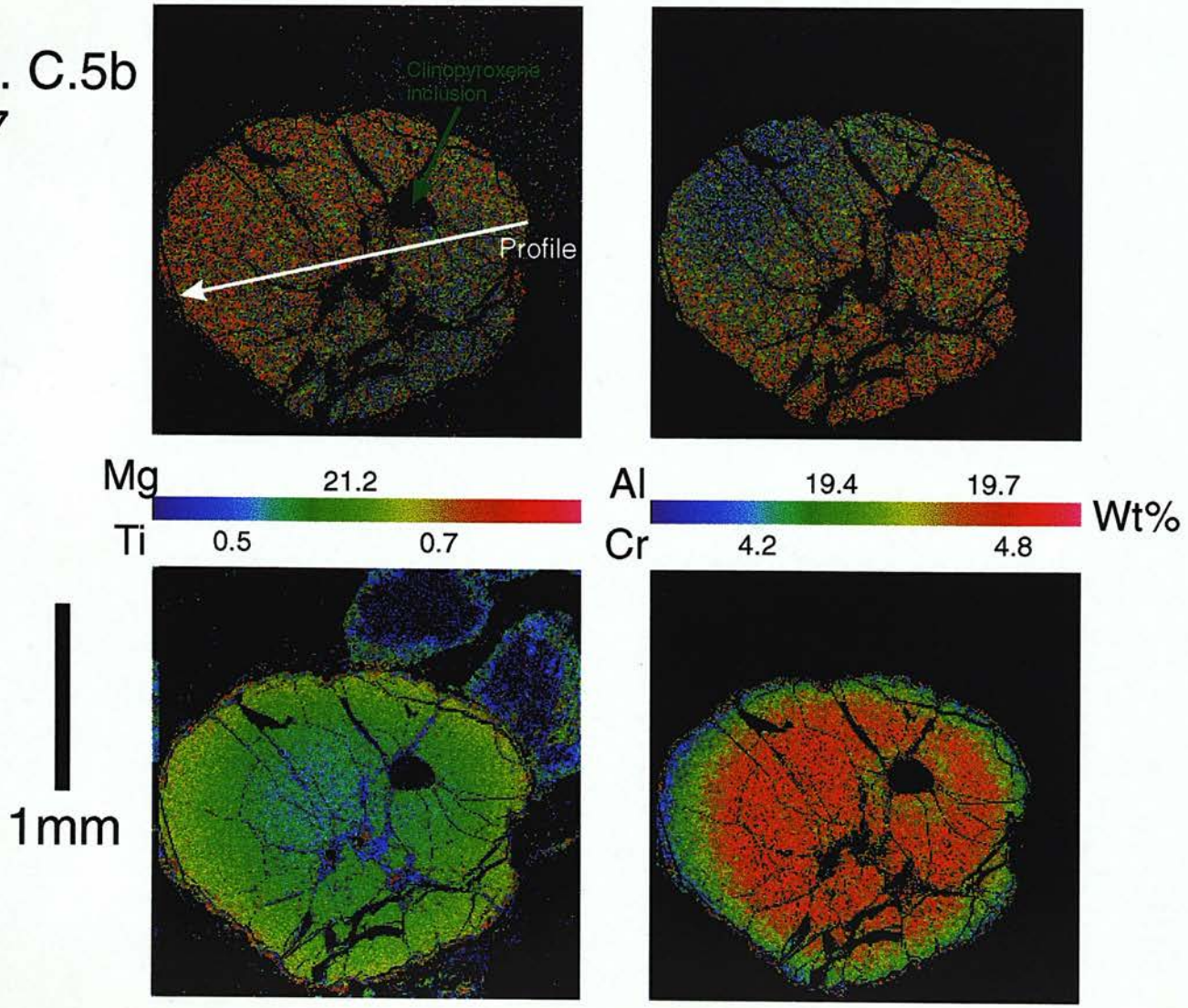
Clinopyroxene inclusion
Profile
Mg
21.2
Ti
0.5
0.7
Al
19.4
19.7
Cr
4.2
4.8
Wt%
1mm

Fig. C.6 J38

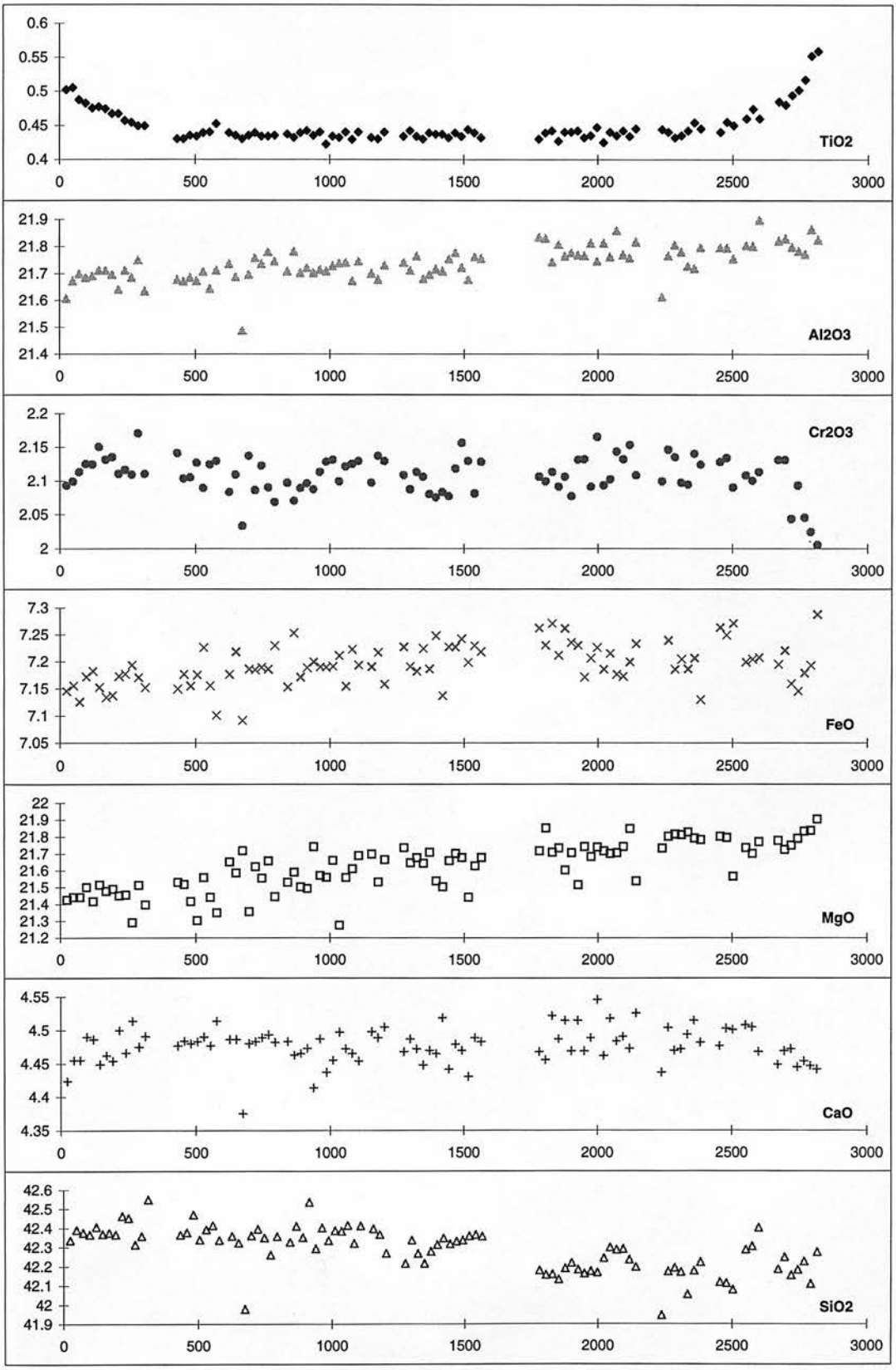
TiO2
Al2O3
Cr2O3
FeO
MgO
CaO
SiO2
0
500
1000
1500
2000
2500
3000

Fig. C.7a J107 -1

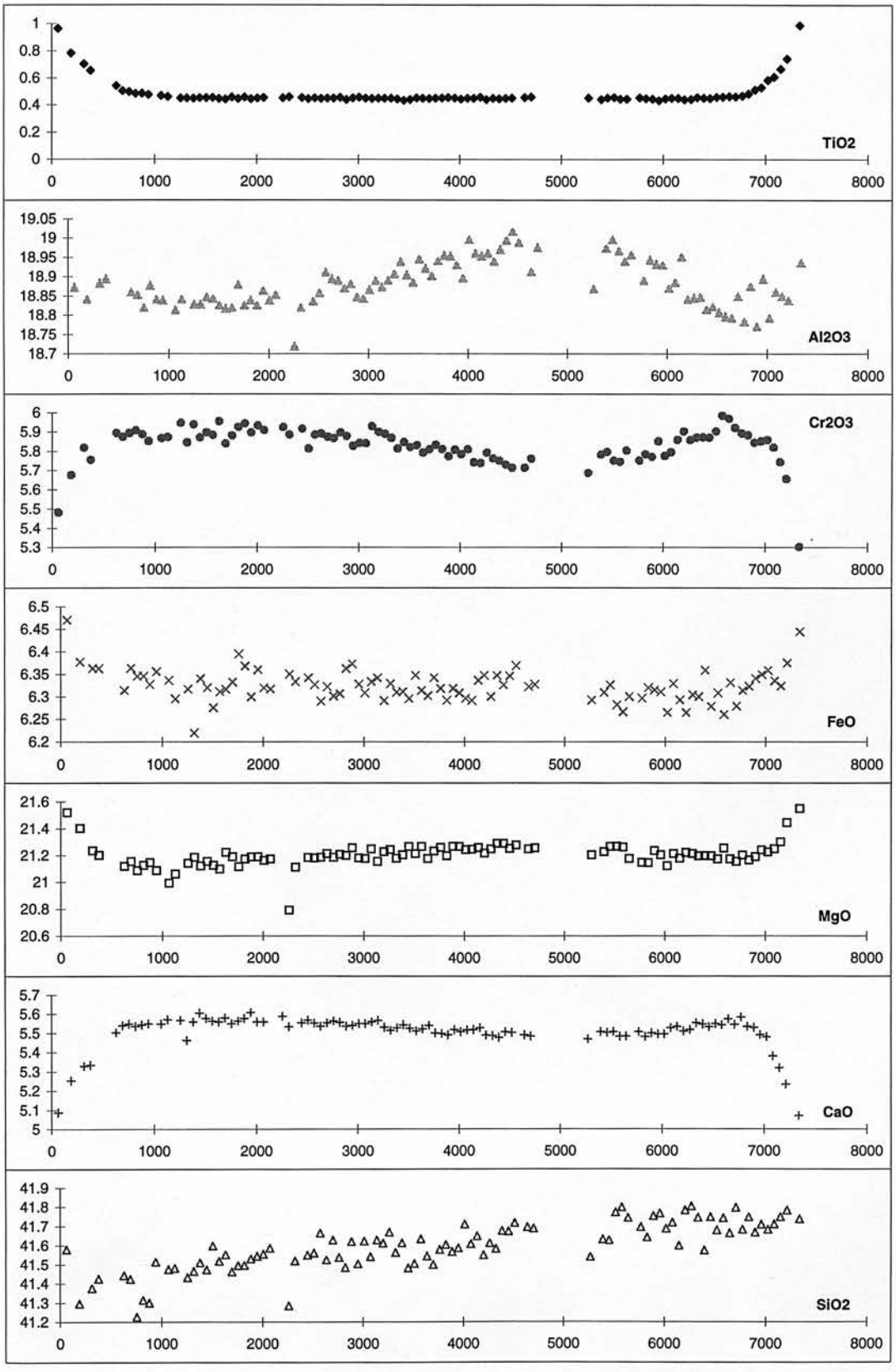

H:\J5rn5.xls

Fig. C.7b J107 -2

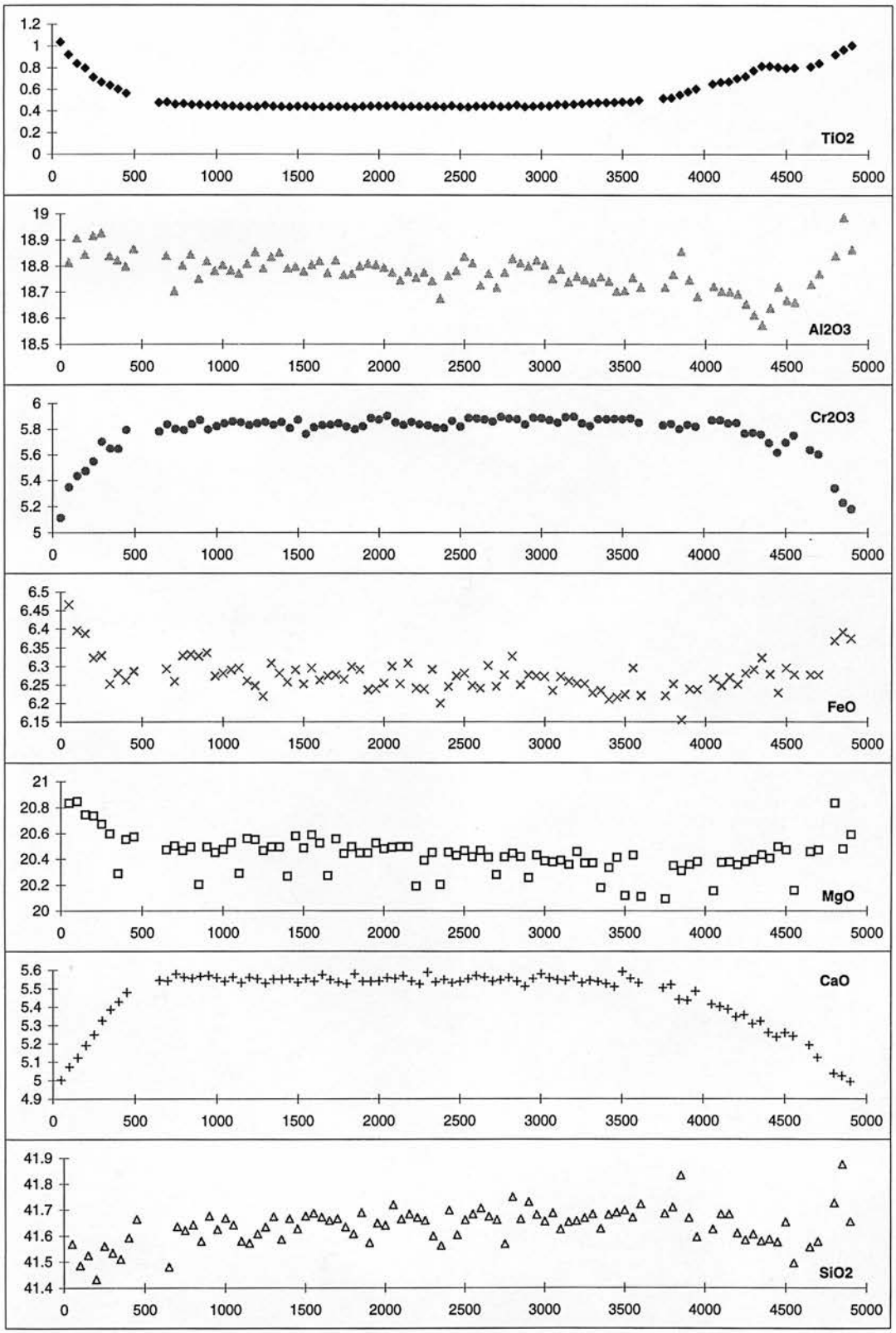

Fig. C.7c
J107

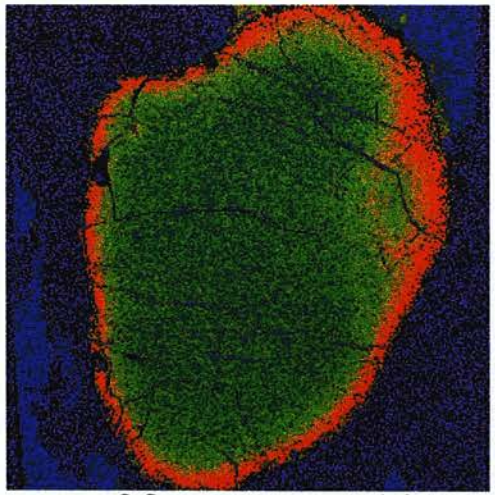

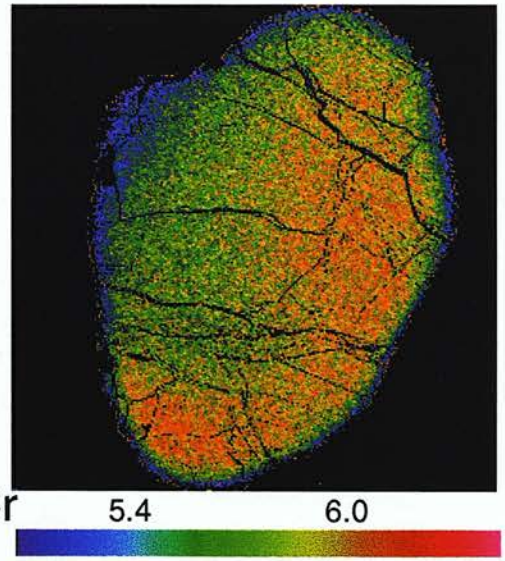

Fig. C.8 J110

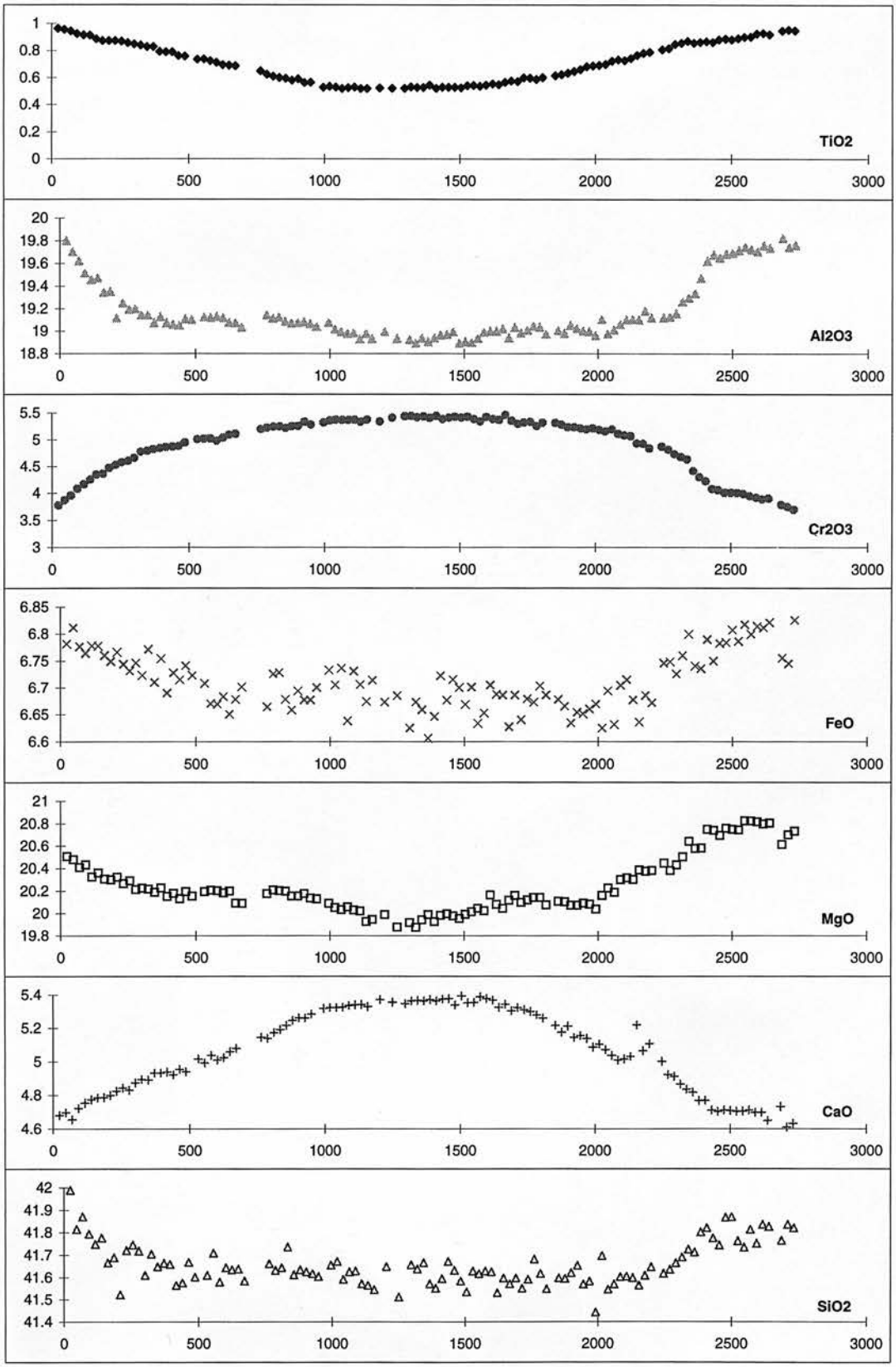

H:\j5rn9.xls

Fig. C.9a J112

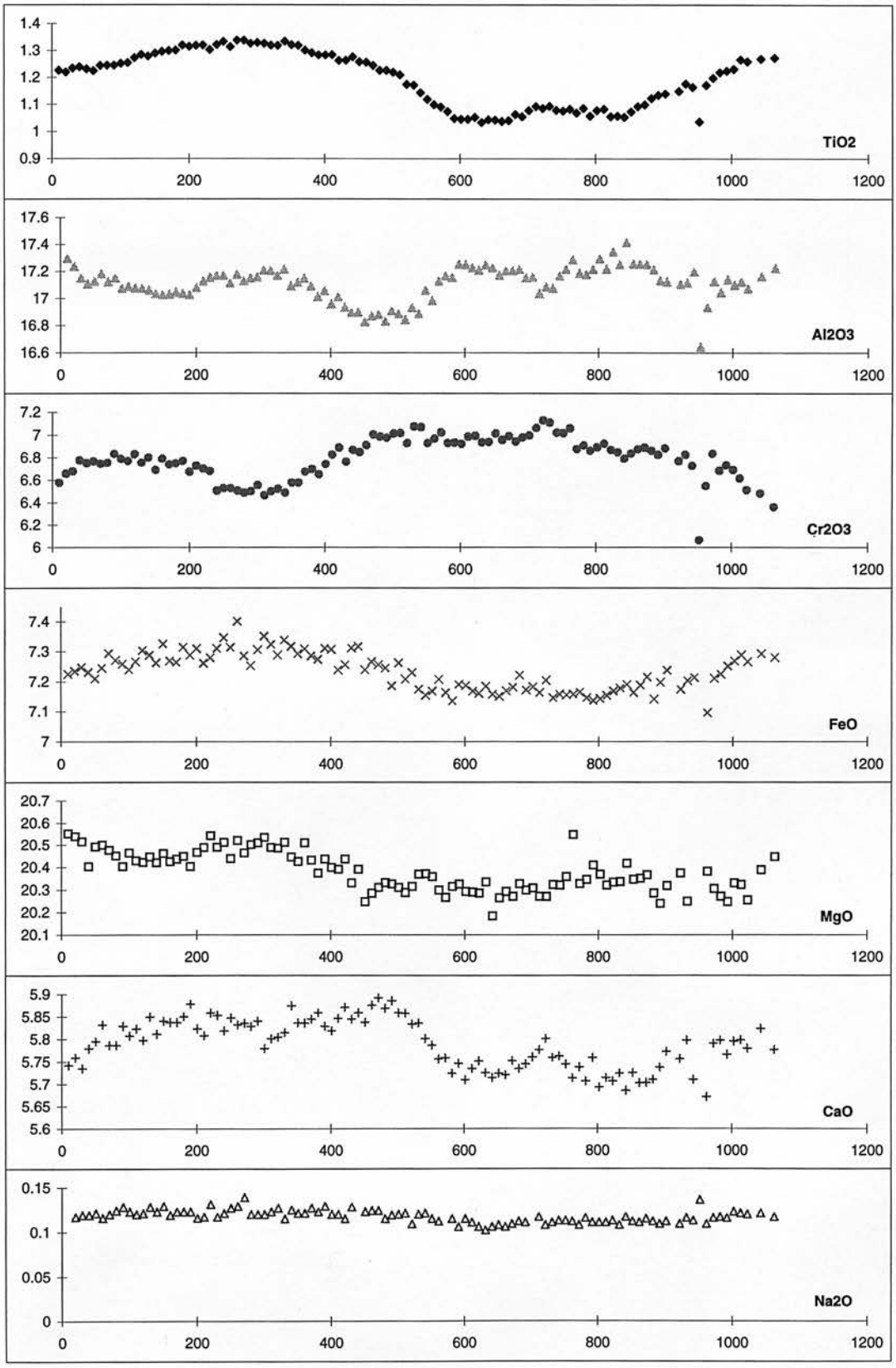

H:\j5run36.xls

Fig. C.9b
J112

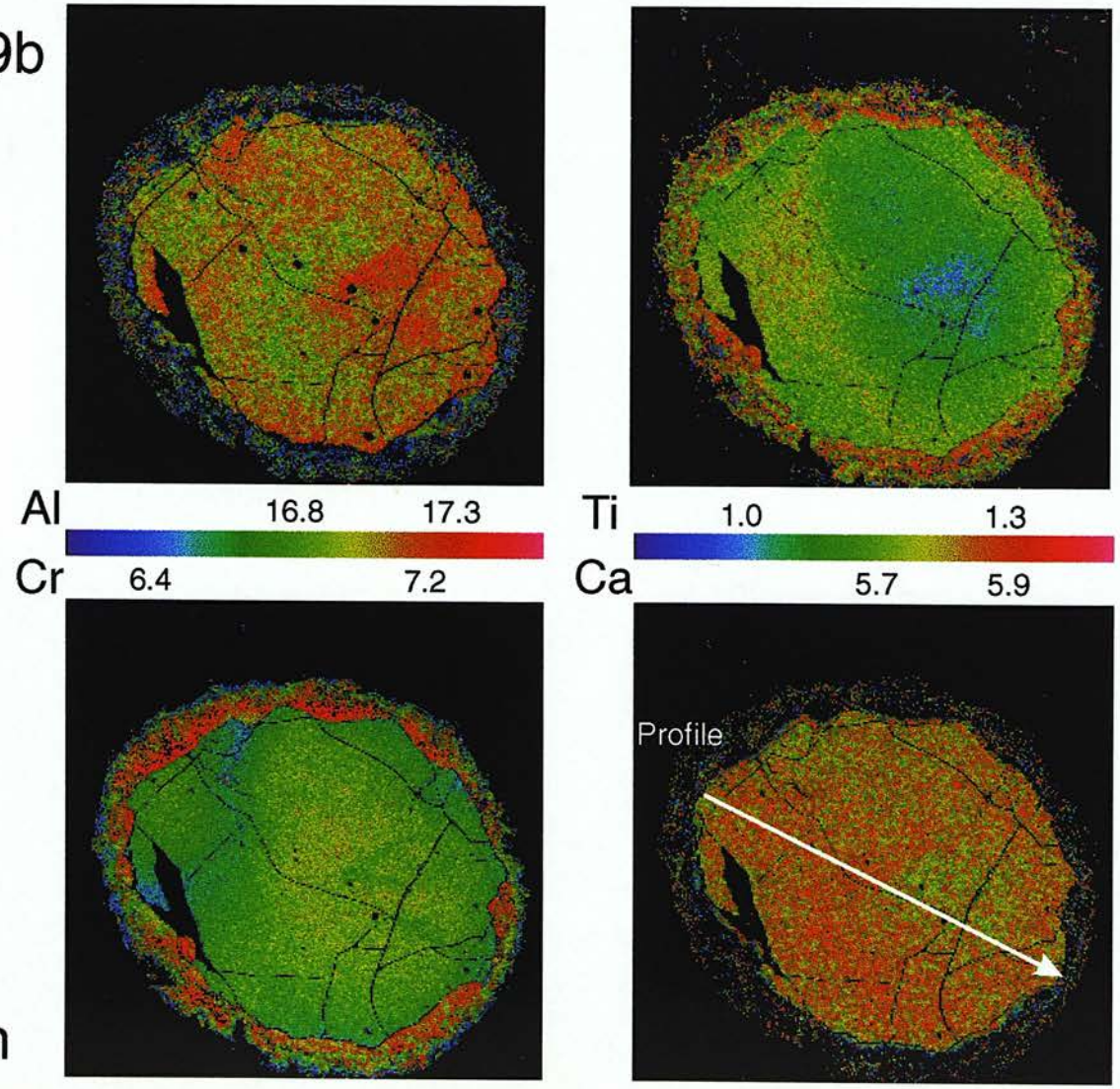

Fig. C.9c J112a

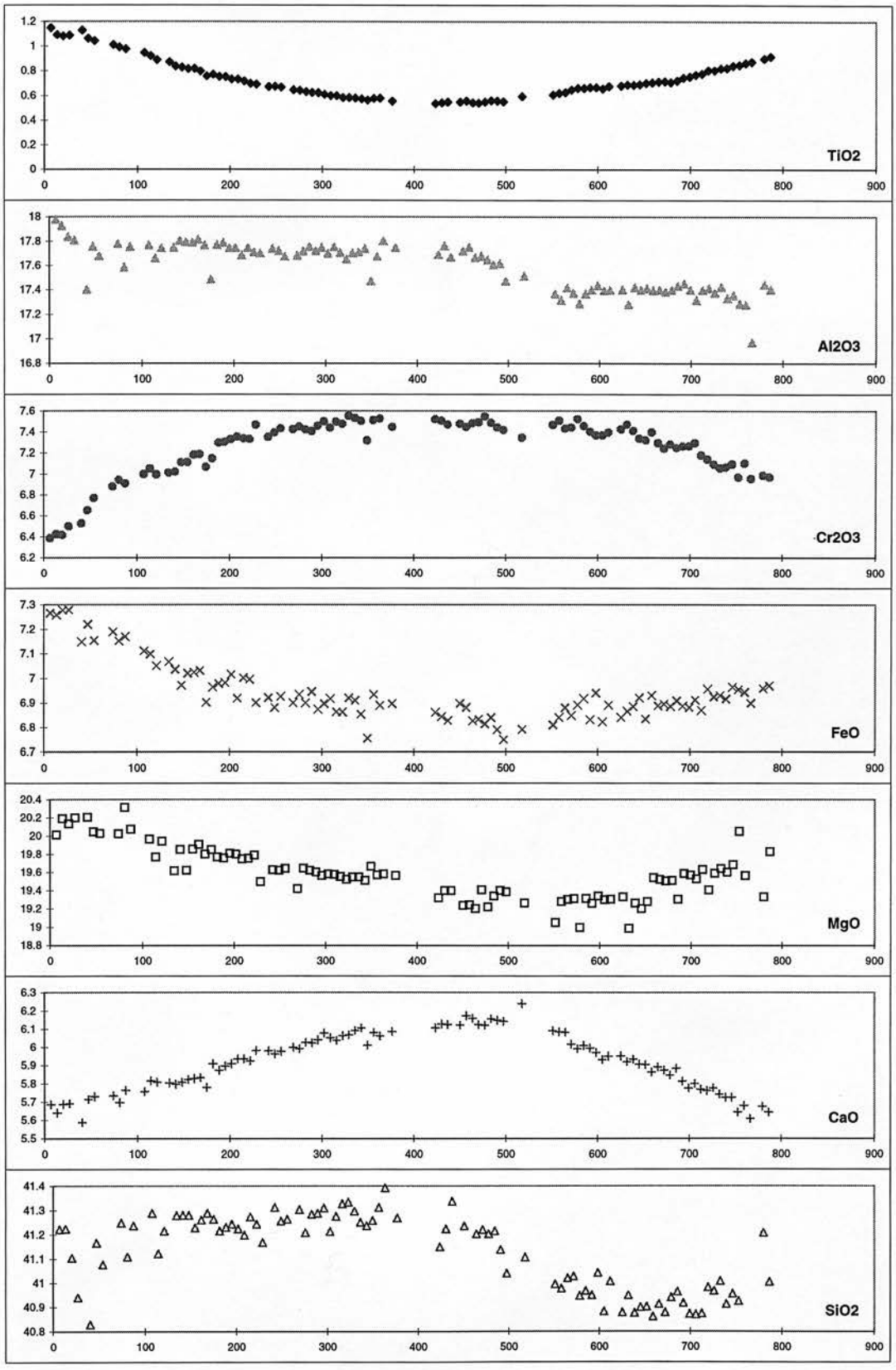

H:\j5rn2.xls

Fig. C.10a J115 -1

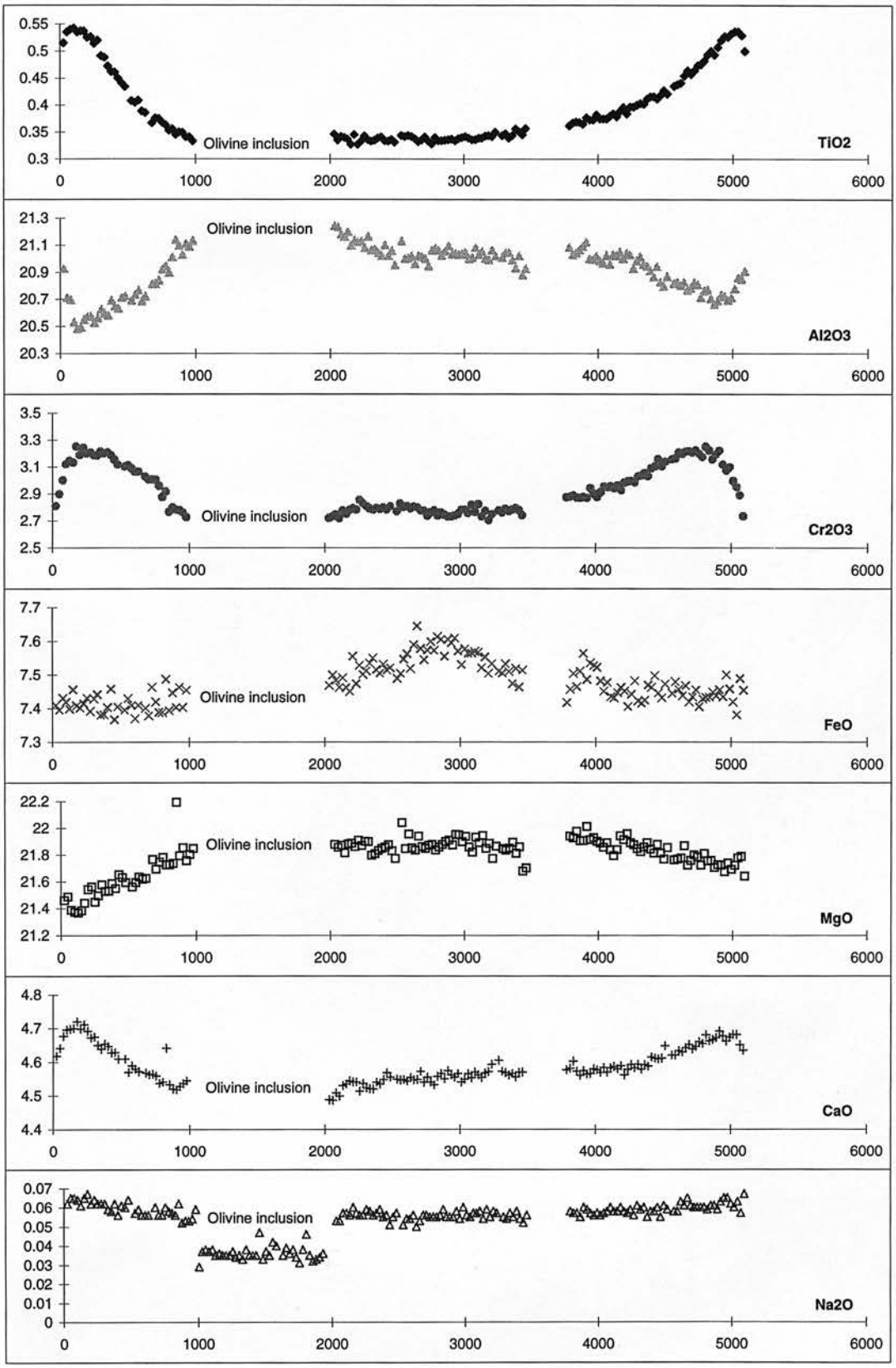

H:\Jag4run4.xls

Fig. C.10b J115 -2

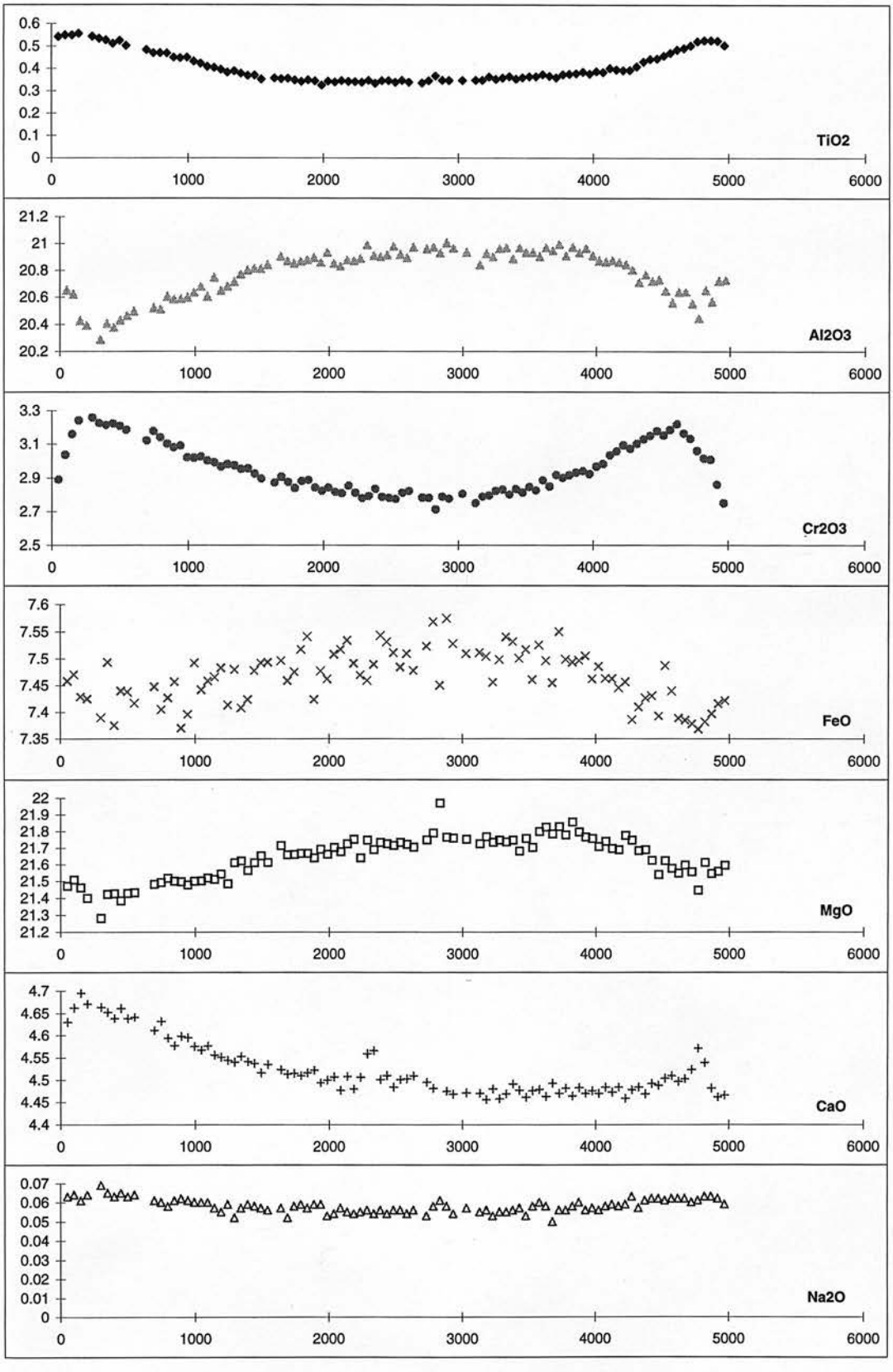

H:\jag4run5.xls

Fig. C.10c
J115

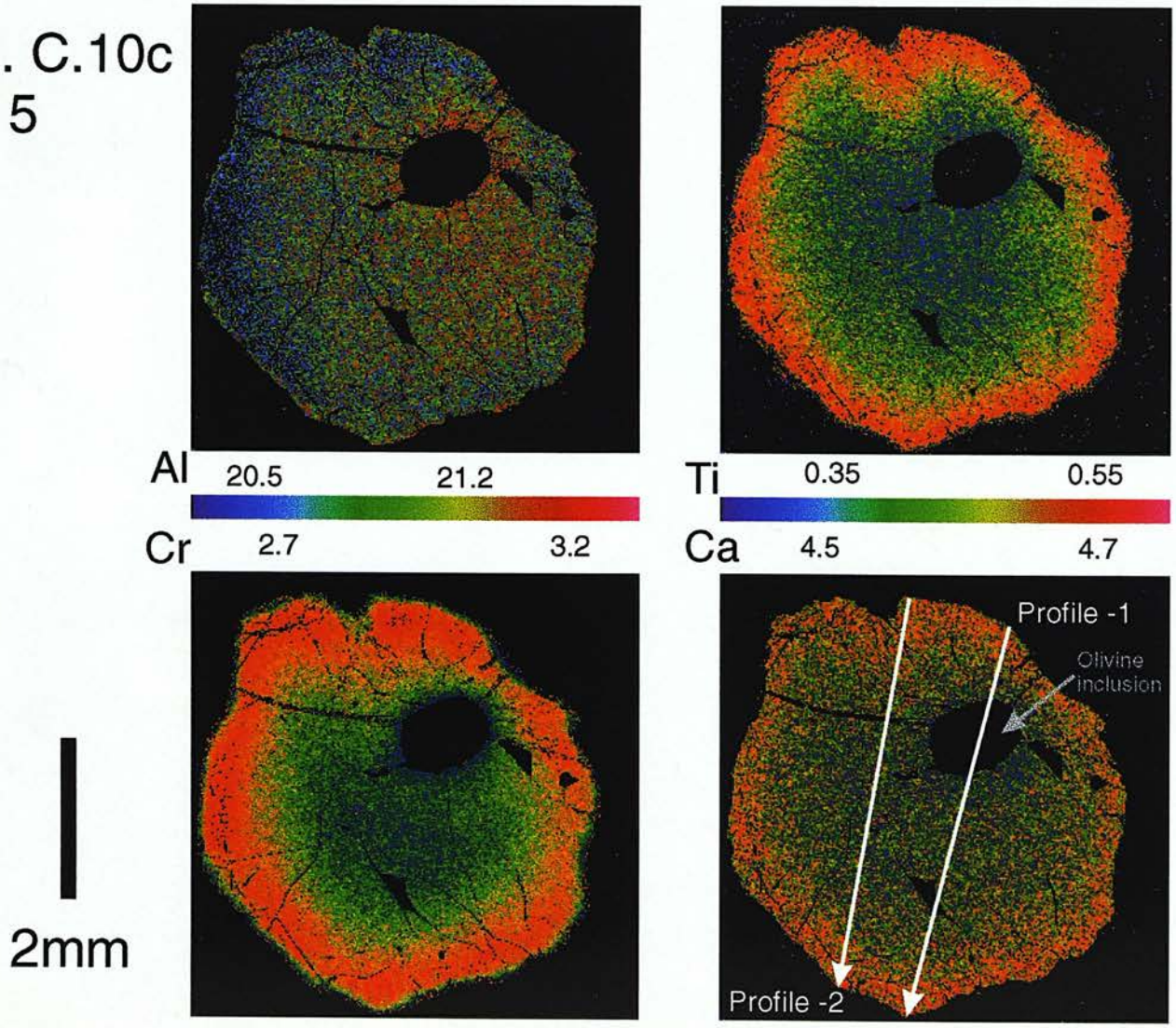

Fig, C.11a J121

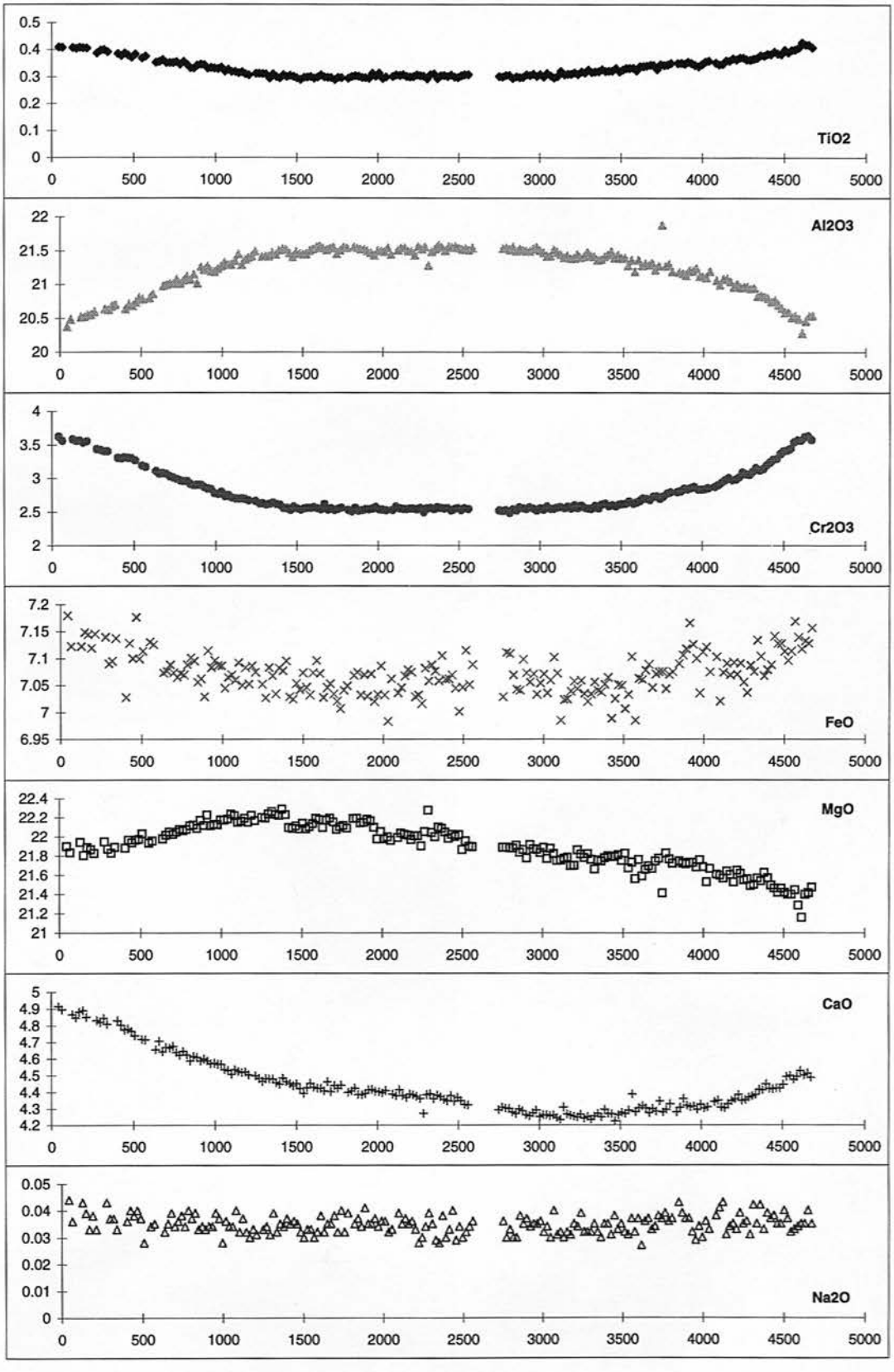

Fig. C.11b J121A

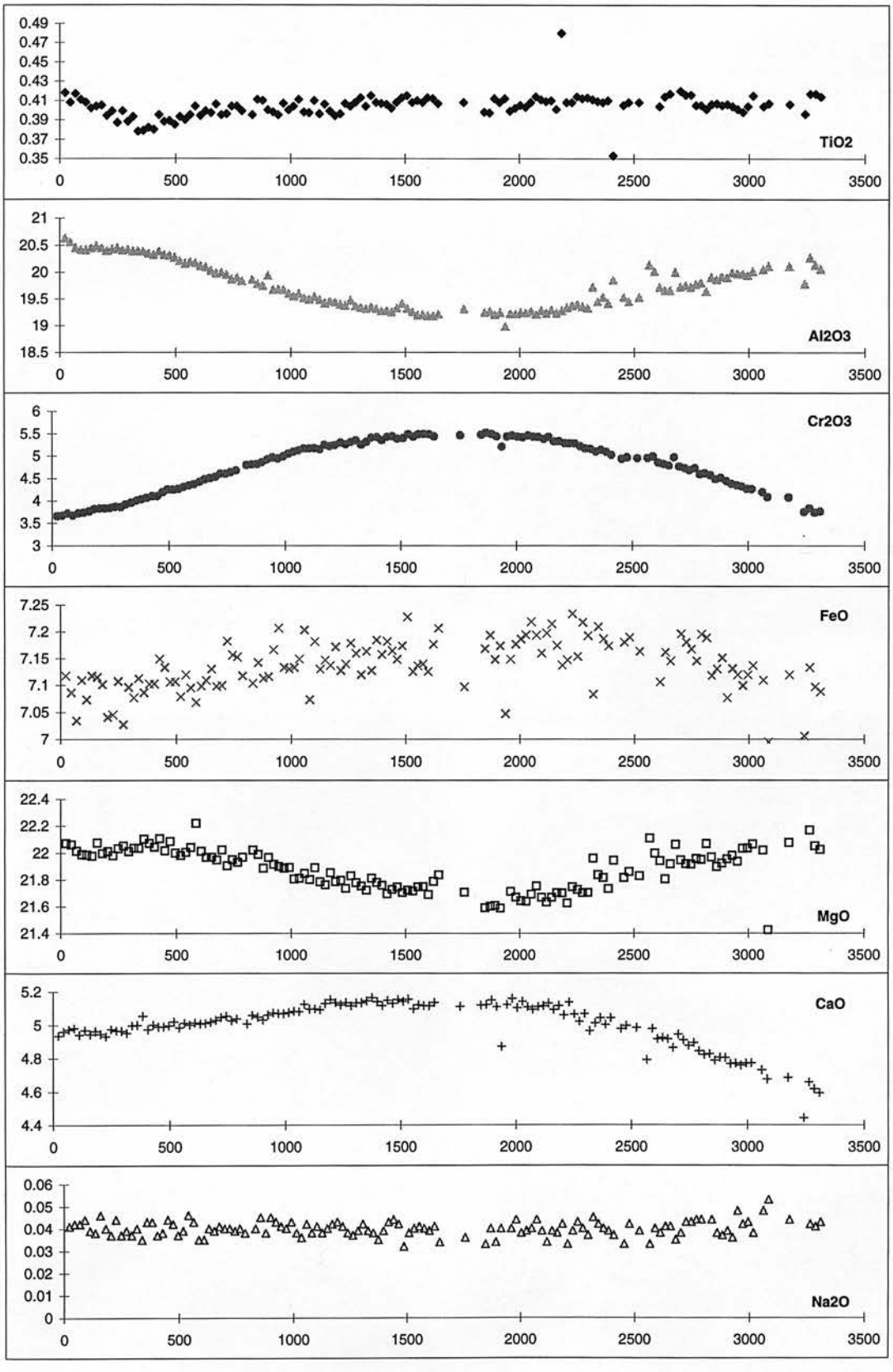

Fig. C.11c
J121A

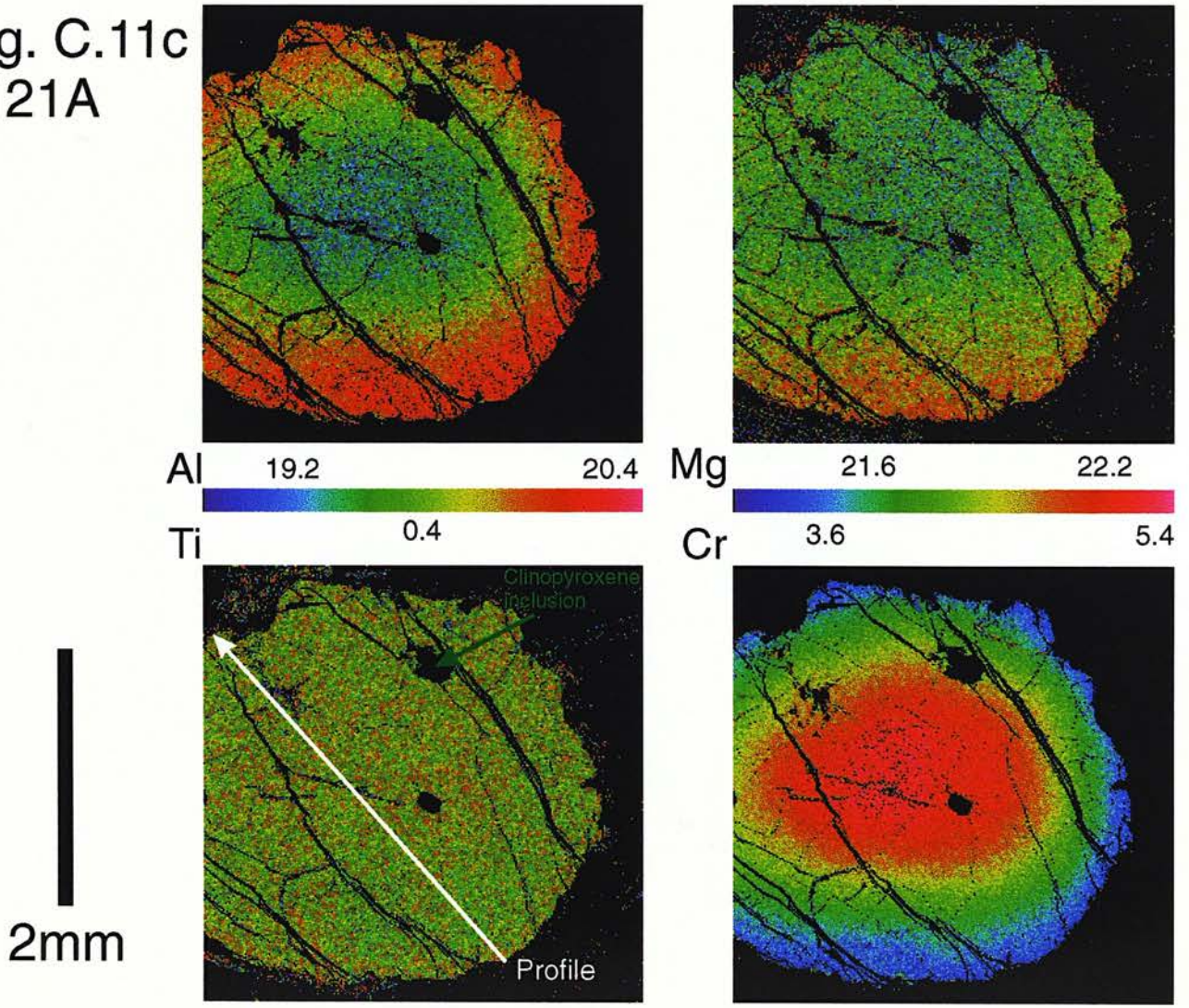

Fig. C.12a J145

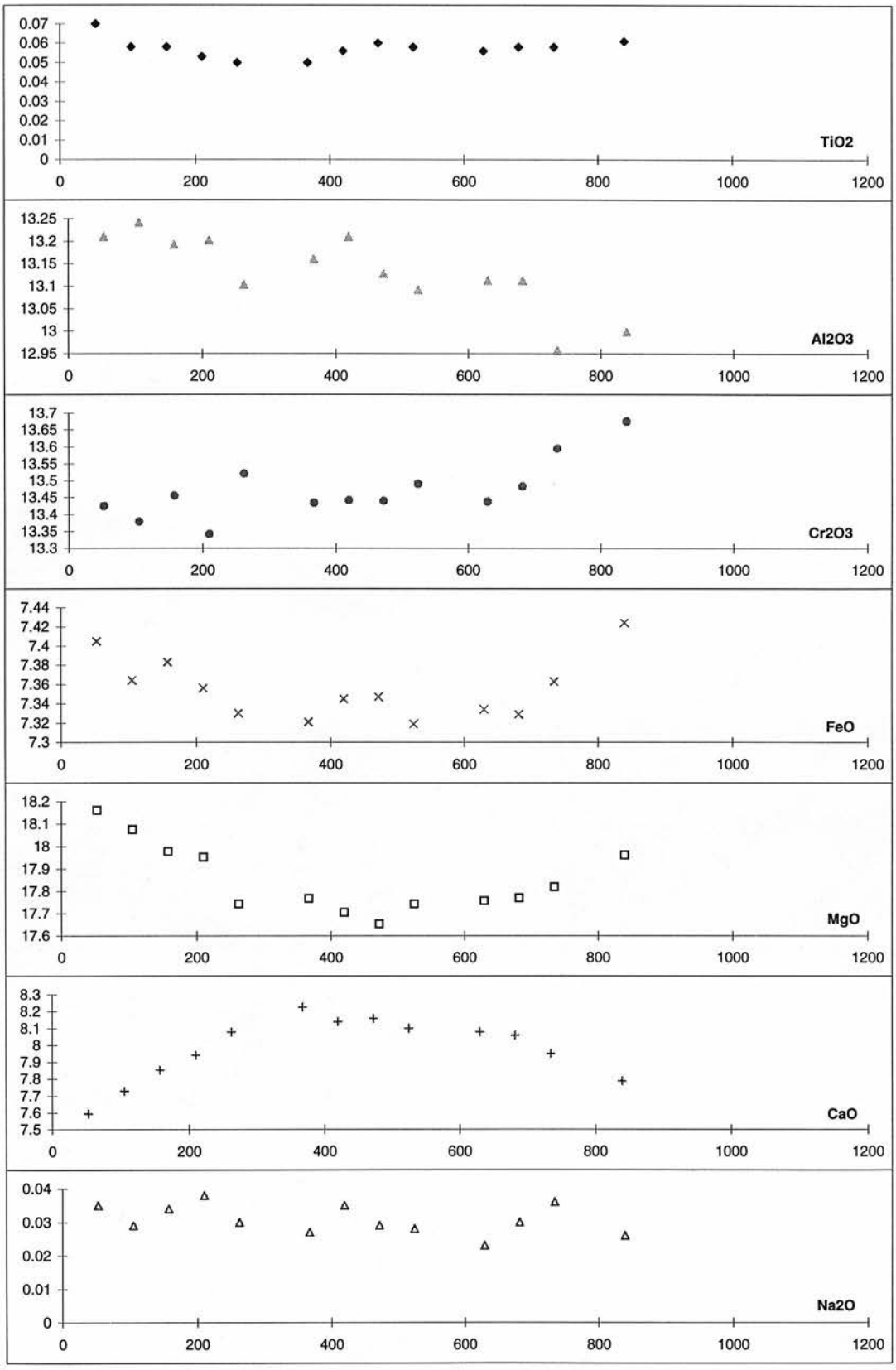

H:\jag12r12

Fig. C.12b
J145

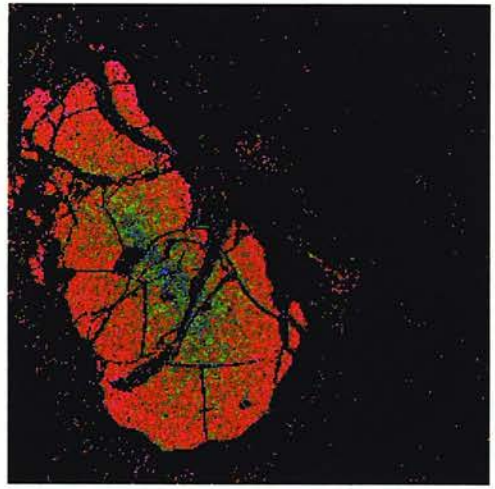

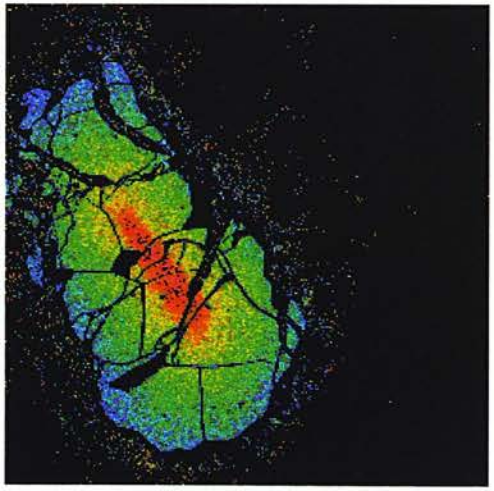

Mg 17.6 18.1 Ca 7.5 8.3 Wt%

Fe 7.30 7.45

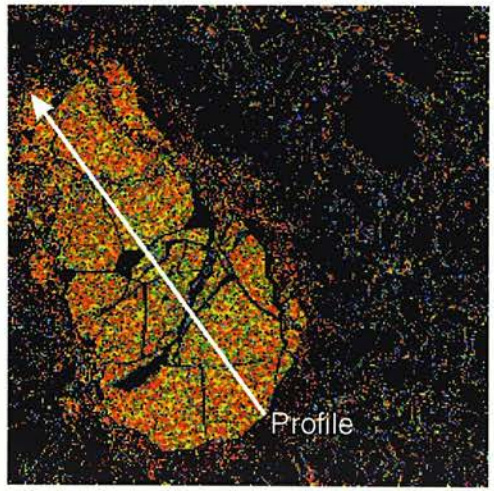

1mm

Fig. C.13a JJG1776

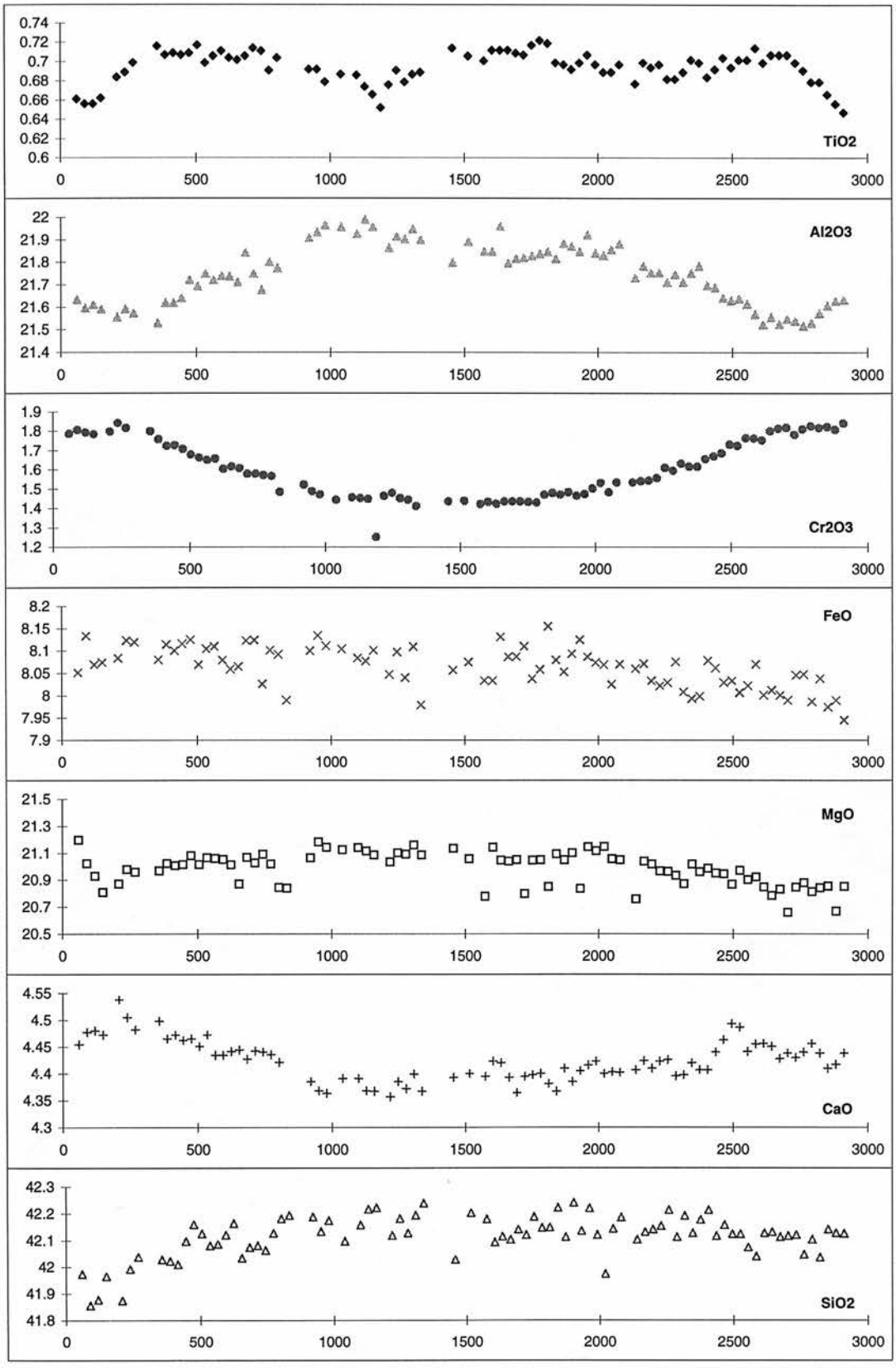

H:\j5rn20.xls

Fig. C.14a JJH11 GarnetA

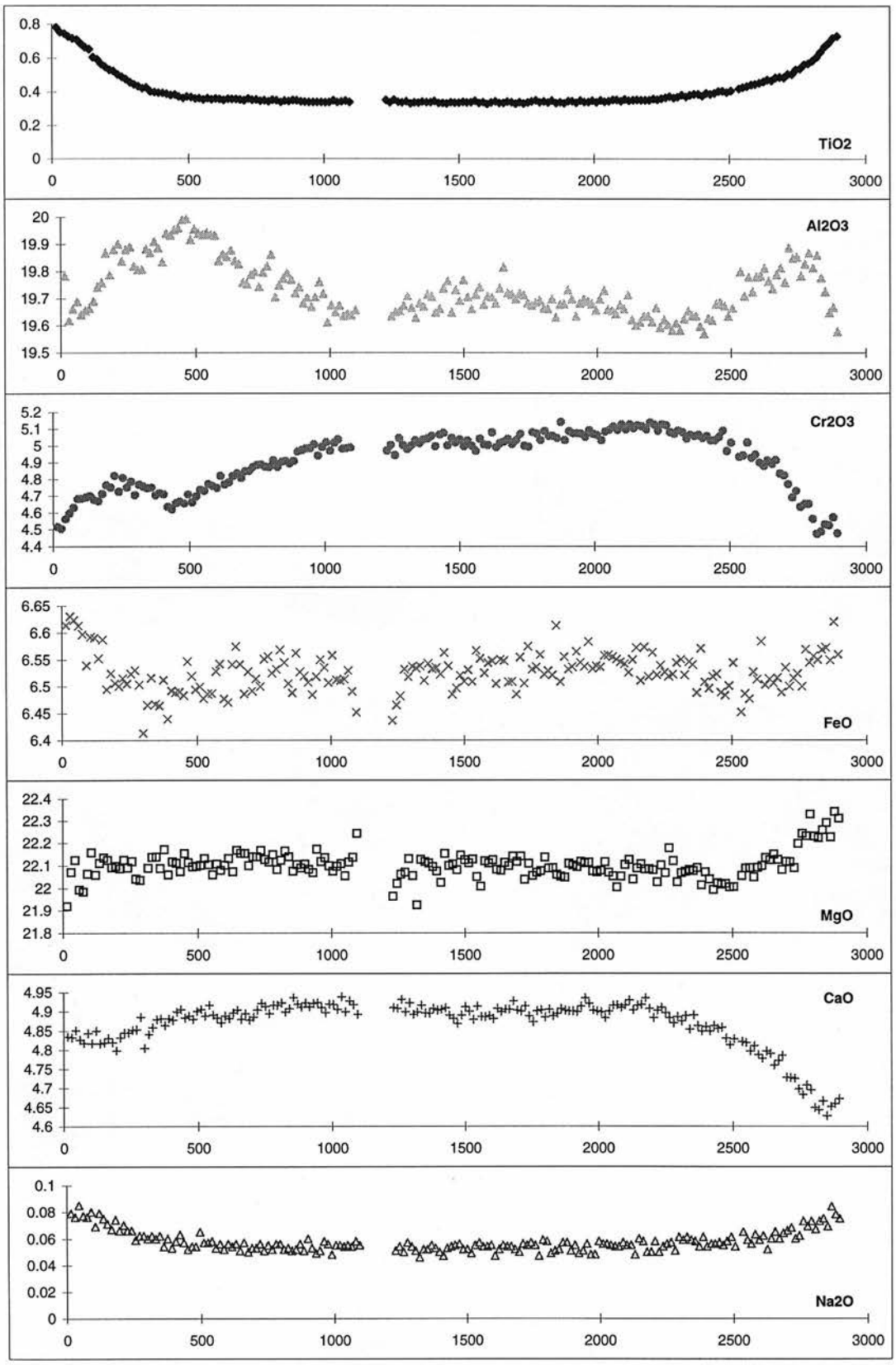

H:\jag12r1.xls

Fig. C.14b
JJH11
Garnet A

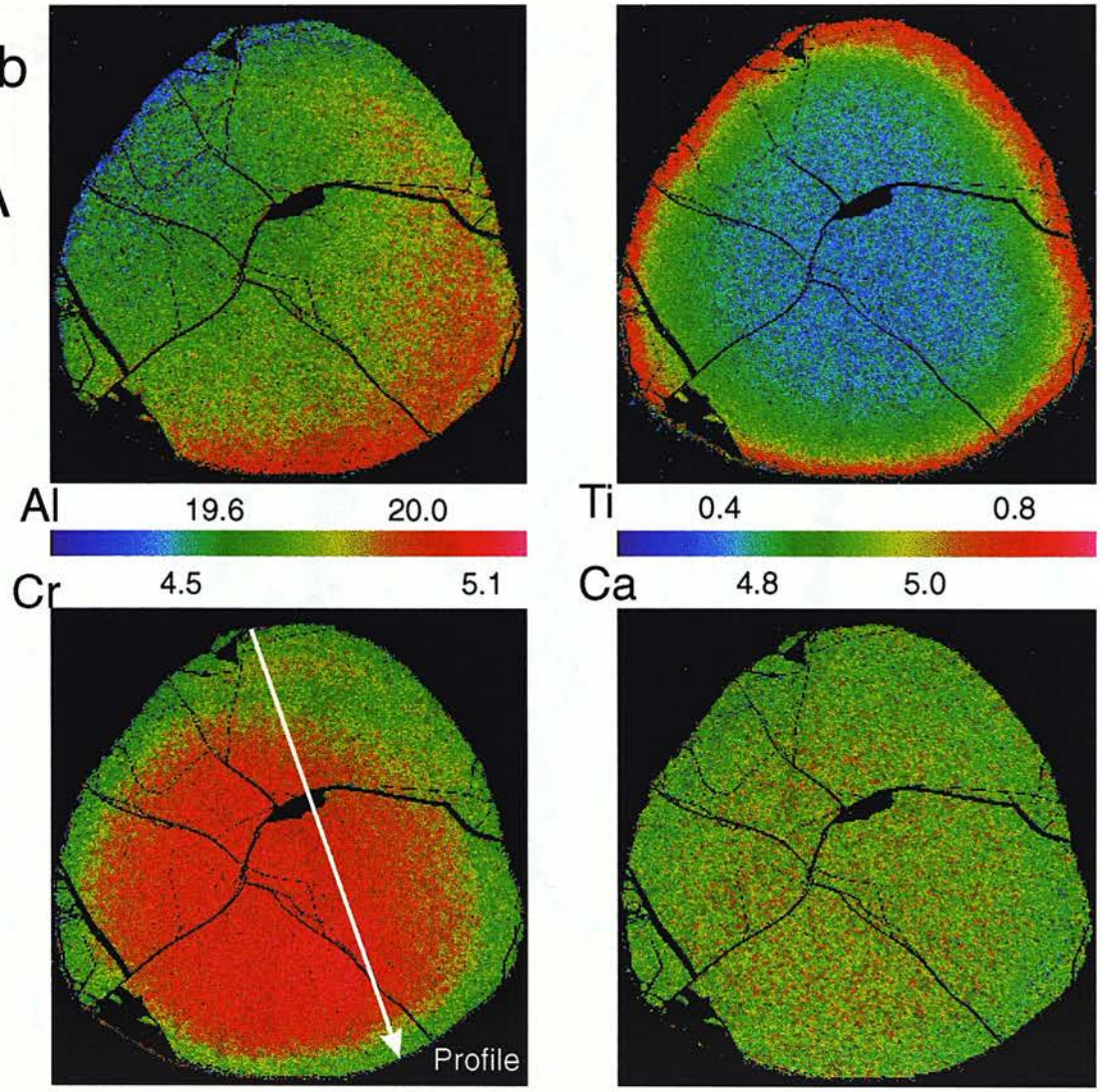

Fig. C.14c JJH11 Garnet B

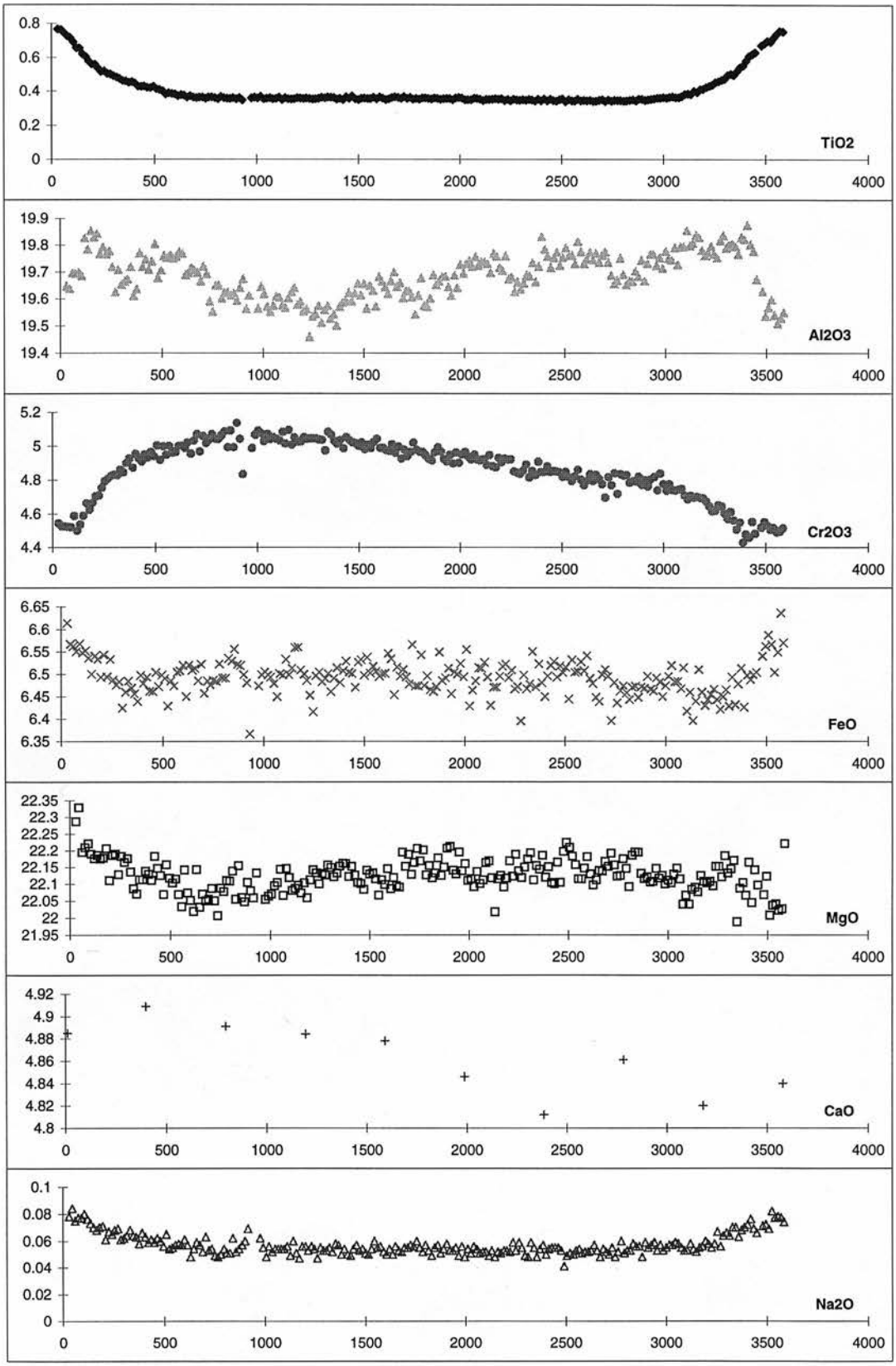

H:\jag12r2.xls

Fig. C.14d
JJH11
Garnet B

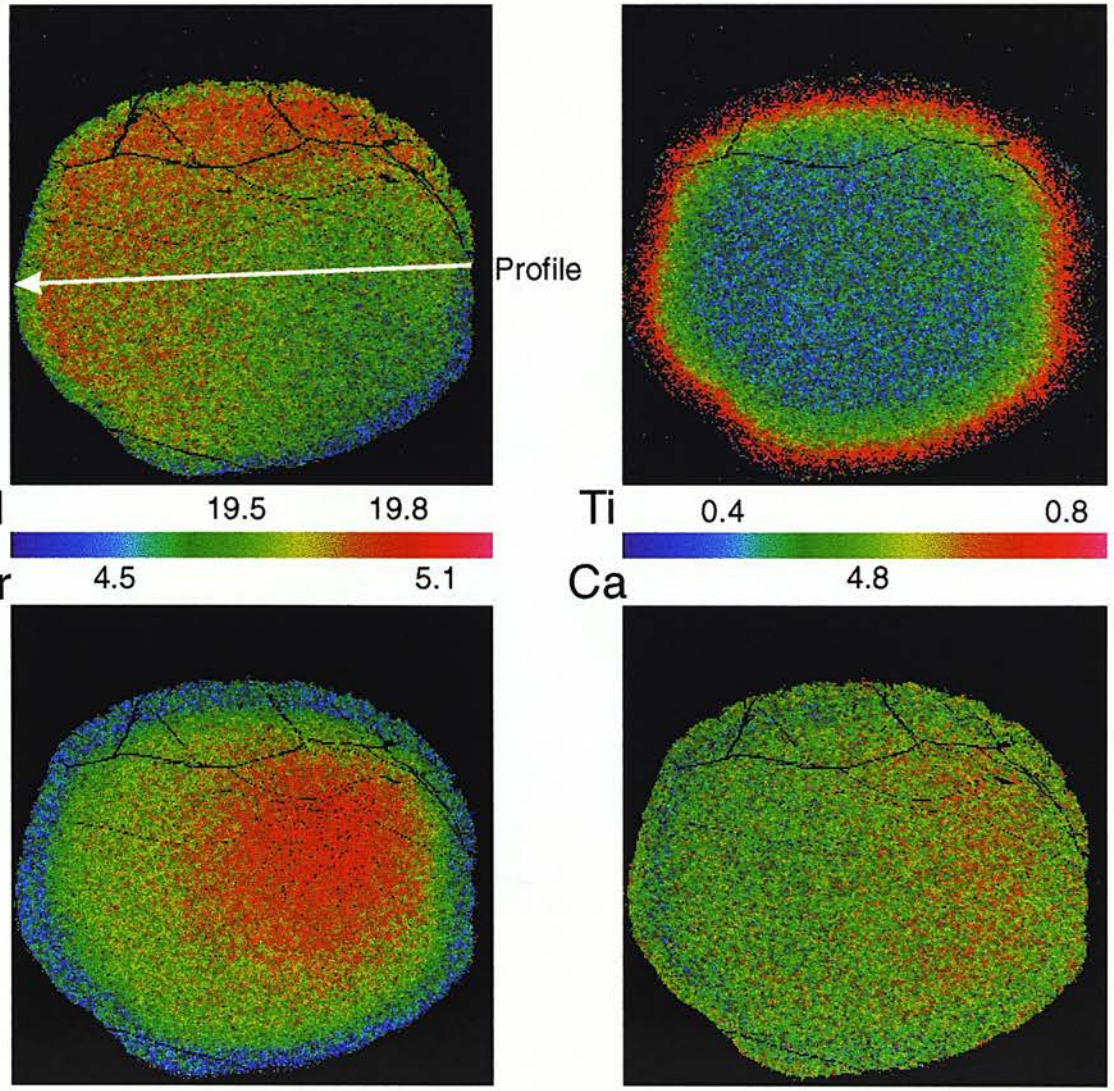

Fig. C.15a JJH19 -1

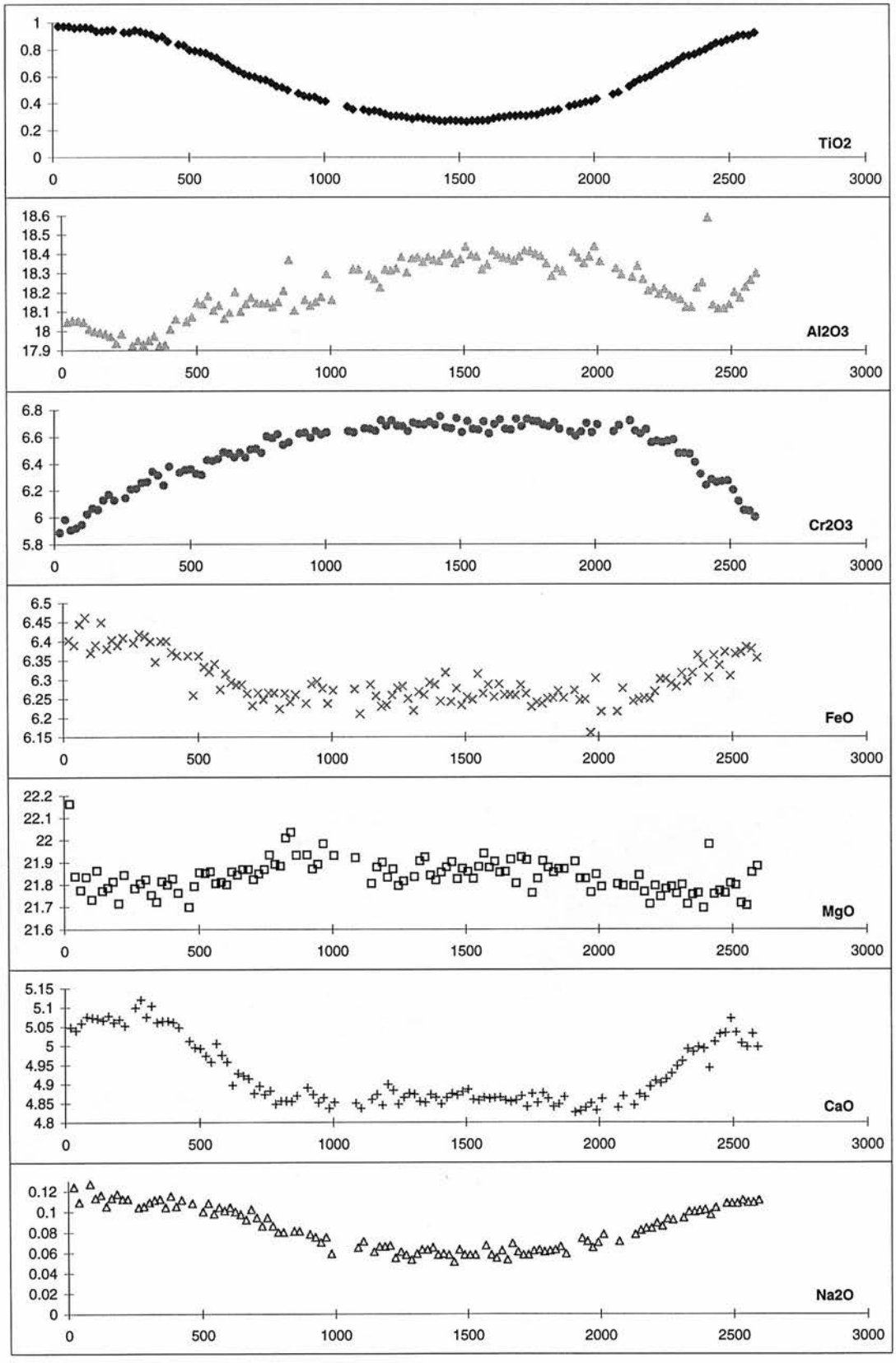

H:\j5run33.xls

Fig. C.15b JJH19 -2

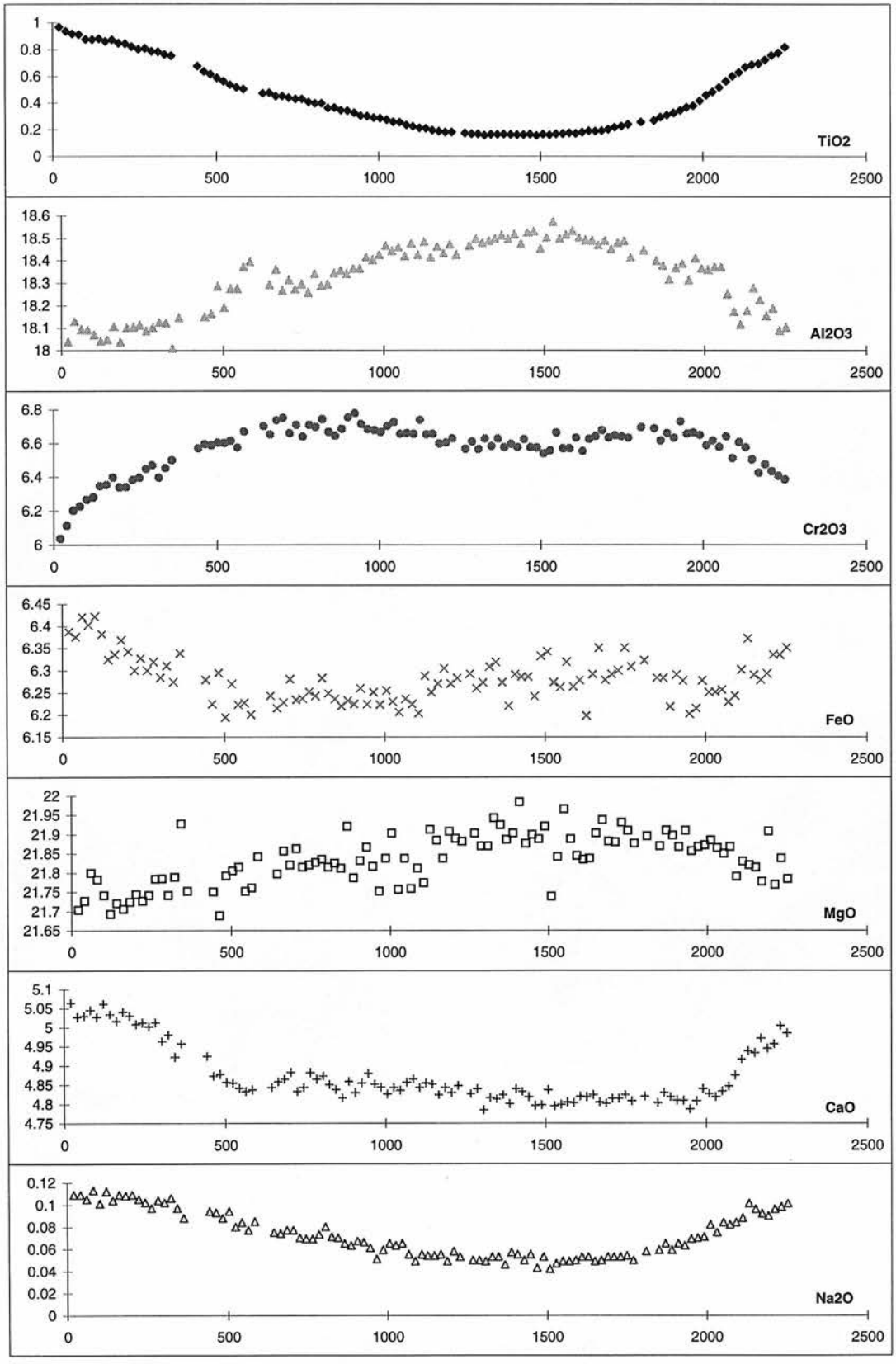

H:\j5run34.xls

Fig. C.15c
JJH19

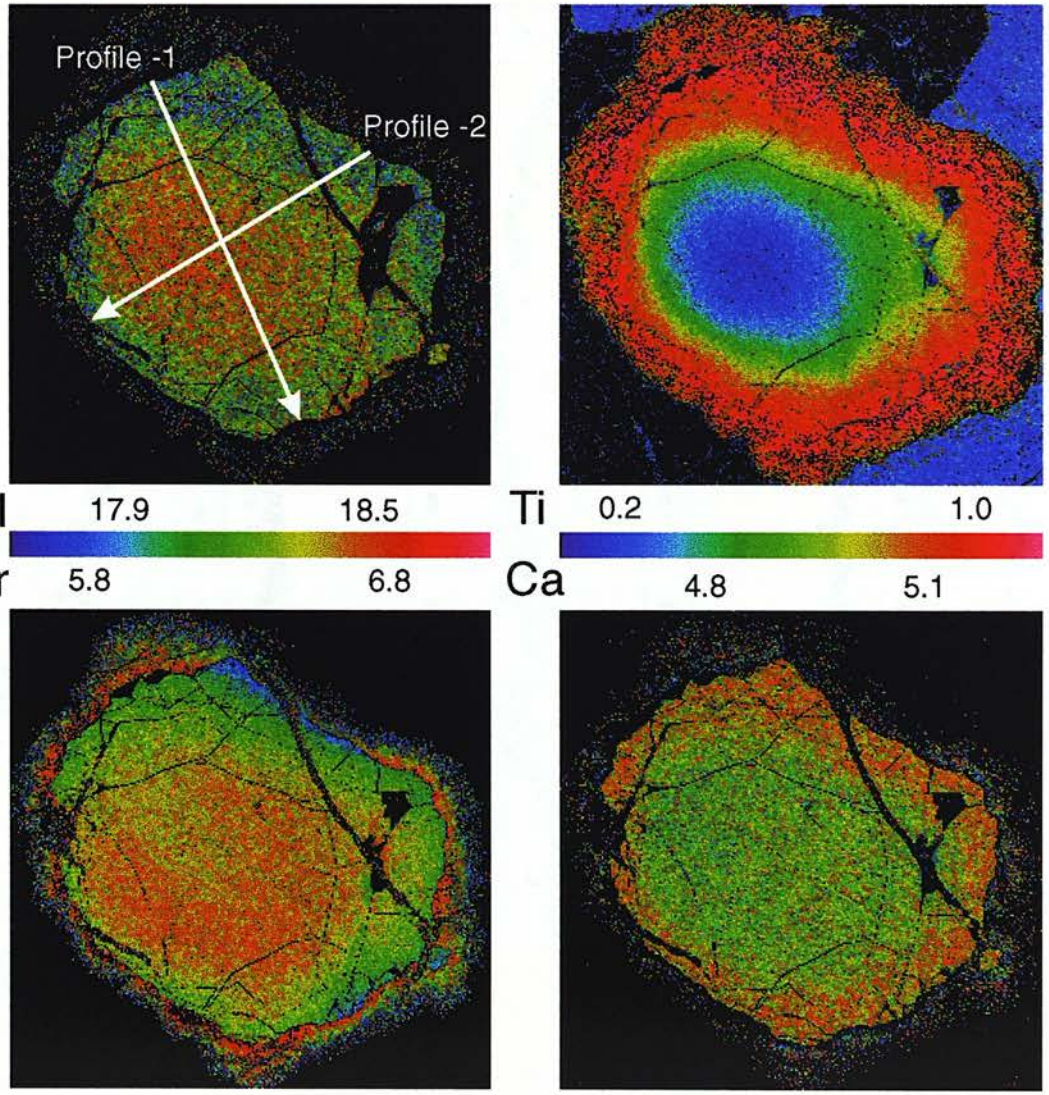

Fig. C.16a JJH37 Garnet A

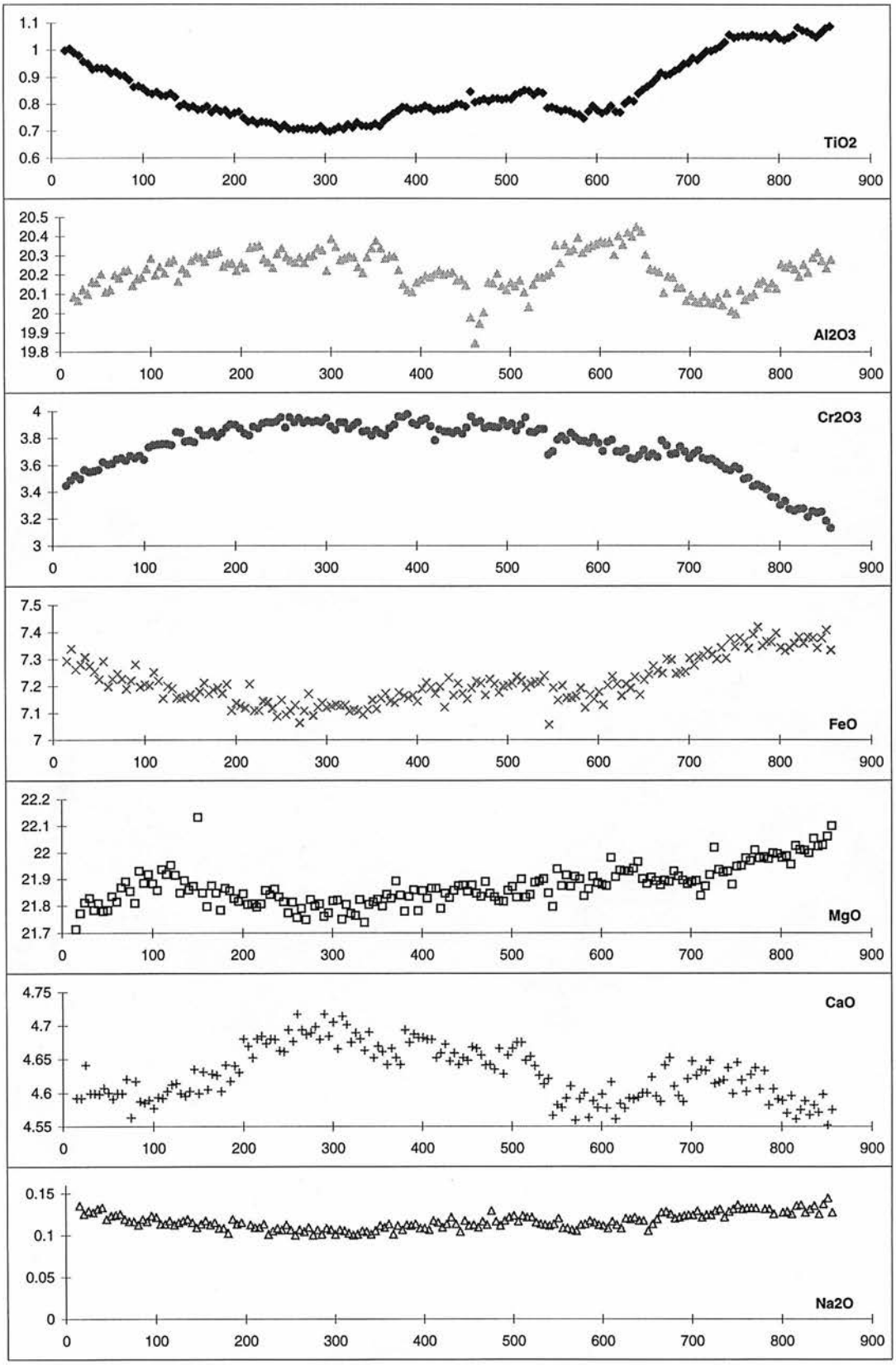

H:\j5run35.xls

Fig. C.16b
JJH37
Garnet A

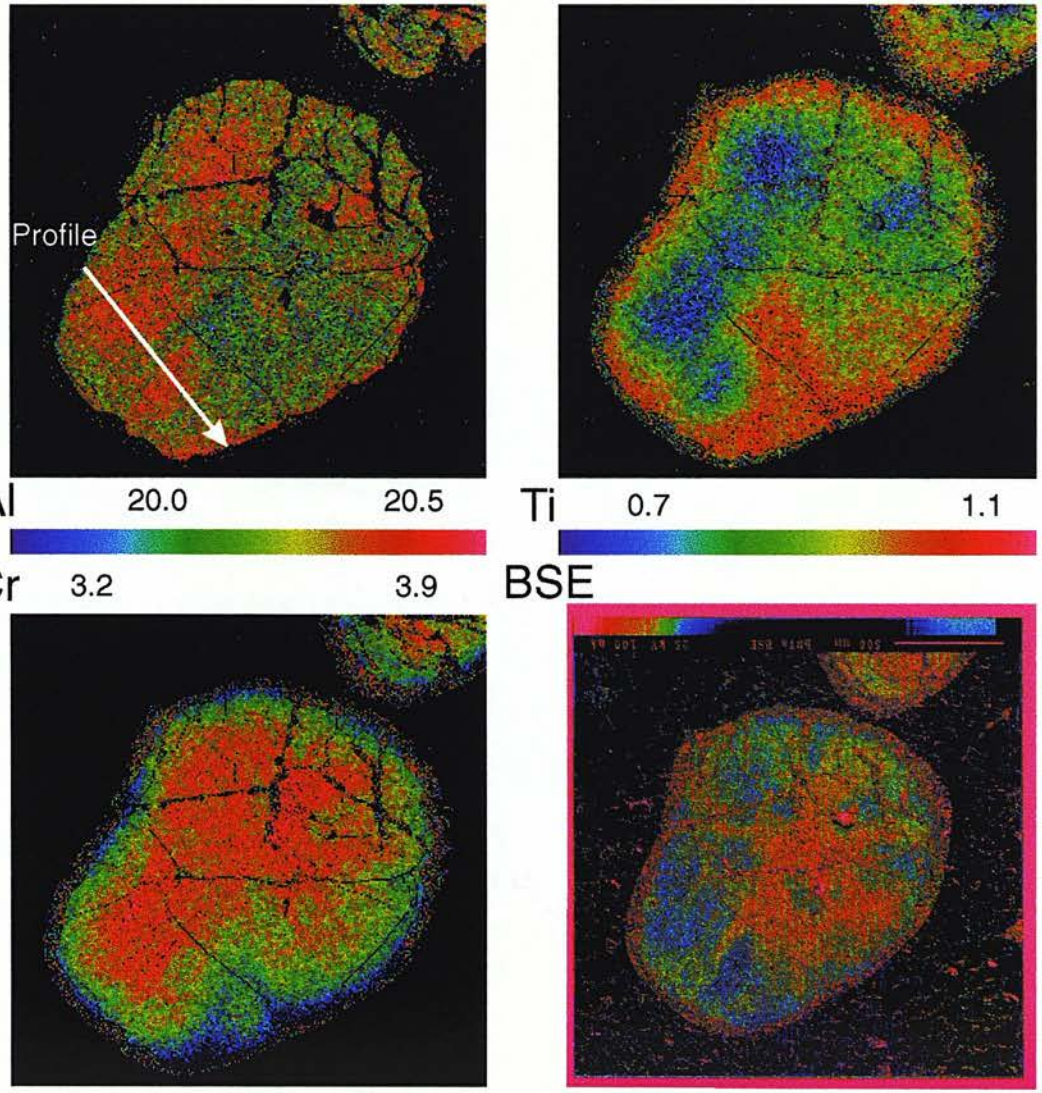

Fig. C.17a JJH37 GarnetB -1

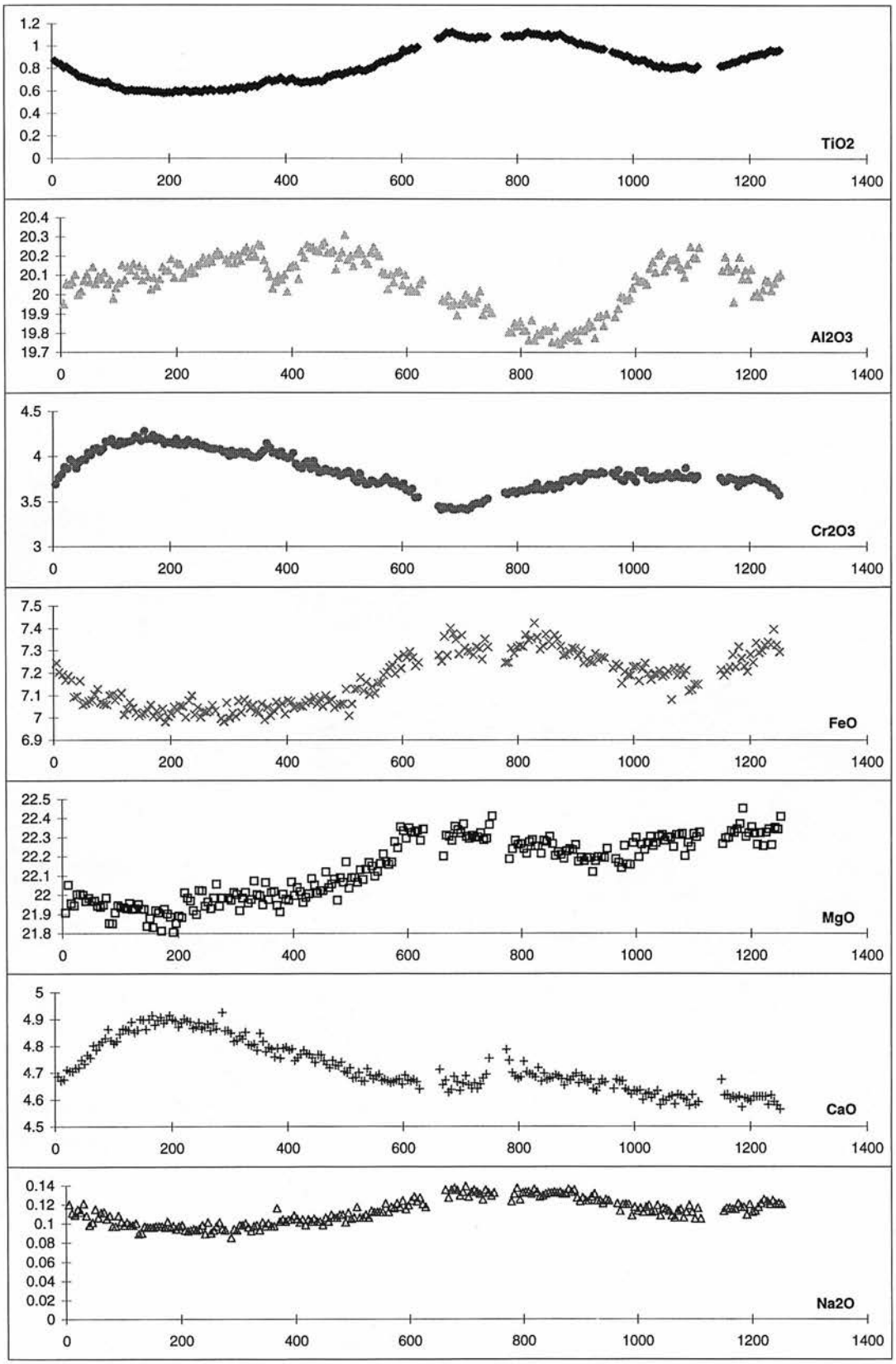

H:\j5m37.xls

Fig. C.17b JJH37 GarnetB -2

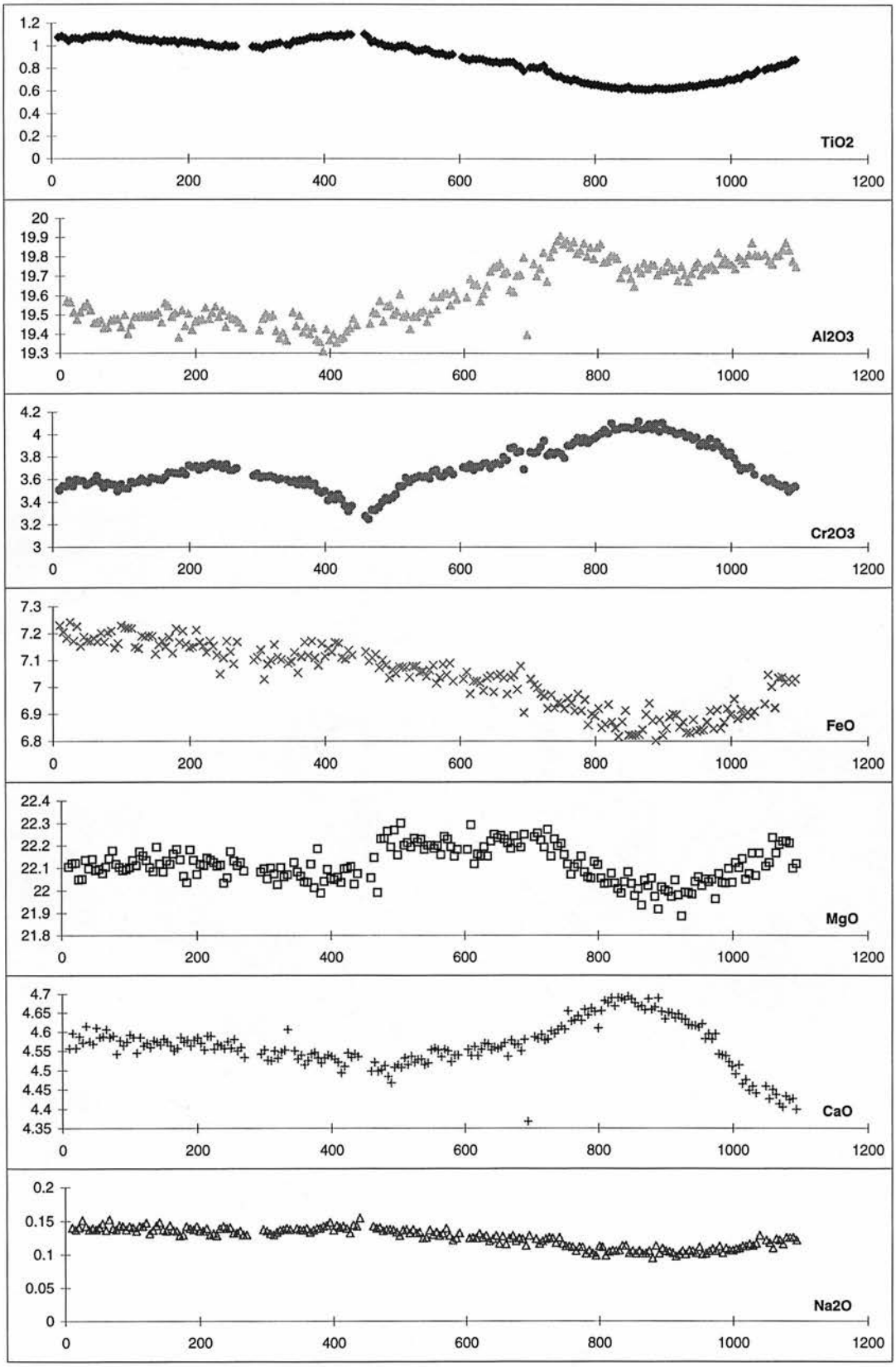

h:\j5rn38.xls

Fig. C.17c
JJH37
Garnet B

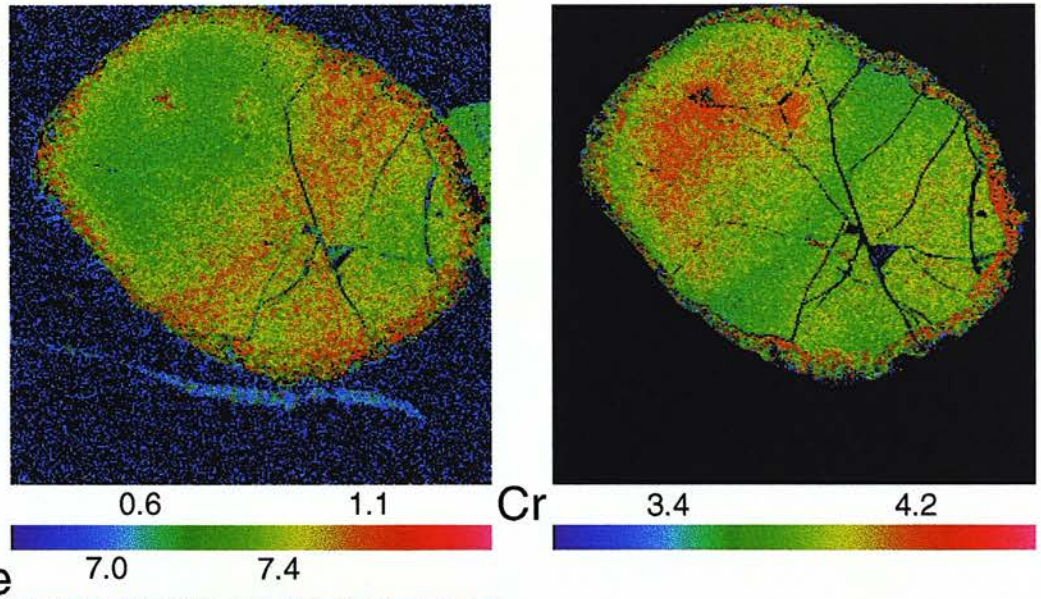

Fig. C.18a JJH37 GarnetC

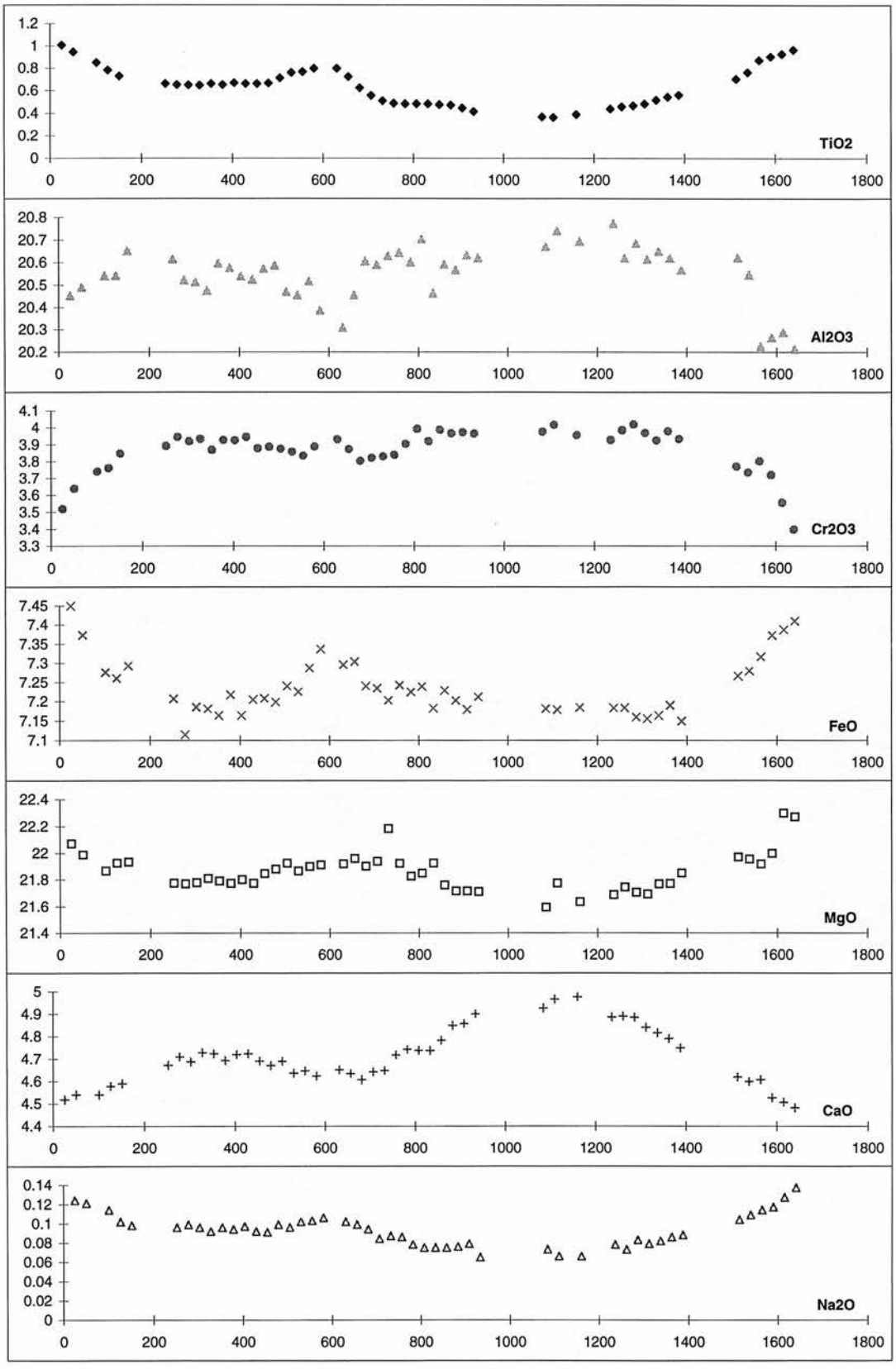

jag12r5.xls

Fig. C.18b
JJH37
Garnet C

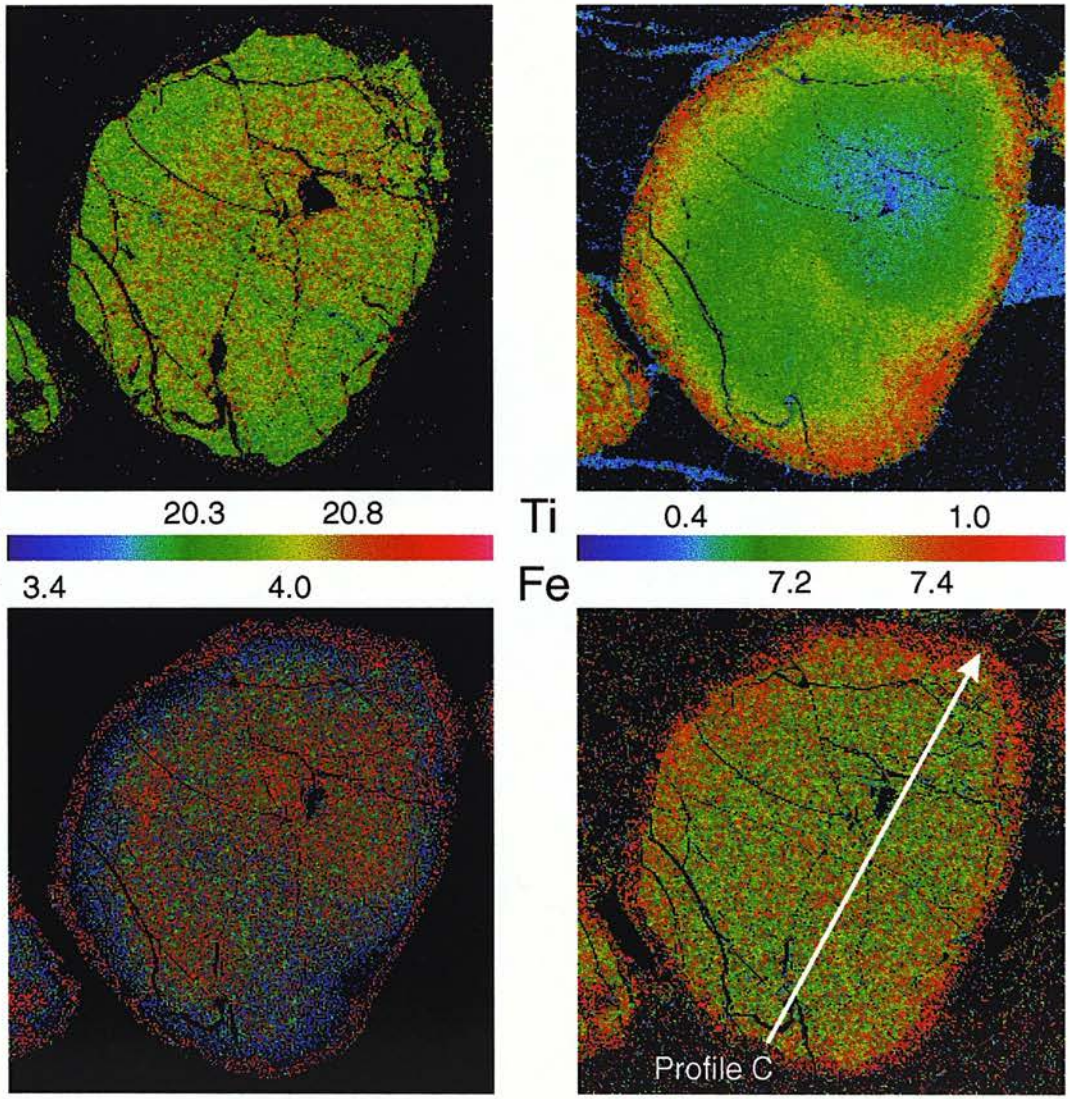

Fig. C.19a JJH37 GarnetD

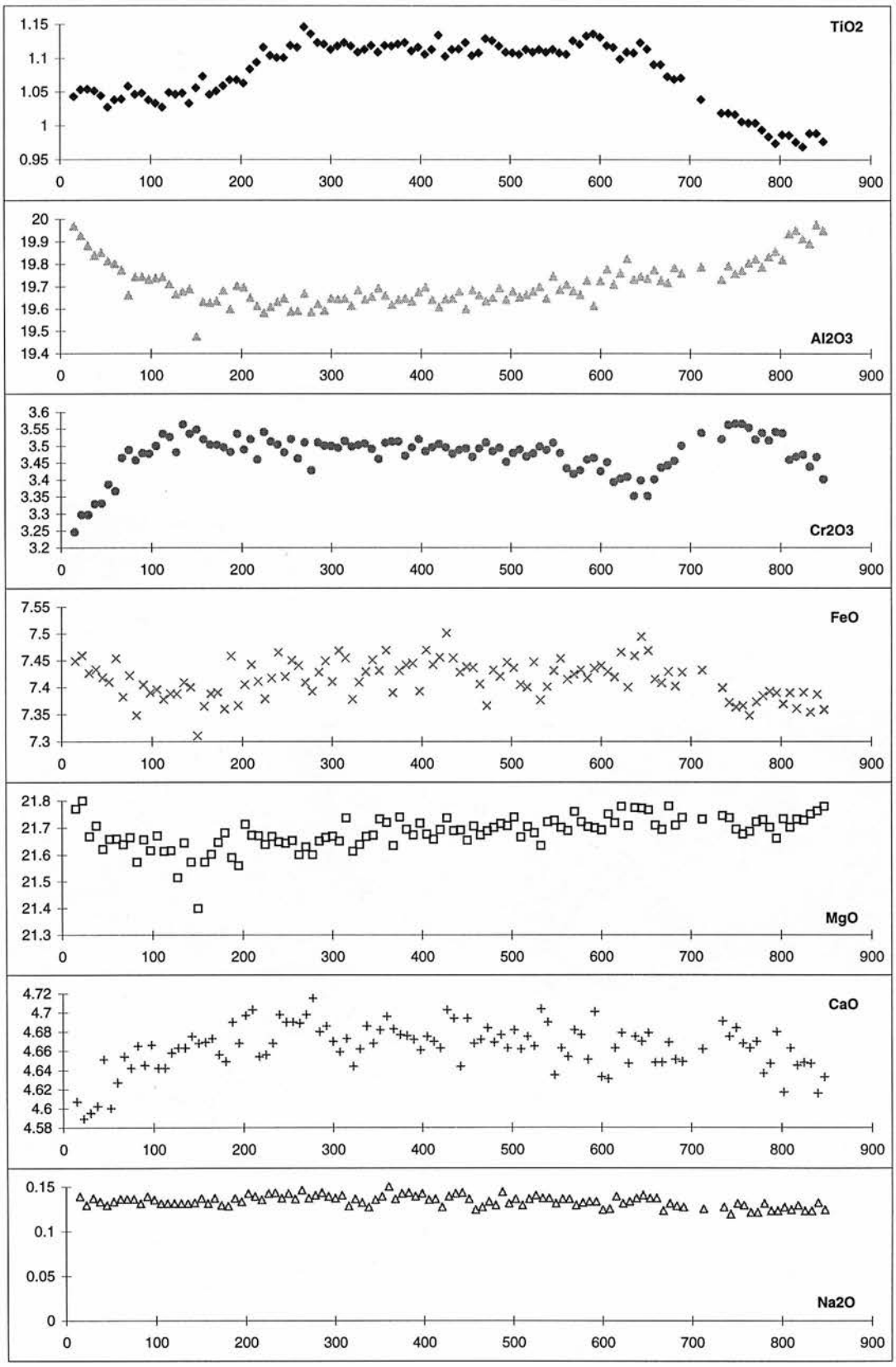

Fig. C.19b
JJH37
Garnet D

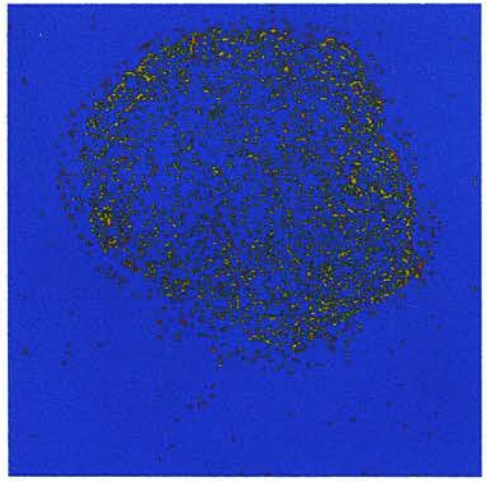

Al 19.6 20.0

Cr 3.3 3.5

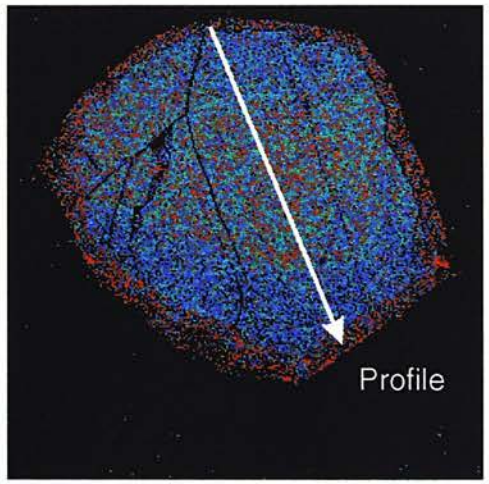

Ti 1.0 1.1

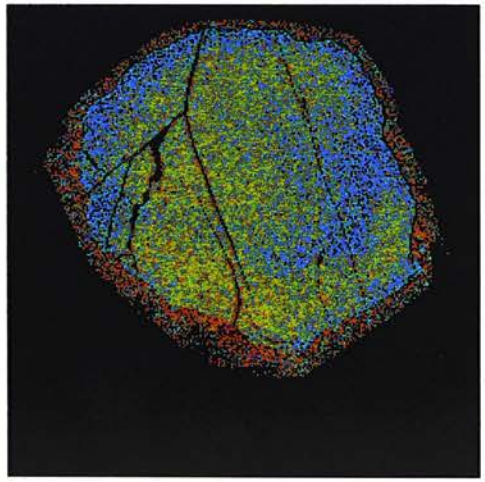

1mm

Fig. C.20a JJH37 GarnetE

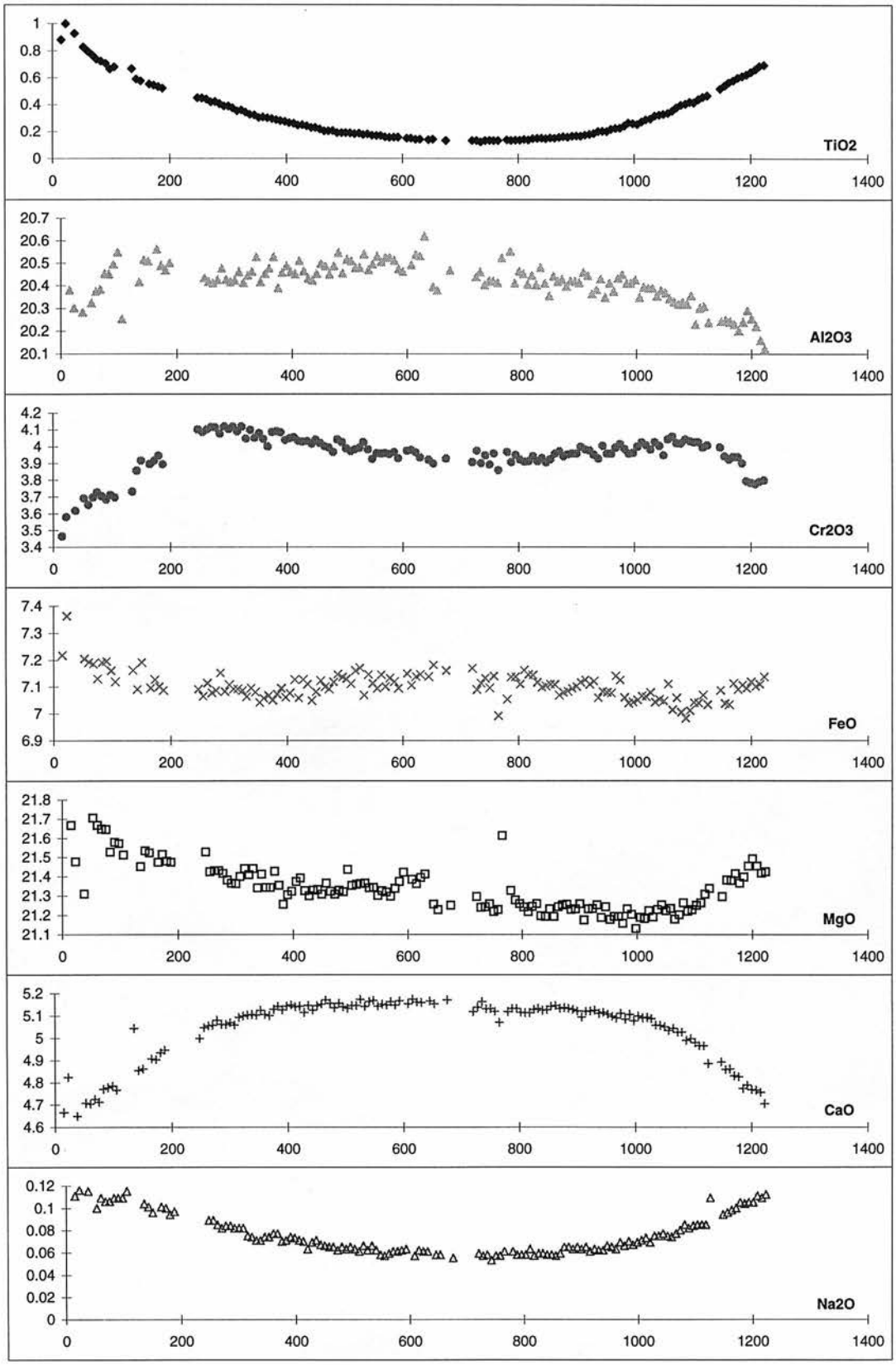

H:\jag8run2.xls

Fig. C.20b
JJH37
Garnet E

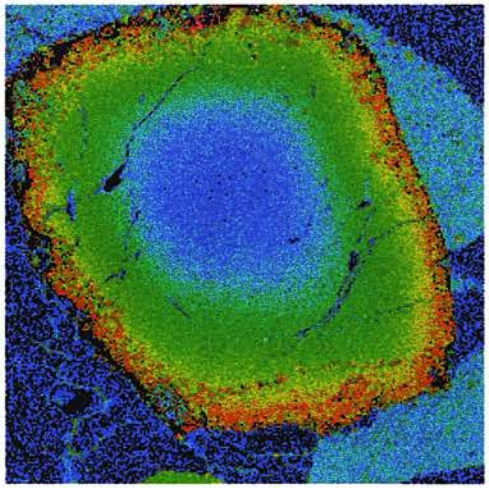

Ti 0.1 1.0

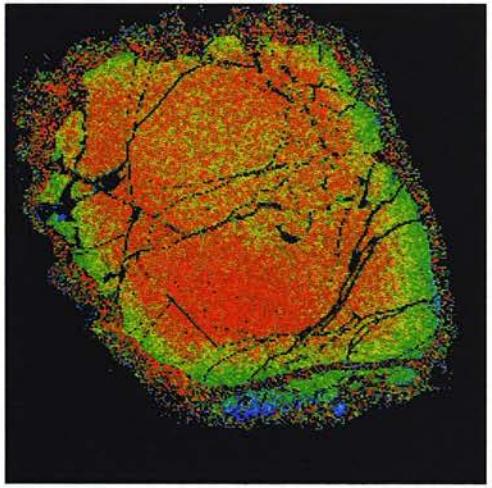

Cr 3.4 4.1

Ca 4.6 5.1

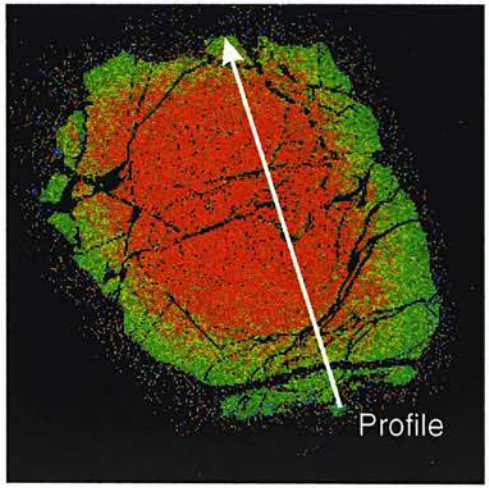

1mm

Fig. C.21a JJH37 Garnet F

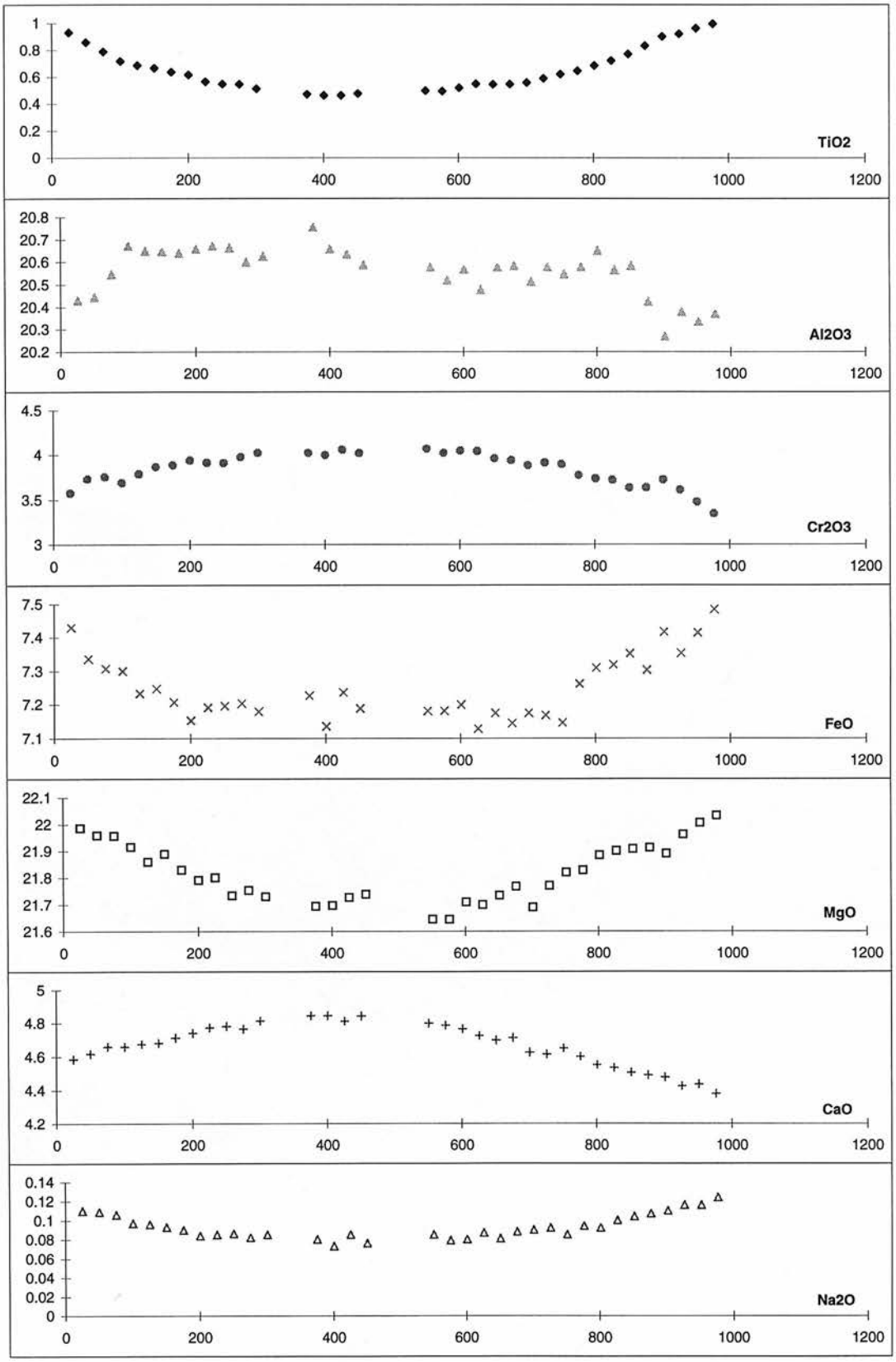

H:\jag12r6.xls

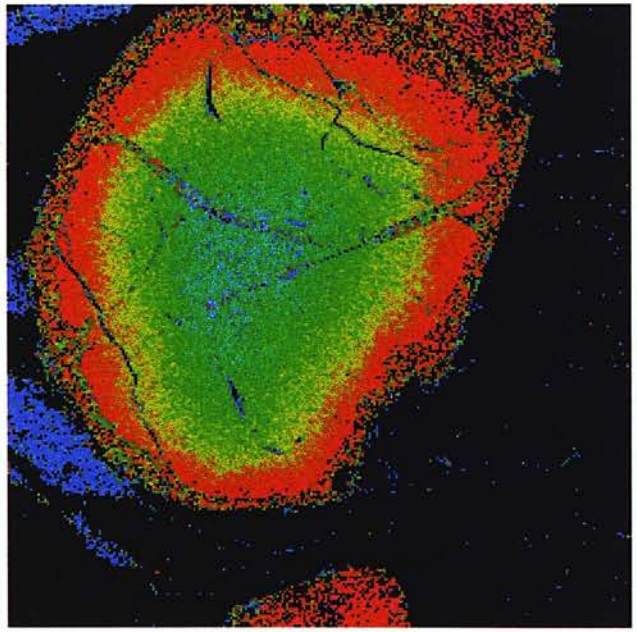

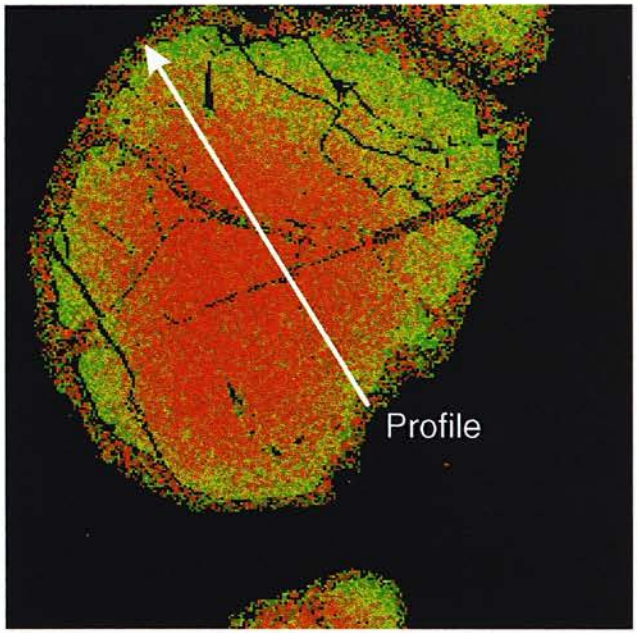

Ti

0.5 1.0

Cr

3.3 4.0

Fig. C.21b
JJH37
Garnet F

1mm

Fig. C.22a JJH37 Garnet G

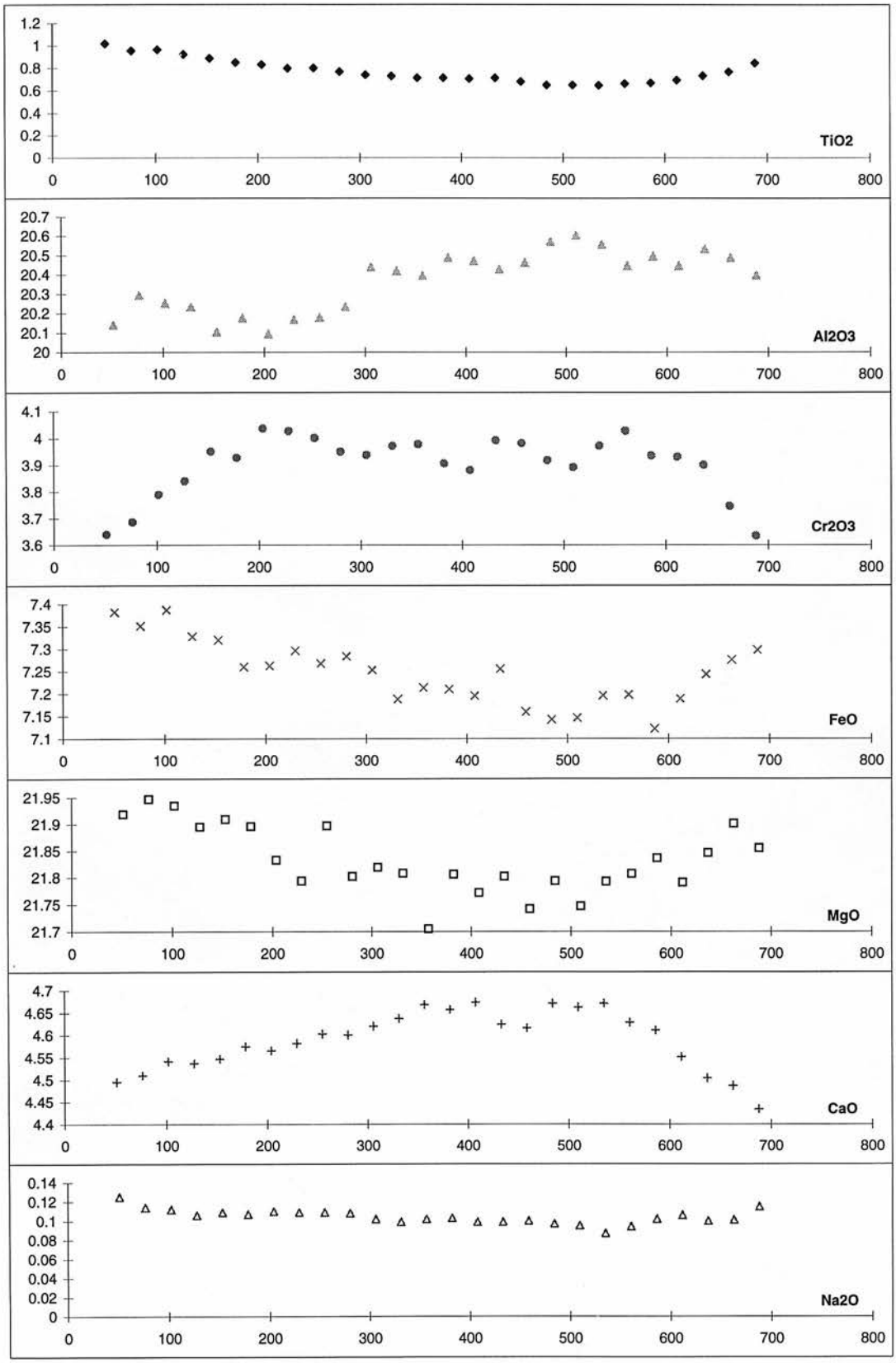

H:\jag12r7.xls

Fig. C.22b
JJH37
Garnet G

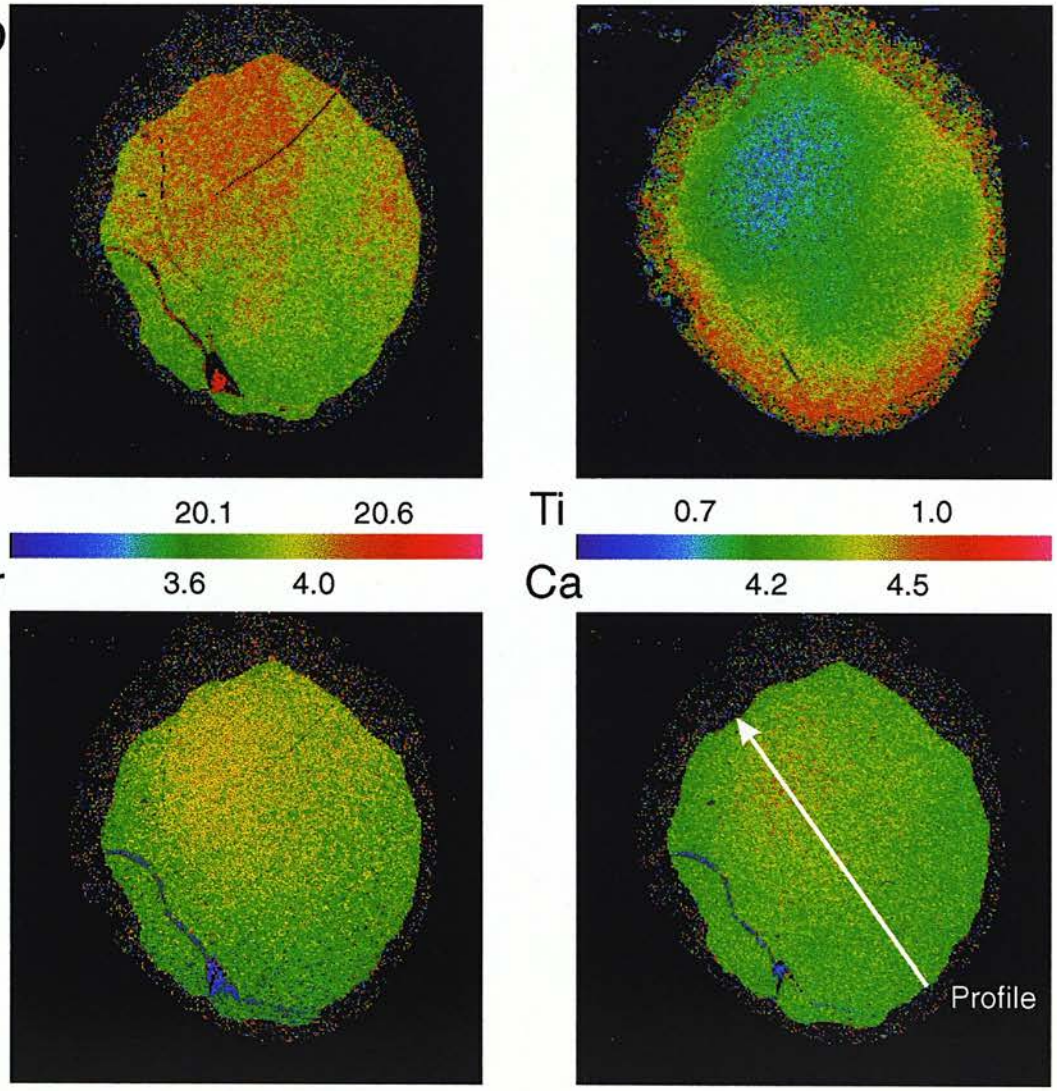

Fig. C.23a JJH37 GarnetH

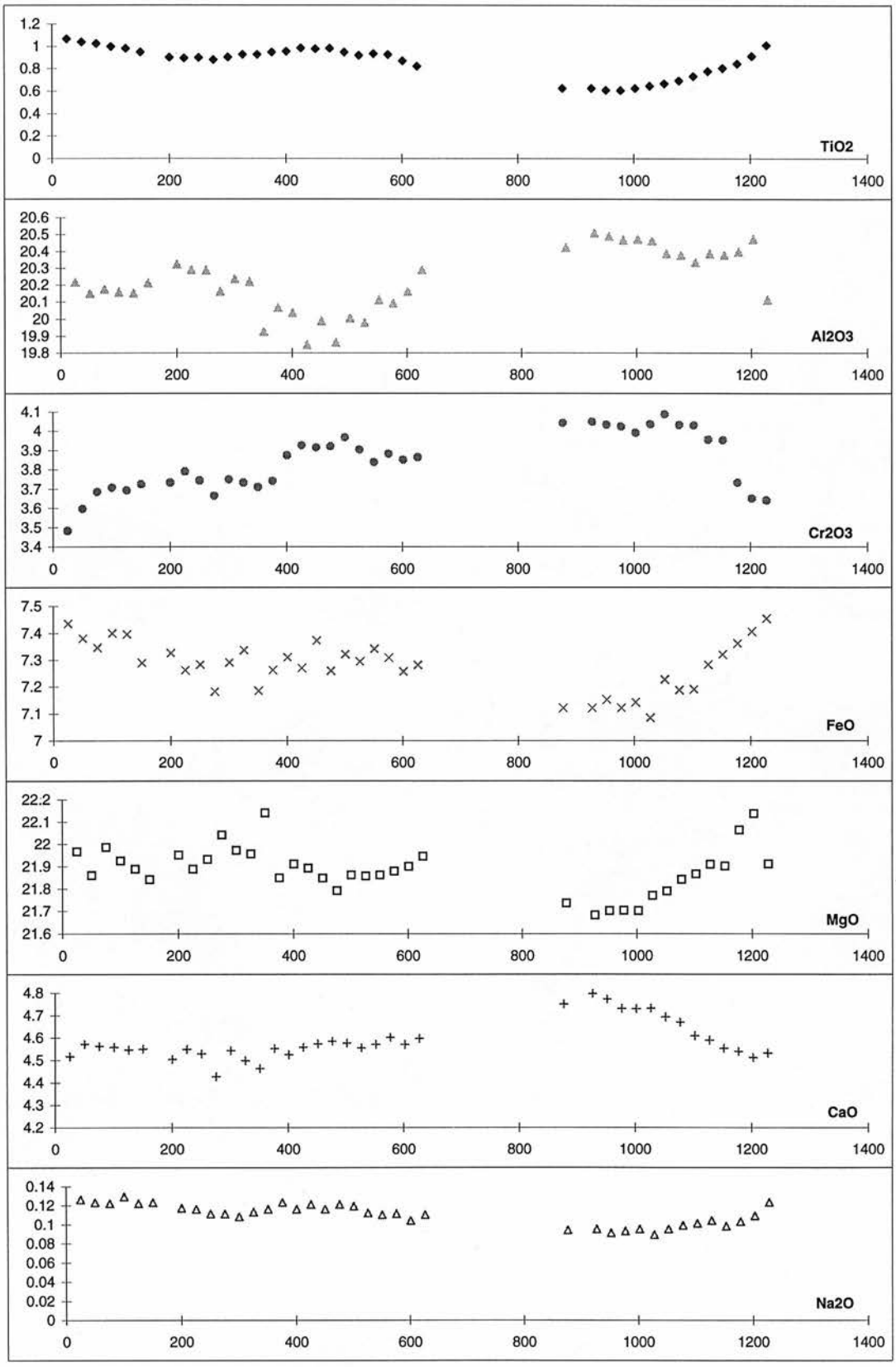

H:\jag12r8.xls

Fig. C.23b
JJH37
Garnet H

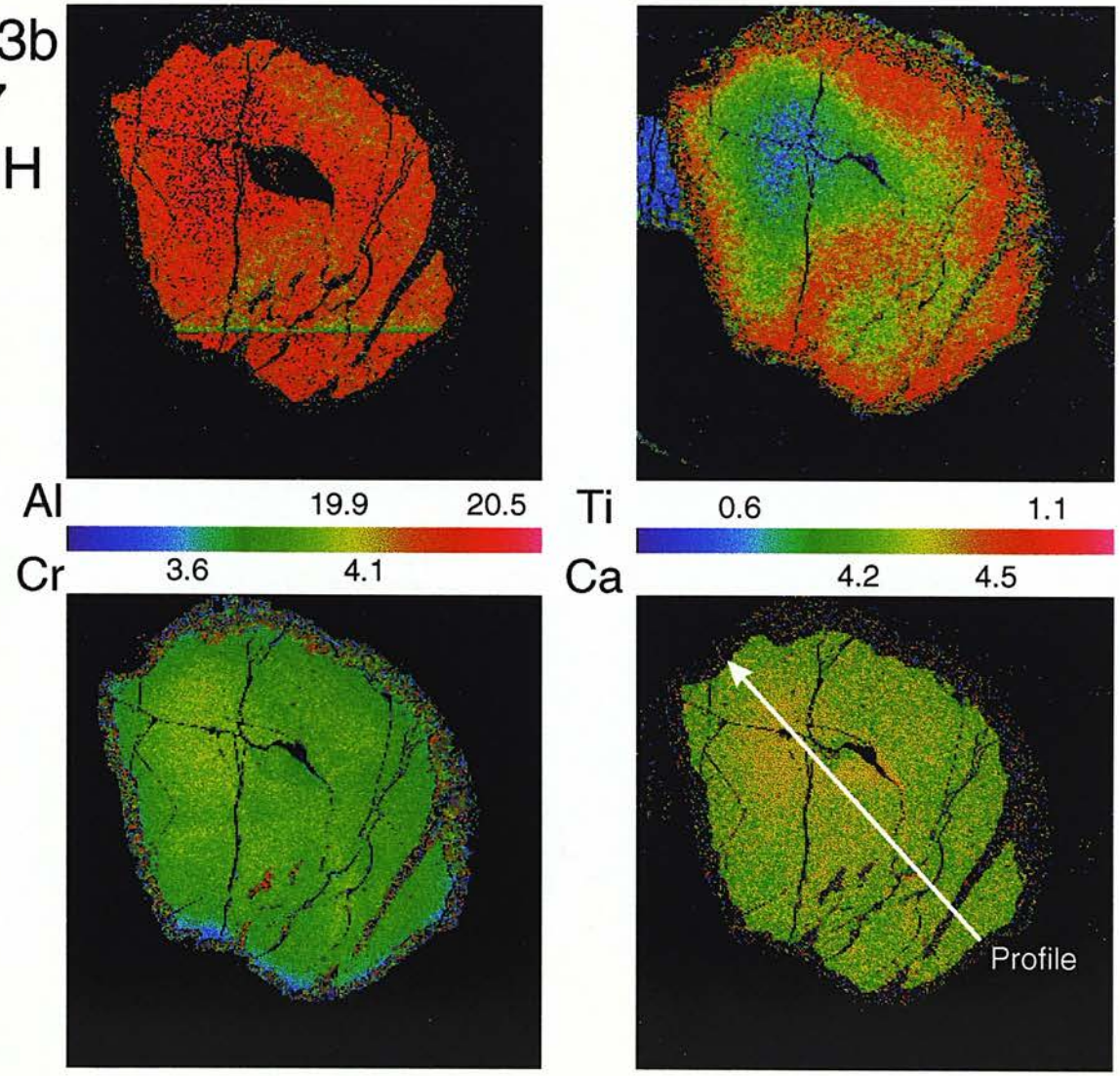

Fig. C.24a JJH37 Garnet I

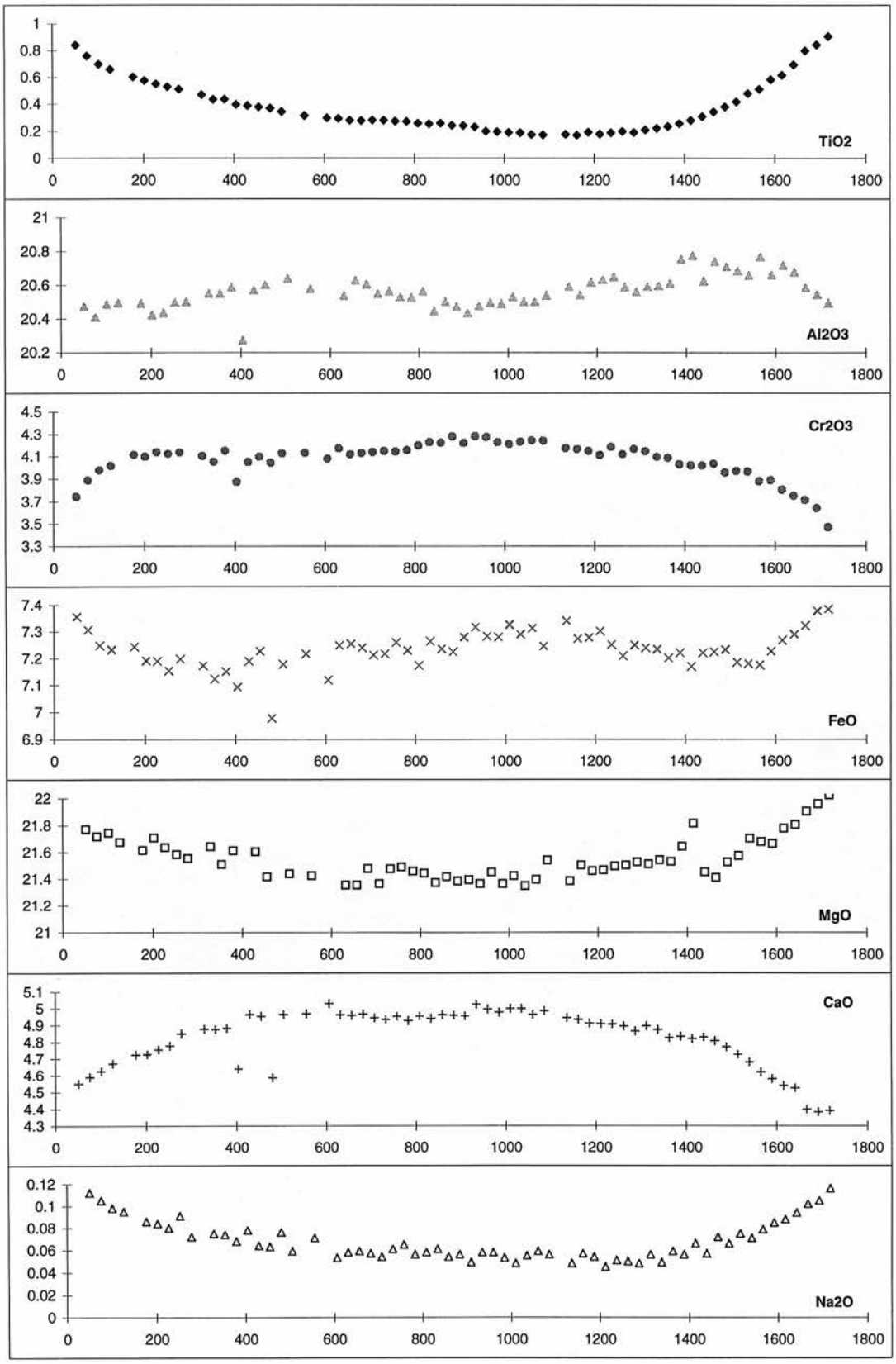

H:\jag12r9.xls

Fig. C.24b
JJH37
Garnet I

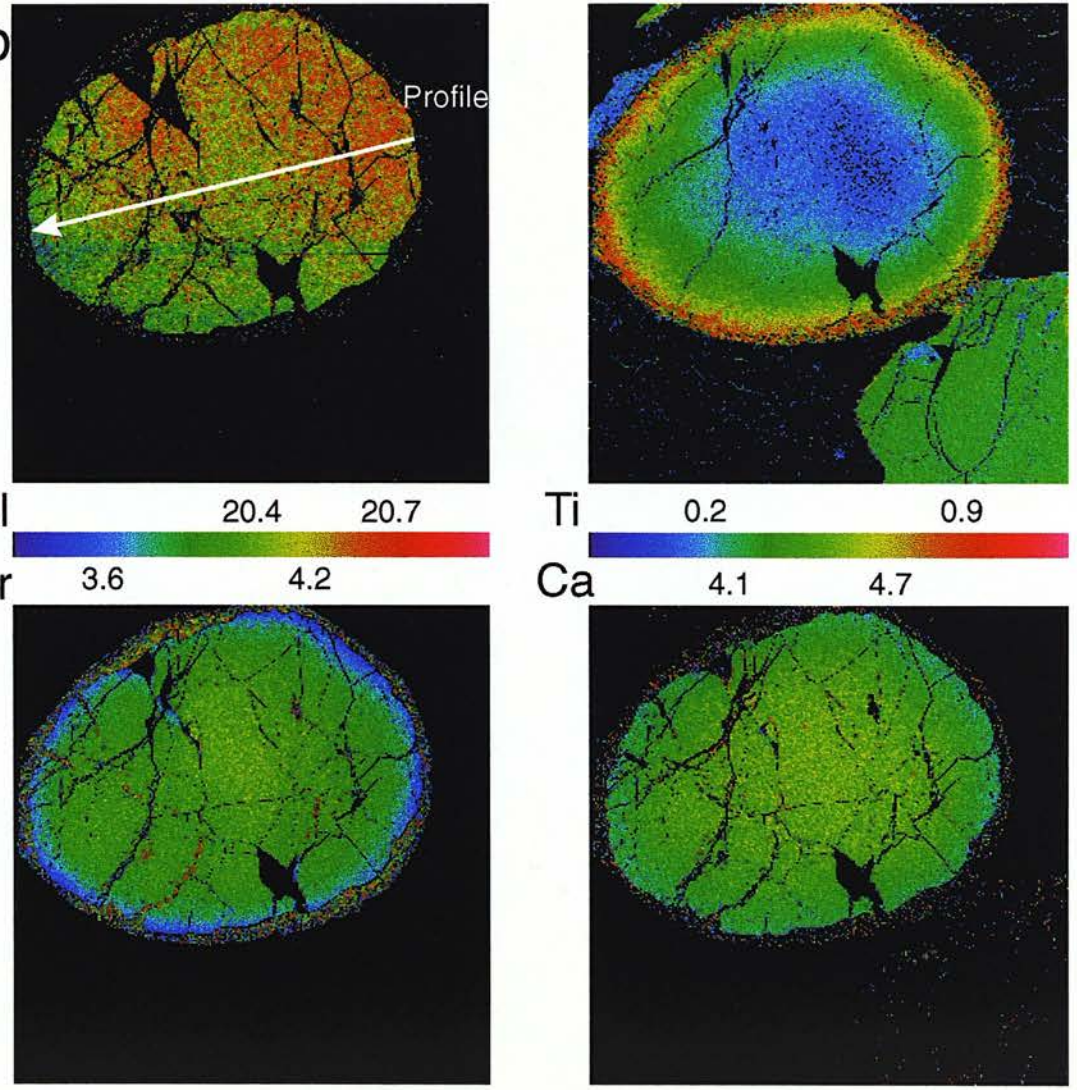

Fig. C.25a J146

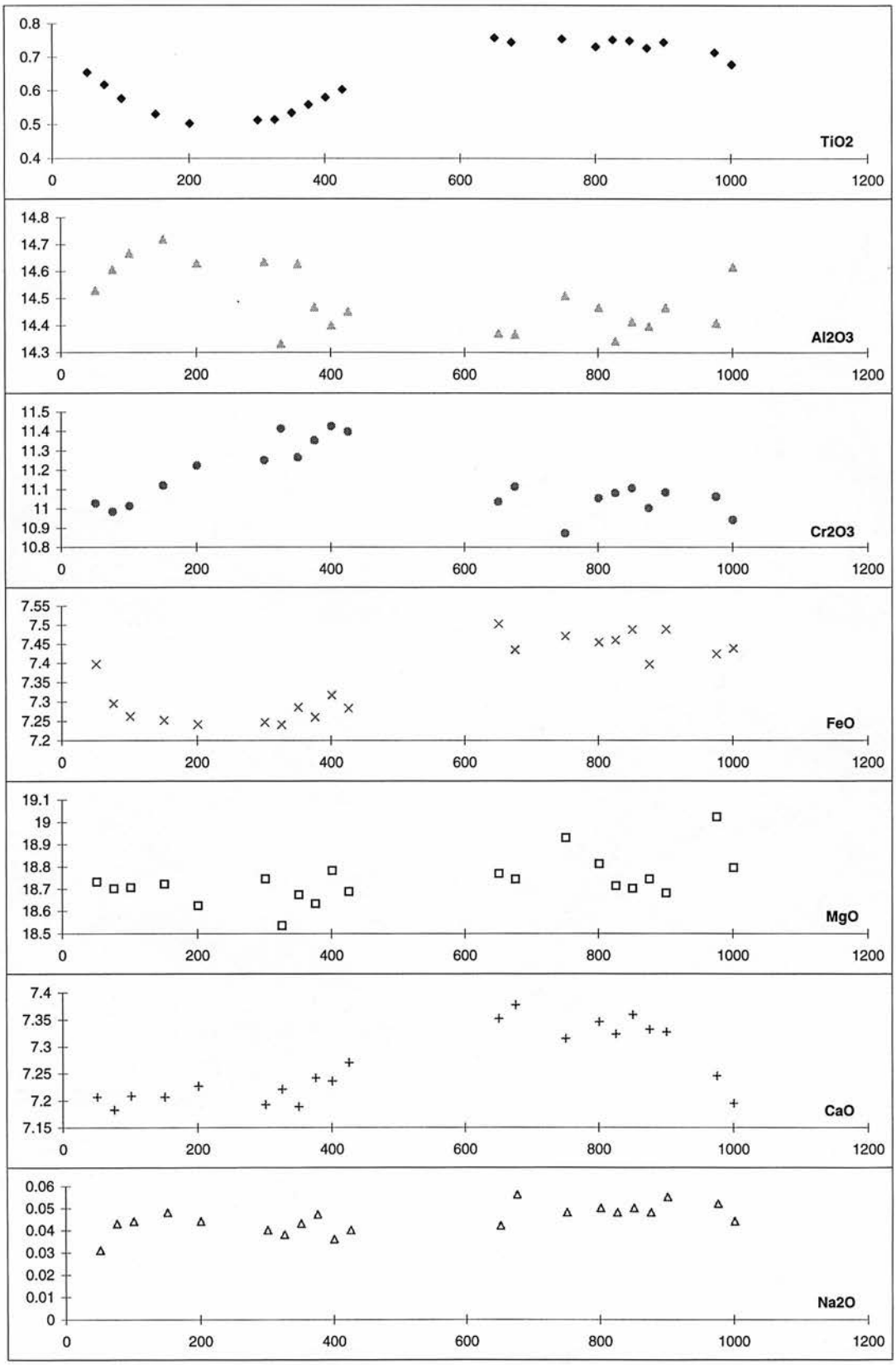

Fig. C.25b
J146

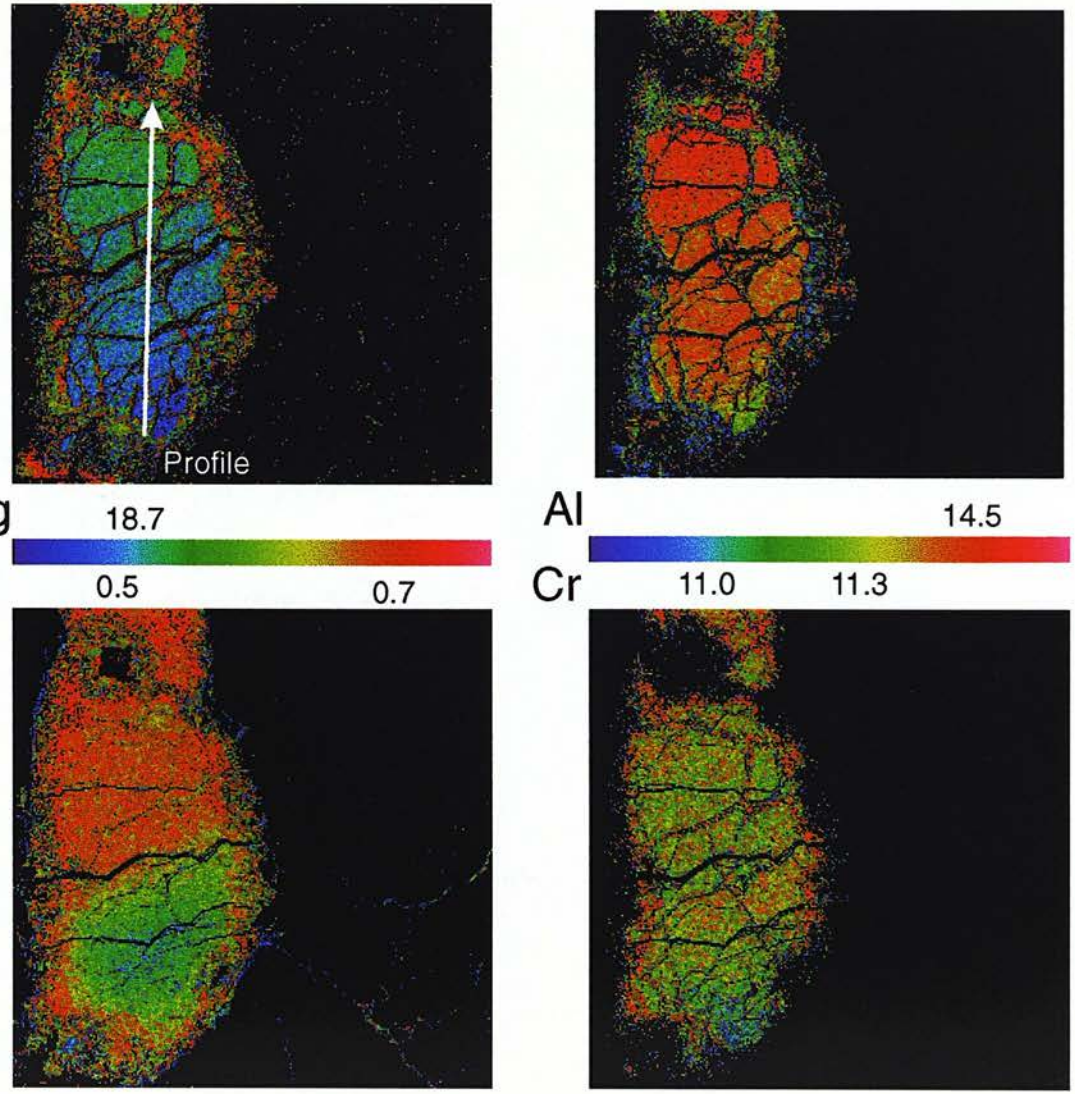

Fig. C.26a JJG1728 -1

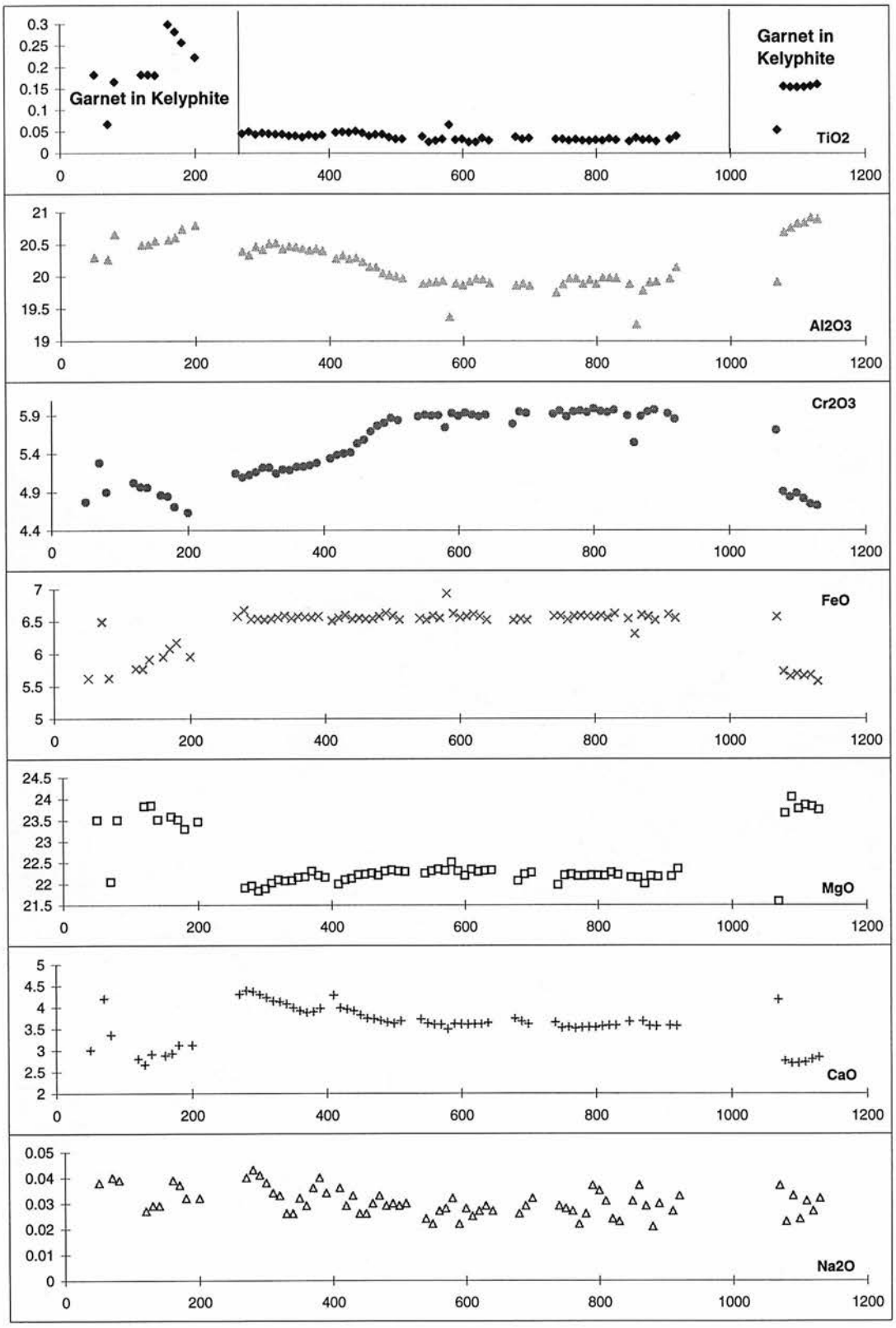

H:\jag12r13.xls

Fig. C.26b JJG1728 -2

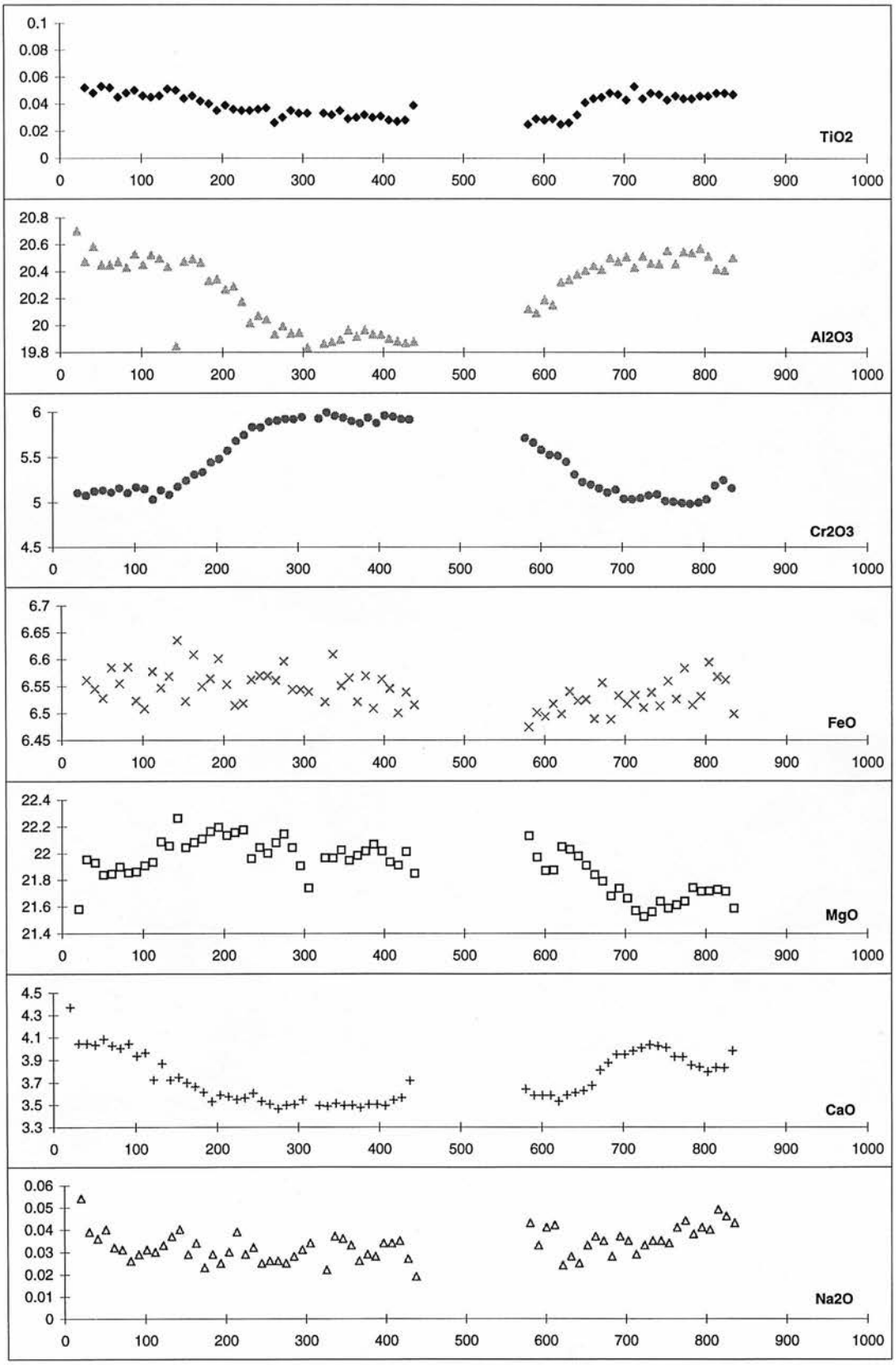

H:\jag12r14.xls

Fig. C.26c
JJG 1728

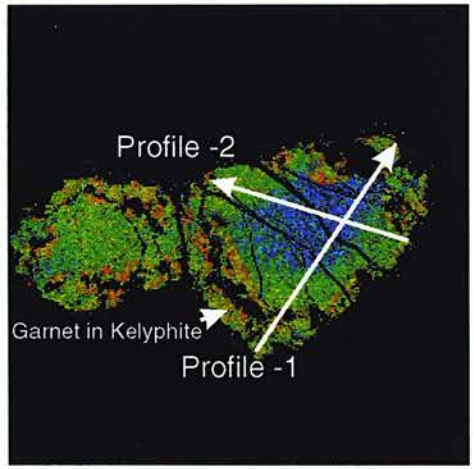

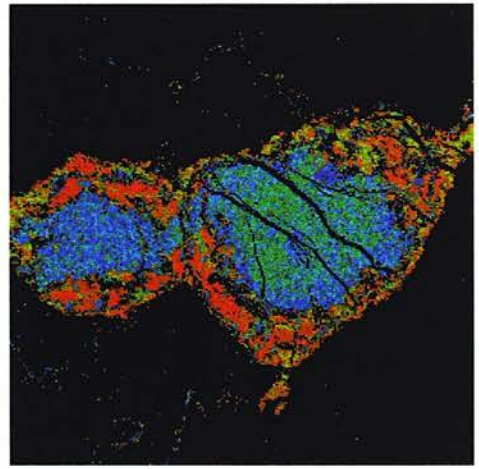

Al 19.7 20.4

Mg 22.1 22.5

Cr 5.1 6.1

Ca 3.7 4.2

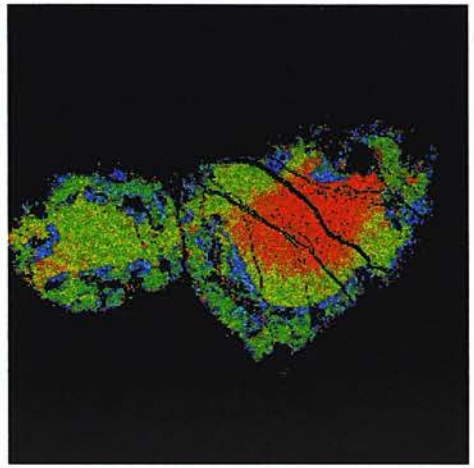

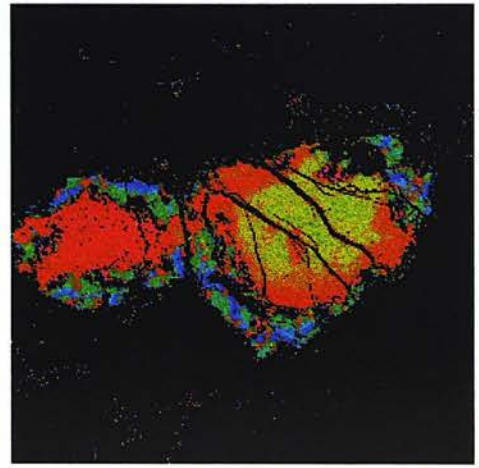

1mm

Fig. C.27a JJG2469 Garnet A

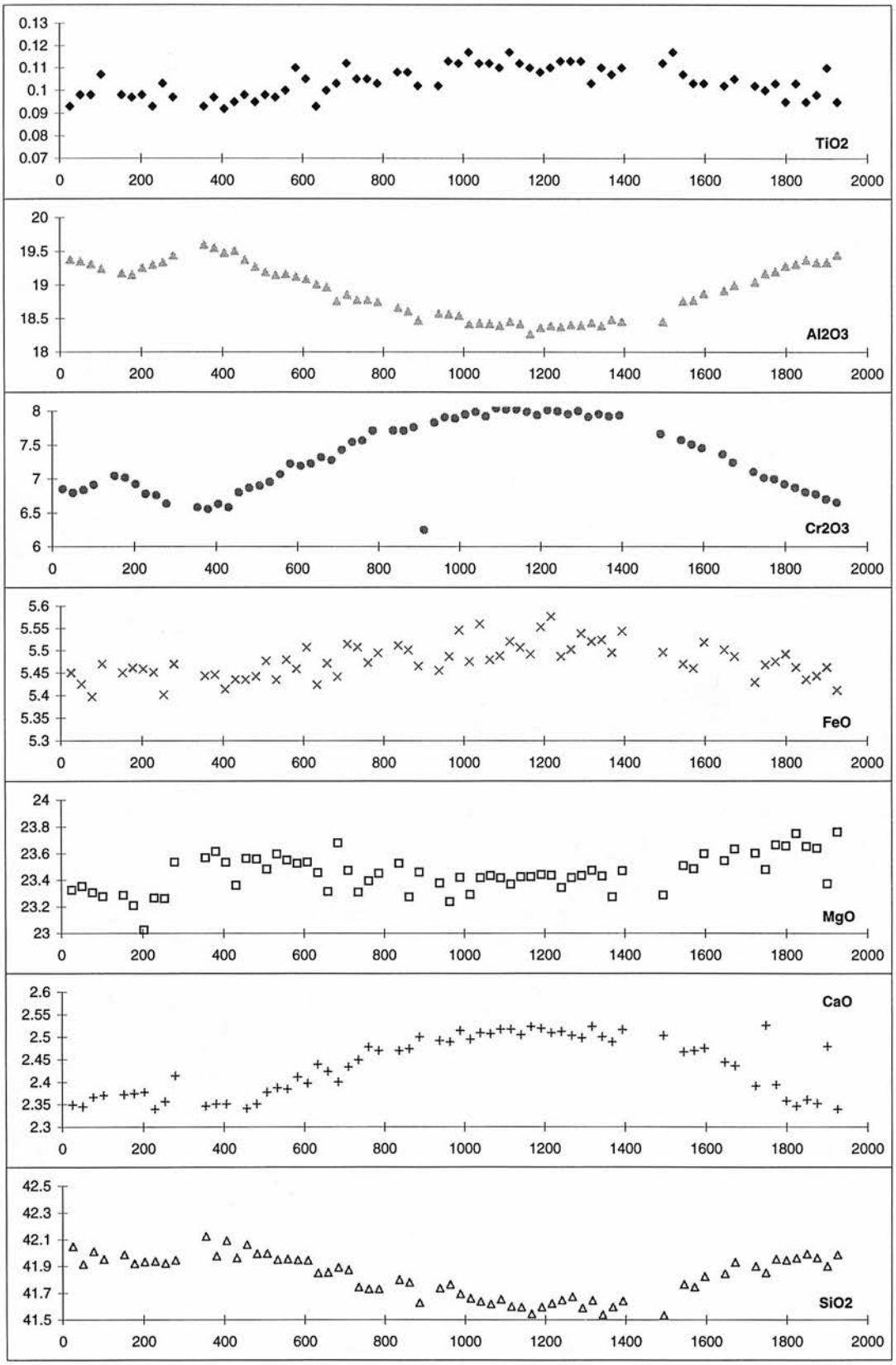

H:\j5rn22.xls

Fig. C.27b JJG2469 Garnet B

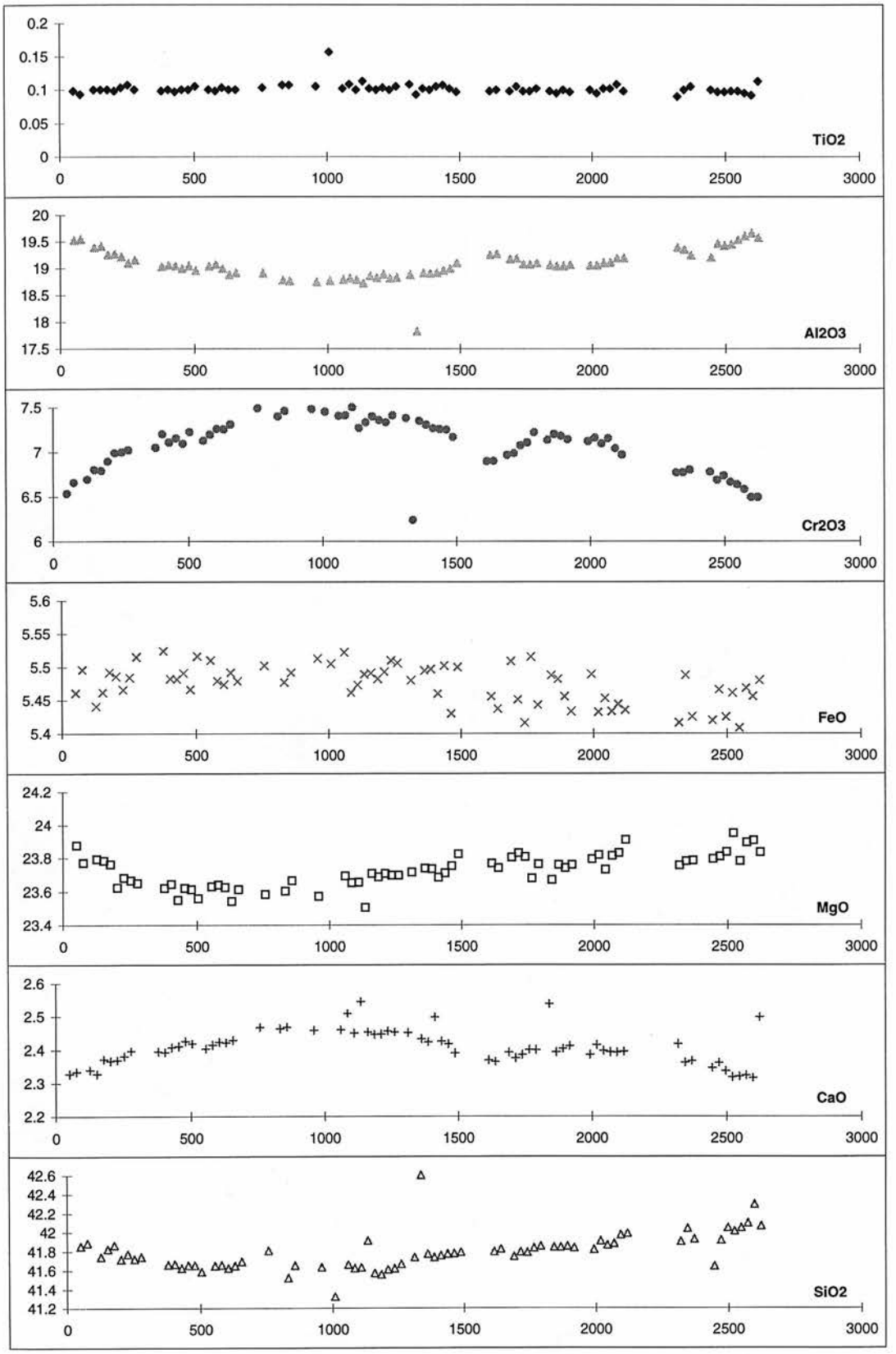

H:\j5rn23.xls

Appendix D

Ion Probe Trace Element Analysis

	September_94	January_96
Primary Beam Polarity	Negative	Negative
Primary Ion Beam	O-	O-
Accelerating Voltage	10kV	10kV
Beam Current	8nA	15nA
Secondary Beam Polarity	Positive	Positive
Offset	~78V	~78V
Energy Window	±19eV	±19eV
No of Cycles	10	8
Count time per cycle	5s (10s for Nb, Ce, Nd, Sm, Eu)	5s
Deadtime	32ns	14ns

Table AD.1 Ion probe operating conditions for trace element analysis sessions in September 1994 and January 1996.

Element	Mass	Interference	Notes
Si	30		Ratio Mass
Fe + Si	84		Correction for Fe + Si combinations on Rb
Rb	85	Fe + Si	
Sr	88		
Y	89		
Zr	90		
Nb	93	Zr + H	
Zr + H	95		Correction for Zr + H on Nb
	130.5		Background measurement
Ba	138		
La	139		
Ce	140		
Nd	143		
Sm	149		
Eu	151	BaO	If 151 or 153 Eu measured only, BaO calculated as fixed ratio
	153	BaO	If both measured BaO calculated by simultaneous equations
BaO	154		Major BaO mass
Gd	156	CeO	Used for Ce/CeO calculation
	157	PrO	
	158	CeO + NdO	
Tb	159	NdO	
Dy	161	NdO	
Ho	165	SmO	
Er	167	EuO	
Yb	172	GdO	
Lu	175	TbO	
Pb	208		

Table AD2. Mass peaks measured during trace element ion probe analysis. Not all peaks were measured during each session, for example when Pr was measured Gd was measured on 157Gd otherwise measurement was on 158Gd. Masses used for determining mass interferences are also given.

Table AD.3 Analysis of Trace Element Garnet Standard GDD1

	Rb	Sr	Y	Zr	Nb	Ba	La	Ce	Pr	Nd	Sm	Eu	Gd	Tb	Dy	Ho	Er	Yb	Lu
GDD11	0.09	0.19	43.75	40.79	N.D.	0.16	0.02	0.15	0.06	0.69	0.68	0.47	2.60	0.75	6.55	1.96	6.72	9.54	1.70
GDD12	0.11	0.19	44.55	40.31	N.D.	0.32	0.01	0.13	0.07	0.63	0.88	0.45	2.39	0.69	6.83	1.93	6.94	9.16	1.55
GDD13	0.06	0.20	44.43	40.25	N.D.	0.03	0.02	0.13	0.06	0.74	0.88	0.44	2.65	0.74	6.64	1.84	6.72	8.87	1.65
GDD14	0.12	0.21	44.28	39.60	N.D.	0.46	0.02	0.15	0.06	0.76	0.77	0.47	2.53	0.72	6.62	1.87	6.82	9.02	1.58
GDD15	0.11	0.21	44.74	39.64	N.D.	0.42	0.00	0.15	0.05	0.67	0.77	0.46	2.52	0.77	7.22	1.84	7.20	9.64	1.70
GDD16	N.D.	0.19	44.36	38.57	N.D.	0.47	0.01	0.13	0.06	0.62	0.80	0.46	2.62	0.65	6.69	1.89	6.99	8.90	1.56
GDD17	0.22	0.21	44.85	38.97	N.D.	0.40	0.02	0.14	0.06	0.67	0.76	0.49	2.49	0.74	6.87	1.84	7.11	9.58	1.71
GDD18	0.30	0.21	45.94	42.13	N.D.	0.53	0.02	0.15	0.06	0.86	0.85	0.50	2.66	0.80	7.07	2.01	7.36	10.49	1.90
GDD1 Standard Value							0.03				1.05	0.60		0.83				10.30	1.97

	GARNET									CLINOPYROXENE					
Sample No.	J25GT1 (Core)			J75GT1 (Rim)			J110G9 (Rim)			J25C1			J110C16		
Current(nA)	15			15			8			15			8		
	Abun.	% Error	Error	Abun.	% Error	Error	Abun.	% Error	Error	Abun.	% Error	Error	Abun.	% Error	Error
Rb	0.105	2.2	0.002	0.120	2.0	0.002	N.D.			N.D.			N.D.		
Sr	0.060	11.3	0.007	0.416	4.3	0.018	N.D.			319.300	0.2	0.565	81.200	0.6	0.448
Y	2.586	1.5	0.037	22.870	0.5	0.110	19.200	0.8	0.158	0.142	6.9	0.010	3.358	2.2	0.075
Zr	0.230	8.4	0.019	71.080	0.5	0.339	75.000	0.7	0.554	0.592	6.0	0.035	13.830	2.0	0.270
Nb	0.046	5.5	0.003	0.067	6.9	0.005	0.170	10.3	0.018	0.816	3.3	0.027	0.262	11.0	0.029
Ba	0.003	50.0	0.001	0.003	70.7	0.002	N.D.			0.254	8.9	0.023	0.312	13.6	0.042
La	0.029	20.9	0.006	0.013	33.3	0.004	0.008	35.4	0.003	20.480	0.9	0.194	1.630	5.1	0.084
Ce	0.069	10.6	0.007	0.182	6.7	0.012	0.282	11.4	0.032	15.600	0.8	0.128	6.073	2.9	0.176
Pr	0.012	28.9	0.004	0.063	14.3	0.009	0.105	16.0	0.017	0.961	4.2	0.040	1.211	5.7	0.069
Nd	0.081	22.4	0.018	0.818	8.1	0.066	1.230	13.7	0.169	2.566	5.2	0.132	7.222	6.7	0.485
Sm	0.004	40.8	0.002	0.716	7.8	0.056	1.110	13.1	0.145	0.112	20.0	0.022	2.023	11.2	0.227
Eu	0.002	37.8	0.001	0.353	5.9	0.021	0.544	10.3	0.056	0.043	17.4	0.008	0.567	11.5	0.065
Gd	0.049	31.6	0.015	1.984	6.3	0.124	1.970	9.6	0.189	0.620	8.7	0.054	1.826	9.1	0.167
Tb	0.017	25.8	0.004	0.482	5.4	0.026	0.558	7.7	0.043	N.D.			0.124	13.1	0.016
Dy	0.286	15.8	0.045	3.804	4.5	0.169	3.460	7.2	0.251	0.043	21.3	0.009	0.982	12.7	0.125
Ho	0.103	11.9	0.012	0.991	3.9	0.038	0.911	6.3	0.057	0.009	35.4	0.003	0.190	14.3	0.027
Er	0.585	10.7	0.063	3.147	4.6	0.144	2.830	7.5	0.213	0.093	26.7	0.025	0.422	18.9	0.080
Yb	0.797	9.7	0.077	3.853	4.3	0.166	2.510	8.1	0.203	0.166	20.0	0.033	0.508	16.9	0.086
Lu	0.136	12.1	0.016	0.564	5.7	0.032	0.356	10.5	0.037	0.016	35.4	0.006	0.029	28.9	0.008
Pb	N.A.			N.A.			8.840	19.2	1.697	N.A.			3.747	27.7	1.038

Table AD.4 Theoretical precision for trace element analysis by ion probe.
Errors given are for a typical garnet composition at 15nA (J75 garnet) and 8nA (J110 garnet), for a garnet with relatively low trace element concentrations (J25 garnet), for a typical clinopyroxene (J110 clinopyroxene), and a clinopyroxene with relatively low trace element abundances (J25 clinopyroxene). Absolute abundances of the trace elements measured for each analysis are given (in ppm), with theoretical 1σ errors calculated from counting statistics (see text) given in absolute and percentage terms. N.A.- not analysed, N.D.- not detected.

TABLE D.1A Trace Element Composition of Coarse Garnets

	Rb	Sr	Y	Zr	Nb	Ba	La	Ce	Pr	Nd	Sm	Eu	Gd	Tb	Dy	Ho	Er	Yb	Lu	Pb	Notes	istance (µm)
J24																						
J24GT1	N.D.	0.38	5.47	34.34	0.22	0.00	0.04	0.61	0.27	3.02	2.08	0.84	1.88	0.16	0.82	0.21	0.94	1.50	0.22		Core	
J24GT2	0.01	0.34	4.80	39.56	0.17	0.01	0.02	0.39	0.19	2.35	1.97	0.86	2.49	0.20	0.74	0.18	1.02	1.37	0.23		Rim	
J24GT3	N.D.	0.31	5.03	40.16	0.09	0.00	0.02	0.40	0.22	2.14	1.76	0.76	2.36	0.20	0.76	0.20	0.68	1.31	0.25		Core near cpx inclusion	
J24GT4	0.16	0.37	4.49	40.15	0.16	0.01	0.01	0.40	0.19	2.06	1.70	0.79	2.30	0.22	0.73	0.20	0.98	1.30	0.21		Rim	
J25																						
J25GT1	0.10	0.06	2.59	0.23	0.05	0.00	0.03	0.07	0.01	0.08	0.00	0.00	0.05	0.02	0.29	0.10	0.58	0.80	0.14		Core	
J25GT2	0.01	0.03	2.64	0.10	0.10	0.01	0.01	0.02	0.01	0.03	0.00	0.00	0.01	0.01	0.30	0.11	0.47	0.83	0.17		Rim	
J25GT3	0.03	0.03	2.66	0.10	0.09	0.01	0.02	0.02	0.00	0.00	0.01	0.00	0.05	0.02	0.28	0.10	0.55	0.87	0.15		Rim	
J25GT4	0.23	0.02	2.59	0.12	0.07	0.00	0.02	0.04	0.00	0.03	0.00	0.01	0.08	0.01	0.29	0.10	0.42	0.82	0.23		Core	
J25GT5	0.11	0.06	2.60	0.23	0.13	0.02	0.02	0.05	0.00	0.13	0.04	0.02	0.05	0.02	0.22	0.10	0.52	1.06	0.18		Rim	
J25GT6	N.D.	0.02	2.74	0.05	0.06	0.00	N.D.	0.00	0.00	0.02	0.01	0.00	N.D.	0.01	0.22	0.11	0.58	1.12	0.18		Grain 2	
J146																						
J146GT1	N.D.	0.91	2.66	74.94	1.02	0.01	0.07	0.68	0.26	2.94	1.75	0.77	1.83	0.22	0.75	0.12	0.39	0.61	0.10		Core Low Ti	
J146GT2	0.13	1.06	10.90	100.10	1.14	0.08	0.10	0.83	0.31	2.99	1.75	0.74	2.81	0.45	2.71	0.50	1.06	1.28	0.20		Rim	
J146GT3	N.D.	0.85	2.20	69.46	1.02	0.01	0.07	0.74	0.25	2.70	1.88	0.60	1.73	0.16	0.72	0.11	0.32	0.58	0.14		Core Low Ti	
J146GT4	0.24	1.05	11.84	104.20	1.15	0.04	0.08	0.88	0.38	3.05	1.88	0.87	2.69	0.51	2.86	0.51	1.33	1.32	0.18		Core High Ti	
J146GT5	0.03	1.05	5.52	86.01	1.07	0.05	0.12	0.78	0.28	3.10	1.78	0.76	2.26	0.31	1.52	0.21	0.57	0.64	0.12		Rim	
J146GT6	0.13	0.74	1.69	30.92	1.08	0.01	0.07	0.90	0.32	3.39	1.18	0.38	0.75	0.11	0.48	0.06	0.14	0.54	0.08		Core Grain 2	
J146GT7	0.20	0.80	2.08	39.90	0.99	0.01	0.08	0.88	0.37	3.30	1.32	0.43	0.97	0.13	0.74	0.06	0.32	0.43	0.12		Rim Grain 2	
J157																						
J157GT1	0.18	0.34	35.41	132.00	0.23	0.00	0.01	0.39	0.25	3.02	2.67	1.33	5.31	1.21	8.55	1.55	3.03	1.59	0.22		Core	
J157GT2	0.18	0.31	36.28	134.30	0.20	N.D.	0.00	0.35	0.18	2.68	2.63	1.45	5.73	1.23	8.47	1.51	3.03	1.73	0.30		Rim	
J157GT3	0.04	0.32	35.42	134.00	0.20	N.D.	0.01	0.35	0.23	2.98	2.69	1.34	5.51	1.12	8.15	1.45	3.05	1.82	0.32		Core	
J157GT4	N.D.	0.34	35.22	131.70	0.20	0.01	0.02	0.37	0.20	3.15	2.64	1.41	5.37	1.15	8.26	1.47	3.00	1.58	0.31		Rim	
JJG1728																						
1728GT1	0.04	5.56	0.37	3.06	0.38	0.01	1.12	7.66	0.99	3.32	0.36	0.09	0.35	0.02	0.10	0.01	0.06	0.11	0.03		Core	
1728GT2	N.D.	1.30	7.48	79.81	0.20	0.00	0.04	0.86	0.34	2.91	1.70	0.78	2.48	0.43	2.39	0.30	0.46	0.24	0.05		Rim	
1728GT3	0.10	0.57	14.26	123.50	0.17	0.66	0.26	0.60	0.11	0.95	0.80	0.39	2.01	0.50	3.25	0.62	1.36	0.60	0.11		New Growth	
1728GT4	N.D.	5.03	1.10	10.05	0.35	0.02	1.00	6.73	0.90	3.35	0.47	0.14	0.47	0.06	0.36	0.05	0.09	0.14	0.02		Core	
1728GT5	0.09	0.85	8.53	82.26	0.21	0.02	0.02	0.70	0.33	3.48	1.87	0.77	2.51	0.49	2.42	0.33	0.46	0.26	0.03		Rim	
1728GT6	0.28	1.35	5.63	65.56	0.26	2.53	0.07	1.01	0.46	3.55	1.53	0.61	1.93	0.34	1.69	0.24	0.40	0.34	0.06		Rim	
1728GT7	0.01	0.71	3.55	50.76	0.30	0.12	0.05	0.86	0.52	7.55	2.95	0.86	1.84	0.26	1.09	0.13	0.26	0.19	0.03		Core, Grain 2	
1728GT8	0.09	0.52	6.48	81.87	0.23	0.01	0.01	0.44	0.32	4.29	2.44	0.96	2.92	0.44	1.89	0.25	0.33	0.30	0.02		Rim, Grain 2	
1728GT9	0.06	5.38	0.36	3.13	0.42	N.D.	1.21	7.68	0.95	3.45	0.33	0.08	0.35	0.01	0.16	0.02	0.08	0.10	0.03		Core	
JJG1757 (Garnet in phlogopite along grain boundary)																						
1757GT1	N.D.	0.05	0.74	0.90	N.D.	N.D.	N.D.	0.01	N.D.	N.D.	N.D.	0.01	0.04	0.01	0.04	0.02	0.14	0.24	0.04			
1757GT2	N.D.	0.06	1.47	1.02	N.D.	N.D.	0.01	0.02	N.D.	0.01	0.01	0.01	0.06	0.02	0.11	0.08	0.23	0.45	0.11			
JJG1761																						
1761GT1	0.04	0.44	3.16	52.07	0.78	0.01	0.02	0.38	0.23	3.06	2.06	0.93	2.52	0.31	1.02	0.15	0.32	0.42	0.07		Core	
1761GT2	0.14	0.48	3.34	54.42	0.78	0.01	0.03	0.37	0.19	3.34	2.19	0.84	2.94	0.31	1.17	0.17	0.25	0.31	0.04		Rim	
1761GT3	0.02	0.50	3.16	51.50	0.81	0.01	0.03	0.36	0.23	3.07	2.04	0.82	2.69	0.31	0.95	0.13	0.28	0.37	0.06		Core	
1761GT4	N.D.	0.42	3.34	53.93	0.75	0.00	0.03	0.39	0.21	2.68	2.22	0.90	2.84	0.35	1.22	0.15	0.30	0.28	0.05		Rim	
JJG1780 (Garnet remnant in kelyphite)																						
1780GT1	0.17	0.49	26.53	132.70	0.22	0.01	0.03	0.50	0.32	3.58	2.91	1.33	4.76	0.93	6.04	1.02	2.18	1.42	0.23			
1780GT2	N.D.	0.53	23.85	127.80	0.25	0.00	0.03	0.54	0.32	3.96	3.13	1.35	4.32	0.88	5.60	0.88	1.97	1.49	0.18			
1780GT3	N.D.	1.48	7.00	56.18	0.28	0.00	0.09	1.55	0.70	6.27	2.19	0.70	2.21	0.38	1.58	0.24	0.50	0.23	0.01			
1780GT4	N.D.	1.12	10.70	79.91	0.30	0.02	0.06	1.32	0.60	6.12	2.55	1.05	3.42	0.50	2.55	0.39	0.91	0.29	0.10			
1780GT6	0.07	0.71	19.64	110.40	0.24	0.01	0.05	0.72	0.40	4.90	2.74	1.20	3.97	0.80	4.67	0.76	1.67	0.93	0.12			
1780GT7	N.D.	0.40	25.23	131.20	0.19	0.01	0.03	0.41	0.29	4.42	3.06	1.30	4.65	0.94	6.27	1.01	2.34	1.39	0.22			

TABLE D.1A CONT. Trace Element Composition of Coarse Garnets

	Rb	Sr	Y	Zr	Nb	Ba	La	Ce	Pr	Nd	Sm	Eu	Gd	Tb	Dy	Ho	Er	Yb	Lu	Pb	Notes	Distance (µm)
1781GT1	0.20	0.86	1.52	72.21	1.12	N.D.	0.06	0.94	0.39	4.73	2.02	0.44	0.82	0.12	0.42	0.11	0.16	0.48	0.04			
1781GT2	0.16	0.88	3.05	115.50	1.10	0.01	0.07	0.86	0.32	4.23	2.27	0.73	1.84	0.30	1.13	0.17	0.40	0.37	0.07			
1781GT3	0.02	0.72	1.54	87.12	1.09	0.00	0.07	0.88	0.37	4.38	2.27	0.61	1.10	0.14	0.50	0.06	0.17	0.34	0.04			
1781GT4	N.D.	0.91	1.58	54.95	1.08	0.03	0.07	1.00	0.41	5.04	1.79	0.42	0.88	0.10	0.34	0.09	0.26	0.20	0.05			
JJG2469																						
2469BG1	0.11	8.79	5.04	61.30	0.59	0.39	0.27	7.90	3.55	31.20	7.40	1.87	4.52	0.66	1.76	0.47	0.63	0.25	0.00		Rim	
2469BG7	N.D.	8.16	5.16	61.70	0.46	0.05	0.30	7.03	3.38	30.90	5.78	1.53	2.99	0.48	2.04	0.24	0.60	0.72	0.13		Rim	
2469BG5	0.01	9.19	5.35	64.50	0.52	0.06	0.46	7.84	3.76	32.90	5.71	1.46	3.99	0.55	1.52	0.28	0.57	0.65	0.12		Rim	
2469BG4	N.D.	8.99	5.10	61.60	0.43	0.02	0.36	7.09	3.67	30.90	5.48	1.57	3.97	0.51	2.12	0.23	0.59	0.86	0.15		Core	
2469BG3	N.D.	7.57	5.18	60.20	0.38	0.03	0.32	5.82	3.04	27.40	5.87	1.42	3.41	0.49	1.95	0.26	0.33	0.48	0.10		Core	
2469BG6	N.D.	10.10	5.11	61.80	0.44	0.03	0.56	9.89	4.09	33.80	5.21	1.47	3.62	0.43	1.32	0.26	0.63	0.60	0.22		Core	
2469BG2	N.D.	12.40	5.03	62.80	0.81	1.73	0.94	9.87	4.35	33.80	6.64	1.59	3.41	0.53	2.20	0.23	0.69	0.73	0.12		Core	

TABLE D.1B Trace Element Composition of Deformed Garnets

	Rb	Sr	Y	Zr	Nb	Ba	La	Ce	Pr	Nd	Sm	Eu	Gd	Tb	Dy	Ho	Er	Yb	Lu	Pb	Notes	Distance (μm)
J22F/2 (Garnet from thick section J22F/2, second slice through garnet J22F)																						
J22FGT1	0.17	0.47	3.15	25.78	0.35	N.D.	0.04	0.44	0.18	2.08	0.83	0.31	1.05	0.17	0.73	0.12	0.36	0.43	0.06		Core	
J22FGT2	N.D.	0.56	8.13	55.81	0.31	0.00	0.01	0.37	0.12	1.41	1.08	0.48	1.77	0.31	1.94	0.38	0.92	1.02	0.13		Core, High Ti Zone	
J22FGT3	0.20	0.55	3.90	38.56	0.27	0.02	0.03	0.32	0.13	1.56	0.97	0.43	1.51	0.19	0.99	0.13	0.42	0.52	0.08		Rim	
J22FGT4	N.D.	0.48	2.75	23.17	0.39	0.01	0.05	0.39	0.15	1.94	0.92	0.33	0.94	0.14	0.77	0.09	0.31	0.44	0.06		Core	
J22FGT5	0.08	0.56	13.90	61.52	0.28	N.D.	0.03	0.33	0.13	1.34	0.89	0.48	1.65	0.39	2.97	0.56	1.85	1.80	0.30		Rim, High Ti Zone	
J22FGT6	0.20	0.54	16.82	64.10	0.21	N.D.	0.02	0.27	0.14	1.14	0.90	0.46	1.35	0.42	3.15	0.71	2.47	2.18	0.35		Rim	
J22FGT7	0.16	0.58	14.13	62.21	0.23	N.D.	0.04	0.30	0.12	1.23	1.01	0.46	1.89	0.35	2.65	0.51	1.84	1.81	0.26		Rim	
J34 (Garnet A from Thick section J34B)																						
J34BGT6		0.31	13.78	29.56	0.26	N.D.	0.03	0.20		1.03	0.81	0.33	1.58	0.33	2.44	0.60	2.13	2.43	0.44		Rim	10
J34BGT7		0.38	13.67	30.37	0.34	N.D.	0.04	0.25		1.15	0.72	0.41	1.73	0.39	2.28	0.88	2.26	1.66	0.33		Core	1700
J34BGT3		0.39	14.38	31.21	0.30	N.D.	0.00	0.28		0.90	0.88	0.39	1.69	0.43	2.61	0.58	2.04	1.84	0.26		Core	2850
J34BGT5		0.38	13.93	30.94	0.36	0.03	0.03	0.26		0.94	0.81	0.39	1.57	0.39	3.35	0.57	1.99	2.50	0.45		Core	3480
J34BGT1		0.39	14.11	30.73	0.33	N.D.	0.04	0.21		1.05	0.69	0.35	1.72	0.35	2.80	0.64	2.15	2.61	0.39		Core	4080
J34BGT4		0.35	13.97	31.22	0.24	0.02	0.03	0.21		0.74	0.71	0.35	1.63	0.44	3.01	0.68	2.04	2.20	0.42		Core	4580
J34BGT2		0.37	13.66	29.52	0.24	N.D.	0.02	0.24		0.84	0.67	0.34	1.66	0.29	3.00	0.59	2.01	2.43	0.32		Rim	4900
J47																						
J47GT1	N.D.	0.28	15.13	41.66	0.14	0.01	0.01	0.13	0.06	0.62	0.59	0.30	1.35	0.34	2.71	0.71	1.99	1.95	0.37		Core	
J47GT2	N.D.	0.28	15.15	42.37	0.13	0.01	0.01	0.15	0.04	0.68	0.60	0.32	1.35	0.34	2.82	0.70	2.02	2.26	0.40		Rim	
J47GT3	0.15	0.25	15.13	36.95	0.10	0.01	0.01	0.15	0.05	0.48	0.49	0.32	1.29	0.34	2.68	0.62	1.91	2.07	0.37		Core	
J47GT4	0.06	0.24	14.86	37.53	0.12	0.01	0.03	0.13	0.05	0.72	0.55	0.31	1.35	0.29	2.67	0.63	2.04	2.72	0.32		Rim	
J51																						
J51GT1	0.05	0.26	17.81	50.59	0.07	N.D.	0.02	0.13	0.08	0.61	0.60	0.33	1.53	0.38	3.10	0.70	2.55	2.76	0.44		Core	
J51GT2	0.06	0.25	17.46	49.22	0.07	0.00	0.02	0.14	0.04	0.69	0.71	0.35	1.39	0.38	3.03	0.74	2.51	2.72	0.43		Rim	
J51GT3	0.02	0.30	17.65	50.55	0.08	0.00	0.01	0.13	0.06	0.61	0.67	0.35	1.53	0.39	3.18	0.79	2.43	2.91	0.42		Core	
J51GT4	0.04	0.31	17.56	49.82	0.08	0.01	0.02	0.13	0.06	0.63	0.62	0.34	1.40	0.37	2.96	0.77	2.41	2.54	0.41		Rim	
J107																						
J107GT10		0.62	18.70	85.50	0.31	0.02	0.02	0.34		1.37	1.15	0.61	2.63	0.59	3.77	0.85	2.34	2.40	0.40		Rim	50
J107GT12		0.60	15.60	82.50	0.26	0.08	0.03	0.30		1.61	1.69	0.63	2.71	0.51	2.90	0.72	1.65	2.12	0.18		Rim	110
J107BGT3		0.56	12.60	77.10	0.32	0.02	0.06	0.43		1.79	1.73	0.54	2.85	0.49	2.85	0.62	1.90	1.59	0.22		Core	330
J107BGT9		0.53	12.30	74.60	0.38	0.04	0.03	0.44		1.68	1.59	0.56	2.86	0.50	3.02	0.49	1.75	1.55	0.22		Core	500
J107BGT1		0.55	12.20	73.50	0.39	0.02	0.07	0.50		1.84	1.95	0.70	2.74	0.49	3.08	0.56	1.70	1.52	0.21		Core	690
J107GT18		0.58	12.10	72.60	0.49	0.25	0.07	0.42		2.22	1.81	0.69	2.41	0.44	2.90	0.53	1.56	1.68	0.29		Core	1050
J107BGT8		0.55	11.60	72.40	0.41	N.D.	0.03	0.44		2.21	1.32	0.59	2.42	0.64	3.00	0.55	1.82	1.82	0.15		Core	1410
J107GT16		0.55	11.30	71.10	0.30	0.02	0.03	0.45		1.73	1.34	0.57	2.94	0.39	2.60	0.51	1.50	1.90	0.21		Core	1920
J107BGT2		0.57	11.70	71.60	0.37	0.01	0.04	0.45		2.20	1.54	0.63	2.59	0.44	2.82	0.53	1.62	1.70	0.25		Core	2350
J107GT20		0.59	11.70	72.40	0.51	0.02	0.04	0.51		1.98	1.56	0.57	2.77	0.46	2.93	0.52	1.70	1.69	0.23		Core	2730
J107GT11		0.63	11.80	74.20	0.34	0.04	0.04	0.46		1.77	1.82	0.68	2.66	0.55	2.65	0.58	1.33	1.11	0.20		Core	3120
J107GT17		0.60	12.10	75.80	0.29	0.25	0.03	0.53		2.24	1.42	0.67	2.86	0.52	2.78	0.61	1.53	1.64	0.34		Core	3460
J107BGT4		0.66	12.10	77.60	0.30	N.D.	0.03	0.46		1.77	1.51	0.52	3.24	0.46	3.25	0.56	1.22	1.49	0.36		Core	3830
J107GT19		0.50	12.50	81.80	0.47	0.06	0.04	0.44		1.99	1.50	0.75	2.47	0.45	2.67	0.52	1.74	1.49	0.28		Core	4150
J107BGT6		0.68	12.90	81.10	0.30	0.08	0.04	0.40		2.03	1.66	0.55	3.15	0.58	3.26	0.67	1.67	1.58	0.30		Core	4460
J107GT13		0.62	12.90	78.30	0.38	0.04	0.04	0.43		2.03	1.54	0.61	2.82	0.53	3.17	0.52	1.64	1.50	0.31		Core	4860
J107BGT5		0.55	13.80	83.10	0.34	0.02	0.02	0.37		1.30	1.30	0.68	2.68	0.54	3.47	0.57	1.50	1.36	0.36		Core	5240
J107GT15		0.65	17.10	85.90	0.32	N.D.	0.04	0.34		1.41	1.28	0.67	2.69	0.58	4.19	0.80	2.42	2.11	0.42		Rim	5380
J107GT14		0.55	19.00	87.00	0.27	0.02	0.04	0.31		1.38	1.34	0.60	2.54	0.55	4.25	0.82	2.35	2.43	0.45		Rim	5460
J107BGT7		0.52	21.60	88.20	0.27	0.01	0.06	0.34		1.48	1.07	0.61	3.04	0.48	4.61	1.02	3.12	3.15	0.61		Rim	5540

TABLE D.1B CONT. Trace Element Composition of Deformed Garnets

	Rb	Sr	Y	Zr	Nb	Ba	La	Ce	Pr	Nd	Sm	Eu	Gd	Tb	Dy	Ho	Er	Yb	Lu	Pb	Notes	Distance (μm)
J110																						
J110G9		0.52	19.20	75.00	0.17	0.13	0.01	0.28	0.11	1.23	1.11	0.54	1.97	0.56	3.46	0.91	2.83	2.51	0.36	8.840	Rim	110
J110G12		0.58	18.60	72.70	0.17	0.06	0.05	0.33	0.09	1.34	0.87	0.46	2.32	0.37	3.68	0.96	2.70	2.65	0.38	12.900	Rim	180
J110G10		0.71	17.60	70.50	0.20	0.18	0.10	0.31	0.11	1.47	0.80	0.47	1.63	0.46	3.14	0.77	2.65	2.49	0.46	11.300	Rim	300
J110G11		0.62	15.50	64.30	0.20	0.09	0.01	0.29	0.12	1.18	1.08	0.34	1.70	0.40	3.19	0.68	2.37	2.32	0.32	12.200	Core	460
J110G5		1.32	12.00	51.70	0.29	1.17	0.25	0.55	0.14	1.54	0.82	0.46	1.92	0.29	2.53	0.46	1.72	1.38	0.34	14.100	Core	600
J110G15		0.61	12.00	50.10	0.23	0.11	0.04	0.36	0.13	1.40	0.88	0.52	1.67	0.35	2.97	0.49	1.33	1.83	0.33	6.390	Core	730
J110G7		0.53	11.70	39.30	0.31	N.D.	0.02	0.31	0.19	1.17	0.82	0.42	1.17	0.34	2.25	0.51	1.77	2.22	0.29	8.970	Core	890
J110G2		0.50	11.40	37.60	0.36	0.03	0.03	0.44	0.16	1.77	0.96	0.36	1.60	0.33	2.56	0.51	1.56	1.82	0.21	5.780	Core	1390
J110G8		0.54	12.20	44.00	0.23	0.21	0.03	0.35	0.10	1.49	0.85	0.48	1.68	0.33	2.33	0.60	1.72	1.63	0.25	16.900	Core	1780
J110G13		1.60	18.30	70.10	0.44	3.39	0.22	0.56	0.19	1.48	1.12	0.45	1.84	0.38	3.78	0.85	2.06	2.47	0.47	18.300	Core	2160
J110G3		0.44	18.90	69.90	0.24	0.06	0.01	0.23	0.12	1.25	0.86	0.50	2.09	0.48	3.81	0.84	3.34	2.82	0.44	10.600	Rim	2430
J110G14		0.53	18.80	69.20	0.18	0.07	0.03	0.26	0.10	1.03	0.98	0.43	1.87	0.53	3.58	0.90	2.67	3.14	0.53	16.700	Rim	2500
J110G4		0.52	19.30	74.50	0.16	0.06	0.02	0.32	0.10	1.24	1.18	0.49	2.01	0.44	4.38	0.82	2.61	2.85	0.41	9.940	Rim	2580
J110G1		0.55	18.70	73.10	0.20	0.33	0.04	0.22	0.09	1.07	0.92	0.47	1.94	0.57	3.58	0.79	2.52	2.87	0.33	8.610	Rim	2650
J112 (Garnet from Ion Probe Section)																						
J112GT1	N.D.	0.74	12.34	145.20	0.51	0.01	0.04	0.48	0.18	2.06	1.57	0.72	2.91	0.59	3.35	0.54	1.13	1.10	0.17		Core, Low Ti	
J112GT2	N.D.	0.75	16.57	154.60	0.51	0.00	0.04	0.51	0.19	1.95	1.34	0.80	3.21	0.68	4.45	0.68	1.59	1.27	0.20		Core, High Ti	
J112GT3	N.D.	0.79	15.10	152.50	0.46	0.01	0.05	0.48	0.14	1.85	1.59	0.75	3.08	0.62	4.27	0.67	1.63	1.07	0.22		Rim	
J112GT4	0.44	0.71	7.50	130.00	0.42	0.00	0.06	0.38	0.17	1.67	1.47	0.65	2.59	0.44	2.52	0.34	0.69	0.91	0.17		Core, V. Low Ti	
J112GT5	0.14	0.82	14.78	150.60	0.45	N.D.	0.05	0.48	0.17	1.84	1.57	0.76	2.63	0.60	3.81	0.66	1.52	1.19	0.19		Rim	
J112GT7	0.03	0.77	13.21	148.60	0.41	0.00	0.03	0.45	0.17	1.96	1.54	0.72	2.96	0.65	3.48	0.59	1.11	1.07	0.15		Rim	
J115																						
J115G1	N.D.	0.33	14.20	31.40	0.26	0.05	0.02	0.25	0.06	0.92	0.70	0.35	1.46	0.29	2.80	0.61	1.81	2.59	0.36	16.800	Rim	
J115G9	N.D.	0.27	13.10	29.40	0.26	0.12	0.04	0.22	0.06	0.68	0.70	0.36	1.84	0.38	2.21	0.60	1.83	2.15	0.36	7.770	Rim	
J115G11	N.D.	0.29	11.80	22.60	0.28	0.07	0.02	0.22	0.05	0.63	0.59	0.31	0.97	0.33	2.35	0.54	1.48	2.10	0.32	10.400	Rim	
J115G14	N.D.	0.32	11.50	20.80	0.21	0.02	0.03	0.17	0.07	0.82	0.65	0.28	1.50	0.28	2.01	0.54	1.99	1.45	0.35	12.500	Core	
J115G13	0.00	0.27	10.70	17.50	0.21	0.03	0.02	0.14	0.06	0.39	0.75	0.26	0.96	0.30	2.07	0.47	1.55	2.11	0.36	13.800	Core	
J115G12	N.D.	0.28	10.90	16.80	0.29	0.04	0.00	0.18	0.03	0.68	0.44	0.27	1.35	0.22	2.09	0.39	1.58	2.00	0.27	12.800	Core	
J115G3	N.D.	0.29	11.00	15.90	0.30	0.06	0.02	0.17	0.08	0.75	0.54	0.20	0.99	0.23	2.13	0.50	1.73	2.15	0.34	15.300	Core	
J115G7	N.D.	0.29	11.10	14.60	0.24	0.09	0.02	0.21	0.08	0.65	0.52	0.22	1.01	0.29	2.21	0.52	1.69	2.03	0.29	22.300	Core	
J115G2	N.D.	0.27	11.20	14.20	0.28	0.01	0.03	0.19	0.08	0.73	0.46	0.22	0.72	0.21	2.15	0.50	2.03	2.09	0.32	31.700	Core	
J115G8	0.01	0.28	10.90	13.10	0.23	0.10	0.01	0.18	0.07	0.89	0.54	0.20	0.64	0.20	1.86	0.43	1.65	1.69	0.34	54.800	Core	
J115G4	0.03	0.25	11.20	13.90	0.29	0.06	0.03	0.15	0.08	0.80	0.56	0.27	0.82	0.28	1.93	0.50	1.90	2.13	0.30	45.500	Core	
J115G10	0.17	0.26	10.90	15.60	0.30	0.02	0.03	0.17	0.06	0.76	0.58	0.21	0.94	0.18	1.96	0.48	1.65	1.94	0.36	29.900	Core	
J115G16	0.25	0.32	11.40	17.80	0.30	0.06	0.04	0.14	0.08	0.71	0.70	0.26	1.11	0.20	1.85	0.45	1.39	2.15	0.30	20.900	Core	
J115G15	N.D.	0.31	12.10	21.90	0.19	0.04	0.04	0.16	0.07	0.54	0.71	0.30	1.27	0.33	1.99	0.53	1.62	2.47	0.37	16.200	Rim	
J115G6	0.27	0.34	13.30	28.90	0.28	0.04	0.02	0.22	0.09	0.67	0.69	0.38	1.10	0.32	2.72	0.57	1.81	2.25	0.30	18.800	Rim	
J115G5	0.21	0.35	13.80	31.30	0.31	0.05	0.04	0.23	0.09	0.75	0.52	0.40	1.29	0.32	2.05	0.61	1.93	2.15	0.30	16.600	Rim	
J121 (Two Grains from Different Slides)																						
J121GT1	0.10	0.26	10.40	16.99	0.20	0.01	0.02	0.22	0.08	0.78	0.40	0.18	0.82	0.22	1.74	0.44	1.48	1.88	0.32		Core	
J121GT2	0.00	0.32	11.30	31.24	0.30	0.00	0.05	0.29	0.10	1.00	0.60	0.30	1.02	0.25	2.09	0.48	1.55	1.86	0.32		Rim	
J121GT3	0.20	0.26	10.19	15.40	0.19	0.02	0.03	0.21	0.08	0.66	0.47	0.20	0.85	0.24	1.69	0.41	1.52	1.91	0.34		Core	
J121GT4	0.09	0.33	11.27	31.18	0.31	0.01	0.03	0.30	0.11	0.96	0.70	0.29	1.13	0.28	1.87	0.42	1.46	1.75	0.26		Rim	
J121GT5	0.13	0.28	9.85	22.55	0.17	0.01	0.02	0.22	0.09	0.73	0.63	0.23	0.76	0.22	1.75	0.41	1.56	1.65	0.27		Core	
J121GT6	0.11	0.32	10.87	29.98	0.23	0.02	0.04	0.30	0.09	1.05	0.63	0.30	1.24	0.25	2.17	0.44	1.47	1.83	0.34		Rim	
J121AGT1	N.D.	0.36	9.58	24.02	0.41	0.00	0.04	0.36	0.11	1.43	0.69	0.29	1.15	0.24	1.83	0.40	1.00	1.24	0.14		Core	
J121AGT2	N.D.	0.30	11.22	30.73	0.29	0.01	0.04	0.30	0.11	1.00	0.56	0.31	1.15	0.27	1.88	0.45	1.69	1.73	0.24		Rim	
J121AGT3	0.19	0.32	10.79	30.32	0.30	0.00	0.03	0.28	0.10	0.88	0.63	0.26	1.12	0.24	1.97	0.47	1.55	1.64	0.29		Rim	
J121AGT4	N.D.	0.37	10.30	26.66	0.37	0.01	0.06	0.39	0.10	1.17	0.65	0.29	1.31	0.29	2.06	0.45	1.27	1.18	0.19		Core	
J121AGT5	0.11	0.30	11.14	31.41	0.27	N.D.	0.02	0.27	0.10	1.03	0.60	0.26	1.16	0.25	2.08	0.47	1.63	1.89	0.27		Rim	
J121AGT6	0.17	0.28	10.97	31.46	0.32	0.01	0.04	0.29	0.09	0.94	0.56	0.27	1.04	0.26	2.07	0.47	1.33	1.63	0.24		Rim	

TABLE D.1B CONT. Trace Element Composition of Deformed Garnets

	Rb	Sr	Y	Zr	Nb	Ba	La	Ce	Pr	Nd	Sm	Eu	Gd	Tb	Dy	Ho	Er	Yb	Lu	Pb	Notes	Distance (μm)
J145																						
J145GT1	0.17	0.81	0.23	14.39	2.05	0.00	0.19	1.09	0.29	2.45	0.69	0.18	0.28	0.03	0.16	0.01	0.06	0.28	0.06		Core, Grain 1	
J145GT2	0.00	0.92	0.52	66.48	1.81	N.D.	0.12	1.40	0.54	5.20	2.80	0.86	1.76	0.16	0.42	0.02	0.07	0.36	0.06		Rim, Grain 1	
J145GT3	0.02	0.88	0.41	88.87	1.79	0.00	0.16	1.46	0.49	5.35	2.97	1.03	1.84	0.14	0.29	0.03	0.06	0.30	0.08		Core, Grain 2	
J145GT4	0.14	0.85	1.25	130.10	1.73	0.01	0.11	1.30	0.46	5.05	3.43	1.47	3.50	0.32	0.88	0.08	0.09	0.38	0.11		Rim, Grain 2	
J159																						
J159GT1	0.10	0.56	0.23	8.18	1.31	0.06	0.10	0.80	0.22	1.70	0.36	0.09	0.23	0.02	0.09	0.01	0.05	0.15	0.06		Core, Grain 1	
J159GT2	0.06	0.46	0.45	11.58	1.23	0.01	0.10	0.63	0.19	1.13	0.39	0.11	0.14	0.05	0.09	0.01	0.06	0.33	0.07		Rim, Grain 1	
J159GT3	N.D.	0.70	1.29	35.56	1.32	0.06	0.08	0.88	0.31	2.57	1.17	0.37	1.01	0.11	0.51	0.07	0.21	0.19	0.07		Core, Grain 2	
J159GT4	0.07	0.63	1.45	33.49	1.17	0.05	0.09	0.86	0.25	2.48	0.89	0.33	0.92	0.15	0.57	0.07	0.15	0.36	0.06		Rim, Grain 2	
JJG1776																						
1776G3	N.D.	2.94	17.90	48.10	0.40	1.70	0.31	0.66	0.15	0.95	0.62	0.39	1.98	0.47	3.71	0.84	2.55	3.29	0.53		Rim	2540
1776G9	N.D.	1.37	17.40	46.90	0.21	0.13	0.01	0.21	0.04	0.72	0.63	0.45	1.86	0.45	3.35	0.73	2.50	3.03	0.46		Rim	2450
1776G10	N.D.	0.31	17.30	46.60	0.15	0.08	0.02	0.16	0.06	0.91	0.63	0.37	1.46	0.38	3.76	0.65	2.36	2.62	0.57		Rim	2320
1776G1	0.13	0.31	17.30	45.70	0.18	0.04	0.01	0.18	0.08	0.54	0.63	0.47	1.85	0.44	2.79	0.73	2.33	2.93	0.39		Core	2100
1776G11	0.28	0.26	16.40	44.70	0.10	0.05	0.02	0.16	0.04	0.51	0.46	0.45	1.89	0.39	2.57	0.75	2.47	2.66	0.50		Core	1790
1776G4	N.D.	0.25	16.30	44.50	0.08	0.02	0.02	0.13	0.03	0.65	0.71	0.26	2.04	0.44	3.12	0.74	2.58	2.45	0.52		Core	1500
JJH19																						
JJH19GT1	0.15	0.63	12.33	57.46	0.29	0.01	0.03	0.34	0.12	1.62	1.00	0.46	1.75	0.35	2.70	0.52	1.33	1.29	0.20		Rim	
JJH19GT2	N.D.	0.46	2.64	15.85	0.39	0.01	0.03	0.44	0.18	2.31	0.99	0.36	1.15	0.15	0.83	0.10	0.20	0.28	0.05		Core	
JJH19GT4	0.21	0.59	7.65	49.30	0.27	0.00	0.03	0.31	0.12	1.39	0.96	0.46	1.69	0.29	1.60	0.31	0.51	0.59	0.12		Rim	
JJH19GT5	N.D.	0.47	2.81	24.44	0.30	0.01	0.03	0.34	0.14	1.48	1.08	0.40	1.03	0.15	0.86	0.12	0.30	0.37	0.06		Core	
JJH19GT6	0.07	0.61	11.86	56.87	0.30	0.01	0.03	0.39	0.14	1.49	1.11	0.49	1.84	0.40	2.55	0.45	1.24	1.18	0.17		Rim	
JJH19GT7	N.D.	0.45	2.70	16.87	0.32	0.00	0.03	0.41	0.17	2.15	1.07	0.37	0.95	0.13	0.80	0.11	0.23	0.22	0.07		Core	
JJH37 (Various Garnet Grains from One Slide)																						
JJH37AG1	0.44	0.52	12.59	71.49	0.20	0.02	0.02	0.25	0.09	1.08	0.91	0.43	1.72	0.44	2.87	0.53	1.66	1.42	0.20		Core, High Z, Grain A	
JJH37AG2	0.11	0.68	12.24	68.25	0.16	0.05	0.03	0.21	0.08	0.93	0.79	0.39	1.39	0.37	2.96	0.57	1.21	1.23	0.24		Rim, Grain A	
JJH37GB1	N.D.	0.39	3.54	27.25	0.13	0.01	0.02	0.20	0.08	0.86	0.50	0.19	0.44	0.07	0.57	0.16	0.56	0.86	0.13		Core, Grain B	
JJH37GB2	0.05	0.42	7.21	42.80	0.09	0.00	0.02	0.19	0.06	0.86	0.64	0.30	0.85	0.26	1.63	0.28	0.89	1.11	0.18		Rim, Grain B	
JJH37GB3	N.D.	0.48	14.79	69.88	0.20	0.01	0.02	0.25	0.09	1.05	0.82	0.40	1.76	0.38	2.97	0.65	1.69	1.79	0.24		Core, High Ti, Grain B	
JJH37GB4	N.D.	0.50	17.01	73.78	0.14	0.00	0.02	0.26	0.07	0.87	0.95	0.43	1.94	0.43	3.23	0.71	2.05	2.01	0.34		Core, High Ti, Grain B	
JJH37GB5	0.02	0.41	4.85	33.42	0.13	0.01	0.02	0.20	0.06	0.82	0.56	0.23	0.72	0.14	1.01	0.19	0.55	0.86	0.18		Core	
JJH37GB6	0.05	0.44	12.28	58.40	0.14	0.00	0.01	0.21	0.07	0.92	0.85	0.42	1.46	0.38	2.57	0.47	1.67	1.46	0.27		Rim	
JJH37GB7	N.D.	0.46	16.50	75.60	0.13	-9.66	0.02	0.25	0.09	1.06	0.91	0.44	1.85	0.46	3.50	0.73	2.02	2.13	0.27		Core, High Ti, Grain B	
JJH37GB8	0.07	0.45	16.10	72.28	0.17	0.00	0.03	0.25	0.08	1.05	0.79	0.40	1.73	0.43	3.00	0.70	1.89	1.92	0.29		Core, High Ti, Grain B	
JJH37DG1	0.02	0.53	18.69	81.14	0.17	0.02	0.01	0.28	0.12	1.27	0.89	0.46	2.05	0.48	4.07	0.81	2.28	2.12	0.35		Core, Grain D	
JJH37DG2	0.14	0.50	13.95	68.58	0.16	0.03	0.03	0.25	0.09	0.94	0.73	0.42	1.68	0.39	3.08	0.59	1.76	1.80	0.24		Rim, Grain D	
JJH37DG3	N.D.	0.49	18.96	80.40	0.22	0.01	0.04	0.25	0.11	1.20	0.92	0.50	1.80	0.50	3.39	0.80	2.58	2.28	0.35		Core, Grain D	
JJH37DG4	0.08	0.51	14.60	70.75	0.18	0.03	0.04	0.25	0.11	1.01	0.93	0.45	1.56	0.44	2.80	0.66	1.82	1.59	0.25		Rim, Grain D	
JJH37EGT1	0.16	0.35	3.26	9.24	0.23	0.01	0.03	0.30	0.11	0.89	0.33	0.08	0.15	0.05	0.51	0.11	0.55	0.99	0.17		Core, Grain E	
JJH37EG2	0.11	0.43	5.68	41.25	0.17	0.01	0.03	0.19	0.09	0.98	0.59	0.31	1.02	0.21	1.06	0.20	0.86	1.26	0.18		Rim. Grain E	
JJH37EG3	0.09	0.31	3.15	7.18	0.22	0.01	0.04	0.29	0.11	0.77	0.28	0.06	0.33	0.04	0.59	0.15	0.63	0.87	0.16		Core, Grain E	
JJH37EG4	0.30	0.47	10.10	55.61	0.13	0.00	0.03	0.22	0.10	0.86	0.75	0.35	1.31	0.30	2.32	0.49	1.07	1.31	0.25		Rim, Grain E	

TABLE D.1C Trace Element Composition of Cr-poor Megacryst Garnets

	Rb	Sr	Y	Zr	Nb	Ba	La	Ce	Pr	Nd	Sm	Eu	Gd	Tb	Dy	Ho	Er	Yb	Lu	Pb	Notes	Distance (μm)
J74																						
J74GT1	0.12	0.57	25.06	87.38	0.11	0.00	0.05	0.34	0.15	1.27	1.14	0.58	2.58	0.58	4.67	1.09	3.65	3.39	0.58		Core	
J74GT2	0.07	0.61	24.73	85.51	0.11	0.03	0.04	0.36	0.16	1.47	1.04	0.56	2.19	0.60	5.26	1.06	3.87	3.87	0.54		Rim	
J74GT3	0.01	0.58	23.74	79.79	0.10	0.03	0.04	0.29	0.15	1.20	1.13	0.51	2.06	0.56	4.14	1.03	3.25	3.44	0.62		Core	
J75																						
J75GT1	0.12	0.42	22.87	71.08	0.07	0.00	0.01	0.18	0.06	0.82	0.72	0.35	1.98	0.48	3.80	0.99	3.15	3.85	0.56		Rim	
J75GT2	0.01	0.36	21.38	62.91	0.07	0.00	0.03	0.17	0.06	0.86	0.77	0.37	1.85	0.46	3.93	0.89	3.08	3.32	0.57		Core	
J75GT3	0.05	0.37	21.43	59.30	0.07	0.01	0.02	0.19	0.06	0.77	0.63	0.32	1.64	0.42	3.71	0.89	3.04	3.28	0.49		Core	
J75GT4	0.08	0.37	20.86	61.72	0.08	0.01	0.02	0.19	0.08	0.78	0.72	0.39	1.56	0.41	3.71	0.89	3.03	3.33	0.45		Rim	

TABLE D.2A Trace Element Composition of Coarse Clinopyroxenes

	Rb	Sr	Y	Zr	Nb	Ba	La	Ce	Pr	Nd	Sm	Eu	Gd	Tb	Dy	Ho	Er	Yb	Lu	Pb	Notes	Distance (μm)
J24																						
J24C1	N.D.	1185.00	0.41	31.60	1.53	0.07	26.70	90.85	12.40	44.95	6.29	1.33	2.23	0.14	0.62	0.05	0.07	0.25	0.00		Inclusion in gnt.	
J24C2	N.D.	1234.00	0.39	33.60	1.79	0.06	30.46	101.90	13.59	49.55	6.64	1.50	2.71	0.10	0.30	0.01	0.17	0.28	0.01		Inclusion in gnt.	
J25																						
J25C1	N.D.	319.30	0.14	0.59	0.82	0.25	20.48	15.60	0.96	2.57	0.11	0.04	0.62	N.D.	0.04	0.01	0.09	0.17	0.02			
J25C2	N.D.	204.00	0.13	0.53	0.77	0.25	17.64	13.05	0.93	1.96	0.21	0.04	0.89	0.01	0.12	0.00	0.13	0.19	N.D.			
JJG1728																						
1728C1	N.D.	242.50	4.11	189.10	1.34	12.16	4.61	18.74	3.59	21.20	5.60	1.77	5.02	0.55	2.48	0.25	0.42	0.15	0.02			
1728C2	N.D.	286.00	4.38	196.70	4.55	42.19	8.23	25.06	4.37	24.46	5.85	1.72	5.03	0.62	2.62	0.23	0.35	0.16	0.01			

Table D.2B Trace Element Composition of Deformed Clinopyroxenes

	Rb	Sr	Y	Zr	Nb	Ba	La	Ce	Pr	Nd	Sm	Eu	Gd	Tb	Dy	Ho	Er	Yb	Lu	Pb	Notes	Distance (μm)
J47																						
J47C1	N.D.	81.25	2.70	11.52	0.27	0.17	1.84	6.30	1.02	5.64	1.59	0.52	1.46	0.21	0.92	0.15	0.23	0.24	0.02		Inclusion in gnt.	
J47C2	N.D.	79.96	2.70	11.27	0.28	0.16	1.86	5.76	1.00	5.60	1.63	0.52	1.63	0.21	0.81	0.13	0.34	0.34	0.04			
J51																						
J51C1	N.D.	93.78	3.41	16.26	0.22	0.22	1.85	6.64	1.19	6.47	1.76	0.60	1.78	0.23	1.17	0.21	0.30	0.40	0.02			
J51C2	N.D.	96.18	3.57	16.52	0.30	0.64	1.91	7.10	1.24	6.91	1.91	0.61	1.67	0.22	1.17	0.16	0.43	0.43	0.04			
J110																						
J110C16	N.D.	81.20	3.36	13.83	0.26	0.31	1.63	6.07	1.21	7.22	2.02	0.57	1.83	0.12	0.98	0.19	0.42	0.51	0.03	3.747		
J110C17	N.D.	83.66	3.13	12.92	0.29	0.22	1.51	5.81	1.11	6.35	1.96	0.57	2.11	0.20	1.23	0.15	0.13	0.35	0.10	4.731		
J110C18	N.D.	82.06	3.44	13.36	0.22	0.30	1.70	5.94	1.09	5.81	2.10	0.54	1.61	0.22	1.02	0.18	0.59	0.16	N.D.	9.000		
J112																						
J112C1	N.D.	103.20	2.06	20.73	0.42	0.19	2.02	7.44	1.37	7.86	1.94	0.59	1.62	0.18	0.94	0.11	0.22	0.29	N.D.			
J112C2	N.D.	104.80	2.04	21.13	0.34	0.22	2.18	7.49	1.31	7.68	2.11	0.61	1.95	0.23	1.05	0.11	0.21	0.14	0.01			
J115																						
J115C17	0.02	54.17	2.13	3.00	0.22	0.38	1.18	3.68	0.54	3.38	1.28	0.32	1.14	0.13	0.96	0.07	0.22	0.16	0.02	6.254		
J115C18	N.D.	53.53	2.10	3.13	0.27	0.32	1.15	3.39	0.59	3.15	1.13	0.39	0.91	0.09	0.64	0.07	0.40	0.33	0.06	8.044		
J115C19	N.D.	53.20	1.97	2.93	0.19	0.34	1.07	3.51	0.50	2.79	1.35	0.27	0.97	0.16	0.66	0.16	0.33	0.47	0.04	11.560		
J115C20	N.D.	51.48	2.01	2.64	0.18	0.46	1.16	3.25	0.54	3.03	0.69	0.32	1.26	0.15	0.49	0.10	0.22	0.35	4.70	5.973		
J121																						
J121C1	N.D.	63.50	1.16	1.82	0.14	0.26	1.29	4.51	0.72	3.91	0.83	0.28	0.81	0.09	0.57	0.06	0.25	0.31	0.05			
J121C2	N.D.	63.20	1.25	1.99	0.18	0.40	1.48	4.57	0.76	4.24	0.95	0.26	0.86	0.10	0.57	0.09	0.32	0.46	0.05			
JJG1776																						
1776C12A		84.70	3.06	10.90	0.23	0.42	1.89	6.77	1.19	6.17	1.74	0.65	0.71	0.23	0.97	0.16	0.18	0.23	0.01			
1776C13		87.40	3.05	12.80	0.27	0.26	1.97	6.75	1.19	7.20	1.78	0.47	1.16	0.24	1.21	0.18	0.34	0.34	0.01			
1776C14		89.20	2.99	13.50	0.30	0.24	2.10	7.43	1.31	7.62	1.57	0.63	2.47	0.28	0.99	0.16	0.39	0.24	0.02			
JJH37																						
JJH37C1	N.D.	86.42	3.50	18.64	0.20	0.22	1.76	6.42	1.20	6.70	1.76	0.61	1.72	0.23	1.11	0.18	0.37	0.35	0.03			
JJH37C2	N.D.	86.97	3.16	15.65	0.21	0.37	1.95	6.64	1.09	6.38	1.76	0.62	1.86	0.24	1.37	0.16	0.39	0.41	0.02			

Appendix D: Spidergrams showing Trace Element Compositions

The results of the ion microprobe trace element analysis of samples from the Jagersfontein suite are presented on chondrite normalised 'spidergrams' in Figs. D.1-26. Results for garnet and clinopyroxene for each sample are given on separate plots. The plots follow the element arrangement preferred by Harte et al. (1993). This arrangement is based on the REE plot with LREE to the left of the diagram. The largest ion Sr is placed to the left of the REE, and Y, Zr and Nb are placed to the right, in order of decreasing size. The plots use the chondrite elemental abundances proposed by Anders and Grevesse (1989, Table 1).

Symbols used:-

Garnet Rim Compositions: Black Crosses

Garnet Core Compositions: Grey Triangles

Cross-cutting Features in Garnet Cores: Black Circles

Clinopyroxene Compositions: Grey Squares

Note for samples J145 (Fig. D.25) and J159 (Fig. D.26) where two grains were analysed, compositions for one grain are represented by filled symbols, the other by open symbols.

Trace Element Profiles

The results of trace element traverses across garnet grains are given in Figs. D.27-32. For each traverse the compositions of Ce, Gd, Ho, Yb, Y, Zr, and Nb are shown. Trace element compositions are given in ppm, and the distance of the profile is measured in μm. The profile shown for each sample represents a rim to rim traverse across a grain, with the exception of JJG1776 (Fig. D.31) and JJG2469 (Fig. D.32) garnets where the traverses are between one rim and the core of the grain. Estimates of the precision of each analysis are given as $\pm 1\sigma$ error bars based on counting statistics.

Spidergrams showing rare earth element melt compositions

The results of partition coefficient calculations to determine hypothetical melt compositions in equilibrium with Jagersfontein minerals are given as chondrite normalised 'spidergrams' in Figs. D. 33-57 (see Chapter 7 for details of calculation). The construction of these diagrams is similar to that of the mineral composition spidergrams (Figs. D.1-26). Note however that these plots only give REE compositions, and melt compositions in equilibrium with garnet and clinopyroxene for a particular sample are plotted on the same diagram. The symbols used are the same as in the mineral composition diagrams (see above).

Fig. D.1a J24 Garnet

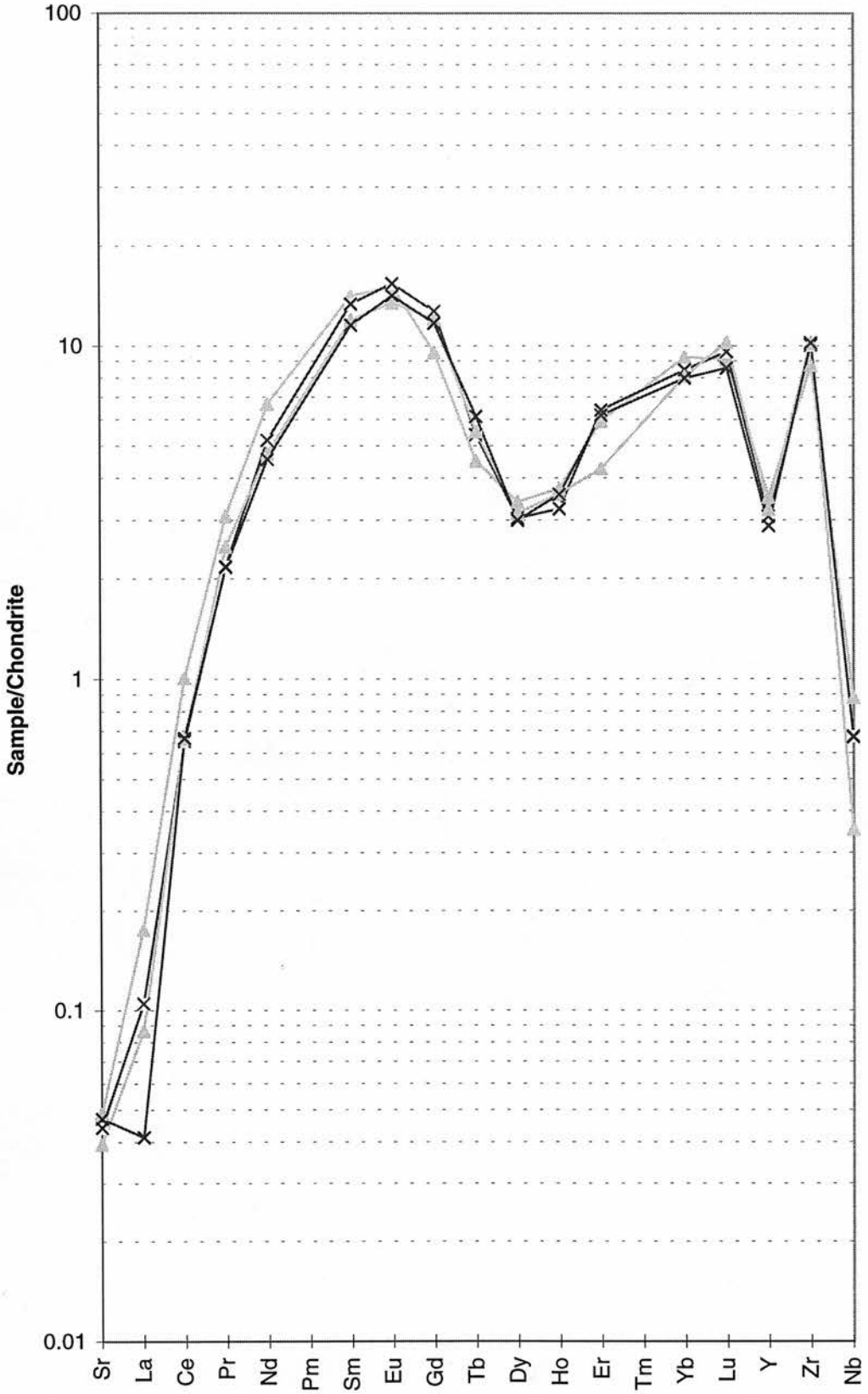

c:\simon\traces\J24gt.xls

Fig. D.1b J24 Clinopyroxene

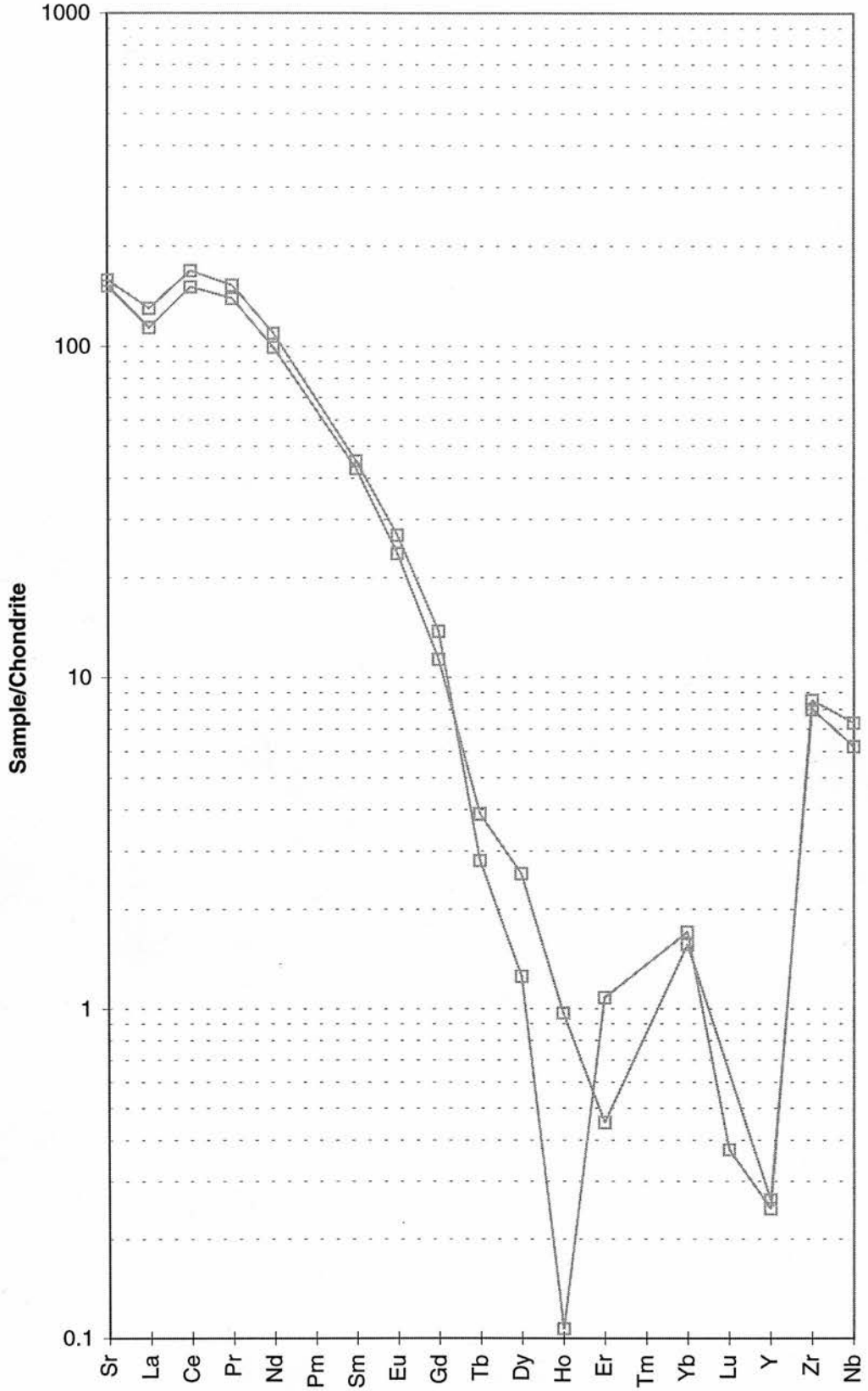

c:\simon\traces\J24c.xls

Fig. D.2a J25 Garnet

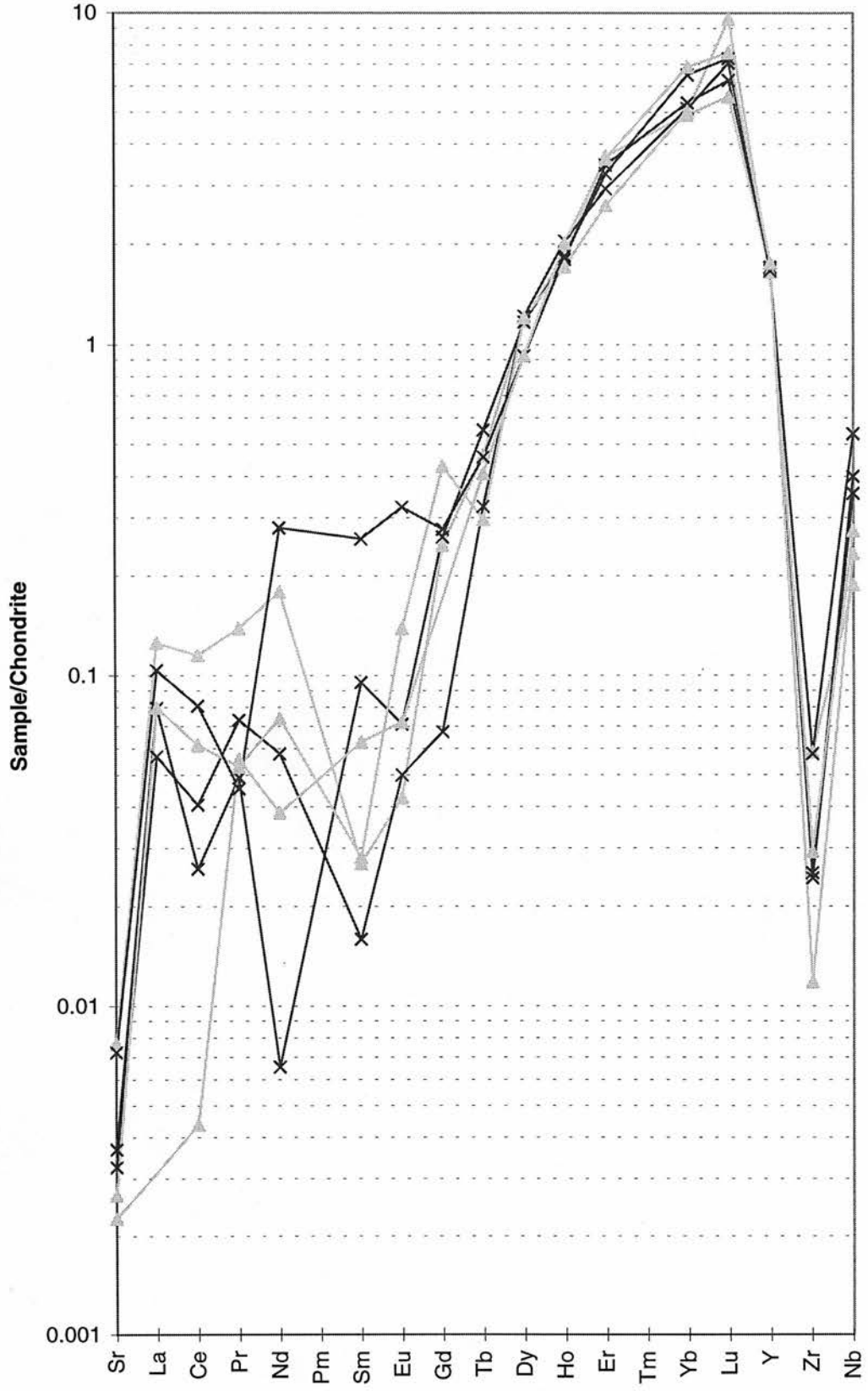

c:\simon\traces\j25gt.xls

Fig. D.2b J25 Clinopyroxene

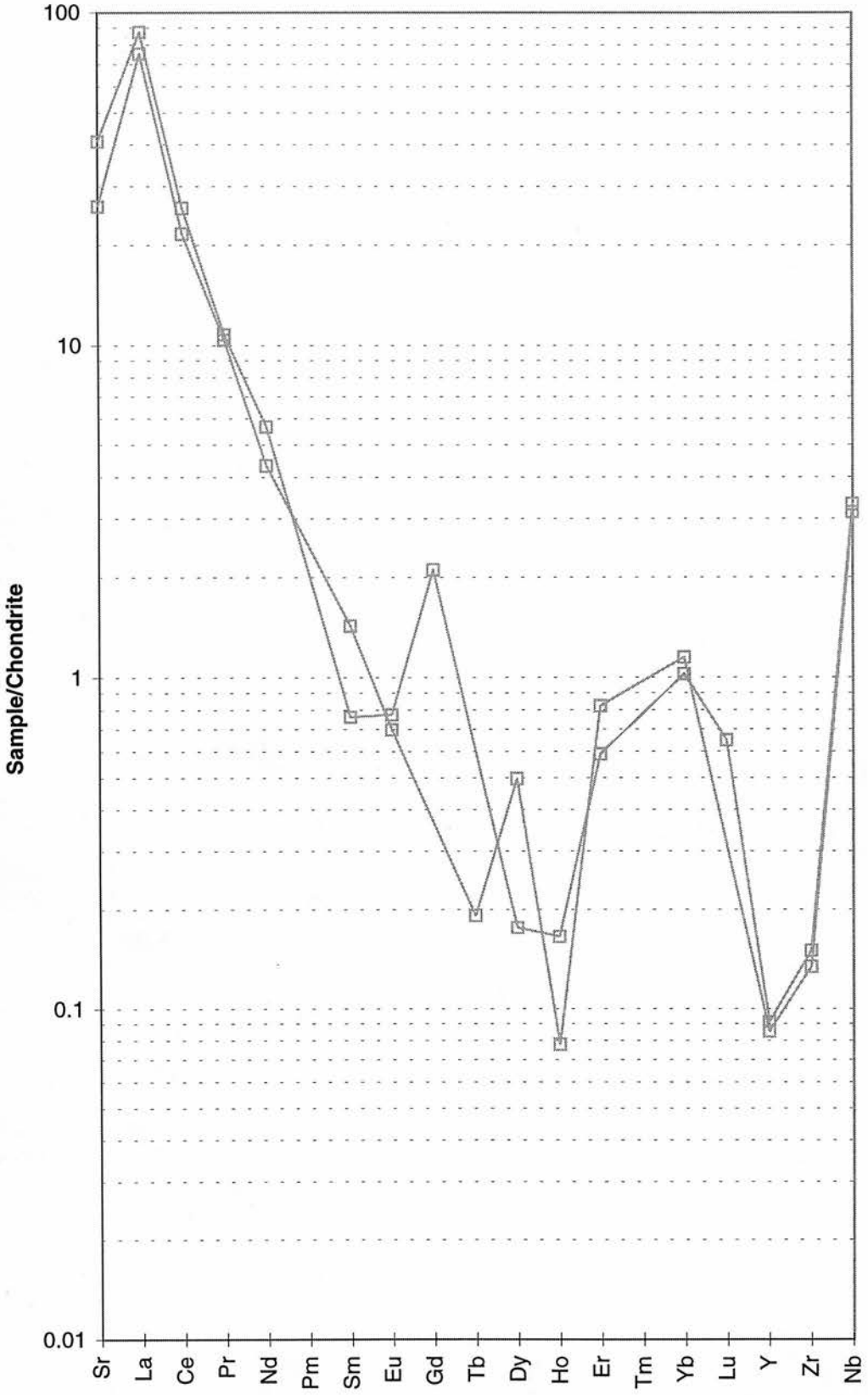

c:\simon\traces\J25c.xls

Fig. D.3 J146 Garnet

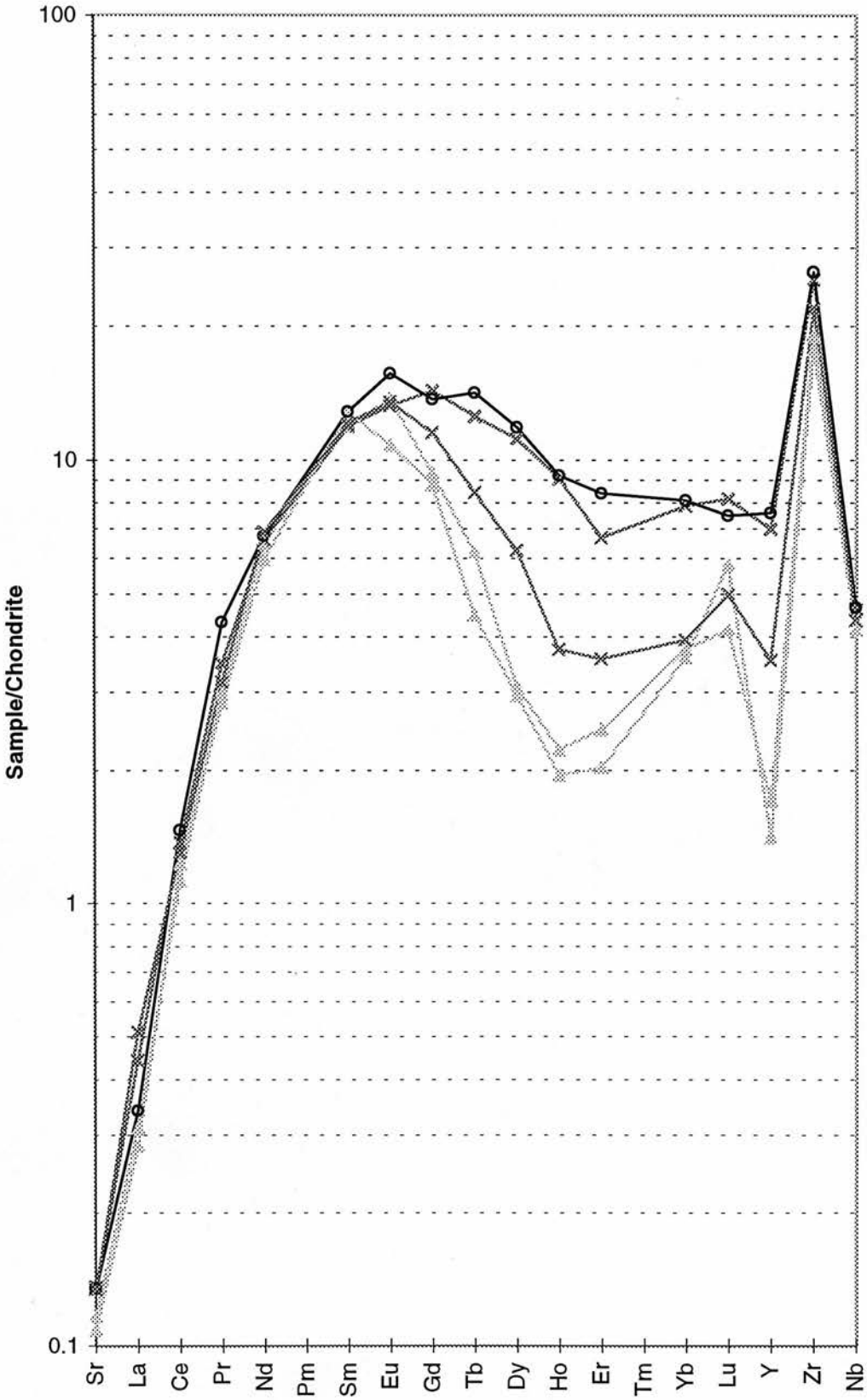

c:\simon\traces\J146gt.xls

Fig. D.4 J157 Garnet

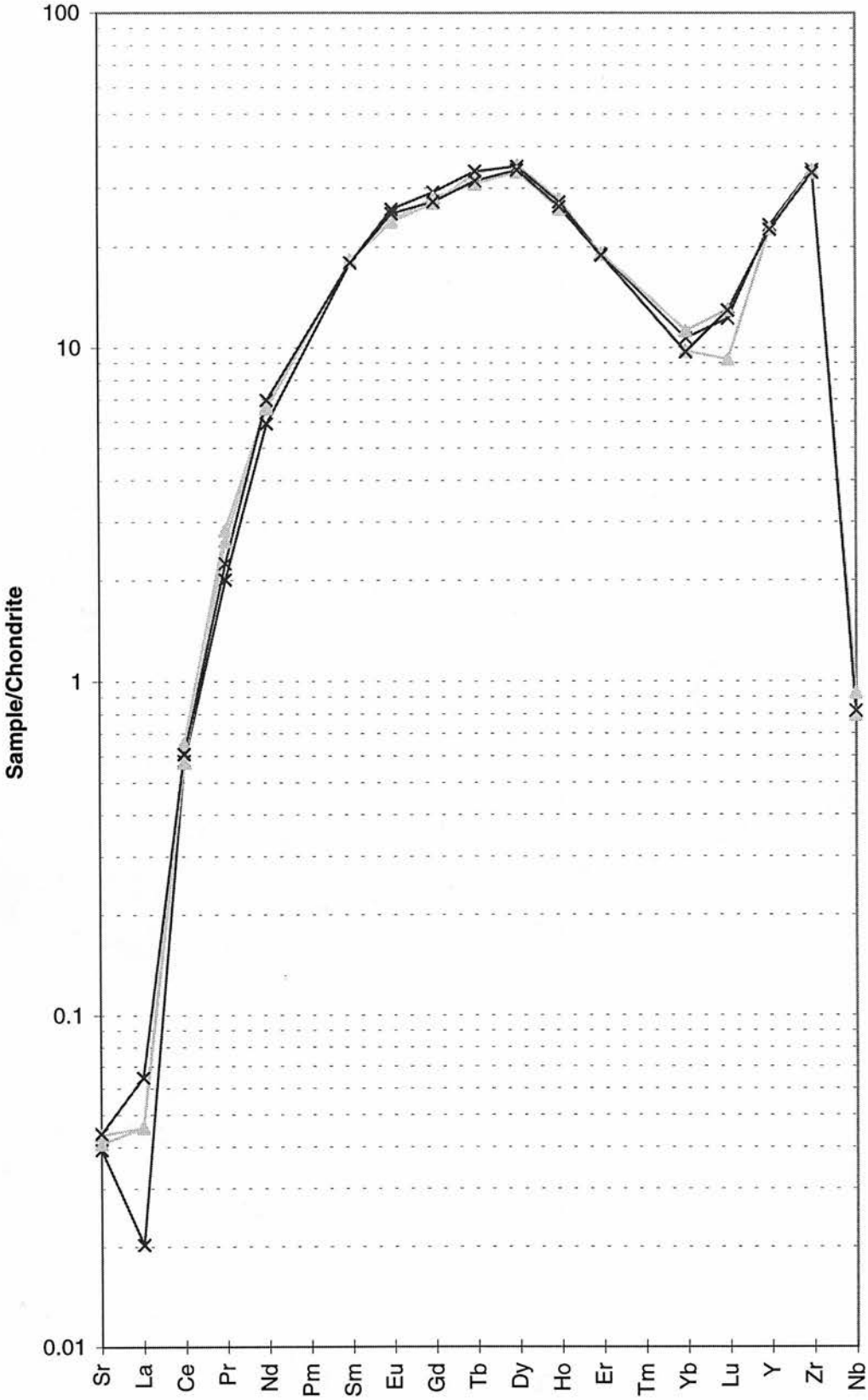

c:\simon\traces\J157gt.xls

Fig. D.5a JJG1728 Garnet

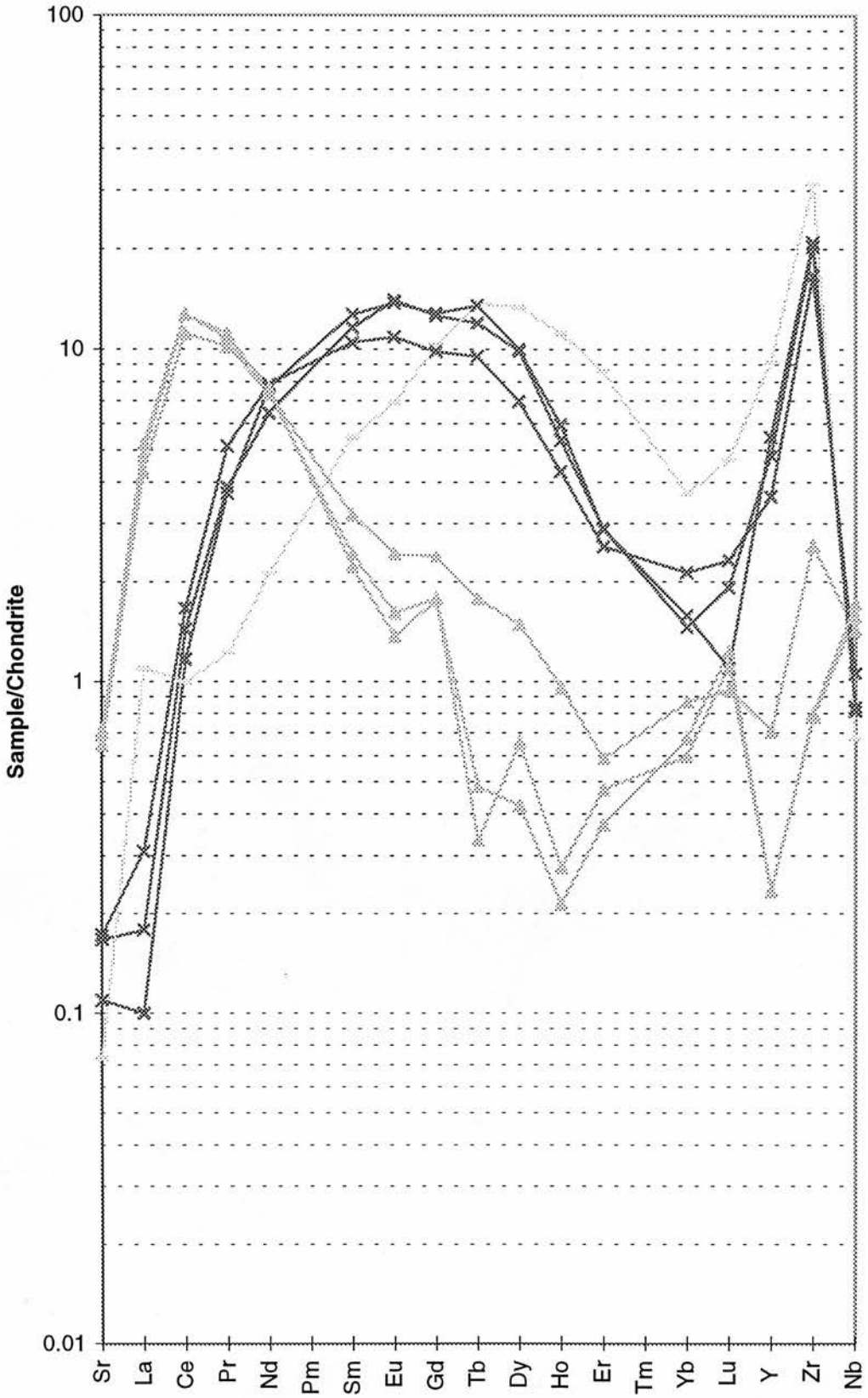

c:\simon\traces\1728gt.xls

Fig. D.5b JJG1728 Clinopyroxene

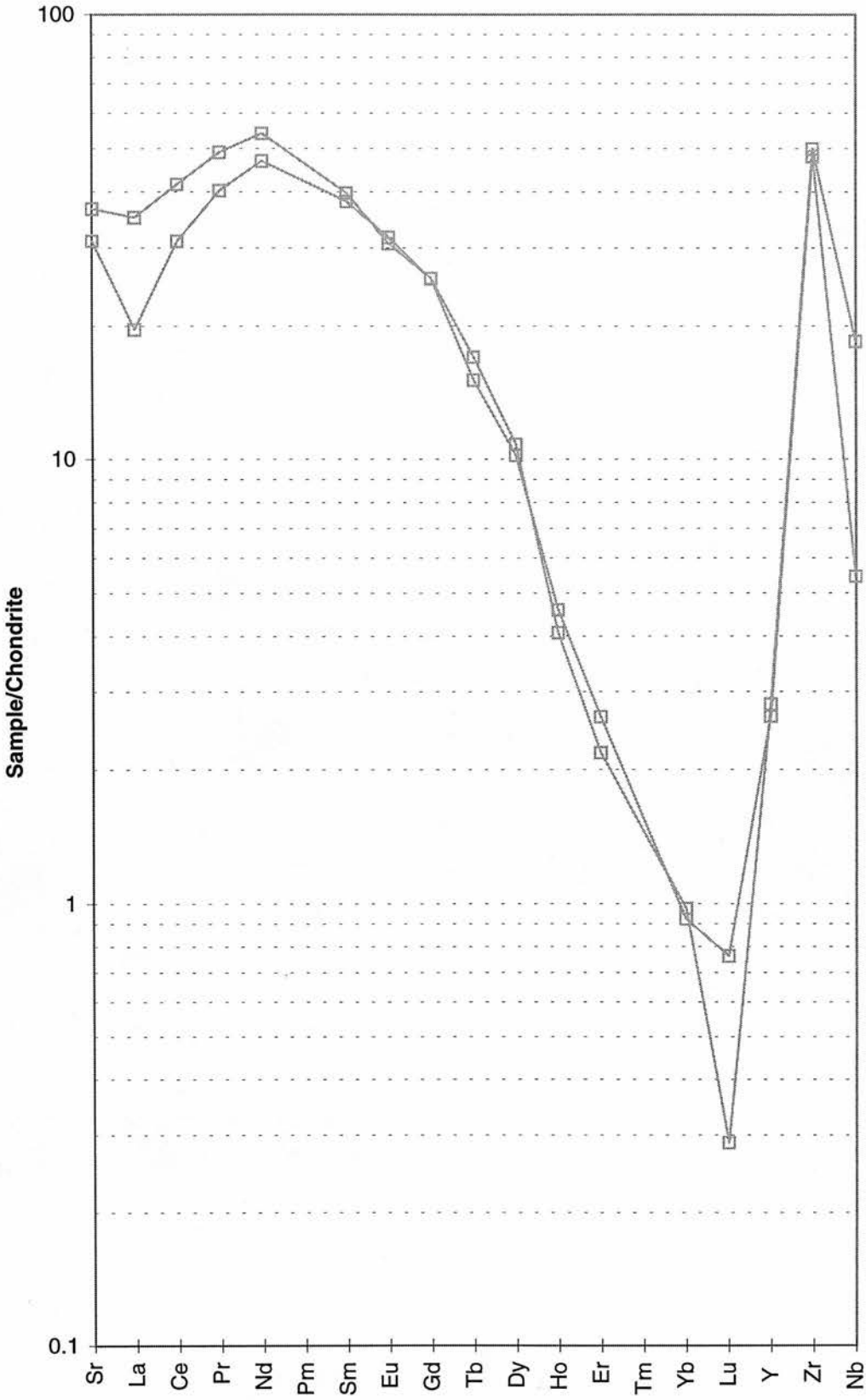

c:\simon\traces\1728c.xls

Fig. D.6 JJG1757 Garnet

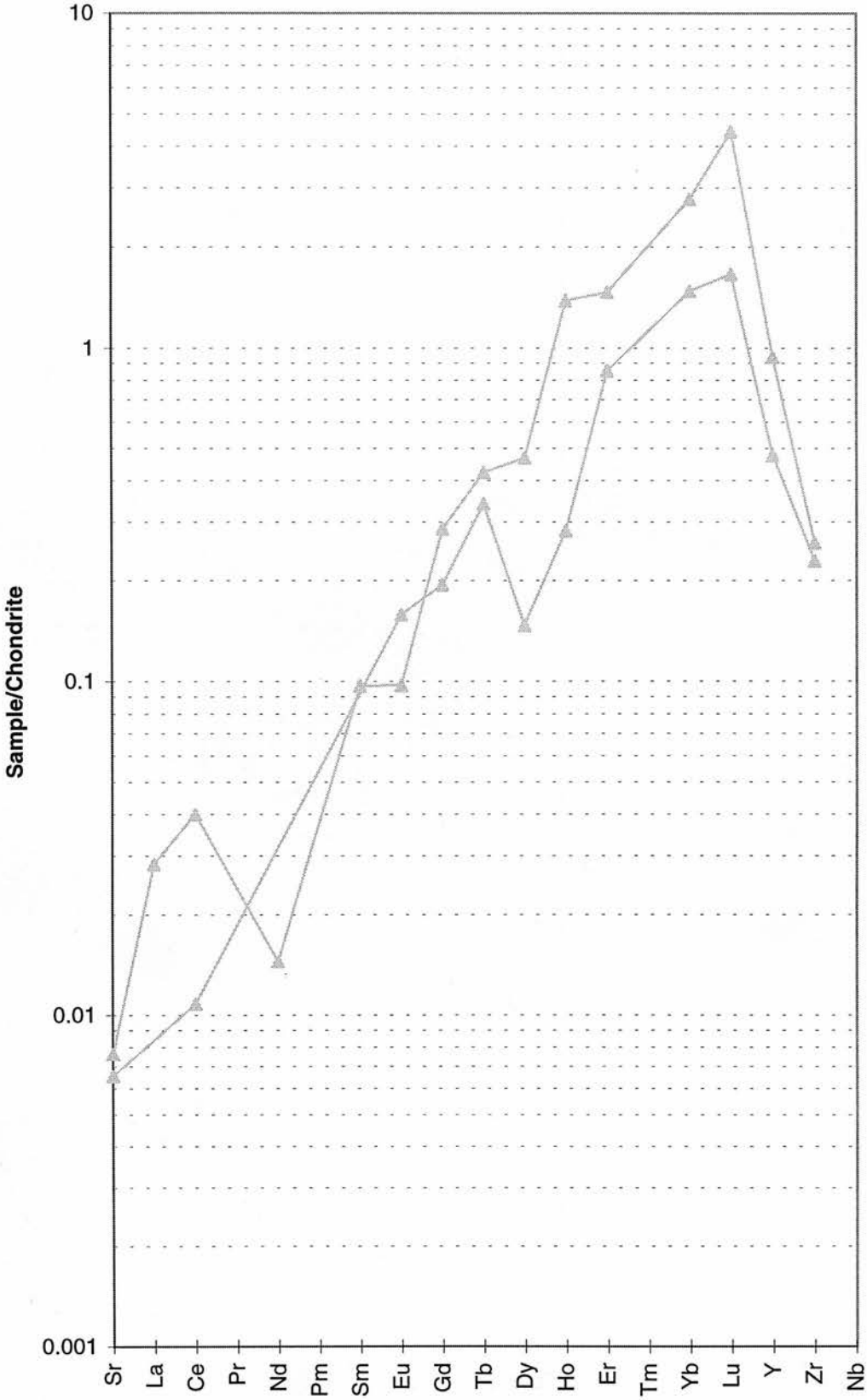

c:\simon\traces\1757gt.xls

Fig. D.7 JJG1761 Garnet

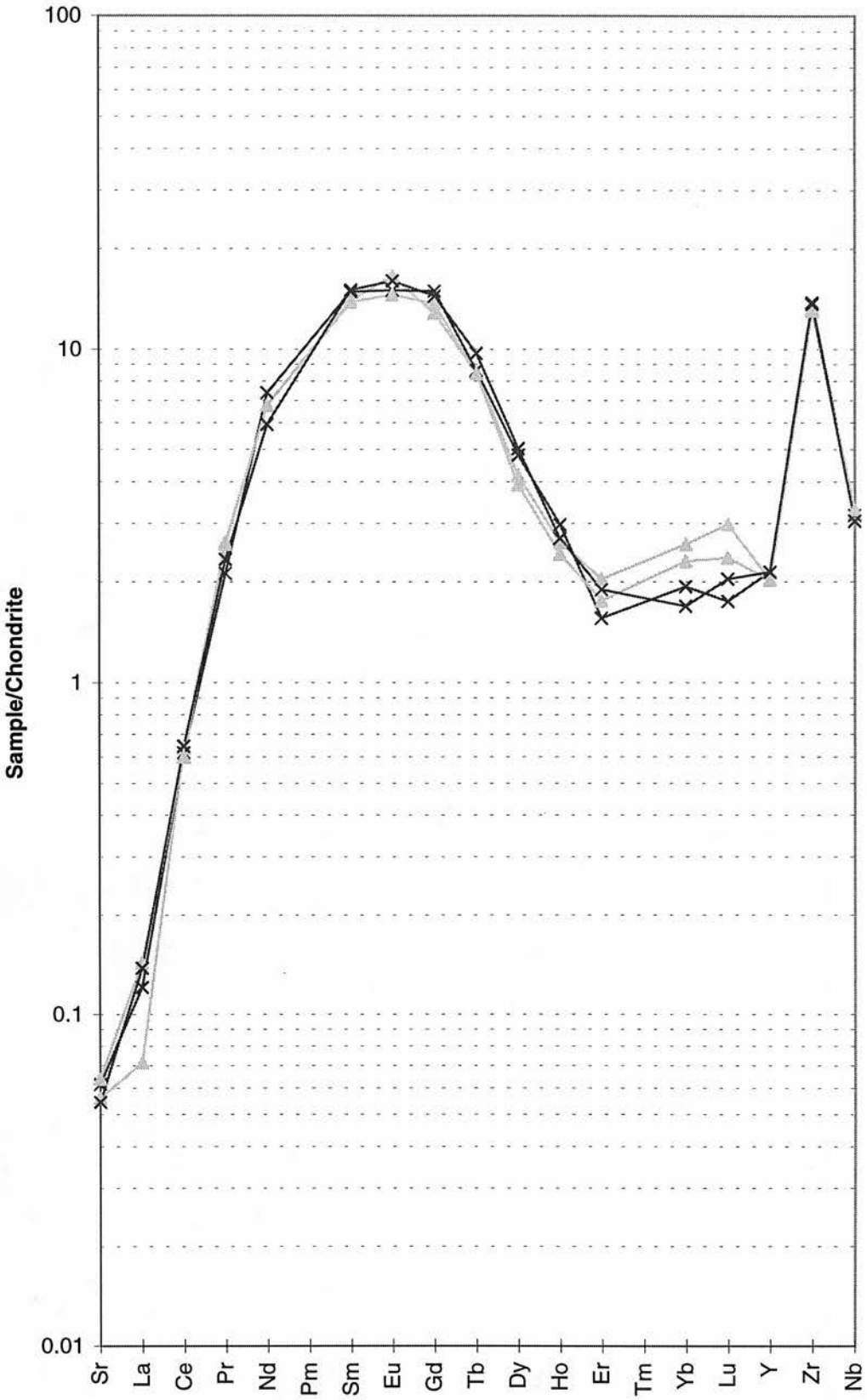

c:\simon\traces\1761gt.xls

Fig. D.8 JJG1780 Garnet

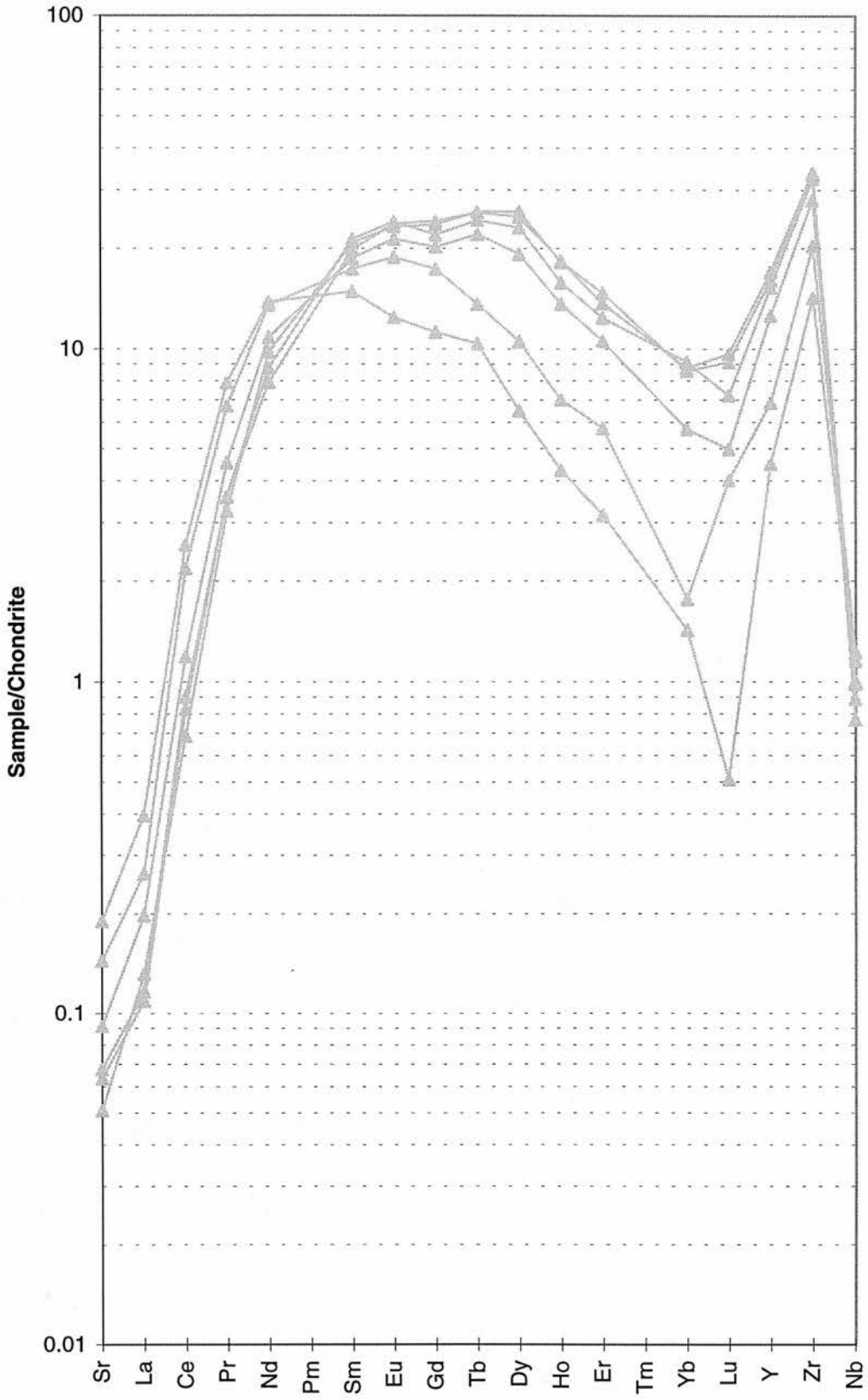

c:\simon\traces\1780gt.xls

Fig. D.9 JJG1781 Garnet

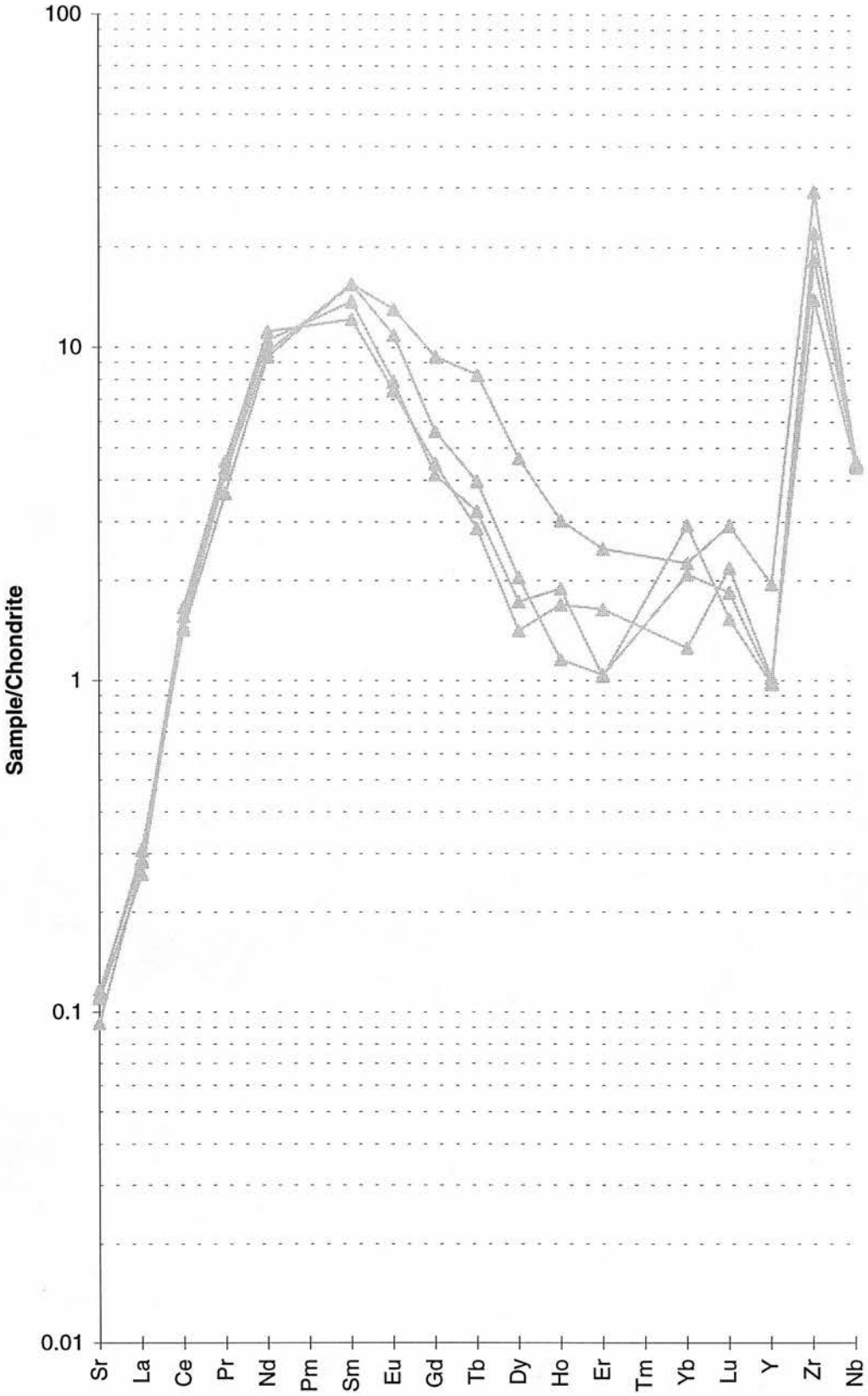

c:\simon\traces\1781gt.xls

Fig. D.10 JJG2469 Garnet

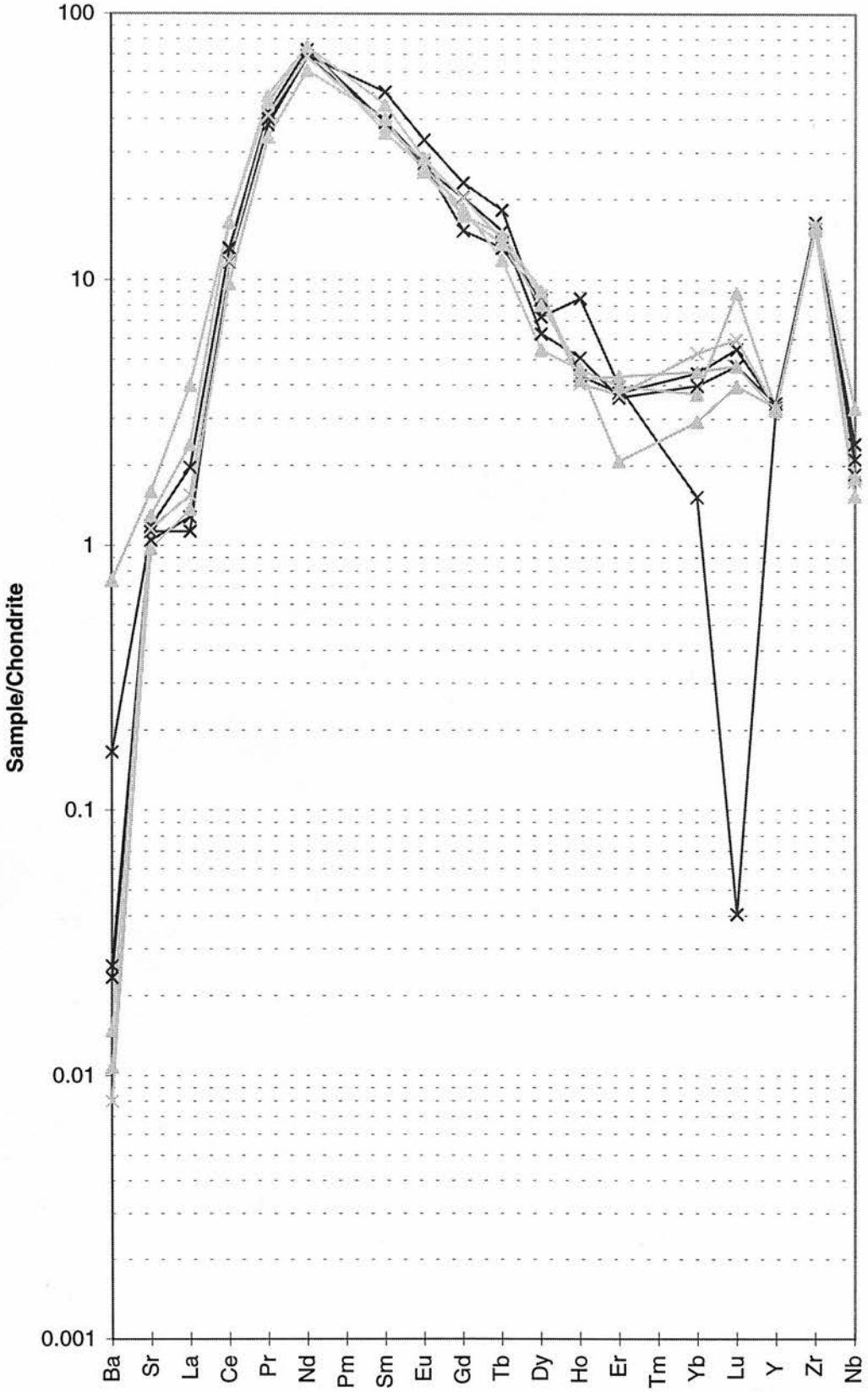

c:\simon\traces\2469bgt.xls

Fig. D.11 J22F/2 Garnet

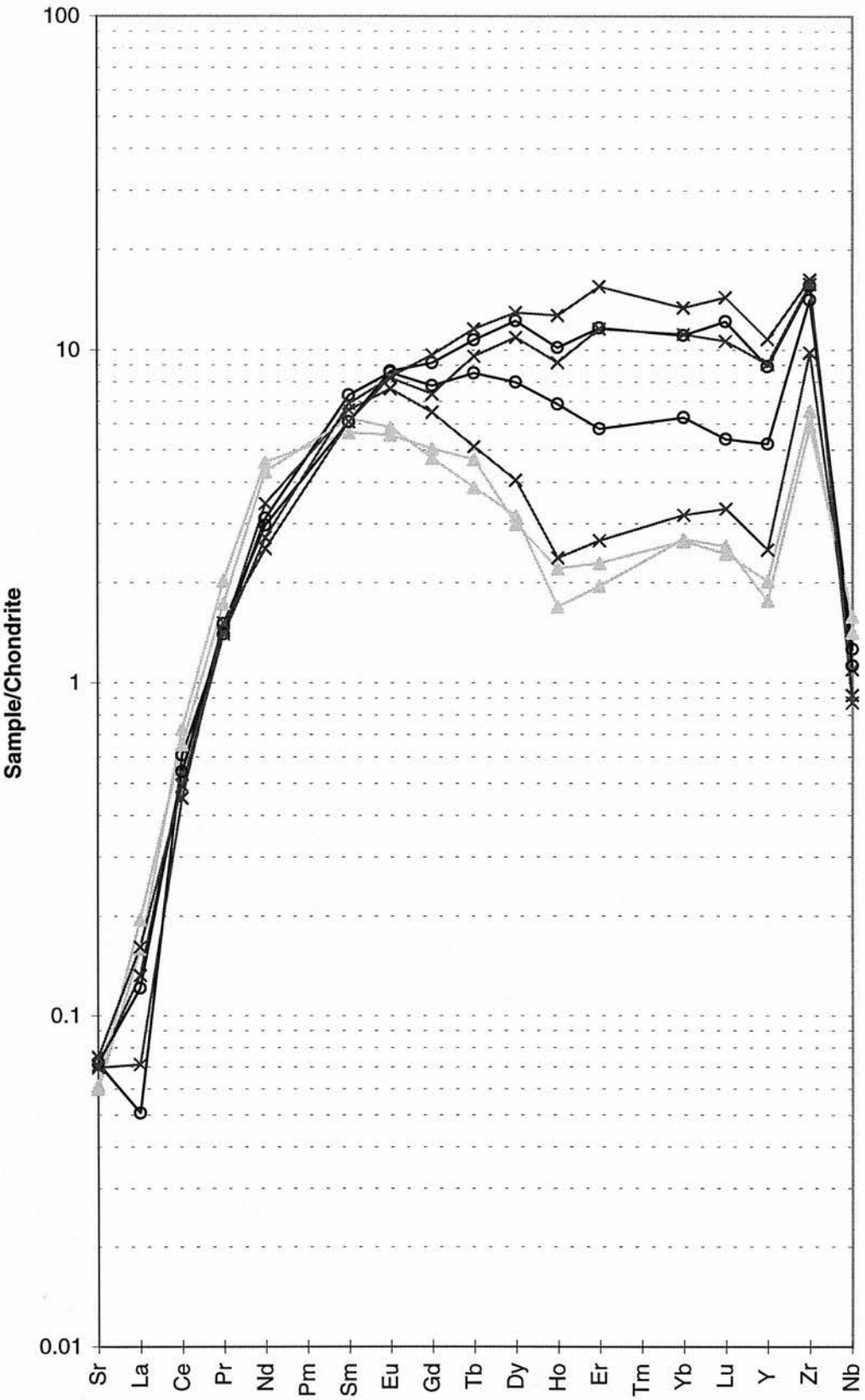

c:\simon\traces\j22f2gt.xls

Fig. D.12 J34B GarnetA

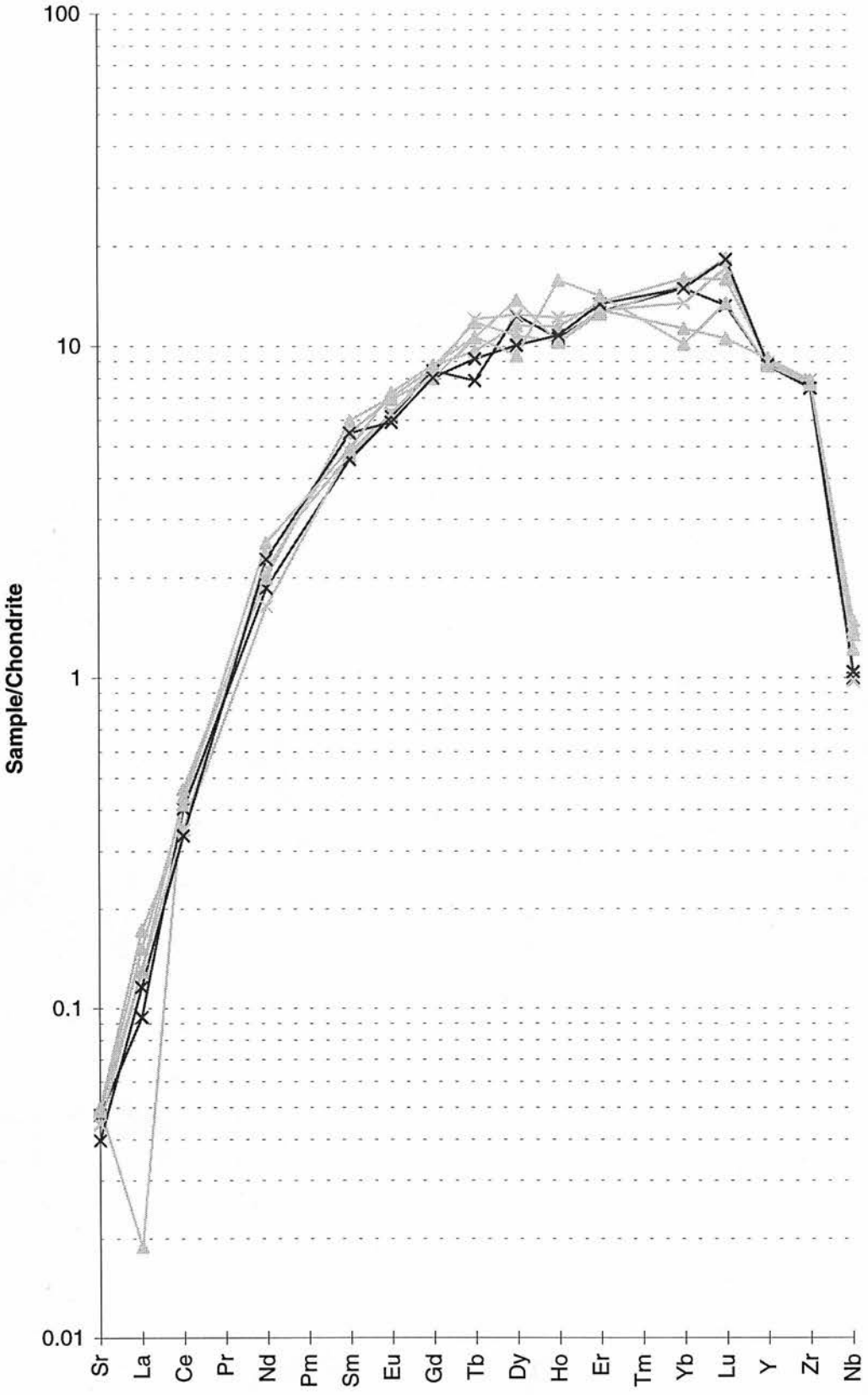

c:\simon\traces\J34bgt.xls

Fig. D.13a J47 Garnet

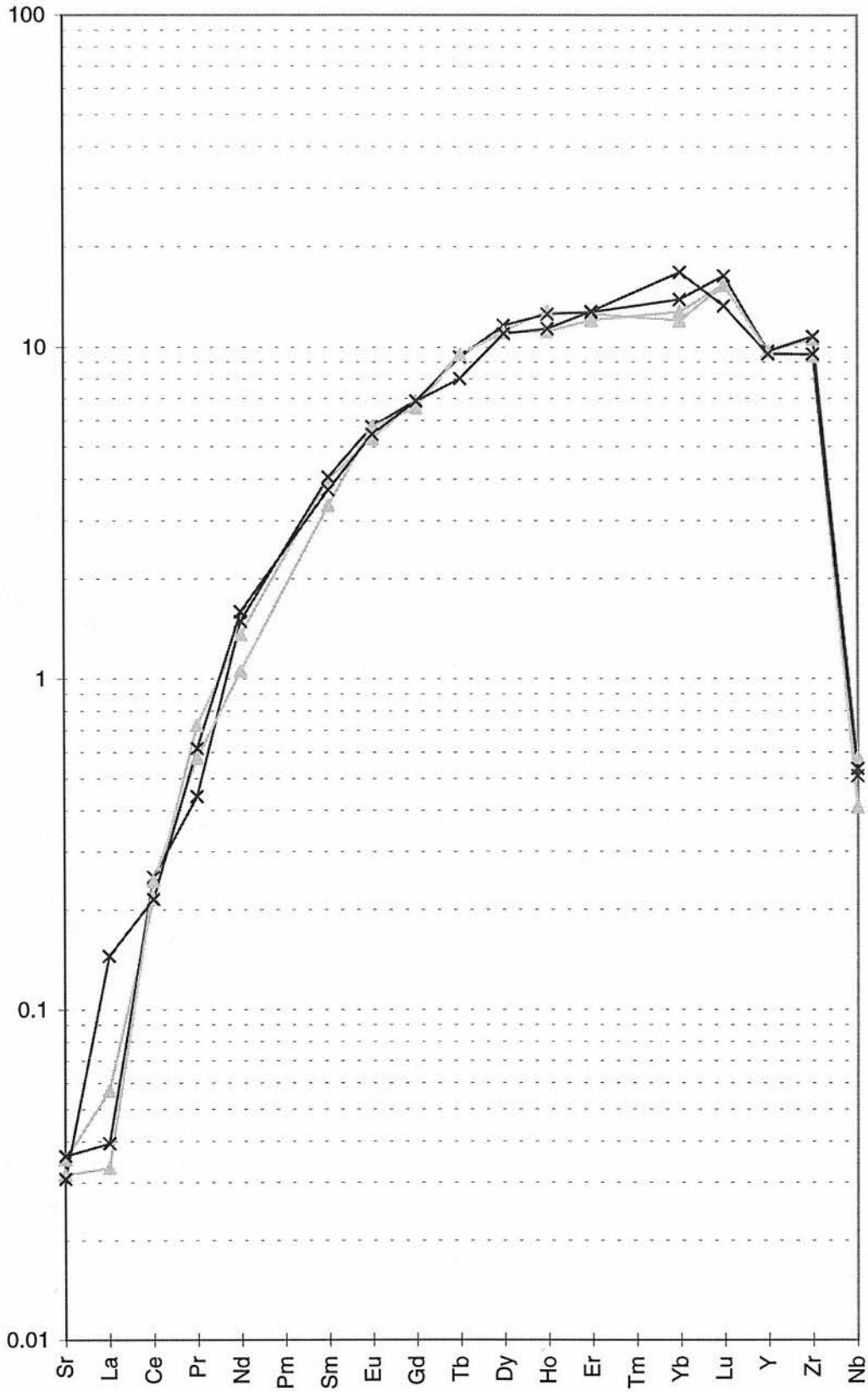

c:\simon\traces\J47gt.xls

Fig. D.13b J47 Clinopyroxene

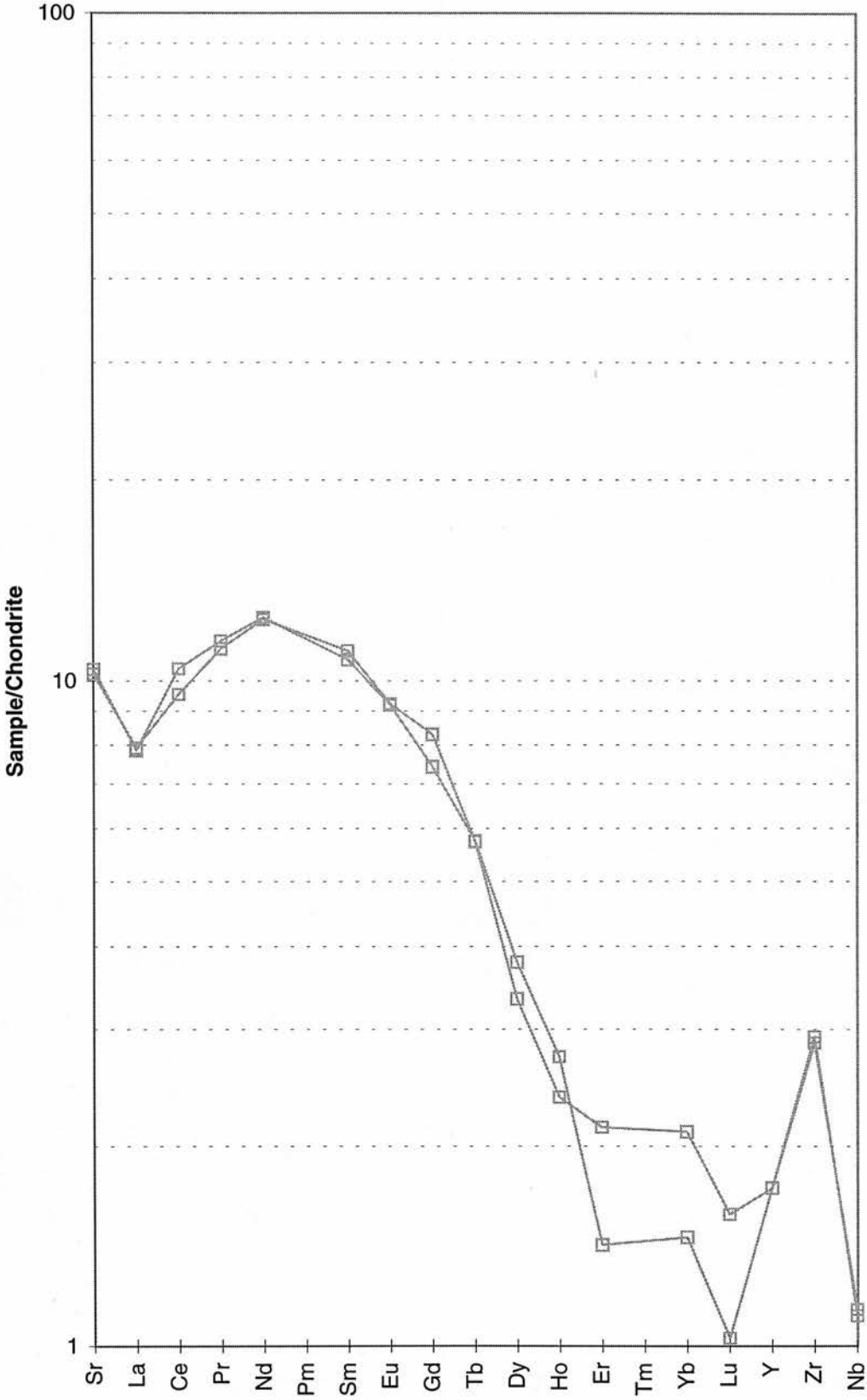

c:\simon\traces\J47c.xls

Fig. D.14a J51 Garnet

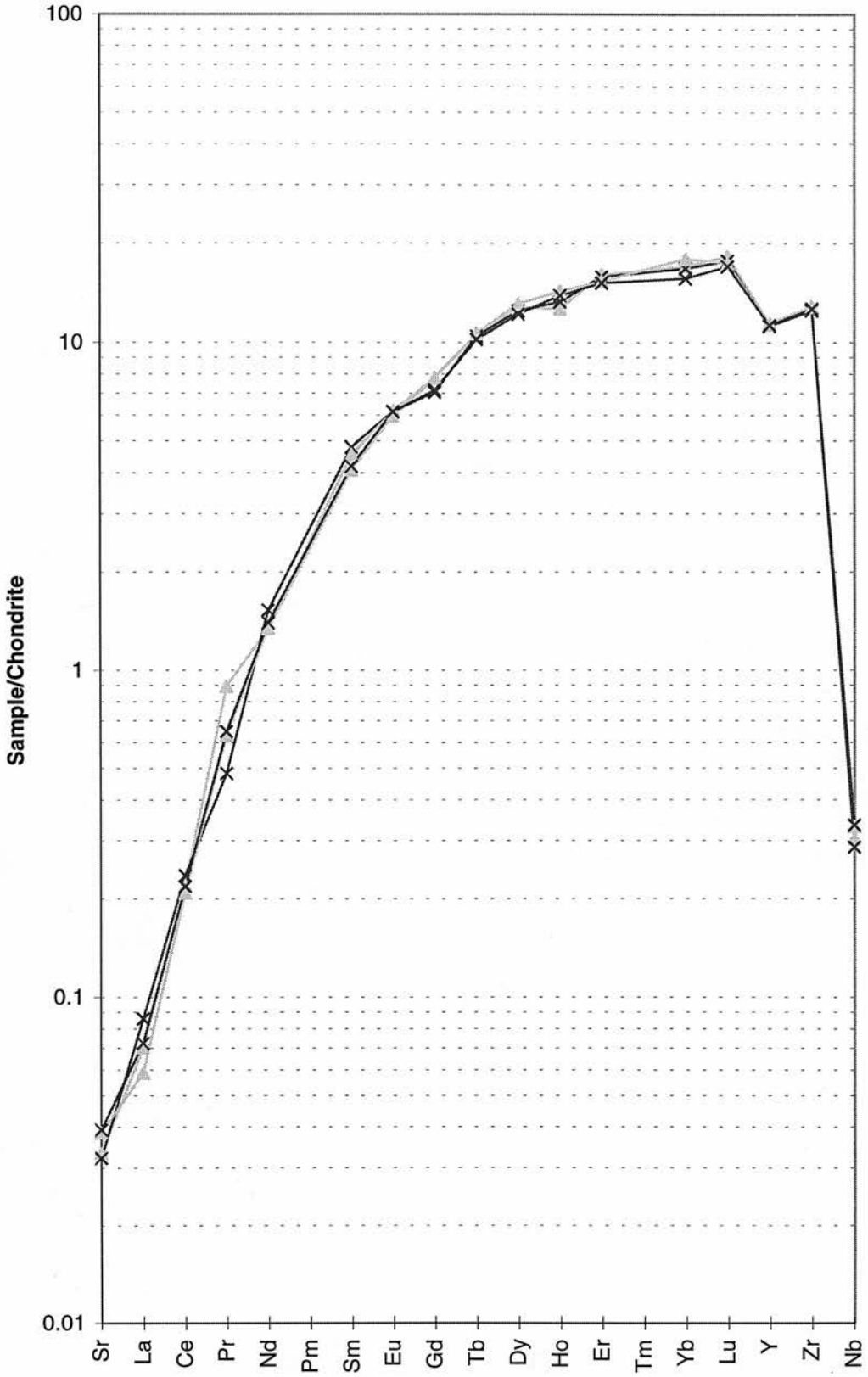

c:\simon\traces\J51gt.xls

Fig. D.14b J51 Clinopyroxene

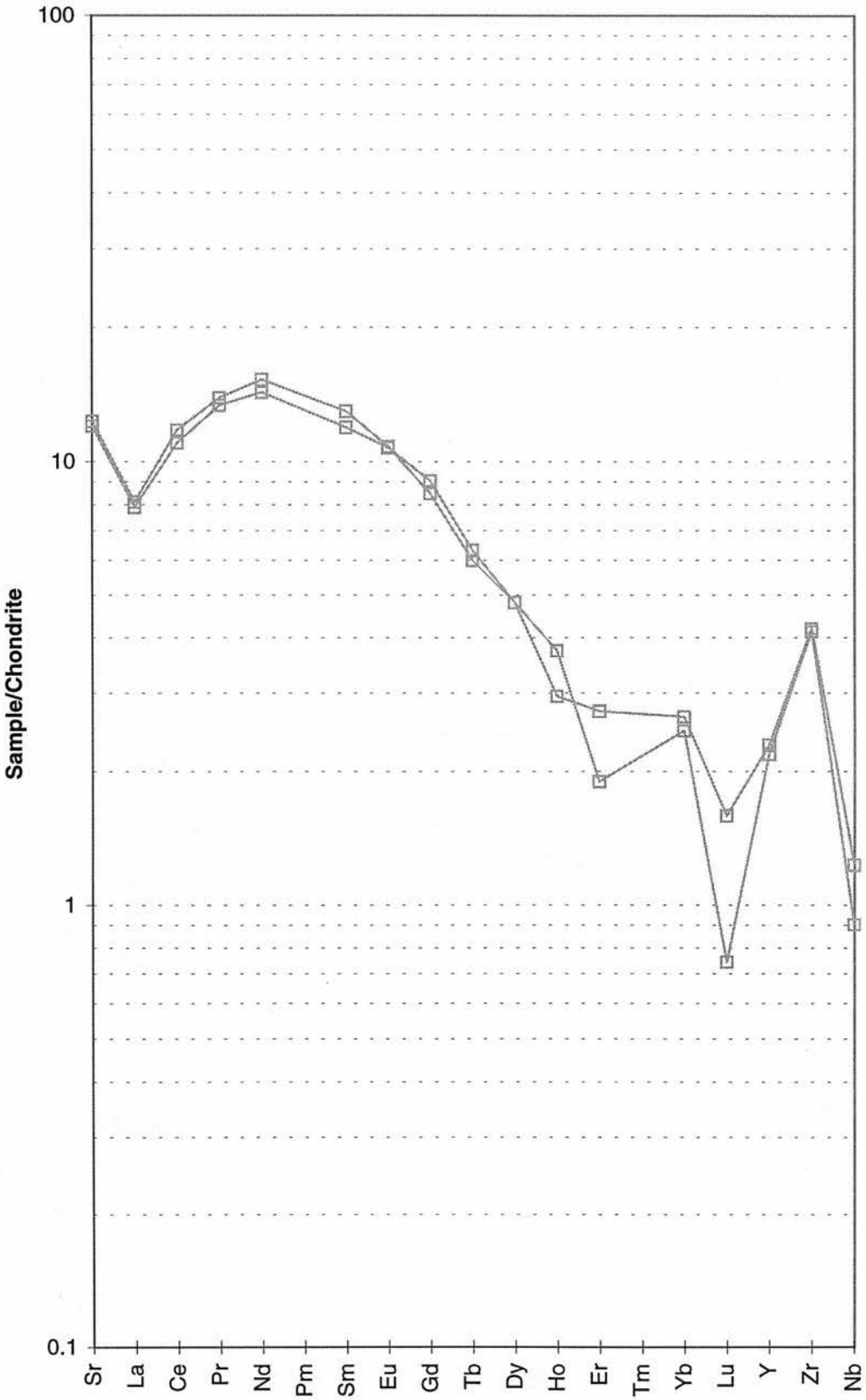

c:\simon\traces\J51c.xls

Fig. D.15 J107 Garnet

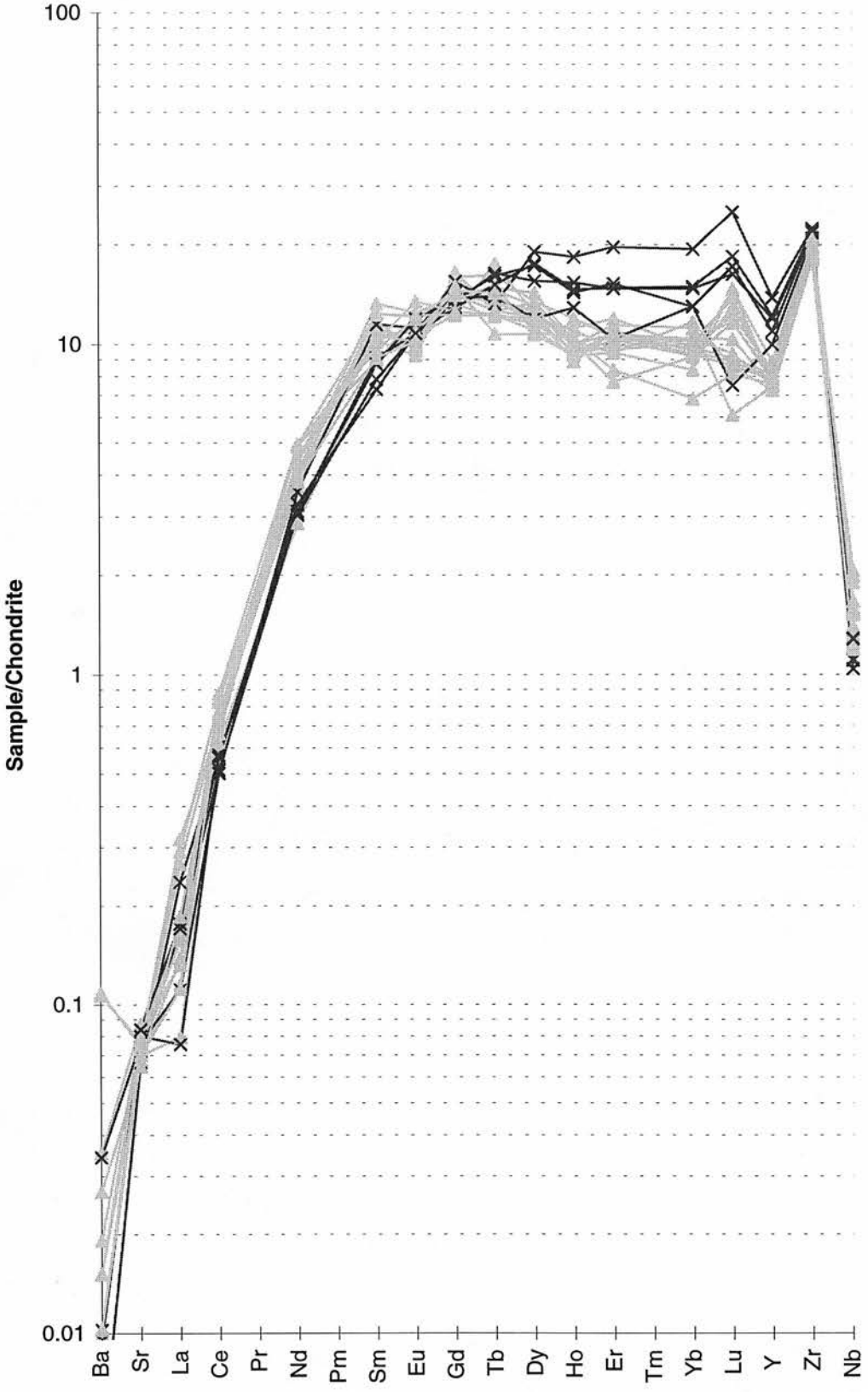

c:\simon\traces\J107bgt.xls

Fig. D.16a J110 Garnet

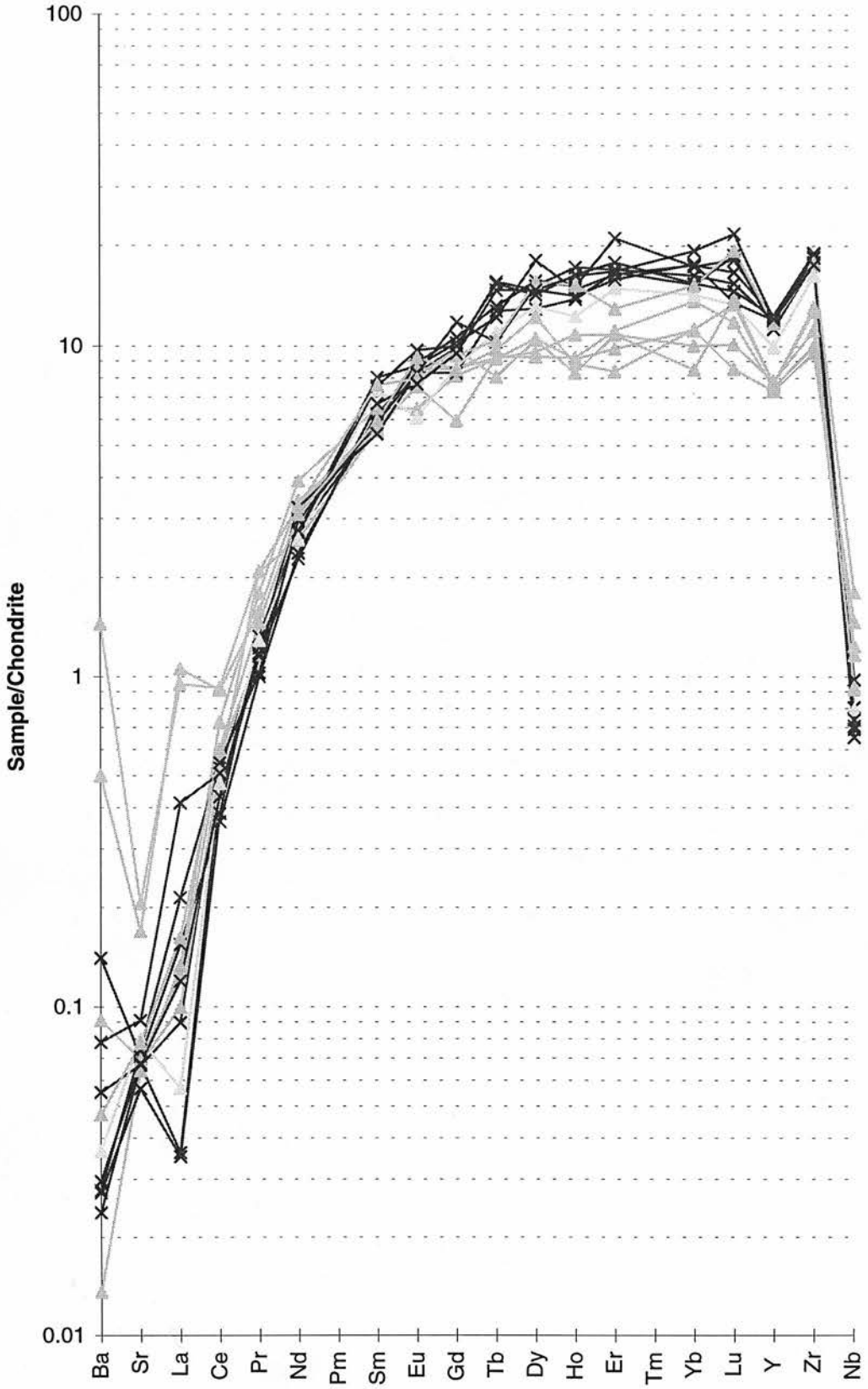

c:\simon\traces\J110gt.xls

Fig. D.16b J110 Clinopyroxene

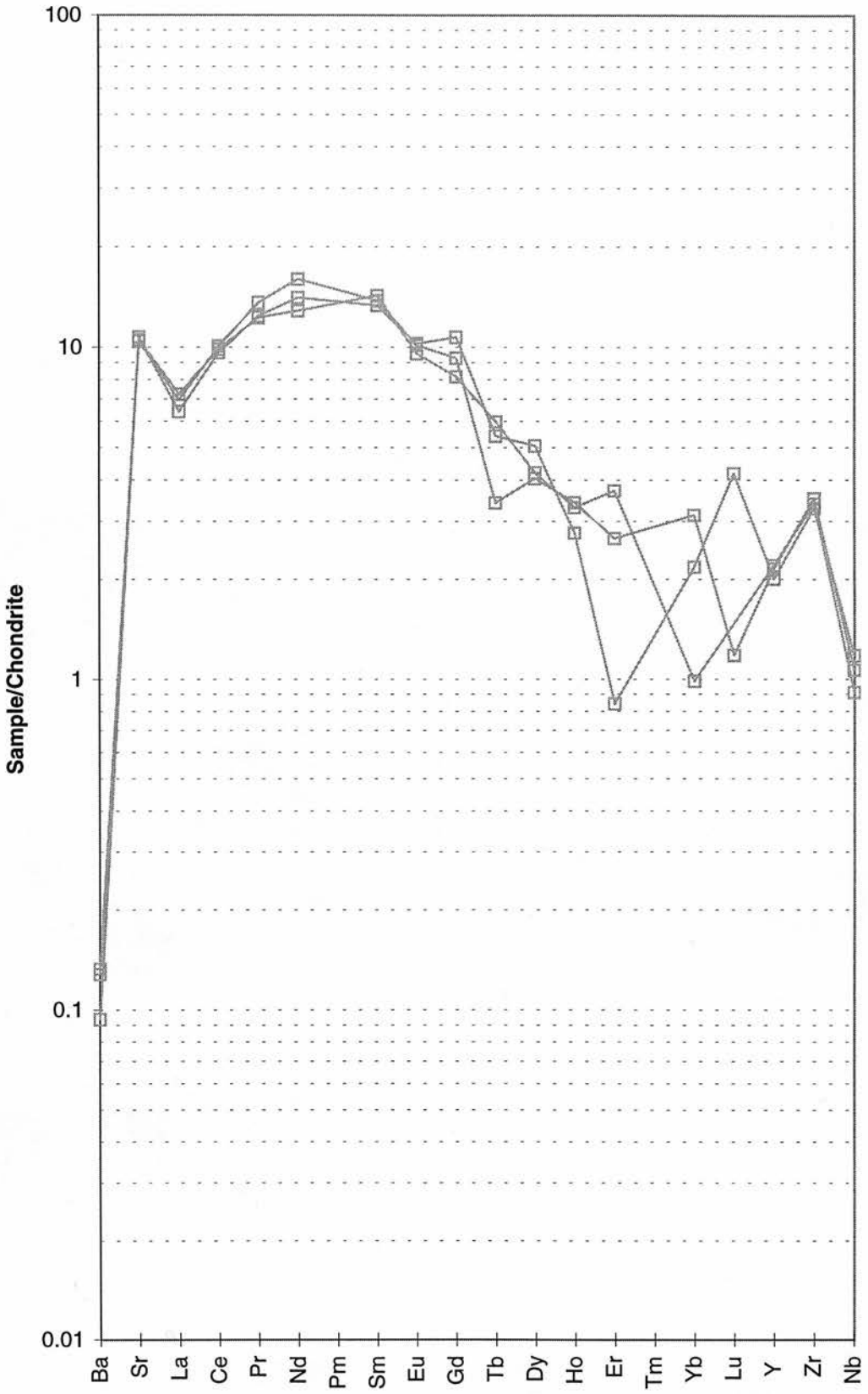

c:\simon\traces\J110c.xls

Fig. D.17a J112 Garnet

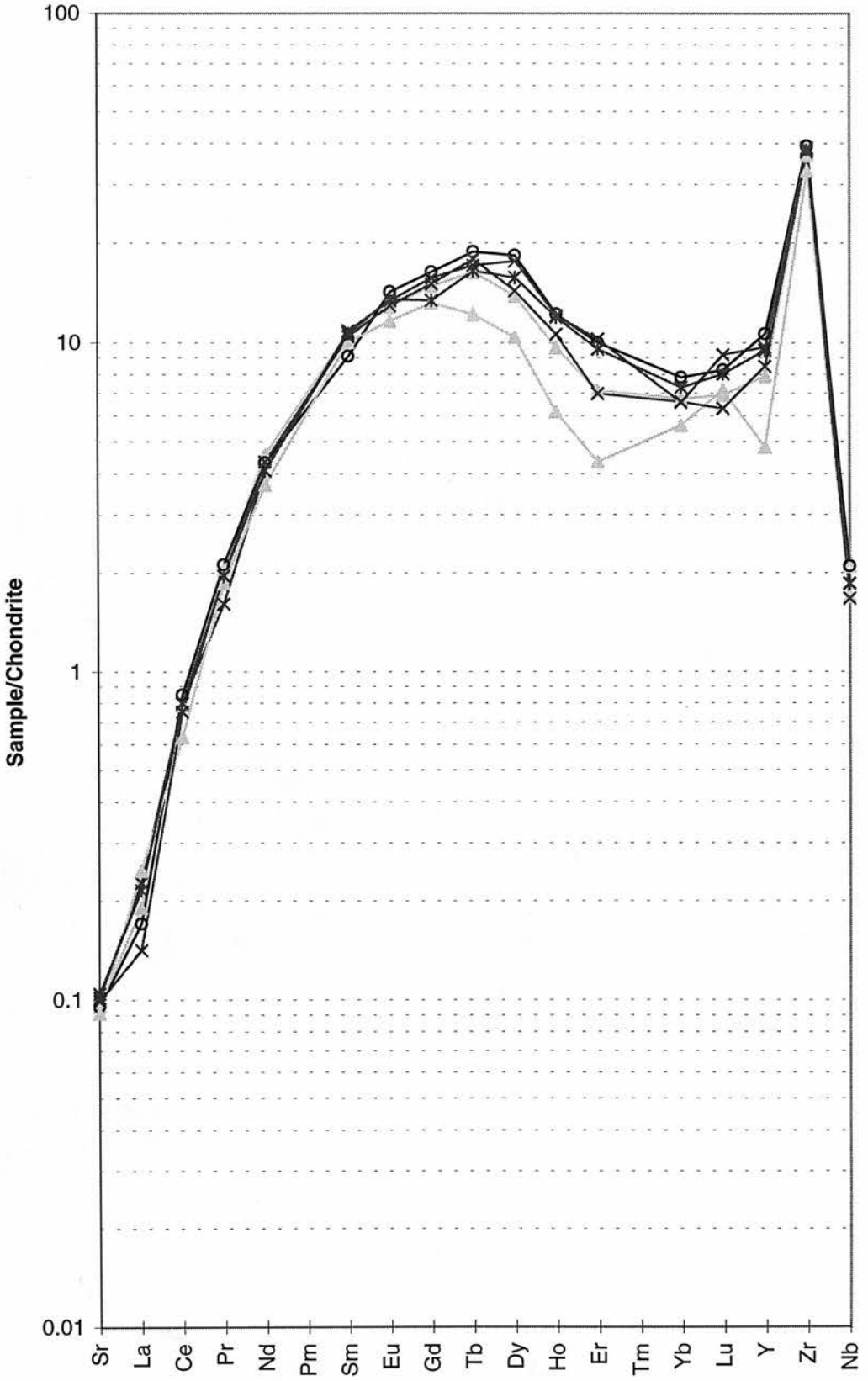

c:\simon\traces\J112gt.xls

Fig. D.17b J112 Clinopyroxene

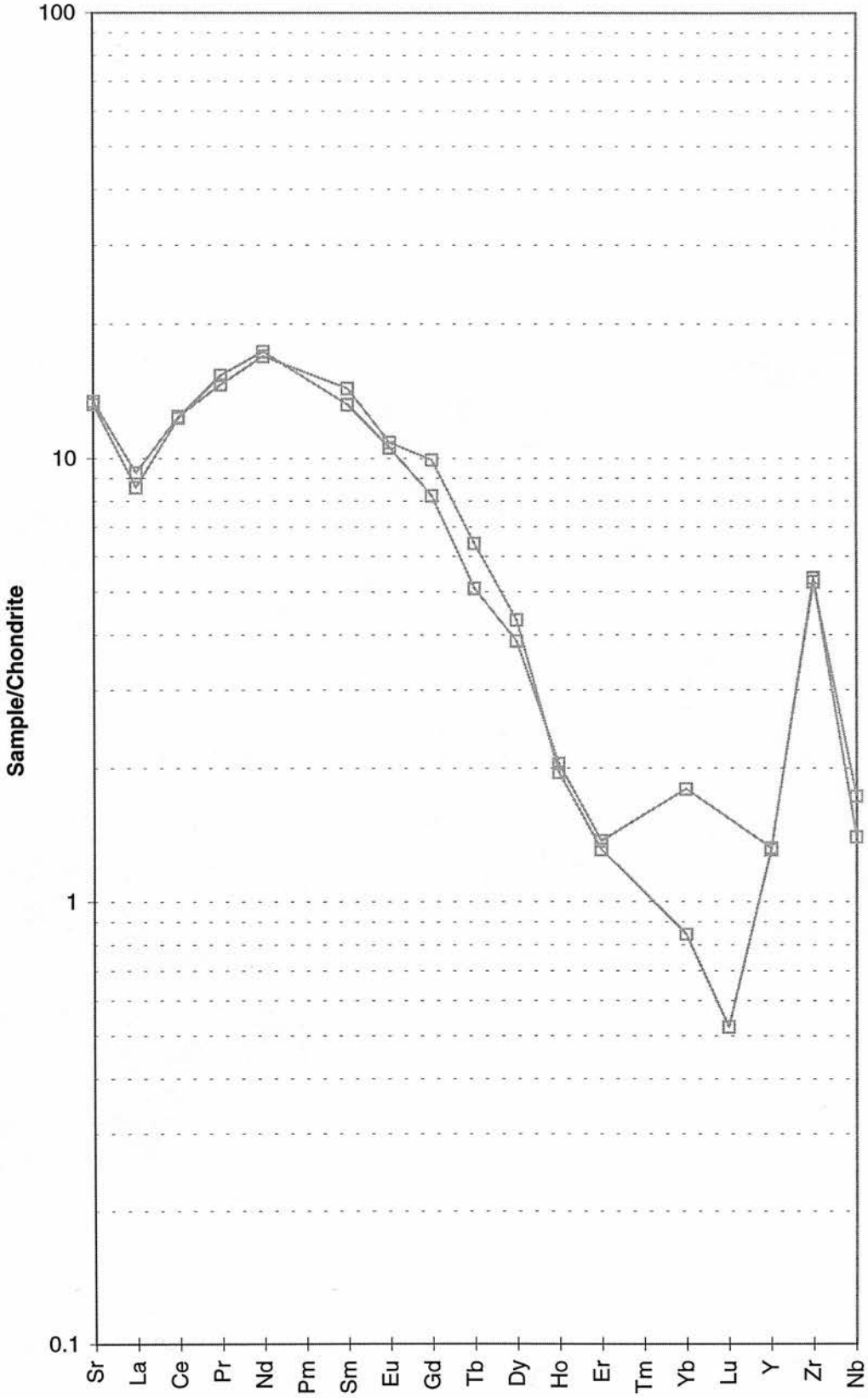

c:\simon\traces\J112c.xls

Fig. D.18a J115 Garnet

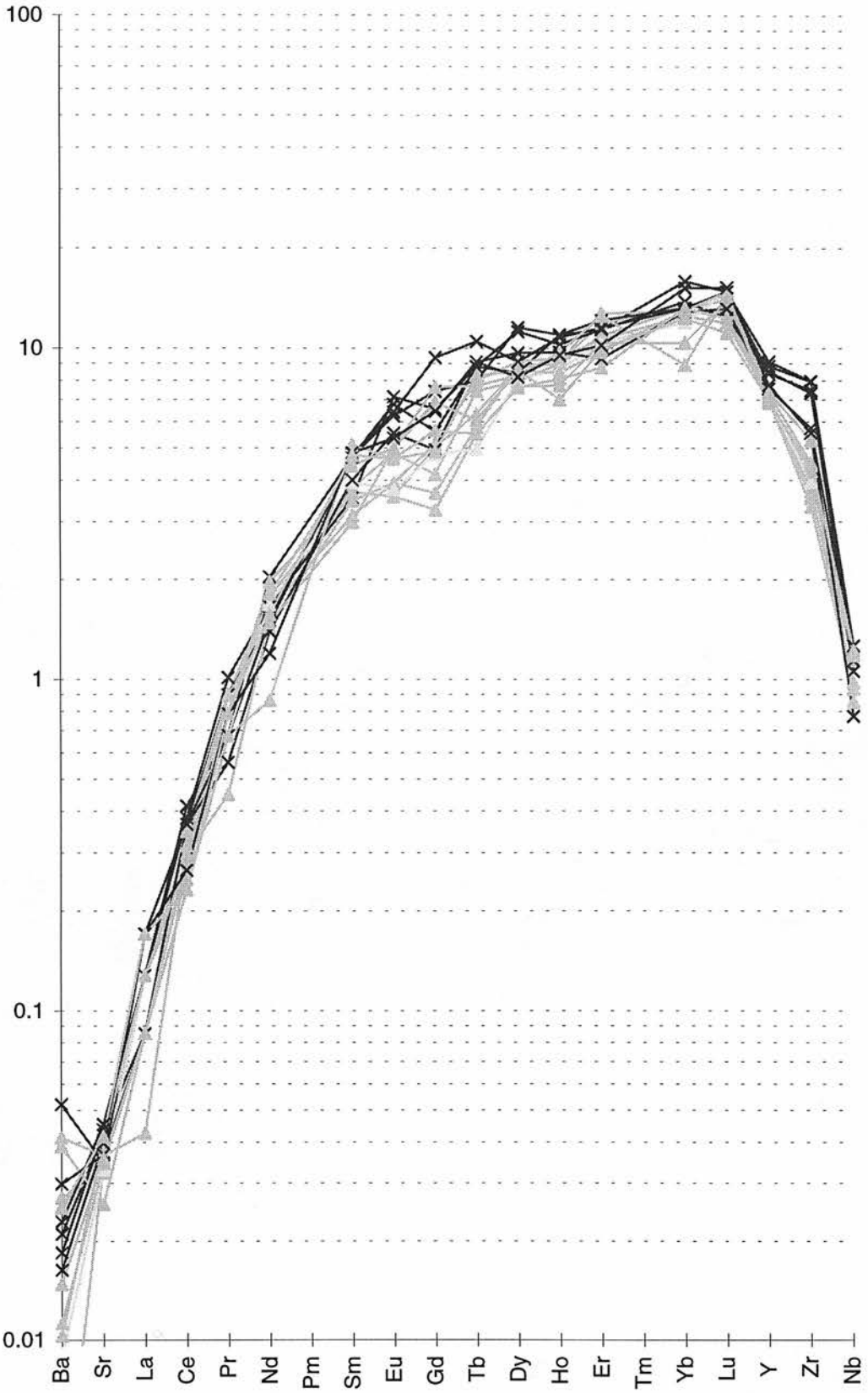

c:\simon\traces\J115gt.xls

Fig. D.18b J115 Clinopyroxene

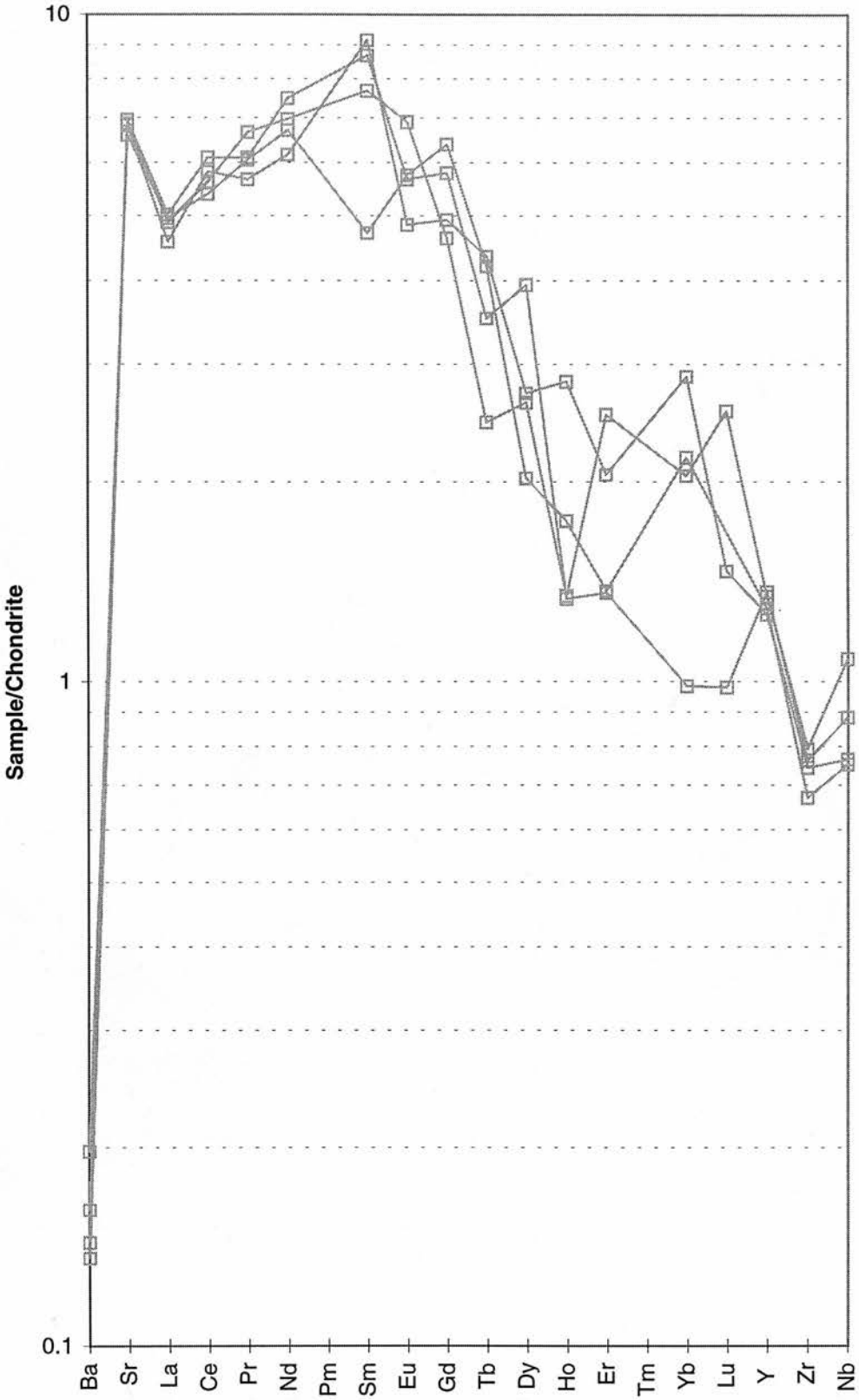

c:simon\traces\J115c.xls

Fig. D.19a J121 Garnet

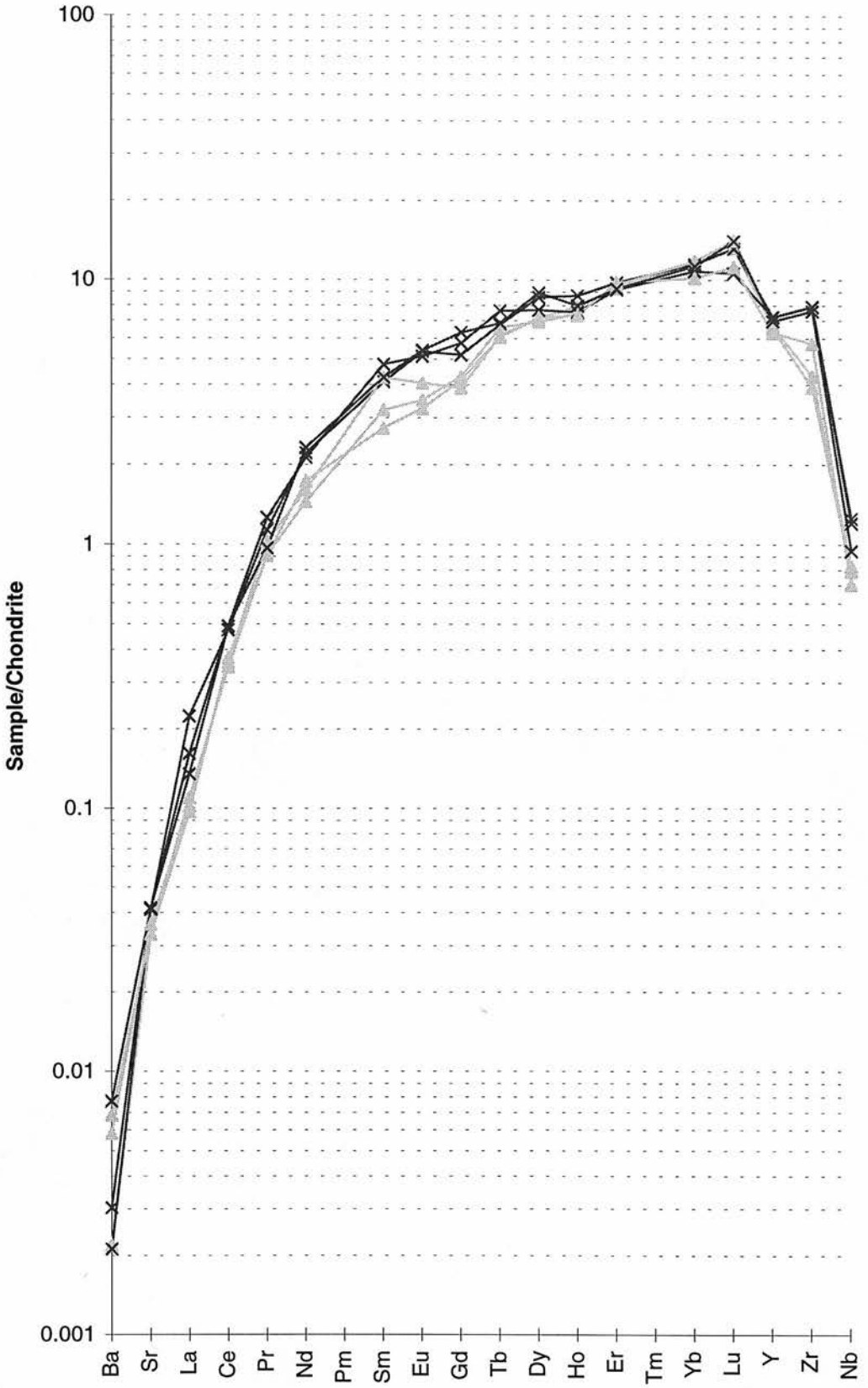

c:\simon\traces\J121gt.xls

Fig. D.19b J121a Garnet

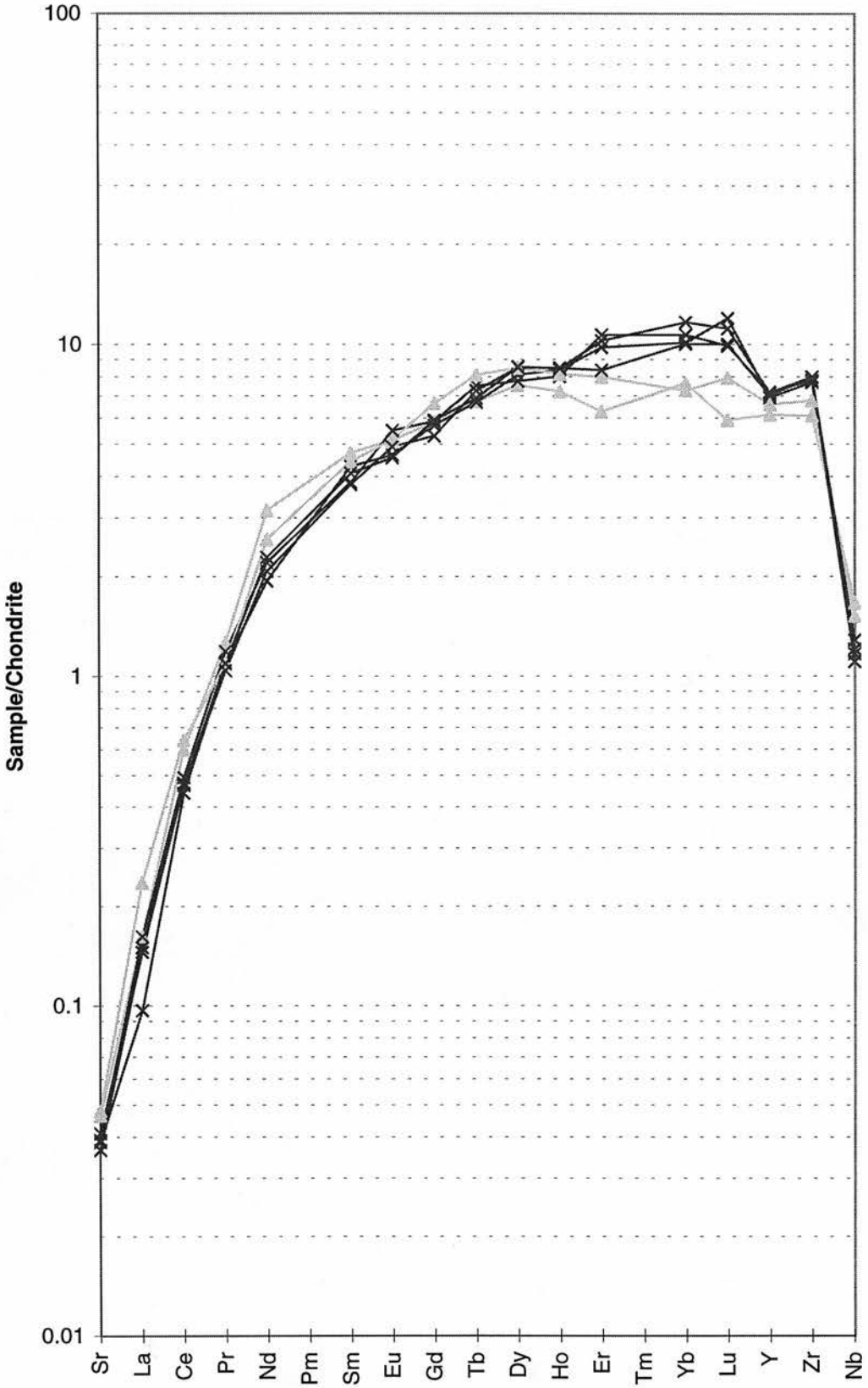

c:\simon\traces\J121agt.xls

Fig. D.19c J121 Clinopyroxene

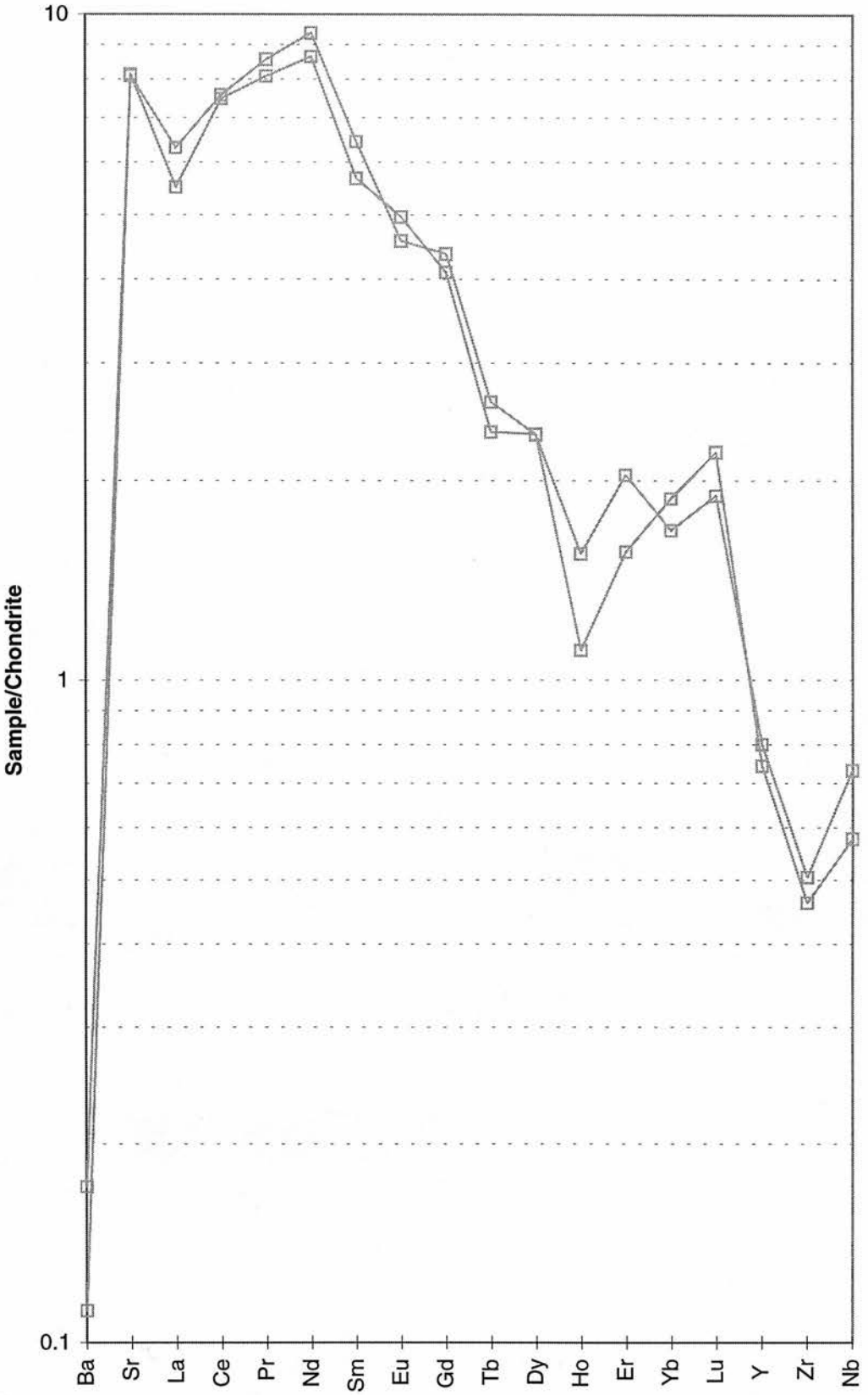

c:\simon\traces\J121c.xls

Fig. D.20a JJG1776 Garnet

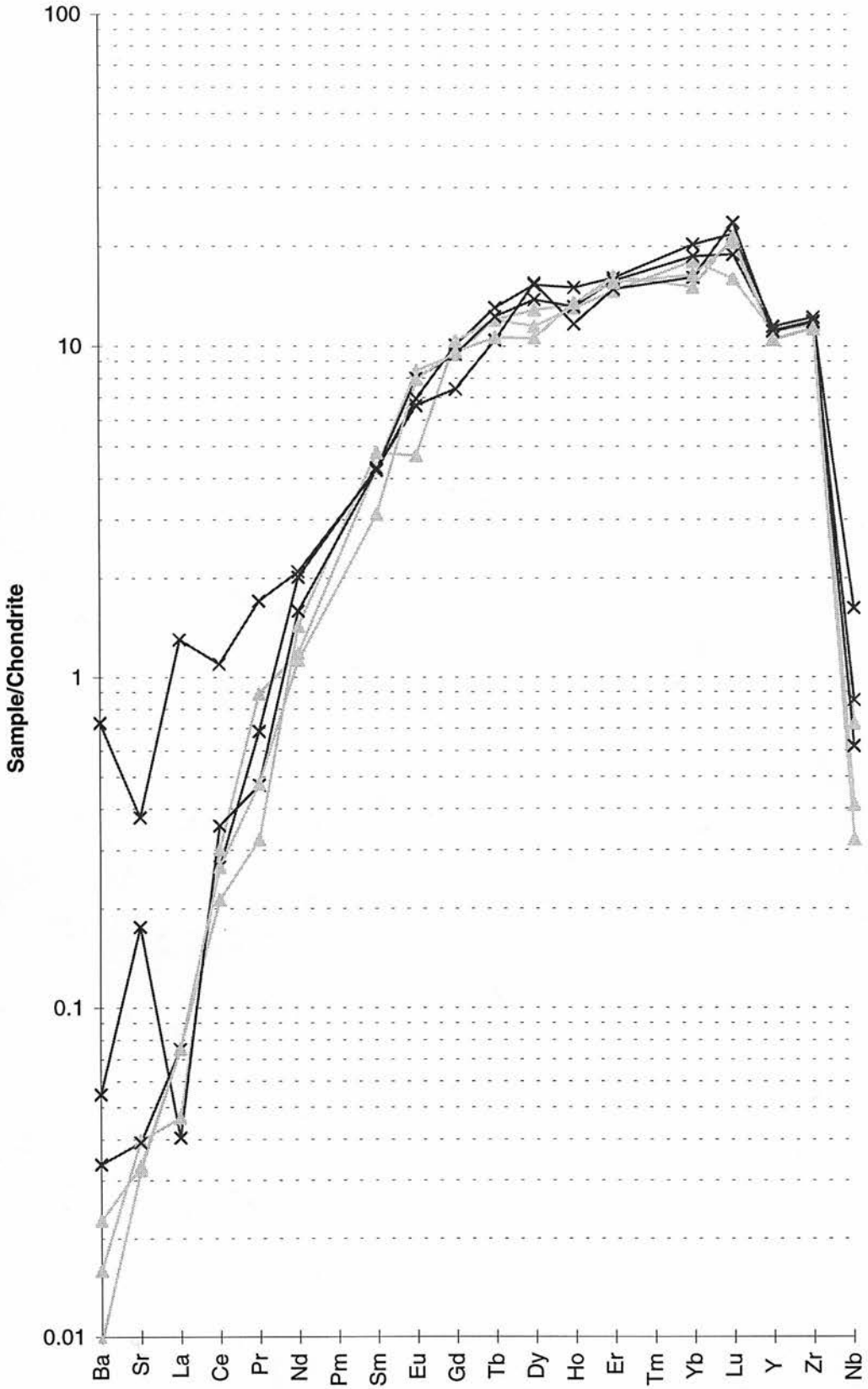

c:\simon\traces\1776gt.xls

Fig. D.20b JJG1776 Clinopyroxene

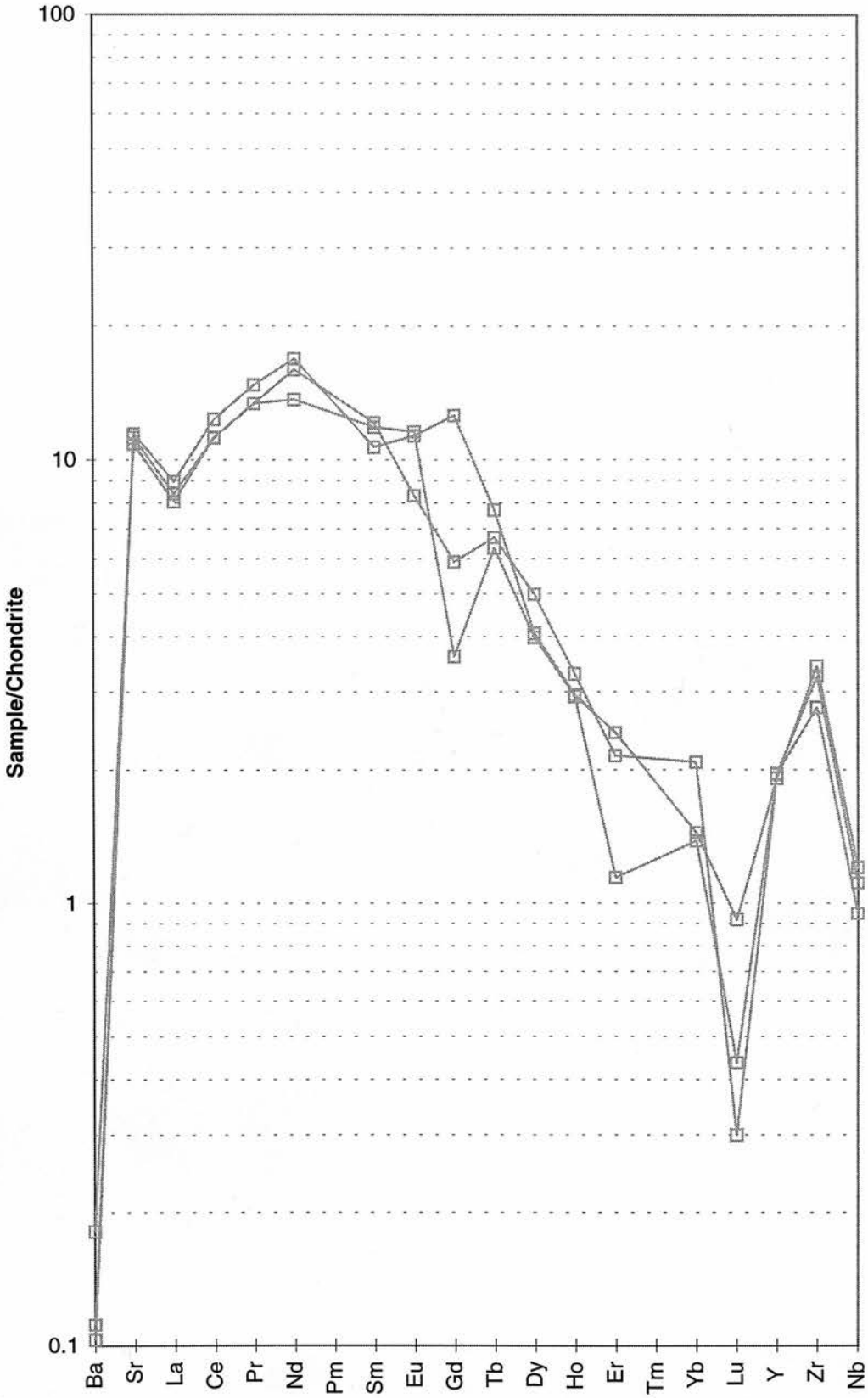

c:\simon\traces\1776c.xls

Fig. D.21 JJH19 Garnet

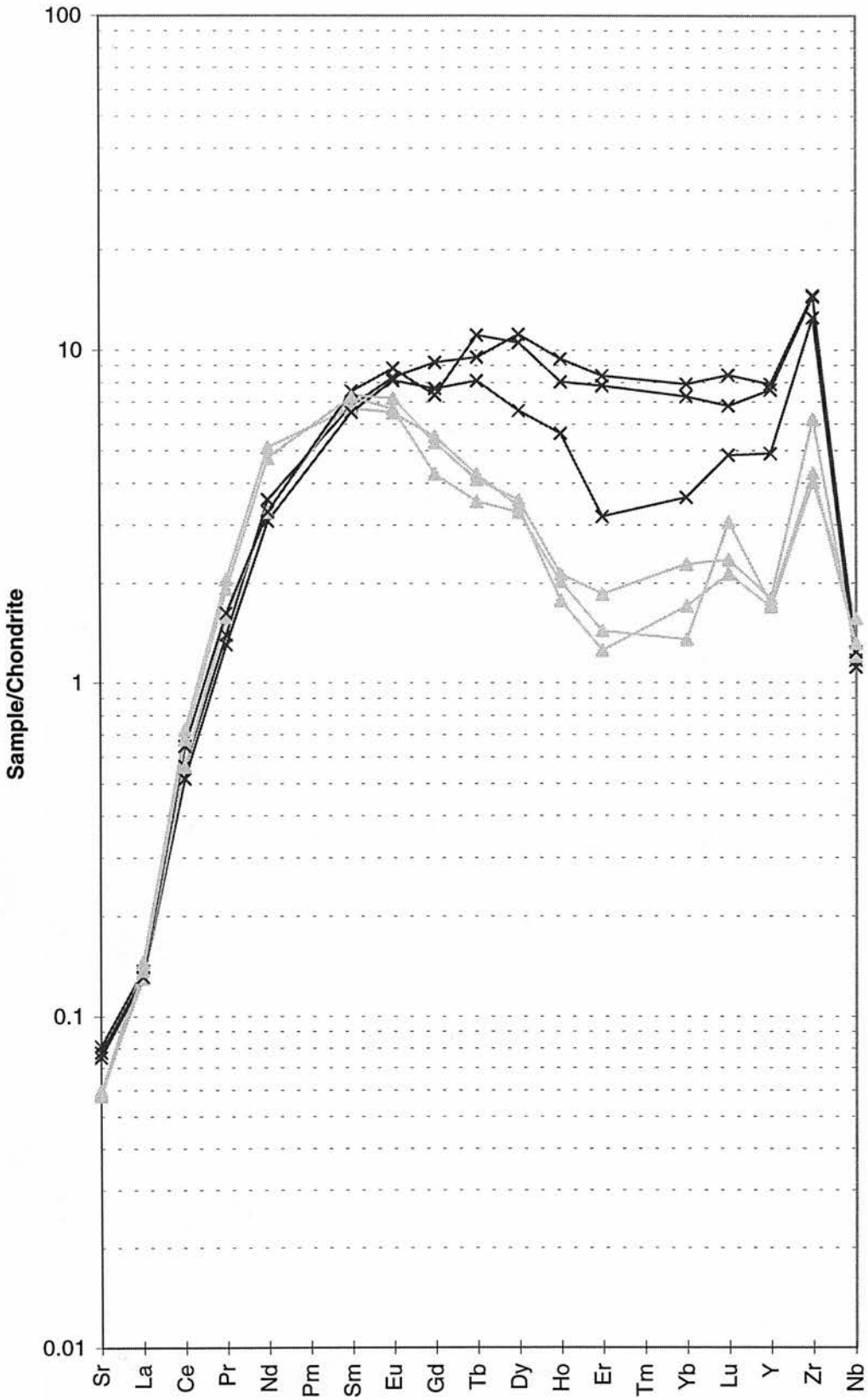

c:\simon\traces\jjh19gt.xls

Fig. D.22a JJH37 Garnet A

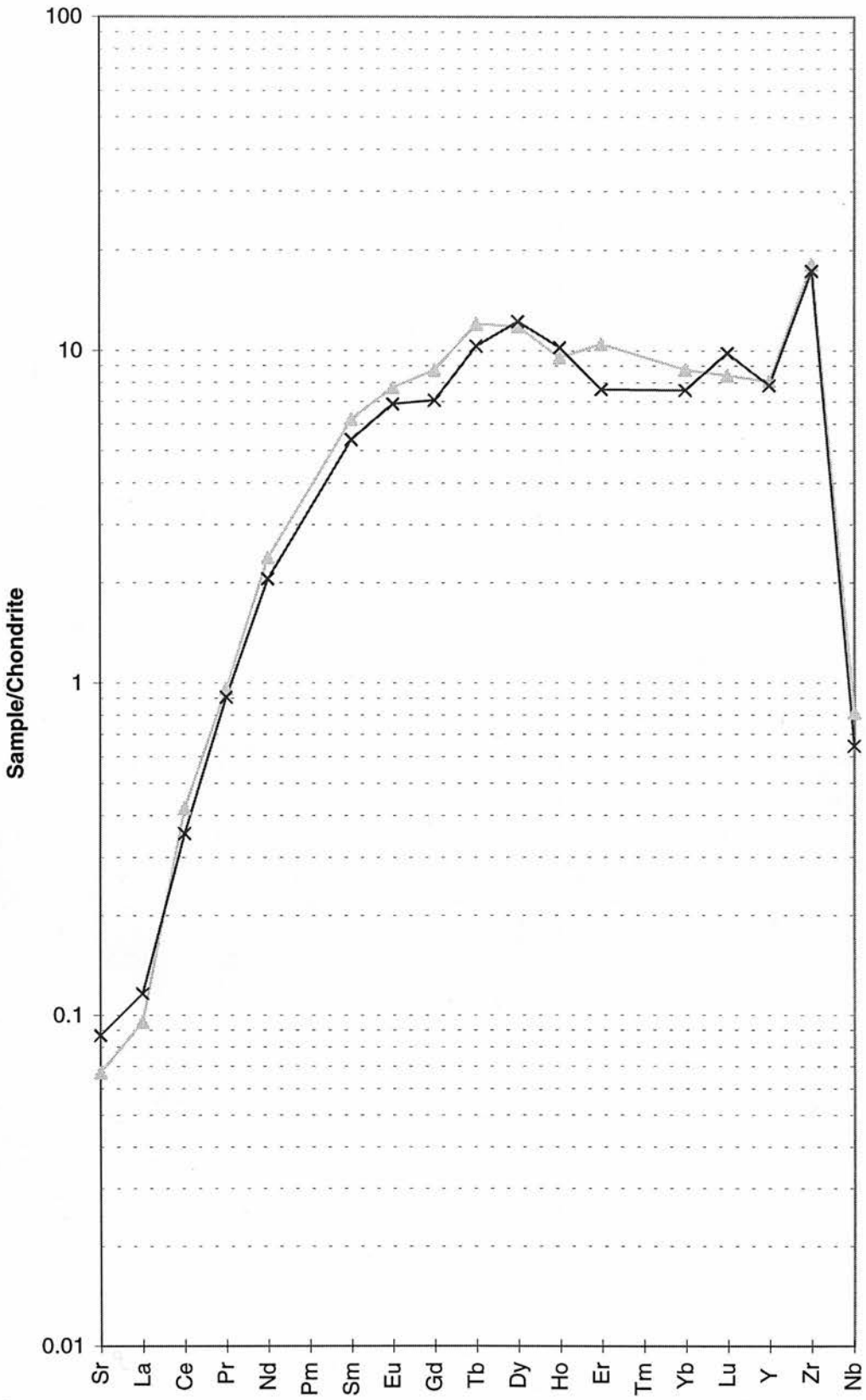

c:\simon\traces\jjh37ag.xls

Fig. D.22b JJH37 Garnet B

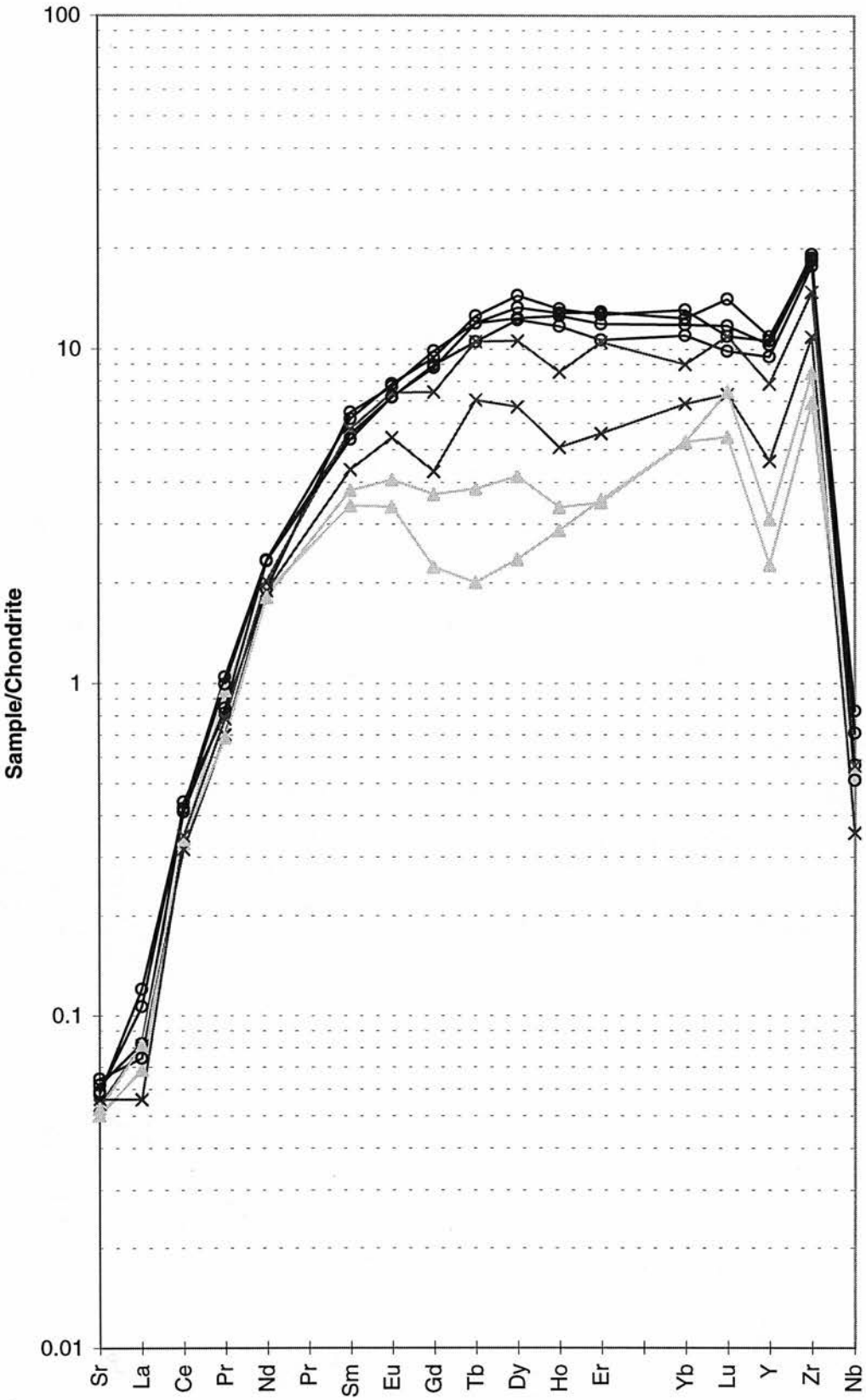

c:\simon\traces\JJH37.xls

Fig. D.22c JJH37 Garnet D

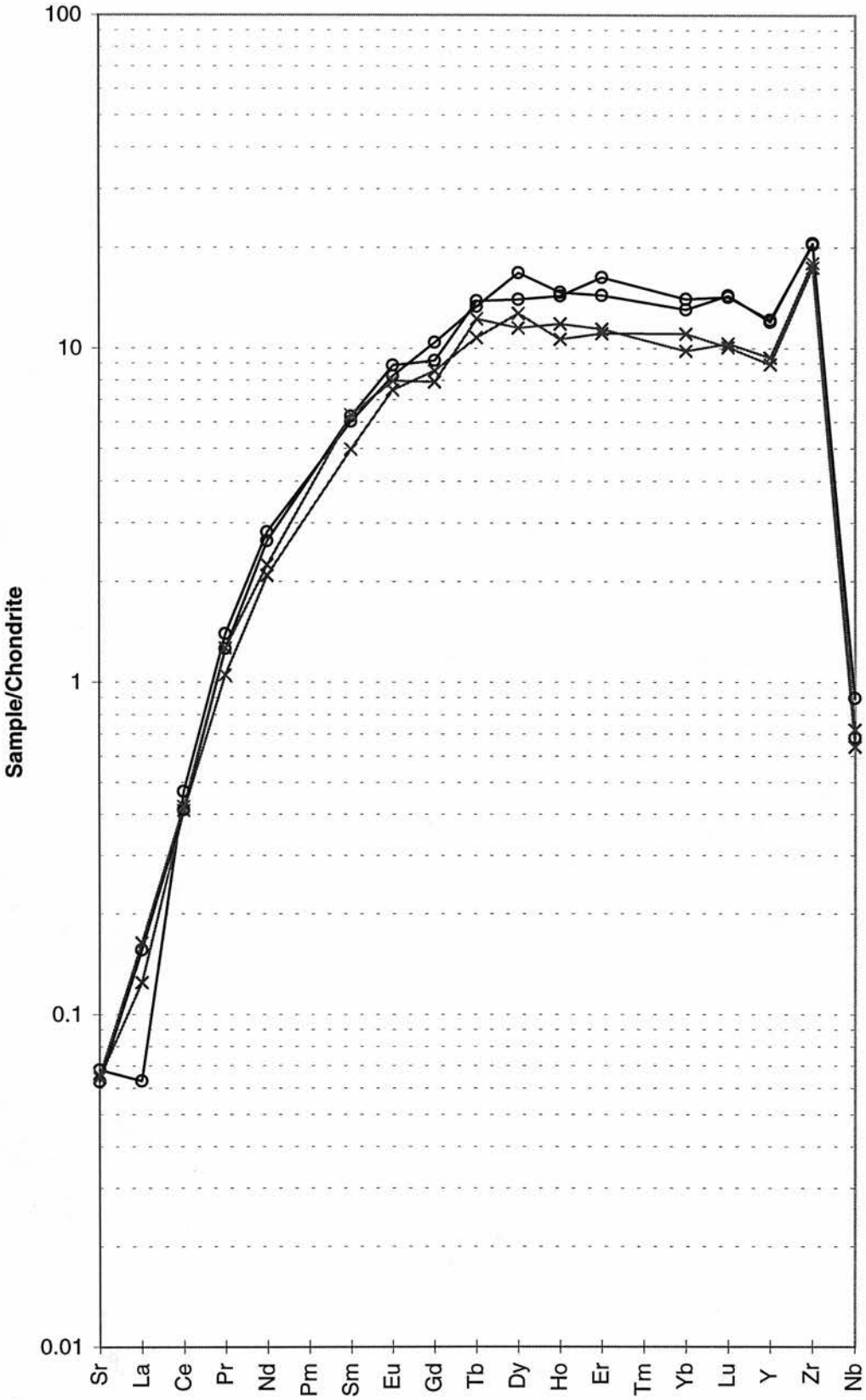

c:\simon\traces\jjh37dg.xls

Fig. D.22d JJH37 Garnet E

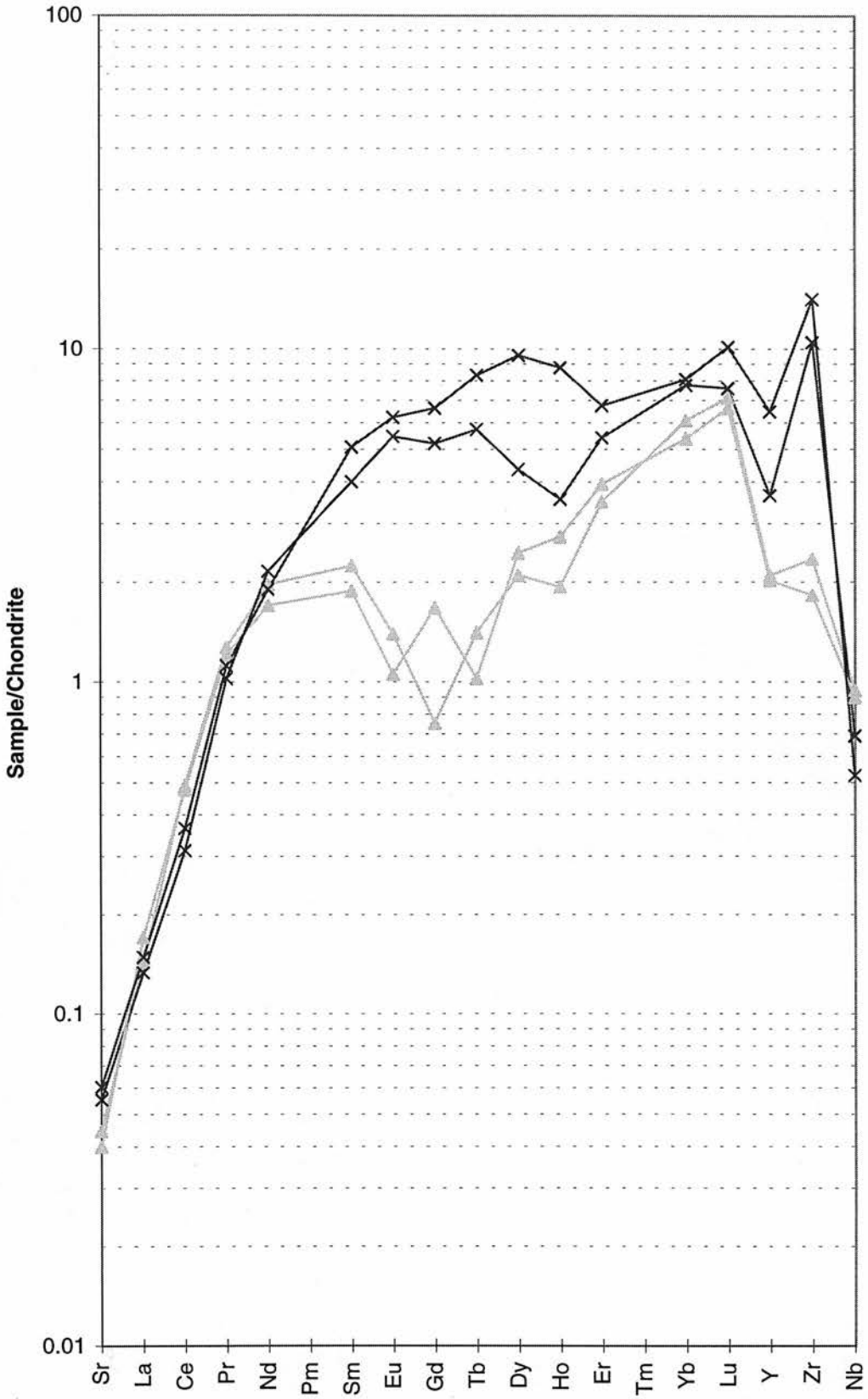

c:\simon\traces\jjh37eg.xls

Fig. D.22e JJH37 Clinopyroxene

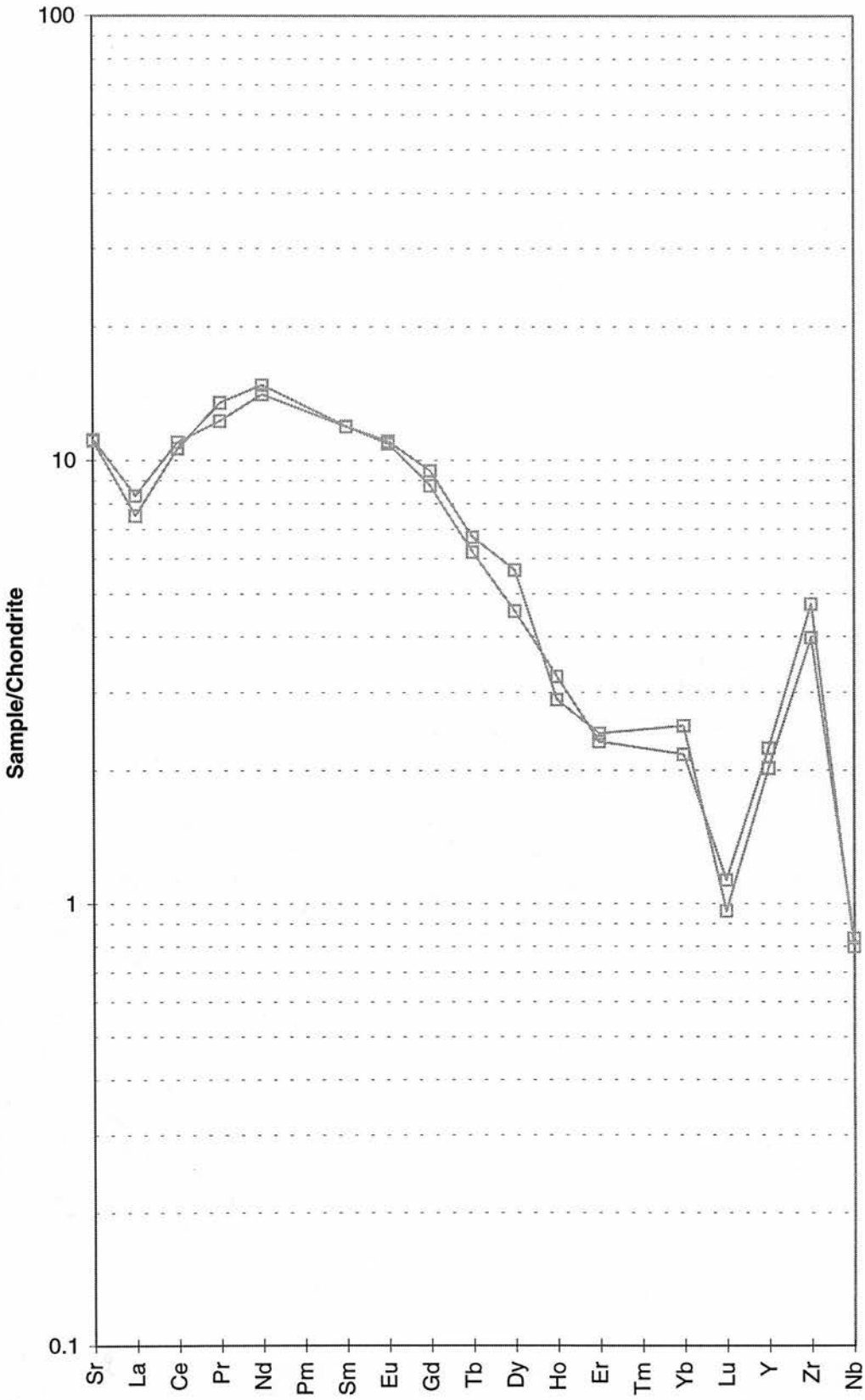

c:\simon\traces\jjh37c.xls

Fig. D.23 J74 Cr-poor Garnet Megacryst

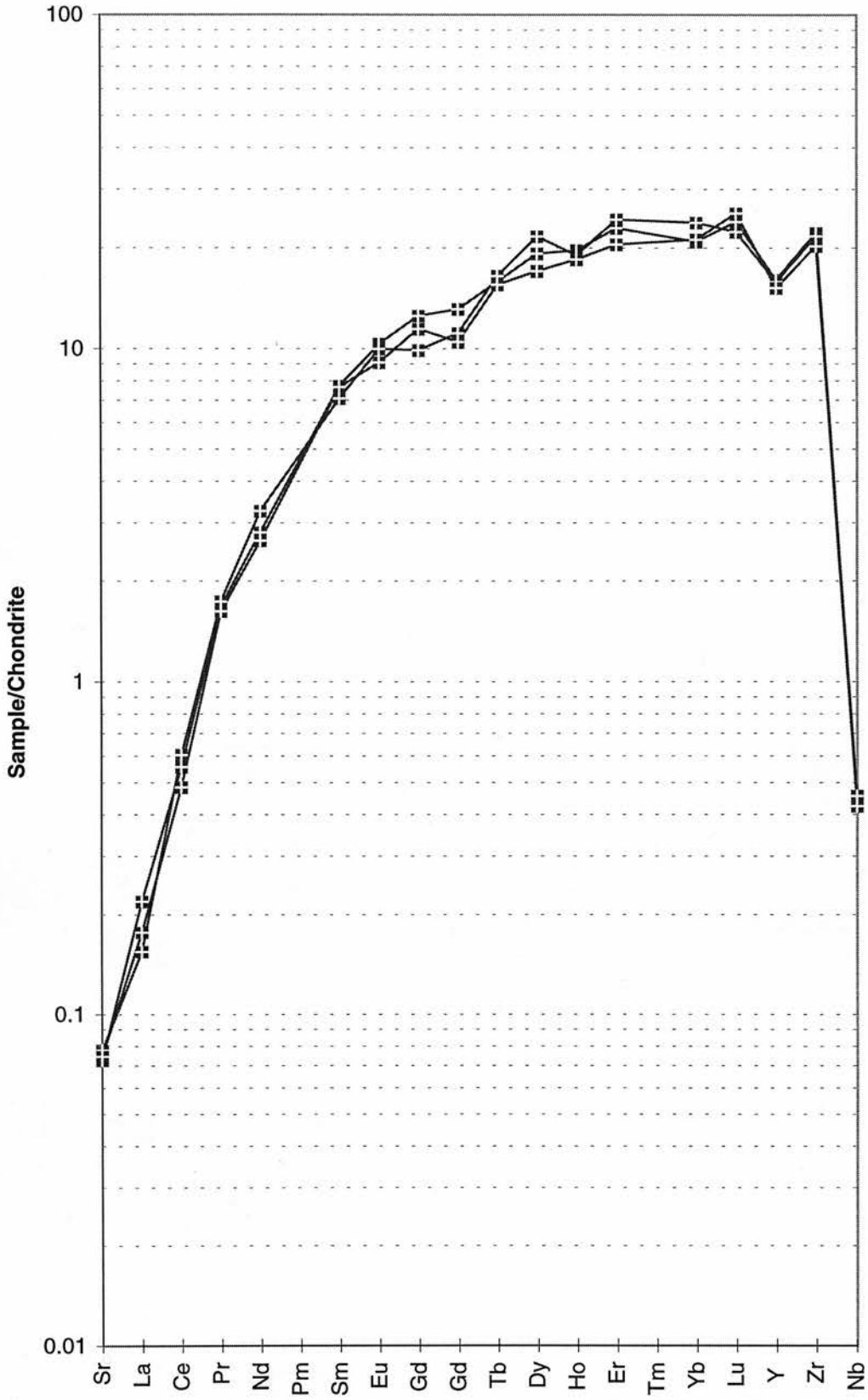

c:\simon\traces\J74gt.xls

Fig. D.24 J75 Cr-poor Garnet Megacryst

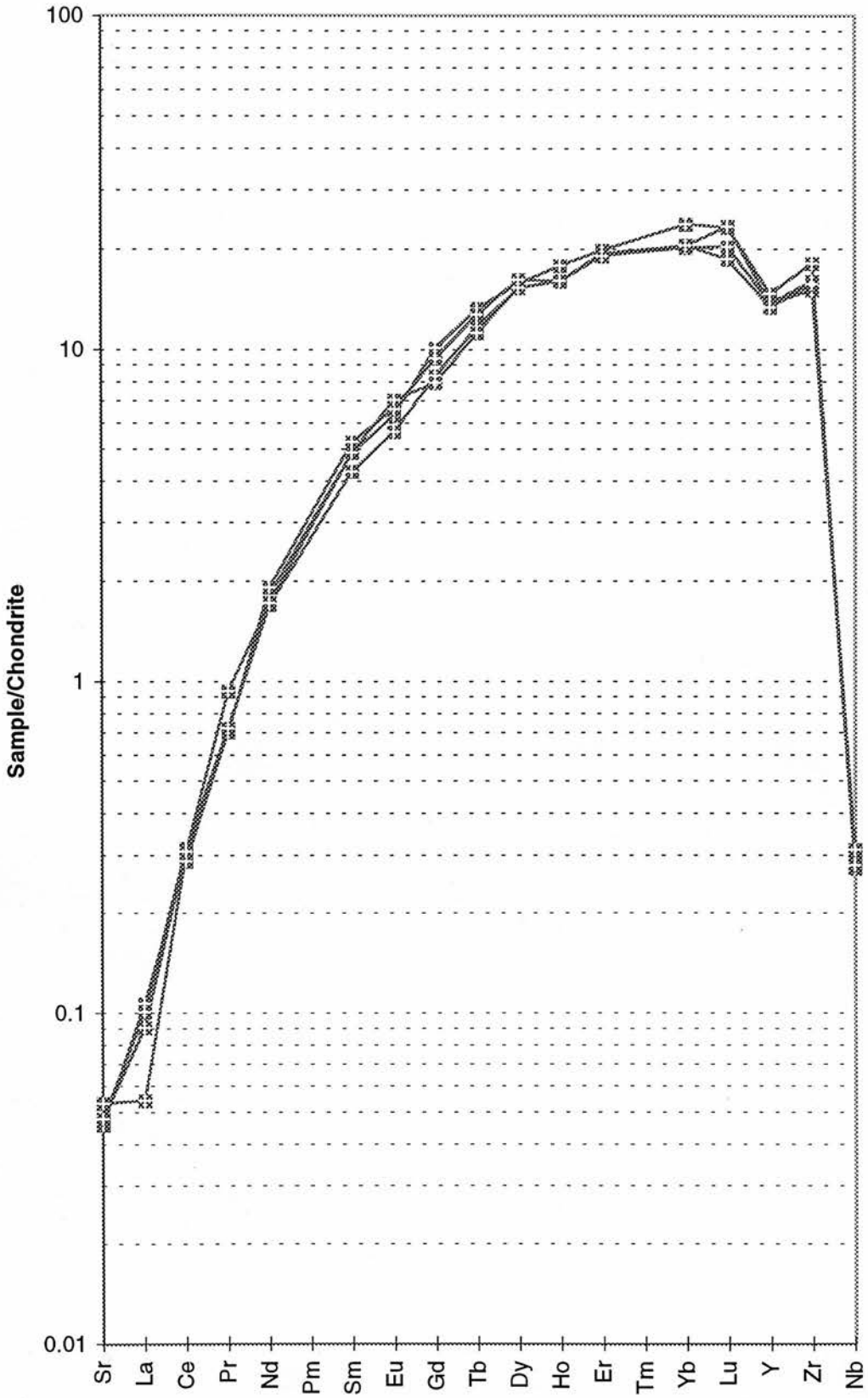

c:\simon\traces\J75gt.xls

Fig. D.25 J145 Garnet (two grains)

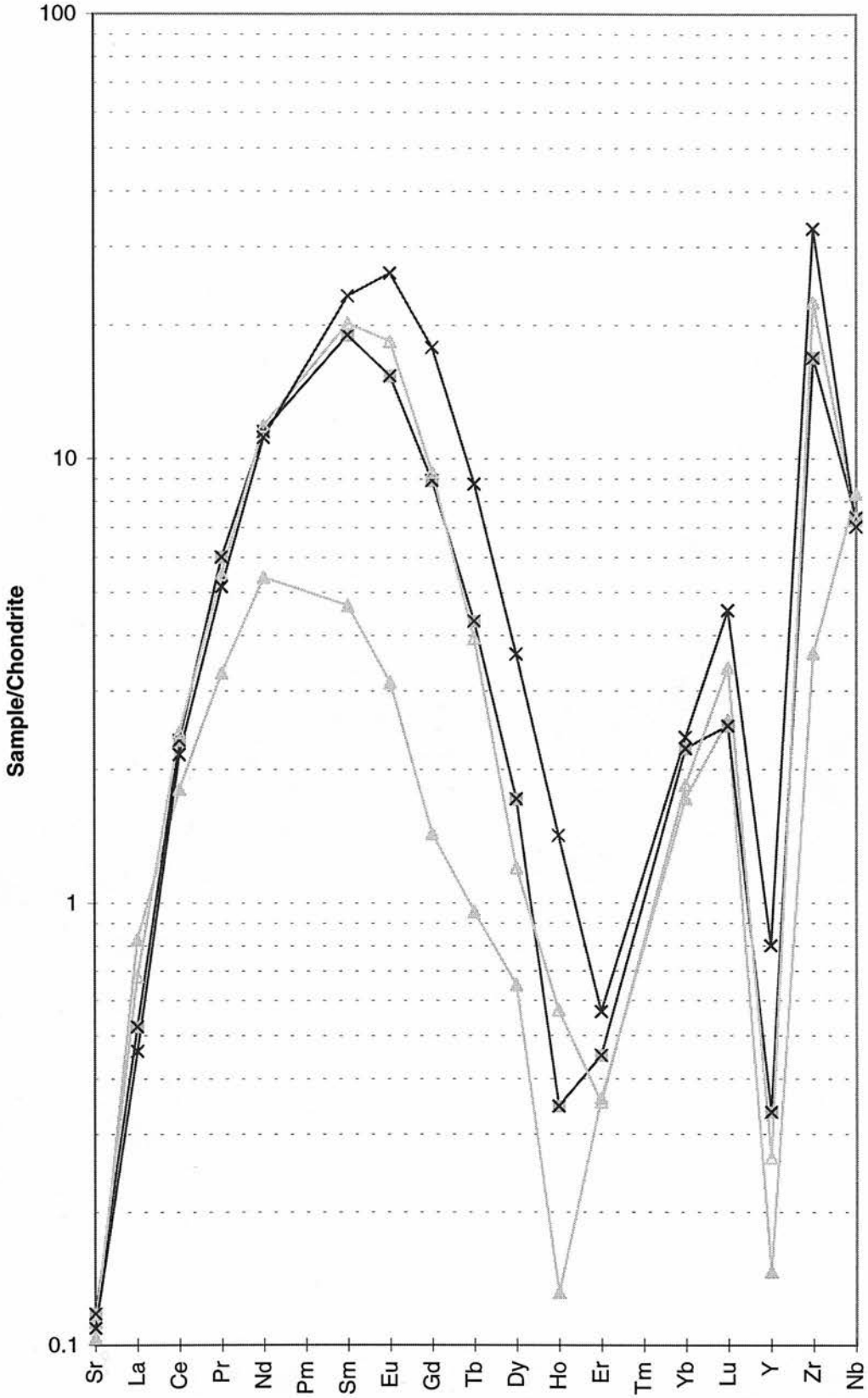

c:\simon\traces\J145gt.xls

Fig. D.26 J159 Garnet (two grains)

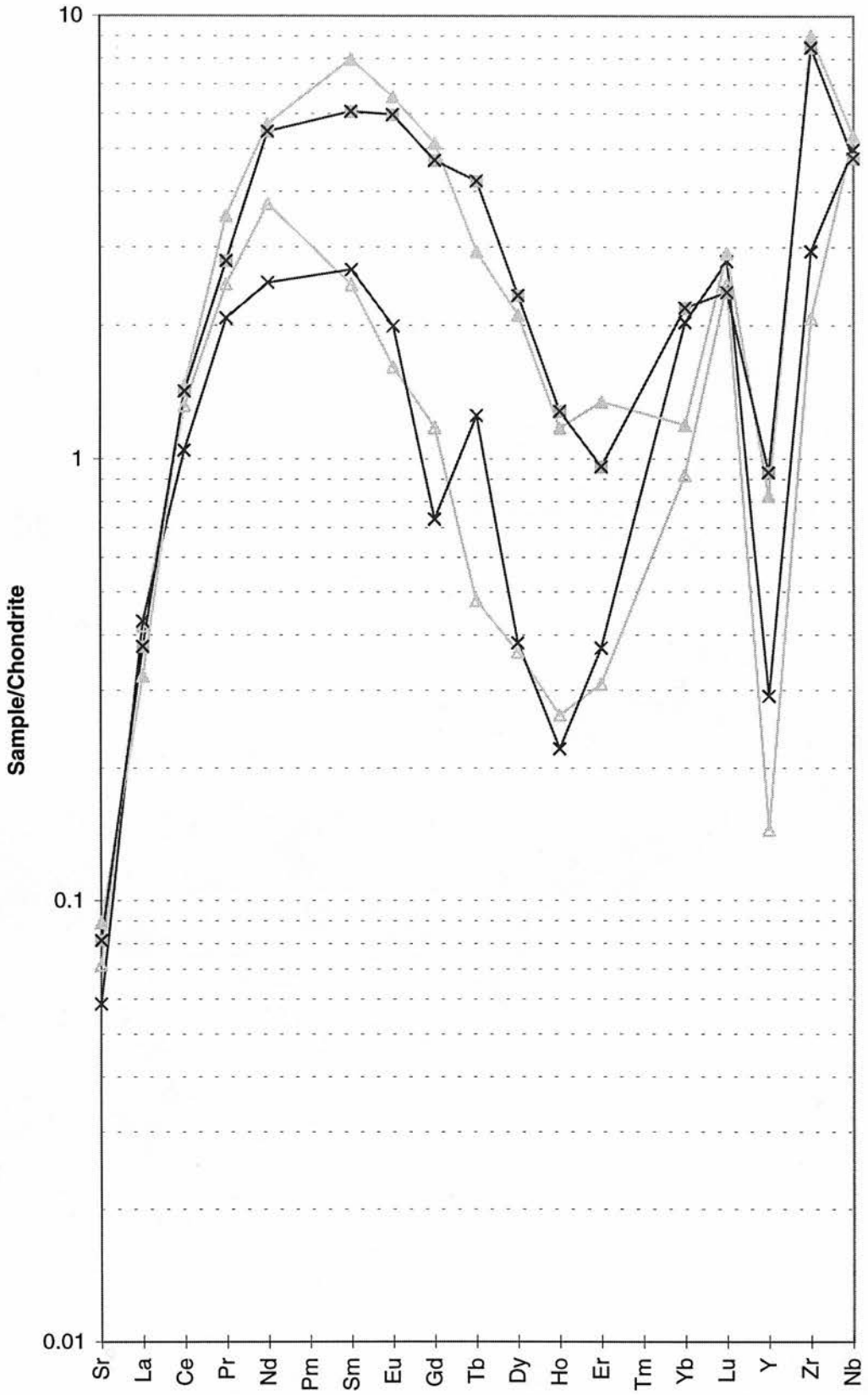

c:\simon\traces\J159gt.xls

Fig. D.27 J34B Garnet A

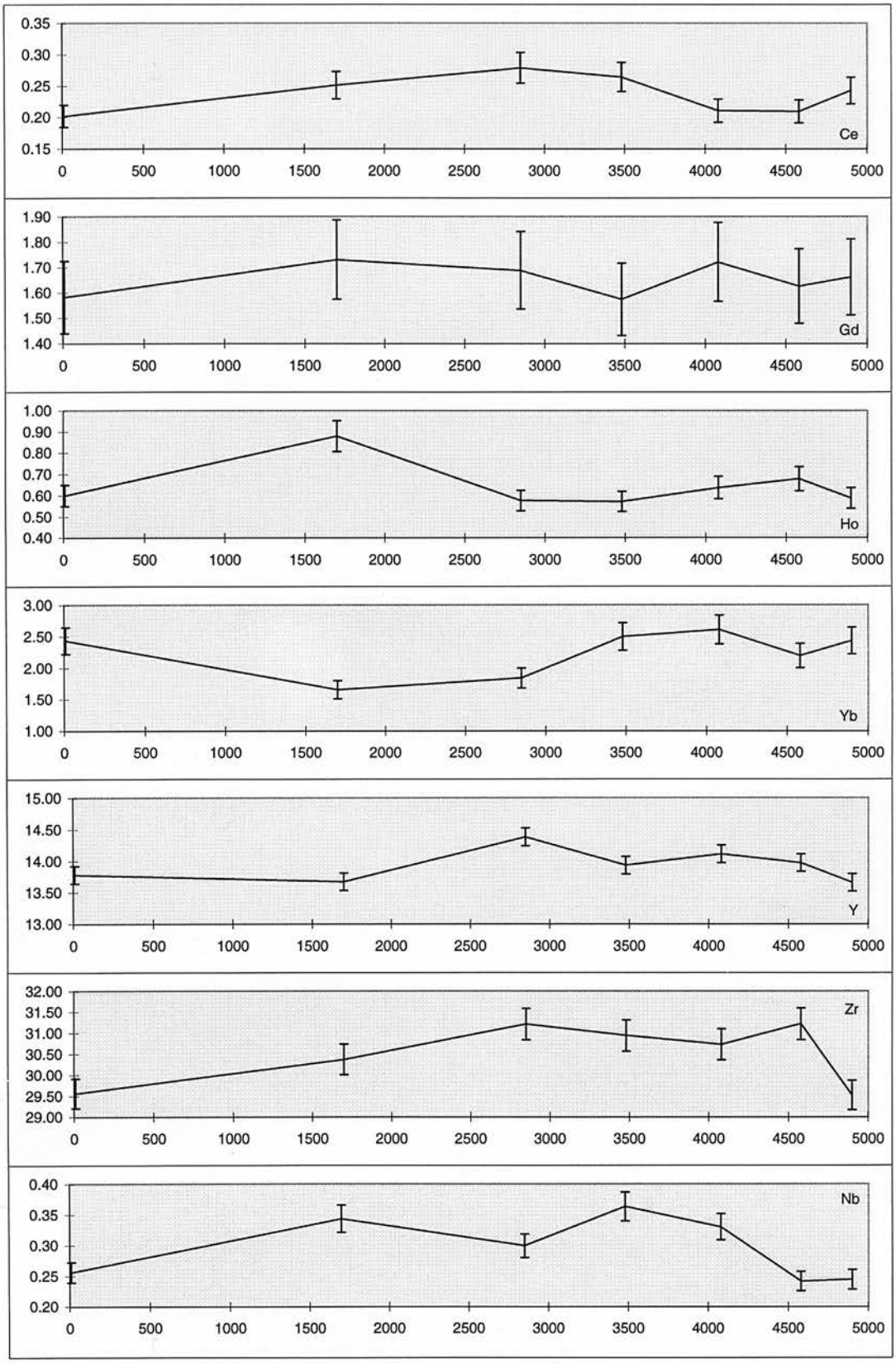

Fig. D.28 J107 Garnet

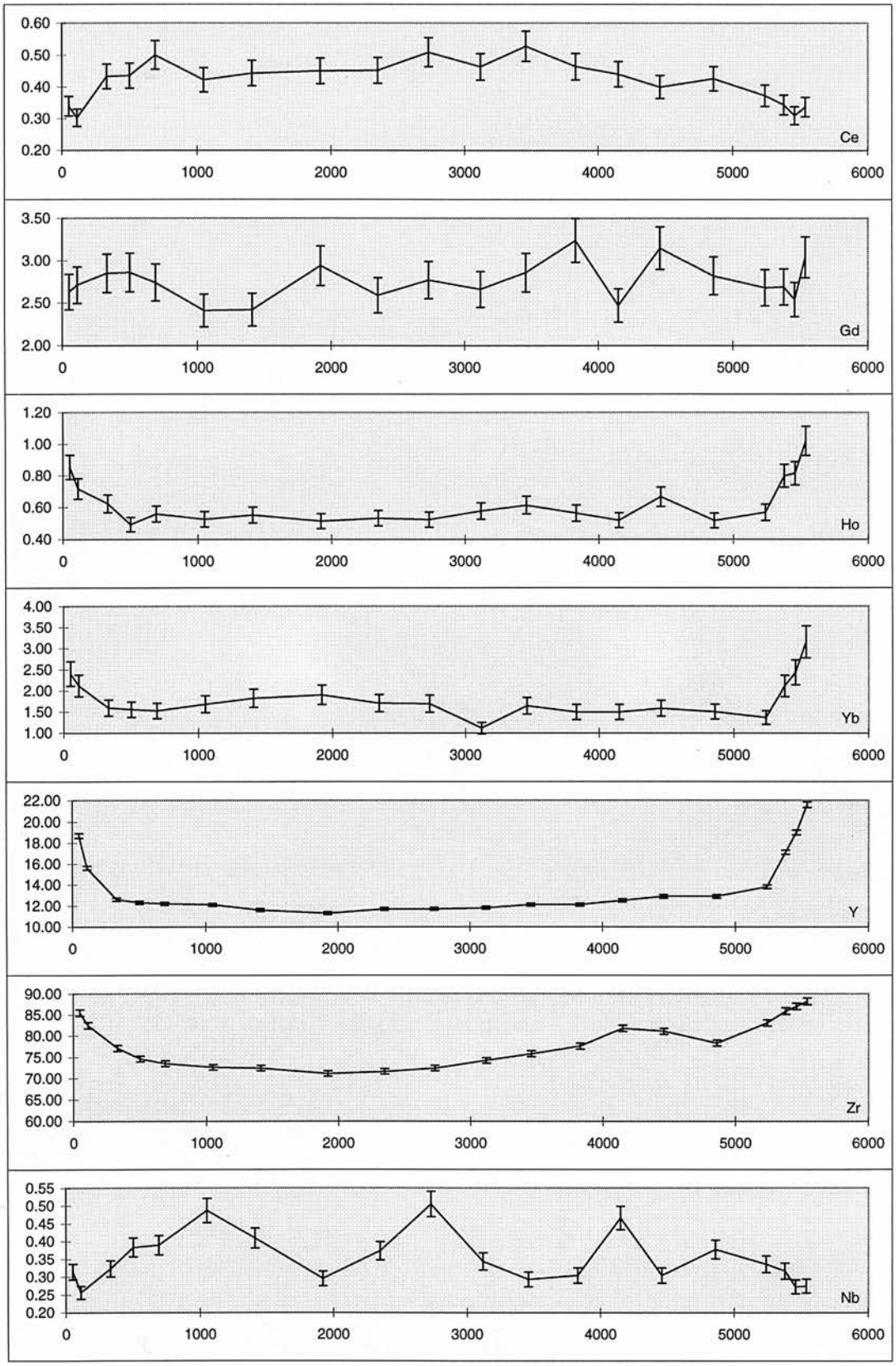

c:\simon\traces\j107v.xls

Fig. D.29 J110 Garnet

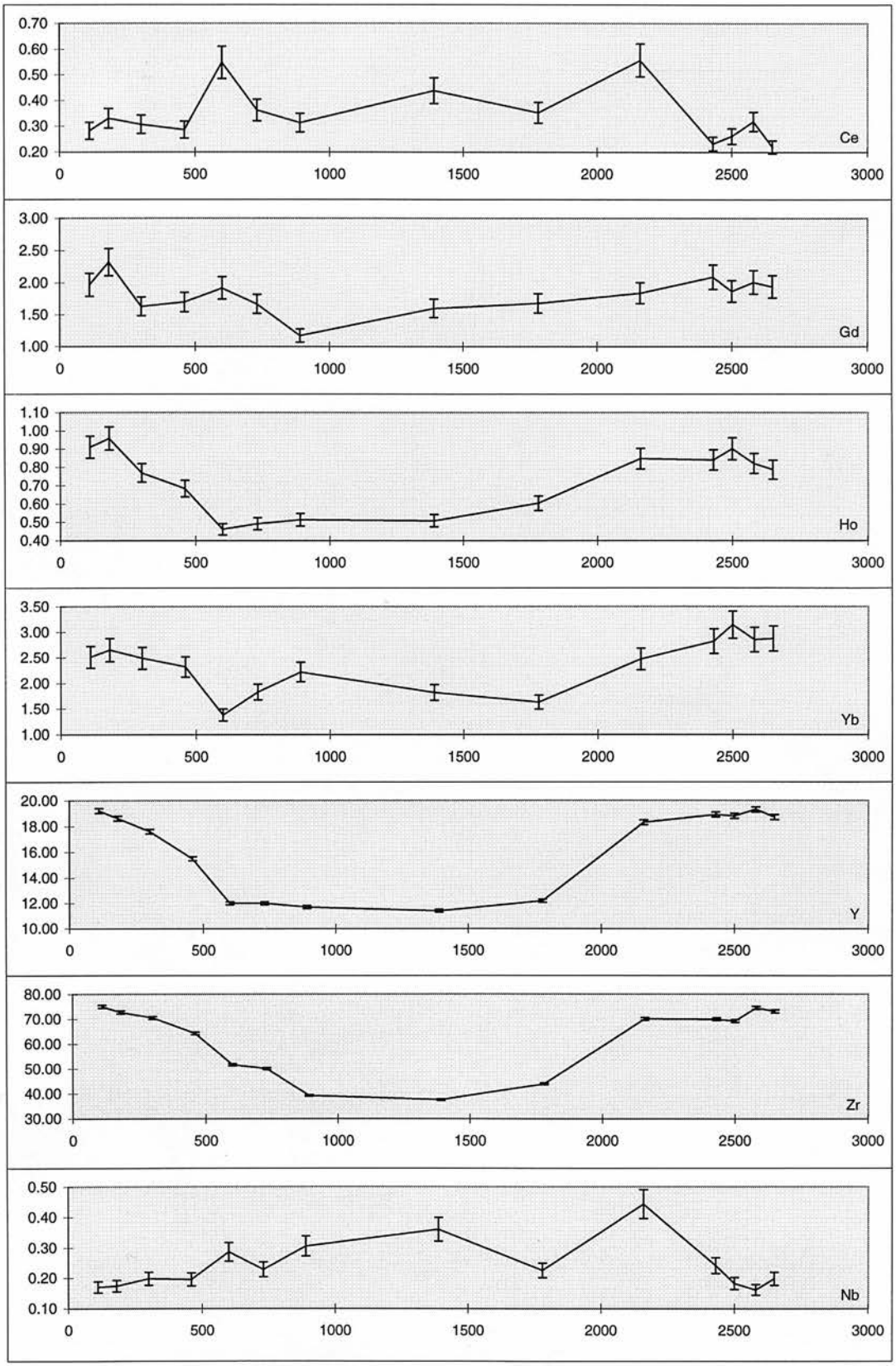

Fig. D.30 J115 Garnet

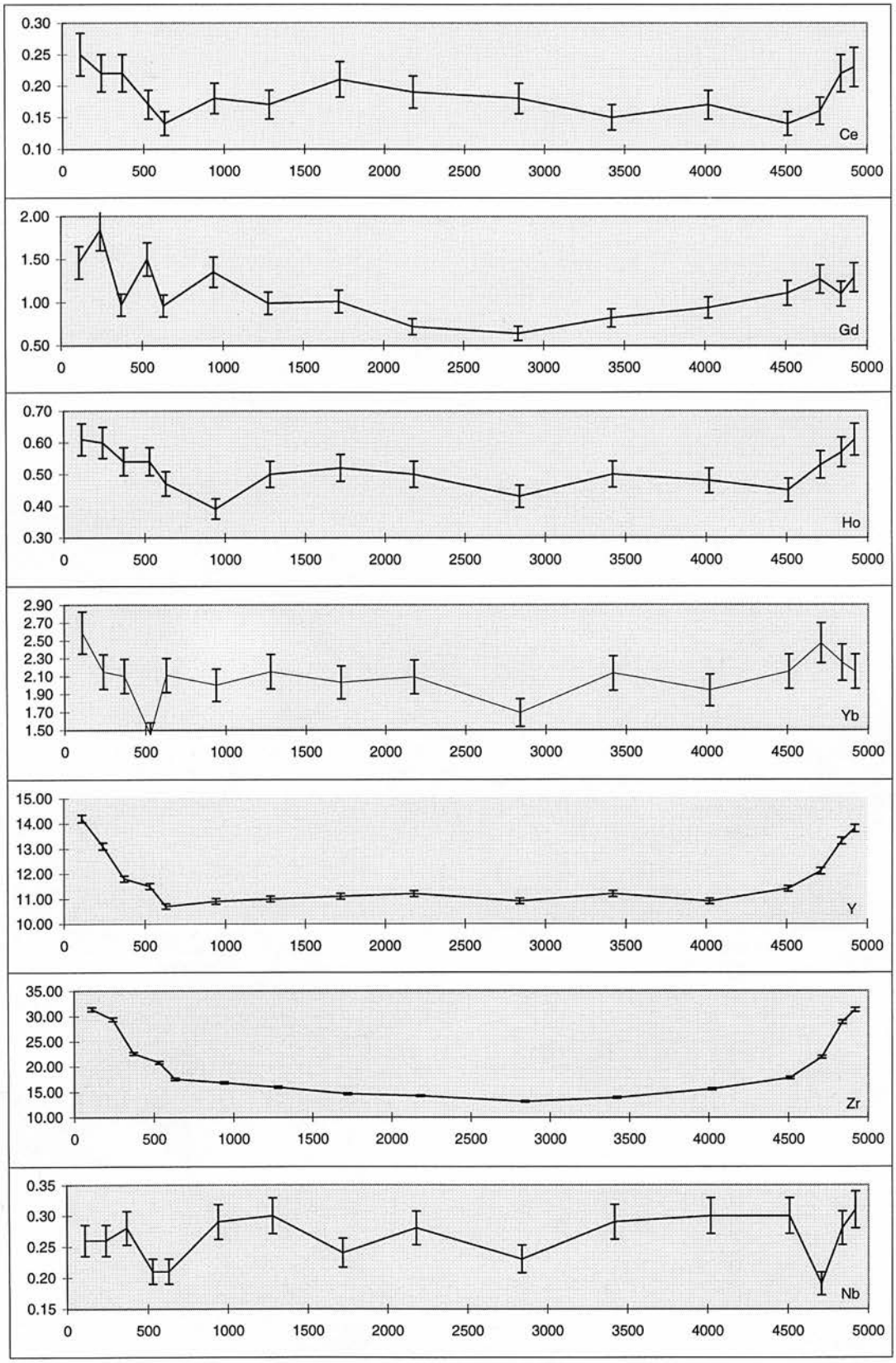

c:\simon\traces\J115v.xls

Fig. D.31 JJG1776 Garnet

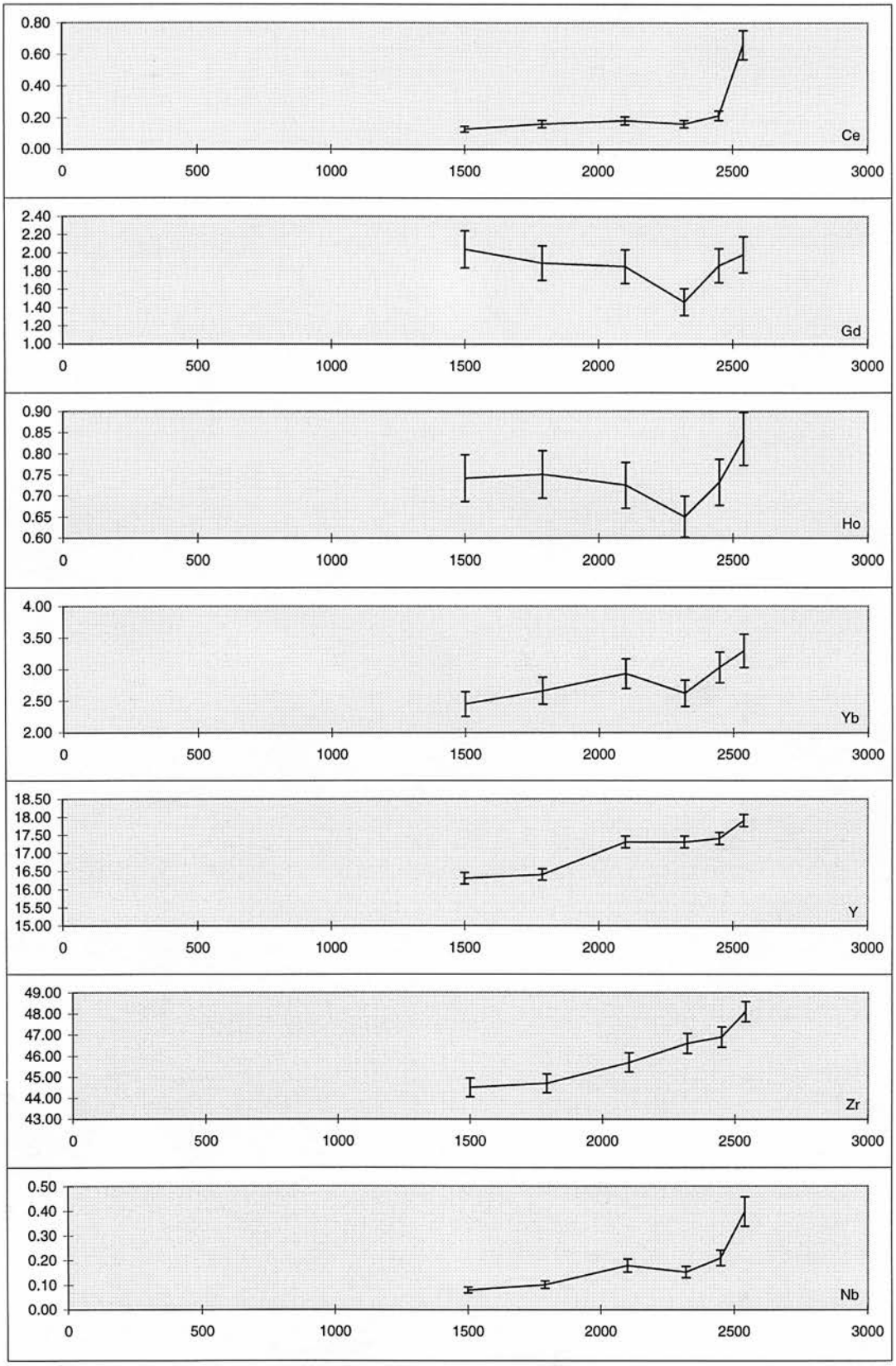

Fig. D.32 JJG2469 Garnet

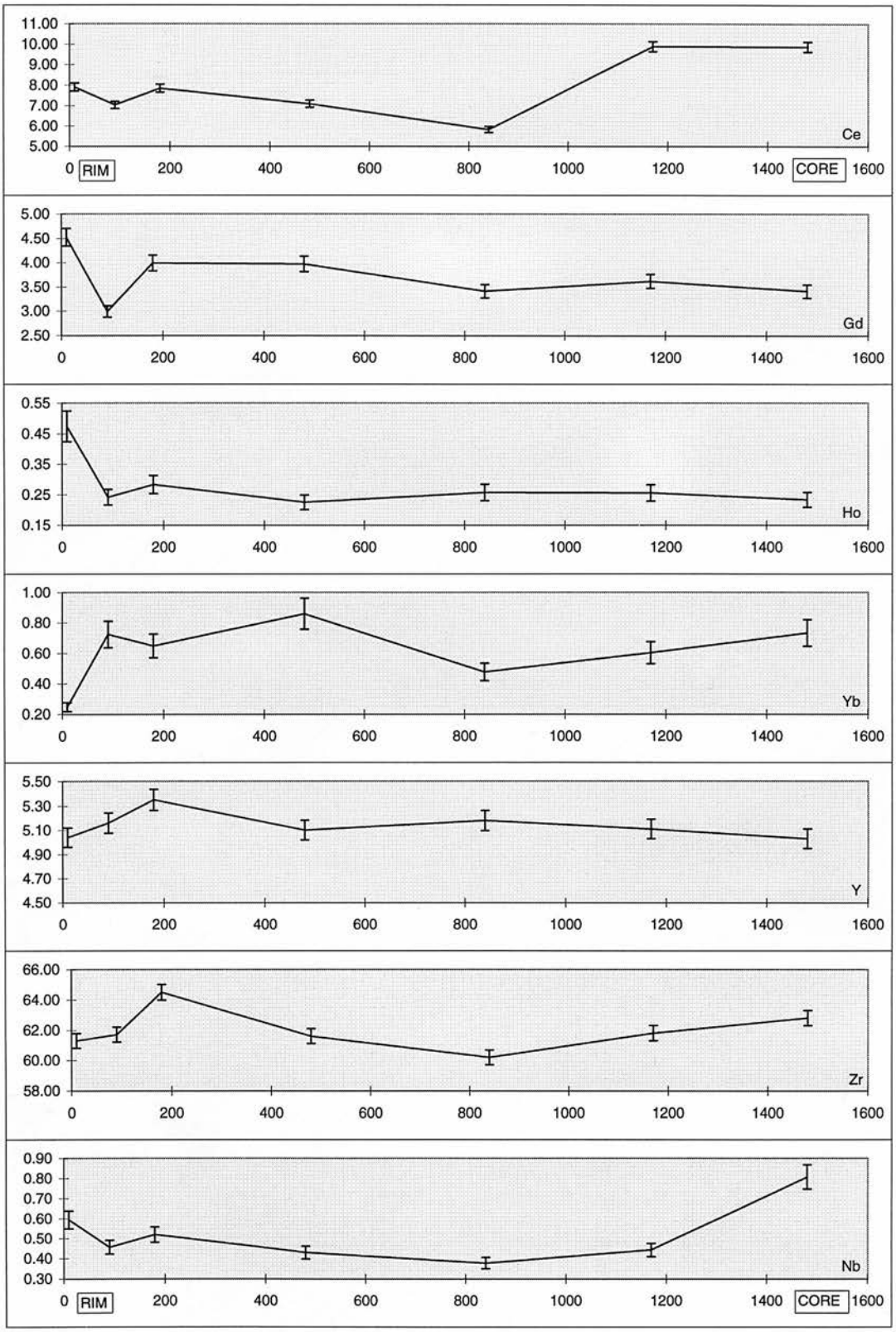

Fig. D.33 J24 'melt'

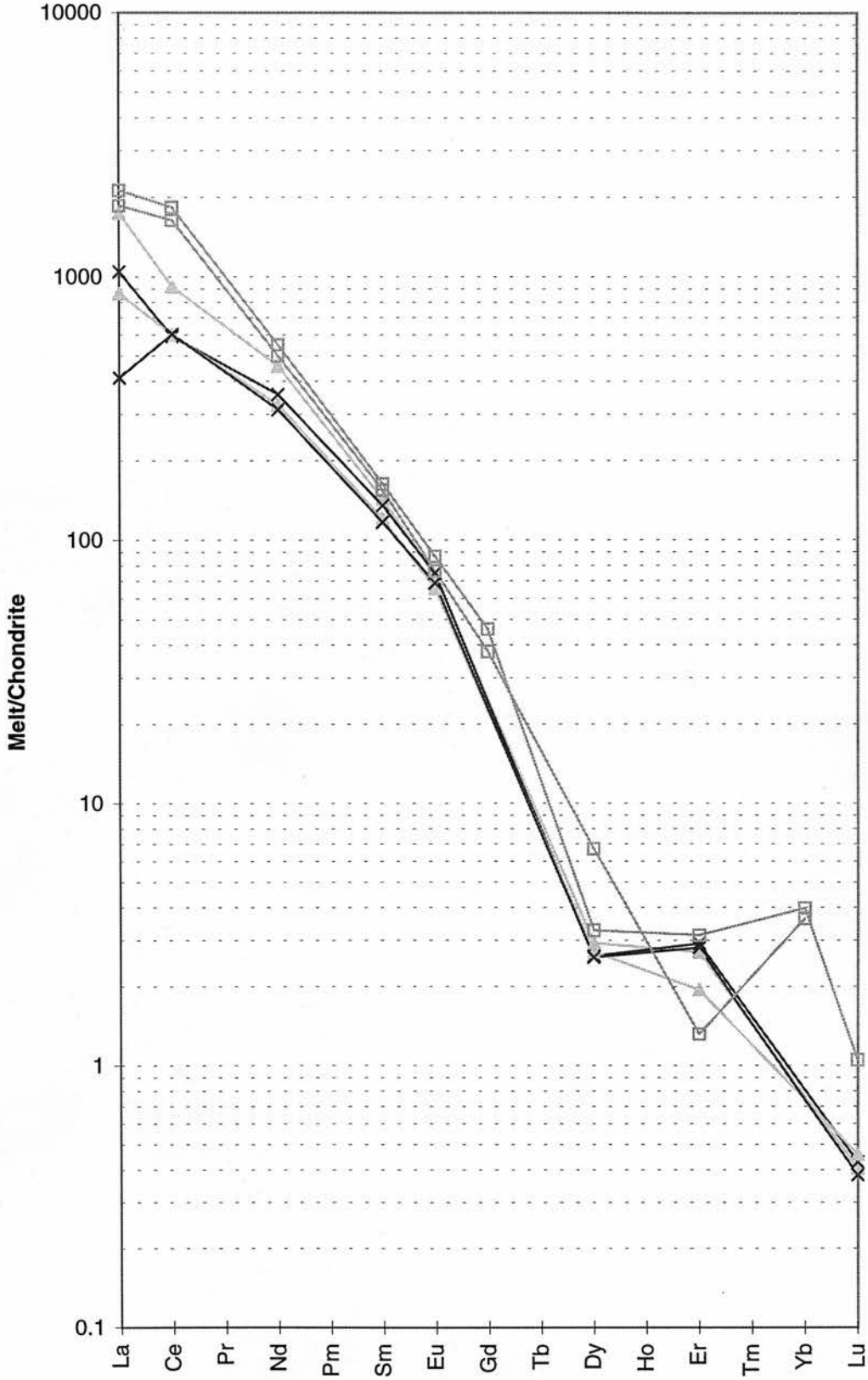

C:\simon\traces\melts\
j24g.xls

Fig. D.34 J25 'melt'

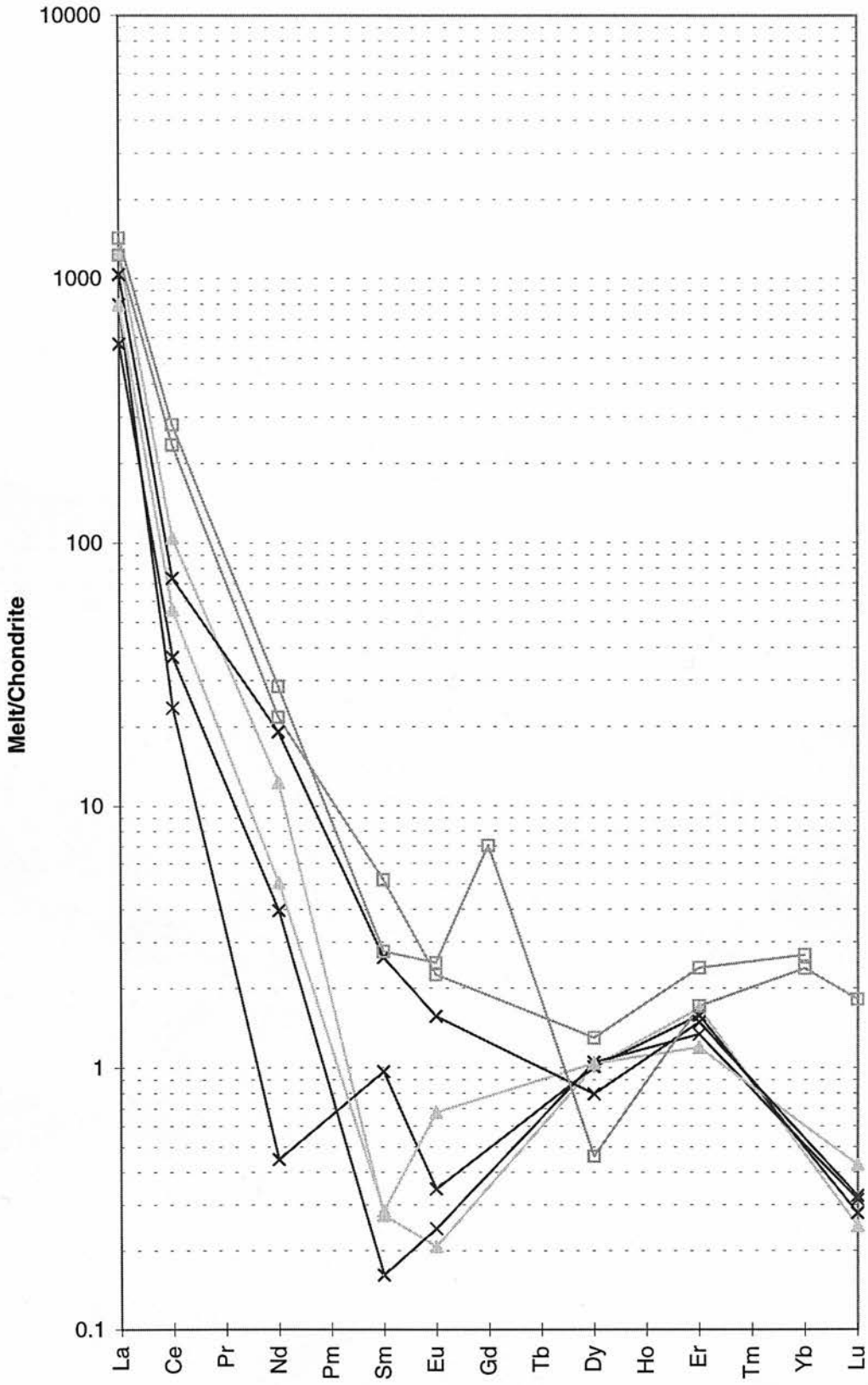

C:\simon\traces\melts\
J25g.xls

Fig. D.35 J146 'melt'

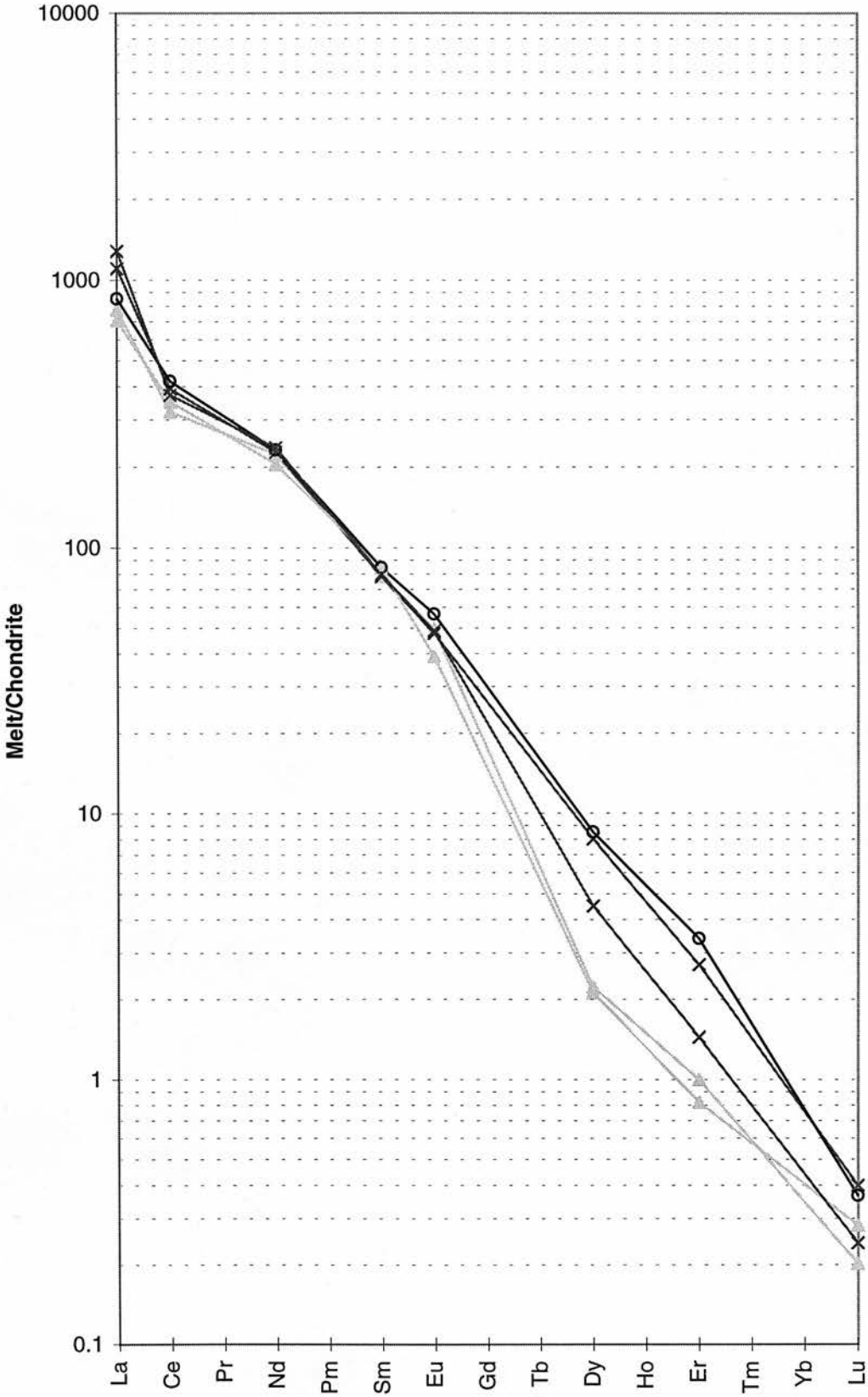

C:\simon\traces\melts\
j146g.xls

Fig. D.36 J157 'melt'

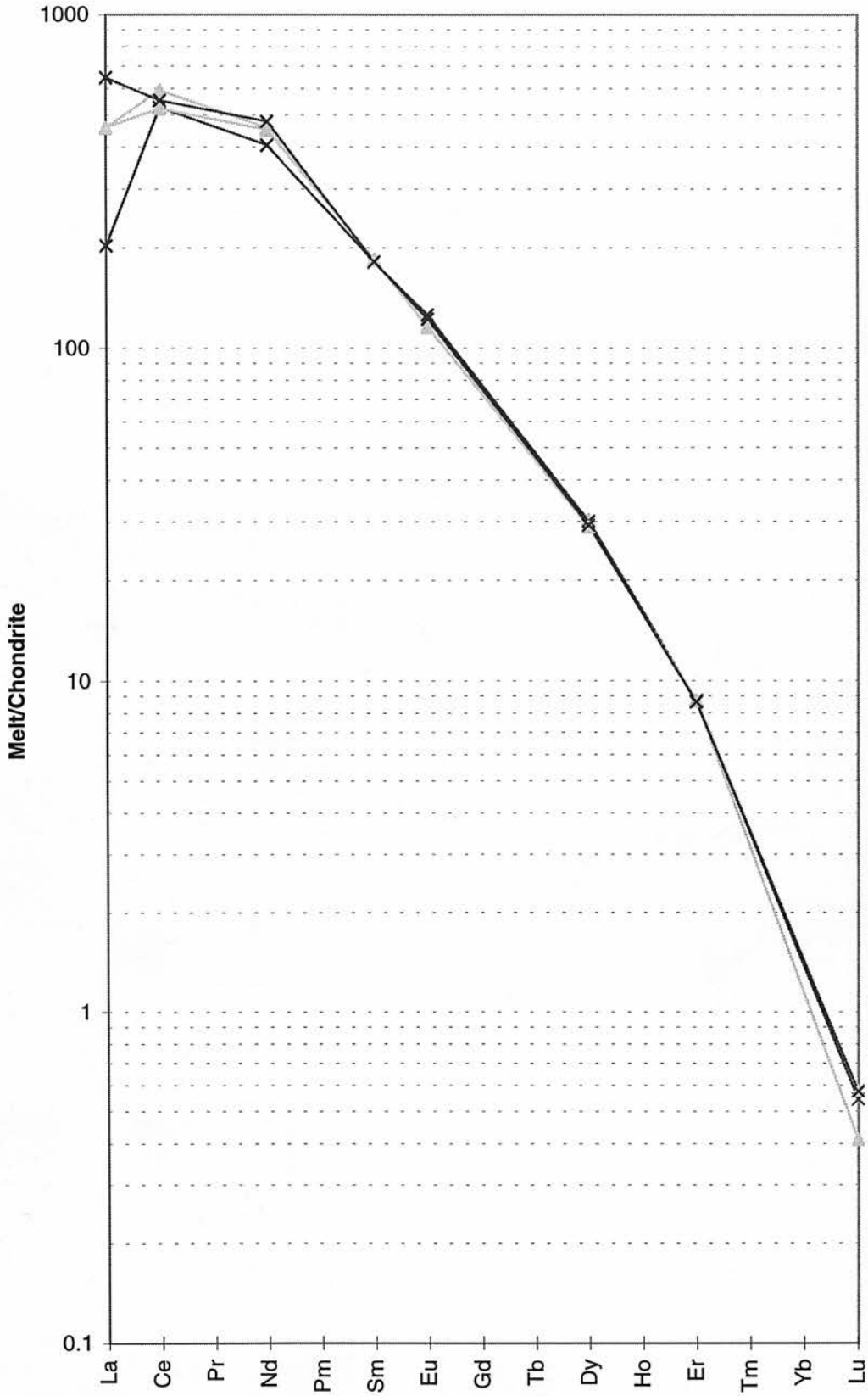

C:\simon\traces\melts\
J157g.xls

Fig. D.37 JJG1728 'melt'

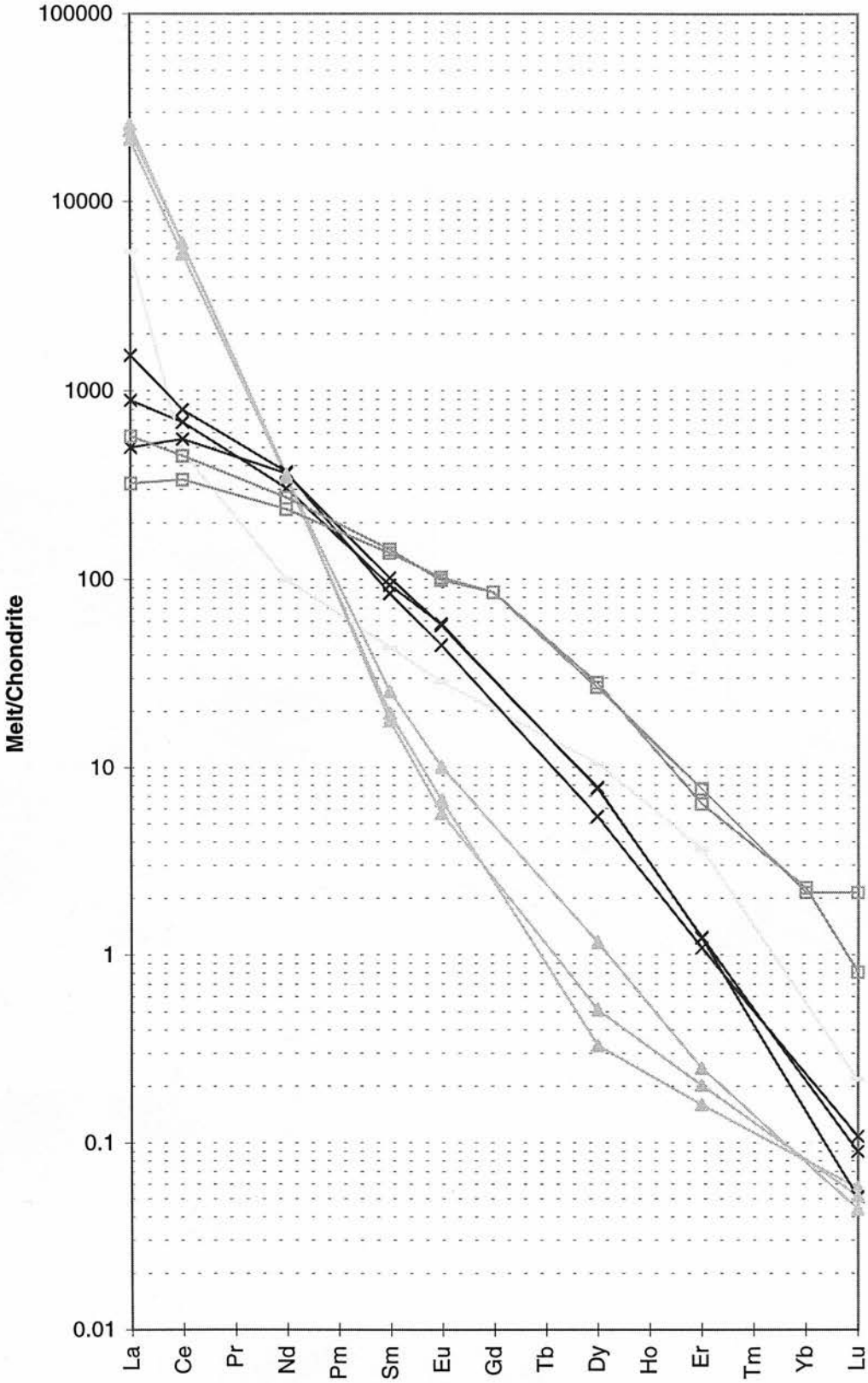

C:\simon\traces\melts\
1728g.xls

Fig. D.38 JJG1757 'melt'

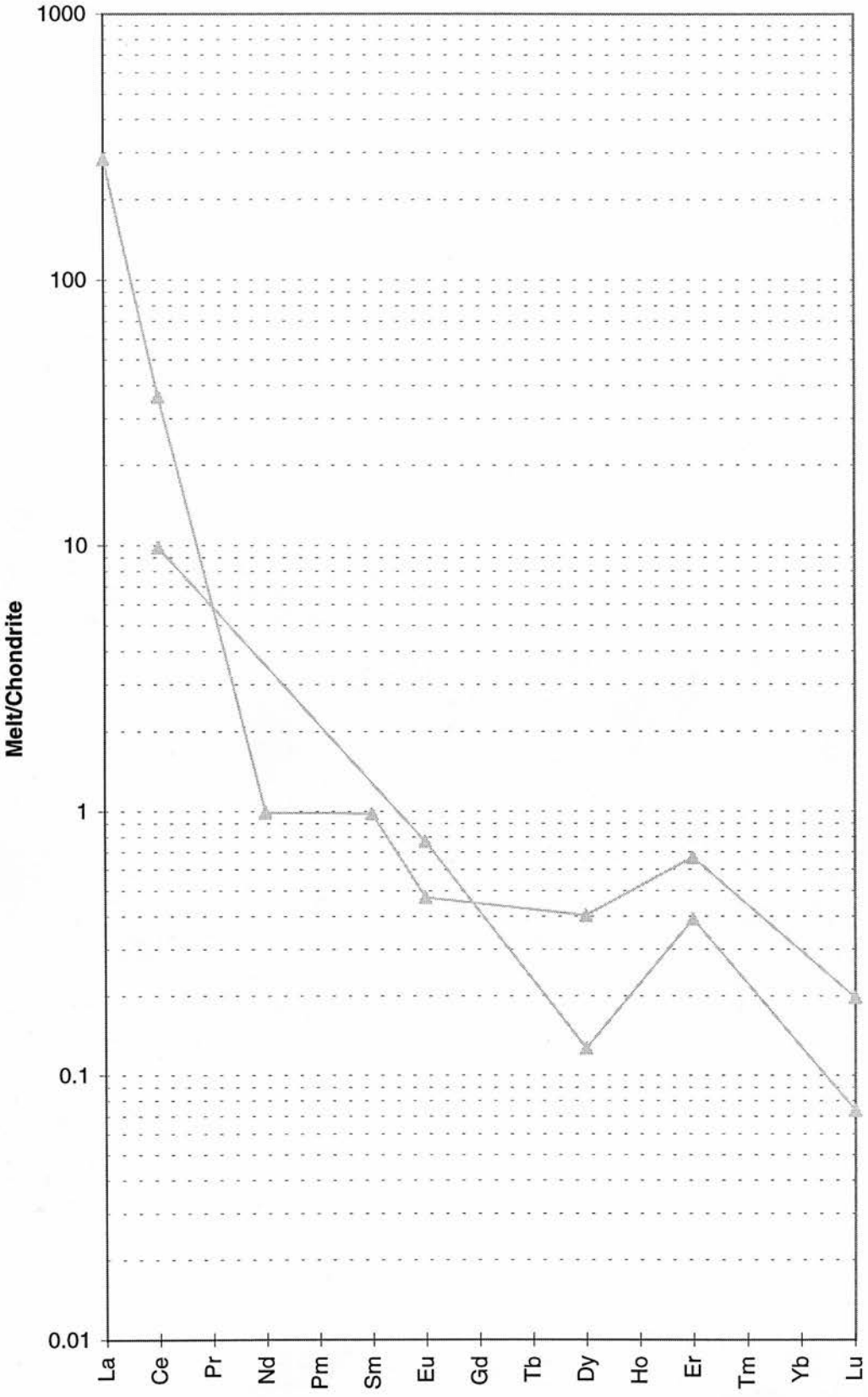

C:\simon\traces\melts\
1757g.xls

Fig. D.39 JJG1761 'melt'

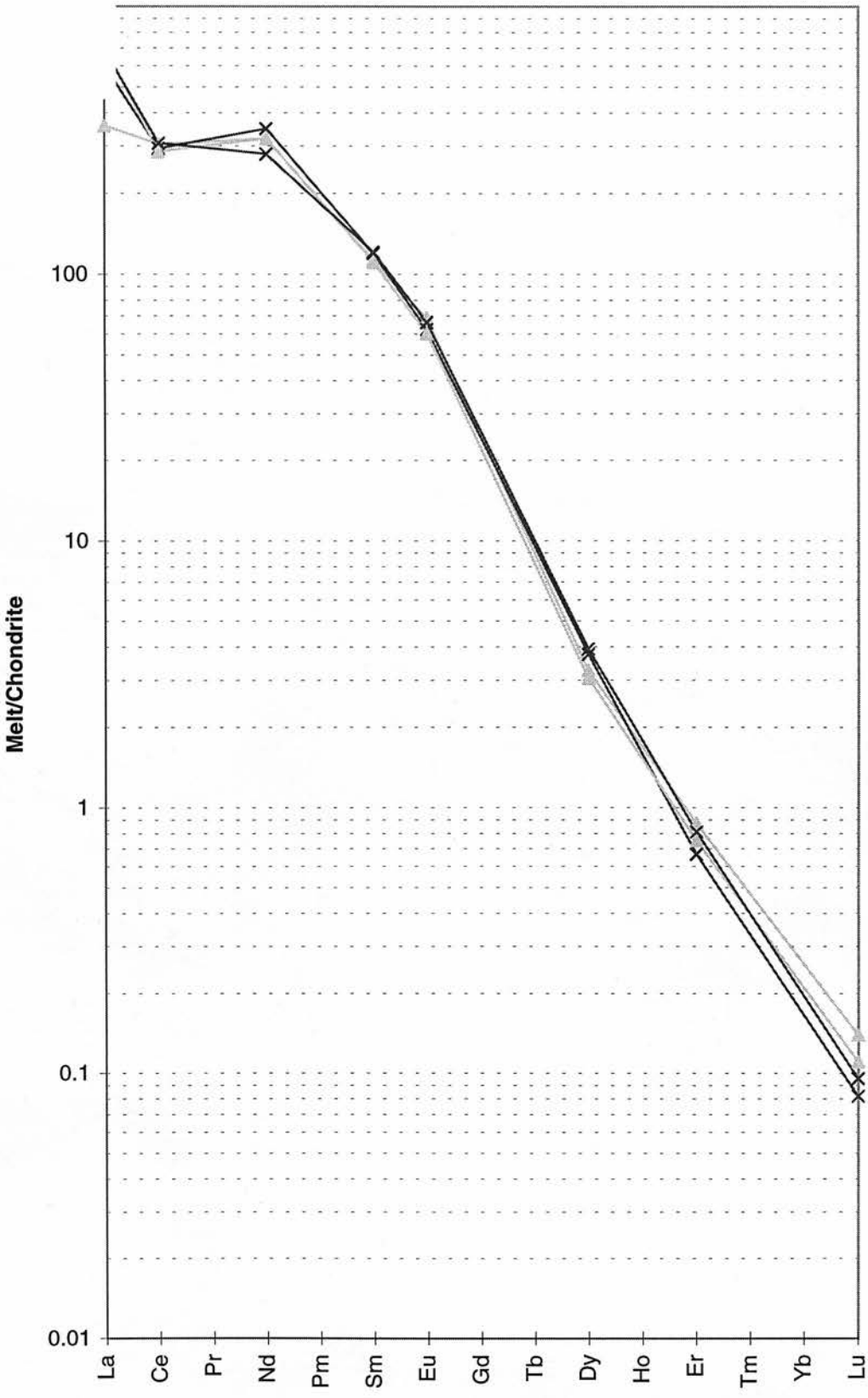

C:\simon\traces\melts\
1761g.xls

Fig. D.40 JJG1780 'melt'

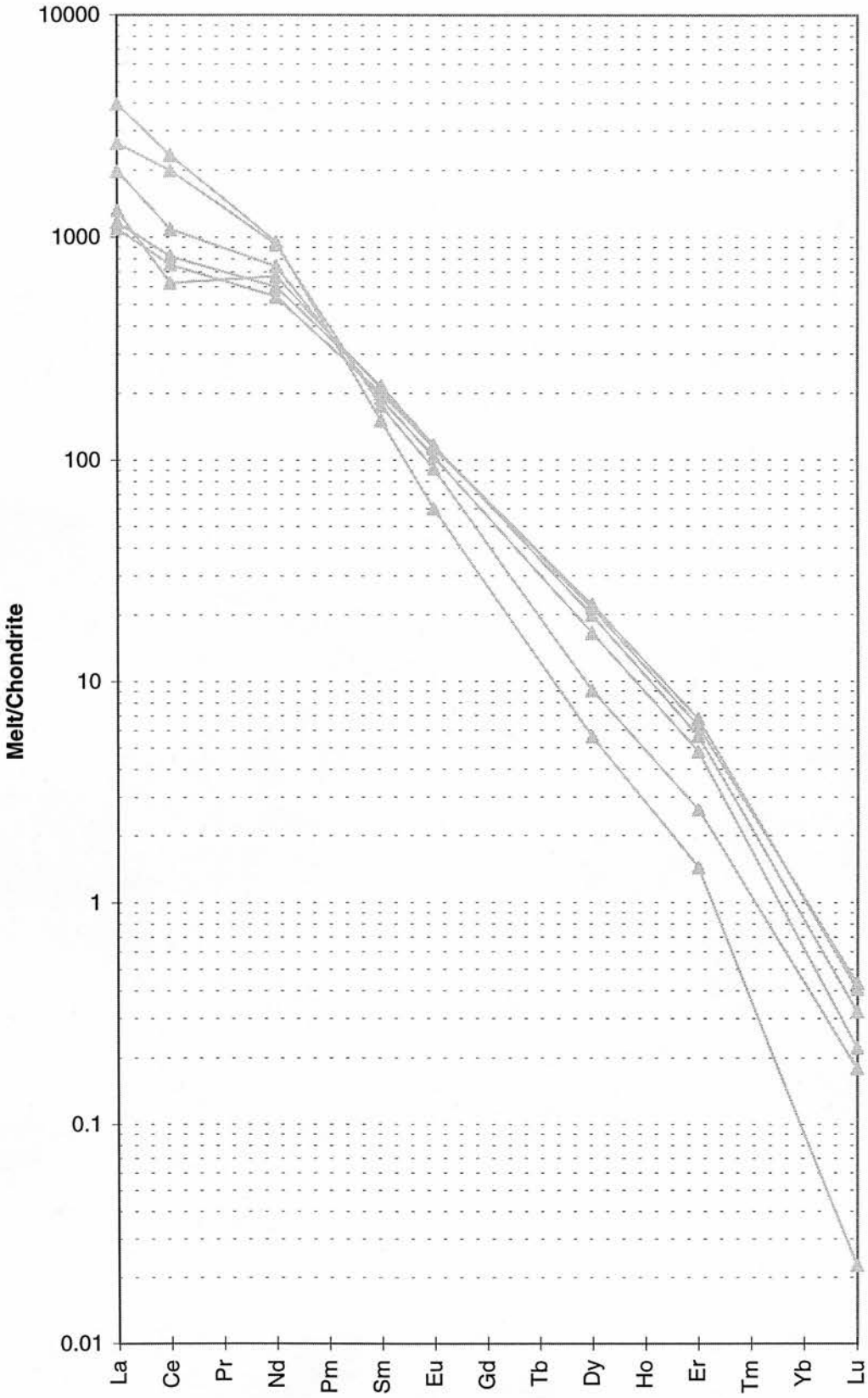

C:\simon\traces\melts\
1780g.xls

Fig. D.41 JJG1781 'melt'

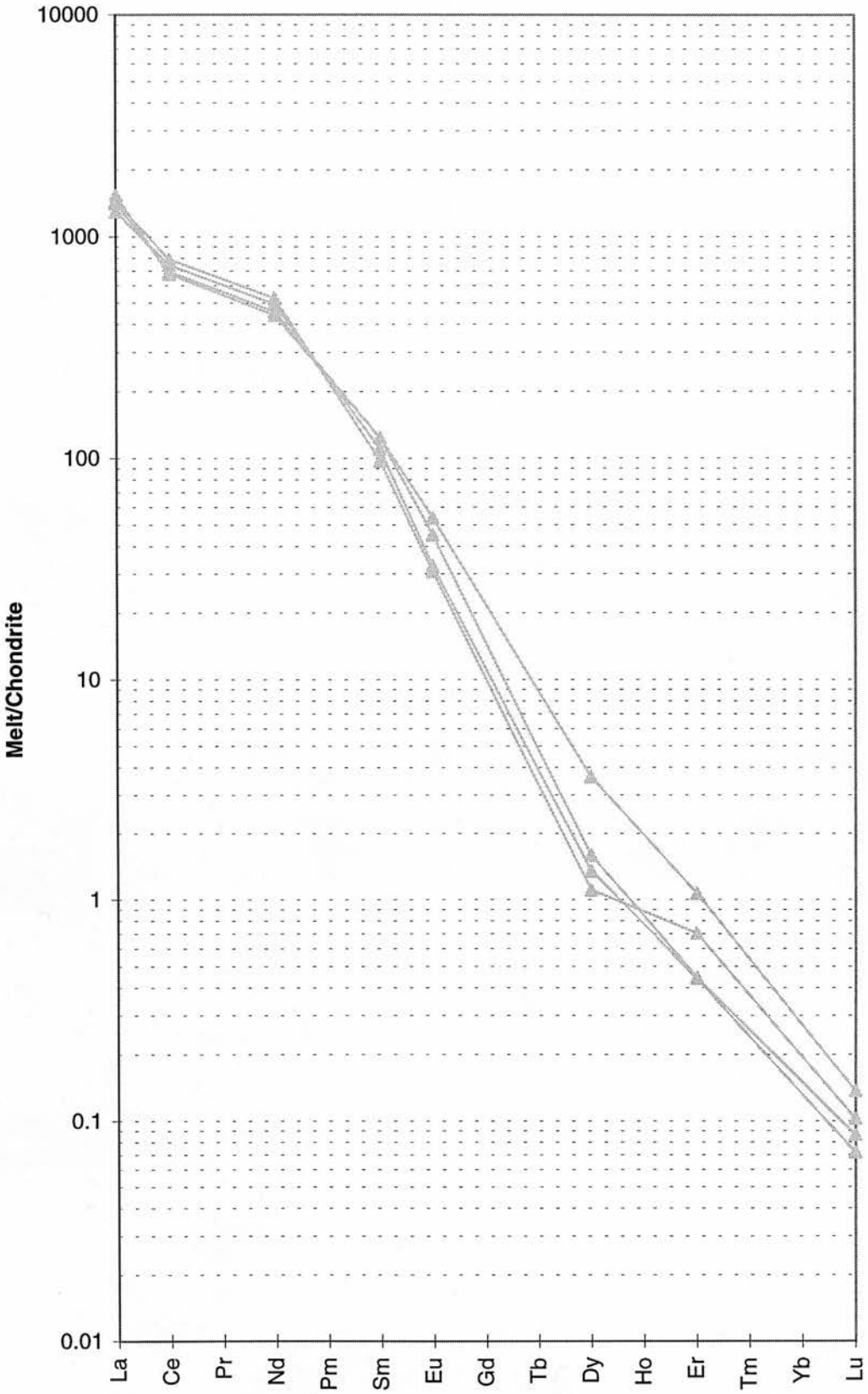

C:\simon\traces\melts\
1781g.xls

Fig. D.42 JJG2469 'melt'

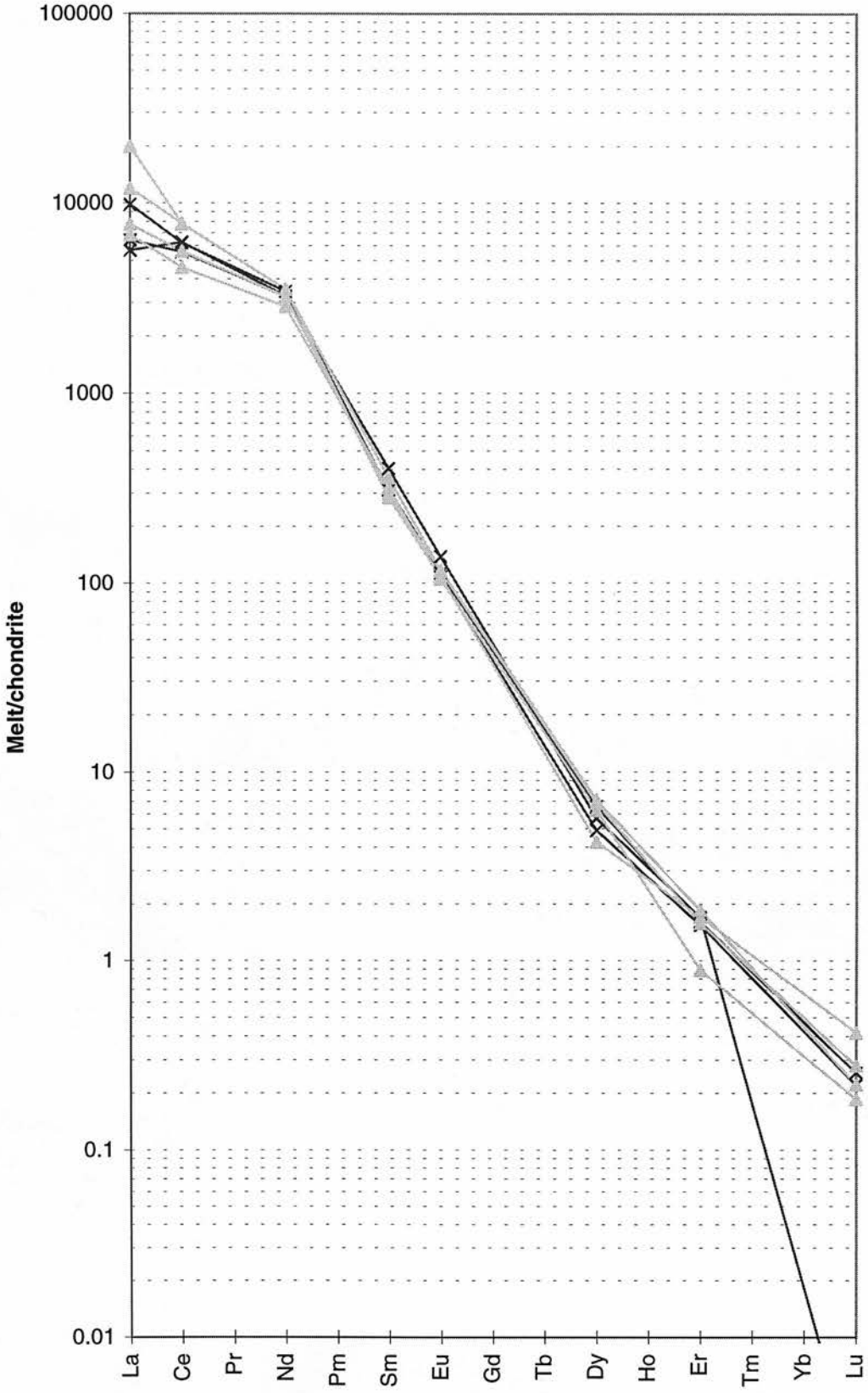

C:\simon\traces\melts\
2469g.xls

Fig. D.43 J22F/2 'melt'

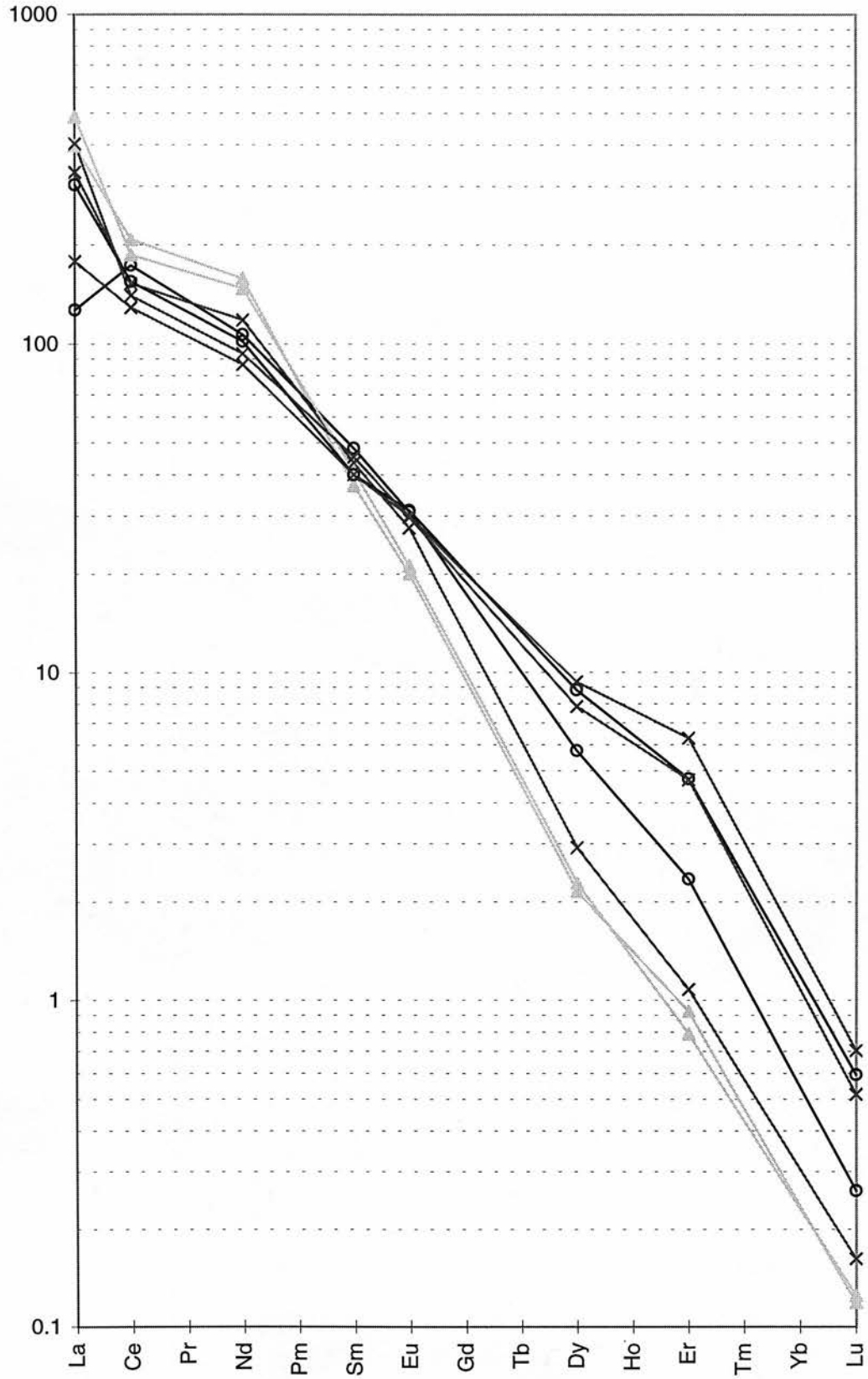

C:\simon\traces\melts\
j22f2g.xls

Fig. D.44 J34 'melt'

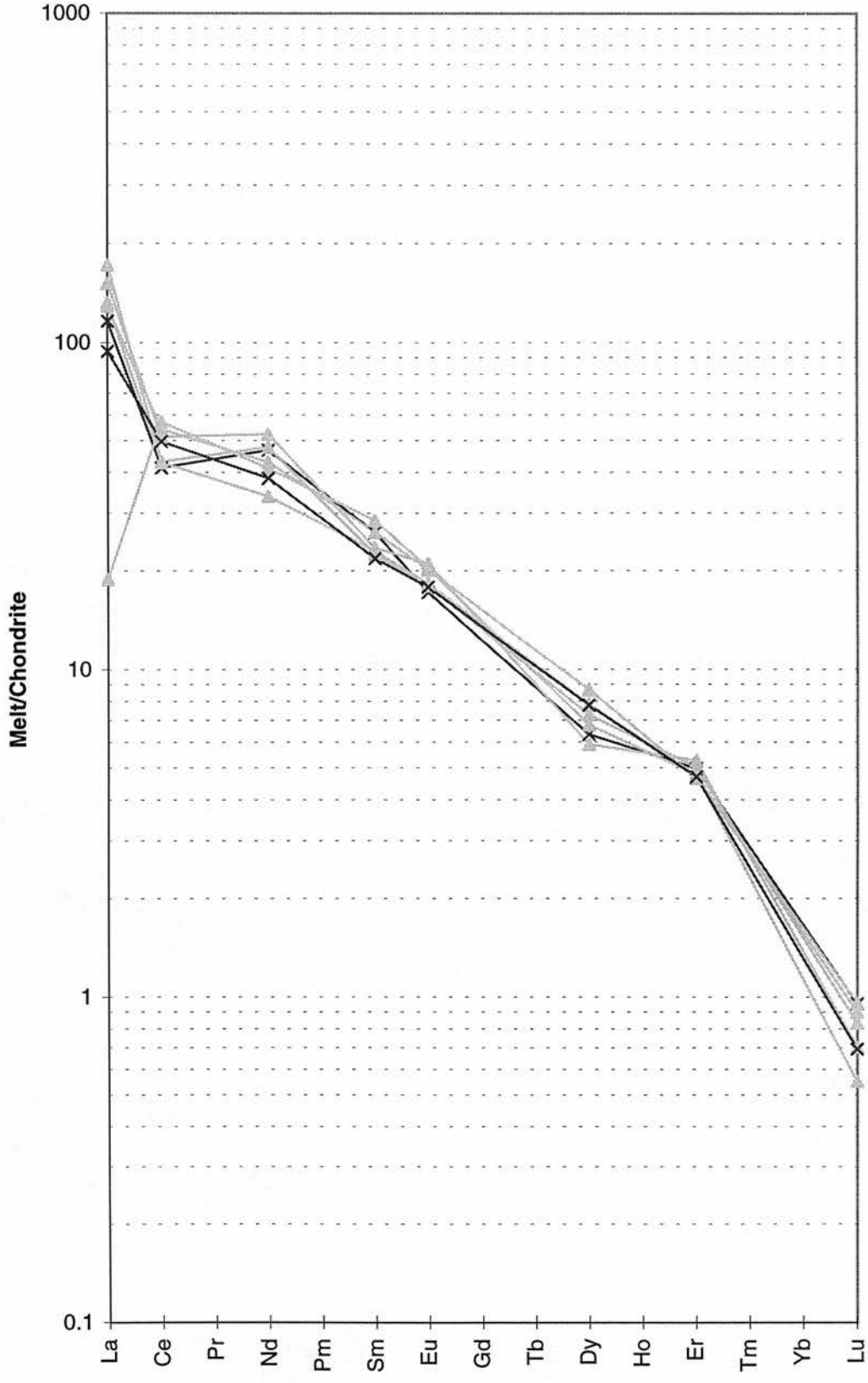

C:\simon\traces\melts\
j34g.xls

Fig. D.45 J47 'melt'

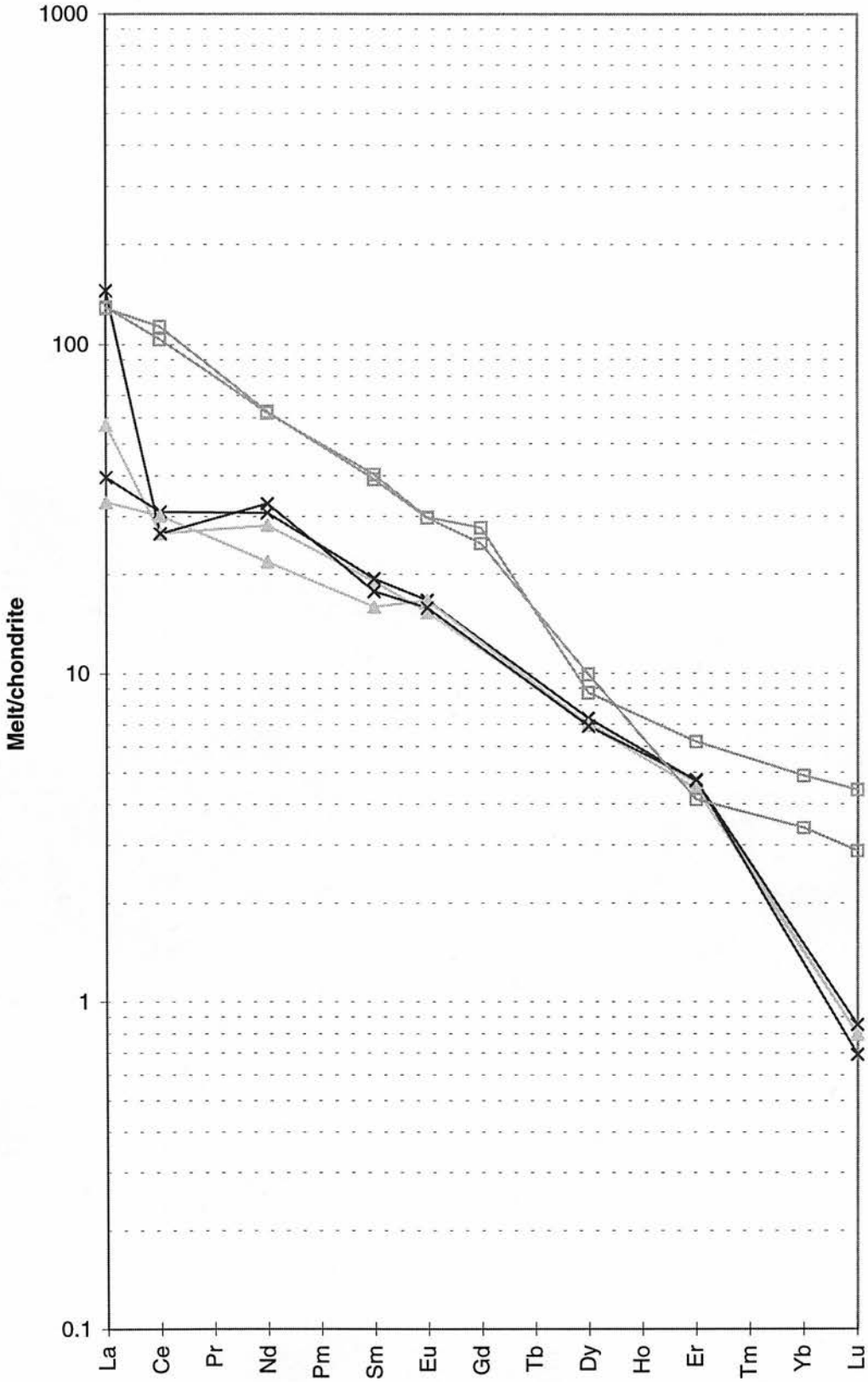

C:\simon\traces\melts\
J47g.xls

Fig. D.46 J51 'melt'

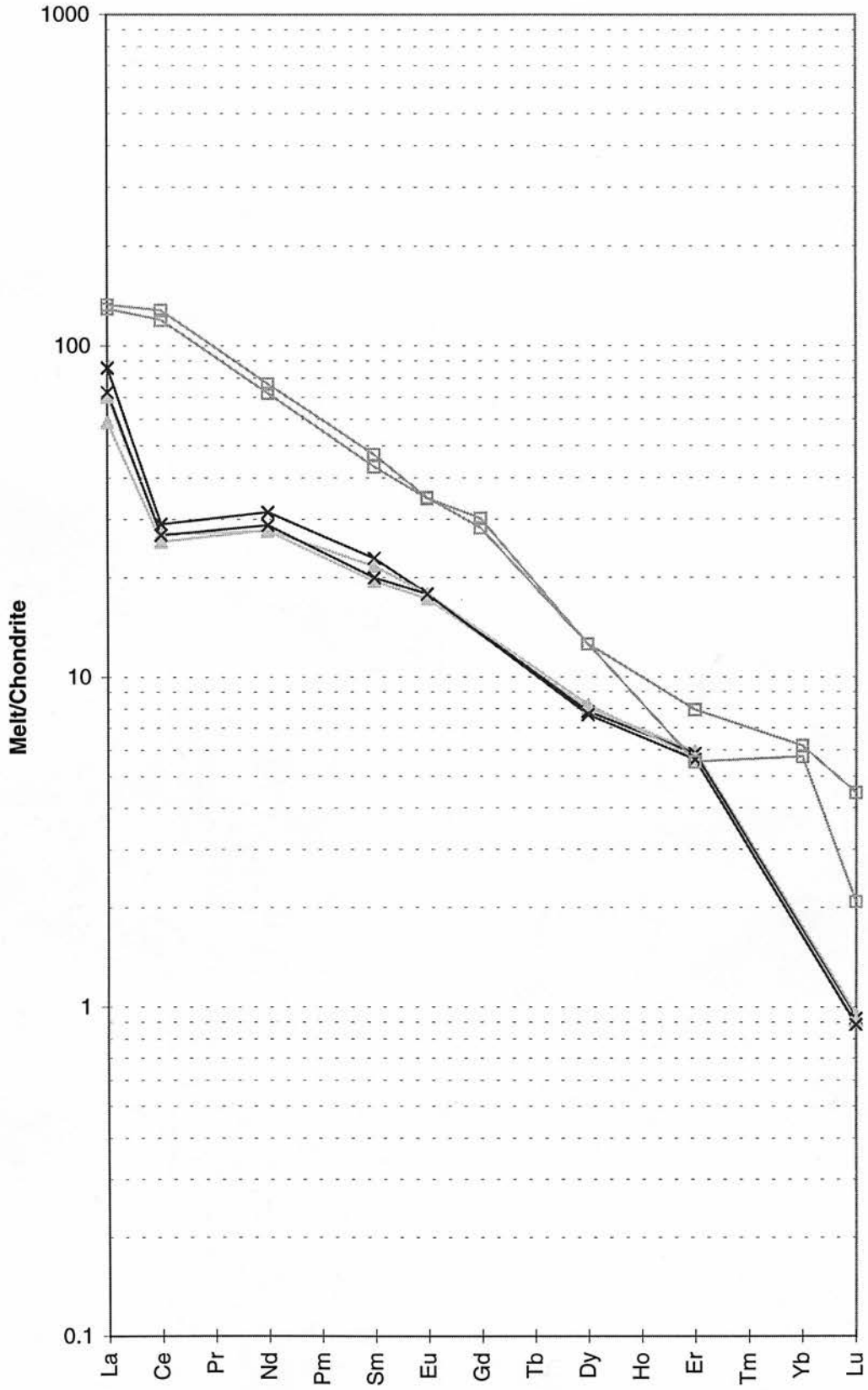

C:\simon\traces\melts\
j51g.xls

Fig. D.47 J107 'melt'

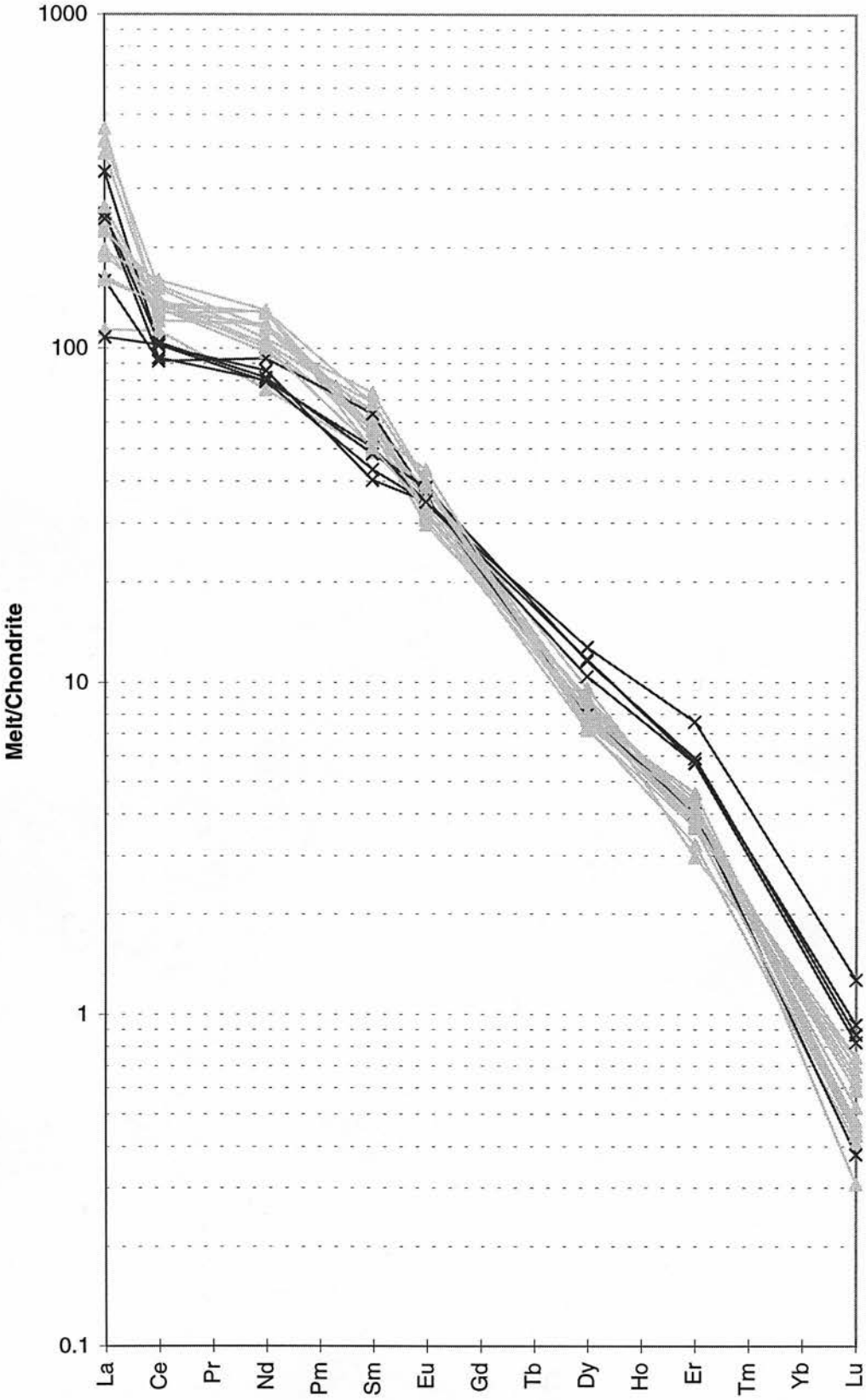

C:\simon\traces\melts\
j107g.xls

Fig. D.48 J110 'melt'

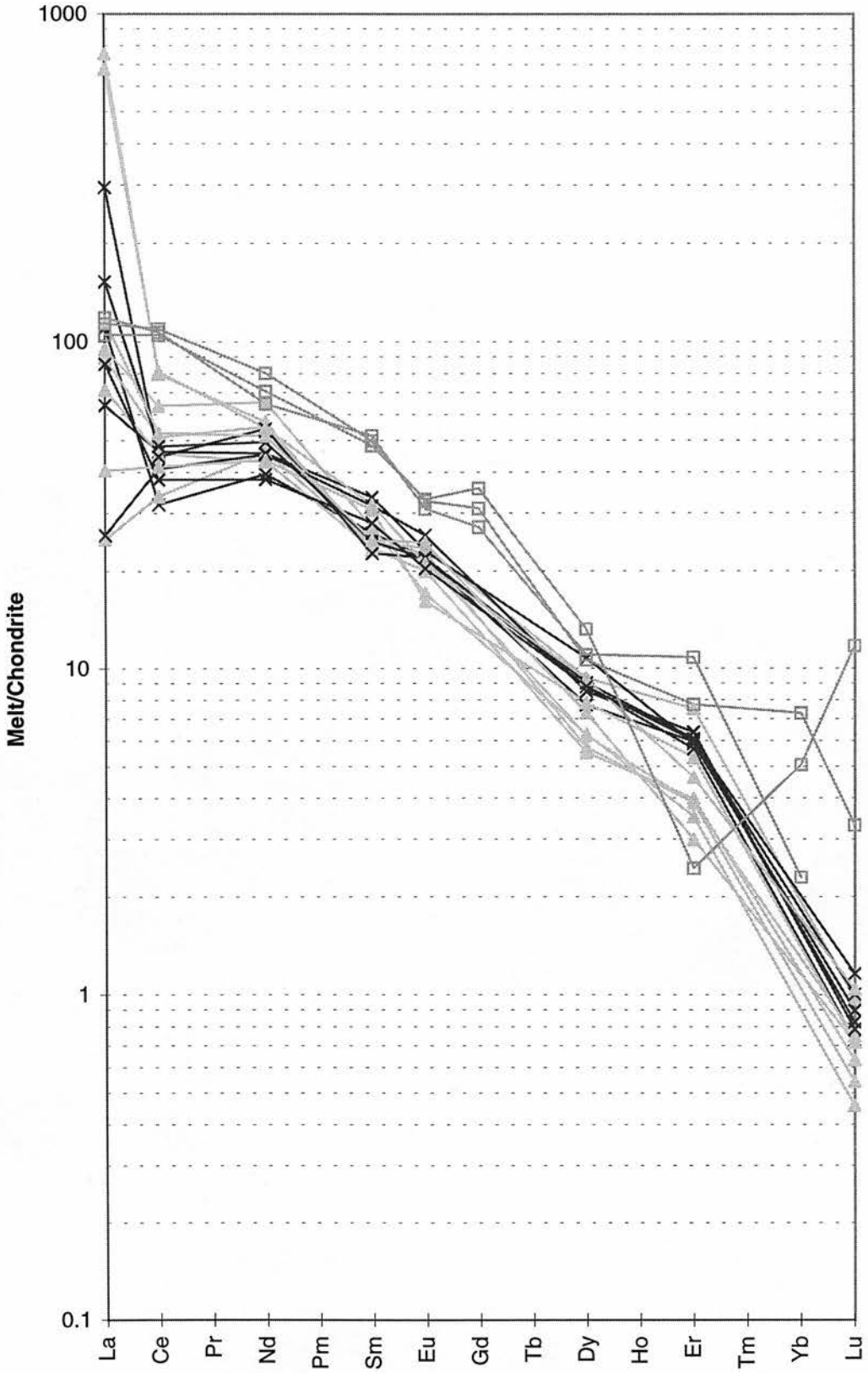

C:\simon\traces\melts\
j110g.xls

Fig. D.49 J112 'melt'

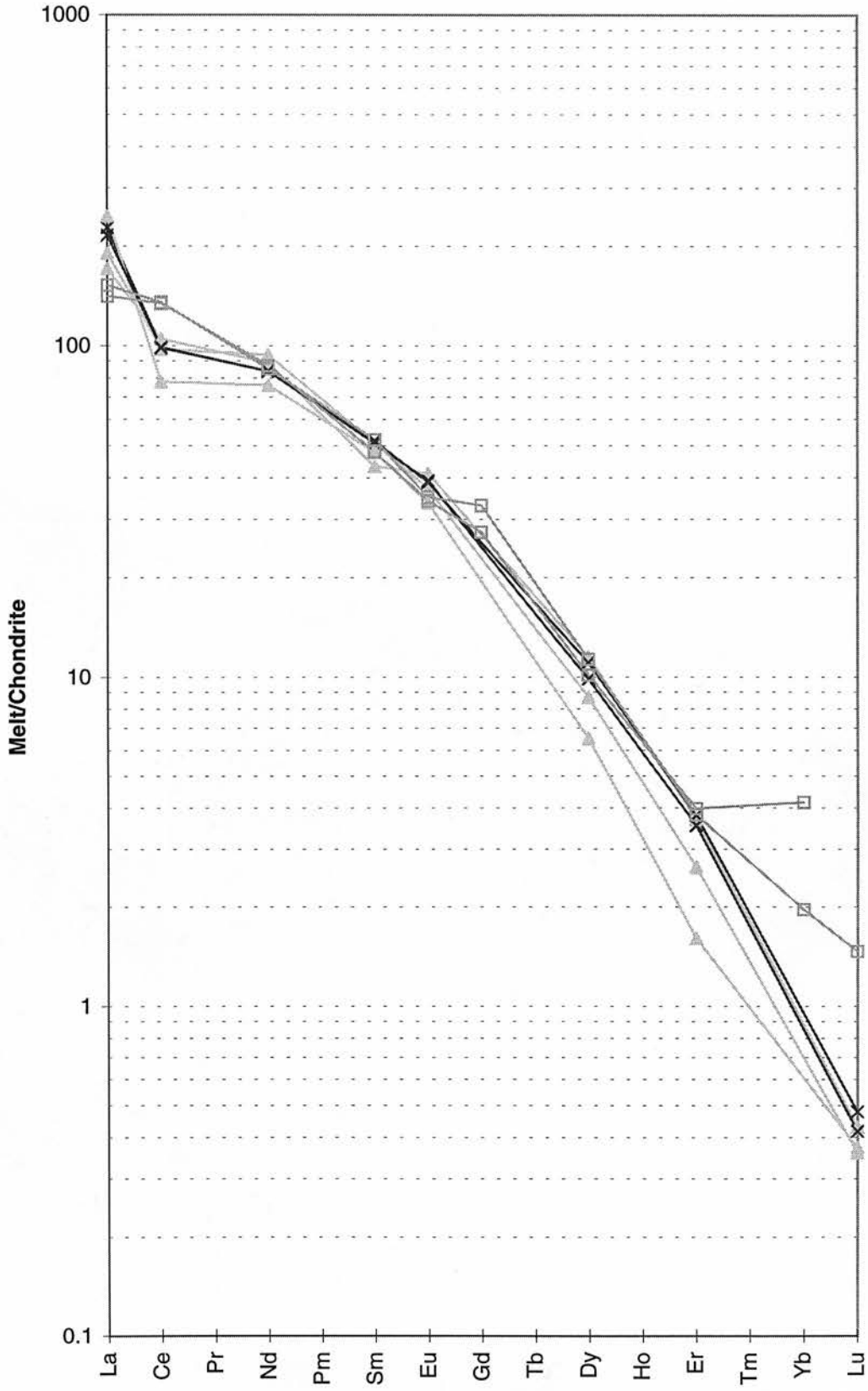

C:\simon\traces\melts
J112g.xls

Fig. D.50 J115 'melt'

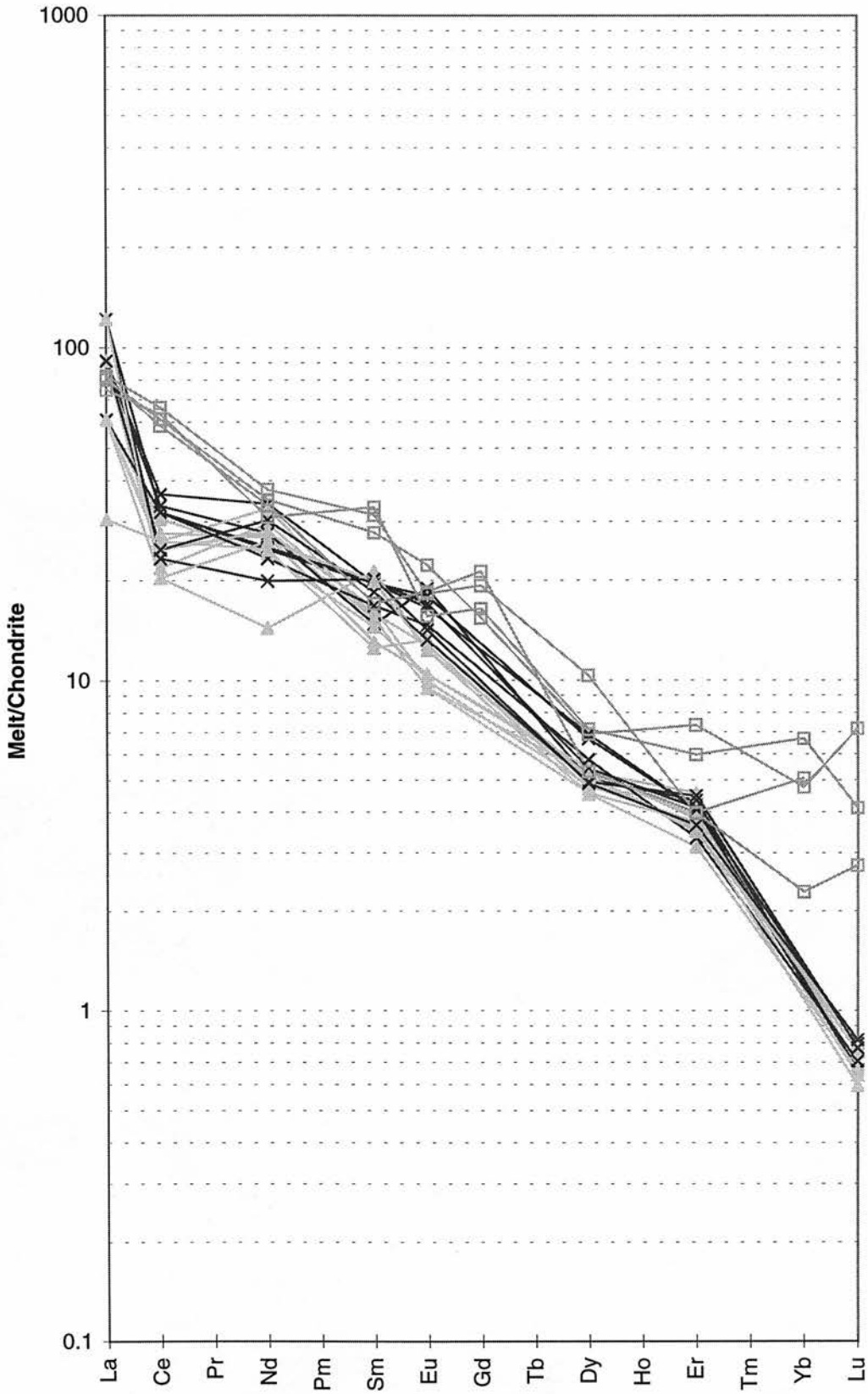

C:\simon\traces\melts\
J115g.xls

Fig. D.51 J121 'melt'

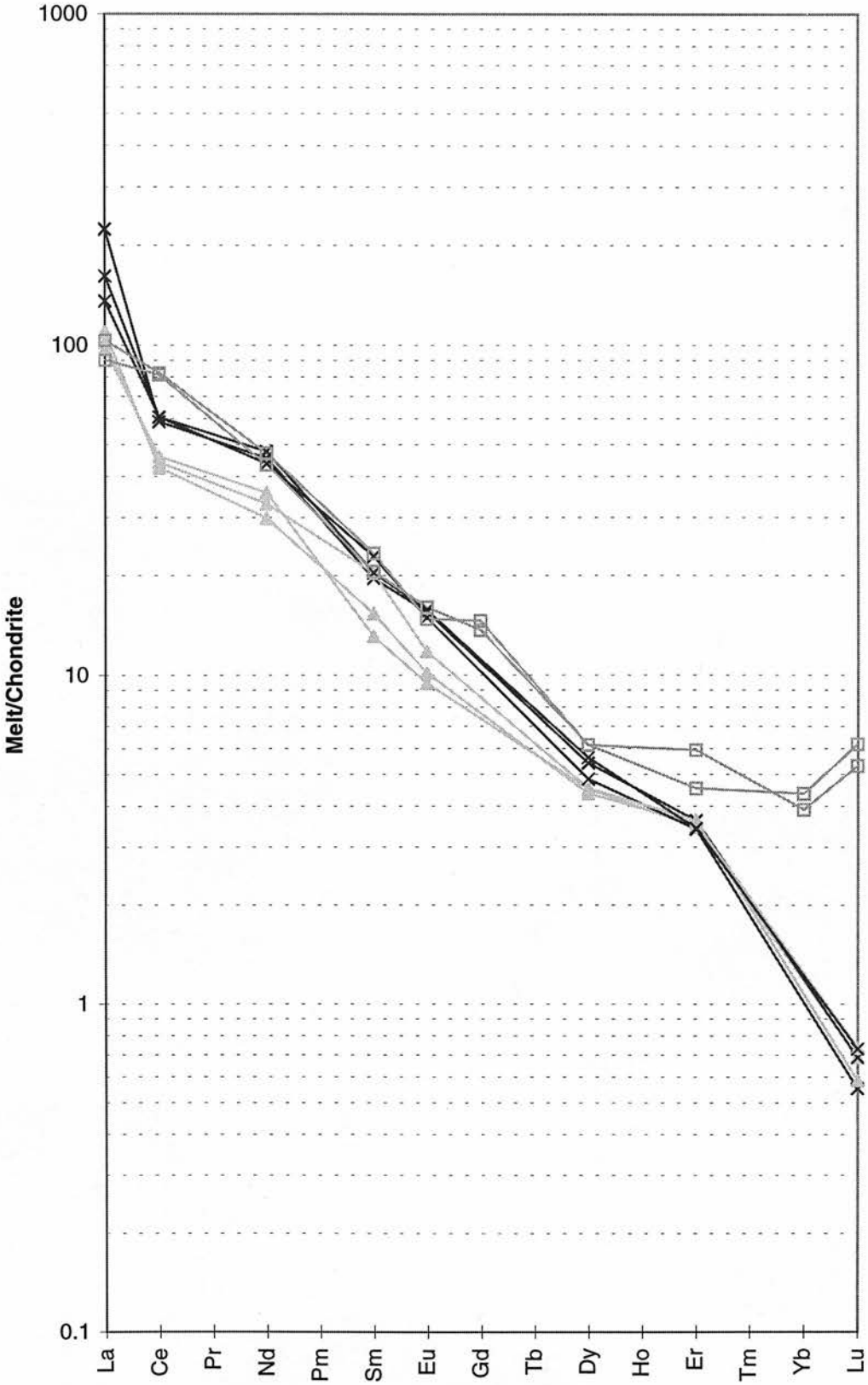

C:\simon\traces\melts\
J121g.xls

Fig. D.52 J145 'melt'

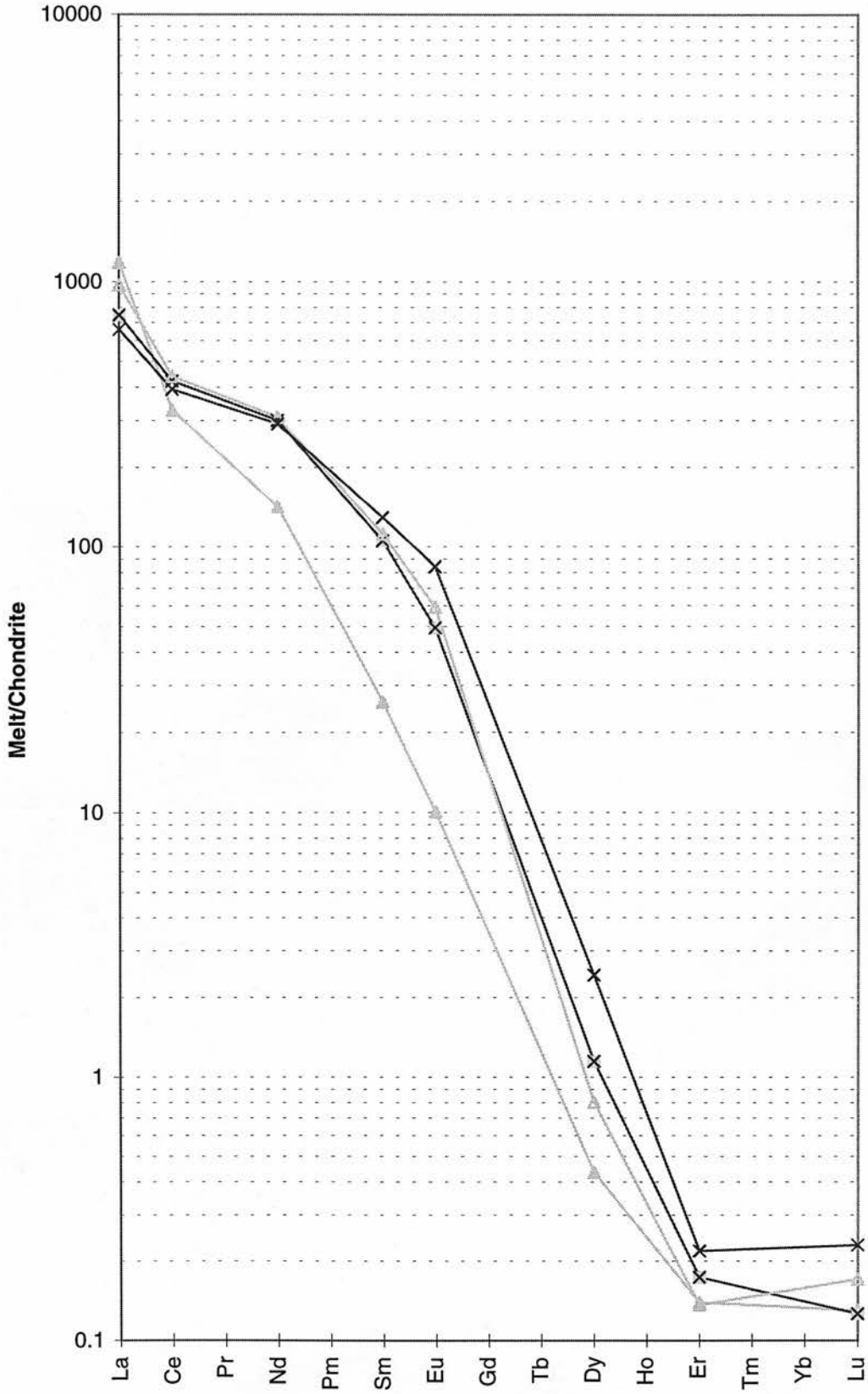

C:\simon\traces\melts\
J145g.xls

Fig. D.53 J159 'melt'

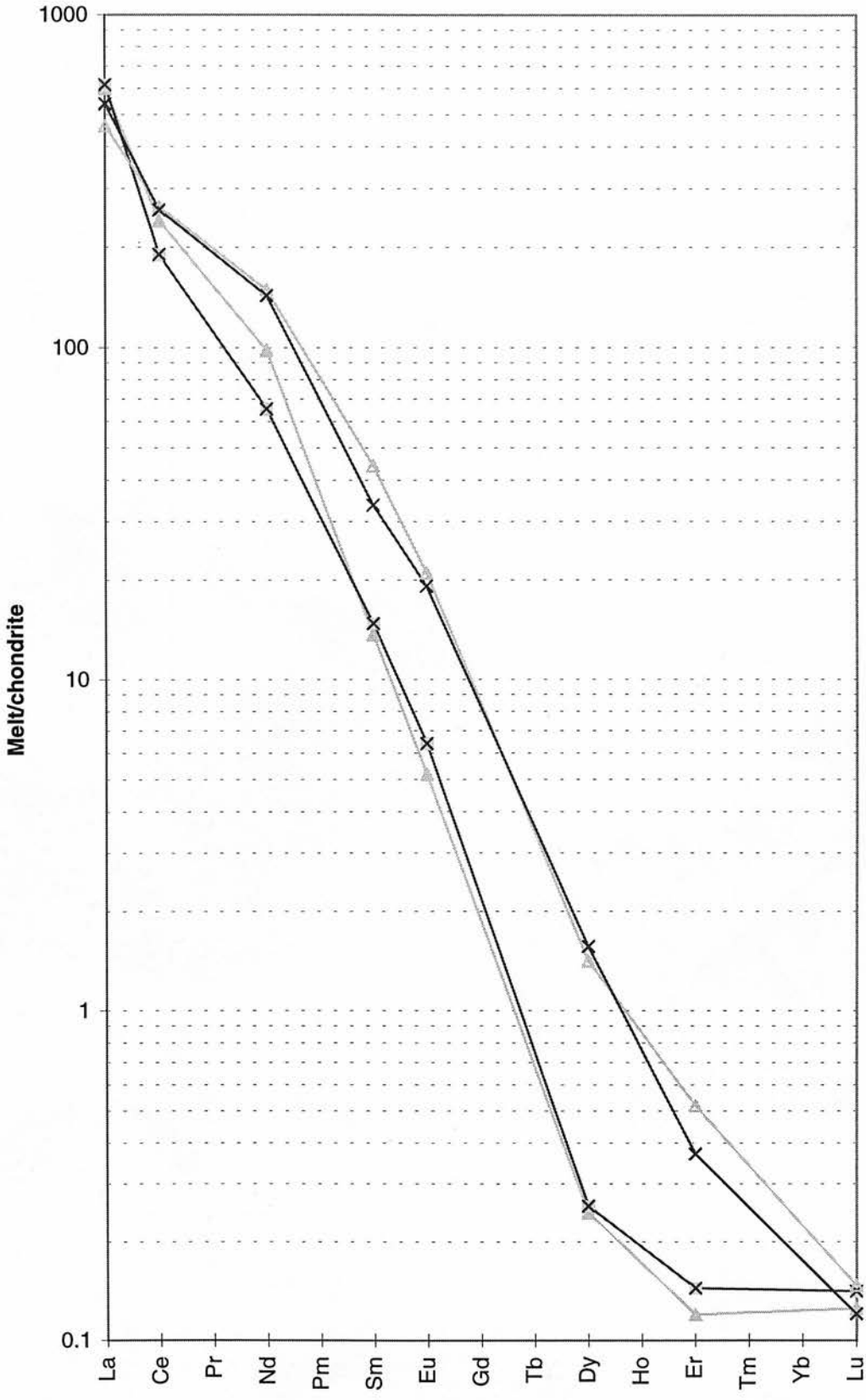

C:\simon\traces\melts\
J159g.xls

Fig. D.54 JJG1776 'melt'

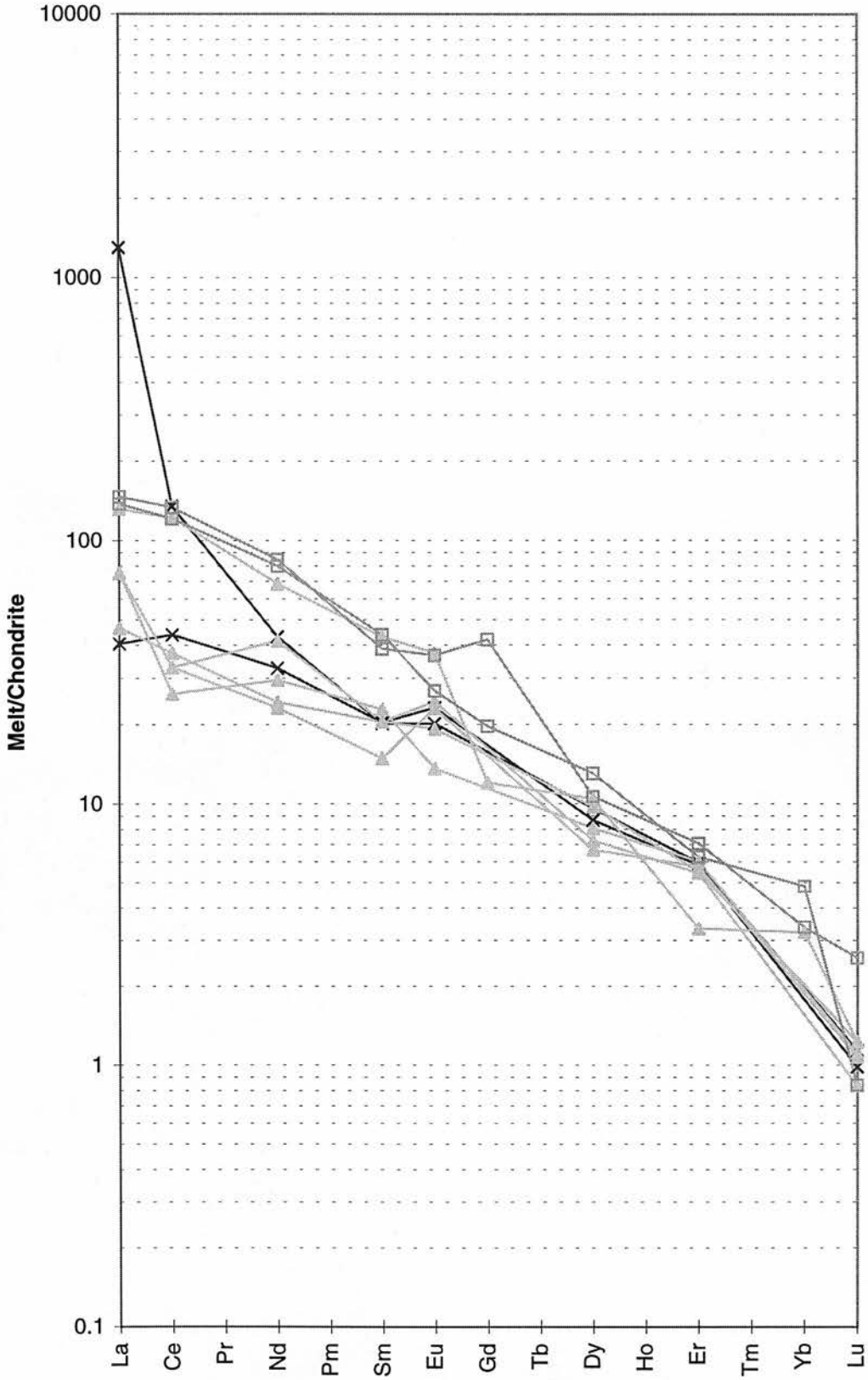

C:\simon\traces\melts\
1776g.xls

Fig. D.55 JJH19 'melt'

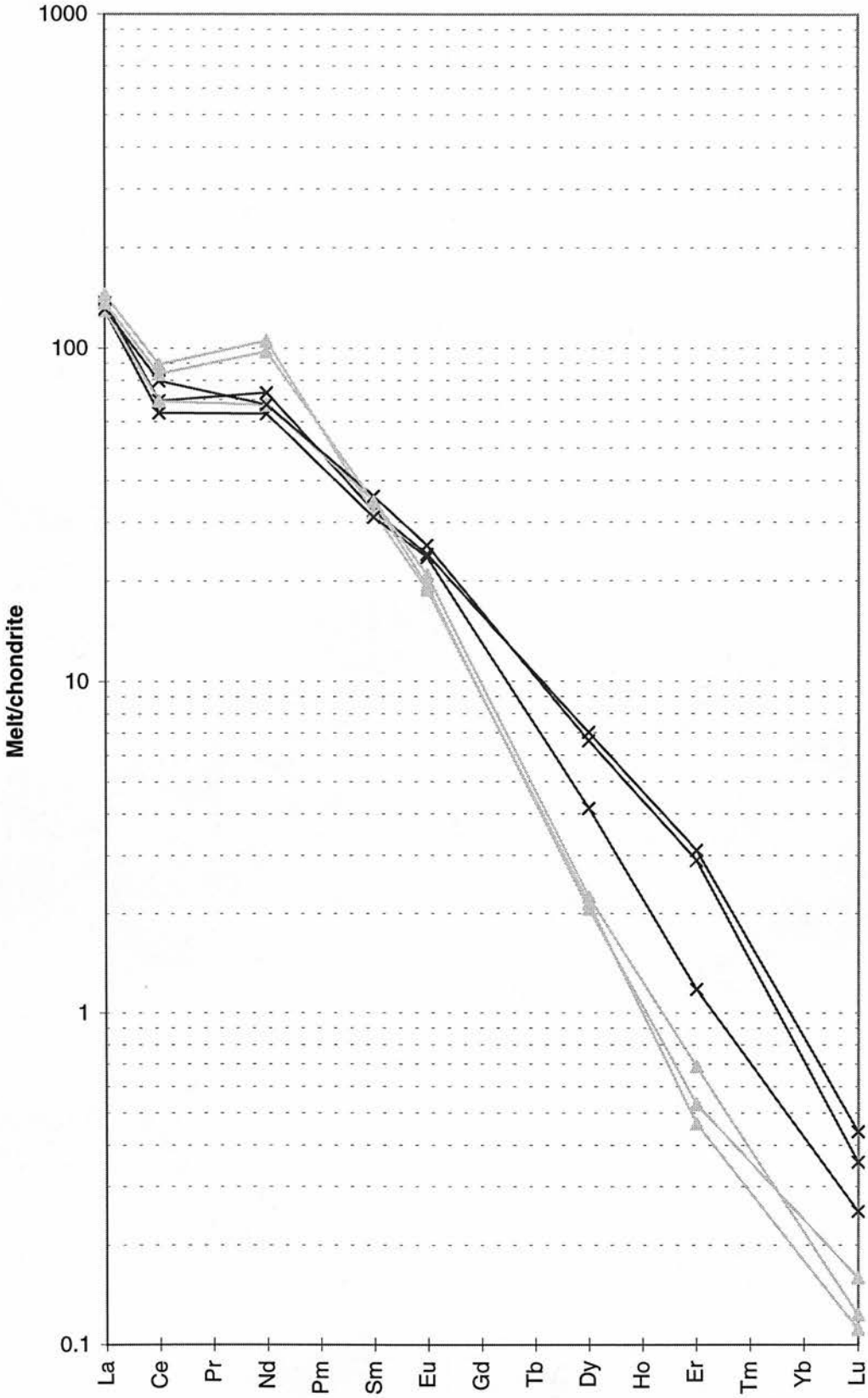

C:\simon\traces\melts
jjh19g.xls

Fig. D.56 JJH37 'melt'

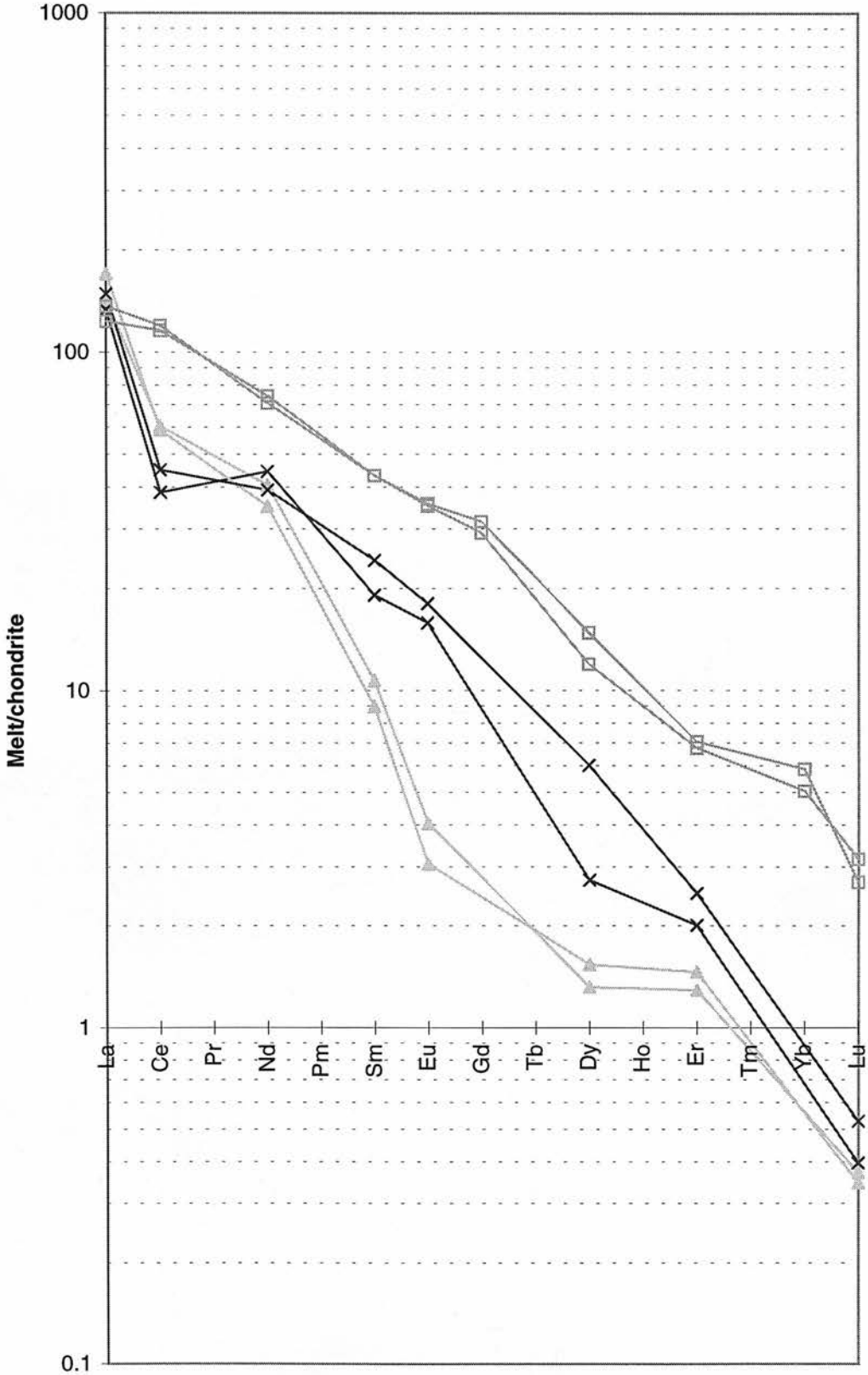

C:\simon\traces\melts
JJH37g.xls

Fig. D.57 Megacryst 'melt'

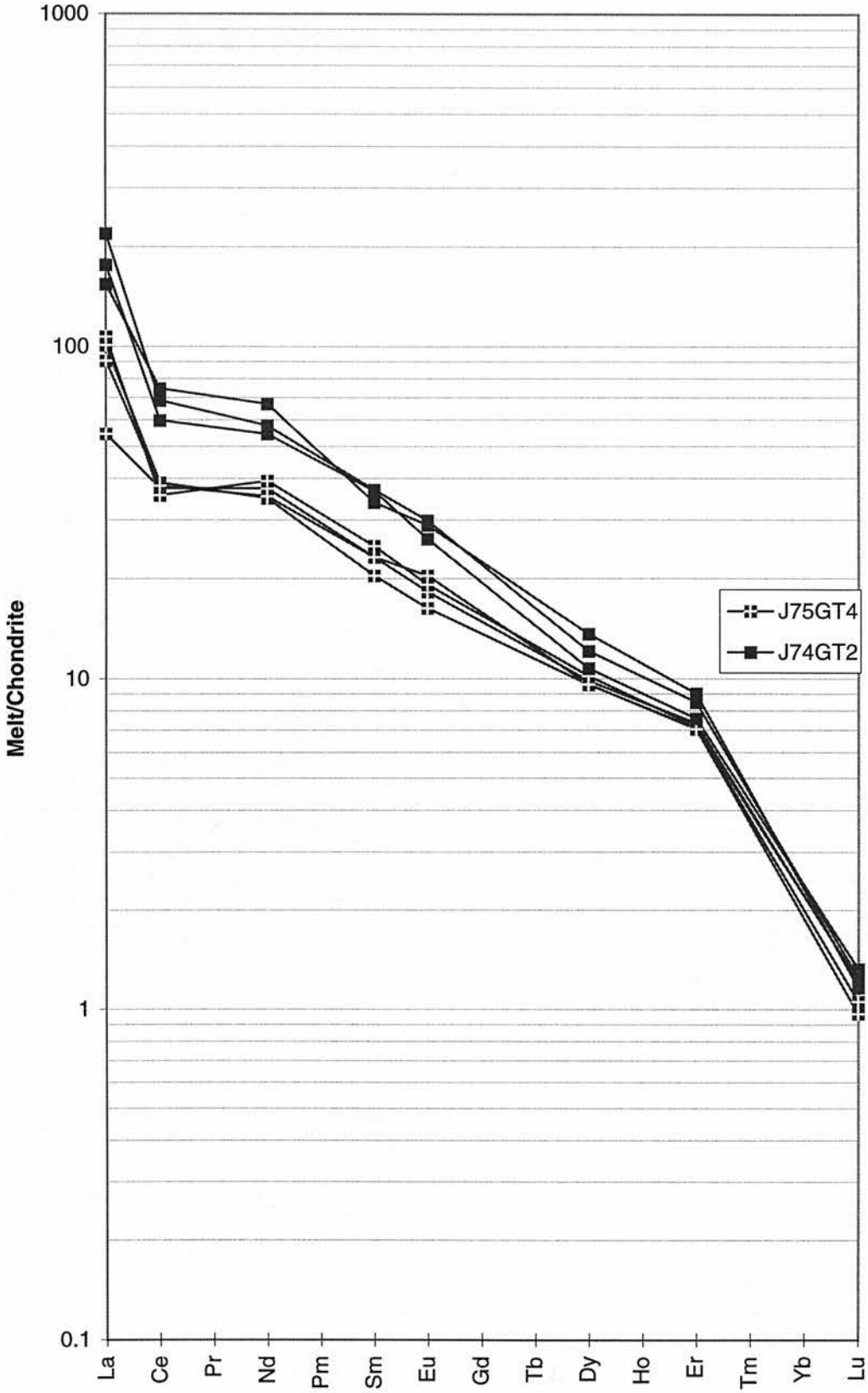

C:\simon\traces\melts\
j75g.xls

Appendix E

Laser Fluorination Oxygen Isotope Analysis

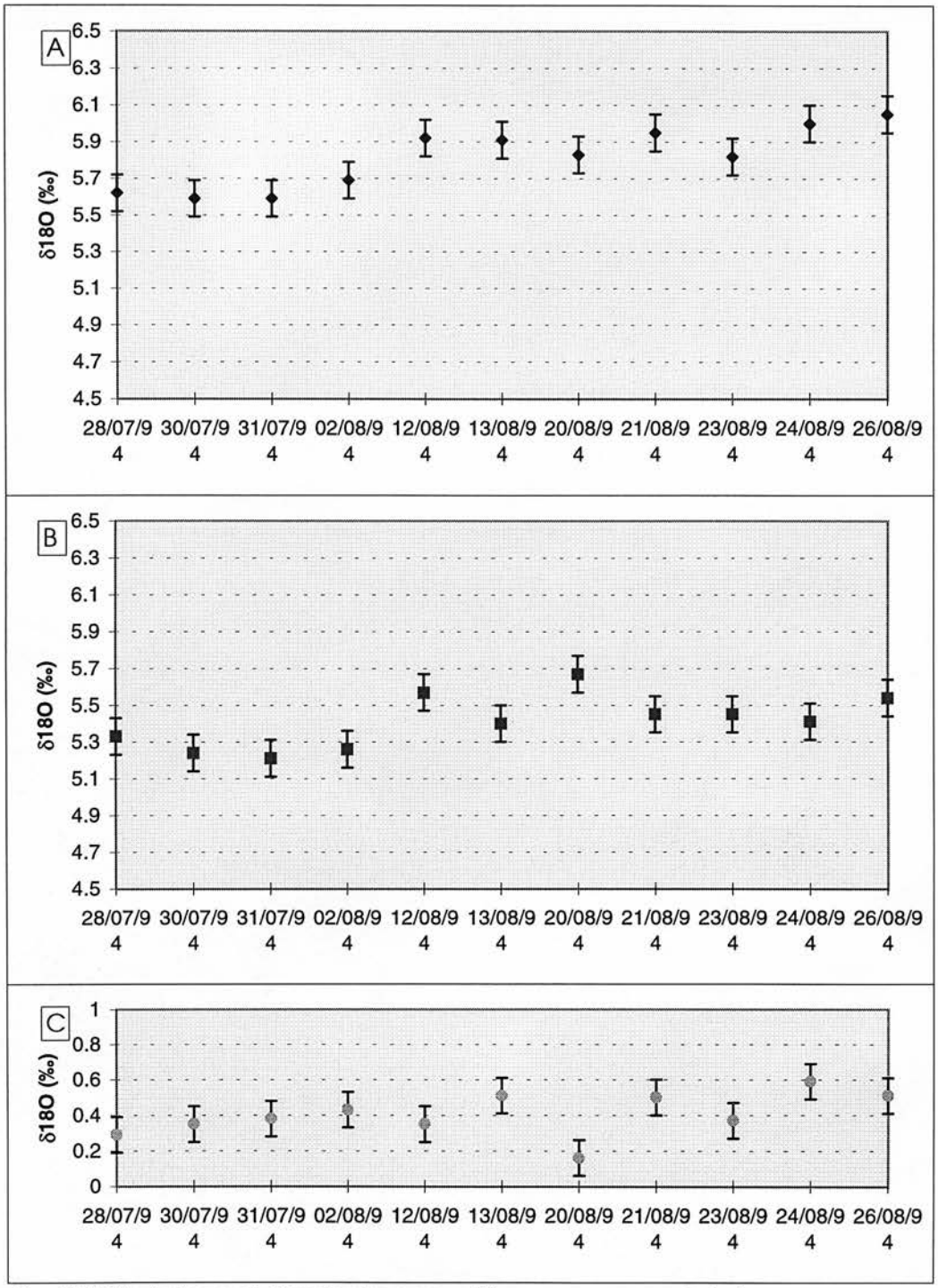

Fig. AE1 Variations of standard compositions as measured during different analysis sessions. A. shows variation in UWGMG-2 garnet standard, and B. shows variation in KHOL olivine standard. Error bars are ±0.1 per mil. representing typical 1σ precision for laser fluorination oxygen isotope analysis. C. shows δ18O UWGMG2 - δ18O KHOL for each session. With the exception of session 20/08/94 relative compositions measured for both standards are equivalent.

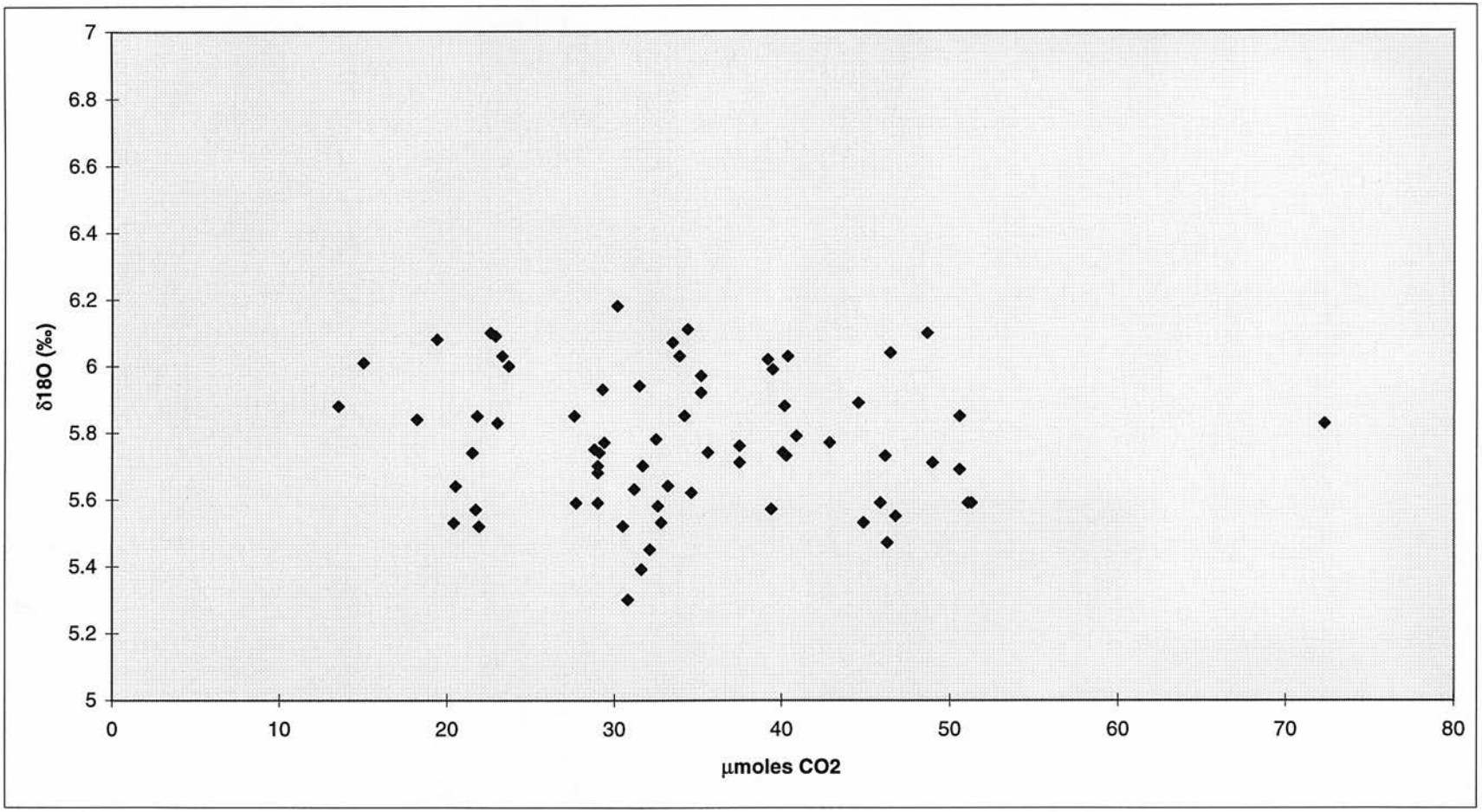

Fig. AE2 Variation of oxygen isotope composition measured for UW-GMG2 garnet standard with sample size. Sample size is given in terms of μmoles of CO2 formed from the oxygen liberated from the sample. Data are for all the analysis sessions from 6/7 to 26/8/1994.

Table E.1 Oxygen Isotope Compositions of Olivines

Sample Number	$\delta^{18}O$ (per mil-SMOW)	Number of Analyses (n)	σ_{n-1}
DEFORMED			
J22E (neoblast)	5.30	2	0.15
J26B (porphyroclast)	5.27	4	0.15
J31 (neoblast)	5.29	2	0.02
J34B (neoblast)	5.34	3	0.16
J36 (neoblast)	5.12	2	0.15
J37 (porphyroclast)	5.10	3	0.16
J37 (neoblast)	5.04	1	
J38 (neoblast)	5.08	3	0.21
J105 (porphyroclast)	5.27	6	0.16
J105 (neoblast)	5.17	2	0.03
J107B (neoblast)	5.05	2	0.25
J110 (noeblast)	5.30	1	
J112 (porphroclast)	5.12	3	0.10
J112 (neoblast)	4.82	2	0.15
J115 (neoblast)	4.96	2	0.38
J119 (porphroclast)	5.45	3	0.33
J119 (neoblast)	5.26	3	0.43
J145 (porphroclast)	5.20	3	0.19
J145 (neoblast)	5.48	1	
J159 (neoblast)	4.92	2	0.47
JJG1776 (porphyroclast)	5.37	1	
JJG1776 (neoblast)	5.40	2	0.06
COARSE			
J11	5.03	3	0.12
J12B	5.22	1	
J53	5.57	5	0.15
J154	5.39	4	0.19
JJG8	5.21	2	0.48
JJG853	5.07	2	0.40
JJG1778	5.09	3	0.08
JJG1795	5.39	2	0.37
JJG2469B	5.45	3	0.30

Table E.2 Oxygen Isotope Compositions of Orthopyroxenes

Sample Number	$\delta^{18}O$ (per mil-SMOW)	Number of Analyses (n)	σ_{n-1}
DEFORMED			
J22E	5.42	7	0.19
J26B	5.33	3	0.05
J31	5.28	5	0.21
J34B	5.67	3	0.14
J36	5.60	4	0.07
J37	5.14	2	0.11
J38	5.51	15	0.10
J105	5.43	5	0.20
J107B	5.74	2	0.25
J110	5.43	3	0.08
J112	5.31	3	0.28
J115	5.01	4	0.16
J119	5.66	15	0.14
J145	5.54	4	0.31
J159	5.51	5	0.39
JJG1776	5.54	3	0.28
COARSE			
J12B	5.57	4	0.37
J28	5.83	7	0.14
J53	6.04	7	0.10
J154	5.88	19	0.14
JJG8	6.02	3	0.06
JJG1778	5.60	6	0.21
JJG1795	5.74	11	0.30

Table E.3 Oxygen Isotope Compositions of Clinopyroxenes

Sample Number	$\delta^{18}O$ (per mil-SMOW)	Number of Analyses (n)	σ_{n-1}
DEFORMED			
J26B	5.12	2	0.17
J34B	5.38	1	
J36	5.18	3	0.17
J38	5.07	3	0.36
J105	4.79	2	0.14
J115	4.98	1	
J119	5.10	7	0.14
JJG1776	5.20	4	0.16
COARSE			
J12B	5.05	7	0.19
JJG853	4.94	5	0.18
JJG1795	4.96	8	0.17

Table E.4 Oxygen Isotope Compositions of Garnets

Sample Number	$\delta^{18}O$ (per mil-SMOW)	Number of Analyses (n)	σ_{n-1}
DEFORMED			
J22E	5.50	23	0.29
J26B	5.54	2	0.04
J31	5.32	4	0.15
J34A	5.59	12	0.17
J34B	5.37	7	0.21
J36	5.57	21	0.23
J37	5.30	2	0.18
J38	5.66	8	0.20
J105	5.44	8	0.24
J107B	5.55	9	0.12
J110	5.38	2	0.07
J115	5.18	5	0.20
J119	5.53	15	0.21
JJG1776	5.62	7	0.25
COARSE			
J53	5.78	1	
JJG2469B	5.14	6	0.23

Table E.5 Oxygen Isotope Compositions of Hydrous Minerals

PHLOGOPITE Sample Number	$\delta^{18}O$ (per mil-SMOW)	Number of Analyses (n)	σ_{n-1}
COARSE			
J154 (Secondary)	5.43	5	0.58
JJG8	5.75	3	0.30
JJG1795	5.72	11	0.32

SERPENTINE Sample Number	$\delta^{18}O$ (per mil-SMOW)	Number of Analyses (n)	σ_{n-1}
DEFORMED			
J26B	2.26	1	
J34B	3.75	1	
J37	2.84	1	
J105	1.63	1	
J145	3.22	1	
COARSE			
JJG2469B	0.21	1	

Appendix F

SIMS Oxygen Isotope Analysis

TABLE AF.1. Major element compositions of standard and unknowns for ion-probe analysis.

	KHOL	J119 Ol. Porph.	J119 Ol. Neoblast	J119 Gnt.	J119 Gnt.
	n=13	n=6	n=3	n=91	n=82
SiO_2	39.93	39.96	40.04	41.30	41.38
TiO_2		0.03	0.04	0.67	0.67
Al_2O_3		0.04	0.04	21.34	21.36
Cr_2O_3				1.93	1.92
MgO	48.64	49.17	49.32	21.85	21.81
CaO	0.13	0.06	0.06	4.49	4.48
MnO	0.17	0.11	0.11	N. A.	N. A.
FeO	10.67	9.89	9.93	8.11	8.10
NiO	0.33	0.31	0.34	N. A.	N. A.
Na_2O		0.04	0.04	0.09	0.09
TOTAL	99.87	99.61	99.92	99.78	99.81
Mg No.	89.04	89.86	89.84		

N. A. Not Analysed
Major elements by W. D. S. analysis on Cameca Camebax, at the University of Edinburgh, beam current 20nA for olivine, 80nA for garnet, 20kV, PAP correction.

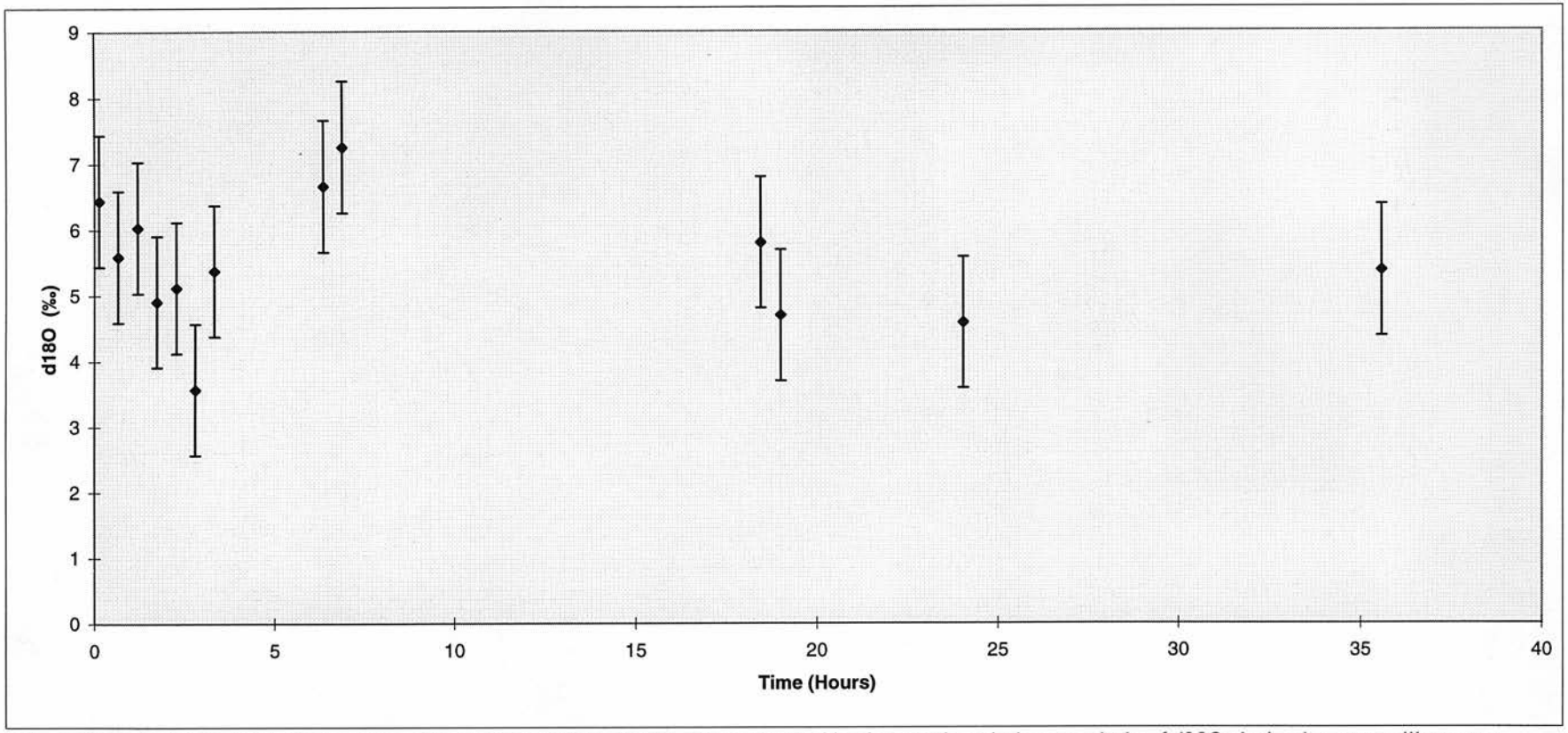

Fig. AF.1 Variation in δ18O with time of the KHOL olivine standard measured by ion probe during analysis of J119. Actual compositions are normalised so the average composition of the standard is δ18O= 5.49 per mil. (as measured by laser fluorination). Error bars represent ±1.0 per mil. precision for each analysis, as determined by counting statistics. There is no consistent drift in the measured oxygen isotope ratio with time, and therefore no drift correction is needed for data manipulation. The standard deviation of the analysis (±0.98 per mil.) is exactly as expected from counting statistics.

TABLE F.1A. Ion Probe Data for sample J119.- olivine analysis

Analysis No.	$\delta^{18}O$ (per mil.-SMOW)	Error (per mil)	Notes
J119OL1	4.2	1.00	Neoblast
J119OL2	5.0	0.97	Neoblast
J119OL5	4.2	0.97	Neoblast
J119OL7	5.5	1.05	Neoblast
J119OL8	5.9	1.00	Neoblast
J119OL9	5.3	1.00	Neoblast
J119OL13	4.7	0.97	Neoblast
J119OL16	4.0	1.03	Neoblast
J119OL17	5.0	1.06	Neoblast
J119OL21	4.1	1.06	Neoblast
J119OL22	5.3	1.10	Neoblast
J119OL23	3.8	0.97	Neoblast
J119OL29	4.8	0.94	Neoblast
J119OL30	6.1	0.99	Neoblast
J119OL34	4.8	1.12	Neoblast
J119OL3	6.1	1.03	Porphyroclast
J119OL4	4.8	0.97	Porphyroclast
J119OL6	6.2	0.96	Porphyroclast
J119OL10	4.2	1.04	Porphyroclast
J119OL11	5.1	0.99	Porphyroclast
J119OL12	4.2	1.08	Porphyroclast
J119OL14	5.7	1.06	Porphyroclast
J119OL15	5.5	1.07	Porphyroclast
J119OL20	6.9	1.05	Porphyroclast
J119OL24	5.4	1.05	Porphyroclast
J119OL25	5.5	1.02	Porphyroclast
J119OL26	4.6	1.04	Porphyroclast
J119OL27	4.4	1.08	Porphyroclast
J119OL28	4.8	1.05	Porphyroclast
J119OL31	4.0	1.04	Porphyroclast
J119OL32	5.7	1.05	Porphyroclast
J119OL33	5.9	1.08	Porphyroclast
J119OL35	4.1	1.04	Porphyroclast
J119OL36	3.0	1.17	Porphyroclast
J119OL18	4.6	1.09	Tablet
J119OL19	4.4	1.04	Tablet

TABLE F.1B.- Ion Probe Data for sample J119.- garnet analysis.
(Garnet grains One and Two have been analysed see Fig. 8.8a,b)

Analysis No.	$\delta^{18}O$ (per mil.-SMOW)	Error (per mil)	Notes
J119GT2	5.5	1.12	Garnet 1
J119GT3	3.5	0.99	Garnet 1
J119GT4	7.3	1.12	Garnet 1
J119GT6	3.4	1.05	Garnet 1
J119GT7	4.3	1.00	Garnet 1
J119GT8	6.0	1.06	Garnet 1
J119GT9	5.2	1.04	Garnet 1
J119GT10	6.6	1.07	Garnet 1
J119GT11	6.0	0.99	Garnet 1
J119GT12	6.6	1.03	Garnet 1
J119GT13	6.9	0.98	Garnet 1
J119GT14	6.0	0.99	Garnet 1
J119GT15	6.9	1.09	Garnet 1
J119GT16	5.7	1.04	Garnet 1
J119GT17	2.9	1.02	Garnet 1
J119GT18	6.2	1.02	Garnet 1
J119GT19	4.9	0.96	Garnet 1
J119GT20	6.2	1.07	Garnet 1
J119GT21	4.6	1.04	Garnet 2
J119GT22	5.8	1.05	Garnet 2
J119GT23	4.2	1.04	Garnet 2
J119GT24	6.8	1.07	Garnet 2
J119GT25	5.6	1.09	Garnet 2
J119 GT26	5.3	1.11	Garnet 2
J119GT27	5.1	1.01	Garnet 2
J119GT28	5.5	0.99	Garnet 2
J119GT30	4.7	1.03	Garnet 2
J119GT31	4.9	1.07	Garnet 2
J119GT32	7.1	1.10	Garnet 2
J119GT33	6.6	1.00	Garnet 2
J119GT34	4.8	1.06	Garnet 2
J119GT35	6.0	1.07	Garnet 2